PhD-FSTM-2023-002
The Faculty of Science, Technology and Medicine

DISSERTATION

Defence held on 09/01/2023 in Luxembourg

to obtain the degree of

DOCTEUR DE L'UNIVERSITÉ DU LUXEMBOURG

EN BIOLOGIE

by

Giulia PAGANO
Born on 15th June 1993 in city of Terlizzi, (Italy)

ROLE OF AHR, HIF-1α AND IL-27 IN T-CELL-MEDIATED IMMUNITY IN CHRONIC LYMPHOCYTIC LEUKEMIA

Dissertation defence committee

Dr Jérôme Paggetti, dissertation supervisor
Group leader, Tumor Stroma Interactions
Luxembourg Institute of Health, Luxembourg

Dr. Elisabeth Letellier, chair
Assistant Professor, Group leader, Molecular Disease Mechanisms Group
University of Luxembourg, Luxembourg

Dr. Eric Eldering, vice-chair
Professor, Department of Experimental Immunology
University Medical Centers, Amsterdam

Dr. Bassam Janji
Group leader, Tumor Immunotherapy and Microenvironment
Luxembourg Institute of Health, Luxembourg

Dr. Martina Seiffert
Group leader, Immune Modulation in Cancer
German Cancer Research Center (DKFZ), Germany

Affidavit

I hereby confirm that the PhD thesis entitled “Role of AHR, HIF-1α and IL-27 in T-Cell-mediated Immunity in Chronic Lymphocytic Leukemia” has been written independently and without any other sources than cited. All necessary ethical approvals have been obtained in accordance with the law (on the use of clinical samples and on the Care and Use of laboratory animals, where applicable).

Luxembourg, 25/11/2022

Giulia Pagano

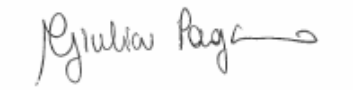

Acknowledgments

I cannot believe these years passed by so fast. I still remember my first days, arriving to work before 9am (madness), getting to know the people in the corridors of Bam, and pretending to understand the multilingual jokes. Four year after here I am, in front of the last white page, thinking about this amazing journey, and I want to express my gratitude towards the people who made the these years so incredible.

Needless to say, the biggest thank you goes to Jerome and Etienne, who welcomed me in their lab in the best way possible. I could not have undertaken this journey without your advice and your guidance. Thank you for making me feel I could always count on you.

TSIs, what can I say… every day side by side, "in happiness and in pain, in sickness and in health". We have gone through a pandemia and a European Cup, and we still enjoy being together. Sandrine, Anne, Ernesto, Elodie, Chloe, Vanessa, Hugo, sharing time with you has been great. Susanne, thank you for hosting me at your place over a beer, for the plants, for the bike, and for all the laughs in the office.

I am particularly grateful to Marina, for teaching me everything in the lab, for our endless conversations in front of the ARIA, for starting the projects I worked on during these four years. Working with you has been of great motivation.

And a warm thank you goes to Tea, for her patience and for her trust. It was great to count on such a motivated and enthusiastic master student for this PhD project.

Of course, thanks to Pablo and Titiksha, for all we shared in these years and in these months. Even during tough moments, I felt your support and guidance.

This journey would not have been so cool without my little sister Iria. I feel very proud of being able to stand you 24/7 in the office, in the lab and at home. And I am not mentioning in Costa Rica, in Galicia, in Asturias, in Cantabria, in Andalucia, in Madrid and in Puglia ☺. Thank you from the bottom of my heart for the time we spent together, for being so enriching for my life, I wish I could bring you with me on the other side of the ocean. Well, maybe it is not a good idea to fly again together over the Atlantic, but I promise my house will always be open for you, wherever it will be.

Simone, Lars and all the DoCR community, I am extremely grateful for all the efforts you made in creating a great environment that made me happy to go to work every day.

Simone, I would also like to express my gratitude for being such an inspiring scientist.

This endeavor would not have been possible without the financial support of Televie. Thank you for giving me the opportunity of pursuing science in such a great place as LIH.

Ilaria, thank you for being a great friend and roommate. For embracing all my extravagant ideas with your amazing enthusiasm (I still cannot believe you said yes to adopting a dog), I felt welcomed and loved. And an immense thank you to Andrea, for the great time we had, for the aperitivi on the terrace and our long conversations.
To the LIH-PhD community, thank you for all the time spent and all the beers drunk together. Malina, Yolanda, Hugo, Carina, Mohammad, Miriam and the beach volley crew, it was therapeutic to share the PhD-related pain.

I feel an immense gratitude for my Luxembourgish family.
Pietro, you gave me an amazing welcome when I landed here. Thank you for all the times I could count on you. To Maria and Esperanza, thank you for all the adventures we shared, from Costa Rica to Castellana Grotte. And to Elisa, Giulia, Ruben, Andrea, for all the fun, all the love, all your support. Shameek, Deborah, Alexej, Luca, Steffi, Tommy, Inés, for your contagious enthusiasm.
So many times after a night out together I thought I was so lucky in having you all in my life.

Thanks to Imma, for being my ally during a very hard time. I consider our friendship one of the best things Milan gave me. And to my friends in Castellana, Maria Serena, Minga, Toni, Nanni, Stefano and all the crew. The appointments we gave to each other during these years made it even more beautiful to go back home.

To my Elena, for your ability in erasing the 2000 km of land that separate us. For being a constant presence in my life and always reminding me what sisterhood means. You are of great inspiration.

Cano Galià, trimoncello, I will not say a lot here (also, as you would tell me, “we are in the area”). There are so many reasons why I would like to thank you, but I will just mention one: thank you for the possibility we gave to each other to say everything else outside of this PhD thesis. Our space and time are a blessing.

To my lovely family, to mum and dad for your constant trust, for the education I had thanks to your support, for reminding me I have big wings but also strong roots. I am deeply grateful to my brother Mario, for all the times he stood by my side when I needed him, and for the most beautiful song he wrote about us.

You all made this PhD an amazing journey.
Wholeheartedly thank you, merci, gracias, obrigada, danke, grazie.

Contents

Summary

Chronic Lymphocytic Leukemia (CLL) represents the most frequent leukemia in adults and it is considered a deadly incurable disease. This cancer is characterized by an accumulation of abnormal, apoptosis-resistant B lymphocytes in the blood and lymphoid organs of patients. CLL progression is highly dependent on complex interactions between tumor cells and the tumor microenvironment (TME). Indeed, CLL cells can modify stromal cells and immune cells to promote the survival of the leukemic clone and to escape from the immune system surveillance.

Among the different immune cells of the TME, regulatory T cells (Tregs) play a crucial role in cancer progression, including CLL. This T-cell subpopulation is a subtype of $CD4^+$ T cells with immunosuppressive abilities, mainly inhibiting other T cells and dendritic cells through different mechanisms. For this reason, Treg inhibit the anti-tumor immune response during cancer development, resulting in a pro-tumoral effect. We previously extensively characterized the immune microenvironment of pre-clinical CLL mouse models and described a significant increase in the Treg subsets with an enhanced immunosuppressive and activated phenotype compared to non-leukemic animals. In addition, $TIGIT^+$ Tregs are more immunosuppressive than their $TIGIT^-$ Treg counterparts and express higher levels of several transcription factors, including AHR and HIF-1α, both involved in the cellular response to microenvironment-mediated stimuli.

The first part of the present project focused on investigating the role of AHR and HIF-1α in the suppressive ability of Tregs during CLL development. For this purpose, we generated conditional knock-out mice (cKO) lacking *Ahr* or *Hif1α* genes exclusively in Tregs ($Foxp3^{YFP\text{-}Cre}Ahr^{fx/fx}$ and $Foxp3^{YFP\text{-}Cre}Hif1\alpha^{fx/fx}$ mice). After having characterized these mice at steady state, adoptive transfer of CLL cells was performed into cKO and control mice, revealing that CLL growth in cKO mice was drastically delayed compared to the control mice and immune checkpoints expression was decreased in Tregs of cKO mice compared to controls. Very interestingly, the decrease in CLL development was mitigated when $CD8^+$ T cells were depleted. Despite not observing differences in the CLL progression when AHR and HIF-1α are depleted in CLL cells, we could observe a decreased CLL development when injecting WT mice with AHR and HIF-1αinhibitors compared to untreated controls, highlighting that AHR and HIF-1α are fundamental in mediating CLL development by acting on the tumor microenvironment with the regulation of the anti-tumoral immune response.

Similarly, injection of B16F10 melanoma cells into cKO and control mice resulted in decreased tumor load in absence of AHR and HIF-1α, confirming the impacted suppressive ability of Tregs when the two transcription factors are depleted in Tregs in a solid malignancy. We then evaluated the phenotype and the suppressive ability of *ex vivo* induced Tregs (iTregs) by flow cytometry and

suppression assay, respectively, observing an increased proliferation of $CD8^+$ T cells in the presence cKO Tregs. Finally, by inspecting the metabolic behavior of KO and control iTregs, we observed an altered oxygen consumption rate and glutamine uptake in absence of the two TFs. Altogether, these results indicate that AHR and HIF-1α act as fundamental transcription factors for the suppressive ability of Tregs both *in vivo* and *ex vivo*, highlighting their key role in CLL development and unravelling their potential as therapeutic targets during CLL progression.

The second part of this project focuses on Interleukin 27 (IL-27), which belongs to the family of IL-12 heterodimeric cytokines. IL-27 is composed of two subunits: IL-27p28 (P28) and Epstein-Barr-virus-induced molecule 3 (EBI3), and is mainly produced by antigen presenting cells. Within the TME, this cytokine has pleiotropic functions, having either pro-tumoral or anti-tumoral roles in different tumoral contexts. Here we wanted to investigate the role of IL-27 during CLL development and for this purpose, we used the *Eμ-TCL1* and *Ebi3*$^{-/-}$ transgenic mouse models as well as clinical samples from CLL patients. The adoptive transfer of CLL cells in *Ebi3*$^{-/-}$ and control mice revealed a strong anti-tumor activity of IL-27 in CLL, as its absence led to a decreased anti-tumor immune response and enhanced immunosuppressive TME. In addition, using RNA sequencing, we could identify $CD8^+$ T cells as the T-cell subtype mainly affected by IL-27 depletion, characterized by major transcriptional changes associated with T-cell activation, proliferation, and cytotoxicity. In line with these findings, an increased cytotoxicity of *ex vivo*-cultured $CD8^+$ T cells was observed in presence of IL-27 using murine and human primary cells. Moreover, *in vivo* neutralization of IL-27 during CLL development partially recapitulated the enhanced leukemia progression observed in *Ebi3*$^{-/-}$ mice. In accordance with the anti-tumoral role of IL-27 during CLL progression, we also observed decreased levels of this cytokine during CLL development in both pre-clinical murine and patient samples. Altogether, these data demonstrate the anti-tumoral role of IL-27 in CLL development by promoting $CD8^+$ T-cell-mediated anti-tumor immunity, as well as establish this cytokine as a potential immunotherapeutic agent in CLL.

List of abbreviations

α-KG	α-ketoglutarate
ADCC	Antibody-Dependent cellular Cytotoxicity
ADM	Adrenomedullin
AHR	Aryl Hydrocarbon Receptor
AHRR	AHR Repressor
AML	Acute Myeloid Leukemia
AP-1	Activator Protein 1
APC	Antigen-Presenting Cell
ARNT	AHR Nuclear Translocator
AT	Adoptive Transfer
aTreg	Activated Regulatory T cells
BAK	BCR-Associated Kinase
BCL-2	B-Cell Lymphoma-2
Bcl-xL	B-cell lymphoma-extra large
BCR	B-cell Receptor
bHLH-PAS	helix–loop–helix/Per-ARNT-SIM
BIRC3	Baculoviral IAP Repeat Containing 3
BiTE	Bispecific T-cell Engager
BM	Bone Marrow
BR	Bendamustine and Rituximab
Bregs	Regulatory B-cells
BTK	Bruton's Tyrosine Kinase
BTKi	BTK inhibitors
cAMP	Cyclic adenosine monophosphate
CAR	Chimeric Antigen Receptor
CBC	Complete Blood Count
CBP	CREB-binding protein
CCCP	Carbonyl cyanide m-chlorophenyl hydrazone
CCL	Chemokine (C-C motif) Ligand
CCR	C-C Motif Chemokine Receptor
CDKN2A	Cyclin Dependent Kinase Inhibitor 2A
CDR	Complementarity-Determining Regions
CFB-β	Core Binding Factor-β

cKO	Conditional Knock Out
CLL	Chronic Lymphocytic Leukemia
CNS	Conserved Non-coding DNA Sequence
CRC	Colorectal Cancer
CREB	c-AMP Responsive Element Binding Protein
CTL	Cytotoxic T Lymphocyte
CTLA-4	Cytotoxic T Lymphocyte Associated Protein 4
CXCL	Chemokine (C-X-C motif) Ligand
CXCR	C-X-C Motif Chemokine Receptor
CYP1A1	Cytochrome P450 Family 1 Subfamily A Member 1
DC	Dendritic cell
del	Deletion
DLBCL	Diffuse Large B-cell Lymphoma
dLN	Draining Lymph Node
DN	Double Negative
DNAM-1	DNAX accessory molecule
DP	Double Positive
DRE	Dioxin-Responsive Elements
EBI3	Epstein-Barr Virus Induced 3
EMT	Epithelial-Mesenchymal Transition
Eomes	Eomesodermin
EVs	Extracellular Vescicles
FAO	Fatty Acid Oxidation
FCR	Fludarabine, Cyclophosphamide and Rituximab
FDC	Follicular Dendritic Cell
FICZ	6-formylindolo[3,2-b]carbazole
FIH	Factor Inhibiting HIF-1α
FOXO	Forkhead box O
FOXP3	Forkhead Box P3
GBM	Glioblastoma
GC	Germinal Center
GEP	Gene Expression Profiling
GITR	Glucocorticoid-Induced TNFR-Related protein
GLUT-1	Glucose Transporter-1

GP130	Glycoprotein130
Gzm	Granzyme
HAP	Hypoxia-Activated Prodrugs
Hb	Hemoglobin
HC	Healthy Controls
HCC	Hepatocellular Carcinoma
HDAC	Histone Deacetylase
HIF	Hypoxia Inducible Factor
HLA	Human Leucocyte Antigens
HRE	Hypoxia Responsive Elements
HSC	Hematopoietic Stem Cell
HSP90	Heat shock protein 90
IC	Immune Checkpoint(s)
ICB	Immune Checkpoint Blockade
ICOS	Inducible T-cell Costimulator
IDO	Indoleamine 2,3-dioxygenase
IFN	Interferon
Ig	Immunoglobulin
IGHV	Immunoglobulin Heavy Variable
IGHV-M	IGHV-Mutated
IGHV-U	IGHV-Unmutated
IL	Interleukin
IL-27Rα	IL-27 Receptor Subunit α
IL-2Rα	IL-2 Receptor Subunit α
IPEX	Immunodysregulation polyendocrinopathy enteropathy X-linked
IPI	International Prognostic Index
IRF4	Interferon Regulatory Factor 4
IS	Immunological Synapse
ITAM	Immunoreceptor-Tyrosine-based-Activation-Motif
iTr35	Inlerleukin-35-producing Regulatory T cells
iTregs	Induced Regulatory T cells
JAK	Janus kinase
KLRG1	Killer Cell Lectin Like Receptor G1
Kyn	Kynurenine

LAG-3	Lymphocyte-Activation Gene 3
LCK	Lymphocyte-specific protein tyrosine Kinase
LC-MS	Liquid Chromatography Mass Spectrometry
LN	Lymph node
LPS	Lypopolisaccarides
mAB	Monoclonal Antibody
MBL	Monoclonal B-cell Lymphocytosis
MDSC	Myeloid Derived Suppressor Cell
MHC	Major Histocompatibility Complex
miRNA	microRNA
MPEC	Memory-Precursor Effector Cells
MSC	Mesenchimal Stem Cell
NFAT	Nuclear Factor of Activated T cells
NF-κB	nuclear factor kappa-light-chain-enhancer of activated B cells
NK	Natural Killer
NLC	Nurse-like Cell
NLS	Nuclear Localization Signal
Nrp1	Neuropilin1
NSG	NOD-scid IL-2Rγ^{null}
nTregs	Natural Regulatory T cells
OCR	Oxygen Consumption Rate
ODD	Oxygen-dependent Degradation Domain
OS	Overall Survival
OSCC	Oral Squamous Cell Carcinoma
OXPHOS	Oxidative Phosphorylation
PB	Peripheral Blood
PBMCs	Peripheral Blood Mononuclear Cells
PD-1	Programmed cell Death protein 1
PD-L	Programmed death-ligand
PHD	Prolyl-4-hydroxylase
PI3K	Phosphatidylinositol 3-kinases
PKC	Protein Kinase C
RA	Retinoic Acid
RAG	Recombination Activating Genes

ROR1	Receptor Tyrosine Kinase Like Orphan Receptor 1
RORγt	Retineic-acid-receptor-related orphan nuclear receptor γ
RT	Richer Transformation
rTregs	Resting Regulatory T cells
SCA-1	Stem Cell Antigen-1
SF3B1	Splicing Factor 3b Subunit 1
SLEC	Short-Lived Effector Cells
SMAD	Small Mother Against Decapentaplegic
SNP	Single-Nucleotide Polymorphism
SOCS3	Suppressor Of Cytokine Signaling 3
SP	Single Positive
STAT	Signal Transducer and Activator of Transcription
Syk	Spleen tyrosine kinase
TAM	Tumor-Associated Macrophages
T-bet	T-box transcription factor TBX21
TCA	Tricarboxylic Acid
TCDD	2,3,7,8-Tetrachlorodibenzo-p-dioxin
Tconv	Conventional T cells
TCR	T-Cell Receptor
TDO	Tryptophan 2,3-Dioxygenase
Teff	Effector T cells
Tex	Exhausted T cells
TF	Transcription Factor
TGF-β	Transforming growth factor β
Th	Helper T cell
TIGIT	T-cell immunoreceptor with Ig and ITIM domains
TIL	Tumor-Infiltrated Lymphocyte
TIM-3	T-cell immunoglobulin and mucin containing protein-3
TLR	Toll-Like Receptor
TMB	Tumor Mutational Burden
TME	Tumor Microenvironment
Tmem	Memory T cells
TNF	Tumor Necrosis Factor
TNFR2	Tumor Necrosis Factor Receptor type II

TNFRSF	TNF Receptor Superfamily Member 18
TOX	Thymocyte Selection Associated High Mobility Group Box
Tr1	Type 1 Regulatory T cells
TregP	Regulatory T cell precursor
Tregs	Regulatory T cells
Trp	Tryptophan
TTFT	Time To First Treatment
VCAM1	vascular cell adhesion molecule 1
VEGF	Vascular Endothelial Growth Factor
VHL	von Hippel-Lindau tumor-suppressor protein
WGS	Whole Genome Sequencing
WT	Wilde Type
XAP2	Human hepatitis B virus X-associated protein
XRE	Xenobiotic-Responsive Elements
ZAP70	Zeta Chain Of T-cell Receptor Associated Protein Kinase 70

List of figures

List of publications

Giulia Pagano, Marina Wierz, Iria Fernandez Botana, Susanne Gonder, Ernesto Gargiulo, Etienne Moussay*, Jérôme Paggetti*.
Microenvironment-regulated Transcription Factors AHR and HIF-1α Expression in Tregs Promotes CLL Progression by impairing CD8⁺ T-cell mediated Anti-Tumor Immunity.
HemaSphere 2022, doi: 10.1097/01.HS9.0000843444.44618.2.

Giulia Pagano†, Iria Carmen Botana†, Marina, Wierz, Philipp Roeßner, Bin Qu, Alan Ramsay, Stamatopoulos Basile, Martina Seiffert, Jerome Paggetti*, Etienne Moussay*.
EBI3/IL-27 Depleted Microenvironment Favours Tumour Progression in Chronic Lymphocytic Leukaemia.
HemaSphere 2022, doi: 10.1097/01.HS9.0000845280.88682.06

Agnieszka Goral, Malgorzata Firczuk, Klaudyna Fidyt, Marta Sledz, Francesca Simoncello, Karolina Siudakowska, **Giulia Pagano**, Etienne Moussay, Jérôme Paggetti, Patrycja Nowakowska, Stefania Gobessi, Joanna Barankiewicz, Aleksander Salomon-Perzynski, Federica Benvenuti, Dimitar G Efremov, Przemyslaw Juszczynski, Ewa Lech-Maranda, Angelika Muchowicz.
A Specific CD44lo CD25lo Subpopulation of Regulatory T cells Inhibits Anti-Leukemic Immune Response and Promotes the Progression in a Mouse Model of Chronic Lymphocytic Leukemia.
Frontiers in Immunology, 2022, doi: 10.3389/fimmu.2022.781364

Susanne Gonder, Anne Largeot, Ernesto Gargiulo, Sandrine Pierson, Iria Fernandez Botana, **Giulia Pagano**, Jerome Paggetti,1,* and Etienne Moussay1,*.
The Tumor Microenvironment-Dependent Transcription Factors AHR and HIF-1α Are Dispensable for Leukemogenesis in the Eμ-TCL1 Mouse Model of Chronic Lymphocytic Leukemia.
Cancers, 2021, doi: 10.3390/cancers13184518

Susanne Gonder†, Iria Fernandez Botana†, Marina Wierz†, **Giulia Pagano**, Ernesto Gargiulo, Antonio Cosma, Etienne Moussay1*, Jerome Paggetti1* and Anne Largeot1*.
Method for the Analysis of the Tumor Microenvironment by Mass Cytometry: Application to Chronic Lymphocytic Leukemia.
Frontiers in Immunology, 2020, doi: 10.3389/fimmu.2020.578176

Giulia Pagano†, Anne Largeot†, Susanne Gonder, Etienne Moussay*, Jerome Paggetti*.
The B-side of Cancer Immunity: The Underrated Tune.
Cells, 2019, doi: 10.3390/cells8050449

Introduction

1. T-cell biology in health and cancer

The ability of T cells to respond on a broad amount of antigens is dependent on the huge repertoire of unique T-cell receptors (TCRs) that are produced through DNA rearrangement and casual chain pairing (Venturi and Thomas, 2018). During an immune response, antigen-presenting cells (APCs) are able to process pathogens or antigens released from cancer cells and load their fragments on **major histocompatibility complex (MHC)** molecules of class I or II, recognized by $CD8^+$ or $CD4^+$ T cells, respectively (Hennecke and Wiley, 2001). In humans, MHC complexes were discovered on leukocytes and for this reason are called human leucocyte antigens (HLA) (Thorsby, 1984). Upon antigen processing, APCs load a fragment of the antigen on the membrane associated to the MHC, forming the MHC/antigen complex that binds to the TCR of naïve T cells and leads to T-cell activation. The stable interaction between a T cell and an APC is defined as **immunological synapse (IS)** (Alarcon *et al.*, 2011), and is constituted by a membrane structure at the T cell-APC interface.

1.1 STRUCTURE OF THE T-CELL RECEPTOR

The TCR is composed of two chains and the majority of human T cells (95%) carry a TCR composed by α and β chains, while a 5% of T cells express a TCR with γ and δ chains (Attaf *et al.*, 2015). The two chains are associated with four CD3 subunits (ε, γ, δ and ζ), organized into three dimers (εγ, εδ and ζζ) (Mariuzza *et al.*, 2020) (**Figure 1**). Since the TCR is unable of independent intracellular signaling, the interactions between the TCR and the CD3 subunits are fundamental for translating the TCR-MHC binding to CD3-mediated signal transduction that leads to T-cell activation (Wucherpfennig *et al.*, 2010). Of note, the TCR/CD3 complex contains Immunoreceptor-Tyrosine-based-Activation-Motif (ITAM) regions, which are phosphorylated by different tyrosine kinases upon T-cell activation and lead to initiation of the downstream TCR signaling cascade (Samelson, 2002). Each of TCR heterodimeric chains contains a variable domain, a constant domain, a connecting region (also named the hinge region) and a transmembrane domain (Mariuzza *et al.*, 2020) (**Figure 1**). Within the variable regions, TCRs present three different hypervariable regions, also named complementarity-determining regions (CDR) (Wong *et al.*, 2019), which represent the portion that physically interacts with the antigen. Within the trans-membrane domains of both chains, instead, there are positively charged amino acids residues, which favour the interaction between the TCR heterodimer and the CD3 complex (Blumberg *et al.*, 1990).

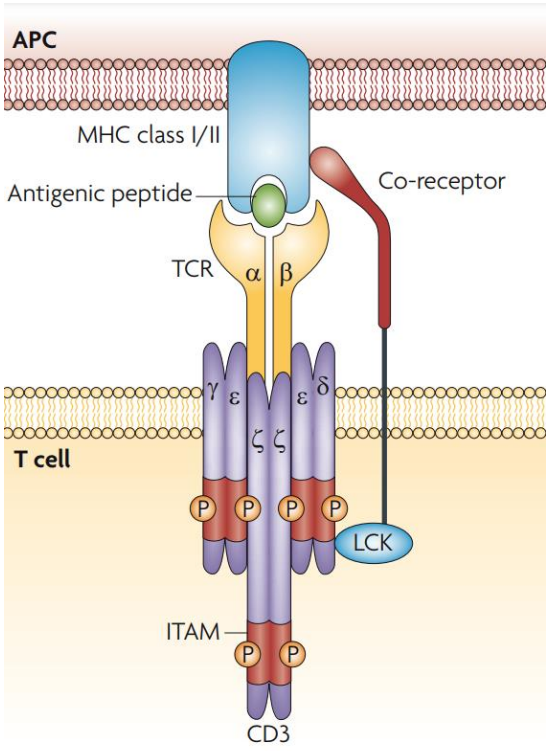

Figure 1. **The structure of the TCR.** The TCR is composed by two chains linked by a disulfide bond. Each region contains a variable domain, a constant domain, a hinge region and a transmembrane domain. The TCR interacts with three complexes of CD3 molecules, fundamental for the signal transduction process that leads to T-cell activation. APC = Antigen Presenting Cell; LCK = lymphocyte-specific protein tyrosine Kinase. Figure taken from (Gascoigne, 2008).

1.2 T-CELL DEVELOPMENT

T cells originate from hematopoietic stem cells in the bone marrow (BM) and the precursors of these lymphocytes migrate and mature in the thymus. These precursors, also defined as thymocytes, go through different maturation steps, and can be recognized through the expression of several extracellular markers (Spits, 2002). Thanks to the thymic microenvironment and the presence of non-hematopoietic cells, T cells differentiate and undergo both positive and negative selection through a process known as **thymic education (Figure 2)** (Takahama, 2006). At the beginning of this process, T-cell precursors do not express CD4 and CD8 co-receptors and for this reason are defined as double negative (DN) T cells (Famili *et al.*, 2017). During this phase, VDJ recombination occurs by initially re-arranging the TCR-β chain (Chen *et al.*, 2021). This event requires the activation of two Recombination Activating Genes (RAG) 1 and 2 (Jones and Gellert, 2004) and, once completed, generates the pre-TCR by assembling the recombined β chain with the pre-TCR-α chain (Shah and Zuniga-Pflucker, 2014). After the pre-TCR interacts with CD3 molecules, T cells receive signals that lead to their survival, proliferation, and recombination of the α chain (Dave, 2011; Livak and Schatz, 1996). Once the fully recombined TCR is assembled, the up-

regulation and expression of both CD4 and CD8 co-receptors makes these cells double positive (DP), able to interact with the epithelial cells of the cortical area of the thymus (Ellmeier *et al.*, 1999). Cortical epithelial cells highly express MHC class I and class II molecules associated with self-peptides, and their interaction with DP T cells drives different selection processes: the vast majority of DP T lymphocytes (~90%) expresses TCRs able to interact very poorly with the self-peptide–MHC ligands and for this reason T cells carrying these TCRs die by neglect. On the other hand, ~7% of immature T cells carry TCRs with very strong affinity for self-ligands, which could cause autoimmunity in case they were allowed to migrate into the periphery. For this reason, a very efficient binding between the TCR and the self-peptide–MHC complex leads to negative selection by apoptosis (**Figure 2**). In this scenario, very few thymocytes express a TCR that generates an intermediate signaling after the recognition with the self-antigens (~3%), and these cells undergo positive selection towards either $CD4^+$ or $CD8^+$ T cells (Breed *et al.*, 2018; Merkenschlager *et al.*, 1997; von Boehmer *et al.*, 1989).

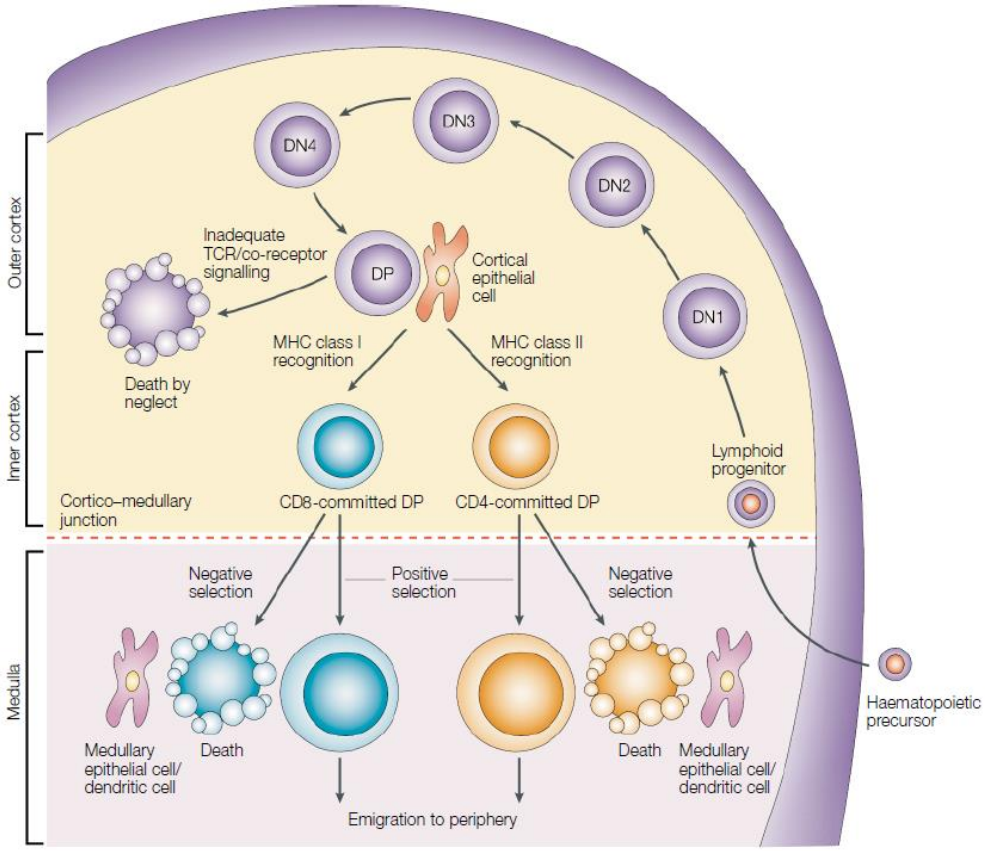

Figure 2. **Key steps of T-cell development in the thymus.** Hematopoietic progenitors develop in the BM and migrate to the thymus. Initially lymphoid progenitors do not express TCR, nor CD4 and CD8 co-receptor, and for this reason are defined as Double Negative cells (DN). Once DN cells further develop, they express both CD4 and CD8 co-receptor, and are defined as Double Positive (DP) cells. DP T cells present a fully rearranged and mature TCR and are selected via different mechanisms (apoptosis, death by neglect or positive selection) based on the affinity by which their TCR is able to bind to self-antigen–MHC complexes. T cells that express TCRs able to recognize MHC class I develop into $CD8^+$ T cells, instead the ones expressing TCRs specific for

MHC class II become $CD4^+$ T cells. Single positive (SP) T cells are mature and able to migrate in the periphery to secondary lymphoid tissues. Figure taken from (Germain, 2002).

In the light of this scenario, it is important to describe the T-cell fate decision of single positive (SP) $CD4^+$ T cells. These T cells include two different subsets: conventional T cells (Tconv) and regulatory T cells (Tregs), which will be extensively described in the paragraphs below. The different outcomes between Tregs and Tconv of SP $CD4^+$ T cells are based on the TCR affinity and in the efficiency in binding self-peptides presented by thymic APCs (Pohar *et al.*, 2018). Intermediate TCR signals are fundamental in promoting the differentiation of $CD4^+$ SP T cells into Tregs (Li and Rudensky, 2016), with a mechanism defined as "two-step process". As first, TCR signaling promotes the upregulation of CD25, together with Glucocorticoid-Induced TNFR-Related protein (GITR), OX40 (CD134) and Tumor necrosis factor (TNF) receptor type II (TNFR2), generating $CD25^+$ Forkhead Box P3 $(FOXP3)^-$ Treg cell precursors ($CD25^+$ $FOXP3^-$ TregP) (Kumar *et al.*, 2019; Santamaria *et al.*, 2021; Schuster *et al.*, 2019).

The second step of Treg maturation occurs when $CD25^+$ TregP start to express FOXP3, becoming fully matured Tregs (Lio and Hsieh, 2008). This process mainly relies on the effect of two cytokines, interleukin (IL)-2 and IL-15, which play a central role in FOXP3 upregulation (Apert *et al.*, 2018) and are able to rescue Treg precursors from apoptosis by promoting the expression of *B-cell lymphoma 2* (*Bcl-2*) (Cheng et al., 2013), an anti-apoptotic molecule. Burchill and colleagues have shown that mice lacking those cytokines do not undergo the process of Treg maturation and present severe autoimmunity (Burchill *et al.*, 2007), as Tregs are involved in self-tolerance regulation.
It is important to highlight that an alternative pathway of Treg development has been recently demonstrated with the identification of precursor Tregs expressing low levels of FOXP3 and lacking CD25 expression ($CD25^-$ $FOXP3^{low}$ TregP) (Tai *et al.*, 2013). Both precursors equally contribute in generating mature Tregs and they both rely on IL-2 and IL-15 for further development into mature Tregs. The main differences between the two precursors reside in their affinity for self-antigens (with $CD25^+$ TregP having a higher affinity than $FOXP3^{low}$ TregP) (Santamaria *et al.*, 2021) and, accordingly, in their different TCR repertoire. Very importantly, Tregs can also be generated in the periphery from Tconv in specific environmental conditions, and in this case they are defined as induced Tregs or iTregs (Lee *et al.*, 2011), which will be discussed in section 1.4c.

1.3 REGULATION OF T-CELL RESPONSE THROUGH IMMUNE CHECKPOINTS

For controlling the functional outcome of TCR signaling, T-cell response is tightly regulated by receptor-ligand interactions at the cell surface level. For this purpose, T cells present several co-stimulatory and co-inhibitory receptors, which cover a fundamental role in T-cell biology as they

ultimately control the T-cell fate (Chen and Flies, 2013). These receptors are defined as **immune checkpoints (IC)** and are considered modulators of the immune response (a summary of the most important IC is depicted in **Figure 3**). The IC-mediated regulation is fundamental because in absence of co-stimulation, T cells enter in an anergic state, which represent a condition of hypo-responsiveness, whereas without co-inhibition, hyper-activated T cells induce autoimmune diseases by recognizing self-components (Schietinger and Greenberg, 2014). The repertoire of immune checkpoints is very versatile and the ligands of these receptors have been found on the membrane of nearly every cell type, although the highest concentration of ligands is present on **APCs** (Shibru *et al.*, 2021). These cells represent a heterogeneous group composed of dendritic cells (DCs), macrophages and B cells that is able to process and present antigens to T cells. In particular, APCs, together with tissue-specific epithelial cells, are the only cells that carry both MHC class I and II, and for this reason they are able to present the antigen to both $CD4^+$ and $CD8^+$ T cells (Gaudino and Kumar, 2019).

The majority of co-stimulatory receptors belong either to the Immunoglobulin (Ig) superfamily or to the TNFR superfamily. Among the Ig superfamily ones, the most important involved in T-cell activation is **CD28**, which has been extensively studied and characterized over the past decades. Without CD28 co-stimulation, TCR signaling often causes the anergy or apoptosis of T cells (Esensten *et al.*, 2016); in fact, CD28 has a key function in promoting the proliferation of both effector T cells and Tregs, since it is also known to stabilize the anti-apoptotic molecule B-cell lymphoma-extra large (Bcl-xL) (Boise *et al.*, 1995). Very importantly, CD28 signaling also promotes cytokine production, in particular IL-2, while promoting the cytoskeletal reorganization at the IS upon MHC/antigen complex binding (Riha and Rudd, 2010). The ligands of this co-stimulatory molecule are CD80 and CD86 (which together are referred to as B7 ligands) and are present on the surface of APCs, implying that a co-stimulatory signal is transmitted upon the interaction between the TCR and the MHC/antigen complex (Lim *et al.*, 2012). Inducible T-cell COStimulator (ICOS) is a co-stimulatory IC belonging to the same family, presenting a similar structure to CD28 and has a non-redundant role in activating T cells and promoting $CD4^+$ T-cell proliferation (Mesturini *et al.*, 2006). The expression of this IC is enhanced upon TCR engagement, and its ligand is ICOSL, expressed by APCs. Co-stimulatory IC that belong the TNFR superfamily, instead, are **GITR**, **4-1BB** (CD137) and **OX40** (Croft, 2003; Ward-Kavanagh *et al.*, 2016). In general, these receptors present pro-inflammatory functions and are specific for T-cell expansion and survival.

It is important to highlight that several IC display pleiotropic functions in the regulation of the T-cell response, meaning that they can mediate activating or inhibitory signals depending on the T-cell

subtype and/or the differentiation stage. One example is represented by the Cytotoxic T Lymphocyte Associated Protein 4 (**CTLA-4**) IC, which belongs to the Ig superfamily. The ligands of this receptor are CD80 and CD86, meaning that it competes with CD28 for their binding, although CTLA-4 has a stronger affinity for these molecules than CD28 (Sansom, 2000). Of note, while T cells constitutively express CD28, the expression of CTLA-4 is induced upon T-cell activation in order to control an excessive tissue inflammation (Perkins *et al.*, 1996). Thus, upon activation, CTLA-4 interferes with CD28 signaling and transmits an inhibitory signal to T cells that results in the inhibition of IL-2 accumulation and cell cycle arrest (Krummel and Allison, 1996). While in $CD8^+$ T cells and in Tconv CTLA-4 engagement mediates an inhibitory signal, this IC is constitutively expressed in Tregs and has a crucial role in promoting Treg immunosuppression (Jago *et al.*, 2004). Another important IC is T-cell immunoreceptor with Ig and ITIM domains **(TIGIT),** which works with a similar mechanism than CD28 and CTLA-4. TIGIT, in fact, is upregulated by TCR engagement and competes with the co-stimulatory IC DNAX accessory molecule (DNAM)-1 and CD96 (TACTILE) for binding to the ligands CD155 and CD112 (Sanchez-Correa *et al.*, 2019), although it has a much higher affinity. TIGIT inhibits effector T-cell functions, while in Tregs it enhances their activation and immunosuppressive phenotype. In addition, TIGIT also promotes the production in DCs of IL-10, a cytokine with immunosuppressive functions (Zhang *et al.*, 2020a).

A very well characterized and pleiotropic co-receptor is Programmed cell Death protein 1 **(PD-1)**, which is expressed upon T-cell activation and is positively regulated by transcription factors (TFs) as Forkhead box O (FOXO)1 and AHR in $CD8^+$ T cells (Liu *et al.*, 2018; Staron *et al.*, 2014). PD-1 is heterogeneously expressed on different T-cell subsets: in the early stages of T-cell activation, PD-1 binds to the ligands PD-L1 or PD-L2 present on DCs and is important for T-cell activity (Ahn *et al.*, 2018). Nonetheless, PD-1 also inhibits TCR signaling to attenuate the T-cell response (Li *et al.*, 2021b), leading to the suppression of T-cell proliferation and survival. On the contrary, PD-1 expression on Tregs promotes their development and expansion, and confers immune suppressive capacities (Cai *et al.*, 2019). Similar to PD-1, also Lymphocyte-activation gene 3 **(LAG-3)** represents an IC with different functions in specific T-cell subtypes: in activated T cells, LAG-3 reduces T-cell activity since its ligand is MHC class II (Maruhashi *et al.*, 2018), while in Tregs it promotes cell differentiation (Huang *et al.*, 2004). Nonetheless, the role of LAG-3 in Tregs remain controversial, as some studies highlight its role in enhancing Treg proliferation and function (Maruhashi *et al.*, 2018), while others show the impacted Treg functionality *in vivo* upon LAG-3 depletion in Tregs. Lastly, it is important to mention the co-inhibitory IC T-cell immunoglobulin and mucin containing protein-3 **(TIM-3)**, discovered in the early 2000s and involved in the suppression of both $CD8^+$ and

CD4⁺ T-cell function (Das *et al.*, 2017). Similarly to other IC, TIM-3 expression in Tregs enhances the suppressive abilities (Banerjee *et al.*, 2021).

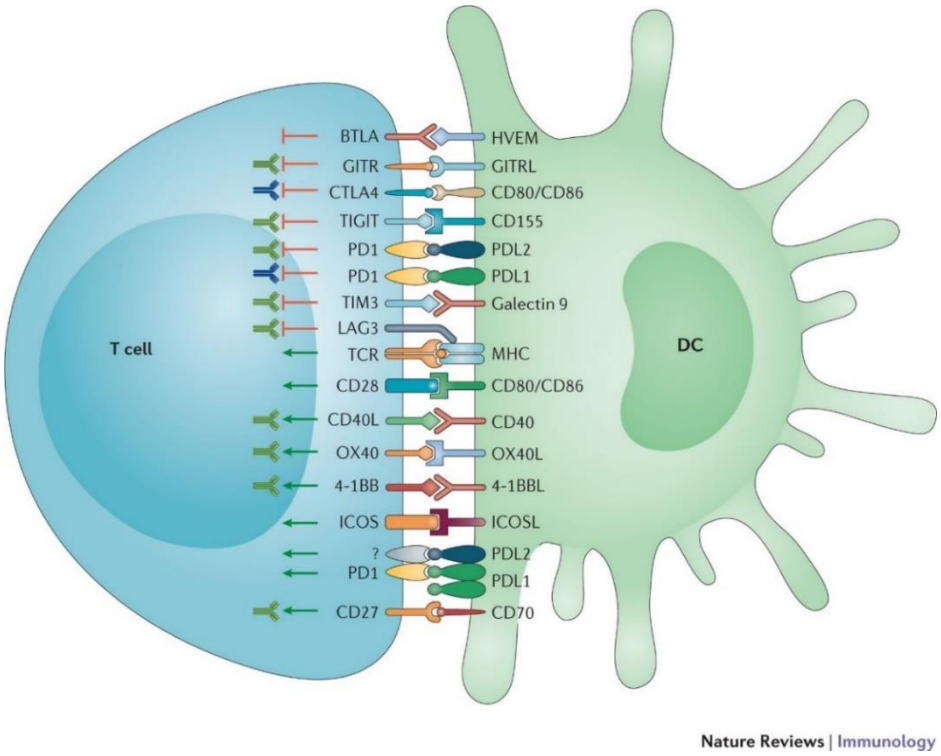

Figure 3. **Summary of the most important immune checkpoints expressed on T cells and their corresponding receptors on APCs.** DCs, as main regulators of the adaptive immune response in T cells, express the ligands of immune checkpoint co-receptors that are present on the T-cell surface. IC are required for fine-tuning of T-cell responses and based on the balance between co-stimulatory and co-inhibitory IC, T cells are activated (indicated by green arrows) or inhibited (indicated by inhibitory red arrows). Antibody symbols represent IC pathways undergoing evaluation in clinical trials. Green antibodies indicate IC pathways in clinical trials for cancer, dark blue indicate those in clinical use for cancer. Figure taken from (Wykes and Lignani, 2018).

1.4 TYPES OF T CELLS

1.4a CD8⁺ T cells

CD8⁺ T cells, also named cytotoxic T cells or cytotoxic T lymphocytes (**CTLs**) have the potential to recognize short peptides associated with MHC-I molecules, which are present on the cell surface of all nucleated cells (Zhang and Bevan, 2011).

CD8⁺ T-cell activation and function

CD8⁺ T cells are the main players of T-cell-mediated immune defense against intracellular pathogens and for tumor surveillance. When naïve CD8⁺ T cells get activated upon TCR binding to the MHC-I/antigen complex, they are able to directly induce the apoptosis of the target cells (Cassioli and Baldari, 2022). At first, CTLs secrete **perforin** to create holes on the cell surface of the target cells. Subsequently, they release serine proteases, as **granzyme (Gzm) A and B**, able to cleave proteins involved in the normal cell maintenance and induce the death of the target cell by

apoptosis (Cullen and Martin, 2008). CTLs are also able to induce apoptosis via **Fas-Fas ligand (FasL) interactions**. Indeed, the binding of FasL with the Fas receptor expressed by target cells, causes a signaling cascade that leads to the apoptosis of the target cell through caspases engagement (Hassin *et al.*, 2011). Very importantly, $CD8^+$ T cells are also able to indirectly kill target cells through the secretion of pro-inflammatory cytokines such as **TNF-α, IL-2 and INF-γ**, which activate other immune cells and stimulate the phagocytic activity of macrophages (Cox *et al.*, 2011).

Moreover, once activated, $CD8^+$ T cells undergo drastic modifications in their metabolism, for example by enhancing the intake of amino acids, iron and glucose. The enhanced glucose uptake correlates with the metabolic change from oxidative phosphorylation (OXPHOS) to glycolysis, to sustain the high cell division rate (Michalek and Rathmell, 2010). Highly activated $CD8^+$ T cells also need to mediate several signals, which comprise the one mediated by the TCR, the costimulatory signals (e.g. OX40 and CD28), and the pro-inflammatory cytokines as IL-12, type-I interferon (IFN) and IL-2 (Mescher *et al.*, 2006).

$CD8^+$ T-cell subsets

It is important to underline that at the peak of the primary response to pathogens or cancer cells, there are several subsets of antigen-induced $CD8^+$ effector T cells, which differ both phenotypically and functionally. In fact, upon antigen encounter, short-lived effector cells (SLEC) are generated and then undergo apoptosis when the infection finishes (Amoah *et al.*, 2013). On the other side, memory precursor effector cells (MPEC) survive the infection and give rise to the population of memory cells (Joshi *et al.*, 2007). In general, **naïve, effector and memory T cells** (Teff and Tmem, respectively) are defined by the expression of different markers, including CD62L (involved in tissue homing) and CD44 (considered an activation marker) (Sckisel *et al.*, 2017).

Role of $CD8^+$ T cells in cancer

In order to describe the complex relationship between cancer cells and immune cells, more than two decades ago, Dunn and colleagues elaborated the concept of **immunoediting** (Dunn *et al.*, 2002), consisting in three phases: the first one, the elimination phase, in which NK cells and $CD8^+$ T cells kill tumor cells. The second, called the equilibrium stage, where a balance between immune cells and tumor cells is maintained. The third, defined as escape phase, happening when the immune system is unable to destroy the tumor and the pathology becomes clinically manifested. Very importantly, the concept of immunoediting considers the evidence that the immune system is a double-edged sword in tumor control, as it can limit but also promote tumor development (Lakshmi Narendra *et al.*, 2013).

During an anti-tumor immune response, a series of events occur leading to the activation and expansion of immune cells in a process defined as **Cancer-Immunity Cycle** (Chen and Mellman, 2013)**.** In this process, tumor cell genomic instability leads to apoptosis and release of antigens by cancer cells, which are captured by APCs, in particular DCs. Upon antigen processing, DCs move into the draining lymph nodes (dLNs) and present the MHC/tumor antigen complex to naïve T cells, inducing T-cell priming and effector T-cell activation. In this way, $CD8^+$ T cells can reach the tumor site where they clonally expand and give rise to the cytotoxic immune response.

Since T cells need to migrate to the tumor site to start an efficient immune response, T-cell trafficking into tumors is a crucial event for malignant cells elimination (Slaney *et al.*, 2014). Based on the tumor infiltrated lymphocytes (TILs) rate, it is possible to divide tumors into "hot", infiltrated by T cells, and "cold", where T-cell infiltration is lacking (Duan *et al.*, 2020). In the first ones, the expression of different chemokines and cytokines attracts T cells to the tumor site (Karin, 2021), instead in cold tumors immune cells are not able to enter the malignant core. Very importantly, T-cell infiltration correlates with increased tumor mutational burden (TMB) and improved patient survival and response to treatment in many cancer types (Li *et al.*, 2021a). The TMB represents the number of genomic mutations in cancer cells and is used as a biomarker for T-cell infiltration (Mi *et al.*, 2020), as tumor cells with a high TMB have the potential to generate a higher number of neoantigens and attract more immune cells to the tumor site.

1.4b $CD4^+$ T cells

$CD4^+$ T cells are involved in both humoral and cell-mediated immunity and they are fundamental for controlling the immune response (RV *et al.*, 2012). Also referred to as "helper" T cells, these lymphocytes are able to bind to MHC-II, which is only expressed by APCs. Among those, DCs represent the most important APCs, as they have an enhanced ability to stimulate naïve T cells compared to B cells and macrophages (Bromley and Dustin, 2002).

$CD4^+$ T-cell activation and function

Once Tconv recognize MHC-II/antigen complex on DCs, the interaction between CD40L expressed by Tconvs and CD40 by DCs promotes DCs maturation and thereby enhances their antigen presenting and co-stimulatory activity (Ma and Clark, 2009). In particular, CD40-CD40L interaction causes the secretion of chemokines (e.g. CCL3), which attract CTLs and facilitates $CD8^+$ T-cell priming (Honey, 2006). Additionally, thanks to $CD4^+$ T-cell activity, DCs upregulate the co-

stimulatory molecules CD80 and CD86 (Carenza *et al.*, 2019), and release type I IFN (Montoya *et al.*, 2002), which enhances their functional activation, together with the cytokines IL-12 and IL-15, known to promote CTL proliferation and differentiation (Mitchell *et al.*, 2010).

$CD4^+$ T-cell subsets

Once Naïve $CD4^+$ T cells get activated, they mature into different subsets depending on the specific cytokines that are released in the microenvironment, as well as on the concentration of antigens, type of APC, and engagement of co-stimulatory receptors (Ashkar *et al.*, 2000; Tao *et al.*, 1997). In presence of IL-12 and IFN-γ, $CD4^+$ T cells mature into T helper (Th) 1 cells, which are characterized by the expression of the TF ***T-BET*** and induce cytokine secretion and activation of macrophages (Trinchieri *et al.*, 2003). Instead, IL-4 promotes Th2 development via STAT6, which upregulates the Th2-specific TF ***GATA3*** (Zhu *et al.*, 2001), while IL-1, IL-6, IL-23 and TGF-β promote the formation of Th17 cells (Volpe *et al.*, 2008), selectively expressing the TF ***ROR-γt***. More recently, it was discovered another T helper subset, named Th9, which develops in presence of IL-4 and TGF-β, secretes IL-9 and is characterized by the expression of the TF ***SPI-1*** (Veldhoen *et al.*, 2008b). Lastly, in presence of IL-2, IL-10 and TGF-β, naïve $CD4^+$ T cells differentiate into peripheral Tregs, also named induced Tregs (Chen *et al.*, 2003), which will be extensively discussed in the paragraph 1.4c. Each $CD4^+$ T-cell subset has a specific function during infection or in cancer development, presenting either pro-inflammatory or anti-inflammatory characteristics. Among the cell types with pro-inflammatory functions, Th1 cells mainly produce IFN-γ and TNF-α, crucial for activating macrophages and maintaining inflammation (Calmon-Hamaty *et al.*, 2011; Murray *et al.*, 1985). Th2 cells, instead, are able to release IL-5, IL-13 and IL-4 (an important survival inducer for B cells), and are crucial for destroying extracellular parasites (Sokol *et al.*, 2009), while Th17 cells, which produce IL-17, IL-21 and IL-22, are required to destroy extracellular bacteria and fungi (Annunziato *et al.*, 2007). Finally, Th9 cells secrete IL-9 and in mice also IL-10 and are involved in inflammatory diseases, autoimmune diseases and tumors. Th1, Th2, Th17 and Th9 cells are defined as **"conventional" T cells (Tconv)**, while Tregs, which mainly secrete anti-inflammatory cytokines, are not included within the Tconv category because of their immunosuppressive ability.

It is important to highlight that cytotoxic $CD4^+$ T cells have been observed in different immune responses (Takeuchi and Saito, 2017). Similar to $CD8^+$ CTLs, this subset is characterized by the ability to secrete GzmB and perforin and to induce the apoptosis of target cells in a MHC class II-specific way.

Role of CD4⁺ Tconv in cancer

CD4⁺ T cells mediate anti-tumor immunity in different ways. First, some Tconv subsets can directly kill tumor cells through cytolytic mechanisms (Cachot *et al.*, 2021), but they mainly act indirectly by modulating the tumor microenvironment-mediated response. In secondary lymphoid organs, Tconv have the essential role of increasing the magnitude of CTL response. As already mentioned, the binding of CD40L on Tconv to CD40 on DCs promotes DC maturation, increasing their antigen presenting and co-stimulatory abilities towards CD8⁺ T cells (Bennett *et al.*, 1998), hence promoting tumor-specific CTLs proliferation and maturation into effector or memory T-cell phenotype. Additionally, Tconv mediate the upregulation of the co-stimulatory molecules CD80 and CD86 on the surface of DCs, and promote cytokine release by DCs to favour CTL survival and differentiation (Castellino *et al.*, 2006). In presence of Tconv, CD8⁺ T cells present enhanced cytotoxicity with increased secretion of the pro-inflammatory cytokines IFN-γ and TNF-α and decreased expression of inhibitory IC (Ahrends *et al.*, 2017). Within the tumor microenvironment (TME), Tconv release different pro-inflammatory cytokines, that attract and activate several immune cells: release of IL-2, for example, recruits NK cells and promote their cytotoxic ability (Dobrzanski, 2013). Moreover, activated CD4⁺ Th1 cells secrete IFN-γ that activates pro-inflammatory M1 macrophages (Corthay *et al.*, 2005). It is important to underline that the main anti-tumoral effects of Tconv are mediated by the Th1 subset. Th17 cells also participate in anti-tumoral immunity, despite having a controversial role in cancer development (Bailey *et al.*, 2014).

1.4c Regulatory T cells

One of the most important ways that our immune system adopts to avoid the excessive activation (defined as **immunological self-tolerance**) is to produce a subset of CD4⁺ T cells called regulatory T cells (Tregs), specialized in immune suppression (Rocamora-Reverte *et al.*, 2020). Discovered in 1995 by Sakaguchi et al, Tregs have a fundamental role in self-tolerance mechanisms and in controlling autoimmunity, in fact they have the ability to suppress the activation, survival and function of other immune cells (mainly lymphocytes) (Sakaguchi *et al.*, 1995). Tregs were initially characterized by their constitutive expression of CD25, also named IL-2 Receptor α (IL-2Rα), which is the high-affinity chain of the IL-2 receptor. Almost a decade later, in 2003, it was discovered that this T-cell subset presents the unique expression of the lineage-specific TF **Forkhead Box P3 (Foxp3)** (Fontenot *et al.*, 2003), since *Foxp3*KO mice developed a lethal autoimmune disease. Very importantly, both mice and humans having a loss-of-function mutation in the *FOXP3* gene locus suffer of a severe, T-cell–dependent, lymphoproliferative, immune-mediated pathology (named immune dysregulation, polyendocrinopathy, enteropathy, and X-linked inheritance, or IPEX)

(Brunkow *et al.*, 2001; Gambineri *et al.*, 2003). Since *FOXP3* gene resides in the X-chromosome in both species, this pathology only happens in mice carrying a hemizygous/homozygous mutation, while heterozygous females are phenotypically healthy.
However, especially in humans, FOXP3 and CD25 alone are not sufficient to identify Tregs, as they are also expressed by different subpopulation of Tconv, despite at lower levels. As Tconv require IL-7 much more than Tregs, the IL-7 receptor α chain CD127 is used together with FOXP3 and CD25 to better discriminate Tconv and Tregs (Wing *et al.*, 2019).

Another fundamental molecule for Treg function is **IL-2**, explaining the constitutive expression of the α-chain of IL-2 receptor, CD25 by Tregs. Although IL-2 plays a crucial role in T-cell activation and differentiation, it was observed that IL-2-deficient mice do not present severe defects in T-cell functionality (Kneitz *et al.*, 1995; Kung *et al.*, 1998). Instead, IL-2-KO mice were developing autoimmune-related disorders and lymphoproliferative disease (Malek *et al.*, 2002), and in humans impacted CD25 expression correlates with IPEX syndrome and severe autoimmunity (Caudy *et al.*, 2007). It is believed that there is a negative feedback mechanism to control the T-cell activation through IL-2: produced by activated non-Tregs, IL-2 fuels Treg activation and expansion, which in turn restricts the proliferation of non-Tregs (Popmihajlov and Smith, 2008). Moreover, the constitutive expression of CD25 allows Tregs to scavenge IL-2 from the microenvironment, as they do not produce their own supply.

Treg classifications

Tregs represent a heterogeneous and dynamic subpopulation of T cells. It is possible to classify Tregs based on their origin into two main subsets: thymus-derived Tregs, also named natural Tregs (**nTregs**), and peripherally differentiated or induced Tregs (**iTregs**), which are generated in the periphery from mature $CD4^+$ Tconv or *in vitro* in presence of polarizing conditions (Togashi *et al.*, 2019). The majority of Tregs present in the blood and in lymph nodes (LNs) are nTregs, which constitutively express FOXP3 and preferentially recognize self-antigens (Workman *et al.*, 2009). Instead, iTregs are specifically engaged upon recognition of *de novo* antigens as allergens, food or during cancer development.
Very importantly, natural Tregs rely on IL-2 for their survival and they expand more in presence of high doses of this cytokine. At the same time, IL-2 promotes TGF-β-dependent differentiation of Tconv into iTregs, while inhibiting the differentiation of native T cells in Th17 (Zhou *et al.*, 2008). Both Treg subpopulations share the same mechanisms of action and express CD25, FOXP3 and the co-receptors GITR and CTLA-4 (discussed in details in the following paragraph). Instead, the expression of Neuropilin 1 (Nrp1), a multifunctional receptor that binds isoforms of Vascular

Endothelial Growth Factor (VEGF) and TGF-β, is restricted to nTregs (Vignali *et al.*, 2008). Another nTreg-specific marker is represented by Helios, a TF involved in lymphocyte development (Kaser *et al.*, 2015). In addition, the stability of *Foxp3* gene expression differs between nTregs and iTregs, as it has been shown that FOXP3 expression in iTregs is transient due to a different epigenetic profile.

Both *in vitro* and *in vivo* studies have shown that, apart from strong TCR signaling and specific co-stimulation, high levels of TGF-β and retinoic acid can induce *Foxp3* expression in naive $CD4^+$ T cells in the periphery. Indeed, the TGF-β receptor (TGF-βR) signaling is indispensable for the majority of the *Foxp3* induction in peripheral $CD4^+$ T cells (Freudenberg *et al.*, 2018). Upon TGF-β binding, the signal transducer molecules SMADs get activated and bind to the CNS1 in the *Foxp3* gene, inducing FOXP3 expression in naive $CD4^+$ T cells, hence boosting their differentiation of these cells into Tregs in peripheral tissues and *in vitro (Fantini et al., 2004; Schlenner et al., 2012)*. During Treg polarization, IL-2 is also essential for TGF-β-mediated induction of *Foxp3* both *in vivo* and *in vitro*, as it promotes the STAT5-dependent activation of *Foxp3* and contributes to cell survival and proliferation (Mahmud *et al.*, 2013). In addition, IL-2 limits the differentiation of activated $CD4^+$ T cells into Th17. Instead, Retinoic acid (RA) enhances the development of iTregs starting from naive $CD4^+$ T cells (Liu *et al.*, 2015c). This might be due to the ability of RA to increase SMAD recruitment upon TGF-βR engagement or to inhibit inflammatory cytokine signaling that negatively regulates *Foxp3* expression (Xiao *et al.*, 2008). In addition, RA can influence the epigenetic changes of the CNS2 region and promote *FOXP3* transcription in Tregs precursors. Finally, RA supports nTregs stability *in vivo* by opposing to the Treg cell-inhibiting cytokine IL-6 (Zhou *et al.*, 2010).
From a functional point of view, human Tregs can be recognized through the expression of CD45RA, FOXP3 and CD25: $CD45RA^+$ $FOXP3^{low}$ $CD25^{low}$ are **resting Tregs**; $CD45RA^-$ $FOXP3^{high}$ $CD25^{high}$ are **activated/effector Tregs**, and $CD45RA^-$ $FOXP3^{low}$ $CD25^{low}$ represent the **non Tregs** (Simonetta and Bourgeois, 2013). In a similar way, murine Tregs are classified into resting or activated Tregs based on the expression of CD62L and CD44, with $CD62L^{high}$ $CD44^{low}$ used to identify resting Tregs, and $CD62L^{low}$ $CD44^{high}$ that define activated Tregs (van der Veeken *et al.*, 2016).

In both humans and mice there are several subsets of Tregs that do not express CD4 and FOXP3 Treg markers, but some of them use the same immunosuppression mechanisms. Among those, the ones better characterized are Type 1 regulatory T cells (**Tr1**), a subset of $CD4^+$ $FOXP3^-$ cells characterized by the production of high levels of IL-10. Tr1 cells are mainly responsible of controlling infection and autoimmunity (Song *et al.*, 2021), and this subset is present in both humans and mice. Other Treg subsets are: **Th3** cells, which secrete high amount of TGF-β and some of them express FOXP3; **iTr35 $FOXP3^-$ Tregs**, which secrete the immunosuppressive cytokine IL-35 (Collison *et al.*,

2007); **$CD8^+$ Tregs**, a small population of $CD8^+$ T cells with immunosuppressive abilities; **$CD4^-$ $CD8^-$ γδ T cells**, associated with immunosuppression in different contexts, including cancer development (Pinheiro *et al.*, 2012). Finally, **Th1-like Tregs** (T-bet^+ $IFN\gamma^+$ $FOXP3^+$), **Th2-like Tregs** ($GATA3^+$ Interferon Regulatory Factor 4 $(IRF4)^+$ $IL\text{-}4^+$ $FOXP3^+$) and **Th17-like Tregs** ($IL\text{-}17^+$ $ROR\gamma t^+$ $FOXP3^+$), mainly present in the TME, display either pro-inflammatory or anti-inflammatory properties and are important in targeted therapy during tumor development (Li *et al.*, 2020).

Mechanisms of suppression

During the last decade, several experiments analyzing the transcriptional profile and protein expression of Tregs revealed the mechanisms used by Tregs to exert their immunoinhibitory functions towards other immune cells, which are summarized in **Figure 4**.

First, different secreted proteins were identified as involved in Treg cell-mediated suppression, including **IL-10, TGF-β and IL-35** (Schmidt *et al.*, 2012). Tregs produce high quantity of either membrane-bound or soluble TGF-β, and blocking this cytokine partially eliminates T-cell suppression *in vitro* in murine and human T cells (Budhu *et al.*, 2017; Gorelik and Flavell, 2000).

The second mechanism of immunosuppression occurs through cytolysis: in humans, Tregs produce and release **GzmA and B** upon stimulation of CD3 and CD46, resulting in the induction of apoptosis in the target cells, represented mainly by T cells and DCs. (Grossman *et al.*, 2004). Of note, in mice only GzmB is responsible of mediating this process (Cao *et al.*, 2007).

Tregs can also metabolically regulate the function of target cells through cell surface molecules such as **CD39 and CD73**, two ectoenzymes that mediate the conversion of ADP/ATP to AMP and AMP to adenosine, respectively (Allard *et al.*, 2017). Consequently, the depletion of ATP from the microenvironment causes a shift from an ATP-driven pro-inflammatory response to an anti-inflammatory environment (Workman *et al.*, 2009). Tregs were also shown to directly inhibit effector T cells by transferring the inhibitory molecule cAMP to effector T cells by **gap junctions** (Sojka *et al.*, 2008). In addition, adenosine in the microenvironment negatively affects the function of DCs. Another metabolic suppressive mechanism used by Tregs is through the **consumption of IL-2** (due to high CD25 expression), which causes the starvation of activated effector T cells that need this cytokine to survive (Thornton and Shevach, 1998).

As previously discussed, Tregs are also able to modulate T-cell response by indirectly controlling the activation of APCs through the constitutive expression or **upregulation of IC**. For instance, LAG-3 has a high binding affinity with MHC class II, and the binding of the MHC molecule on immature DCs with LAG-3 leads to the inhibition of DCs maturation (Liang *et al.*, 2008). Moreover, other co-inhibitory receptors, such as CTLA-4 and TIGIT, are highly expressed on Treg cells and negatively

impact DCs activation while causing the production of immunosuppressive cytokines (Sojka *et al.*, 2008). In fact, CTLA-4 binds to CD80/CD86 on DCs and suppresses DC maturation and T-cell priming.

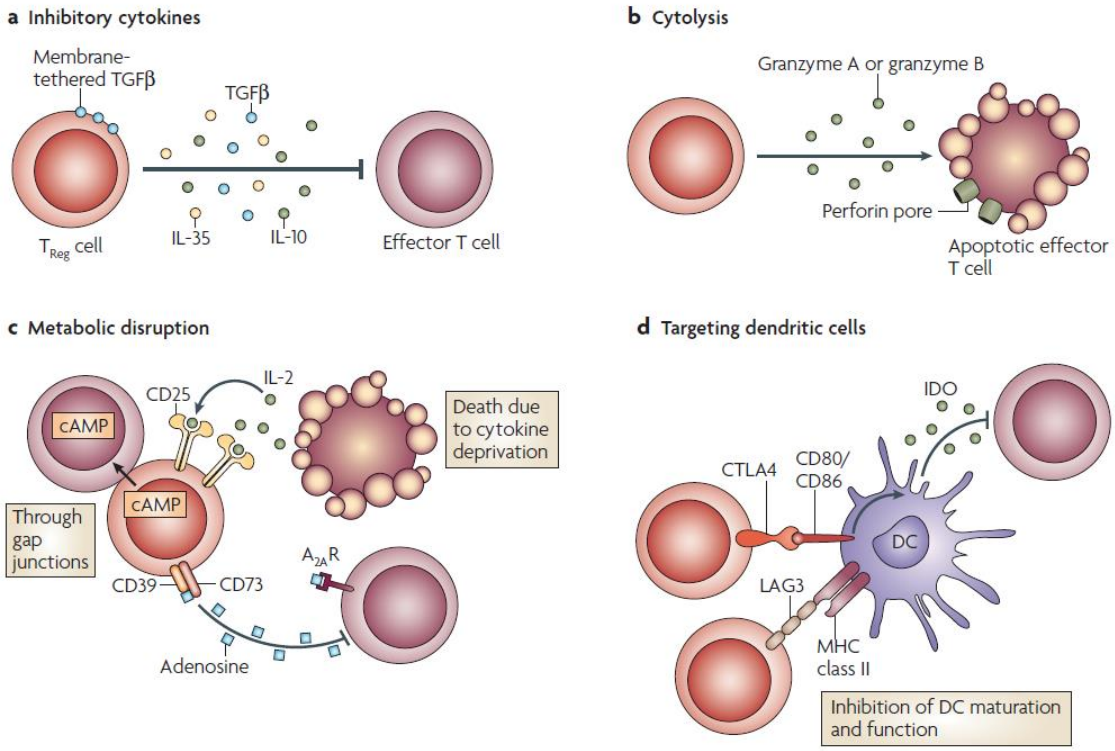

Figure 4. **Infographic of the immunosuppressive mechanisms used by Tregs to regulate immune responses.** a) IL-10, IL-35 and TGF-β are the most important inhibitory cytokines released by Tregs. b) Cytolysis includes GzmA- and GzmB-dependent apoptosis. c) Metabolic regulation includes high-affinity CD25-dependent IL-2 depletion, inhibition mediated by cyclic AMP (cAMP), and immunosuppression through CD39 and/or CD73. d) Upregulation of immune checkpoints inhibits T-cell activity and DCs maturation and function. Picture taken from (Vignali *et al.*, 2008)

Transcriptional activity of FOXP3

It is now clear that FOXP3 is the key TF in determining the identity and function of regulatory T cells. Among the most important activated genes, **FOXP3 directly regulates *CTLA-4, IL-2RA, TNFRSF18, NRP1 and IL-10*** in a cell-intrinsic manner (Georgiev *et al.*, 2019). At the same time, FOXP3 represses the transcription of genes normally activated upon TCR engagement in naive and effector T cells: this is the case of *GATA3 and RORγt*, which expression is inhibited by FOXP3 to avoid the differentiation into Th2 and Th17 cells, respectively (Chapoval *et al.*, 2010; Ichiyama *et al.*, 2008). From a molecular point of view, FOXP3 is able to positively and negatively regulate the transcription of target genes because it promotes epigenetic remodeling of specific target loci. In fact, binding of FOXP3 to target genes correlates with an increase in activating or inhibitory histone modifications (Li *et al.*, 2007).

Regulation of FOXP3 gene

Especially in nTregs, FOXP3 expression is regulated by different TF, which can bind either the *FOXP3* promoter or the CNS regions to promote or retain FOXP3 expression (Colamatteo *et al.*, 2019). In particular, the FOXO proteins FOXO1 and FOXO3 regulate *FOXP3* expression by interacting with *FOXP3* promoter or with other regulatory regions of the gene (Ohkura and Sakaguchi, 2010). Another fundamental TF is c-Rel, a member of the NF-κB family that participates in controlling FOXP3 expression in nTreg cells (Hovelmeyer *et al.*, 2022). Of note, in both humans and mice, after TCR engagement and co-stimulation, TFs such as NFAT and AP-1 interact with and activate *FOXP3* promoter (Mantel *et al.*, 2006). Finally, nTreg cells present a demethylation of CpG islands when several TFs are recruited at *FOXP3* locus, including STAT5, the Core Binding Factor β (CBF-β), the c-AMP responsive element binding protein (CREB), and FOXP3 itself (Sekiya et al., 2016).

Role of regulatory T cells in cancer

To escape the immune surveillance, tumor cells promote the establishment of an immunosuppressive microenvironment. For this purpose, tumor cells recruit and/or induce myeloid derived suppressor cells (MDSCs) and Tregs, defined as immunosuppressive cell types (Lindau *et al.*, 2013). Due to their immunosuppressive abilities, Tregs are able to inhibit the antitumor immunity, and for this reason, they have a strong **pro-tumoral role**, helping tumor cells to develop and proliferate (Li *et al.*, 2020). The first piece of evidence of the pro-tumoral role of Tregs was obtained in 1999 by Shimizu et al., who observed an improved anti-tumor immunity upon $CD25^+$ Treg cell depletion in a murine model of melanoma (Shimizu *et al.*, 1999). However, increased Treg number correlates with good prognosis in tumors characterized by sustained chronic inflammation, such as colon, bladder or breast cancer, because in these cases Tregs suppress the tumor-promoting inflammation (Greten and Grivennikov, 2019).

Within the TME, there is an overall increase of intratumor Tregs numbers and this phenomenon is due to several reasons. The first one relies on the fact that tumor cells can recruit nTregs at the tumor site through chemokine receptors, such as CCR4 (Nagarsheth *et al.*, 2017). As such, in melanoma and hematological malignancies, nTregs are recruited into tumors by chemotactic signaling, as key chemokines (mainly CCL17 and CCL22) are produced by MDSCs, stromal cells and tumor cells (Faget *et al.*, 2011; Higuchi *et al.*, 2019; Lim *et al.*, 2008). Moreover, MDSCs can induce Treg activation through CD40/CD40L, PD-1/PD-L1, and CD80/CTLA-4 binding (Byrne and Vonderheide, 2016; Kochetkova *et al.*, 2010; Yang *et al.*, 2006). The second reason for Treg accumulation in the TME is the conversion of naïve T cells (or more rarely Th17 cells) into iTregs (Wang *et al.*, 2019b). These cells are induced by TME-mediated signals, including the release of

tumor antigens, the presence of cytokines such as TGF-β. Once polarized, iTregs can inhibit the antitumor immune response of Teff, DCs and NK cells through several mechanisms that result in tumor progression (Li *et al.*, 2020). For example, in human acute myeloid leukemia (AML), Tconv differentiate into iTregs thanks to the production of Indoleamine 2,3-Dioxygenase (IDO), an enzyme able to convert Tryptophan (Trp) into Kynurenine (Kyn). Kyn is the ligand of a membrane-associated TF called Aryl hydrocarbon receptor (AHR), which binds to *FOXP3* and stabilizes its expression (Arandi *et al.*, 2018). Furthermore, exosomes secreted by tumor cells are able to induce iTregs and are associated with impaired anti-tumor immune response (Whiteside, 2013). The last reason for Treg accumulation within the TME is the capacity of Treg cells to adapt their metabolism to the TME conditions. Recent studies showed that Tregs present low expression of the glucose transporter GLUT-1 on their surface together with enhanced OXPHOS activity when compared to Teff (Gerriets *et al.*, 2016). Indeed, Tregs favorably rely on fatty acid oxidation (FAO) and OXPHOS, especially in hypoxic environments with low-glucose and high-lactate availability, very common in the context of both solid tumors and hematological malignancies (Angelin *et al.*, 2017). This metabolic advantage is mainly regulated by the expression of FOXP3, which is responsible of inhibiting the transcription of glycolytic enzymes-related genes and of MYC, involved in glycolysis.

Tumor-infiltrating Tregs display greater immunosuppressive activity when compared to other systemic Tregs, have an enhanced proliferating phenotype and are highly immunosuppressive, as demonstrated by the increase in $Ki67^+$ Tregs in murine models of lung cancer (Kamada *et al.*, 2019) and by the co-expression of IC such as CTLA-4, TIGIT, PD-1, ICOS and GITR in different tumors (Kim *et al.*, 2020). Similarly to non-cancerous conditions, Tregs expressing CTLA-4 interact with CD80 and CD86 expressed by DCs causing the downregulation of DC activity in tumors (Tekguc *et al.*, 2021). Likewise, LAG-3 molecules expressed by Tregs interact with MHC II molecules on DCs, hampering their APC abilities (Liang *et al.*, 2008). Moreover, DC tolerance is also induced through IDO upregulation, which is induced by Tregs and favors an increased production of IL-10 and indirect induction of T-cell apoptosis (Schmidt *et al.*, 2012). As in non-tumoral contexts, tumor-infiltrated Tregs secrete TGF-β, IL-10, and IL-35, able to specifically hamper antitumor immunity while suppressing antigen presenting abilities by DCs and $CD4^+$ Th activation (Whiteside, 2013). While TGF-β mainly inhibits $CD8^+$ T-cell and DC activity, IL-10 and IL-35 induce intratumor T-cell exhaustion by promoting IC upregulation and the transcriptional rearrangements that characterize $CD8^+$ TILs exhaustion (Yan *et al.*, 2022).

1.5 T-CELL EXHAUSTION

T-cell exhaustion is a definition used to describe a terminal state of T-cell response to chronic antigen stimulation. Despite T-cell infiltration within tumors represents a positive prognostic factor in patients, the chronic exposure of T cells to tumor antigens causes a state of non-responsiveness or hypo-responsiveness in which T cells are "exhausted" (Pauken and Wherry, 2015). $CD8^+$ exhausted T cells (Tex) were identified in both solid and hematological tumors, such as melanoma and Chronic Lymphocytic Leukemia (CLL). Within the TME, Tex present several characteristic features, such as progressive impairment of their effector functions, upregulation and co-expression of several IC, altered expression of TFs, and metabolic dysfunction (Balkhi, 2020). Importantly, Beltra *et al.* recently identified *in vivo* 4 different stages of $CD8^+$ T-cell exhaustion during prolonged exposure to viral agents, highlighting the gradual loss of functionality between the different stages that correlate with IC upregulation and transcriptional and epigenetic changes (Beltra *et al.*, 2020a). Exhausted T cells belonging to the first 3 stages are not completely dysfunctional, as they retain suboptimal but crucial activity that limits cancer progression and can be therapeutically used with immunotherapy (Beltra *et al.*, 2020a; Xia *et al.*, 2019).

Regarding the sustained upregulation and co-expression of several IC, Tex gradually start to co-**express several inhibitory receptors**, including PD-1, LAG-3, TIM-3, 2B4, CD160 and TIGIT. Notably, these IC are also expressed by activated and functional CTLs, and this is the reason why only the co-expression of several IC is highly associated with a dysfunctional and exhausted phenotype (Blackburn *et al.*, 2009). For example, PD-1 alone is also upregulated by activated T cells and plays a fundamental role in tuning the immune response in physiological conditions. Furthermore, recent studies have contributed to differentiate Teff from Tex as the first ones express low levels of PD-1, while the second ones present a high expression of this IC (Pellegrino *et al.*, 2019). The third characteristic of Tex is their altered expression of different TFs. Tex transcriptional profiling, in fact, revealed that that Tex have an **altered expression of key TFs**, in particular of T-bet and eomesodermin (Eomes), normally involved in the differentiation of Teff and Tmem (Buggert *et al.*, 2014). Another TF recently described as Tex specific is TOX, as *Tox*-deficient CTLs fail to differentiate into Tex but are able to develop into Teff and Tmem (Scott *et al.*, 2019).

Lastly, exhausted T cells are characterized by **metabolic rearrangements**. While naïve T cells mainly rely on OXPHOS to generate energy, Teff mainly use aerobic glycolysis in order to produce ATP, which is fundamental to support their high energetic effector activity (Patsoukis *et al.*, 2016). Once memory T cells develop, they switch again to OXPHOS and to fatty acid oxidation (FAO) for their survival. In contrast, Tex present a dysfunctional metabolism, as reflected by decreased glycolysis, and increased anabolic pathways. Very interestingly, these metabolic alterations are linked to IC expression (Bengsch *et al.*, 2016). Notably, recent studies highlighted the importance of the

epigenetic signature in T-cell exhaustion. PD-1 locus, for example, is transiently demethylated in activated Teff, but completely demethylated in Tex, resulting in the constitutive expression of PD-1 in Tex (Sen *et al.*, 2016).

1.6 CANCER IMMUNOTHERAPY

Immunotherapy is a treatment used in oncology that sustains the immune system in fighting against tumor cells. Therapeutically, the re-activation of the immune system in tumors is achieved in different ways, for example using chimeric antigen receptor (CAR) T cell or CAR-NK therapy, cancer vaccines, immunomodulatory drugs, oncolytic viruses, or specific antibodies used with the purpose of redirecting T cells against cancer cells. Among those, immune checkpoint blockade (ICB) is an incredible advance in cancer immunotherapy (Waldman *et al.*, 2020), as witnessed by the 2018 Nobel Prize Award in Physiology and Medicine to James Allison and Tasuku Honjo for their studies of the ICB anti-CTLA-4 and anti-PD-1. Two other strategies adopted as immunotherapeutic agents are bi-specific antibodies, which bind two different antigens or epitopes, and the Bispecific T-cell Engagers (BiTE), able to recognize simultaneously an antigen on tumor cells and a surface molecule on T cells.

1.6a Immunotherapy strategies targeting Teff

IC inhibitors work by blocking the immune checkpoints present on the T-cell surface to avoid its binding to the respective ligand. In this way, it prevents the "off" signal to be sent, allowing effector T cells to be active in the TME and kill cancer cells (Franzin *et al.*, 2020).

In 2011, the FDA approved the first IC inhibitor, an **anti-CTLA-4** antibody (ipilimumab), introduced as a therapeutic drug for the treatment of melanoma (Savoia *et al.*, 2016). Few years later, in 2014, the FDA authorized the usage of another checkpoint inhibitor, **anti-PD-1** (Pembrolizumab), for the treatment of advanced melanoma (Burns *et al.*, 2016). In a similar way, very recently, the FDA approved the IC inhibitor **anti-PD-L1** (Atezolizumab) for bladder cancer patients (Inman *et al.*, 2017). Since the introduction of IC inhibitors in the clinic, several clinical trials were conducted to evaluate the efficacy of the ICB compared to the standard treatment of different hematological malignancies (e.g. Hodgkin lymphoma and CLL) and solid tumors (among others, advanced hepatocellular carcinoma, HCC, and colorectal cancer, CRC) (Qin *et al.*, 2019).

In some cases, a single IC inhibitor did not show any clinical improvement compared to other therapies, as it happened with the administration of anti-PD-1 to CLL patients (Ding *et al.*, 2017), probably because the inactivation of a single immune checkpoint triggers the activation of other co-receptors in T cells as a compensatory mechanism (Postow *et al.*, 2015). Instead, in some tumors

the combination of different IC inhibitors has been clinically approved since it showed an increased survival benefit for cancer patients. This is the case of the dual CTLA-4/PD-1 blockade for the treatment of advanced melanoma (Wolchok *et al.*, 2013), which has been authorized by FDA in 2015. Since 2020, dual immunotherapy of anti-PD-1/CTLA-4 is also used to treat HCC and advanced lung cancer (Liu *et al.*, 2021). Several clinical trials are currently ongoing to the efficacy of the combination of different IC inhibitors, including TIGIT, LAG-3, PD-L1, VISTA and TIM-3 (Barrueto *et al.*, 2020). Very importantly, beside the tumor cell intrinsic biomarkers, several studies highlighted the importance of the TME composition in influencing the therapeutic response to ICB. Crucial factors within the TME that influence the success of ICB therapy are the infiltration rate of immune cells, the expression of IC by T cells and NK cells, and the TMB (Petitprez *et al.*, 2020).

1.6b Immunotherapy strategies targeting Tregs

Cancer immunotherapies such as CTLA-4 and PD-1 ICB frequently cause autoimmune-related issues (Burke *et al.*, 2021). Very often, the efficiency of the anti-tumor response upon ICB is associated with the development of autoimmunity, especially upon depletion of systemic Tregs. For this reason, researchers focus on finding effective ways to restore a functional anti-tumor immunity by targeting tumor infiltrated Tregs without interfering with systemic Tregs. For this purpose, one strategy adopted is to target only effector Tregs, which are highly suppressive, proliferative, and susceptible to apoptosis. Good candidates are represented by **chemokines receptors**, which are predominantly expressed by effector Tregs. Since the recruitment of Tregs to the cancer site is dependent on the expression of CCR4 ligands secreted by other cells within the tumor, the usage of anti-CCR4 antibody effectively depletes effector Tregs while increasing the induction of $CD4^+$ and $CD8^+$ effector T cells. Based on these studies, phase I clinical trials using an anti-CCR4 monoclonal antibody (mAb) were initiated in patients with solid tumors and resulted in enhanced antitumor immune responses, although the majority of patients did not respond to the treatment (Saito *et al.*, 2021; Sugiyama *et al.*, 2013a). Several *in vivo* studies and clinical trials also investigated the effect of **anti-CD25** (daclizumab) administration, showing a stabilization of the disease and effective generation of CTLs upon depletion of CD25 in breast cancer patients (Rech and Vonderheide, 2009; Shimizu *et al.*, 1999). However, Cohan *et al.* demonstrated that daclizumab targeted both effector T cells and Treg cells, as CD25 is also expressed by activated T cells (Cohan *et al.*, 2019). Solomon *et al.* showed the efficacy of Treg depletion through a new anti-CD25 antibody (RG6292) that does not interfere with IL-2 signaling in Teff (Solomon *et al.*, 2020). Together with antibody-mediated Treg depletion treatments, some studies focused on small molecule drugs able to target Tregs. One example is the administration of low doses of cyclophosphamide for prolonged time, which

selectively blocks highly activated Tregs within the tumor tissues, and reactivates an anti-tumor immunity in metastatic colorectal cancer patients (Scurr *et al.*, 2017).

Since Tregs constitutively express CTLA-4, recent studies have investigated the possibility that anti-**CTLA-4 mAb** mainly binds to Treg cells, hence causing an increase of the anti-tumor immune responses in an indirect way (Simpson *et al.*, 2013). Indeed, the clinical efficacy of Ipilimumab in cancer patients strongly correlates with a decreased Treg number at the tumor site (Hodi *et al.*, 2010). To this regard, it was recently demonstrated in a mouse model of B-cell lymphoma that ICB interfered with Treg-mediated immunosuppression, reducing FOXP3, CD25 and IL-10 expression upon treatment together with decreased immunosuppressive capacity (Bauer *et al.*, 2021). Lastly, a new approach used to neutralize intratumoral Tregs is to **convert them into Teff**. Since epigenetic modifications are fundamental for maintaining Treg phenotype and activity, small drugs against molecules involved in epigenetic remodeling (e.g. EZH2) have been used to target tumor-specific Tregs, inducing an increased tumor-specific immune response while avoiding systemic autoimmunity (Wang *et al.*, 2018a).

2. Chronic Lymphocytic Leukemia

2.1 DISEASE OVERVIEW

Chronic Lymphocytic Leukemia (CLL) represents the most frequent adult leukemia in the western world, accounting for 38% of the total leukemia diagnoses, and it is characterized by the clonal accumulation of B cells (Hallek and Al-Sawaf, 2021). CLL is roughly 20 times more frequent in Western countries than in the East ones (Burger, 2020), implying that not only genetic aspects, but also environmental-related causes affect the development of this disease. In addition, CLL mainly affects elderly people, as the diagnosis mainly occurs among people aged between 65 and 74. More males than females are affected (1.9:1) and the incidence of CLL did not vary in the last twenty years (https://seer.cancer.gov/statfacts/html/clyl.html). Nonetheless, the mortality for CLL has been decreasing in the last decades: the 5-year relative survival of CLL patients was at 68.1% in 1975 and it has been stably increasing up to 87.2% between 2011 and 2017. The disease usually has a slow course, but it can also have a faster progression, and either relapse or mutate into an aggressive malignancy, similar to Diffuse Large B-cell Lymphoma (DLBCL), process referred to as Richter transformation (RT).

Thanks to large-scale DNA-sequencing studies and epigenomic analyzes in the last decade, deep knowledge regarding the pathogenesis of CLL has been achieved, and a high amount of mutations has been discovered to drive the disease progression.

2.2 CELL OF ORIGIN AND CLONAL EXPANSION

During CLL progression, mature $CD19^+$ $CD23^+$ $CD5^+$ B cells clonally proliferate and accumulate in the blood, BM, and secondary lymphoid organs. CLL cells have a homogeneous morphology and immunophenotype, however this disease is considered as clinically heterogeneous, since some patients never need to be treated, while in other cases there is an aggressive disease correlating with poor response to treatment (Chiorazzi and Ferrarini, 2011).

Over the decades, different studies proposed several cell types as the healthy counterpart of CLL cells. At first, according to the mutations of the immunoglobulin heavy-chain variable (IGHV) genes, CLL can be divided into two groups: **unmutated (U) or mutated (M)**. The IGHV region is defined as unmutated when it has more than 98% of IGHV identity with the germline, while it is defined as mutated when there is more than 2% of deviation. IGHV-U and IGHV-M CLL patients vary in their clinical outcome, in fact IGHV-M CLL patients have a better prognosis then IGHV-U ones (Rotbain *et al.*, 2020). According to several studies, this difference is most likely due to the fact that IGHV-U CLL cells mainly express low affinity and polyreactive B-cell receptors (BCRs), while IGHV-M CLLs normally carry oligoreactive and monoreactive BCRs (Chiorazzi and Ferrarini, 2011; Garcia-Munoz

et al., 2012). Moreover, while IGHV-U CLL cells arise from B cells that have not entered the germinal center (GC), IGHV-M cells originate from post-GC B cells, and acquire somatic hypermutations and class switch recombination signatures. It is still under debate whether IGHV-U cells derive from naïve B cells or antigen-experienced B cells that did not enter the GC reaction, but several studies point towards the evidence that both CLL types arise from antigen-experienced B cells, as they express the memory cell marker CD27 (Bosch and Dalla-Favera, 2019; Tangye *et al.*, 1998).

Despite the recent advances, the cellular origin of CLL and its clonal evolution mechanisms are still under debate. The main discussion concerns the stage of B cell development from which CLL cells originate (pre- GC, post- GC or GC- independent B cells) and the type of cell that carries the first mutation (HSCs or mature B cells).

2.3 GENOMIC, GENETIC AND EPIGENETIC ABNORMALITIES

CLL is not characterized by a specific genetic event, and this type of leukemia carries several genetic mutations that can synergically contribute to induce the development and progression of CLL (Guieze and Wu, 2015). Nonetheless, there are recurrent genetic and epigenetic abnormalities that lead to the dysfunction of common pathways. First of all, the vast majority of CLL patients (up to 80%) present at least one of four chromosomal abnormalities, with the most frequent being the deletions of 13q (**del13q**), which happens in 50-60% of CLL patients (Srinivasan *et al.*, 2020). This lesion is more present in IGHV-M CLL patients than in IGHV-U ones and, among all the deletions, it is the only one associated with the better prognosis (Khalid *et al.*, 2021). This deletion involves the miR-15/16 locus, encoding for the miR-15 and miR-16 miRNAs, which are two tumor suppressor miRNAs. Their depletion results in the overexpression of the anti-apoptotic gene *BCL-2* and in the loss of control in the genes involved in the G0/G1–S cell cycle phases. Among the other most frequent deletions, the trisomy 12 is associated with RT, (Strati *et al.*, 2015); the **del11q** causes the deletion of ATM (fundamental tumor suppressor gene involved in the DNA damage response) (Stankovic and Skowronska, 2014), and the **del17p** cause the deletion of the tumor suppressor gene *TP53*.

At the genetic level, thanks to whole-genome sequencing (WGS) of CLL patients, more than 40 mutated driver genes have been described in CLL. The most common mutated gene at the time of diagnosis is ***NOTCH1***, an oncogene able to contribute to CLL cells survival and resistance to apoptosis. *NOTCH1* mutations are also associated with poor outcome and resistance to treatment (Rosati *et al.*, 2018; Rossi *et al.*, 2012a). As already mentioned, another important lesion involves the ***TP53*** gene, fundamental in the DNA damage response. Mutations in this gene are present in almost 10% of CLL patients at the time of diagnosis but this percentage goes up to 50% in patients with relapsed or refractory CLL, with *TP53* mutation correlating with bad prognosis and

chemoresistance. Among the most mutated gene, there is also *Splicing Factor 3b Subunit 1 (**SF3B1**)*, encoding for a protein involved in the spliceosome machinery, mutated in 10% of CLL cases (Wang *et al.*, 2011). Moreover, two very important mutations regards the NF-κB pathway, in particular *Baculoviral IAP Repeat Containing 3* (***BIRC3***) mutations, found in 2.2–4.3% of diagnosed CLL patients (Diop *et al.*, 2020), and ***MYD88***, found in almost 3% of patients with CLL (Baliakas *et al.*, 2015), both leading to the constitutive activation of NF-κB (Mansouri *et al.*, 2016).

At the epigenetic level, it has been shown that CLL cells present a general state of hypomethylation together with local hypermethylation (Guieze and Wu, 2015), and changes in the epigenetic state of CLL cells are associated with tumor progression (Smith *et al.*, 2015).

2.4 ROLE OF BCR SIGNALING IN CLL

B cell proliferation is mediated by the engagement of the BCR and activation of downstream pathways, and gene expression studies revealed that the pathways downstream to BCR activation are the most upregulated in CLL cells in LNs (which represent one of the most important reservoir of the disease) (Herishanu *et al.*, 2011). This characteristic highlights that the BCR has a fundamental role in the pathogenesis and disease progression of CLL, and this leukemia is often defined as a **BCR-dependent malignancy** (Burger and Chiorazzi, 2013). As already mentioned, there are differences in the clinical outcome of CLL patients based on the mutational status of the IGVH, and these differences have been linked to the BCR reactivity. Unmutated BCRs are more reactive towards different antigens (including self-antigens), giving rise to a strong BCR activation and resulting in a worse clinical outcome, while mutated BCRs have a more restricted antigen repertoire to which they are able to respond and give rise to a less aggressive disease with a better prognosis (Stevenson *et al.*, 2011). Approximately 30% of CLL patients present almost-identical BCR (defined as stereotypical), implying that there are common antigens able to initiate the disease and promote its progression (Ten Hacken *et al.*, 2019).

The activation of CLL cells is mainly caused by the interaction with T cells and a subtype of macrophages defined as nurse-like cells (NLCs). In fact, there are no activating pathway mutations in untreated CLL patients, implying that the BCR activation in CLL normally occurs in an antigen-dependent way (Gaidano and Rossi, 2017). BCR mutations are very rare in CLL, underlining the importance of the surrounding cells in activating and promoting CLL-BCR engagement (Svanberg *et al.*, 2021). Moreover, BCRs of CLL cells can be activated by different autoantigens, including molecules present on the cell membrane during apoptosis (e.g. cytoskeletal proteins like vimentin, IgG, DNA, microbial antigens and fungal antigens) (Hoogeboom *et al.*, 2013).

2.5 CLINICAL PRESENTATION AND DIAGNOSIS

Before the development of a manifest and symptomatic CLL, in the peripheral blood (PB) of patients (at this stage still asymptomatic), there is an accumulation of a clonal B cell population. This asymptomatic preclinical state is defined as monoclonal B cell Lymphocytosis (MBL) (Strati and Shanafelt, 2015), and it has been recently shown that some CLL clonal subtypes are detectable up to 16 years before CLL diagnosis (Kolijn *et al.*, 2022). Clinically, MBL is defined when the number of B cells accumulating in the bloodstream of patients goes up to 5,000 clonal B cells/µl of PB and it theoretically precedes every case of CLL in patients. CLL diagnosis occurs once the B cell number passes this threshold, and in presence of other molecular features.

At the moment of diagnosis, CLL patients can be either asymptomatic (in fact in many cases CLL is discovered during a routine blood test) (Zelenetz *et al.*, 2015), or present symptoms as enlarged LNs, splenomegaly, fatigue, weight loss, excessive night sweats, increased frequency of infections due to hypogammaglobulinemia (decreased antibodies production) (Kipps *et al.*, 2017). A complete blood count (CBC) test, together with flow cytometry, reveals an increased number of B cells (more than 5000/µl of PB), that very often express low levels of surface Ig, with either κ or λ light chains, due to the clonal nature of CLL cells expansion (Garcia-Munoz *et al.*, 2012). Flow cytometry analysis of the PB can confirm the expression of CLL antigens, as CD5, CD19 and CD23, together with low levels of CD20 (Hallek, 2019; Marti *et al.*, 1992). In case of an enlarged LN, a biopsy can be performed for suspected lymphoma. Within the LNs, CLL cells organize in pseudofollicles or proliferation centres, where they proliferate and receive stimuli from the surroundings cells (Herndon *et al.*, 2017). Even if it is not required for CLL diagnosis, a BM biopsy can be performed, and it often shows increased percentage of mature lymphocytes, as CLL cells infiltrate the BM (Rozman *et al.*, 1981).

2.6 STAGING

In order to divide CLL patients in different stages of disease progression, two staging systems are widely used. The first one, named Rai staging system, is mostly used in the United States of America, while the Binet classification is commonly used in Europe (Gupta *et al.*, 2021; Kay *et al.*, 2022). Regardless the method, both staging systems define three main groups with different clinical outcomes.

The **Rai staging system** is based on lymphocytosis and it stratifies CLL patients in:

- Low-risk (stage 0): patients who have lymphocytosis without cytopenia and present leukemic cells in the blood and/or BM (lymphoid cells >30%).

- Intermediate risk (stage I or II): patients with lymphocytosis without cytopenia. In case of lymphadenopathy CLL is considered at stage I, if splenomegaly and/or hepatomegaly is present, it is considered at stage II.
- High-risk (stage III or IV): patients with lymphocytosis and cytopenia, disease-related anemia (stage III) and thrombocytopenia (stage IV).

The **Binet staging system** relies on how many areas are involved, and considers the concentration of haemoglobin (HB) and platelets:

- Stage A: up to 2 enlarged sites, without cytopenia, with Hb ≥10 g/dL and platelets ≥ 100×10^9/L.
- Stage B: 3 or more enlarged sites, without cytopenia, with Hb ≥10 g/dL and platelets ≥ 100×10^9/L.
- Stage C: cytopenia, Hb of less than 10 g/dL and/or a platelets count of less than 100×10^9/L.

In the last years, fast progresses have been made in CLL treatments, and for this reason these two staging systems are not enough to stratify patients in prognostic subgroups. For this reason, in 2016 an international consortium established a new prognostic score: the CLL International Prognostic Index (**CLL-IPI**) (International-CLL-IPI-working-group, 2016). This score classifies patients based on five independent prognostic factors, which are TP53 status (deletion and/or mutation), IGHV mutational status (mutated vs unmutated), concentration of serum β2-microglobulin , Binet or Rai clinical stage, and age (<65 years or >65 years). Based on these criteria, patients are separated in 4 groups based on the prognostic score with different 5-years survival: low-risk, intermediate-risk, high-risk and very high-risk.

2.7 RICHTER TRANSFORMATION

CLL patients can develop an aggressive form of large cell lymphoma, named Richter Transformation (RT), in 2-10% of cases (Tadmor and Levy, 2021). RT consists in a transformation of CLL cells into DLBCL (in 95-99% of the cases) or in Hodgkin's variant of RT (0.5-5%). RT might develop in previously untreated patients, although it is more common to arise in patients following therapy (with a ratio of 1:3, respectively) (Wang *et al.*, 2020a). Moreover, it has been shown that the treatment of CLL patients with purine nucleoside analogues (the most used being Fludarabine) increases the risk of developing RT (Molica, 2010).

Regarding the genetic characteristics, at the moment of diagnosis there are some single nucleotide polymorphisms that positively correlate with a higher risk of RT (e. g. SNP in *CD38* or *BSL2* genes) (Tadmor and Levy, 2021). Moreover, patients carrying an unmutated IGHV and/or stereotyped BCR

are at higher risk of developing RT (Rossi *et al.*, 2009; Timar *et al.*, 2004). Very recently, it was shown that a higher complexity in the karyotype correlates with an increased risk of RT (Visentin *et al.*, 2022). Some of the genetic aberrations that increase the risk to develop RT include *TP53* and *CDKN2A* inactivation (Chigrinova *et al.*, 2013), MYC overexpression and NOTCH1 mutation (Parikh and Shanafelt, 2014). Of note, the probability of CLL patients carrying NOTCH1 mutations to develop RT is much higher (45%) compared with those without this mutation (4%) (Rossi *et al.*, 2012b).

2.8 CURRENT TREATMENTS AND CLINICAL TRIALS

Improvements made in the treatments of patients drastically improved the overall survival (OS) in the last three decades (Hallek and Al-Sawaf, 2021). Nonetheless, CLL is still considered an incurable disease for patients who do not receive allogeneic stem cell transplantation (Sharma and Rai, 2019).

2.8a Chemoimmunotherapy

Before new therapeutic agents were introduced, about 20 years ago, CLL was mainly treated with chemotherapy, including alkylating agents (with the most used being **cyclophosphamide** or **chlorambucil**), nucleoside analogues (e.g. **fludarabine**) and glucocorticoids, with younger and fit patients usually receiving a more intense therapy than elderly ones. With the advances of immunotherapy, anti-CD20 antibodies were included (as **Rituximab**) (Hillmen *et al.*, 2015) and the chemoimmonotherapy became the standard therapy before the introduction of newly discovered agents. In fact, the treatment with Fludarabine, Cyclophosphamide and Rituximab (**FCR**) became the front-line therapy used for young and fit patients (Fischer *et al.*, 2016), while Bendamustine together with Rituximab (BR) was normally given to less fit and elderly patients (Eichhorst *et al.*, 2016; Fischer *et al.*, 2011). Patients with low-risk CLL have better remissions upon FCR treatment, especially in case of IGHV-mutated CLL (Thompson *et al.*, 2016), while higher-risk patients have worst remissions. The FCR therapy is now implemented by changing Rituximab with more efficient anti-CD20 antibodies as **Obinutuzumab** or **Ofatumumab**, reducing the number of cycles.

2.8b Agents targeting signaling pathways in CLL cells and in the TME

Given the importance that BCR signaling holds for the survival and proliferation of CLL cells, new therapeutic approaches have been implemented for CLL patients. Different BCR-associated kinases (BAKs), such as Bruton-tyrosine kinase (BTK), Spleen tyrosine kinase (Syk), Zeta Chain Of T-cell Receptor Associated Protein Kinase 70 (ZAP70), Lyn and phosphatidylinositol 3-kinase (PI3K) mediate the signals coming from the BCR in CLL cells (Robak and Robak, 2013). In fact, the

introduction of compounds targeting these kinases (alone or in combination with chemotherapy or immunotherapy) can be considered a turning point in the treatment of B cell malignancies (Patel and Pagel, 2021).

In general, BTK inhibitors (BTKi) cause a shutdown of BCR signaling in CLL cells, inhibit chemotaxis towards CXCL12 and CXCL13, decrease survival and proliferation signals and increase apoptosis. The first BTK inhibitor, **Ibrutinib**, covalently binds the BTK kinase, which is upstream of the other kinases LYN and SYK and has a fundamental role in tissue homing of CLL cells while inducing apoptosis of CLL cells (Burger *et al.*, 2017). Different clinical trials have demonstrated an increase in overall and progression-free survival of patients treated with ibrutinib in different cases: relapsed or refractory disease, elderly patients, in case of the del17p, and in previously untreated patients (Timofeeva and Gandhi, 2021). **Acalabrutinib**, a second-generation BTK inhibitor, is more selective for BTK than ibrutinib and it has high response rate in relapsed/refractory CLL patients (Byrd *et al.*, 2016). Other BTK inhibitors as Pirtobrutininb and Zanubrutinib are also currently studied in phase 1/2 clinical trials (Mato *et al.*, 2021; Tam *et al.*, 2019; Xu *et al.*, 2020). Since several studies showed an increased incidence of atrial fibrillations or ventricular arrhythmias in patients treated with ibrutinib (Lipsky and Lamanna, 2020). Other inhibitors are then considered for patients at risk for cardiac arrhythmias.

Another kinase inhibitor used to treat CLL patients is **Idelalisib**, which is a reversible inhibitor of PI3K and inhibits BCR signaling and homing of CLL cells, while inducing their apoptosis (Hoellenriegel *et al.*, 2011). A phase 3 trial demonstrated that Idelalisib combined with rituximab increases the progression free survival when compared with rituximab alone (Furman *et al.*, 2014). Nonetheless, Idelalisib shows frequent side effects and lower efficacy than BTK inhibitors (Ghia *et al.*, 2020), so it is mainly used when patients have intolerable side effects due to BTK inhibitors. Another PI3K inhibitor, **Duvelisib,** was approved for relapsed/refractory CLL patients (Flinn *et al.*, 2018).

Since CLL cells upregulate the anti-apoptotic molecule BCL-2, **Venetoclax** (BCL-2 inhibitor) is commonly used to treat CLL and other leukemias. After two clinical trials showing the increased survival of patients treated with Venetoclax (Fischer *et al.*, 2019; Seymour *et al.*, 2018), this inhibitor has been FDA-approved in combination with Rituximab as frontline treatment of untreated CLL and as a treatment of relapsed CLL. The combination of Venetoclax with Obinutuzumab is also approved as first-line treatment for patients with del17p/TP53 as well as for physically unfit patients since it showed very good efficacy in the CLL14 clinical trial (Al-Sawaf *et al.*, 2020). In general, Venetoclax represents a very important alternative when kinase inhibitors show unacceptable side effects or for patients who developed resistance to kinase inhibitors due to mutations at the inhibitor-binding sites (Sedlarikova *et al.*, 2020). Another compound used in high-risk patients is **Lenalidomide**, a thalidomide analogue that has immunomodulatory and anti-inflammatory effects. A combination

with Rituximab showed a good overall response rate in relapsed/refractory CLL patients (Badoux *et al.*, 2013).

2.8c Cell therapy

Due to the acquired resistance to BTK inhibitors and venetoclax that CLL patients can develop, **allogenic hematopoietic stem cell (HSCs) transplantation** remains the only therapy able to cure CLL patients. Nonetheless, given the side effects related to the transplantation, such as the graft versus host disease and severe infections, HSCs transplantation is only considered for selected young and fit patients with high risk disease, who include a minority of CLL patients, especially in case of relapsed CLL (Gladstone and Fuchs, 2012). Another cell therapy that gave very good efficacy implies the usage of **CAR T cells** with specificity for CD19, a B cell specific antigen. A very recent study showed a decade-long CLL remission in two patients upon treatment with CAR T cells (Melenhorst *et al.*, 2022). In addition, **CAR-NK** cells might become another cellular therapy, due to the positive results obtained in safety and efficacy (Liu *et al.*, 2020).

2.8d Clinical trials

Several clinical trials are ongoing in CLL patients, with the aim of finding curative therapies and develop treatments that work when others fail. The majority of clinical trials investigates new compounds, including new kinase inhibitors. Several clinical trials are also evaluating the combination of different compounds that are currently used in the treatment of CLL patients, including CART-T and CAR-NK cell therapy (https://www.lls.org/leukemia/chronic-lymphocytic-leukemia/treatment/clinical-trials). Moreover, different monoclonal antibodies that target CLL-specific antigens are being tested such as UC-961, which targets ROR1, or milatuzumab to target CD74 (ID NCT00603668). Importantly, immune checkpoint blockade represents a promising clinical strategy in CLL, and several clinical trials are ongoing. For example, anti-PD-1 (Pembrolizumab, Nivolumab) in combination with the kinase targeting molecules idelalisib or ibrutinib are being evaluated for their efficacy (NCT02332980; NCT02420912). In addition, LAG-3, has being targeted with a blockade antibody, as a monotherapy or in combination with anti-PD-1, in CLL and other B cell malignancies (NCT02061761).

2.9 CLL PRECLINICAL MODEL: A FOCUS ON *Eμ-TCL1* MICE

Different mouse models have been generated in order to recapitulate different genetic aberrations present in CLL patients. Among those, the **Eμ-TCL1 mouse model** is the most widely used in preclinical research (Bresin *et al.*, 2016). Eμ-TCL1 mice, also referred to as TCL1, overexpress the

human oncogene *TCL1* under the expression of VH-promoter-IgH-Eμ-enhancer, resulting in the overexpression of this gene in all B cells (Bichi *et al.*, 2002). In CLL patients, this oncogene is overexpressed in the vast majority of cases and correlates with an aggressive course of the disease (Herling *et al.*, 2005).

TCL1 is involved in different signaling pathways, and the better characterized is the PI3K pathway, with TCL1 binding to AKT1/2 kinases and leading to cell proliferation and survival (Paduano *et al.*, 2018). In addition, TCL1 has been described to activate the NF-κB pathway in CLL cells (Pekarsky *et al.*, 2008).

In 2014, Simonetti et al. compared several different mouse models used to study CLL, each recapitulating a different feature of the human disease (Simonetti *et al.*, 2014). The Eμ-TCL1 model is the one better recapitulating the aggressive form of human CLL, in particular the one with the most similar immunophenotype, BCR repertoire and disease progression. Similarly to CLL patients, CLL cells in the TCL1 mouse models undergo a clonal expansion of $CD19^+$ $CD5^+$ B cells, characterized by unmutated IGHV, enhanced proliferation and increased AKT phosphorylation, recapitulating an aggressive form of human CLL (Bresin *et al.*, 2016). CLL cells in TCL1 mice are p53 wild type (WT) and are initially able to respond to fludarabine, but drug resistance develops after the treatment (Johnson *et al.*, 2006). Importantly, TCL1 overexpression in this model has 100% disease penetrance, meaning that all the mice carrying the TCL1 oncogene will develop CLL. In the TCL1 model, CLL cells can be detected at first in the peritoneum when the mice are 2 months old. Afterwards, within 4 months, CLL cells start to accumulate in the spleen and after 6-8 months they appear in the PB and in the BM (Hofbauer *et al.*, 2011). In TCL1 mice, CLL development is usually followed by a monthly bleeding and FACS analysis of the PB. This technique is used to monitor CLL development although the spleen represents the main reservoir of the disease in mice (Patrussi *et al.*, 2019), contrary to what happens in CLL patients, where the accumulation of CLL cells mainly occurs in LNs.

Notably, the CLL cells from sick TCL1 mice can be transferred into syngeneic WT mice to enhance the disease progression and mimic the clonal evolution of leukemic cells (Bresin *et al.*, 2016). This model is defined as **Adoptive Transfer (AT)-TCL1**, and the disease progression is much faster compared to the transgenic TCL1 mice (it occurs within few weeks), making this model more convenient for shorter studies.

2.10 TUMOR MICROENVIRONMENT IN CLL

The tumor microenvironment (TME) represents a complex and evolving entity that is composed by tumor cells, immune cells, stromal cells, endothelial cells, blood vessels, the extracellular matrix and other non-cellular factors (such as circulating DNA, exosomes, apoptotic bodies and secreted

factors) (Baghban *et al.*, 2020). The interactions that occur between the tumor cells and the TME are dynamic, as tumor cells are able to shape and control the function of their environment, favoring signal networks that are able to promote drug resistance, metastasis and cancer progression (Arneth, 2019; Khalaf *et al.*, 2021; Neophytou *et al.*, 2021).

CLL cells rely for their survival and proliferation on the stimuli provided by the TME (Burger and Gribben, 2014; Dubois *et al.*, 2020) (**Figure 5**). Indeed, when cultured *in vitro*, CLL cells die by apoptosis within few hours, but this time can be prolonged when they are co-cultured with stromal cells (Burger *et al.*, 2000; Simon-Gabriel *et al.*, 2018). Moreover, CLL cells show differences depending on the various compartments in which they are located. Circulating CLL cells in the PB are not proliferating, their cell cycle is arrested in the G0/G1 phase and they show prolonged survival and defects in apoptosis (Herishanu *et al.*, 2013). Instead, CLL cells proliferate via BCR-mediated NF-κB activation when they receive stimuli from the TME within the secondary lymphoid tissues and BM (Damle *et al.*, 2010; Soma *et al.*, 2006). In line with these dynamics, several drugs inhibiting chemokines and BCR-mediated signaling in CLL cells (e.g. BTK and PI3K inhibitors) are able to impact CLL trafficking and modify the interactions between CLL cells and stromal cells (Andritsos *et al.*, 2010; Ponader *et al.*, 2012). Fundamentally, apoptosis, chemoresistance and tumor expansion of CLL cells are mainly due to the interaction between CLL cells and non-malignant cells within lymphoid tissues (Herishanu *et al.*, 2011).

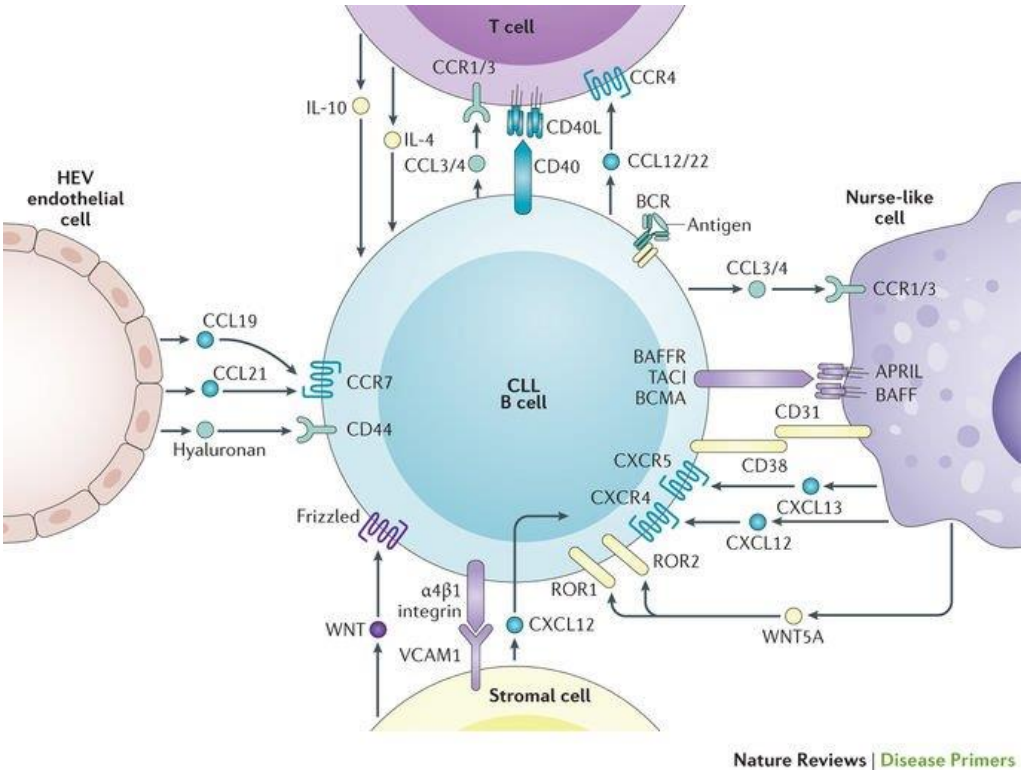

Figure 5. **Schematic summary of the different immune cells found in the CLL microenvironment.** CLL homing to the LNs is mediated by several chemokines released mainly by NLCs. Within the lymphoid tissues, different chemokines produced by NLCs and stromal cells promote B cell survival and proliferation. Not only paracrine signals, but also direct contact between cells promote CLL survival (e.g. VCAM1-VLA4 interaction between stromal cells and CLL cells, respectively). CLL cells, on the other side, secrete factors able to recruit immune cells in the TME. Within the lymphoid tissues, CLL cells are exposed to external or self-antigens able to increase the activation status of CLL cells. Figure taken from (Kipps *et al.*, 2017)

2.11 CELL TYPES IN CLL TUMOR MICROENVIRONMENT

Several cell types contribute to CLL stimulation and proliferation within the secondary lymphoid organs. The roadmap of the CLL microenvironment is being described, and the signaling pathways contributing to CLL homing, survival and proliferation are being elucidated. Very importantly, these discoveries provide solid bases for the development of new therapeutic agents against the TME.

2.11a Stromal cells

Stromal cells represent a very heterogeneous population with immunomodulatory properties, able to secrete factors that modulate cell homing and with differentiation potential (Wilson *et al.*, 2019). In the BM, **mesenchymal stem cells** (MSCs) belong to a population of $CD45^-$ non immune cells that in normal conditions supports hematopoietic progenitor cells and maintain the physiological architecture (Kandarakov *et al.*, 2022). In CLL patients, MSCs secrete factors that promote survival and migration of CLL cells while inducing the up-regulation of ZAP70 and CD38 (Trimarco *et al.*, 2015), considered markers of aggressive CLL development (D'Arena *et al.*, 2007; Rassenti *et al.*,

2008). Very importantly, MSCs have been shown to promote the downregulation of CD20 on the surface of CLL cells, feature associated with resistance to anti-CD20 antibody treatment (Marquez *et al.*, 2015). Different works also demonstrated the role of exosomes in CLL. Exosomes, also named extracellular vesicles (EVs) are able to carry different molecules (e.g. RNA, DNA, proteins, lipids) and transport them between different cell types. MSCs-derived EVs protect leukemic cells from apoptosis and promote migration of CLL cells (Crompot *et al.*, 2017). Also CLL cells can activate stromal cells through protein kinase C (PKC)-βII and activation of NF-κB (Lutzny *et al.*, 2013). CLL cells induced retinoic acid signaling in stromal cells, affecting chemokine secretion and lymphocytes chemoattraction (Farinello *et al.*, 2018). Moreover, EVs are fundamental for CLL cells to modulate the surrounding microenvironment: exosomes are able to transfer miRNAs in the stromal cells and induce an inflammatory phenotype similar to cancer-associated fibroblasts (Paggetti *et al.*, 2015).

Among stromal cells, it is important to highlight the presence of **Follicular Dendritic cells** (FDCs). In healthy conditions, the main function of FDCs is to capture antigens and present them to B cells circulating in the GC (Kranich and Krautler, 2016). In CLL patients, FDCs also accumulate in the BM (Chilosi *et al.*, 1985) and can interact with CLL cells through different molecules and receptor/ligand couples such as vascular cell adhesion molecule 1 (VCAM1)-VLA-4 (Kim *et al.*, 1994).

2.11b Myeloid cells

In physiological conditions, myeloid cells are CD14-expressing cells crucial for the functioning of innate and adaptive immunity, but they are also considered fundamental players in the CLL microenvironment. Many studies consider myeloid cells as a double-edged sword in CLL development. On one side, they include antigen-presenting cells (e.g. macrophages and DCs) which are fundamental for initiating and amplifying the anti-tumor immune response; on the other side they are widely described as having tumor-promoting activities. In fact, besides several *in vitro* works that highlighted the importance of these cells (Burger, 2011), *in vivo* studies have demonstrated that the depletion of monocytes, macrophages and granulocytes is able to control CLL growth (Galletti *et al.*, 2016; Hanna *et al.*, 2016; Jitschin *et al.*, 2014). Among myeloid cells, the most important subtypes in CLL pathophysiology are monocytes, NLCs, neutrophils and DCs.

Monocytes originate in the BM and migrate in the periphery. They are divided into human inflammatory monocytes and patrolling monocytes, with the inflammatory ones being $CD16^{-}$ and expressing high levels of CD14. Murine monocytes, instead, are characterized by the expression of Ly6 and CD43, the inflammatory ones are $Ly6C^{high}$ $CD43^{low}$, and the patrolling ones are $Ly6C^{low}$ $CD43^{high}$.

Gustafson *et al.* described a correlation between the monocyte count in the PB and a decreased time of progression of CLL (Gustafson *et al.*, 2012). Moreover, in the Eμ-TCL1 model Hanna *et al.*

showed the accumulation of monocytes in many organs of diseased mice (Hanna *et al.*, 2016) with a phenotype of patrolling monocytes ($Ly6C^{low}CD43^{high}$).

The **tumor-associated macrophages (TAMs)** are a macrophage subpopulation mainly characterized by an immunosuppressive and M2-like phenotype. The polarization of macrophages in M2-like TAMs can be due to different cytokines secreted or metabolites accumulated in the TME. In 2016, Hanna *et al.* showed an accumulation of macrophages in the peritoneum and spleen of Eμ-TCL1 mice compared to healthy controls (HC), and these cells exhibited a M2-like phenotype and upregulation of PD-L1 (Hanna *et al.*, 2016).

Very importantly, a special subset of macrophages is defined as **nurse-like cells (NLCs)** in the context of CLL development. NLCs represent specialized cells that differentiate from monocytes and are able to protect CLL cells from spontaneous apoptosis *in vitro* (Burger *et al.*, 2000). Within the following years, this model was widely used as an *in vitro* model to mimic the TME of CLL and to test different drugs (Ponader *et al.*, 2012; Schulz *et al.*, 2013).

Several studies on CLL patients have shown how monocytes isolated from healthy donors are able to differentiate into NLCs when co-cultured with CLL cells, promoting the survival of malignant cells *ex vivo* (Tsukada *et al.,* 2002).

Among myeloid cells, **DCs** were also shown to contribute to CLL cells survival. In a recent study, Barak *et al.* showed that BM dendritic cells (BMDCs) accumulate in the BM of CLL patients and of TCL1 mice and promote CLL cell survival and proliferation (Barak *et al.*, 2020). In addition, the depletion of BMDCs in mice is able to control CLL development. In patients DCs in the PB present an immature phenotype and have an altered functionality (Orsini *et al.*, 2003).

A very heterogeneous population found in CLL is composed by **myeloid-derived suppressor cells (MDSCs)**. MDSCs express high levels of IDO1 and inhibit the anti-tumor immune response (Jitschin *et al.*, 2014) and their accumulation in the PB correlates with bad prognosis (Liu *et al.*, 2015a).

2.11c Non-malignant B-cells

During the anti-tumor immune response, B cell activation leads to the differentiation of these cells into antibody-producing plasma cells. Antibodies are able to recognize tumor antigens and mediate the humoral immune response. Nonetheless, we have recently reviewed (reported in annex III) how B cells have both pro- and anti-tumoral role in cancer, with regulatory B cells (Bregs) being the most important mediators of B cell pro-tumoral activity (Largeot *et al.*, 2019). In CLL, the role of non-malignant B cells is poorly characterized. It is known that B cells acquire cytotoxic activity upon IL-21 stimulation, and in CLL cells stimulated with IL-21 are able to induce the apoptosis of non-stimulated ones in a GzmB-mediated mechanism (Jahrsdörfer *et al.*, 2006). The most common

feature related to B cells in CLL patients is hypogammaglobulinemia, a reduction of soluble IGs that is associated with poor prognosis (Andersen *et al.*, 2016).

2.11d NK cells

NK cells have a very important role in anti-tumor immunity, especially because they are able to directly kill tumor cells by recognizing specific molecules released by tumor cells but also by antibody-dependent cellular cytotoxicity (ADCC), which is able to recognize fragments of antibodies attached to the target cells. In the context of CLL, the role of NK cells remains quite controversial. While some studies reported impaired cytotoxicity in NK cells of CLL patients, (Katrinakis *et al.*, 1996; Wurzer *et al.*, 2021), other ones demonstrated that NK functions are unaltered in CLL patients and can be restored after cytokine treatment (Guven *et al.*, 2003; Veuillen *et al.*, 2012). In the same direction, other works showed that in CLL patients there is an increased number of NK cells in the PB and it predicts good prognosis (Wang *et al.*, 2018b).

2.11e T cells

CD8⁺ T cells

Although alterations of T cells in CLL patients were already observed in 1974 (Catovsky *et al.*, 1974), Hermann *et al.* were the first ones to observe a specific increase of $CD8^+$ T cells in CLL patients, which was leading to an inverted proportion of the physiological CD4:CD8 ratio (Herrmann *et al.*, 1982). This inverted ratio was then found to correlate with shorter time to first treatment (TTFT) and shorter OS (Nunes *et al.*, 2012) and is also present in leukemic TCL1 mice (McClanahan *et al.*, 2015).

Phenotypically, CLL patients present a higher percentage of antigen-experienced effector and memory $CD8^+$ T cells together with an increase in PD-1^+ $CD8^+$ T cells (Palma *et al.*, 2017), which is believed to correlate with an enhanced activation status of this T-cell subset. Moreover, in several *in vivo* studies, it was reported that there is an oligoclonal expansion of $CD8^+$ T cells in CLL (Blanco *et al.*, 2018), supporting the idea of an active anti-tumor immune response. Thanks to the analysis of $CD8^+$ T-cell TCRs isolated from CLL patient PB or spleens of AT-TCL1 mice, it was possible to demonstrate an increase in clonal $CD8^+$ T cells with a restricted TCR repertoire (Hanna *et al.*, 2019b; Vardi *et al.*, 2017b). As such, some T-cell clones are CLL-specific and are shared among different patients, especially the ones presenting the same BCR stereotype (Vardi *et al.*, 2017a). It is believed that CLL patients present T cells that specifically recognize leukemic antigens.

Hanna *et al.* demonstrated that $CD8^+$ T cells are able to contain CLL development in the AT model of TCL1, leading to an increased survival of diseased mice in presence of $CD8^+$ T cells (Hanna *et al.*,

2019b). In line with this work, Asslaber *et al.* demonstrated that leukemic conditional KO mice lacking IRF4 in B cells showed enhanced CLL development, as IRF4-deficient CLL cells downregulated MHC molecules and caused a reduced activation of $CD8^+$ T cells (Asslaber *et al.*, 2019).

Despite the numerous evidence of an efficient anti-tumor immune activity of $CD8^+$ T cells in both CLL patients and leukemic mice, several studies demonstrated their dysfunctional status in CLL patients, which contributes to tumor progression. First of all, $CD8^+$ T cells from CLL patients and cultured *ex vivo* present a decreased proliferative and cytolytic activities (Riches *et al.*, 2013) and have an impaired formation of the IS with CLL cells (Ramsay *et al.*, 2008). In addition, together with high levels of PD-1 in $CD8^+$ T cells, CLL patients also present increased expression of different immune checkpoints, such as TIM-3 (Taghiloo *et al.*, 2017), Killer Cell Lectin Like Receptor G1 (KLRG1) (Göthert *et al.*, 2013) and CTLA-4 (Motta *et al.*, 2005), pointing towards an exhausted phenotype of $CD8^+$ T cells in CLL. Our group could confirm these findings in leukemic TCL1 mice, showing an enrichment of exhausted $CD8^+$ T cells that express high levels of PD-1, LAG-3, TIM-3, and CTLA-4 when compared to HC (Wierz *et al.*, 2018). Very interestingly, targeting two immune checkpoints (PD-1 and LAG-3) could restore a functional anti-tumor immune response, implying that $CD8^+$ T cells are not completely dysfunctional in leukemic mice, but retain a sub-functional activity that can be restored with a therapeutic approach both in mice and humans (Riches et al., 2013; Wierz et al., 2018). For this reason, $CD8^+$ T cells of CLL patients are defined as "pseudoexhausted" and accumulate more in LN rather than in PB (de Weerdt *et al.*, 2019). Importantly, we and others demonstrated the role of CLL-derived EVs in hampering T-cell activation and metabolism while promoting their exhaustion and formation of Tregs (Bottcher *et al.*, 2022; Gargiulo *et al.*, 2022a).

$CD4^+$ T cells

As it happens with $CD8^+$ T cells, CLL patients also present increased antigen-experienced effector and memory $CD4^+$ T cells. Despite expressing high levels of the IC PD-1 and TIGIT (Catakovic *et al.*, 2017; Elston *et al.*, 2020), CLL-associated $CD4^+$ T cells present a higher expression of HLA and Ki-67 compared to healthy individuals, suggesting a strongly activated phenotype (Palma *et al.*, 2017). Nonetheless, $CD4^+$ T cells seem to have an active role in CLL development, as demonstrated by the requirement of co-injecting activated $CD4^+$ T cells in NOD-scid IL-2Rγ^{null} (NSG) mice together with CLL cells for a successful leukemia engraftment (Bagnara *et al.*, 2011). In addition, it was recently shown that CLL growth is dependent on $CD4^+$ T cells in the TCL1 model since this T-cell subset supports the proliferation of CLL cells (Grioni *et al.*, 2021). In line with these findings, in CLL patients

the increased number of $CD4^+$ T cells correlates with BCR characteristics such as the IGHV mutational status (Zaborsky *et al.*, 2015).

Gene expression profiling (GEP) of T cells in CLL patients demonstrated an accumulation of both Th1 and Th2 cells in the blood of CLL patients compared to healthy individuals (Catakovic *et al.*, 2017; Palma *et al.*, 2017), with Th1 accumulation correlating with a more progressed disease. More recently, an accumulation of $Tbet^+$ Th1-like T cells rather than Th2 cells was shown through expression analysis of T cells in patients and TCL1 mice (Roessner *et al.*, 2020).

Regulatory T cells

An increased frequency and number of Tregs can be found in the PB of CLL patients compared to HC (Biancotto *et al.*, 2012; Giannopoulos *et al.*, 2008; Gorgun *et al.*, 2005), and this accumulation is even more enhanced in LN of CLL patients (de Weerdt *et al.*, 2019). Moreover, there is an unbalance between $CD4^+$ T-cell subsets, as the ratio of Treg/Th17 cells in the PB of CLL patients is inverted, with Tregs accumulation correlated with disease progression (Pang *et al.*, 2016). Notably, we recently added another evidence in the contribution of Tregs in CLL development *in vivo* (see annex II). By depleting Tregs in DEREG mice injected with CLL cells, we observed a reduced CLL development together with the expansion of functional $CD8^+$ T cells compared to leukemic mice with functional Tregs (Goral *et al.*, 2022). In addition, we observed a CLL-specific Treg subpopulation ($FOXP3^+$ $CD44^{low}$ $CD25^{low}$) that accumulates along with CLL progression in Eμ-TCL1 mice and that mainly affects $CD8^+$ T cells in an antigen-specific manner.

It is important to underline that CLL-associated Tregs are more suppressive than normal Tregs (Lad et al., 2018) and secrete higher amounts of the anti-inflammatory cytokines IL-10 and TGF-β (Beyer et al., 2005; Biancotto et al., 2012). Furthermore, they present an increased expression of maturation markers such as CD103 and KLRG1, activation markers including CD69 and GITR, and suppressive markers such as CTLA-4 and PD-1 (Hanna *et al.*, 2019a; Roessner and Seiffert, 2020).

In line with these findings, we observed similar characteristics in leukemic mice, where Tregs present enhanced expression of immunosuppressive and activation markers such as PD-1, KLRG1, LAG-3 and CTLA-4 (Wierz *et al.*, 2018). Moreover, it was shown that Tregs and Th17 cells of CLL patients overexpress TIM-3 compared to HC (Pang *et al.*, 2021) and this overexpression correlates with a decrease in IFN-γ and increase in IL-10 in the serum of CLL patients (De Matteis *et al.*, 2018).

As in many other tumors, Tregs appear as an attractive therapeutic target in CLL. Indeed, treatment of CLL patients with chemotherapy such as fludarabine causes a decrease in Treg number (Beyer *et al.*, 2005). Other drugs used in CLL therapy such as the immunomodulatory lenalidomide and the BCL-2 inhibitor Venetoclax have a negative impact on Treg numbers. In line with this observation,

very recently Liu *et al.* explored the role of this anti-apoptotic molecule in T cells within the TME of CLL patients and demonstrated that T cells of CLL patients expressing BCL-2 correlate with an immunosuppressive TME characterized by enhanced activation of Tregs and $CD8^+$ T-cell exhaustion (Liu *et al.*, 2022). Very interestingly, inhibitors of PI3Kδ kinase, which mainly target BCR signaling of CLL cells, decrease the Treg count in CLL patients (Hanna *et al.*, 2019a). In order to test a new therapeutic approach in leukemic mice, Hanna *et al.* used an antibody against CD25 in TCL1 mice in order to deplete Tregs in CLL. Although this method did not target $CD25^-$ Tregs and depleted $CD25^+$ non-Tregs, it resulted in the increase of anti-tumoral $CD8^+$ T cells activation and functional activity (Hanna *et al.*, 2019a). However, the depletion of $CD25^+$ cells was not able to control CLL growth, suggesting that a more specific approach to target Tregs is needed which should include $CD25^-$ Tregs and spare $CD25^+$ effector T cells.

3. Role of TME-specific factors in tumor-stroma interactions

3.1 THE ARYL HYDROCARBON RECEPTOR (AHR) TRANSCRIPTION FACTOR

The aryl hydrocarbon receptor (AHR) is a ligand-dependent TF, activated by several diverse synthetic and natural compounds. When inactive, AHR is a signal sensor present in the cytoplasm, which translocates into the nucleus upon binding to its ligands.

3.1a Structure and activation of AHR

AHR belongs to the family of helix-loop-helix-PERARNT-SIM (bHLH-PAS) domain-containing TFs (Denison *et al.*, 2002; Schmidt and Bradfield, 1996) mediating the response to toxic agents in immune cells (Denison and Heath-Pagliuso, 1998; Denison *et al.*, 2002). The ligand with the highest-affinity for AHR is 2,3,7,8-tetrachlorodibenzo-p-dioxin (TCDD), an environmental contaminant. In addition, ligands of AHR include tryptophan-derived metabolites such as 6-formylindolo[3,2-b]carbazole (FICZ) (Rannug and Rannug, 2018) and kynurenine (Kyn) (Opitz *et al.*, 2011), fundamental in regulating several mechanisms, comprising immune cell development (Gasiewicz *et al.*, 2014) and tumor growth (Murray *et al.*, 2014).

Inactive AHR is found in the cytoplasm, in a proteic complex comprising 90-kDa heat shock protein (HSP90), which maintains AHR in a conformation for an appropriate binding of its ligands; the co-chaperones protein p23, the c-Src kinase, and the human hepatitis B virus X-associated protein (XAP2) (**Figure 6**) (Tappenden *et al.*, 2013). The interactions between the chaperone complex and AHR makes AHR inactive and in a stable conformation with a high-binding affinity for ligand while maintaining the TF in the cytoplasm (Denison *et al.*, 2002). Once AHR binds an exogenous or endogenous ligand, it undergoes conformational changes that make it detach from the proteins p23 and XAP2. Then, AHR exposes its Nuclear Localization Signal (NLS), and is imported in the nucleus by interacting with importin β (Chan *et al.*, 1994; Tsuji *et al.*, 2014). Once in the nucleus, AHR dissociates from the protein complex and is available for dimerizing with **ARNT** (AHR nuclear translocator). This dimer activates the transcription of different genes by interacting with specific DNA recognition sites (DNA consensus motif 5'-TNGCGTG-3') named Dioxin- or Xenobiotic-Responsive Elements (DRE or XRE) (**Figure 6**) (Bacsi and Hankinson, 1996; Seok *et al.*, 2017). The target genes of AHR include several enzymes able to metabolize xenobiotic molcules, such as cytochrome P450 family-1 subfamily-A polypeptide-1 (CYP1A1) (Larigot *et al.*, 2018). Other target genes are *NOLC1, POLR1B, NDRG1*, involved in metabolic changes and protein synthesis, while *BLIMP1, IL1, IL6, IL17A* and *IL-22* are target genes involved in inflammation processes (Bock, 2019).

In order to overcome potential negative consequences due to chronic AHR activation, its expression is tightly regulated: the AHR repressor (AHRR) competes with AHR for binding to ARNT and inhibits the AHR/ARNT complex by affecting its transcriptional functionality (Mimura *et al.*, 1999). Moreover, AHR is degraded via the 26S proteasome (**Figure 6**) (Davarinos and Pollenz, 1999). Very importantly, AHRR is a transcriptional target of AHR, and the degradation mediated by 26S proteasome is activated by AHR engagement.

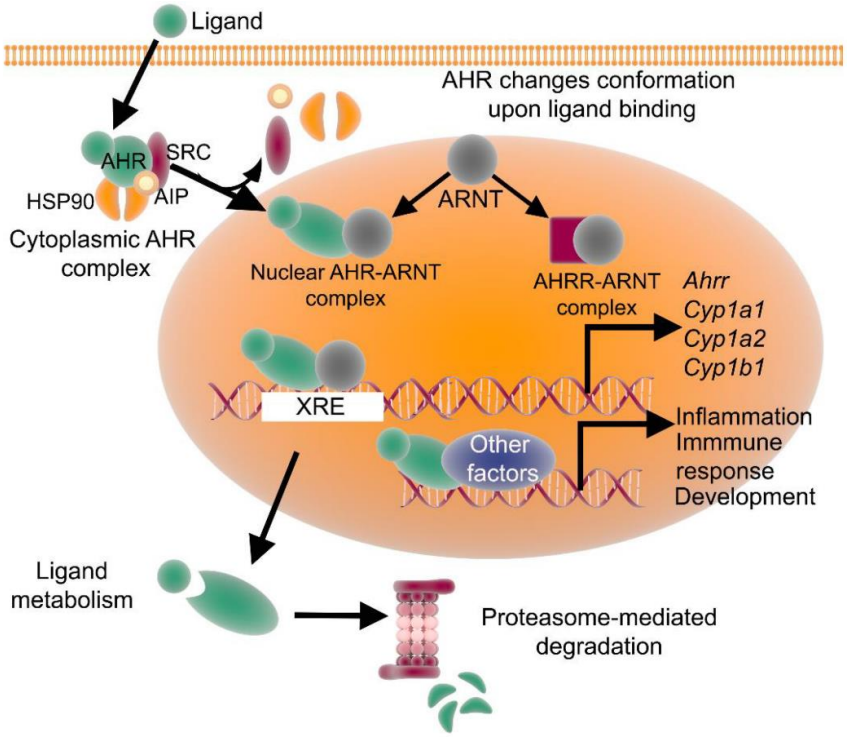

Figure 6. **The AHR signaling pathway**. Non-activated AHR is in the cytoplasm in association with a complex composed by HSP90, AIP and SRC. Upon ligand binding, conformational modifications lead to AHR translocation to the nucleus, where AHR binds its dimerization partner ARNT and recognizes XRE regions of target genes, mainly involved in metabolic changes. AHR can also induce transcription of genes that regulate development of immune cells and inflammation. As a regulation mechanism, AHRR, a target gene of AHR, competes with AHR to bind ARNT and gives rise to the complex AHRR-ARNT, transcriptionally inactive. Once the transcriptional complex is disrupted, AHR is translocated into the cytoplasm and degraded via proteasome.
AHR: aryl hydrocarbon receptor; AHRR: AHR repressor; ARNT: AHR nuclear translocator; and XRE: xenobiotic response element. Figure taken from (Choudhary and Malek, 2020).

3.1b Role of AHR in T cells

Very importantly, AHR activity is known to regulate the immune cell activity, in particular it affects $CD4^+$ T-cell development (Gagliani *et al.*, 2015). Moreover, different ligands of AHR can have diverse effects on Th cell development and Treg differentiation, pointing out the fine-tuning that this TF receives for the binding to its ligands (Al-Ghezi *et al.*, 2019; Quintana *et al.*, 2008). As first, AHR expression varies within the different $CD4^+$ T-cell subsets, with Th17 cells and Tregs (including

FOXP3$^+$ Tregs and TR1) having the highest AHR expression, while naïve, Th1 and Th2 CD4$^+$ T cells exhibit no or very limited AHR expression (Stockinger *et al.*, 2014).

During **Th17 cell differentiation**, AHR is upregulated and is responsible for the expression of IL-17A, IL-17F, while promoting the binding of RORγt to the *IL-22* promoter (Veldhoen *et al.*, 2008a; Yeste *et al.*, 2014). In presence of TGF-β and IL-6, the AHR ligand FICZ promotes the generation of Th17 cells both *in vitro* and *in vivo* (Quintana *et al.*, 2008). Besides having a role in Th17 development, AHR promotes the expression of CD39 in these cells and is also involved in the switch of Th17 cells into IL-10-producing TR1 cells (Gagliani *et al.*, 2015).

AHR is also important for **Treg development**. Indeed, in presence of TCDD and TGF-β, AHR promotes regulatory T-cell differentiation both *in vitro* and *in vivo,* as it modulates FOXP3 expression (Funatake *et al.*, 2005). The same effect is observed in presence of Kyn and 2-(1'H-indole-3'-carbonyl)-thiazole-4-carboxylic acid methyl ester (ITE), both metabolites of the Trp pathway that promote Treg expansion (de Araújo *et al.*, 2021; Mezrich *et al.*, 2010; Quintana *et al.*, 2010). In Tregs, AHR also controls the expression of IL-10 and CD39. Very importantly, in mouse splenocytes, AHR expression is linked to highly immunosuppressive TIGIT$^+$ Tregs, that are specialized in controlling Th1 and Th17 effector cells and express higher levels of AHR compared to TIGIT$^-$ Tregs (Joller *et al.*, 2014). As already mentioned, depending on the ligand, AHR can also inhibit FOXP3$^+$ Treg differentiation and boost Th17 differentiation (Kimura *et al.*, 2008).

AHR activation also promotes effector T-cell apoptosis *in vivo*, causing an increase in Treg percentage (Stockinger *et al.*, 2009). These differences are due to ligand-specific responses of AHR (that cause diverse effects on T-cell development), and to the different AHR expression among Treg subsets in tissues. Very importantly, AHR-expressing Tregs had enhanced *in vivo* suppressive ability compared to Ahr-KO Tregs in a T-cell transfer model of colitis (Goettel *et al.*, 2016). It is evident how the effects of AHR on FOXP3$^+$ Tregs are determined by the experimental approaches used in different studies, most likely recapitulating tissue-specific differences in producing diverse AHR agonists.

AHR activation in DCs is also able to indirectly induce Treg formation. Once AHR is activated in DCs, it promotes IDO1 expression, which is the key enzyme responsible in converting Trp into Kyn. In this way, DCs produce Kyn, which enhances TGF-β-driven Treg cell induction (Nguyen et al., 2010; Vogel et al., 2008). Indeed, DCs lacking AHR do not boost Treg development and promote Th17 cell differentiation *in vitro* (Nguyen et al., 2010). In a recent paper, Cui and colleagues demonstrated also *in vivo* that AHR-activated DCs can promote the differentiation of Treg cells and improve colitis in mice (Cui *et al.*, 2022).

3.1c AHR activation in cancer

AHR expression is higher in almost 70% of different tumors cells compared to healthy tissues. Indeed, *AHR* transcript is overexpressed in many malignancies, including breast cancer (Li *et al.*, 2014), lung cancer (Su *et al.*, 2013), oral squamous cell carcinoma (OSCC) (Stanford *et al.*, 2016) and glioblastomas (GBM) (Lim *et al.*, 2022). Very importantly, the endogenous agonist Kyn has a fundamental role in tumor development. As already mentioned, Kyn originates from Trp in a reaction catalyzed by IDO1, IDO2 and tryptophan 2,3-dioxygenase 2 (TDO2). Since the genes encoding for these enzymes are target genes of AHR, AHR activation leads to more AHR ligands production in an amplification loop that sustains AHR constitutive activation in cancer (Wang *et al.*, 2020b). Indeed, enhanced Trp metabolism is one of the hallmarks of GBM and increased Kyn/Trp ratio is associated with poor prognosis in GBM patients (Hornyak *et al.*, 2018). In addition, AHR activation by Kyn in the TME enhances Treg differentiation in glioma and is linked to immunosuppression (Gabriely *et al.*, 2017). Beside IDO1, IDO2 and TDO2, which are overexpressed in tumors (Ye *et al.*, 2019), another enzyme, named IL4I1, was recently found to catalize the conversion of Trp in indole metabolites and kynurenic acid, which are able to activate AHR (Castellano *et al.*, 2021; Sadik *et al.*, 2020), potentially explaining the lack of success of IDO inhibitors in different clinical trials. The imporance of this enzyme in tumor development was also confirmed in CLL as IL4l1 levels are increased in the serum of leukemic mice compared to HC (Sadik *et al.*, 2020).

Several studies contributed to demonstrate that the activation of Kyn-AHR signaling axis has a crucial role in tumor development, particularly influencing TME-infiltrated T cells. Indeed, AHR reduced the cytotoxicity and induces apoptosis of $CD8^+$ T cells (Greene *et al.*, 2019), while enhancing the recruitment of immunosuppressive TAMs (Takenaka *et al.*, 2019). Indeed, through *ex vivo* and *in vivo* experiments, it was shown that activated $CD8^+$ T cells stimulate the release of Kyn produced by tumor cells, as Kyn is transferred into $CD8^+$ T cells and activates AHR with a consequent PD-1 upregulation (Liu *et al.*, 2018). Moreover, the blockade of this pathway in mice led to enhanced efficacy of antitumor adoptive T-cell therapy. This pathway also promotes Treg and TAM synergic immunosuppressive effect in a melanoma mouse model. In fact, blocking AHR with an antagonist in tumor-bearing mice decreased Treg and TAM populations, limited tumor progression and improved the efficacy of PD-1 blockade therapy (Campesato *et al.*, 2020a). Very interestingly, AHR depletion in cancer cells also led to a decrease in immune checkpoint expression of $CD4^+$ T cells (PD-1, LAG-3, CTLA-4, CD39), in macrophages and MDSCs (CD39) compared to mice injected with AHR-WT cancer cells. Our group performed a similar experiment by depleting AHR in CLL cells in the TCL1 model, as reported in the Annex I section (Gonder *et al.*, 2021). In both cases, we could not observe

differences in CLL development between AHR-WT and AHR-KO leukemic cells, highlighting the peculiar dynamics of each tumor and the impact that cancer cells have on immune cells in different TMEs.

3.1d AHR as a therapeutic target

Based on the pro-tumoral role that AHR expression has in tumor development, AHR inhibitors were tested in preclinical models and are now entering clinical trials. The usage of AHR antagonists is mainly intended to reactivate the immune response by acting on cytotoxic T cells and by decreasing immunosuppression mediated by Tregs, MDSCs and, indirectly, by DCs. First of all, targeting AHR is considered a pursuable strategy to activate the immune system in gliomas (Lim *et al.*, 2022) as the AHR antagonist CH-223191 inhibits the proliferation and invasiveness of glioma cells *in vitro* by controlling TGF-β signalling (Gramatzki *et al.*, 2009). In addition, inhibiting AHR in mice reduced Treg- and macrophages-mediated immunosuppression in melanoma (Campesato *et al.*, 2020a). There are also FDA-approved molecules that could be used as treatment for cancer patients. One of those is clofazimine, an anti-leprosy drug, is a potent AHR antagonist and demonstrated clinical improve in multiple myeloma patients (Bianchi-Smiraglia *et al.*, 2018).

To test the direct effect of AHR inhibition in cancer, two phase 1 clinical trials have been started. The first one is a non-randomized clinical trial where the goal is to evaluate the toxicity and tolerability of an AHR inhibitor, BAY2416964, in 114 patients with untreatable advanced solid tumors (lung cancer, colorectal cancer, and head and neck cancer) (NCT04069026). The second one aims at determining the toxicity and tolerability of another AHR inhibitor, KYN-175, in 53 patients having advanced solid tumors (NCT04200963).

Due to the important role of IDO and TDO enzymes in the Kyn-AHR axis and their upregulation in several tumors, many clinical trials were initiated using IDO and TDO as tumor immunotherapy targets and are still in progress (Balachandran *et al.*, 2011; Litzenburger *et al.*, 2014; Pilotte *et al.*, 2012). Nonetheless, several trials initiated to evaluate the efficacy of IDO inhibition in different tumors failed, most likely because of the presence of other compensatory enzymes able to produce AHR-activating metabolites (Sadik *et al.*, 2020; Tang *et al.*, 2021). For this reason, AHR direct inhibition may offer a better approach for tumor immunotherapy, by targeting not only tumor-specific immunity but also cancer cells.

3.2 HYPOXIA AND HYPOXIA INDUCIBLE FACTOR-1A

Hypoxia is a common feature in cancer, and occurs as cancer cells grow rapidly, thereby causing a limited oxygen availability, while the blood flow is also impaired due to abnormal blood vessel

formation. Hypoxia-inducible factors (HIF) are widely recognized for being the major TFs involved in the hypoxic response, and their role in cancer is crucial for metabolic remodeling, glucose uptake, proliferation, metastasis development and angiogenesis, in both solid tumors and hematological malignancies (Lee *et al.*, 2020). The members of HIF family are HIF1, HIF2 and HIF3, heterodimers composed by α and β subunits. The α subunits are proteins present in the cytoplasm, regulated by oxygen levels, whereas the β subunits are constitutively expressed nuclear proteins, and not oxygen-sensitive (Wang *et al.*, 1995). HIF-1α and HIF-2α are mainly responsible of the transcriptional activity of HIF factors when in complex with HIF-1β (also known as ARNT) and HIF-2β, respectively (Keith *et al.*, 2011). Nonetheless, the two TFs have different functions and only partially overlap, with HIF-1α being the main responsible for activating transcriptional responses under hypoxia and regulating glycolytic genes (Saito *et al.*, 2015). Of note, HIF-1α controls the expression of severals genes specific for several processes, including angiogenesis and O_2 supply (*EPO, VEGF*), stemness and self-renewal (*ADM, TGFa*), proliferation (*TGFB3, ITF*), and metabolism (*GLUT1, PHD, BNIP3*) (Dengler *et al.*, 2014).

William G. Kaelin, Jr., Peter Ratcliffe and Gregg Semenza gave the most important contribution in understanding HIF engagement in response to low oxygen and the molecular mechanisms by which cells can sense O_2. Thanks to these fundamental discoveries, these researchers were awarded the Nobel Prize in in Physiology or Medicine in 2019.

3.2a Structure and activation of HIF-1α

As already mentioned, HIF-1 is a heterodimeric TF consisting of a constitutive β-subunit and an oxygen-sensitive α-subunit (Forsythe *et al.*, 1996). Both HIF-1α and HIF-1β belong to the bHLH-PAS protein family of TFs and regulate the transcription of hypoxia-inducible genes (Semenza *et al.*, 1997). In normoxic conditions, prolyl-4-hydroxylases (**PHDs**) enzymes hydroxylate HIF-1α through O_2 and 2-oxoglutarate substrates on two proline residues of HIF-1α, Pro402 and Pro564, located in its oxygen-dependent degradation domain (ODD) (Schofield and Ratcliffe, 2005) (**Figure 7A**). Hydroxylated HIF-1α is bound by the von Hippel–Lindau tumor suppressor protein (**pVHL**), a component of an E3 ubiquitin-protein ligase that mediates HIF-1α degradation via the ubiquitin-proteasome system (Huang *et al.*, 1998; Maxwell *et al.*, 1999). Since HIF-1α hydroxylation only occurs in a condition with sufficient oxygen, HIF-1α is stabilized in hypoxic conditions due to the inhibition of PHDs and inability of pVHL to recognize unhydroxilated HIF-1α (Palazon *et al.*, 2014; Ziello *et al.*, 2007). In this way, HIF-1α migrates in the nucleus and together with the HIF-1β subunit creates the transcriptionally active HIF-1 complex (Pagé *et al.*, 2002). Of note, HIF-1β, also named ARNT, is the dimerization partner of both AHR and HIF-1α and the crosstalk between these two

pathways could have a wide influence on several cellular mechanisms that involve the activation of these two TFs.

Very importantly, HIF-1α also contains two transcriptional activation domains (C-TAD and N-TAD) that are essential for the interaction with co-activator proteins, CREB-binding protein (CBP) and p300 (Freedman *et al.*, 2002). These two activators are necessary for the interaction between HIF-1α and the hypoxia responsive element (HRE)-binding regions of the target genes (**Figure 7A**). Indeed, another oxygen-dependent regulation of HIF-1α activation occurs through the control of HIF-1α and p300 interaction. Under normoxic conditions, the asparaginyl hydroxylase Factor Inhibiting HIF-1α (FIH) hydroxylates HIF-1α, inhibiting the interaction between p300 and HIF-1α and leading to HIF-1α transcriptional inactivation (Lando *et al.*, 2002). As HIF-1α expression is enhanced upon acetylation, another way of inhibiting HIF-1α accumulation is achieved by inhibiting its acetylation (Jeong *et al.*, 2002).

Noteworthy, in addition to hypoxia, other stimuli such as growth factors, hormones, and cytokines induce HIF-1α stabilization under normal oxygen conditions during inflammation, infection and cancer. For example, NF-κB is fundamental for orchestrating the immune reaction to infection, and induces HIF-1α activation in macrophages (Rius *et al.*, 2008). Whereas in T cells, TCR engagement, IL-6 and TGF-β induce *HIF1α* mRNA and protein accumulation (**Figure 7B**), in particular in Th17 cells (Dang *et al.*, 2011; Nakamura *et al.*, 2005). In addition, p300 is able to stabilize HIF-1α by acetylation in both normal and hypoxic conditions.

3.2b Role of Hif-1α in T cells

HIF-1α affects the development and activity of several T-cell subpopulations in both presence and absence of oxygen. For example, during naïve $CD4^+$ T-cell differentiation, a metabolic change is required to promote different glycolytic activities (van der Windt and Pearce, 2012). The glycolysis demand changes in Th1, Th2, Th17, and Treg cells, and Th17 present the highest glycolytic rate and Tregs displaying the least (Shi *et al.*, 2011). During Th1 development, HIF-1α seems to have different roles: increased glycolysis is essential for Th1 cell differentiation (Michalek *et al.*, 2011; Shi *et al.*, 2011), but also hypoxia inhibits IFN-γ production in Th1 cells, repressing their function (Shehade *et al.*, 2015). A clearer picture is depicted in Th17 cells, where HIF-1α is involved in IL-17 upregulation and *RORγt* expression (Zhang *et al.*, 2020c).

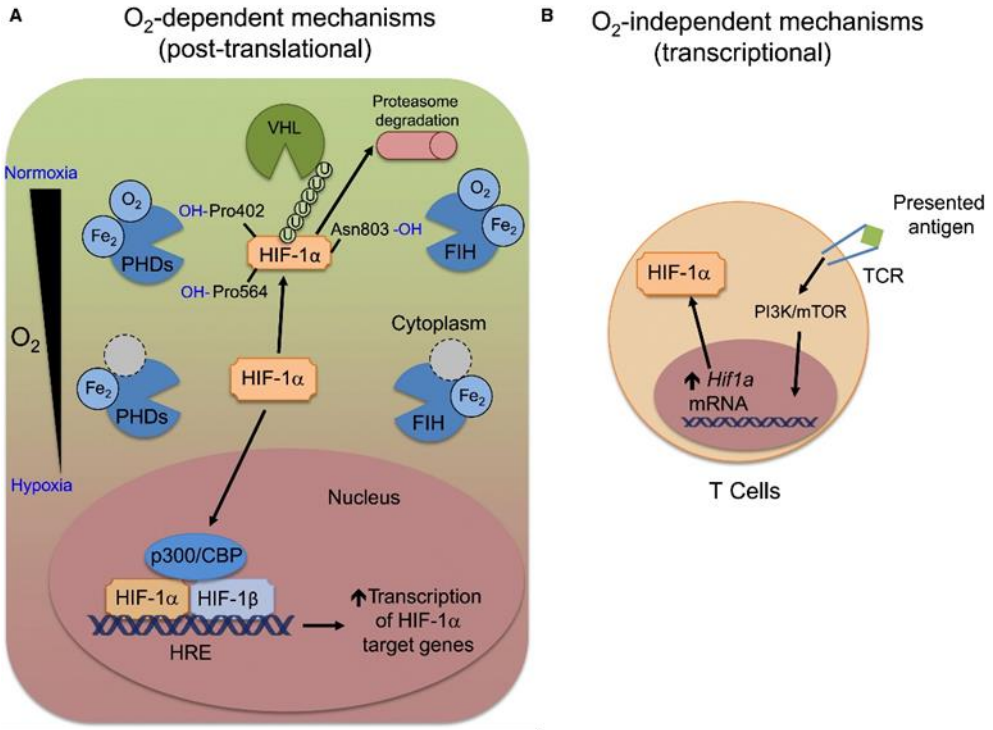

Figure 7. **HIF-1α stabilization in immune cells**
(A) O_2-dependent mechanism. In presence of O_2, HIF-1α is hydroxylated by PHDs and polyubiquitinated by VHL, resulting in proteasomal-mediated HIF-1α degradation. In addition, FIH hydroxylates HIF-1α, blocking its interaction with p300/CBP, essential for HIF-1α activation. In presence of low oxygen levels, PHDs and FIH activity are inhibited, allowing HIF-1α activation.
(B) O_2-independent mechanism. In T cells, TCR engagement upon recognition of the MHC/antigen complex leads to HIF-1α stabilization even in normoxia. This mechanism is thought to be mediated by PI3K and mTOR activation. Figure adapted from (Palazon *et al.*, 2014)

In Treg cells, HIF-1α plays a complex role, as different studies showed opposite roles of HIF-1α during Treg development and function. Of note, *FOXP3* promoter contains a HRE binding site, and HIF-1α was shown to promote Treg differentiation, while low oxygen levels enhance FOXP3 expression (Ben-Shoshan *et al.*, 2008; Clambey *et al.*, 2012). In line with these findings, Joller and colleagues showed that highly suppressive murine TIGIT$^+$ Tregs express high levels of *Hif1a* compared to their TIGIT$^-$ counterparts (Joller *et al.*, 2014). Nonetheless, Dang *et al.* also showed that HIF-1α directly interacts with FOXP3, increasing its degradation via proteasome and repressing Treg development, which suggests a complex role of HIF-1α in the development and function of Tregs. In a conditional knock-out mouse model, HIF-1α upregulation was mimicked by selective depletion of VHL in Tregs. Indeed, Tregs constitutively expressing HIF-1α presented increased IFN-γ production together with a decreased FOXP3 expression, which caused a decreased number of FOXP3$^+$ Tregs and increased Th1-like effector T cells (Lee *et al.*, 2015a). Furthermore, HIF-1α stabilization caused a more severe inflammation in an *in vivo* colitis model, while silencing HIF-1α in the cKO mice restored Treg functionality and balanced the inflammatory effects (Lee *et al.*,

2015a). Similarly, HIF-1α accumulation (achieved by knocking-out PHDs) inhibits Treg development and enhances Th1 cells functional activity (Clever *et al.*, 2016).

Very importantly, Hif-2α is also fundamental for Treg function. Indeed, Hsu and colleagues demonstrated that this transcription factor is indispensable for regulatory T cell function (Hsu *et al*., 2020). Using $Foxp3^{Cre}Hif2a^{fx/fx}$ mice, the authors observed that HIF-2α-KO Treg cells have impaired ability to suppress colitis and reprogram into IL-17 secreting cells. Of note, they observed that HIF-1α expression is increased in HIF-2α-KO Treg cells.

HIF-1α, together with AHR, plays also a pivotal role in Tr1 differentiation. In particular, Mascanfaroni and colleagues demonstrated *in vitro* an opposing role of AHR and HIF-1α in Tr1 development (Mascanfroni *et al.*, 2015). While HIF-1α expression at the early stages of Tr1 development promotes AHR inactivation and mediates an enhanced glycolytic metabolism, at a later point AHR inhibits HIF-1α and controls Tr1 metabolism via STAT3/CD39 upregulation. Furthermore, CD39 upregulation promotes HIF-1α degradation and promotes the late stages of Tr1 development, highlighting the opposite role of HIF-1α over the different phases of Tr1 development. In this context, this phenomenon was attributed to the competition between HIF-1α and AHR for binding their common dimerization co-factor HIF-1β/ARNT (Zhang *et al.*, 2022). While HIF-1α dimerizes with ARNT to promote glycolysis, AHR interacts with ARNT to promote the expression of Tr1-specific genes like *IL-10*, *IL-21*, and *EntPD-1* (Apetoh *et al.*, 2010).

HIF-1α is also important during $CD8^+$ T-cell activation, as it is crucial for the glycolysis increase in cytotoxic T cells following TCR engagement (Gupta *et al.*, 2020). At the same time, HIF-1α promotes $CD8^+$ Teff and Tmem differentiation by upregulating pro-inflammatory cytokines (IFN-γ, TNF-α), GzmB and IC (GITR, OX40, PD-1) and HIF-1α depletion inverts this process (Palazon *et al.*, 2017).

3.2c Hif-1α activation in cancer

Hypoxia is a hallmark of cancer and HIF-1α plays a role in several aspects of tumor development (Jing *et al.*, 2019), such as tumor cell metabolic adaptation to the TME, angiogenesis, epithelial-mesenchymal transition (EMT), tumor cell survival, communication between tumor cells, and epigenetic rearrangements (Bosco *et al.*, 2020; Qiu *et al.*, 2017). At the same time, hypoxia allows tumor cells to proliferate and metastasize while making an unfavorable environment for immune cells that are involved in the anti-tumor immune response (Abou Khouzam *et al.*, 2020).

In CLL patients, Griggio *et al*. demonstrated that TP53 mutations correlate with higher HIF-1α accumulation and activity (Griggio *et al.*, 2020) and TP53 is a target of HIF-1α, although this interaction has been poorly characterized. In CLL patients, HIF-1α upregulation is also due to VHL

dysfunction, which is dependent on the accumulation of miR-155 (Ghosh *et al.*, 2009). Moreover, HIF-1α upregulation also depends on TME-mediated signals: PI3K/ERK pathway is activated in CLL cells upon contact with stromal cells and leads to HIF-1α expression (Seiffert, 2020). In addition, chemokine receptors (e.g. CXCR4) and adhesion molecules are known to be induced by HIF-1α (Valsecchi *et al.*, 2016). In line with this, targeting HIF-1α in CLL mice inhibits chemotaxis and CLL cell adhesion to stroma, and enhances survival of immunodeficient mice. Very importantly, we show that depletion of HIF-1α in leukemic cells *in vivo* did not affect leukemogenesis (Annex I) (Gonder *et al.*, 2021), confirming that non-leukemic cells play a role in HIF-1α engagement and suggesting that HIF-specific drugs might act mainly on TME cells rather than on CLL cells.

Besides its role in tumor cells, hypoxia dampens the antitumor immunity, mainly interfering with the cytotoxic activity of $CD8^+$ Teff. In particular, deletion of the *HIF1α* gene in activated T cells enhances T-cell expansion and IFN-γ secretion, thus influencing T-cell responses, implying that HIF-1α is able to inhibit T-cell function in hypoxia (Reyes *et al.*, 2020). Nonetheless, cKO mice lacking HIF-1α in $CD8^+$ T cells *in vivo* display enhanced tumor development compared to WT mice, together with loss of anti-tumor activity of $CD8^+$ T cells (Palazon *et al.*, 2017).

PD-L1 is also upregulated on macrophages, DCs, and MDSCs during hypoxia, and this effect is dependent on HIF-1α. In addition, HIF-1α and PD-L1 are upregulated in MDSCs of different tumors, finally leading to T-cell exhaustion and tumor progression. PD-L1 blockade in MDSCs *ex vivo* in hypoxia enhanced the ability of MDSCs to activate T cells, meaning that PD-L1 upregulation via HIF-1α in MDSCs represses T-cell activity (Noman *et al.*, 2014).

Very importantly, within the TME hypoxia drives immunosuppression by enhancing Treg, MDSCs and TAM function. Indeed, besides directly affecting FOXP3 expression via HIF-1α, tumor-associated hypoxia also attracts Tregs into the TME regulating Treg chemotaxis. For example, Facciabene and colleagues demonstrated in ovarian cancer that hypoxia enhances the secretion of CCL28, thus promoting Treg recruitment (Facciabene *et al.*, 2011).

Of note, Hif-2α has a very important role in cancer development, with some functions partially overlapping the ones of Hif-1α, while others diverging through different regulation of distinct target genes (Keith *et al.*, 2011).

Another line of research that we recently reviewed focuses on the role of hypoxia on B cell function in the TME (described in annex III). In particular, the depletion of GLUT-1 in B cells, a HIF-1α target gene, hampers B cell proliferation and antibody production abilities in cancer, while it is believed that sustained hypoxia promotes the immunosuppressive functions of Bregs (Largeot *et al.*, 2019).

3.2d Hif-1α as a therapeutic target

The modulation of the HIF pathway with drugs is a promising tool in cancer therapy. In the last years, several studies showed different effects of drugs on HIF pathway, alone or in combination with other compounds, and some of them are now in clinical trials. Available drugs have different approaches in targeting the HIF pathway and prevent its activation: they can affect either its heterodimerization, transcription, translation, stability, target genes, or transcriptional activity. To inhibit HIF heterodimerization, HIF-1α-derived peptides have been developed (Makino *et al.*, 2001), which compete with endogenous HIF-1α to bind to the dimerization partners and co-activators, and result in HIF-1α reduction activity. This can be also mediated by targeting the PAS domains of both HIF-1α and HIF-2α, thanks to antioxidant agents (Gao *et al.*, 2007). Other pathways targeted by drugs are related to *HIF* transcription and translation processes. To inhibit its transcription different compounds are used, such as GL331 (Chang *et al.*, 2003), anthracyclines (Pang *et al.*, 2017) and YC-1, which show specificity for the different HIF isoforms. For example, in macrophages YC-1 is specific for HIF-1, but not for HIF-2 (Strowitzki *et al.*, 2019). Another path to target HIF is by interfering with its stability, using inhibitors that promote HIF degradation. This effect is achieved by disrupting the complex of proteins that interact with HIF-1α and stabilize it, as the HSP90/HDAC6 complex (Kovacs *et al.*, 2005). This complex can be targeted using different histone deacetylase (HDAC) inhibitors, as MPT0G157 (Huang *et al.*, 2015).

New molecules used to target HIF also include hypoxia-activated prodrugs (HAPs) (Wilson and Hay, 2011), which are only active in hypoxic cells and are able to induce cell death in a selective manner. Among those, TH-302 is the most advanced HAP, as it is currently in phase III clinical trial for patients with pancreatic cancer and sarcoma (Borad *et al.*, 2015; Chawla *et al.*, 2014).

3.3 IL-27 AND ITS PLEIOTROPIC EFFECTS

3.3a Structure and function of IL-27

IL-27 is a heterodimeric cytokine belonging to the IL-12 family, which includes IL-12, IL-27, IL-35, and IL-39. It is composed by two subunits, Epstein-Barr virus–induced gene 3 (**EBI3**) **and p28** (Pflanz *et al.*, 2002). The combination of different subunits produces different cytokines, for example EBI3 can also dimerize with another subunit, p35, to form IL-35, an immunosuppressive cytokine mainly released by Tregs (Kourko *et al.*, 2019).

The major producers of IL-27 are activated APCs, in particular DCs, monocytes, and macrophages, but B cells can also release this cytokine. IL-27 production is triggered by the activation of Toll-Like Receptors (TLR) through the binding of different agonists, including lipopolysaccharides (LPS) and CpG (Guzzo *et al.*, 2012; Povroznik and Robinson, 2020). LPS promotes the expression of IL-27, in

particular the p28 subunit, by activating MyD88/NF-κB pathway (Wirtz *et al.*, 2005). This pathway is also activated by the IFN-γ secreted by T and NK cells, which in APCs promotes the expression of IFN-γ regulatory factors (IRFs) that enhance IL-27 production (Zhang *et al.*, 2010). In addition, p28 expression is enhanced by IFN-α/IFN-β through IRF1 activation and STAT1/STAT2/IRF9 recruitment (Molle *et al.*, 2007a).

The receptor of IL-27 is also heterodimeric and includes glycoprotein 130 (**gp130**) **and** Interleukin 27 Receptor Subunit Alpha (**IL-27Rα**, also named WSX-1) subunits (Pflanz *et al.*, 2004). Since the majority of immune cells express gp130, the specificity of IL-27 binding depends on the co-expression with WSX-1 (Villarino *et al.*, 2005). Both subunits are necessary for activating the JAK/STAT pathway, in particular STAT1 and STAT3 which are the most important mediators of signal transduction upon IL-27 binding (Pflanz *et al.*, 2004).

IL-27 mainly affects T cells, and IL-27Rα expression is high in effector T cells, memory T cells and Tregs, while it is low in naïve T cells. NK cells also express high levels of IL-27 receptor (Morita *et al.*, 2021). In $CD4^+$ T cells, IL-27 has mainly a pro-inflammatory role and is considered one of the most important inflammatory mediator for Th1 differentiation and IFN-γ production. In Th1 cells, IL-27 promotes T-bet and IL-12Rβ2 expression, which are necessary for Th1 differentiation (Lucas *et al.*, 2003). In this context, WSX-$1^{-/-}$ mice were more prone to major infections and this was correlating with a decreased IFN-γ production in Th1 cells (Larousserie *et al.*, 2004). Nonetheless, a recent paper demonstrated that IL-27 acts as an immunoregulatory cytokine that suppresses inflammation in Th cells by promoting IL-10 expression in Th subsets (Zhang *et al.*, 2020b).

In $CD8^+$ T cells, IL-27 enhances the function of CTL cells via IFN-γ upregulation (Wang *et al.*, 2017) and induces GzmB and perforin production in a STAT1-dependent manner (Morishima *et al.*, 2005a). In addition, IL-27 is used as an adjuvant during vaccination because it promotes the expansion of antigen-specific $CD8^+$ T cells. (Kilgore *et al.*, 2020). Liu and colleagues also demonstrated *in vivo* that IL-27 promotes Stem cell antigen-1 (Sca-1) expression, hence favouring $CD8^+$ Tmem development (Liu *et al.*, 2017).

Of note, IL-27 also enhances B cell growth and survival, and IL-27Rα is upregulated only in naïve and memory B cells, as GC B cells do not express it (Larousserie *et al.*, 2006). In mouse spleens, IL-27 favours Ig class switching of B cells by promoting STAT1/T-bet pathway independently of IFN-γ (Yoshimoto *et al.*, 2004).

However, IL-27 also demonstrates anti-inflammatory and immune inhibitory activities, especially regarding the inhibition of Th2 and Th17 T-cell subsets. Consistently, IL-27 impedes Th17 cell development in several ways, including the inhibition of IL-6, while promoting the production of IL-

17 (Liu and Rohowsky-Kochan, 2011). IL-2 production in $CD4^+$ Tconv is also inhibited by IL-27, mainly by inducing Suppressor Of Cytokine Signaling 3 (SOCS3), thus limiting T-cell responses (Owaki *et al.*, 2006). In addition, IL-27 promotes the development of immune-regulatory Tr1 cells (Chihara *et al.*, 2016).

3.3b Role of IL-27 in cancer development

IL-27 has a complex effect on the anti-tumor immune response, and during the last decade, it was described having both pro- and anti-tumoral roles. This dichotomy may be explained by the diverse functions that IL-27 displays in the immune response but also by the different technical approaches used both *in vivo* and *in vitro* to manipulate IL-27 expression. Indeed, in order to deplete IL-27 *in vivo*, different models were used, such as mice deficient in a receptor subunit (e.g. IL-27R$\alpha^{-/-}$ mice) or mice lacking one of the cytokine subunit, EBI3, or p28 ($EBI3^{-/-}$ or $p28^{-/-}$ mice). Of note, each model recapitulates IL-27 depletion, but other cytokines are also affected, in particular the ones sharing the same subunits or the same receptor. Due to the complexity and peculiarity of each tumor, IL-27 might have opposite roles according to the tumor type and composition of the TME.

IL-27 exerts its anti-tumoral role by inhibiting cancer cells, or indirectly by activating several immune cells. For instance, IL-27 inhibits the proliferation of murine and human melanoma cells through a STAT1-dependent mechanism (Yoshimoto *et al.*, 2008). IL-27 also directly causes cancer cell death in prostate tumor, ovarian cancer and multiple myeloma (Cocco *et al.*, 2010; Di Carlo *et al.*, 2014). In line with an anti-tumor role, IL-27 mRNA expression decreases in CLL cells isolated from leukemic patients compared to HC. (Manouchehri-Doulabi *et al.*, 2020).

In T cells, IL-27 promotes survival and cytotoxic function of $CD8^+$ T cells, thus favouring the anti-tumor immune response (Liu *et al.*, 2013a; Salcedo *et al.*, 2004). In addition, IL-27 enhances the production of IFN-γ, perforin, and GzmB via STAT1/T-bet upregulation (Morishima *et al.*, 2005a). Very importantly, by injecting IL-27-overexpressing GBM and colon cancer cells in mice (Hisada *et al.*, 2004; Salcedo *et al.*, 2004), they lose their tumorigenic ability. Some mice were able to completely eliminate IL-27-expressing tumor cells while developing CTL-mediated immunity to tumor antigens and IFN-γ production in both models. A recent study on melanoma patients revealed that high EBI3 expression correlates with longer OS and a favourable $CD8^+$ TILs profile, suggesting the potential use EBI3 as a novel biomarker (Yonekura, 2022). In addition, $EBI3^{-/-}$ mice have enhanced melanoma growth compared to WT mice that correlates with impaired antitumor T-cell responses (Liu *et al.*, 2015b).

The anti-tumor effect of IL-27 might also be due to its role in $CD4^+$ T cells. Since IL-27 is involved in the differentiation of Th1 and Th2 cells, it is able to shift the $CD4^+$ T-cell development towards Th1 cells, promoting the anti-tumor activity of this subpopulation (Kourko *et al.*, 2019). In addition, IL-27 affects Treg development and function (Huber *et al.*, 2008). By overexpressing IL-27 *in vivo* via a recombinant vector, Zhu *et al.* showed that IL-27 inhibits Treg proliferation (Zhu *et al.*, 2018).

Taken together, these studies highlight the role of IL-27 as an anti-tumor cytokine able to promote CTL survival, proliferation and differentiation into memory effector T cells. In addition, IL-27 promotes anti-tumor immune responses mediated by Th1 cells, and inhibits Treg development.

For these reason, IL-27 has a therapeutic potential in cancer immunotherapy, since its activity mainly promotes Th1 and CTL antitumor responses, which lead to tumor regression. In addition, IL-27 promotes NK cell cytotoxic activity toward cancer cells (Nicholson *et al.*, 2019), and this evidence is supported by several studies in different cancer settings (Cocco *et al.*, 2012; Oniki *et al.*, 2006), including CLL (Hemati *et al.*, 2020). Indeed, NK cells isolated from CLL patients and stimulated *ex vivo* with IL-27 exhibited enhanced cytotoxic activity compared to untreated cells (Hemati *et al.*, 2020).

Nonetheless, different studies also demonstrated the pro-tumoral role of IL-27. Indeed, tumor cells can secrete IL-27 and an accumulation of this cytokine correlates with advanced gastropharingeal cancer (Diakowska *et al.*, 2013) and melanoma (Gonin *et al.*, 2013). In addition, in $EBI3^{-/-}$ and IL-$27R\alpha^{-/-}$ mice it was demonstrated that IL-27 depletion affects Treg activity and CD39 production and results in decreased tumor growth, suggesting a role of IL-27 in promoting Treg immunosuppressive function. By injecting melanoma cells in IL-$27R\alpha^{-/-}$ and WT mice, Chihara and colleagues demonstrated with single cell (sc)RNA-seq of CD8+ TILs that the expression of TIM-3, LAG-3, and TIGIT was reduced in IL-27R-deficient mice. In addition, the same group demonstrated that IL-27 induces a co-inhibitory gene program in $CD8^+$ and $CD4^+$ TILS in melanoma (Chihara *et al.*, 2018).

Beyond the pleiotropic effect of this cytokines, it is important to underline that the discrepancies between different studies are also due to the differences in the models, in the experimental settings, together with the intrinsic differences in tumors and in the composition of the TME.

Scope and aims

The central insight underlying this PhD project consists of the notion that Chronic Lymphocytic Leukemia (CLL) represents a microenvironment-dependent disease, in which a complex cross-talk between CLL cells, immune cells and cytokines present in the tumor microenvironment (TME) is crucial for CLL progression.

Within the TME, regulatory T cells (Tregs) represent a subtype of $CD4^+$ T cells with immunosuppressive abilities, causing the evasion of cancer cells from the immune system and having a pro-tumoral role in CLL and other malignancies (Goral *et al.*, 2022; Kim *et al.*, 2020). Moreover, in a study from our group performed on a pre-clinical model of CLL, we described an increase in the percentage of Tregs with an enhanced immunosuppressive and activated phenotype compared to Tregs from non-leukemic animals (Wierz *et al.*, 2018). Interestingly, $TIGIT^+$ Tregs are more immunosuppressive than their $TIGIT^-$ Treg counterparts and express higher levels of several transcription factors, including AHR and HIF-1α (Joller et al., 2014), both involved in the cellular response to microenvironment-mediated stimuli.

In this context, in a first part, the aim of the PhD project is to investigate the role of these two transcription factors, AHR and HIF-1α, in the suppressive ability of Tregs during CLL development. For this purpose, we used the most validated murine model to mimic this disease (*Eμ-TCL1* mice) in control (*Foxp3*$^{YFP/CRE}$) and conditional knock out mice (*Foxp3*$^{YFP/CRE}$*Ahr*$^{fx/fx}$ and *Foxp3*$^{YFP/CRE}$*Hif1α*$^{fx/fx}$), which lack either AHR or HIF-1α only in Tregs. AHR and HIF-1α are both involved in the metabolic response to microenvironment-mediated stimuli during cancer development (Anderson, 2020; Roy *et al.*, 2020), regulate immune checkpoint expression in immune cells and cancer cells (Hu *et al.*, 2021; Liu *et al.*, 2018), and have fundamental roles in CLL progression (Sadik *et al.*, 2020; Valsecchi *et al.*, 2016). In this scenario, the initial hypothesis underlying this project was that these two transcription factors (TFs) also regulate the suppressive function of Tregs during CLL development, and that their absence impacts on the phenotype, immunosuppressive ability and metabolic behavior of Tregs, unravelling their potential as therapeutic targets during CLL progression.

The second part of this project focused on the study of Interleukin 27 (IL-27) in the progression of CLL. IL-27 is a heterodimeric cytokine composed of two subunits: IL-27p28 (P28) and Epstein-Barr-virus-induced molecule 3 (EBI3) (Yoshida and Hunter, 2015), produced by different cells of the TME (Kourko *et al.*, 2019). IL-27 has recently gained considerable therapeutic attention, but its effects reportedly differ among malignancies, as it is described as a cytokine with pleiotropic functions in tuning the anti-tumor immune response (Beizavi *et al.*, 2021). We then wanted to test the effect of

this cytokine during CLL development and its impact on anti-tumor immune response. To this aim, we used *Ebi3*$^{-/-}$ transgenic mice, which lack the EBI3 subunit of IL-27. We investigated the role of this cytokine during CLL progression in several murine models and experimental settings. We also wanted to identify the main cellular target of IL-27 among the different cells composing the TME and to test the role of this cytokine on the functionality of the target cells. Another fundamental aim of this project was to analyze the concentration of this cytokine in leukemic mice and CLL patients, with the long-term goal of establishing this cytokine as a potential immunotherapeutic agent in CLL.

Experimental data

Part I - Microenvironment-Regulated Transcriptions Factors AHR and HIF-1α Expression in Regulatory T cells promotes Chronic Lymphocytic Leukemia Progression by impairing $CD8^+$ T-cell-mediated Anti-Tumor Immunity

Preface

Different immune cells compose the CLL-TME and some of them have a pro-tumoral role throughout tumor development. Among those, Tregs represent the T-cell subtype involved in suppressing the anti-tumor immune response and promoting tumor development. For this reason, understanding the mechanisms that govern Treg-immunosuppressive functions is fundamental for developing new therapeutic strategies able to inhibit intra-tumoral Tregs and restore a functional anti-tumor immunity.

It was demonstrated that a Treg subset expressing the immune checkpoint (IC) TIGIT showed enhanced immunosuppressive abilities towards $CD4^+$ T cells, both in mice and humans (Joller et al., 2014). Among the different genes overexpressed by murine $TIGIT^+$ Tregs, the transcription factors (TF) Ahr and Hif1a were among the most upregulated ones. Since these two TFs are activated by microenvironment dependent stimuli, we wanted to investigate whether AHR and HIF-1α were involved in maintaining the suppressive phenotype and functions of Tregs during CLL development. AHR and HIF-1α are becoming of great importance in the field of oncoimmunology and have an active role in cancer progression (Balamurugan, 2016; Wang et al., 2020b). Indeed, both TFs are overexpressed and/or chronically active in many tumors, including CLL, DLBCL, T-cell leukemias and some solid tumors. Since promising results were obtained in preclinical models, some clinical trials are evaluating the therapeutic efficacy of AHR or HIF-1α inhibition during cancer development (NCT04999202, NCT04069026, NCT04200963). For these reasons, the main goal of this project was to investigate the role of AHR and HIF-1α in the suppressive abilities of Tregs during CLL development, understanding whether their absence affects the phenotype, immunosuppressive ability and metabolic behavior of Tregs.

State of publication:

The manuscript is in preparation and final experiments are in progress before submission.

For this part of the project, the data represented in the figures were obtained by myself and others as follows:

- Figure 8: Data shown in panels A-E were obtained by Dr. Marina Wierz, former PhD candidate of the Tumor Stroma Interaction (TSI) group at the Luxembourg Institute of Health (LIH). I contributed to Panel F of figure 8.
- Figure 9, 10, 11: I designed and performed the experiments together with Dr. Marina Wierz, and we equally contributed to all the panels of these figures.
- Figure 12: I performed the experiments shown in all the panels together with the help of Iria Fernandez Botana.
- Figure 13: Dr. Agnieszka Goral from the University of Warsaw performed all the experiments shown in this figure.
- Figure 14: I performed the experiments shown in these panels together with Susanne Gonder, PhD candidate of the TSI group at LIH.
- Figure 15: I performed the experiments shown in in panels A-F together with Marina Wierz, while I independently executed the experiments shown in panels G-I.
- Figures 16, 17: the experiments shown in these figures were performed together with Tea Mancuso, master student who was working on this project from January 2020 to September 2020. She produced independently the data shown in panel B of figure 17, and we performed together the experiments of the other panels.
- Figure 18: I contributed to the protocol design and part of the experiments. The analysis of the seahorse experiments (panels B-F) and the analysis of the glutamine tracing experiment (panels G-H) were performed by Mohaned Benzarti, PhD student in the Cancer Metabolism group at LIH.

Material and methods

Animal experiments

All experiments involving laboratory animals were performed in a pathogen-free animal facility with the approval of the Luxembourg Ministry for Agriculture. Eμ-TCL1 mice were kindly provided by Pr. Carlo Croce and Pr. John Byrd (OSU, USA), and obtained from Dr M. Seiffert (DKFZ, Germany). The protocol number for all animal experiments conducted at the Luxembourg Institute of Health is LECR-2018-02. *Foxp3*$^{YFP/Cre}$ mice, *Ahr*$^{fx/fx}$ and *Hif1a*$^{fx/fx}$ mice were purchased form The Jackson Laboratory (MA, USA) and C57BL/6 (WT) mice were from Janviers Labs (France). *Foxp3*$^{YFP/Cre}$ *Ahr*$^{fx/fx}$ and *Foxp3*$^{YFP/Cre}$ *Hif1a*$^{fx/fx}$ conditional knock-out (cKO) mice were obtained by breeding in-house *Foxp3*$^{YFP/Cre}$ mice with *Ahr*$^{fx/fx}$ or *Hif1a*$^{fx/fx}$mice, as described in **Fig.1A**. Experiments with *Rag2*$^{-/-}$ immunodeficient mice were performed in collaboration at the Medical University of Warsaw (Dr. Angelika Muchowicz group).

For experiments with adoptive transfer (AT) of CLL cells, 10x10^6 splenocytes isolated from diseased Eμ-TCL1 mice were injected intraperitoneally (i.p.) in 100μL of DMEM without phenol red. CLL development was monitored by weekly bleeding to determine the percentage of CD5$^+$CD19$^+$ CLL cells in PBMCs by flow cytometry (FC) on a Cytoflex (Beckman Coulter, USA) with CD19-APC and CD5-PE (Biolegend, San Diego, CA, USA) antibodies. For AT in *Rag2*$^{-/-}$ mice, 8x10^6 splenocytes isolated from *Foxp3*$^{YFP/Cre}$, *Foxp3*$^{YFP/Cre}$*Ahr*$^{fx/fx}$ and *Foxp3*$^{YFP/Cre}$*Hif1a*$^{fx/fx}$ were injected into *Rag2*$^{-/-}$ hosts followed by intravenous (i.v.) AT of 5x10^6 CD19$^+$ cells CLL isolated from diseased Eμ-TCL1 mice one day later.

For AHR and HIF-1α *in vivo* inhibition experiments, WT mice were i.p. injected with 10x10^6 splenocytes isolated from diseased Eμ-TCL1 mice. When the frequency of CLL cells in PBMCs reached 5% to 10%, recipient mice were randomized and daily treated with either AHR antagonist (CH-223191, Sigma-Aldrich, Burlington, MA, USA, 10mg/kg per mouse by oral gavage) or HIF-1α dimerization inhibitor (Acriflavine, Sigma-Aldrich, Burlington, MA, USA, 2mg/kg per mouse by i.p. injection).

For melanoma *in vivo* experiment, 2x10^5 B16F10 melanoma cells were subcutaneously (s.c.) injected into the right flank of cKO and control mice. Tumor size was measured in three dimensions using a caliper.

For *in vivo* depletion of CD8$^+$ T cells, recipient mice were injected with 200μg (at day -2 and 0) and 100μg (from day 3 and then every 3 days) of either blocking ab against CD8 (InVivoMAb anti-mouse CD8α, Bioxcell) or isotype control (InVivoMAb polyclonal Armenian hamster IgG, Bioxcell). At day 0, CLL cells (10x10^6/mouse) were injected i.p. in cKO and control mice. All animals used in the experiments were aged between six to ten weeks. Both male and female mice were used, and

age/gender was matched within the same experiment. No impact nor variation was detected in the results because of sex difference.

Validation of mouse models at genomic and transcriptomic levels.

Genomic DNA was extracted from ear snips using Mouse Direct PCR Kit (Biotool) following the manufacturer's instructions. The specific primer sequences were:

Foxp3^{WT}: F: 5'-CCTAGCCCCTAGTTCCAACC-3'; R: 5'-AAGGTTCCAGTGCTGTTGCT-3', product of 408bp;

Foxp3^{Cre}: F: 5'-AGGATGTGAGGGACTACCTCCTGTA-3'; R: 5'-TCCTTCACTCTGATTCTGGCAATT T-3', product of 511 bp;

Ahr: F1: 5'-GTCACTCAGCATTACACTTTCTA-3' F2: 5'-CAGTGGGAATAAGGCAAGAGTGA-3'; R: 5'-GGTACAAGTGCACATGCCTGC-3'. These primers allowed the detection of wild-type (106bp), floxed (140bp), and excised (180bp) alleles.

Hif1a: F: 5'-GGTGCTGGTGTCCAAAATGTAG-3'; R: 5'- ATGGGTCTAGAGAGATAGCTCCACA-3'. These primers allowed the detection of wild-type (212bp) and floxed (232bp) alleles.

Detailed methods are available at (Gonder *et al.*, 2021). Briefly, *Foxp3* and *Ahr* amplification were performed with the following program: 10 cycles (with a decrease of 0.5°C per cycle) of 94°C for 2min and 20s, 65°C for 15s, and 68°C for 10s, 28 cycles of 94°C for 15s, 60°C for 15s, and 72°C for 10s. Upon amplification, PCR products were run on a 3% agarose gel with SYBR™ Safe DNA Gel Stain (ThermoFisher, Waltham, MA, USA) and analysed by Image Quant Las 4000 (GE Healthcare, Chicago, IL, USA).

For *Hif1a* amplification, genomic DNA was isolated using NucleoSpin Tissue Mini kit for DNA from cells and tissue (Macherey-Nagel, Düren, Germany) following the manufacturer's instructions. Taqman Real-time PCR was performed using TaqMan copy number assay Mm00375032_cn with the TaqMan™ Copy Number Reference Assay, mouse, Tfrc (Thermo Scientific, Waltham, MA, USA). The qPCR was run on the QuantStudio™ 3 or 5 (Applied Biosystems, Waltham, MA, USA) with the following program: 50 °C for 2min, 95°C for 10min, 40 cycles of 95°C for 15s, and 60°C for 1min.

RNA from sorted regulatory T cells (Tregs) and conventional T cells (Tconv) was extracted through Nucleozol reagent and the NucleoSpin® RNA Set for NucleoZOL (Macherey-Nagel, Düren, Germany) and quantified by Nanophotometer N60 (Implen, München, Germany). The complementary DNA was produced from 500ng of RNA through FastGene Scriptase II cDNA 5x ReadyMix (Nippon Genetics, Düren, Germany) according to the manufacturer's instructions. Quantitative PCRs were run using Takyon for SYBR Assay Low Rox or Takyon Low Rox Probe 2X mastermix (Eurogentec, Seraing, Belgium). The following primers were used:

Ahr: F: 5'-AGCCGGTGCAGAAAACAGTAA-3' and R: 5'-AGGCGGTCTAACTCTGTGTTC-3';

Hif1a: F: 5'-CCACAGGACAGTACAGGATG-3' and R: 5'-TCAAGTCGTGCTGAATAATACC-3';

Actb: F: 5'-ATCCACACAGAGTACTTGCGCTCA-3' and R: 5'-GCACCACACCTTCTACAATGAGCTG -3'.
In order to quantify the gene expression relative to the hkg *Actb,* comparative Ct method was used.

Cell isolation from spleen and thymus

In order to obtain a single cell suspension, spleens and thymus were isolated from mice upon euthanasia, disocciated in PBS with a syringe plunger and filtered with a 100µm cell strainer. To deplete red blood cells, splenocytes were then lysed with ACK Lysing Buffer (Thermofisher Scientific, Waltham, MA, USA) according to manufacturer's instructions. $CD4^+$ and $CD8^+$ T cells were purified from splenocytes by negative selection using the MojoSort™ Mouse CD4 or CD8 T-cell isolation Kit (Biolegend, San Diego, CA, USA) following the manufacturer's instructions. The purity of isolated cells was verified by FC and isolation efficiency was above 90% for the population of interest.

Processing B16F10 tumors

Tumor mass was isolated from the flank of recipient mice upon euthanasia. Tumors were chopped into small pieces, gently dissociated with a syringe plunger in PBS and passed through a 100µm cell strainer to obtain a suspension of single cells. Immune cells were separated from tumor cells using Percoll® reagent (Sigma-Aldrich, Burlington, MA, USA). Tumor cells were resuspended in 80% Percoll® solution in PBS and 40% Percoll® solution of PBS was gently overlaid on top. Upon centrifugation (16min, 2000g, RT), interphase was collected, $CD4^+$ T cells were isolated via magnetic beads sorting (as previously described) and stained for FC analysis.

Flow cytometry and cell sorting

Staining of extracellular proteins was performed in 100µl of MACS buffer (Miltenyi Biotec) for 30min on ice in the dark. Stained cells were then washed with PBS and live/dead staining was performed using Zombie Fixable Viability Kit (Biolegend, San Diego, CA, USA) according to manufacturer's instructions. For intracellular staining, surface stained cells were fixed and permeabilized with the eBioscience™ Foxp3/Transcription Factor Staining Buffer Set (ThermoFisher Scientific) following the manufacturer's instructions, and were subsequently stained for intracellular antigens. Acquisition was performed on a BD FACSAria™ III Cell Sorter (BD Biosciences) or NovoCyte Quanteon Flow Cytometer (Agilent).

Peripheral blood was directly stained for extracellular antigens for 30min on ice in the dark, red blood cells were then lysed using RBC Lysis/Fixation Solution (Biolegend, San Diego, CA, USA) for 15min in the dark at RT. After washing twice with PBS, samples were acquired and analyzed with CytoFLEX analyzer (Beckman Coulter).

Cell sorting was performed on stained cells using BD FACSAria™ III Cell Sorter (BD Biosciences). Tregs and Tconv were isolated based on YFP expression from $CD4^+$ T cells obtained from *Foxp3*$^{YFP/Cre}$, *Foxp3*$^{YFP/Cre}$*Ahr*$^{fx/fx}$ and *Foxp3*$^{YFP/Cre}$*Hif1a*$^{fx/fx}$ mice.

***Ex vivo* cell culture**

To analyze cytokine release by T cells, splenocytes were isolated from cKO and control mice and cultured *ex vivo* in RPMI medium supplemented with 10% FBS, 1% penicillin, streptomycin, 100nM Phorbol 12-myristate 13-acetate (PMA, Sigma-Aldrich, Burlington, MA, USA), 1µM ionomycin (Sigma-Aldrich, Burlington, MA, USA) and 5µg/ml (1X) Brefeldin A Solution (Biolegend). Cells were incubated for 4h at 1x10^6cells/100µl at 37 °C and 5% CO_2 and subsequently stained for FC analysis.

To perform iTreg polarization, splenocytes were obtained from the different models and $CD4^+$ T cells were sorted by negative selection using Mojosort™ Mouse CD4 T-cell isolation Kit (Biolegend). $CD4^+$ T cells were then cultured in RPMI completed with 10% FBS, 50µM 2-β-mercaptoethanol, 1% penicillin, streptomycin, 100ng/ml Recombinant Human IL-2 (carrier-free) (Biolegend), 20ng/ml Recombinant Mouse TGF-β1 (carrier-free) (Biolegend) and 1nM Retinoic Acid (Sigma-Aldrich, Burlington, MA, USA). Prior to cell culture, 24-well plates were coated with 10µg/ml purified anti-mouse CD3ε antibody (Biolegend) in PBS for 3 hours at 37 °C and 5% CO_2. $CD4^+$ T cells were cultured in pre-coated 24-well plates at 1 x10^6 cells/ml in each well for 4 days and stained for FC analysis at different time points.

For suppression assay experiments, iTreg cells were fed with fresh medium after 72h. After 4 days of polarization, iTregs were harvested and a portion was analyzed by FC to verify polarization efficiency. At the same time, $CD8^+$ T cells were isolated from splenocytes of control *Foxp3*$^{YFP/Cre}$ mice using Mojosort™ Mouse CD8 T-cell isolation Kit (Biolegend) and stained with Tag-it Violet™ Proliferation and Cell Tracking Dye (Biolegend) according to manufacturer's instructions. Stained $CD8^+$ T cells were co-cultured with either control or *Ahr/Hif1a*-KO iTregs at different ratios (indicated in **Fig.10B-C**) in fresh RPMI medium supplemented with 10% FBS, 50µM 2-β-mercaptoethanol, 1% penicillin, streptomycin, IL-2 (10ng/ml), purified anti-CD3 antibody (1µg/ml) and purified anti-mouse CD28 antibody (1µg/ml, Biolegend) for 3 days at 37 °C and 5% CO_2. Subsequently, cells were harvested, stained, and analyzed by FC.

For Seahorse and glutamine tracing experiments, polarized iTregs were harvested after 4 days and a portion was analyzed by FC to verify polarization efficiency. Dead cells were removed from

harvested iTregs to avoid background signals using MojoSort™ Mouse Dead Cell Removal Kit (Biolegend) according to manufacturer's instructions.

Oxygen consumption rate measurement

As previously published (Gargiulo *et al.*, 2022b), to measure the oxygen consumption rate (OCR), we used Seahorse XFe96 Bioanalyser (Agilent) for polarized Tregs isolated from control or cKO mice following manufacturer's instructions. XF Base Assay medium (Agilent) was used to wash cells, and the same medium with 10mM glucose, 1mM sodium pyruvate and 2mM L-glutamine (Gibco), pH 7.4 at 37 °C was used to subsequently seed cells in Seahorse cell culture plates, which were previously coated with Cell-Tak (Corning). Plating concentration of cells was 3.5×10^5cells/well. Plates were then centrifuged for 5min at 300g, RT without breaks. For oxidative stress assay, the drugs Oligomycin (1µM), CCCP (4µM), Rotenone (1µM) and Antimycin A (1µM) (all from Agilent kit) were injected into each well.

Glutamine tracing and metabolites extraction

Stable isotope tracing experiment with [U-^{13}C]-glutamine tracer (Cambridge isotope Laboratories, CLM-1822) was performed as previously described (Gargiulo *et al.*, 2022b). RPMI 1640 medium for SILAC was supplemented with 11.1mM [U-^{13}C]-glutamine, 2mM glucose, 1.15mM arginine, 0.219mM lysine, 10% Fetal Bovine Serum (FBS), 1% Penicillin/Streptomycin (P/S), IL-2 (100ng/ml), purified anti-CD3 antibody (1µg/ml) (Biolegend) and purified anti CD28 antibody (1µg/ml) (Biolegend).

$1x10^6$ cells were resuspended in [U-^{13}C]-glutamine medium and cultured in triplicates in 24-well plates for 48h at 37 °C and 5% CO_2. After 2 days, the packed cell volume (PCV) was calculated to determine cell volume and amount. Cells were then collected and metabolites were extracted by centrifugation at 350g for 5min at 4°C followed by the culture medium storage at -80°C. Wells containing only culture medium were used to calculate basal medium, as these wells were analyzed together with the medium collected from the samples. Cell pellets were then washed with cold PBS and 400µl of extraction fluid [acetonitrile/H2OMQ/methanol (ratio, 3:2:5); liquid chromatography–mass spectrometry (LC-MS) grade solvents)] was added to each cell pellet. Cells were incubated for 10min at 4°C while shaking, and samples were then centrifuged for 10min at 16,100g at 4°C. 100µL of supernatant was transferred to an pre-cooled LC-MS glass vial with inserts and stored at -80°C.

LC-MS Measurements

We followed the analytical conditions as previously published (Meiser *et al.*, 2018). Thermo Vanquish Flex Quaternary LC coupled to a Thermo Q Exactive HF mass spectrometer was used to

perform the metabolomics analyses. Chromatography was performed by using SeQuant ZIC-pHILIC 5µm polymer (150 x 2.1mm) column connected to the corresponding SeQuant ZIC-pHILIC Guard (20 x 2.1mm) pre-column. Column temperature was maintained constant at 45°C, flow rate was 0.2ml/min and the mobile phases consisted of 20mmol/L ammonium carbonate in water, pH 9.2 (Eluent A) and Acetonitrile (Eluent B). The specificities of the method are furhter described in (Kiweler *et al.*, 2022). Data acquisition and analysis were performed via Thermo Xcalibur (Version 4.3.73.11; RRID:SCR_014593) and TraceFinder (Version 4.1) as well as previously descrived computing scripts (Meiser *et al.*, 2018).

Results

1. Generation of Treg-specific *Ahr* and *Hif1a* conditional knock out mice.

In order to investigate the impact of AHR and HIF-1α in regulatory T cells (Tregs) *in vivo*, we generated conditional knock (cKO) out mice lacking *Ahr* or *Hif1a* genes exclusively in Tregs by breeding *Foxp3*$^{YFP\text{-}Cre}$ mice with *Ahr*$^{fx/fx}$ or *Hif1a*$^{fx/fx}$ mice, which carry the exon 2 of the two genes flanked by floxed sequences (**Fig.8A**). To validate the depletion of the two genes at genomic and transcriptomic levels, splenocytes were isolated from cKO and control *Foxp3*$^{YFP\text{-}Cre}$ mice and enrichment of CD4^{+} T cells was obtained with magnetic beads. Subsequently, Tregs (YFP^{+}) and conventional T cells (Tconv, YFP^{-}) were purified by FACS sorting, and DNA and RNA were extracted. WT and floxed alleles were genotyped and, as expected, the exon 2 of *Ahr* was excised only in Tregs of *Foxp3*$^{YFP\text{-}Cre}$ *Ahr*$^{fx/fx}$ mice, while the floxed allele was detectable in both Tconv and Tregs of the cKO mice (**Fig.8B**). Moreover, neither floxed nor excised alleles were detectable in the *Foxp3*$^{YFP\text{-}Cre}$ control mice. Looking at the expression of *Ahr* by RT-qPCR, there was extremely low expression of this gene in Tregs of *Foxp3*$^{YFP\text{-}Cre}$ *Ahr*$^{fx/fx}$ mice compared to Tconv and to control mice (**Fig.8C**). Similar results were found when validating the *Foxp3*$^{YFP\text{-}Cre}$ *Hif1α*$^{fx/fx}$ model, that showed no detectable DNA of *Hif1a* exon 2 in Tregs of *Foxp3*$^{YFP\text{-}Cre}$ *Hif1α*$^{fx/fx}$ mice (**Fig.8D**) and very low expression of *Hif1a* in the Tregs of the cKO model as compared to control mice (**Fig.8E**). Once the mouse models were generated, we could observe that cKO mice were viable, fertile, showed no evident autoimmune-related alteration and exhibit a survival comparable to controls (**Fig.8F**), allowing us to use these models for further *in vivo* and *ex vivo* analysis.

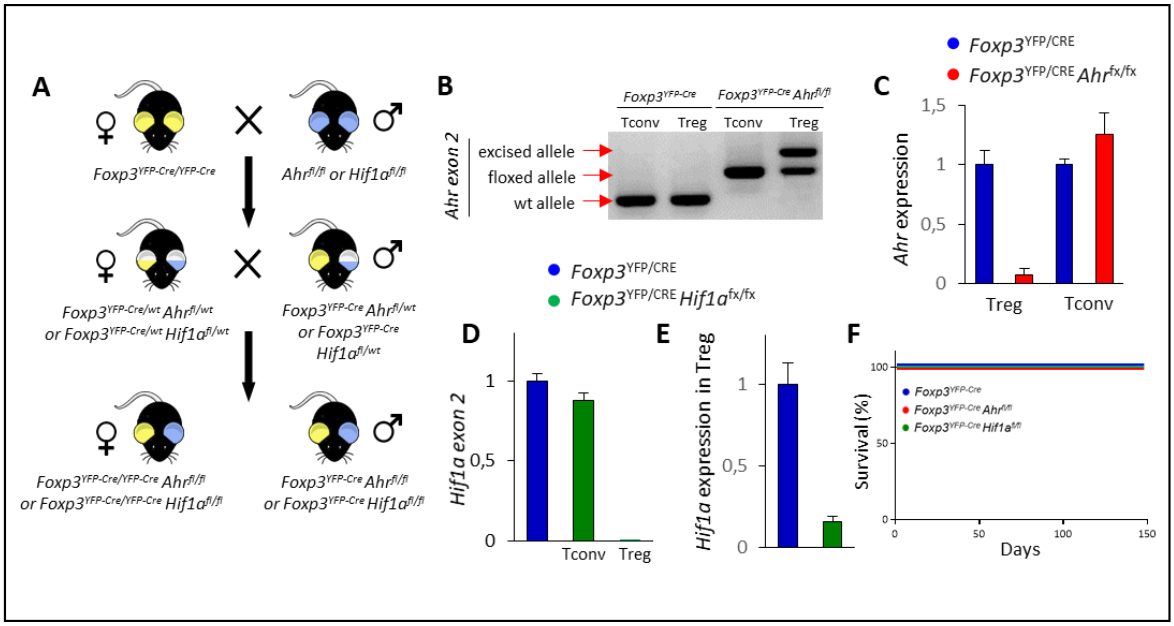

Figure 8: **Generation of Treg-specific *Ahr* and *Hif1a* conditional knock out mice. (A)** Breeding strategy for the generation of the cKO mice. *Foxp3*$^{YFP\text{-}Cre}$ and *Ahr*$^{fx/fx}$ or *Hif1α*$^{fx/fx}$ mice were bred to obtain homozygous females and hemyzygous mice carring floxed sequences in both alleles of the two genes of interest. **(B)**

Representative example for one mouse of the PCR developed to detect the absence of exon 2 of *Ahr* gene on genomic DNA of sorted Tregs obtained from *Foxp3*$^{YFP\text{-}Cre}$ and *Foxp3*$^{YFP\text{-}Cre}$ *Ahr*$^{fx/fx}$ mice. **(C)** Quantification of RNA expression of *Ahr* by RT-qPCR in sorted Tregs obtained from *Foxp3*$^{YFP\text{-}Cre}$ and *Foxp3*$^{YFP\text{-}Cre}$ *Ahr*$^{fx/fx}$ mice (n=3 mice per group). **(D)** qPCR evaluation of the presence of *Hif1a* exon 2 genomic DNA of sorted Tregs obtained from *Foxp3*$^{YFP\text{-}Cre}$ and *Foxp3*$^{YFP\text{-}Cre}$ *Hif1α*$^{fx/fx}$ mice (n=3 mice per group). **(E)** Quantification of RNA expression of *Hifa* by RT-qPCR in sorted Tregs obtained from *Foxp3*$^{YFP\text{-}Cre}$ and *Foxp3*$^{YFP\text{-}Cre}$ *Hif1α*$^{fx/fx}$ mice (n=3 mice per group). **(F)** Survival curve of *Foxp3*$^{YFP\text{-}Cre}$, *Foxp3*$^{YFP\text{-}Cre}$ *Ahr*$^{fx/fx}$ and *Foxp3*$^{YFP\text{-}Cre}$ *Hif1α*$^{fx/fx}$ mice (n=20 per group).

2. *Ahr* and *Hif1a* depletion impacts Treg phenotype while mildly affecting other T cell subpopulations.

In order to investigate the impact of Treg-specific AHR and HIF-1α depletion in different T-cell subpopulations, splenocytes were isolated from cKO and control mice, and then activated *in vitro* to favor cytokine production (**Fig.9A**). As first, we observed that the depletion of both transcription factors (TFs) had a mild impact on the frequency and number of T-cell subpopulations (**Fig.9B-D**). Indeed, a minor increase in Treg frequency was observed in absence of AHR (**Fig.9C**) together with an increase in $CD4^+$ (in particular in Tconv) and $CD8^+$ T-cell number in absence of HIF-1α (**Fig.9D**). Despite the mild differences in Treg percentage and number in the spleen, FOXP3 expression was reduced in Tregs from cKO mice compared to controls (**Fig.9E**), which correlated with a diminution in immunosuppressive markers (CD25 and CD73) in absence of AHR (**Fig.9F**). Very interestingly, AHR depletion caused a significant expansion of TGF-β^+ Tregs without affecting the percentage of IL-10-expressing Tregs (**Fig.9G**), while the expression of the immune chekpoints (IC) TIGIT and CTLA-4 was not affected by AHR and HIF-1α depletion (**Fig.9H**). Since Tregs regulate the activity of $CD4^+$ Tconv and $CD8^+$ T cells, we analyzed the cytokine-producing abilities of Tconv and $CD8^+$ T cells in the cKO mice and observed no differences between the different models (**Fig.9I-J**), demonstrating that lack of AHR and HIF-1α in Tregs does not impact T-cell functionality in a non-tumoral context.

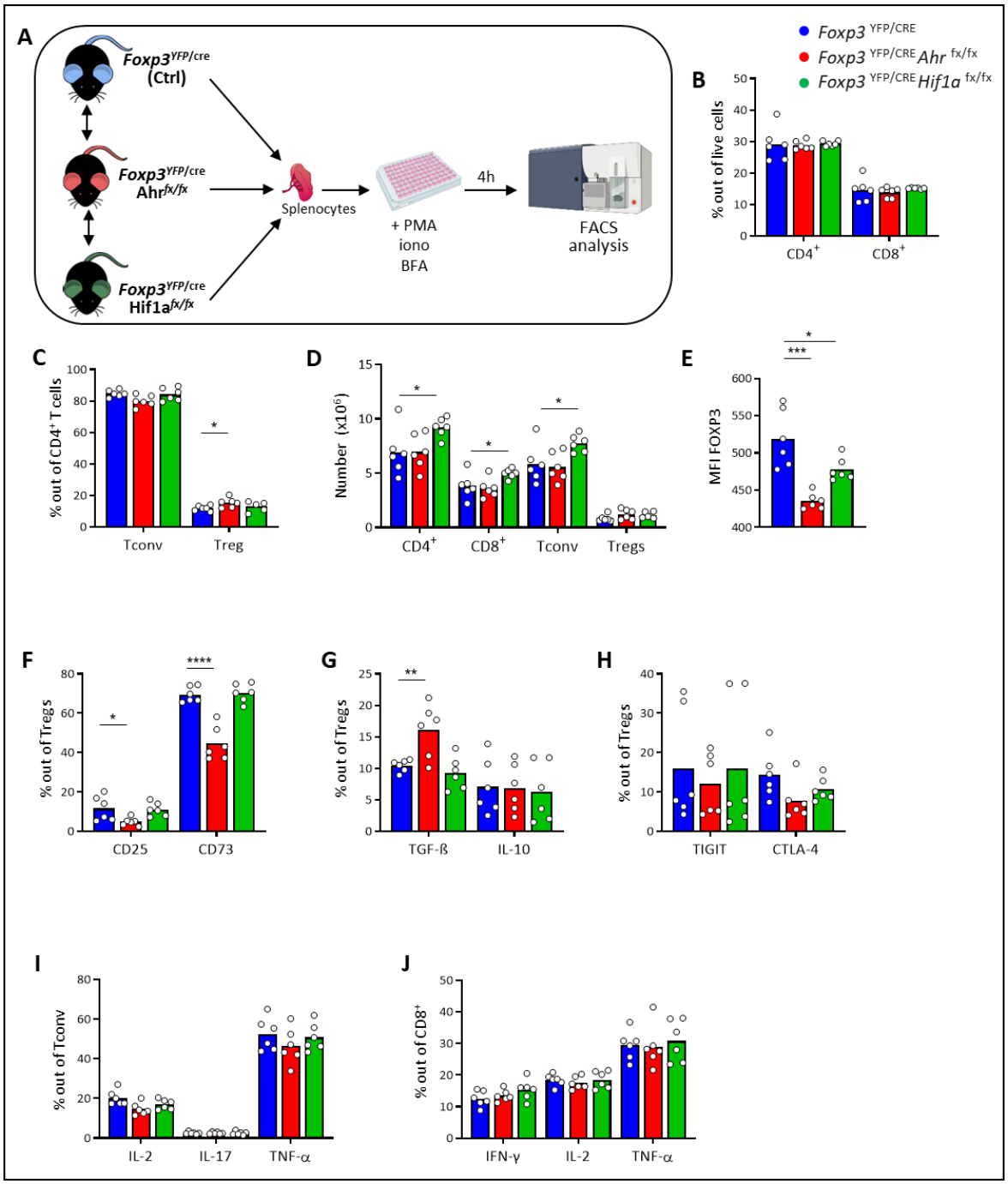

Figure 9: ***Ahr* and *Hif1a* depletion impacts Treg phenotype while mildly affecting other T-cell subpopulations. (A)** Splenocytes were isolated from the three models and *ex vivo* activated for 4 hours before being analyzed by FACS. **(B-J)** FACS analysis of $CD4^+$ and $CD8^+$ T cells upon activation. **(B)** Percentages of $CD4^+$ and $CD8^+$ T cells within live cells and **(C)** frequency of $CD4^+$ Tconv and Tregs in $CD4^+$ global T-cell population. **(D)** Number of cells (in million) of different T-cell subpopulations. **(E)** Expression of FOXP3 in Tregs of the different models. **(F-H)** Frequency of Treg-specific population expressing **(F)** CD25, CD73, **(G)** TGF-β, IL-10, **(H)** TIGIT and CTLA-4. **(I)** Frequency of IL-2, IL-17 and TNF-α –expressing cells in $CD4^+$ Tconv. **(J)** Frequency of IFN-γ, IL-2 and TNF-α-expressing cells in $CD8^+$ T cells. (n=6, * P< .05, ** P< .01, *** P< .001, **** P< .0001, Unpaired T test).

3. *Ahr* and *Hif1a* depletion in Tregs does not affect thymic development of T cells and modestly impacts splenic myeloid cells.

As AHR and HIF-1α are both known to regulate peripheral Treg development and functions in different contexts (Dang *et al.*, 2011; Quintana *et al.*, 2008), we wanted to verify that their depletion in Tregs was not altering the physiological thymic Treg development. For this reason, thymus was isolated from cKO and control mice (**Fig.10A**) and analyzed by flow cytometry. *Ahr* and *Hif1a* depletion in Tregs did not affect the number of thymocytes (**Fig.10B**), nor the frequency and number of Tregs within the thymus (**Fig.10C-D**), suggesting that depletion of these TFs does not alter Treg physiological thymic development. In addition, since different studies highlighted the role of Tregs in affecting myeloid cell activity (Okeke and Uzonna, 2019), we asked whether *Ahr* and *Hif1a* depletion in Tregs had an impact on myeloid cells in the spleen. Spleens were collected from the same mice (**Fig.10A**) and the myeloid compartment was analyzed by flow cytometry (FC). As first, absence of *Ahr* and *Hif1a* did not affect the number of splenocytes (**Fig.10E**). When analyzing the monocytes (gating strategy is depicted in **Fig.10F**), no changes were detectable in the global frequency and number of this population (**Fig.10G-H**), nor in the frequency of patrolling, inflammatory and intermediate monocytes (**Fig.10I**). Nonetheless, *Ahr* and *Hif1a* depletion in Tregs caused a decrease in the number of $Ly6C^{high}$ $CD43^{low}$ inflammatory monocytes compared to controls (**Fig.10J**), as well as intermediate monocytes $Ly6C^{int}$ $CD43^{int}$, which only reached statistical significance for *Ahr* cKO mice. Intermediate monocytes present many features of inflammatory monocytes but do not have patrolling activity (Wolf *et al.*, 2019). Regarding macrophages and DCs present in the spleen (gating strategies are displayed in **Fig.10K and N**), *Ahr* and *Hif1a* depletion in Tregs did not affect their frequency (**Fig.10L and O**) neither their number (**Fig.10M and P**), confirming that lack of the two TFs mildly affects the myeloid cell compartment in the spleen.

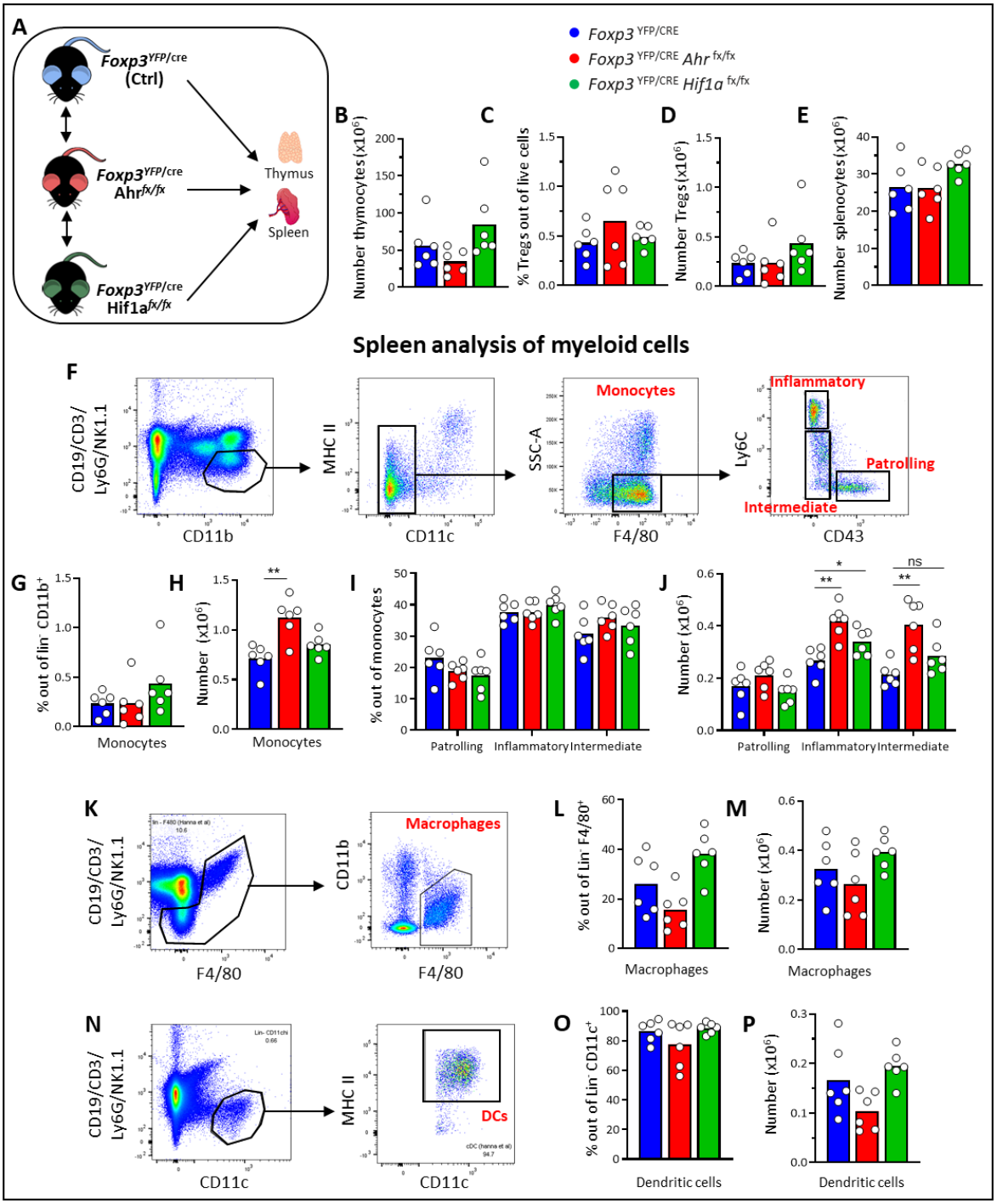

Figure 10: ***Ahr* and *Hif1a* depletion in Tregs does not affect thymic development of T cells and modestly impacts splenic myeloid cells. (A)** Thymus and spleen were isolated from the three models and analyzed by FACS with different antibody panels. **(B)** Number of thymocytes in the three models. **(C-D)** FACS analysis of thymic Tregs. **(C)** Frequency of Tregs in live thymic cells. **(D)** Number of Tregs (in million) in the thymus of the three models. **(E)** Number of splenocytes of cKO and control mice. **(F)** Gating strategy of monocyte analysis. **(G)** Frequency of monocytes in CD19, CD3, Ly6G, NK1.1 (lin)$^-$ CD11b$^+$ cells. **(H)** Number of monocytes. **(I-))** Frequency **(I)** and number **(J)** of indicated subpopulations within monocytes. **(K)** Gating strategy to analyze macrophages. **(L-M)** Frequency **(L)** and number **(M)** of macrophages within lin$^-$ F4/80$^+$ cells. **(N)** Gating strategy for DC analysis. **(O)** Percentage and **(P)** number of DCs in the different groups. (n=6, * P< .05, ** P< .01, Unpaired T test).

4. *Ahr* and *Hif1α* depletion in Tregs delays leukemia development and promotes an anti-tumor T-cell response.

To test the role of AHR and HIF-1α in Tregs during leukemia progression, CLL cells obtained from diseased Eμ-TCL1 mice were adoptively transferred in two independent cohorts of cKO and control mice (**Fig.11A**). To follow the development of CLL in the three models, a weekly bleeding of the recipient mice was performed to detect the presence of circulating leukemic cells ($CD19^+$ $CD5^+$) by FC. In absence of *Ahr* and *Hif1α*, we observed a drastic delay of leukemia outcome (**Fig.11B-C**). In addition, for the second cohort we measured the spleen weight, and cKO mice presented a decrease in this parameter, associated with a decrease in the number of splenocytes compared to controls (**Fig.11E**). In order to decipher the mechanisms by which AHR and HIF-1α pathways in Tregs affect CLL progression, the splenic TME of the recipient mice was analysed by FC. Mice lacking *Ahr* and *Hif1α* in Tregs presented altered $CD4^+$ and $CD8^+$ T-cell frequency (**Fig.11F**), in line with an enhanced anti-tumor immune response compared to their WT counterparts. Surprisingly, there were no differences in the frequency of Tconv and Tregs within $CD4^+$ T-cell population between the different groups (**Fig.11G**), nor in the T-cell numbers (**Fig.11H**). As other T cells, Tregs can be in an activated or resting state (defined as $CD44^{hi}CD62L^{low}$ aTregs or $CD44^{low}CD62L^{hi}$ rTregs, respectively). In line with a decreased immunosuppressive environment in cKO mice, *Ahr* depletion in Tregs caused an expansion in rTregs together with a reduction in aTregs (**Fig.11I**), and the same tendency was observed in *Hif1α* cKO mice. In addition, the frequency of Tregs expressing key immunosuppressive IC, as TIGIT and CTLA-4, was decreased in absence of *Ahr* (**Fig.11J**), while CD25 and CD73 immunosuppressive molecules were not different among the three models (**Fig.11K**). As observed in a non-tumoral context (Fig.9G), *Ahr* depletion caused an increase in TGF-β production also in the leukemic microenvironment (**Fig.11L**), while IL-10 expression did not change among the different mice. When we evaluated the production of key T-cell-related cytokines, we found an enhanced production of IL-17 and TNF-α in Tconv from mice whose Tregs are depleted for *Ahr* and *Hif1α* genes (**Fig.11M**). Interestingly, there were no differences in cytokine production in $CD8^+$ T cells between the models (**Fig.11N**), probably due to the involvement of different molecules (e.g. other cytokines or proteases) that mediate $CD8^+$ T-cell cytotoxic activity in this context. Within the myeloid compartment, there was a shift from patrolling monocytes to inflammatory monocytes in cKO mice (**Fig.11P**), although the frequency of total monocytes was not changing (**Fig.11O**). The frequency of macrophages was not different between controls and cKO mice (**Fig.11Q**), however there was an enhanced frequency of DCs when *Ahr* and *Hif1α* were depleted in Tregs (**Fig.11R**), in line with the effect that Tregs directly exert towards DCs to inhibit their activation. Surprisingly, despite the differences in tumor load, there were no differences in the cell number of myeloid cell subpopulations (**Fig.11S**). All together, these results show that AHR and HIF-1α depletion impairs

Treg immunosuppressive ability, leading to a drastic delay in CLL development in cKO mice, decreased IC expression in Tregs, increased cytokine production in Tconv and enhanced pro-inflammatory TME. We concluded that this effect was due to an impaired suppressive ability of AHR- and HIF-1α KO Tregs in inhibiting anti-tumor T cells, which results in a more efficient T-cell-mediated immune response against CLL cells.

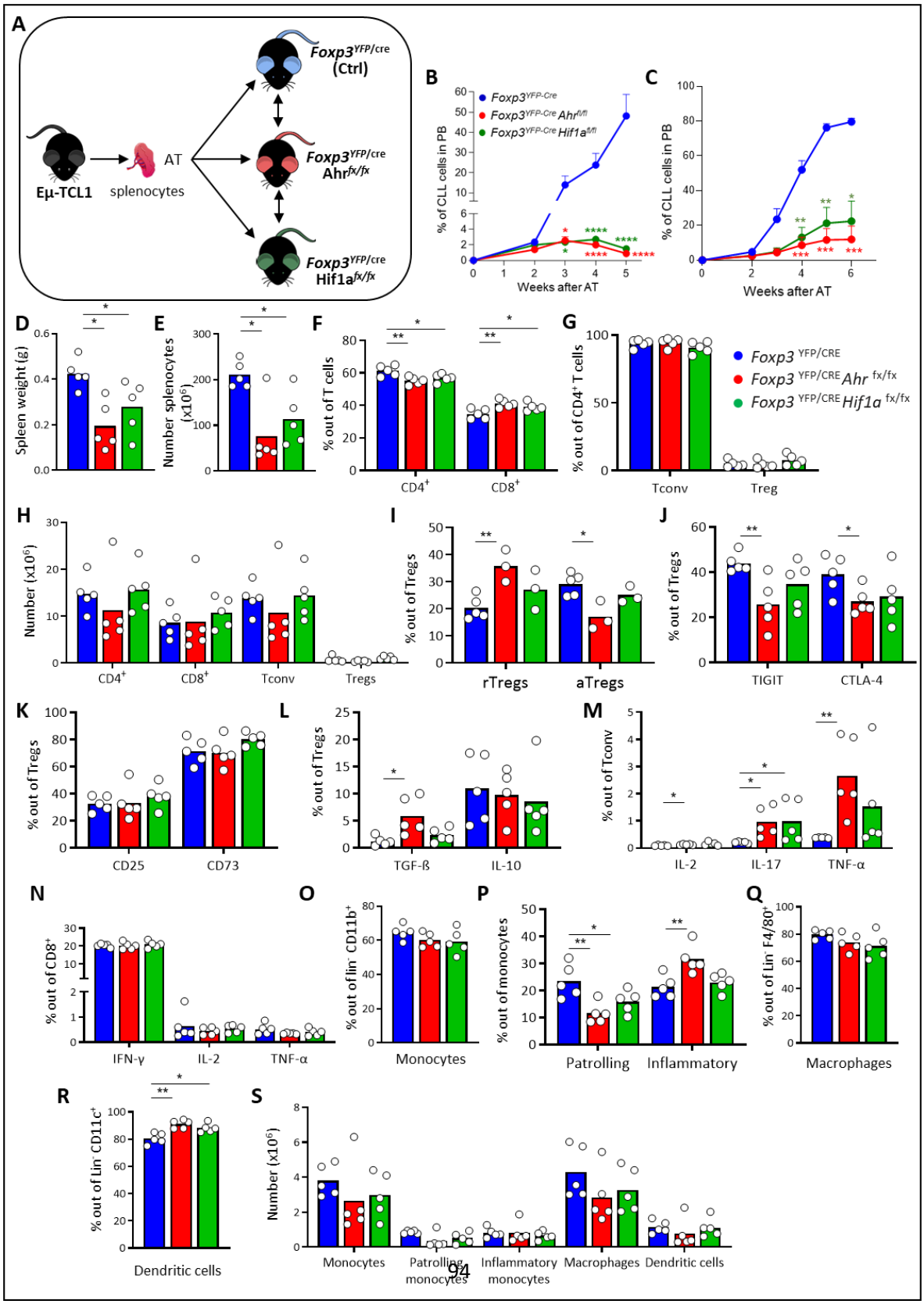

Figure 11: ***Ahr* and *Hif1a* depletion in Tregs delays leukemia development and promotes an anti-tumor T cell response.** **(A)** Two independent cohorts of cKO and control mice were injected with splenocytes derived from diseased Eμ-TCL1 mice. Recipient mice were bled every 7 days to evaluate peripheral disease development. **(B, C)** Percentages of circulating neoplasic $CD19^+CD5^+$ cells detected by FC in **(B)** the first cohort and **(C)** the second cohort. (n=6 per group in the first cohort; n=5 per group in the second cohort, Two-way ANOVA). **(D)** Values of spleen weights for the three goups studied and **(E)** number of splenocytes of the recipient mice. **(F)** Percentage of T-cell subsets and **(G)** frequency of CD4+ T-cell subpopulations in the three models. **(H)** Number of Tcell subpopulations in control and cKO mice.**(I)** Frequency of $CD62L^+$ $CD44^-$ rTregs and $CD62L^-$ $CD44^+$ aTregs in the Treg compartment. **(J-L)** Frequency of Treg-specific population expressing **(J)** the IC TIGIT and CTLA-4, **(K)** the immunosuppressive markers CD25 and CD73 and **(L)** the immunosuppressive cytokines TGF-β and IL-10. **(M)** Frequency of IL-2, IL-17 and TNF-α-expressing cells in $CD4^+$ Tconv. **(N)** Frequency of IFN-γ, IL-2 and TNF-α-expressing cells in $CD8^+$ T cells. **(O)** Frequency of monocytes in the three models within the splenic TME **(P)** Percentage of monocytes subpopulations in the three models. **(Q-R)** Frequency of macrophages **(Q)** and of DCs **(R)** in the recipient mice. **(S)** Number of myeloid cell subpopulations in the three models. FC=flow cytometry; (* P< .05, ** P< .01, Unpaired T test).

5. Delay in CLL development in mice lacking *Ahr* and *Hif1a* in Tregs is mediated by $CD8^+$ T cells.

Both in physiological conditions and during cancer development, Tregs exert their immunosuppressive functions mainly towards $CD8^+$ T cells (Chen *et al.*, 2005; Noyes *et al.*, 2022). We then wanted to investigate whether the delay in CLL development observed in cKO mice was dependent on the effect of Tregs on $CD8^+$ T cells. To address this, $CD8^+$ T cells were depleted *in vivo* in the three models, which were subsequently adoptively transferred with CLL cells (**Fig.12A**). As expected, in mice injected with isotype control, there was a drastic delay in CLL development in the cKO mice (**Fig.12B**), as previously observed (Fig.11B-C), while these differences were highly reduced in absence of $CD8^+$ T cells (**Fig.12C**). When comparing the CLL development of mice with the same genotype in presence or absence of $CD8^+$ T cells (**Fig.12D-F**), we observed that in control mice there were no differences between the two conditions (**Fig.12D**), while significant differences were observed in *Ahr* and *Hif1a* cKO mice (**Fig.12E-F**). These results confirmed that Tregs mediate, at least partially, the decreased CLL development observed in cKO mice through the regulation of $CD8^+$ T-cell activity.

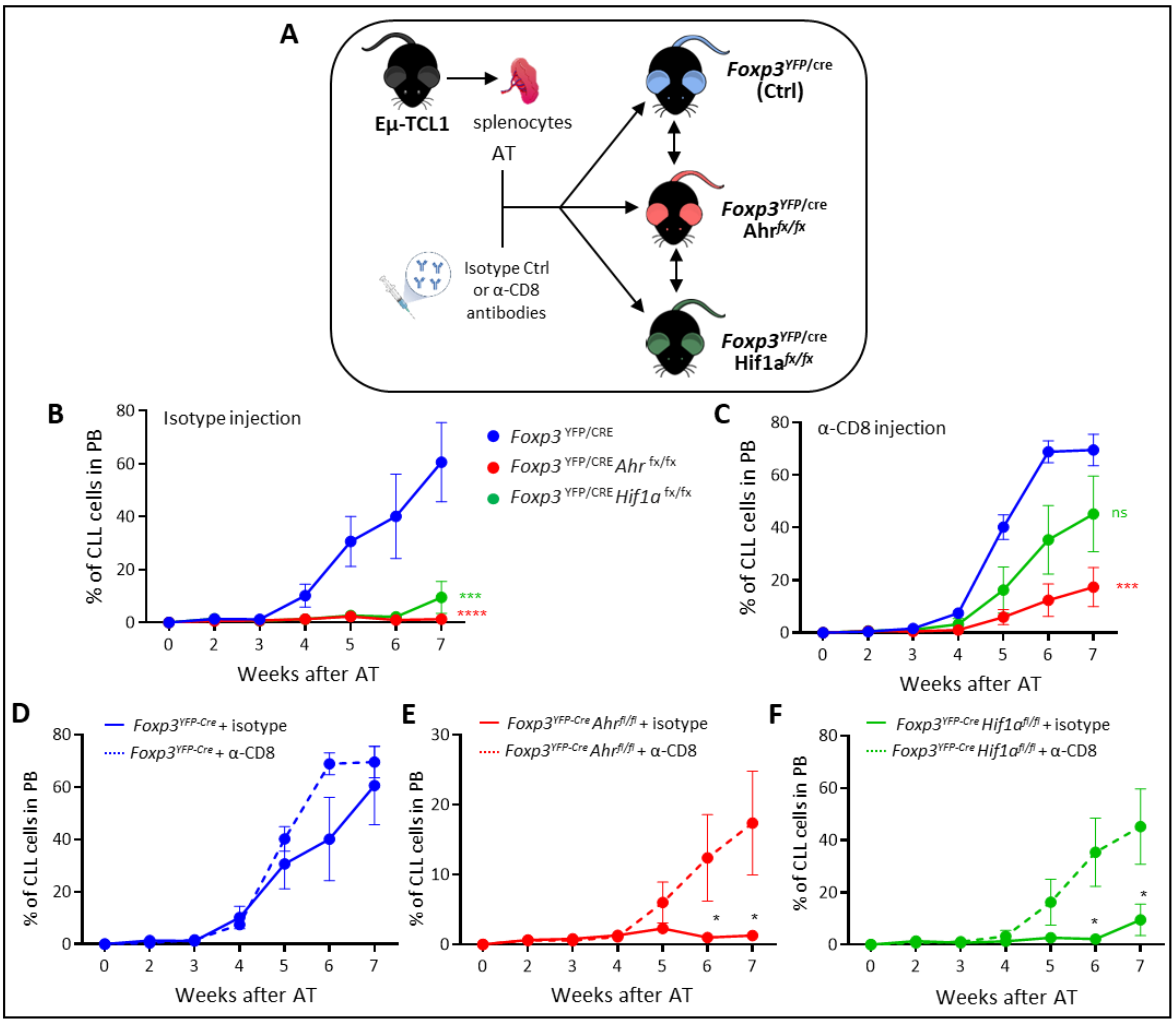

Figure 12: Delay in CLL development in mice lacking *Ahr* and *Hif1a* in Tregs is mediated by CD8⁺ T cells. A) Mice lacking *Ahr* and *Hif1a* in Tregs and control mice were injected with α-CD8 depleting antibodies 2 days before being adoptively transferred with splenocytes derived from a diseased Eμ-TCL1 mouse. Recipient mice were bled every week to evaluate peripheral disease development. **(B-C)** Percentages of circulating neoplasic $CD19^{+}CD5^{+}$ cells detected by FC in mice injected with IgG isotype control **(B)** and mice injected with CD8-depleting antibody **(C)**. **(D-F)** Tumor growth curve comparison between control mice (D), *Ahr* cKO **(E)** and *Hif1a* cKO **(F)** mice injected with isotype control and α-CD8 antibody. FC=flow cytometry; (n=6, * P< .05, ** P< .01, *** P< .001, **** P< .0001, Two-way ANOVA).

6. Injection of cKO- and control-derived splenocytes into *Rag2*$^{-/-}$ mice recapitulates decreased immunosuppressive phenotype of Tregs in absence of *Ahr* and *Hif1a*.

In order to understand whether that the differences observed in Treg phenotype in the AT model (Fig.11I-J) were not dependent on the differences in tumor load between control mice and cKO mice (Fig.11B-C), we isolated splenocytes from the three mouse models and injected them into *Rag2*$^{-/-}$ mice, which lack functional T and B cells. One day after, CLL cells isolated from diseased Eμ-TCL1 mice were adoptively transferred into recipient mice (**Fig.13A**), and three weeks later, mice were euthanized. Importantly, no differences in tumor load were detected in the spleen of recipient mice (**Fig.13B**). To inspect Treg phenotype within recipient mice, CD4^{+} YFP^{+} Tregs were analyzed by FC in the splenic leukemic microenvironment of *Rag2*$^{-/-}$ host mice (representative plot in **Fig.13C**). As first, the frequency of *Ahr*- and *Hif1a*-KO Tregs was decreased compared to controls (**Fig.13D**). Moreover, TIGIT expression in Tregs was reduced in recipient mice injected with cKO-derived splenocytes compared to controls (**Fig.13E**), in line with an increased immunosuppressive phenotype of TIGIT^{+} Tregs (Joller *et al.*, 2014). A similar tendency was observed when analysing the expression of CD69, a T-cell activation marker (**Fig.13F**), and when comparing the frequency of TIGIT^{+} LAG3^{+} Tregs (**Fig.13G**). Very importantly, all these data highlight the relevance of AHR and HIF-1α expression in regulating tumor-specific Treg immunosuppressive activity.

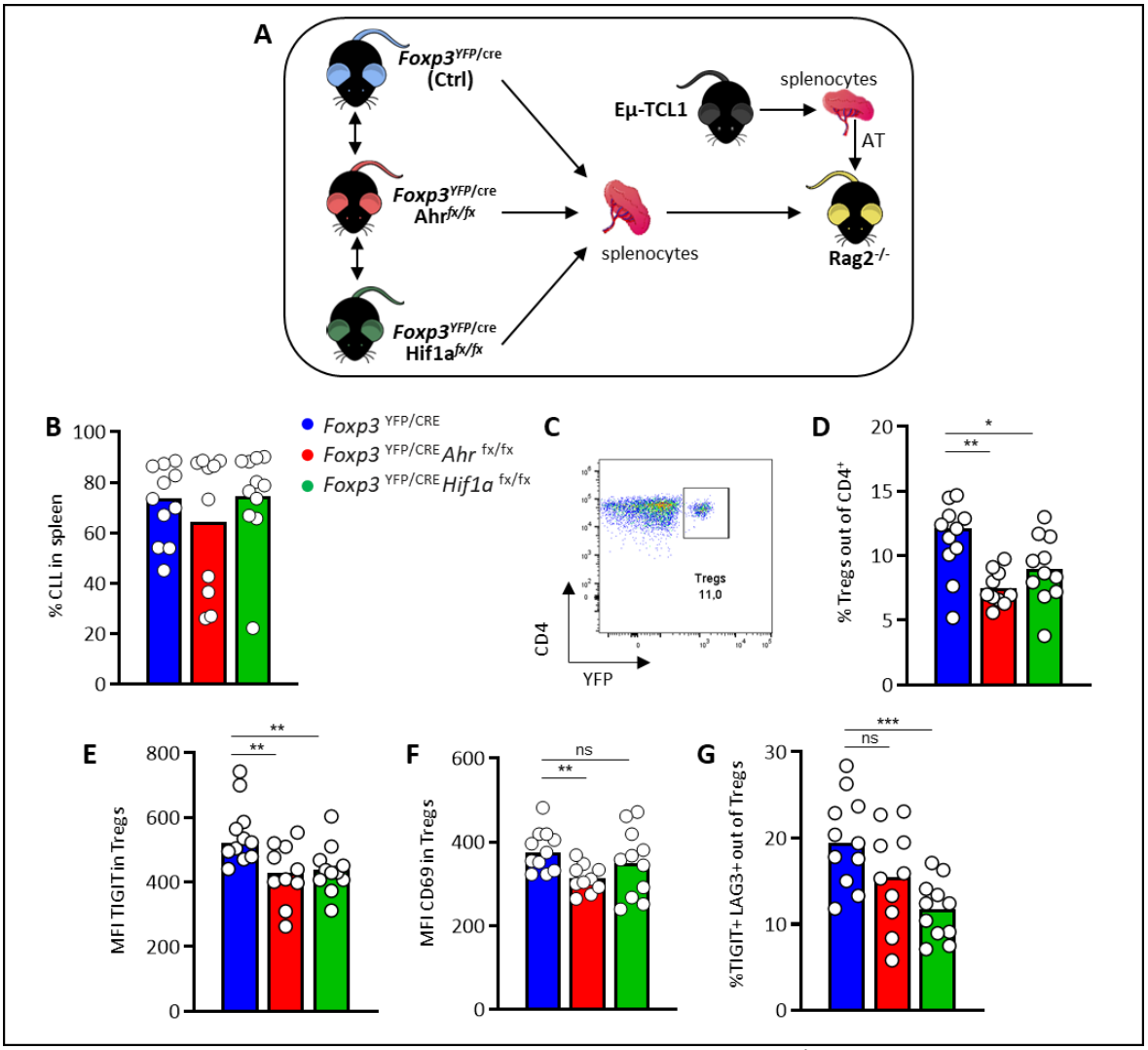

Figure 13: Injection of cKO- and control- derived splenocytes into Rag2$^{-/-}$ mice recapitulates decreased immunosuppressive phenotype of Tregs in absence of *Ahr* and *Hif1a*. (A) Splenocytes were isolated from cKO and control mice and injected into *Rag2*$^{-/-}$ mice. One day after, recipient mice were injected with CLL cells isolated from Eμ-TCL1 mice. **(B)** Percentages of neoplasic CD19^{+}CD5^{+} CLL cells in the spleen of recipient mice upon euthanasia (3 weeks after CLL injection). **(C)** Gating strategy to analyze YFP^{+} Tregs. **(D)** Frequency of Tregs within CD4^{+} T cells in the recipient mice. **(E)** MFI of TIGIT in Tregs in recipient mice injected with splenocytes isolated from the three models. **(F)** MFI of CD69 in Tregs of *Rag2*$^{-/-}$ host mice. **(G)** Frequency of TIGIT^{+} LAG3^{+} Tregs within recipient mice. (n=11 for control and HIF-1α cKO, n=10 for AHR cKO mice, * P< .05, ** P< .01, *** P< .001, Unpaired T test).

7. *In vivo* inhibition of AHR and HIF-1α results in decreased CLL development.

Since *Ahr* and *Hif1a* depletion in Tregs resulted in a drastic delay in CLL development, we evaluated the efficacy of AHR and HIF-1α inhibition *in vivo* during CLL development. For this purpose, WT mice were injected with CLL cells and monitored by weekly analysis of PB to follow leukemia development. When CLL cells started to accumulate in PB (at week 5 after AT), recipient mice were randomized and treated with AHR or HIF-1α inhibitors (**Fig.14A**). Very importantly, inhibition of AHR and HIF-1α recapitulated the decreased CLL development observed in cKO mice (**Fig.14B**) highlighting the pro-tumoral role of these two TFs in CLL leukemogenesis. Since we have previously shown that *Ahr* and *Hif1a* specific depletion in CLL cells does not affect leukemogenesis (Annex I) (Gonder *et al.*, 2021), part I of results, these data also suggest that the inhibition of AHR and HIF-1α reduces CLL development by affecting the TME, in particular Tregs, rather than directly affecting CLL cells.

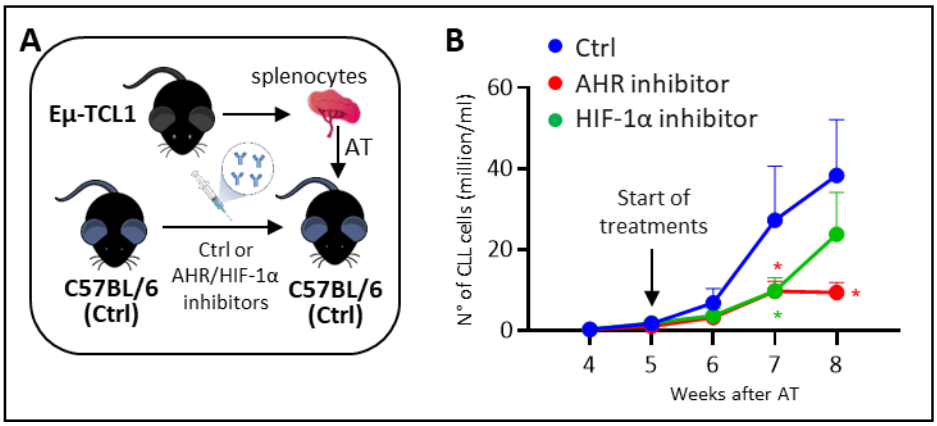

Figure 14: *In vivo* inhibition of AHR and HIF-1α results in decreased CLL development. (A) Splenocytes derived from diseased Eμ-TCL1 mice were injected in WT mice and CLL development was monitored by weekly analysis of PB. Five weeks after AT, mice were randomized and divided in different groups, which received either vehicle, AHR inhibitor (CH-223191) or HIF-1α inhibitor (acriflavin). **(B)** Percentages of circulating neoplasic $CD19^{+}CD5^{+}$ cells detected by FC in mice injected with vehicle or inhibitors. FC=flow cytometry; (n=5,* P< .05, Two-way ANOVA).

8. *Ahr* and *Hif1a* depletion in Tregs delays melanoma development *via* $CD8^+$ T-cell inhibition and causes a reduced expression of immunosuppressive IC in tumor-infiltrated Tregs.

In order to investigate whether the impacted immunosuppressive activity observed upon *Ahr* and *Hif1a* depletion in Tregs was restricted or not to CLL development *in vivo*, syngenic melanoma B16F10 cells were injected in the three models and tumor size was measured over time (**Fig.15A**). As for CLL, a delay in melanoma growth upon Treg-depletion of *Ahr* and *Hif1a* in recipient mice could be observed (**Fig.15B**). We then repeated the injection in a second cohort of control and *Ahr* cKO mice, and could recapitulate the decrease in melanoma development when *Ahr* was depleted in Tregs of recipient mice (**Fig.15C-D**). When analysing tumor-infiltrated aTregs in the second cohort by FC, we observed a decreased expression of immunosuppressive IC TIGIT (**Fig.15E**) and PD-1 (**Fig.15F**), adding more evidences to the role of AHR and HIF-1α in contributing to Treg suppressive activity during tumor development. We then wanted to verify whether Tregs exert their immunosuppressive effect through $CD8^+$ T cells in this context, and for this reason another cohort of cKO and control mice were treated with α-CD8 depleting antibody and subsequently injected with B16F10 melanoma cells (**Fig.15G**). While mice injected with isotype control could recapitulate the delay in melanoma growth observed in the first cohort (**Fig.15H**), these differences were abrogated in absence of $CD8^+$ T cells (**Fig.15I**), demonstrating that the melanoma delay observed in absence of *Ahr* and *Hif1a* is mediated by the effect of Tregs on $CD8^+$ T cells.

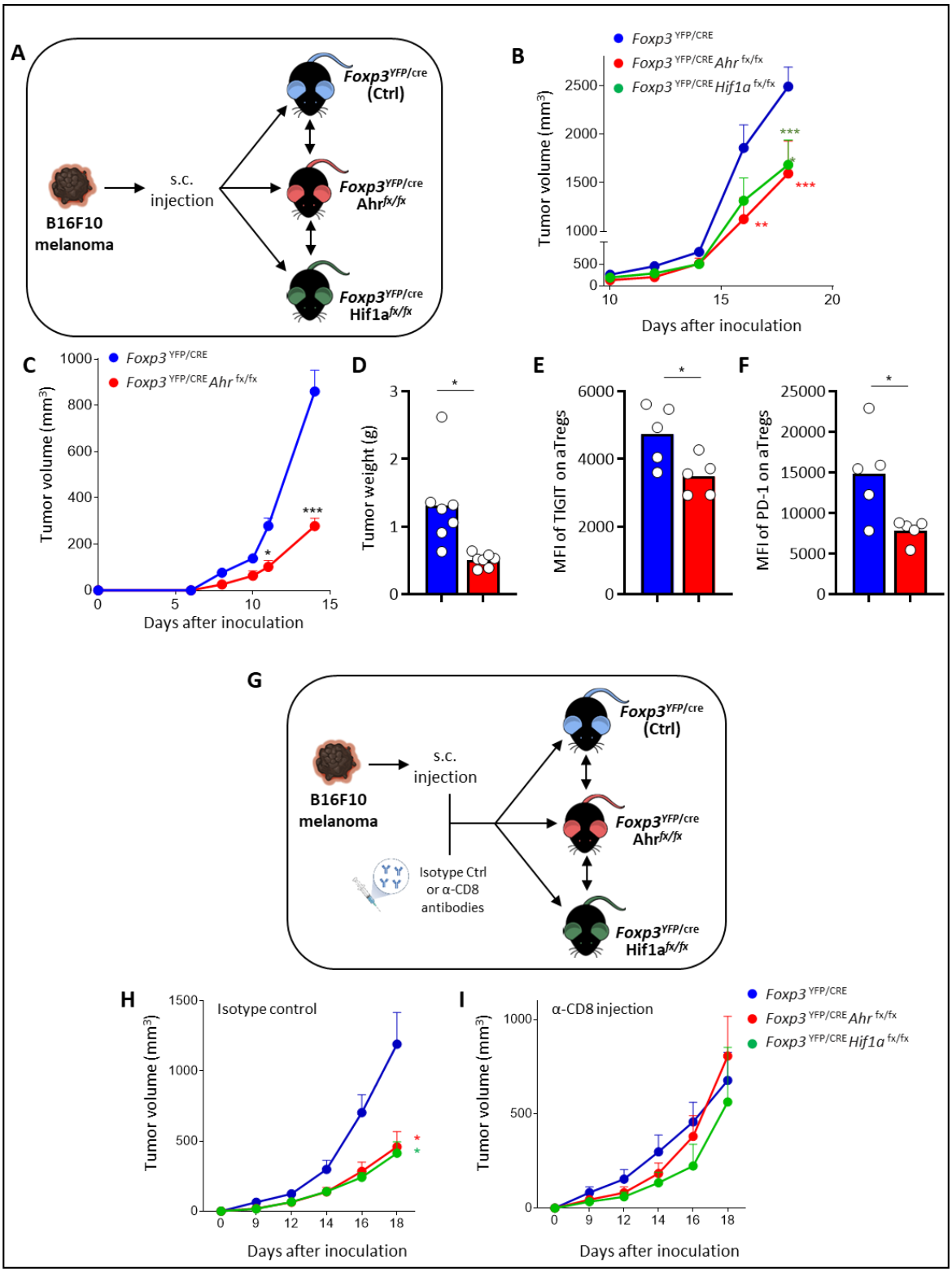

Figure 15: *Ahr* and *Hif1a* depletion in Tregs delays melanoma development via CD8⁺ T-cell inhibition and causes a reduced expression of immunosuppressive IC in tumor-infiltrated Tregs. (A) cKO and control mice were s.c. injected with B16F10 melanoma cells. When tumors became palpable, tumor measurement was performed every 2 days until human endpoint. **(B)** Tumor growth in recipient mice. **(C)** Growth curve of melanoma in a 2nd cohort of AHR cKO and control mice. (n=8 per group for the 1st cohort, n=7 per group for the 2nd cohort, Two-way ANOVA). **(D-F)** Analysis of the 2nd cohort upon euthanasia. **(D)** Tumor weight of the two groups, **(E)** expression of TIGIT in tumor-infiltrated aTregs and **(F)** of PD-1 in the same population. **(G)** cKO and control mice were injected with α-CD8 depleting antibodies 2 days before being s.c. injected with B16F10 melanoma cells. When tumors became palpable, tumor measurement was performed every 2 days

until euthanasia (n=6 per group, Two-way ANOVA). **(H)** Tumor volume of mice injected with isotype control and **(I)** mice injected with α-CD8 depleting antibody. (* P< .05, ** P< .01, *** P< .001, Unpaired T test).

9. *Ahr*- and *Hif1a*-KO iTregs present impacted immunosuppressive phenotype.

It is well established that tumor-infiltrating Tregs can be peripherally induced in the TME and have strong immunosuppressive functions (Li *et al.*, 2020). Both AHR and HIF-1α play an important role in peripheral Treg development (Dang *et al.*, 2011; Quintana *et al.*, 2008), therefore we induced *in vitro* Treg differentiation from $CD4^+$ T cells and characterize them in presence and absence of AHR and HIF-1α. For this purpose, $CD4^+$ T cells isolated from cKO and control mice were polarized *in vitro* for 4 days in presence of TGF-β and retinoic acid (RA) (**Fig.16A**), known to induce Treg differentiation of $CD4^+$ T cells (Schiavinato *et al.*, 2017). We then analysed the polarized/induced Tregs by FC and observed that after 4 days, the vast majority of cells were YFP^+ Tregs (representative plot in **Fig.16B**). Very interestingly, differences were detectable neither in the frequency of YFP^+ ($FOXP3^+$) cells (**Fig.16C**), nor in the percentage of live cells (**Fig.16D**), implying that *Ahr* and *Hif1a* depletion does affect neither the ability of Tconv to differentiate towards Tregs nor Treg viability in polarizing conditions. Nonetheless, we found a decrease in the expression of YFP (FOXP3) in absence of AHR and HIF-1α. FOXP3 is the master TF of Tregs that controls the expression of several genes crucial for their immunosuppressive functions (Ohkura and Sakaguchi, 2020). Indeed, when analysing the expression of different markers, lack of *Ahr* and *Hif1a* caused decreased Ki-67 expression (**Fig.16F**), which was correlated with a decrease in TIGIT, CD44 and IL-10 in KO iTregs compared to controls (**Fig.16G-I**). We also observed a decrease in Granzyme B expression in both *Ahr* and *Hif1a* KO iTregs compared to controls (**Fig.16J**), although the decrease reached statistical significance only in AHR-KO iTregs. Very interestingly, for *Hif1a*-KO iTregs, TGF-β expression was reduced compared to *Hif1a*-WT iTregs. All together, these data demonstrate that *Ahr* and *Hif1a* depletion does not alter the iTreg polarization process of Tconv but impacts the expression of key activation and immunosuppressive molecules, fundamental for the inhibitory functions of Tregs.

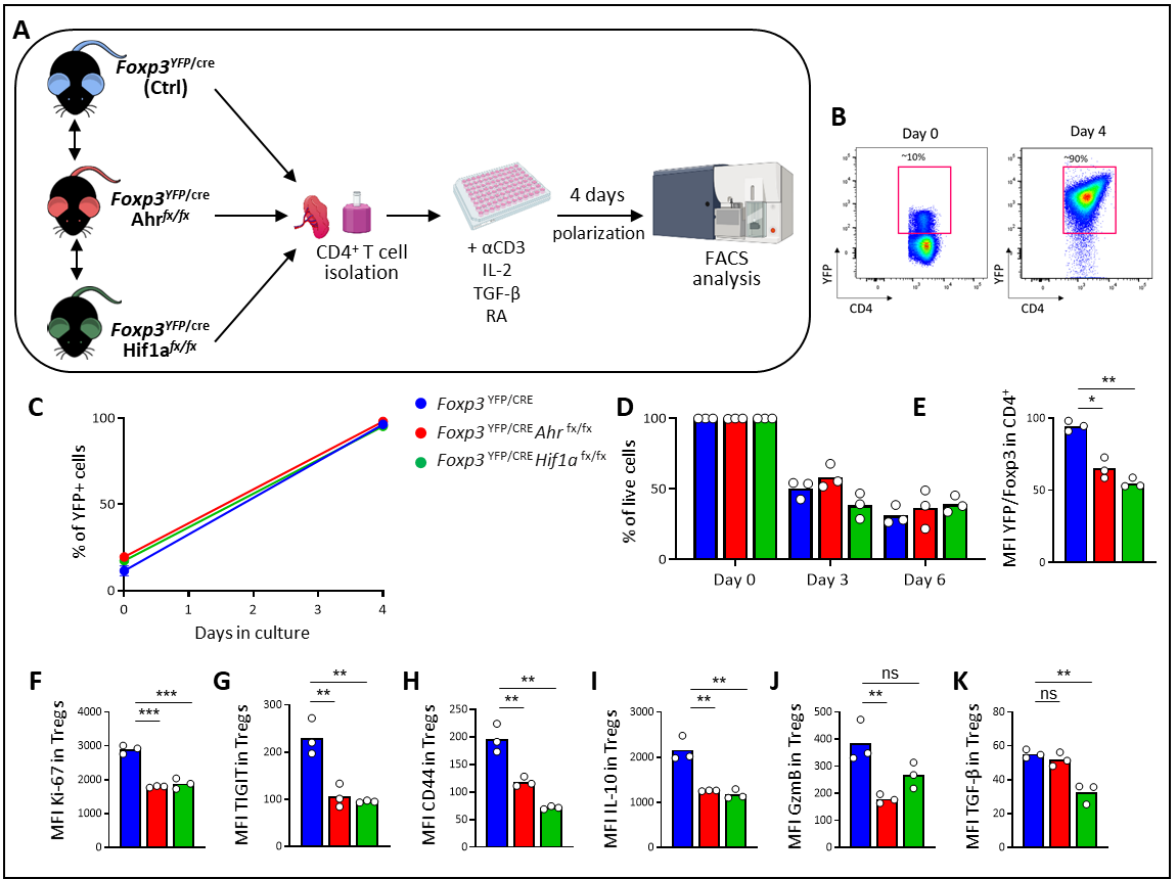

Figure 16: *Ahr*- and *Hif1a*-KO iTregs present impacted immunosuppressive phenotype. (A) Splenocytes were isolated from cKO and control mice and CD4⁺ T cells were sorted through magnetic beads. CD4⁺ T cells were activated *in vitro* in polarizing conditions and iTregs were analysed by FACS after 4 days. **(B)** Representative FACS plot of YFP expression in CD4⁺ T cells at day 0 and after 4 days of polarization. **(C)** Frequency of YFP⁺ Tregs at day 0 and after 4 days of polarization in the different models. **(D-K)** FACS analysis of iTregs after 4 days of polarization. **(D)** Frequency of live cells in the different models among different days of culture. **(E)** Expression of YFP (FOXP3) in *Ahr*-/*Hif1a*-KO iTregs compared to control iTregs. **(F-K)** Expression of indicated markers in iTregs of the different models (n=3, * P< .05, ** P< .01, *** P< .001, Unpaired T test).

10. *Ahr*- and *Hif1a*-KO iTregs have less suppressive abilities towards CD8⁺ T cells.

As our *in vivo* data demonstrated an important role of AHR and HIF-1α in mediating the suppressive ability of Tregs towards CD8⁺ T cells in CLL (and melanoma), and our *in vitro* data showed a decreased immunosuppressive phenotype of KO iTregs, we inspected the suppressive ability of iTregs isolated from the three models using suppression assays. For this purpose, CD4⁺ T cells were isolated from splenocytes of the three models and activated *in vitro* in polarizing conditions. After 4 days of polarization, KO and control iTregs were co-cultured with CD8⁺ T cells isolated from *Foxp3*$^{YFP/Cre}$ mice (**Fig.17A**). In line with a decreased immunosuppressive phenotype of KO iTregs (Fig.16E-K), we observed an increased proliferation of CD8⁺ T cells in presence of KO-iTregs compared to WT iTregs (**Fig.17B-C**), implying that *Ahr*- and *Hif1a*-KO iTregs have dampened suppressive abilities towards CD8⁺ T-cell proliferation compared to their WT counterparts and confirming the involvement of these two TFs in regulating Treg immunosuppressive functions.

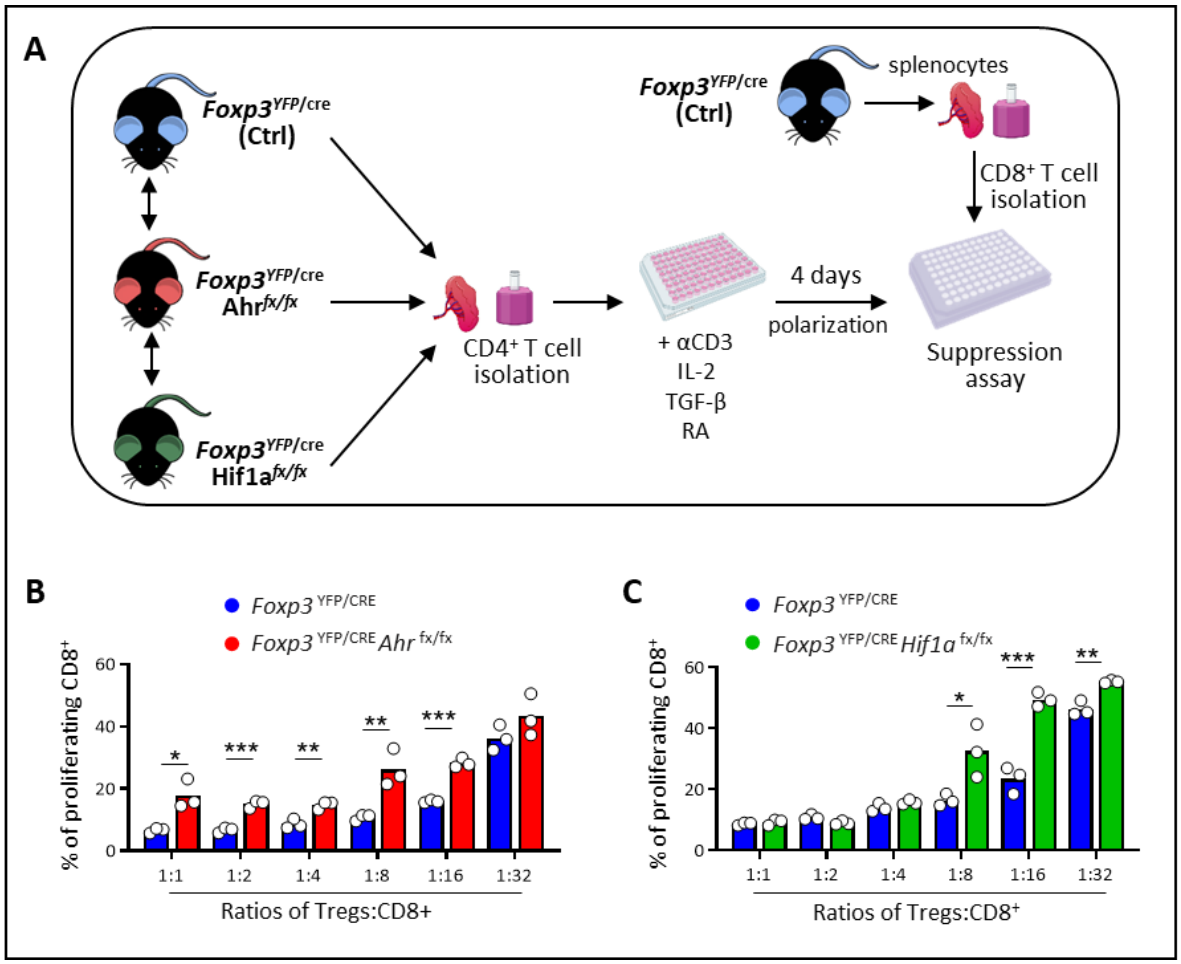

Figure 17: *Ahr*- and *Hif1a*-KO iTregs have less suppressive abilities towards CD8⁺ T cells. (A) Splenocytes were isolated from cKO and control mice and CD4⁺ T cells were sorted through magnetic beads. CD4⁺ T cells were activated *in vitro* in polarizing conditions and iTregs were co-cultured with CD8⁺ T cells isolated from control mice. Prior to co-culture, CD8⁺ T cells were stained with Tag-it violet to track their proliferation *in vitro*. **(B)** Frequency of proliferating CD8⁺ T cells in co-culture with either control or *Ahr*-KO iTregs **(C)** Frequency of proliferating CD8⁺ T cells in co-culture with either control or *Hif1a*-KO iTregs. (n=3, * P< .05, ** P< .01, *** P< .001, Unpaired T test).

11. *Ahr*- and *Hif1α*-KO iTregs present an altered energetic metabolism and glutamine uptake to fuel the TCA cycle.

Given that Tregs have a metabolic advantage in the TME compared to other T cells (Angelin *et al.*, 2017), and that AHR and HIF-1α are both involved in the metabolic adaptation of Tregs to TME-mediated stimuli (Campesato *et al.*, 2020b; Miska *et al.*, 2019), we wanted to inspect the metabolic behavior of *ex vivo* polarized iTregs in absence of the two TFs. For this purpose, upon 4 days of *in vitro* polarization of $CD4^+$ T cells isolated from the three models, we performed a Seahorse analysis and a glutamine tracing experiment of iTregs (**Fig.18A**). The Seahorse Mito Stress assay allowed us to analyze the oxygen consumption rate (OCR) of the cells in different conditions, as a proxy of the dependency on mitochondrial respiration. Very interestingly, there was an increased OCR in *Ahr*- and *Hif1α*-KO iTregs compared to control iTregs, (**Fig.18B**), in particular in basal mitochondrial respiration (**Fig.18C**) and basal oxygen consumption (**Fig.18D**) although a third biological replicate is needed to confirm this tendency. *Hif1α*-KO iTregs also presented an increased maximal respiration (**Fig.18E**) and spare respiratory capacity (**Fig.18F**). It was previously reported that glutamine metabolism plays a key role in Treg differentiation (Klysz *et al.*, 2015; Matias *et al.*, 2021), therefore we wanted to interrogate whether our KO iTregs presented an alteration on their glutamine uptake that could impact their suppressive capacity. [U-^{13}C]-glutamine incorporation into TCA cycle metabolites was determined in iTregs polarized from the three models via metabolite flux analysis by liquid chromatography mass spectrometry (LC-MS). Lack of *Ahr* and *Hif1α* in iTregs caused an increased relative flux of glutamine-derived carbon into citrate and α-ketoglutarate (α-KG) (**Fig.18G**). In line with an increased glutamine flux, KO iTregs presented decreased glucose uptake and lactate release in the cell culture medium (**Fig.18H**), although it reached statistical significance only for *Hif1α*-KO iTregs. In summary, our data shows that *Ahr*- and *Hif1α*-KO iTregs present an increased glutamine uptake for TCA cycle intermediates, increased mitochondrial respiration and decreased glucose uptake and lactate release. This metabolic rewiring observed in the cKO Tregs could be responsible for their lesser immunosuppressive ability in cancer development.

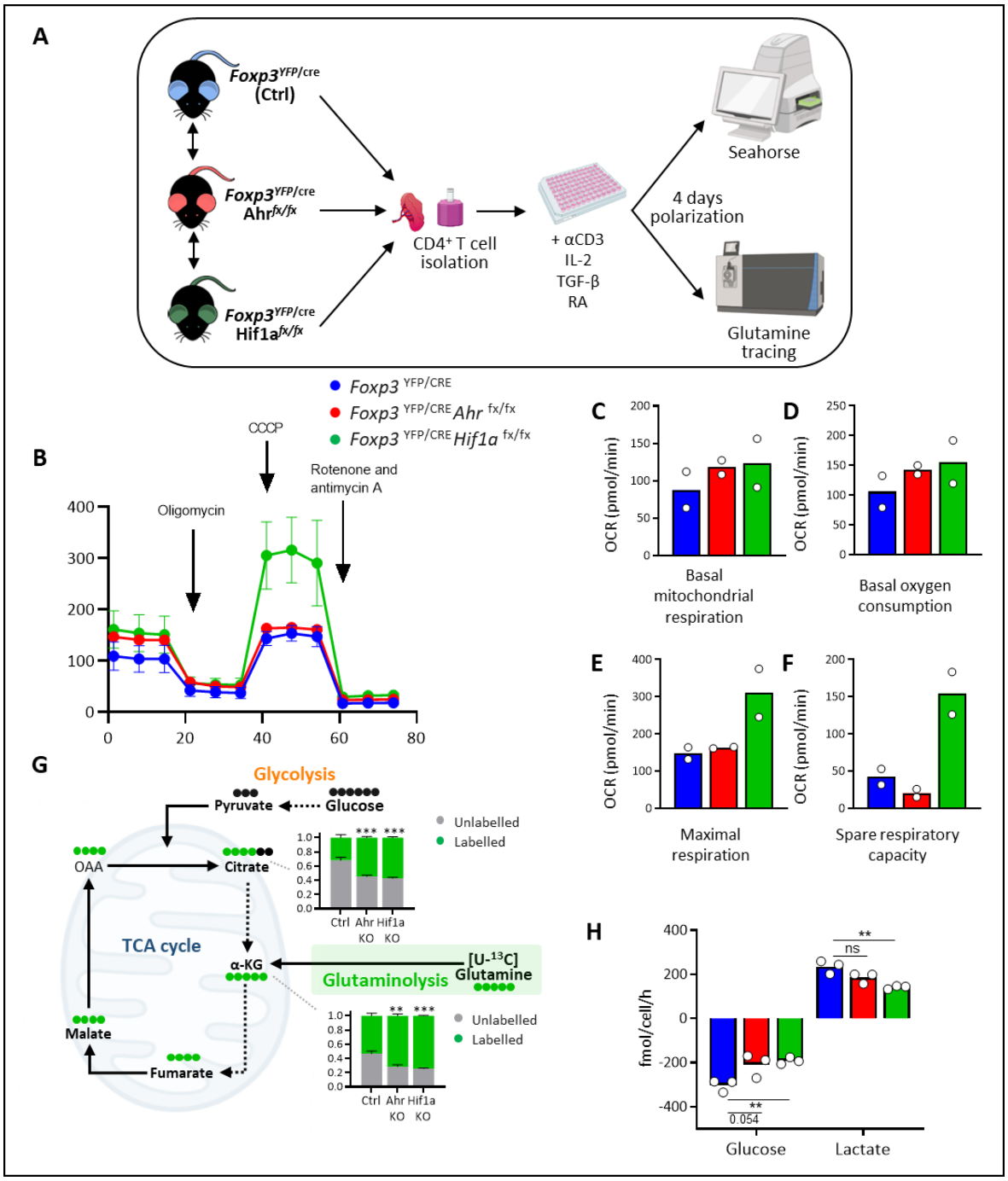

Figure 18: *Ahr*- and *Hif1a*-KO iTregs present an altered energetic metabolism and glutamine uptake to fuel the TCA cycle. (A) Splenocytes were isolated from cKO and control mice and CD4$^+$ T cells were sorted using magnetic beads. CD4$^+$ T cells were activated *in vitro* in polarizing conditions for 4 days and iTregs were subjected to seahorse analysis and glutamine tracing experiment. **(B)** Determination of OCR via seahorse. Basal mitochondrial respiration was initially determined and other parameters (basal oxygen consumption, maximal respiration and spare respiratory capacity) were analysed by adding oligomycin, CCCP and Rotenone/antimycin A, respectively. (n=5, * P< .05, ** P< .01, *** P< .001, Unpaired T test). **(C-F)** Quantification of the four indicated parameters were calculated. **(G)** Schematic representation of [U-^{13}C]-glutamine flux tracing into the TCA cycle and relative incorporation of glutamine derived carbons (labelled) in α-KG and citrate. **(H)** Levels of glucose and lactate measured by mass spectrometry in culture medium in control and KO iTregs cultured for 48h in [U-^{13}C]-glutamine culture medium. Negative value represent consumption. (n=2 for seahorse analysis, n=3 for glutamine tracing, * P< .05, ** P< .01, Unpaired T test).

Conclusions

By depleting AHR and HIF-1α in Tregs, we generated conditional knock out (cKO) mice that lack either TF only in Tregs. We initially evaluated the suitability of these models for further analysis, then adoptive transfer of CLL cells into cKO and control mice was performed, obtaining a drastic delay in CLL growth upon depletion of AHR and HIF-1α, and a decrease in immune checkpoints expression in Tregs compared to controls. In vivo injection of AHR and HIF-1α antagonists recapitulated the decreased CLL development when the two TFs are functionally inactive. Knowing that AHR and HIF-1α depletion in CLL cells does not impact leukemogenesis (Gonder et al., 2021), our findings strongly suggested an important role of AHR and HIF-1α in contributing to the immunosuppressive activity of Tregs during CLL development. Similar results were obtained when injecting B16F10 melanoma cells in the cKO and control mice, with intra-tumoral AHR-KO Tregs expressing less TIGIT and PD-1 compared to WT Tregs. The differences in CLL and melanoma development between WO and cKO mice were lower when $CD8^+$ T cells were depleted, demonstrating the importance of $CD8^+$ T cells in mediating decreased tumor load observed in cKO mice. We then evaluated the suppressive ability of ex vivo induced Tregs (iTregs) via suppression assay, observing an enhanced proliferation of $CD8^+$ T cells in the presence of KO-iTregs. Finally, KO-iTregs showed an altered oxygen consumption rate and glutamine uptake, pointing towards an altered metabolic behaviour of Tregs in absence of the two TFs. Altogether, these results indicate that AHR and HIF-1α play a fundamental role in the suppressive function of Tregs, and are of particular importance for sustaining the immunosuppressive ability of intra-tumor Tregs during CLL development.

Part II - Ebi3/IL-27 depleted microenvironment favors leukemia progression in CLL by impairing $CD8^+$ T-cell-mediated anti-tumor immunity

Preface

The second part of this project focused on the study of Interleukin 27 (IL-27) in the progression of CLL. IL-27 is a heterodimeric cytokine composed of two subunits: IL-27p28 (P28) and Epstein-Barr-virus-induced molecule 3 (EBI3) (Yoshida and Hunter, 2015), produced by different cells of the TME (Kourko *et al.*, 2019). IL-27 has recently gained considerable therapeutic attention, but its effects reportedly differ among malignancies, as it is described as a cytokine with pleiotropic functions in tuning the anti-tumor immune response (Beizavi *et al.*, 2021). We then wanted to test the effect of this cytokine during CLL development and its impact on anti-tumor immune response. To this aim, we used *Ebi3*$^{-/-}$ transgenic mice, which lack the EBI3 subunit of IL-27. We investigated the role of this cytokine during CLL progression in several murine models and experimental settings.

We also wanted to identify the main cellular target of IL-27 among the different cells composing the TME and to test the role of this cytokine on the functionality of the target cells. Another fundamental aim of this project was to analyze the concentration of this cytokine in leukemic mice and CLL patients, with the long-term goal of establishing this cytokine as a potential immunotherapeutic agent in CLL.

For this part of the project, the data represented in the figures were obtained by myself and others as follows:

- Figure 1: I equally contributed to panels A-F together with Dr. Marina Wierz, former PhD student of the TSI group at LIH. Data in the panels G and H were produced by Dr Ernesto Gargiulo, former PhD student in the same group.
- Figure 2: I performed the experiments displayed in panels A-D and G-H. For the panels A and B, the experiments were performed together with Dr. Marina Wierz, while I performed independently the experiment shown in figure G. The data shown in panels E-F were obtained by Dr. Ernesto Gargiulo.
- Figure 3: I performed the experiments displayed in panels A-D together with Iria Fernandez Botana, PhD student in the TSI group at LIH. Dr. Ernesto Gargiulo analysed the data shown in panels E-F of the same figure.
- Figure 4: I independently executed the experiment shown in panel A. The bioinformatic analysis dispayed in panels BG-F was performed by Dr. Etienne Moussay.
- Figure 5: I designed and performed independently the experiments shown in panels A-F. Panel G represents data obtained by our collaborator Dr. Alan Ramsey at King's college of London. Figures represented in Panels H-J were performed by our collaborator Dr. Bin Qu from University of Saarland.
- Figure 6: experiments shown in panel A, C-E I were executed by myself together with Iria Fernandez Botana, while the ELISA shown in panel B was performed by Dr. Basile Stamatopoulos at the Institute Jules-Bordet of Bruxelles. Panels F and G were produced by Dr. Ernesto Gardgiulo.
- Figure S1: experiments shown in panels A-B and E-F were obtained by me and Dr. Marina Wierz, while data present in panels D, G-H were produced by Dr. Ernesto Gargiulo.
- Figure S2: I performed the experiments shown in every panel together with Dr. Marina Wierz.
- Figure S3: the experiments in panels A-C, F-H were executed by me and Dr. Marina Wierz, data shown in panels D-E, I-K were obtained by Dr. Ernesto Gargiulo. The experiment shown in panel L was perfomed by me.
- Figure S4: panels A, D-E were produced by Dr. Ernesto Gargiulo, while data presented in panels B-C were obtained by me and Iria Fernandez Botana.
- Figure S5: all data present in this figure were obtained by Dr. Etienne Moussay.

- Figure S6: the experiment shown in panel A was performed by me. Panels B-C were produced by Dr. Ernesto Gargiulo, while data shown in panel D were obtained by Dr. Bin Qu.
- Figure S7: Dr. Etienne Moussay produced the data shown in panels A and B. Iria Fernandez Botana performed the experiments shown in panels C-F.
- Figure S8: Data shown in panels A-B and F-G were produced by Dr. Ernesto Gargiulo, while the experiments shown in panels C-E were performed by me and Iria Fernandez Botana.

Ebi3/IL-27 depleted microenvironment favors leukemia progression in CLL by impairing CD8$^+$ T-cell-mediated anti-tumor immunity

Giulia Pagano[1,2*], Iria Fernandez Botana[1,2*], Marina Wierz[1,3], Philipp M. Roessner[4], Nikolaos Ioannou[5], Xiangda Zhou[6], Ernesto Gargiulo[1], Susanne Gonder[1,2], Bin Qu[6], Basile Stamatopoulos[7], Alan G. Ramsay[5], Martina Seiffert[4], Anne Largeot[1], Etienne Moussay[1#], Jerome Paggetti[1#]

[1] Tumor Stroma Interactions, Department of Cancer Research, Luxembourg Institute of Health, Luxembourg, Luxembourg

[2] Faculty of Science, Technology and Medicine, University of Luxembourg, Esch-sur-Alzette, Luxembourg

[3] MVZ für Histologie, Zytologie und Molekulare Diagnostik Trier, 54296 Trier, Germany

[4] Molecular Genetics, German Cancer Research Center (DKFZ), Heidelberg, Germany

[5] School of Cancer and Pharmaceutical Sciences, Faculty of Life Sciences & Medicine, King's College London, London, United Kingdom

[6] Biophysics, Center for Integrative Physiology and Molecular Medicine, School of Medicine, Saarland University, Homburg, Germany.

[7] Clinical Cellular Therapy Research Laboratory, Jules Bordet Institute, Brussels, Belgium

* these authors contributed equally.

# these authors share senior authorship.

Correspondence: etienne.moussay@lih.lu; jerome.paggetti@lih.lu

State of publication:

In revision for *Haematologica* journal.

Abstract

Chronic Lymphocytic Leukemia (CLL) cells are highly dependent on interactions with the immunosuppressive leukemic tumor microenvironment (TME) for survival and proliferation. In the search for novel treatments, pro-inflammatory cytokines have emerged as candidates to reactivate the immune system. Among those, IL-27 has recently gained therapeutic attention, but its effects differ among malignancies. Here, we utilized the Eμ-TCL1 and EBI3 knock-out mouse models as well as clinical samples from CLL patients to investigate the role of IL-27 in CLL. Characterization of murine leukemic spleens revealed that the absence of IL-27 leads to enhanced CLL development and to a more immunosuppressive TME in transgenic mice. Gene profiling of T-cell subsets from EBI3 knock-out highlighted transcriptional changes in the $CD8^+$ T-cell population associated with T-cell activation, proliferation, and cytotoxicity. We also observed an increased anti-tumor activity of $CD8^+$ T cells in presence of IL-27 *ex vivo* with murine and clinical samples. Finally, we detected a decrease in IL-27 serum levels during CLL development in both pre-clinical and patient samples. Altogether, we demonstrated that IL-27 has a strong anti-tumorigenic role in CLL and postulate this cytokine as a promising treatment or adjuvant for this malignancy.

Keywords: chronic lymphocytic leukemia, IL-27, Ebi3, tumor microenvironment, $CD8^+$ T-cell, anti-tumor immunity

Introduction

Chronic Lymphocytic Leukemia (CLL) is the most frequent type of adult leukemia in the USA and Europe, affecting mainly older adults over the age of 65 (Swerdlow *et al.*, 2016). Clinically, CLL is defined as a B cell hematological malignancy characterized by an accumulation of abnormal, monoclonal, B-lymphocytes in the peripheral blood (PB) and secondary lymphoid organs of patients (Cree, 2022).

The current standard of care for CLL patients consists of chemotherapy combined with monoclonal antibodies and/or other specific inhibitors. However, this treatment does not have a curative potential, and a significant percentage of patients do not respond or become resistant (Burger, 2020). Consequently, there is a pressing need for the development of novel therapies for advanced and aggressive CLL, which unfortunately remains an incurable disease. CLL cells are highly dependent on interactions with surrounding non-malignant cells for survival and proliferation (Svanberg *et al.*, 2021). In fact, they spontaneously undergo apoptosis in monoculture, but co-culture with accessory cells significantly extends their survival (Asslaber *et al.*, 2013; Burger *et al.*, 2000; Collins *et al.*, 1989). Given the pivotal role of the tumor microenvironment (TME) in CLL, an increasing number of studies are focusing on the identification of micro-environmental signals that could play a role in the pathogenesis of this disease.

Interleukin 27 (IL-27) is a heterodimeric cytokine composed of two non-covalently linked subunits: IL-27p28 (P28) and Epstein-Barr-virus-induced molecule 3 (EBI3) (Yoshida and Hunter, 2015). IL-27 is produced by activated antigen presenting cells (APCs) and it signals through a heterodimeric receptor (IL-27R) that comprises the gp130 and WSX-1 subunits, both essential for efficient signaling (Molle *et al.*, 2007b). IL-27 was initially characterized as being pro-inflammatory, given its ability to promote Th1 immunity. Nevertheless, it was later reported that IL-27 exerts a potent inhibitory role during Th2, Th17 and Treg differentiation. Hence, IL-27 mediates a wide range of functions involved in T-cell-mediated immunity (Fabbi *et al.*, 2017).

Not surprisingly, IL-27 has been reported to have pleiotropic functions in the setting of cancer development in relationship to the biological context and experimental models considered. Most existing evidence refers to the anti-tumor activities of this cytokine (Kourko *et al.*, 2019). IL-27 has been reported to hinder tumor development and progression mainly by modulating the immune landscape surrounding the malignant cells (Hisada *et al.*, 2004). While most evidence points towards the upregulation of Th1 and Cytotoxic T lymphocyte (CTL) responses as the main anti-

tumor contribution of IL-27 to the TME (Liu *et al.*, 2013b; Morishima *et al.*, 2005b; Salcedo *et al.*, 2004), other reports suggest that IL-27 can also mediate NK cell responses and inhibit M2 macrophage polarization (Matsui *et al.*, 2009; Yao *et al.*, 2017). On the other hand, a few studies indicate that IL-27 might also contribute to tumorigenesis in specific settings. For example, elevated IL-27 serum levels are associated with poor prognosis and disease progression in some malignancies such as gastroesophageal cancer, melanoma and adult AML (Ahmed *et al.*, 2019; Diakowska *et al.*, 2013; Gonin *et al.*, 2013). Additionally, IL-27 was found to modulate transcriptional programs and induce the expression of immune-regulatory molecules such as PD-L1 and IDO in human ovarian cancer cells *in vitro* (Carbotti *et al.*, 2015; Chihara *et al.*, 2018).

Given the dynamic nature of cytokine biology, and consistent with a rather variable role in cancer biology, the role of IL-27 and its mechanism of action must be carefully investigated in each malignancy. With this background, we asked whether IL-27 has an effect in the development and progression of CLL. Here, we describe a strong anti-tumorigenic role of IL-27 in CLL in distinct pre-clinical mouse models and patient samples. First, we show that the genetic depletion of the IL-27 subunit *Ebi3* leads to a strongly enhanced CLL development and a more immunosuppressive TME using two *in vivo* approaches. Secondly, we elucidate a mechanism by which IL-27 enhances CD8+ T-cell anti-tumor immunity in CLL, as well as propose and validate several cellular mediators involved in this process. Moreover, we identify a decrease in the circulating levels of IL-27 concomitant with CLL development in both murine and patient samples. We then functionally validate the enhanced anti-tumor ability of $CD8^+$ T cells in the presence of IL-27 both in murine and human samples. Finally, and in accordance to our previous results, IL-27 neutralization recapitulates the enhanced leukemic progression observed in the transgenic mouse models.

Methods

Additional information regarding the materials and methods used in this publication can be found in the supplementary data section.

Patient samples

All experiments involving the use of human samples were conducted in accordance with the declaration of Helsinki and approved by the appropriate local ethics committee: the Jules Bordet Institute ethics committee (Belgium), The Comité National d'Ethique de Recherche (Luxembourg), and the University of Saarland (Germany).

Peripheral blood (PB) samples were obtained from CLL patients and from age-matched healthy donors following informed consent. PB mononuclear cells (PBMC) were isolated from whole blood by density gradient centrifugation using the LeucoSep™ Separation Medium (Greiner Bio-One) as described on the manufacturer's protocol.

Animal experiments

All animal experiments were performed under specific pathogen-free conditions with the approval of the Luxembourg Ministry of Agriculture (#LECR-2018-02 and #LECR-2018-03) and in accordance with the guidelines from the European Union. *Ebi3*$^{-/-}$ (RRID: IMSR_JAX:008701) and *FoxP3*$^{YFP/Cre}$ (RRID: IMSR_JAX:016959) mice were purchased from the Jackson Laboratory (Bar Harbour, ME); and C57BL/6 (MGI: 3028467, RRID: IMSR_JAX:000664) from Janvier Labs (France). *Eμ-TCL1* mice (on C57BL/6 background; MGI: 3527221) were kindly provided by Pr. Carlo Croce and Pr. John Byrd (OSU, OH). The *Eμ-TCL1 Ebi3*$^{-/-}$ strain was generated in-house by crossing *Ebi3*$^{-/-}$ mice with *Eμ-TCL1*, together with *FoxP3*$^{YFP/Cre}$ *Ebi3*$^{-/-}$ mice, obtained by breeding *FoxP3*$^{YFP/Cre}$ and *Ebi3*$^{-/-}$ mice for several generations. *Rag2*$^{-/-}$ mice were held at specific pathogen-free conditions at the central animal facility of the German Cancer Research Centre (DKFZ).

Flow cytometry

Single-cell suspensions were stained with cell-surface antibodies (30min, 4 °C) and washed twice with FACS buffer. For the staining of intracellular proteins, surface-stained cells were fixed (30min, RT) with eBioscience™ Foxp3/Transcription Factor Staining Buffer Set (ThermoFisher Scientific). After additional washing steps, cells were permeabilized using eBioscience™ Permeabilization Buffer (ThermoFisher Scientific) and stained with the intracellular antibody mix (30 min, 4°C). Samples were stored at 4 °C in dark conditions until acquisition. Antibodies used for flow cytometry are listed in Table S1.

Statistical analyses

Sample size was determined based on expected variance of read-out. No samples or animals were excluded from the analyses. Statistical analysis was performed using GraphPad Prism software (version 9.1.2; RRID: SCR_002798). Data are displayed as mean ± standard error of mean (SEM). For the percentage of CLL cells in PB over time, we performed two-way ANOVA followed by multiple comparison test. The unpaired t test was used for the rest of the figures. A p-value lower than 0.05 was considered statistically significant. Significance displayed in each figure is explained in figure legends.

Results

1. EBI3 depletion promotes leukemia development and induces an enhanced immunosuppressive tumor microenvironment.

In order to investigate the role of IL-27 in CLL development, we used *Ebi3*$^{-/-}$ mice, defective in the production of the heterodimeric IL-27. First, we validated the specific deletion of the *Ebi3* subunit via qPCR, and confirmed the suitability of the models for further analyses (**Fig.S1A**). We adoptively transferred (AT) *Ebi3*$^{-/-}$ mice and *Ebi3*$^{+/+}$ mice (WT, used as controls) with two independent clones of CLL cells obtained from the spleen of leukemic Eμ-TCL1 mice. We then followed-up leukemia development in the PB of recipient mice using flow cytometry (FC), which lead to the observation of a strikingly enhanced tumor development in the absence of *Ebi3* (**Fig.1A and S1B**). Consistently, we observed an increased number of splenocytes and spleen weight in mice lacking *Ebi3* (**Fig.1B**). After, we characterized the immune landscape in the splenic CLL TME, focusing on T cells as main mediators of the anti-tumor immune response *in vivo* (Sawant *et al.*, 2019). Interestingly, we found an increased number of CD8$^+$ effector T cells and CD4$^+$ conventional T cells in mice lacking EBI3, while the Tregs number remained stable (**Fig.1C**). Moreover, *Ebi3*$^{-/-}$ mice presented more effector (CD62L$^-$ CD44$^+$) and memory (CD62L$^+$ CD44$^+$) CD8$^+$ T cells, concomitant to a decrease in the frequency of naive cells (CD62L$^+$ CD44$^-$) (**Fig.1D**). In addition, we observed an increased frequency in Ki-67$^+$ CD8$^+$ T cells in *Ebi3*$^{-/-}$ mice (**Fig.1E**). While some immune checkpoints (IC) are expressed by activated CD8$^+$ T cells, only terminally exhausted cells co-express several IC (Palma *et al.*, 2017). Here, we observed an increased percentage of TIGIT$^+$ and PD1^{hi} CD8+ T cells, while no differences were observed in the frequency of PD1^{int} cells (**Fig.1F**). To analyze the functional status of CD8$^+$ T cells, we performed a hierarchical clustering of CD8$^+$ T cells based on marker expression. Seven CD8$^+$ T-cell clusters (C) were identified based on CD44, Ki-67, PD1, IFN-γ, TIGIT and CD62L (**Fig.1G and S1C**). As observed with the conventional FC analysis, in absence of *Ebi3,* there was a decrease in naïve CD8$^+$ T cells (C1) together with an increase in T_{mem} (C3) and T_{eff} cells showing high IC and Ki-67 (**Fig.1H and S1D**), suggesting an exhausted phenotype. As observed for CD8$^+$ T cells, the proportion of antigen-experienced CD4$^+$ conventional T cells (Tconv) was also increased (**Fig.S1E**). Moreover, activated Tregs (aTregs, CD62L$^-$ CD44$^+$, **Fig.S1F**) from leukemic *Ebi3*$^{-/-}$ mice display higher levels of TIGIT and KLRG1 along with increased Ki-67 positivity, thus exhibiting an enhanced immunosuppressive and proliferative phenotype. Clustering of CD4$^+$ T cells revealed the presence of nine clusters (**Fig.S1G-H**), showing that activated and immunosuppressive Tregs were expanded in absence of *Ebi3*. Altogether, these findings suggest an anti-tumor role of EBI3 during CLL development, as its depletion enhances tumor growth, promotes CD8$^+$ T-cell exhaustion and increases Treg immunosuppression.

In parallel, we deeply characterized the immune landscape in *Ebi3*$^{+/+}$ and *Ebi3*$^{-/-}$ mice to confirm that the aforementioned differences in CLL growth were not due to major intrinsic differences between the transgenic strains. We used *Foxp3*$^{YFP/Cre}$ mice to analyze T cells and Treg. As expected, immunophenotyping of *Foxp3*$^{YFP/Cre}$ and *Foxp3*$^{YFP/Cre}$ *Ebi3*$^{-/-}$ splenocytes did not reveal any major difference between *Ebi3*$^{+/+}$ and *Ebi3*$^{-/-}$ mice. We found no statistical differences in the frequency of T cells, NK cells, NK-T cells nor myeloid cells between groups (**Fig.S2A**). Moreover, the analysis of the myeloid cell compartment showed no differences in the frequency of neutrophils, dendritic cells, monocytes nor macrophages (**Fig.S2B**). Only a slight increase/decrease in the frequencies of CD8$^+$ T cells and CD4$^+$ Tconv cells, respectively, was observed, with no differences for Tregs (**Fig.S2C**). To evaluate T-cell functionality between phenotypes, we isolated splenic CD4$^+$ and CD8$^+$ T cells and analyzed IC and cytokines expression following *ex vivo* stimulation for 4h. We did not observe any difference in the frequency of indicated IC and cytokines in CD8$^+$ T cells, CD4$^+$ Tconv cells, nor in Tregs (**Fig.S2D-F**). These results indicate that *Ebi3* depletion does not drastically impact immune cells distribution, effector cytokine secretion and IC expression in T cells, pointing towards a fundamental role of IL-27 in the tumor context rather than in physiological conditions.

2. EBI3 depletion in transgenic *Eμ-TCL1* mice affects mice survival.

To better understand the role of EBI3 during CLL development, we crossed the *Eμ-TCL1* mouse model (referred as T mice) with *Ebi3*$^{-/-}$ mice to generate the Eμ-TCL1 Ebi3$^{-/-}$ mouse model (referred as TE mice) that spontaneously develop CLL in the absence IL-27 production. As opposed to the TCL1 AT model, TE mice lack *Ebi3* expression in all cell types, including CLL cells. We observed a shorter survival for TE mice (median survival of 302 vs 351days, **Fig.2A**) and an increased percentage and number of CLL cells in the PB at earlier time point, although not statistically significant (**Fig.2B and S3A**). The analysis of the splenic TME following euthanasia indicated, despite a similar tumor load (**Fig.S3B-C**), an increased frequency of CD8$^+$ T cells among total T cells in leukemic TE mice (**Fig.2C**), as well as an increase in TIGIT$^+$ CD8$^+$ T cells (**Fig.2D**). Clustering analysis identified six clusters based on CD44, Ki-67, PD1, KLRG1, TIGIT and CD62L expression in CD8$^+$ T cells, as well as an enrichment in proliferative Ki67$^+$ CD8$^+$ T cells (**Fig.2E-F and S3D**). In addition, a general increase in CD8$^+$ T-cell subpopulations expressing several IC was observed in TE mice compared with their *Ebi3*$^{+/+}$ counterpart (clusters C1-C4, **Fig.S3E**), pointing towards a more exhausted phenotype of CD8$^+$ T cells in TE mice. Additionally, We observed a decrease in CD4$^+$ T cells percentage in leukemic mice lacking *Ebi3* compared to *Ebi3*$^{+/+}$ controls (**Fig.S3F**). More precisely, TE mice exhibited a decreased proportion of CD4$^+$ Tconv together with increased frequency of Treg (**Fig.S3G**), which were in turn immunosuppressive, as highlighted by higher expression of CD73 and CTLA4 in absence of *Ebi3*

(**Fig.S3H**). Unsupervised clustering revealed eight $CD4^+$ T-cell clusters (**Fig.S3I-K**). Of particular relevance, a cluster representing highly immunosuppressive Tregs (C1) was enriched in *Ebi3*-deficient leukemic mice. Immunophenotyping of T and TE CLL cells showed that the expression of immunosuppressive cytokines, MHC molecules, activation markers, and IC remained unchanged; suggesting that ebi3 depletion in CLL cells does not play a role in the observed phenotype. (**Fig.S3L**). To investigate whether the effects of *Ebi3* depletion observed *in vivo* were mediated by cells of the TME or by CLL cells themselves, we depleted *Ebi3* exclusively *in* CLL cells. For this purpose, we isolated CLL cells from spleens of diseased T and TE mice and injected them in recipient control $Ebi3^{+/+}$ mice. In this experimental setting, we could not observe any differences in tumor growth in mice injected with $Ebi3^{-/-}$ leukemic cells (**Fig.2G**). Altogether our results indicate that EBI3 depletion in cells of the TME and not in CLL cells favors CLL progression by impacting T-cell-mediated immunity.

3. Specific T-cell-EBI3 depletion promotes leukemia development.

As the AT of EBI3-depleted CLL cells did not impact tumor growth (**Fig.2G**) while substantial changes in T cells were observed upon EBI3 depletion in the AT model and *Eμ-TCL1* model (**Fig.1D-F** and **Fig.2C-D**), we proceeded to specifically investigate the impact of $Ebi3^{-/-}$ $CD3^+$ T cells on CLL development. We used $Rag2^{-/-}$ mice, deficient in producing mature T and B cells. $CD3^+$ T cells were isolated from the spleen of $Ebi3^{-/-}$ and $Ebi3^{+/+}$ mice and intravenously injected in recipient $Rag2^{-/-}$ mice. Recipient mice were subsequently adoptively transferred with *Eμ-TCL1* leukemic cells (**Fig.3A**). Monitoring of leukemic growth in the PB revealed that $Rag2^{-/-}$ mice injected with $Ebi3^{-/-}$ T cells showed an enhanced CLL development compared to mice injected with the WT counterpart (**Fig.3A**). Importantly, the differences observed between the two groups were not due to a variation in the T-cell number throughout the experiment (**Fig.3B**). Consistently, post-euthanasia analysis of the leukemic spleens showed an increase in the percentage of CLL cells in the $Ebi3^{-/-}$ group (**Fig.3C**). Regarding T cells, we did not observe any differences in the frequency of subpopulations (**Fig.3D**). Nonetheless, unsupervised analysis identified 9 clusters of $CD8^+$ T cells (**Fig.3E**), and revealed the expansion of activated/exhausted $CD8^+$ T cells in the mice injected with $EBI3^{-/-}$ $CD3^+$ T cells (**Fig.3F** and **Fig.S4A**). In addition, we identified an increased frequency of Tregs within the $CD4^+$ T-cell population (**Fig.S4B**), as well as a higher percentage $KLRG1^+$ Tregs (**Fig.S4C**). These results indicated an enhanced immunosuppressive ability of Tregs in absence of EBI3. Moreover, unsupervised clustering analysis of analyzing $CD4^+$ T cells identified an accumulation of activated and immunosuppressive Tregs in recipient mice injected with $Ebi3^{-/-}$ T cells (**Fig.S4E**).

4. CD8$^+$ T cells from *Ebi3*$^{-/-}$ mice have altered expression of genes involved in activation and functionality.

As our data demonstrates that IL-27 controls CLL development in a T-cell-mediated mechanism *in vivo*, we proceeded to investigate the transcriptional differences between T cells from *Ebi3*$^{+/+}$ and *Ebi3*$^{-/-}$ mice after *ex vivo* activation (**Fig.4A**). Among the upregulated genes in CD8$^+$ T cells, we identified *Profilin-1* (*Pfn1*) (**Fig.4B-C**), an actin-binding protein and a negative regulator of effector T-cell-mediated cytotoxicity (Schoppmeyer *et al.*, 2017). Amidst the downregulated genes, we found several transmembrane transporters known to mediate T-cell activation (Ren *et al.*, 2017b) (*Slc2a8* and *Slc7a5*, **Fig.4D**). An ontology analysis indicated a reprograming of crucial functions as translation initiation and rRNA processing (**Fig.S5A**). We also compared the gene expression profile with transcriptional signatures of exhausted CD8$^+$ T-cell subsets previously published (Beltra *et al.*, 2020a). We observed that *Ebi3*$^{-/-}$ CD8$^+$ T cells present similarities with progenitor CD8$^+$ exhausted T cells (Tex^{Prog}) but also with more terminally exhausted cells **(Fig.S5B-C)**. Indeed, looking at the third component of the PCA, explaining 13% of the variability, indicated that Ebi3$^{-/-}$ T cells and Tex^{term} present similar gene expression profiles (**Fig.S5C right panel**). Therefore, we selected genes described to mirror T-cell activation and exhaustion and we observed that Ebi3$^{-/-}$ T cells clustered between progenitor and terminally exhausted T cells (**Fig.4E**). The expression of these marker genes also showed differences between *Ebi3*$^{+/+}$ and *Ebi3*$^{-/-}$ T cells, mostly for Tox, Tbet, Il7r, Ccr1 and Pfn1 (**Fig.4F**). Regarding CD4$^+$ Tconv and Treg compartments, gene expression analysis revealed no differences between groups (**Fig.S5D-E**), suggesting that, in absence of *Ebi3*, effector CD8$^+$ T cells are the major T-cell population affected and are less functional when activated *in vitro*.

5. *Ebi3*$^{-/-}$ CD8$^+$ T cells present impacted cytotoxic activity while IL-27 enhances their potential both in murine and human settings.

To functionally characterize *Ebi3*$^{-/-}$ and *Ebi3*$^{+/+}$ CD8$^+$ T cells and validate the gene expression data, we performed *ex vivo* activation of CD3$^+$ T cells for 3 days and analyzed CD8$^+$ T cells by FC and confocal microscopy (**Fig.5A**). In line with previous findings, after 3 days, we could observe a decrease in TOX abundance in *Ebi3*$^{-/-}$ CD8$^+$ T cells (**Fig.5B**). Very interestingly, we could not observe any difference in cytokine production between the two conditions (**Fig.S6A**), whereas after 6 days, *Ebi3*$^{-/-}$ CD8$^+$ T cells presented decreased production of IL-2 and IFN-γ compared to WT cells (**Fig.5C**). Clustering analysis of CD8$^+$ T cells co-expressing different cytokines (C3) appeared significantly reduced (**Fig.5E and S6B-C**), confirming that in absence of *Ebi3*, CD8$^+$ T cells are less polyfunctional. After 6 days of activation, we quantified Profilin1 protein level in CD8$^+$ T cells by immunofluorescence (**Fig.5A**). As expected, the analysis revealed an increase in Profilin1 in *Ebi3*$^{-/-}$ CD8$^+$ T cells (**Fig.5F**). To assess if IL-27 could indeed affect the cytotoxic capabilities of CD8$^+$ T cells,

we performed a cytotoxic assay with WT CD8$^+$ T cells treated with IL-27 for 48h (**Fig.5G**), and sAg-loaded Eμ-TCL1 CLL cells as target cells. We noted an increased cytotoxic ability of CD8$^+$ T cells in presence of IL-27 (**Fig.5G**). To inspect whether the effect of IL-27 on CD8$^+$ T-cell was conserved in human cells, we purified and activated T cells from PBMCs of four healthy donors, and then cultured them in presence or absence of IL-27 for 6 days (**Fig.5H**). T cells were co-cultured with target cells for 30h and the killing efficiency of CD8$^+$ T cells during co-culture was quantified. In line with previous results, we observed a decrease in the percentage of live target cells (**Fig.5I** and**S6D**), translated into an increased killing efficiency of human CD8$^+$T cells in presence of IL-27 for all donors (**Fig.5J**).

6. IL-27 level is reduced in the blood of leukemic mice and CLL patients and IL-27 neutralization enhanced CLL development.

The analysis of several publicly available gene expression datasets revealed a lower *Ebi3* expression in different immune populations between CLL patients and HC (**Fig.S7A**) and between leukemic Eμ-TCL1 and WT mice (**Fig.S7B**). Since a number of studies indicate that IL-27 exerts a direct inhibitory effect on malignant cells (Kachroo *et al.*, 2013), we wanted to assess whether IL-27 could also have a direct anti-tumor effect on CLL cells. Thus, we treated both patient and mouse CLL *samples ex vivo* for 48h with different concentrations of human and murine IL-27 respectively (25 and 50 ng/mL) **(Fig.S7C-F)**. Viability and expression of key immunosuppressive markers were assessed by FC. For all the experiments performed, neither the apoptosis rate nor the expression of immunosuppressive markers of the leukemic cells were significantly altered, suggesting that IL-27 does not impact the viability and the phenotype of CLL cells.

To support our results on *Ebi3* genetic deletion and confirm the implication of IL-27 in CLL progression, we depleted IL-27 *in vivo* in C57BL/6 mice before injecting TCL1 cells. Monitoring leukemic growth in the PB revealed an increase in CLL in mice depleted for IL-27 (**Fig.6C**), consistent with a higher number of CLL cells in the spleen following euthanasia (**Fig.6D**). Despite not observing differences in the frequency of CD8$^+$ T cells between groups, clustering analysis confirmed the enrichment of proliferative and activated CD8$^+$ T cells (Ki-67$^+$ CD44^{hi}) (**Fig.6F-G and S8A-B**), similarly to the adoptive transfer in *Ebi3*$^{-/-}$ mice (Fig.1E). Moreover, we observed a significant decrease in the percentage of CD4$^+$ T cells (**Fig.S8C**), even though the frequencies of Tconv and Treg within the CD4$^+$ T-cell compartment were unaltered between the two groups (**Fig.S8D**). Importantly, Tregs appeared more suppressive and proliferative in IL-27-depleted mice, as demonstrated by the increased percentage of KLRG1 and Ki-67-expressing Tregs (**Fig.S8E**). Analysis of CD4$^+$ T cells confirmed the increased immunosuppressive and activated phenotype of Tregs in absence of IL-27 in recipient mice (**Fig.S8F-G**).

Figure 1

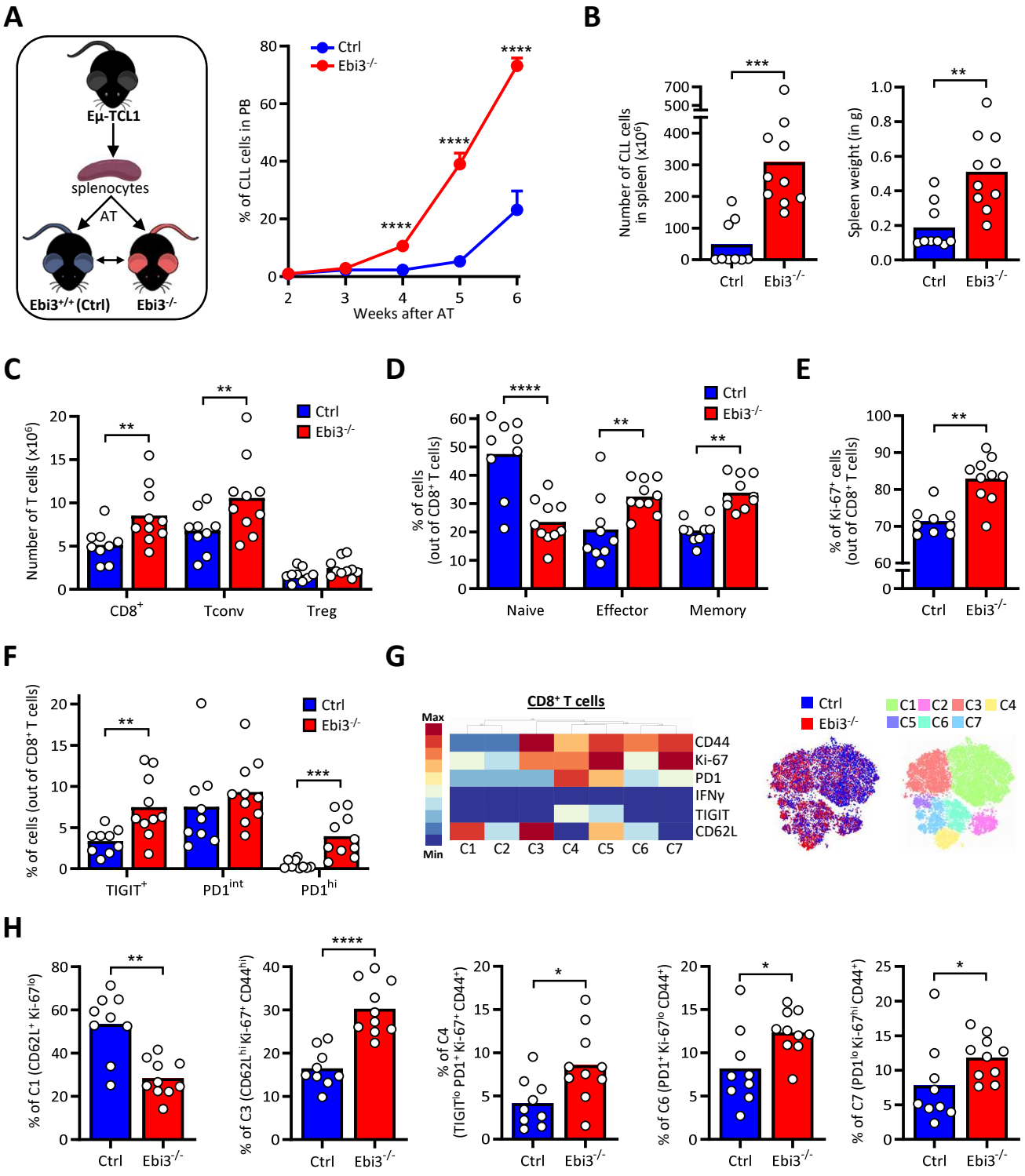
A
Eμ-TCL1
splenocytes
AT
Ebi3+/+ (Ctrl)
Ebi3-/-
% of CLL cells in PB
Ctrl
Ebi3-/-
Weeks after AT
B
Number of CLL cells in spleen (x10^6)
Spleen weight (in g)
C
Number of T cells (x10^6)
CD8+
Tconv
Treg
D
% of cells (out of CD8+ T cells)
Naive
Effector
Memory
E
% of Ki-67+ cells (out of CD8+ T cells)
F
% of cells (out of CD8+ T cells)
TIGIT+
PD1int
PD1hi
G
CD8+ T cells
Max
Min
CD44
Ki-67
PD1
IFNγ
TIGIT
CD62L
C1
C2
C3
C4
C5
C6
C7
H
% of C1 (CD62L+ Ki-67lo)
% of C3 (CD62Lhi Ki-67+ CD44hi)
% of C4 (TIGITlo PD1+ Ki-67+ CD44+)
% of C6 (PD1+ Ki-67lo CD44+)
% of C7 (PD1lo Ki-67hi CD44+)

Figure 2

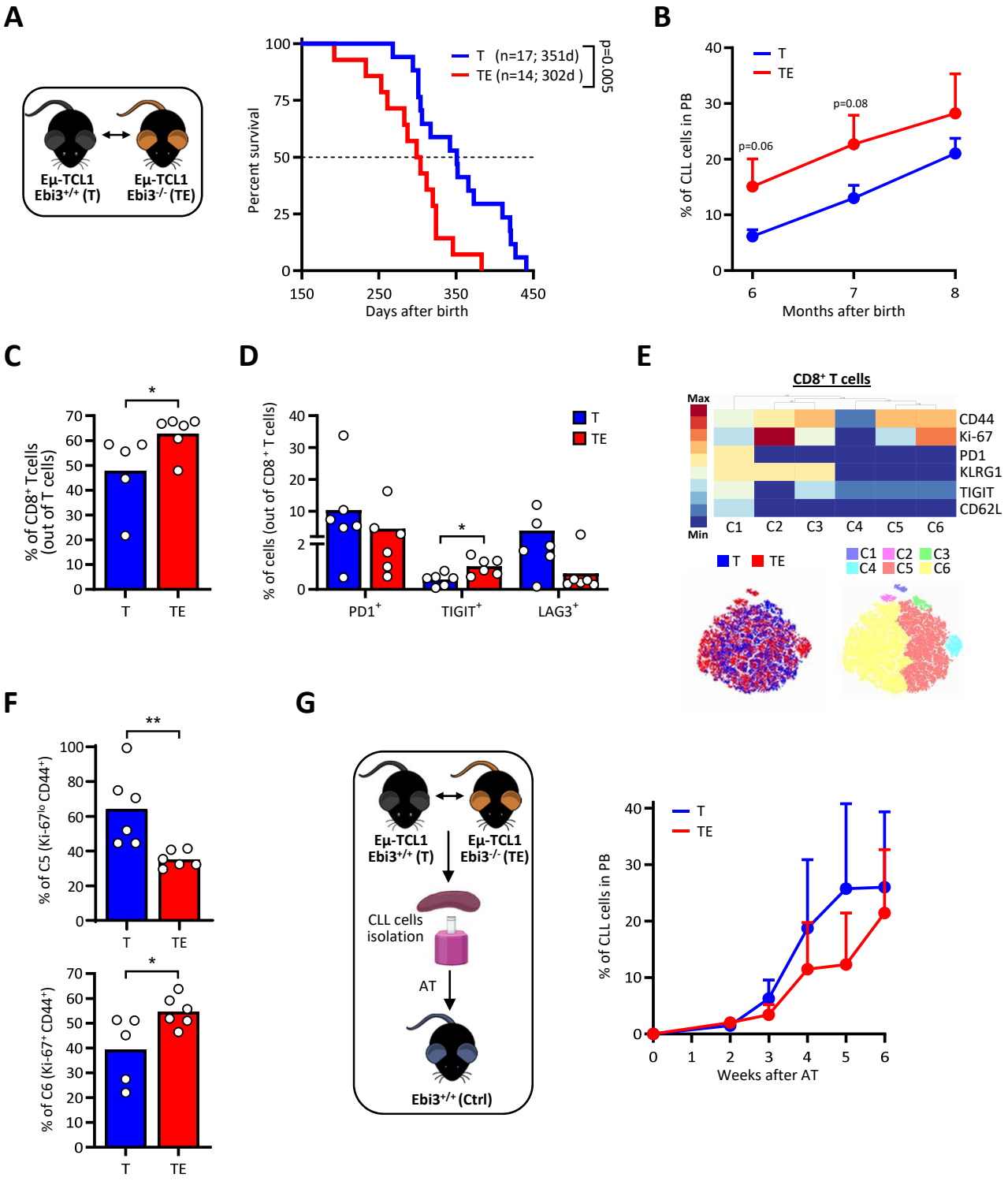
A
Eμ-TCL1 Ebi3+/+ (T)
Eμ-TCL1 Ebi3-/- (TE)
Percent survival
Days after birth
T (n=17; 351d)
TE (n=14; 302d)
p=0.005
B
% of CLL cells in PB
Months after birth
p=0.06
p=0.08
C
% of CD8+ Tcells (out of T cells)
D
% of cells (out of CD8+ T cells)
PD1+
TIGIT+
LAG3+
E
CD8+ T cells
Max
Min
CD44
Ki-67
PD1
KLRG1
TIGIT
CD62L
C1 C2 C3 C4 C5 C6
F
% of C5 (Ki-67lo CD44+)
% of C6 (Ki-67+ CD44+)
G
CLL cells isolation
AT
Ebi3+/+ (Ctrl)
Weeks after AT

Figure 3

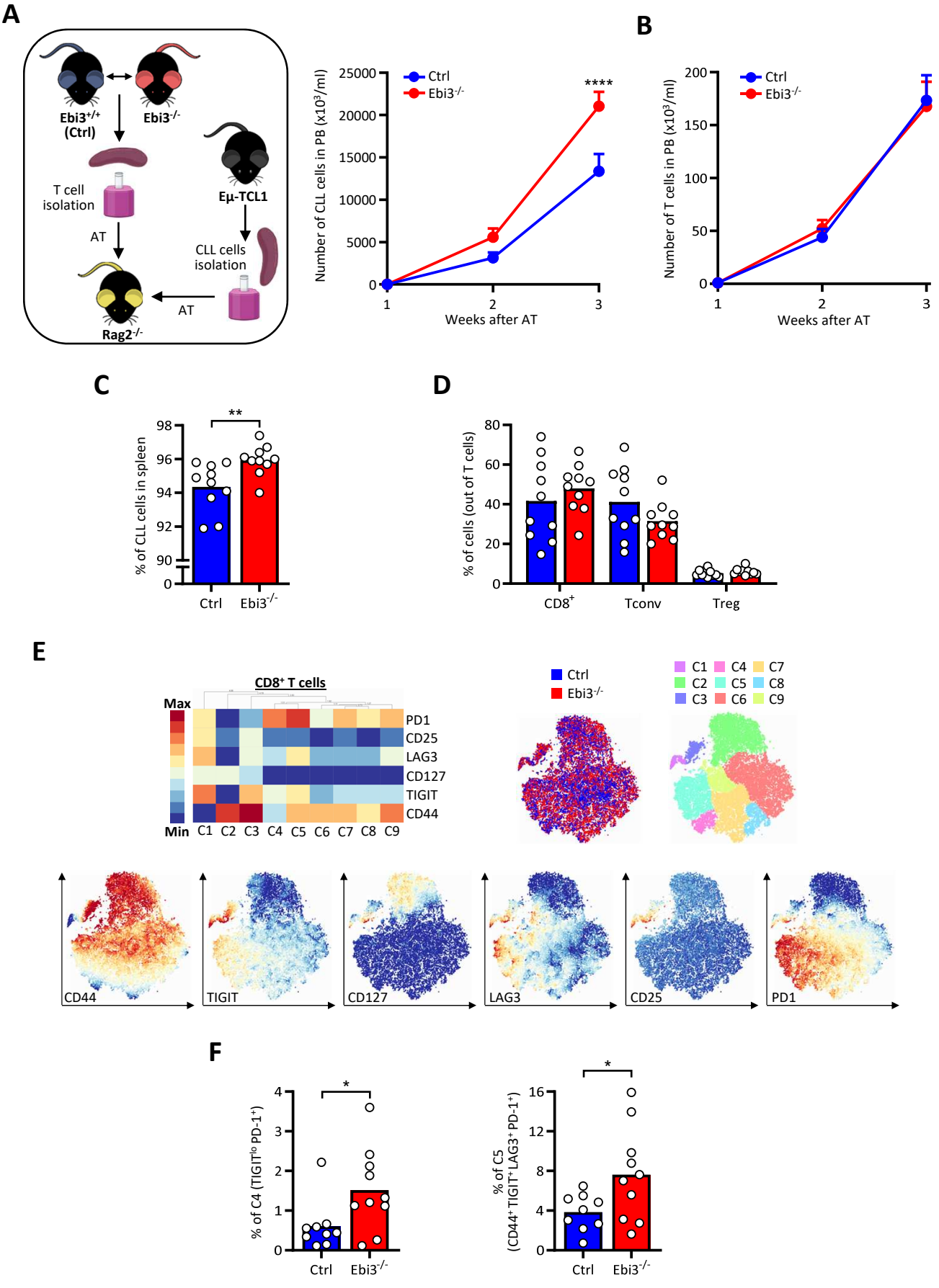
A
Ebi3+/+ (Ctrl)
Ebi3-/-
T cell isolation
AT
Eμ-TCL1
CLL cells isolation
AT
Rag2-/-
B
Number of CLL cells in PB (x10³/ml)
Ctrl
Ebi3-/-
****
Weeks after AT
Number of T cells in PB (x10³/ml)
Weeks after AT
C
% of CLL cells in spleen
**
Ctrl
Ebi3-/-
D
% of cells (out of T cells)
CD8+
Tconv
Treg
E
CD8+ T cells
Max
Min
PD1
CD25
LAG3
CD127
TIGIT
CD44
C1 C2 C3 C4 C5 C6 C7 C8 C9
Ctrl
Ebi3-/-
CD44
TIGIT
CD127
LAG3
CD25
PD1
F
% of C4 (TIGITlo PD-1+)
*
% of C5 (CD44+ TIGIT+ LAG3+ PD-1+)
*

Figure 4

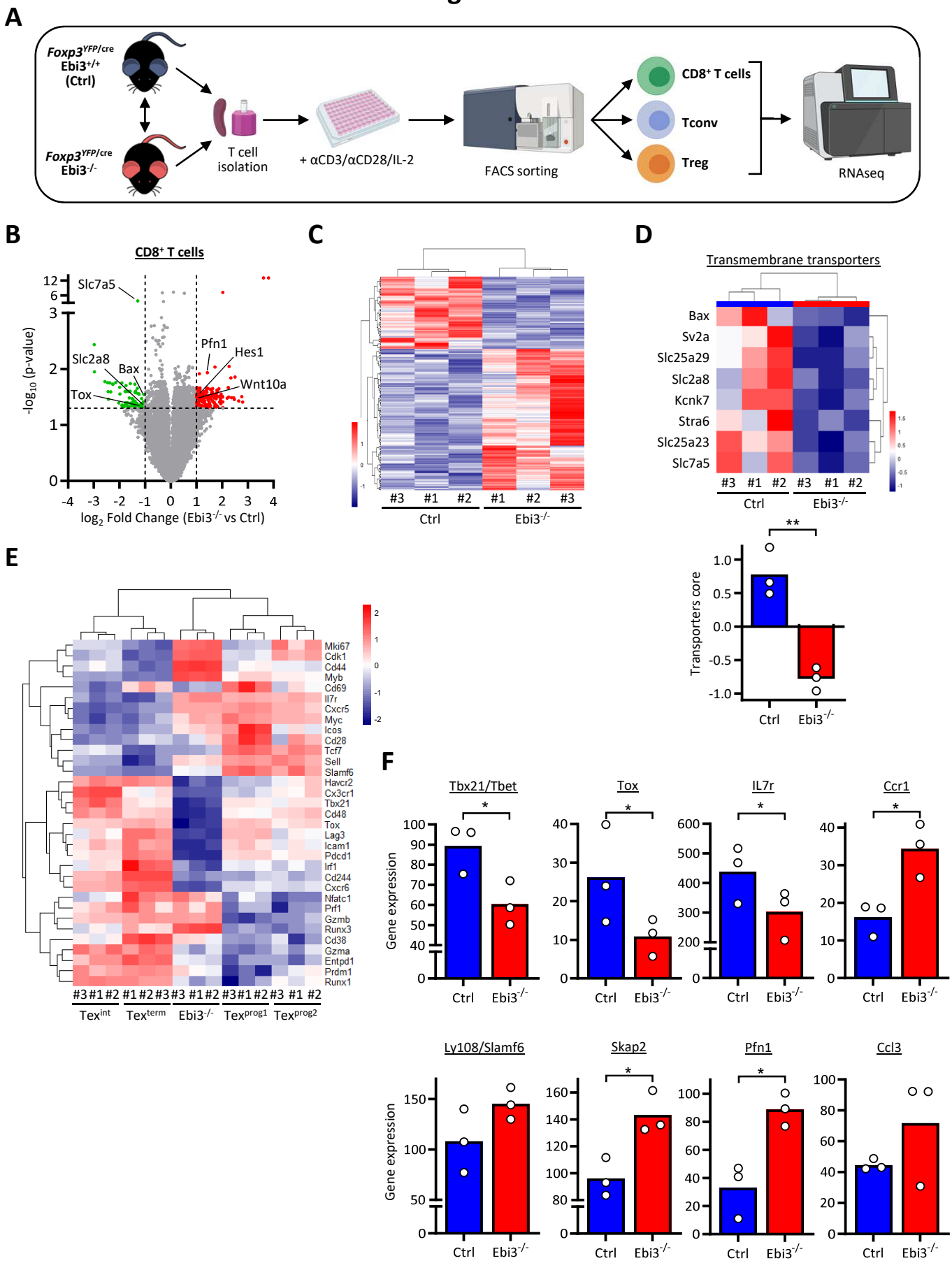
A
Foxp3YFP/cre Ebi3+/+ (Ctrl)
Foxp3YFP/cre Ebi3-/-
T cell isolation
+ αCD3/αCD28/IL-2
FACS sorting
CD8+ T cells
Tconv
Treg
RNAseq
B
CD8+ T cells
-log10 (p-value)
log2 Fold Change (Ebi3-/- vs Ctrl)
Slc7a5
Slc2a8
Bax
Tox
Pfn1
Hes1
Wnt10a
C
Ctrl
Ebi3-/-
D
Transmembrane transporters
Bax
Sv2a
Slc25a29
Slc2a8
Kcnk7
Stra6
Slc25a23
Slc7a5
Transporters core
E
Mki67
Cdk1
Cd44
Myb
Cd69
Il7r
Cxcr5
Myc
Icos
Cd28
Tcf7
Sell
Slamf6
Havcr2
Cx3cr1
Tbx21
Cd48
Tox
Lag3
Icam1
Pdcd1
Irf1
Cd244
Cxcr6
Nfatc1
Prf1
Gzmb
Runx3
Cd38
Gzma
Entpd1
Prdm1
Runx1
Texint
Texterm
Ebi3-/-
Texprog1
Texprog2
F
Tbx21/Tbet
Tox
IL7r
Ccr1
Ly108/Slamf6
Skap2
Pfn1
Ccl3
Gene expression

Figure 5

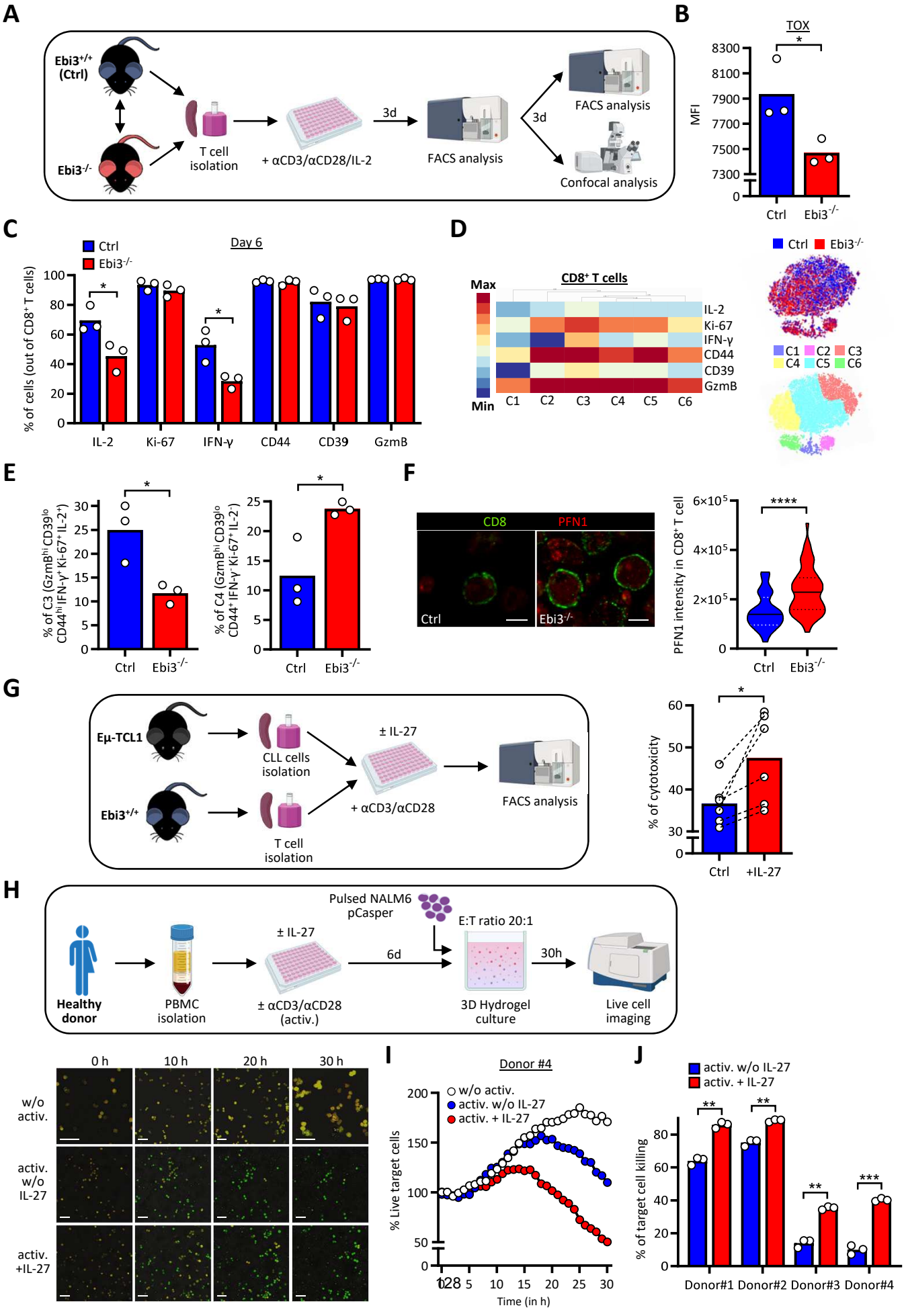
A
Ebi3+/+ (Ctrl)
Ebi3-/-
T cell isolation
+ αCD3/αCD28/IL-2
3d
FACS analysis
3d
FACS analysis
Confocal analysis
B
TOX
MFI
Ctrl
Ebi3-/-
C
Day 6
Ctrl
Ebi3-/-
% of cells (out of CD8+ T cells)
IL-2
Ki-67
IFN-γ
CD44
CD39
GzmB
D
CD8+ T cells
Max
Min
IL-2
Ki-67
IFN-γ
CD44
CD39
GzmB
C1
C2
C3
C4
C5
C6
E
% of C3 (GzmBhi CD39lo CD44hi IFN-γ+ Ki-67+ IL-2+)
% of C4 (GzmBhi CD39lo CD44+ IFN-γ- Ki-67+ IL-2-)
Ctrl
Ebi3-/-
F
CD8
PFN1
Ctrl
Ebi3-/-
PFN1 intensity in CD8+ T cell
G
Eμ-TCL1
Ebi3+/+
CLL cells isolation
T cell isolation
± IL-27
+ αCD3/αCD28
FACS analysis
% of cytotoxicity
Ctrl
+IL-27
H
Healthy donor
PBMC isolation
± IL-27
± αCD3/αCD28 (activ.)
Pulsed NALM6 pCasper
6d
E:T ratio 20:1
3D Hydrogel culture
30h
Live cell imaging
0 h
10 h
20 h
30 h
w/o activ.
activ. w/o IL-27
activ. +IL-27
I
Donor #4
w/o activ.
activ. w/o IL-27
activ. + IL-27
% Live target cells
Time (in h)
J
activ. w/o IL-27
activ. + IL-27
% of target cell killing
Donor#1
Donor#2
Donor#3
Donor#4

Figure 6

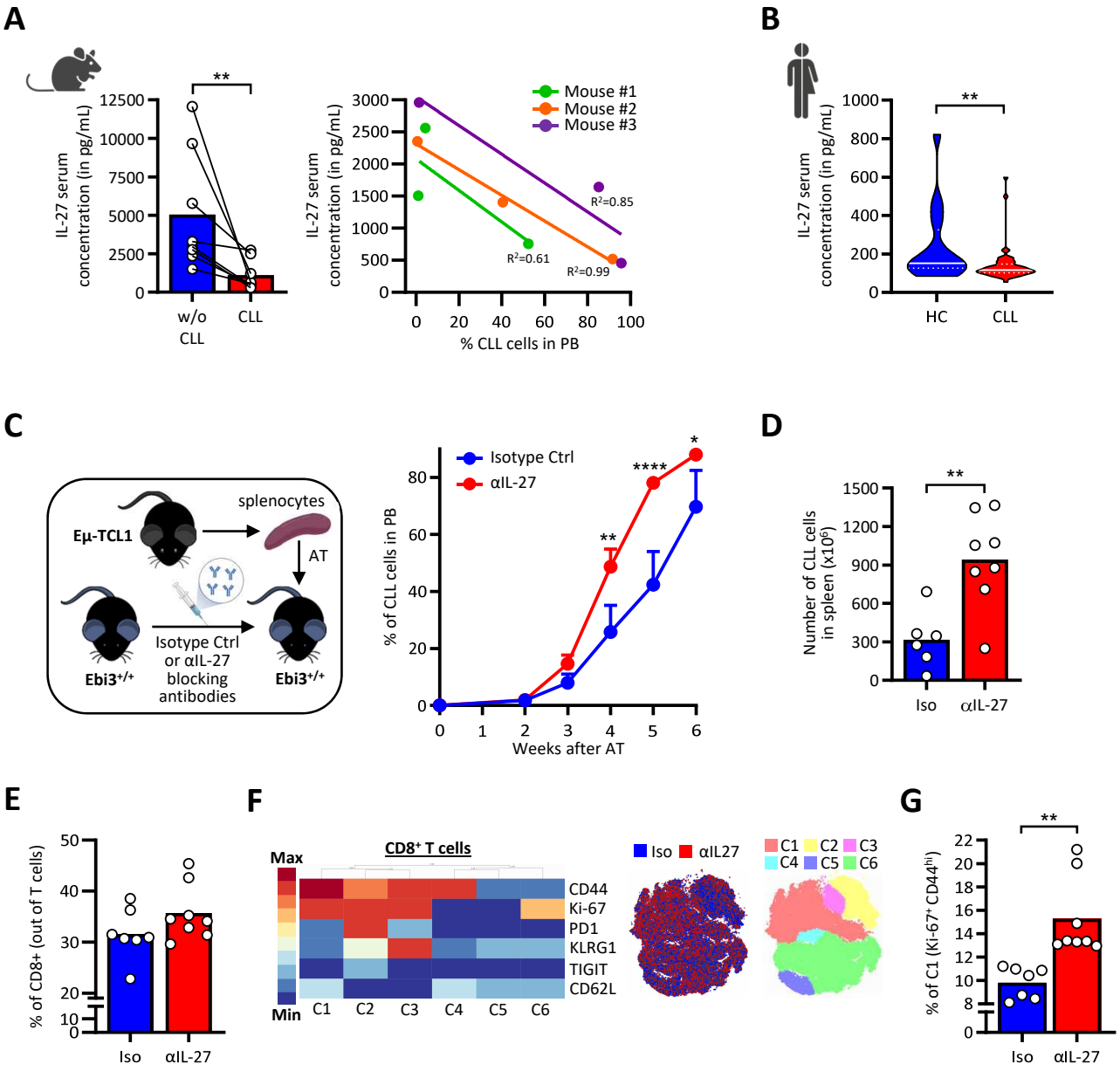
A
B
C
D
E
F
G
IL-27 serum concentration (in pg/mL)
w/o CLL
CLL
Mouse #1
Mouse #2
Mouse #3
R²=0.85
R²=0.61
R²=0.99
% CLL cells in PB
HC
splenocytes
Eμ-TCL1
AT
Isotype Ctrl or αIL-27 blocking antibodies
Ebi3+/+
Isotype Ctrl
αIL-27
% of CLL cells in PB
Weeks after AT
Number of CLL cells in spleen (x10⁶)
Iso
αIL-27
% of CD8+ (out of T cells)
CD8⁺ T cells
Max
Min
CD44
Ki-67
PD1
KLRG1
TIGIT
CD62L
C1
C2
C3
C4
C5
C6
% of C1 (Ki-67⁺ CD44ʰⁱ)

Figure legends:

Figure 1: EBI3 depletion promotes leukemia development and induces an enhanced immunosuppressive tumor microenvironment.

(A) Two cohorts of recipient *Ebi3* $^{-/-}$ and Ctrl mice were injected with splenocytes isolated from leukemic *Eμ-TCL1* mice. Two weeks after adoptive transfer (AT), mice were bled weekly to monitor CLL development in peripheral blood (PB). Percentages of circulating neoplastic $CD5^+$ $CD19^+$ cells were detected by flow cytometry (FC); (n=18 for Ctrl and n=19 for *Ebi3*$^{-/-}$, two-way ANOVA). **(B-H).** For the second experimental cohort, splenic TME was characterized by FC (n=9 for Ctrl and n=10 for *Ebi3*$^{-/-}$). **(B)** Number of $CD5^+$ $CD19^+$ CLL cells in the spleen (left), and spleen weight (right) in *Ebi3*$^{-/-}$ compared to Ctrl mice. **(C)** Cell numbers of $CD8^+$ T cells, $CD4^+$ Tconv, and Tregs in the spleen are compared between the two groups. **(D)** Frequency of cells with a naive ($CD62L^+$ $CD44^-$), effector ($CD62L^-$ $CD44^+$) or memory ($CD62L^+$ $CD44^+$) phenotype among $CD8^+$ effector T cells. **(E)** Percentage of proliferative Ki-67^+ cells among $CD8^+$ effector T cells in the spleen of Ctrl and *Ebi3*$^{-/-}$ mice. **(F)** Frequency of the indicated populations in Ctrl and *Ebi3*$^{-/-}$ $CD8^+$ T cells. **(G)** HSNE clustering analysis of Ctrl and *Ebi3*$^{-/-}$ $CD8^+$ T cells based on CD44, Ki-67, PD1, IFN-γ, TIGIT and CD62L expression measured by FC. **(H)** Percentages of cluster distribution on Ctrl and *Ebi3*$^{-/-}$ $CD8^+$ T cells. Unpaired t test, * $P< .05$, ** $P< .01$, *** $P< .001$, **** $P< .0001$.

Figure 2: EBI3 depletion in transgenic Eμ-TCL1 mice affects mice survival.

(A) Transgenic *Eμ-TCL1* mice were crossed with *Ebi3*$^{-/-}$ mice to obtain leukemic mice deficient in IL-27. Starting at 6 months after birth, mice were bled every month to evaluate peripheral disease development. (T= *Eμ-TCL1* mice; TE= *Eμ-TCL1 Ebi3*$^{-/-}$ mice). Mouse survival was compared between groups (survival curve analysis). **(B)** Percentages of circulating neoplastic $CD5^+$ $CD19^+$ cells were detected by flow cytometry (FC) in peripheral blood (PB) (n=17 for T mice and n=14 for TE mice, two-way ANOVA test). **(C-G)** Leukemic T and TE mice were euthanized and their splenocytes were analyzed using FC. **(C)** Percentage of $CD8^+$ T cells in Ctrl and *Ebi3*$^{-/-}$ $CD3^+$ T cells. **(D)** Frequency of the indicated populations in T and TE $CD8^+$ T cells. (n=6 for T group and n=6 for TE group). **(E-F)** HSNE clustering analysis of T and TE $CD8^+$ T cells based on CD44, Ki-67, PD1, KLRG1 and CD62L expression measured by FC. **(E)** Heatmap comprising the clusters generated by HSNE and HSNE plots depicting the expression of each individual marker. **(F)** Percentages of $CD8^+$ T-cell clusters distribution in T and TE mice. **(G)** Leukemic *Eμ-TCL1* mice and *Eμ-TCL1 Ebi3* $^{-/-}$ mice were euthanized, and CLL cells were isolated from splenocytes. Isolated CLL cells were adoptively transferred into WT mice. Recipient mice were bled weekly to evaluate peripheral disease development. Percentages of circulating neoplastic $CD5^+$ $CD19^+$ cells were detected by FC. (n=12 mice divided in 6 groups. Each

group of 2 animals received one independent CLL clone coming from diseased T or TE mice). Unpaired t test, * *P*< .05, ** *P*< .01.

Figure 3: Specific T-cell-EBI3 depletion promotes leukemia development.

(A) Ctrl and *Ebi3*$^{-/-}$ mice were euthanized, and CD3^{+} T cells were isolated from the splenocytes. Recipient *Rag2*$^{-/-}$ mice were injected with either Ctrl (n=10) or *Ebi3*$^{-/-}$ CD3^{+} T cells (n=10) and subsequently injected with splenocytes derived from leukemic *Eμ-TCL1* mice. Experimental mice were bled weekly to evaluate peripheral disease development. Number of circulating neoplastic CD5^{+} CD19^{+} cells is shown in the two groups (two-way ANOVA test). **(B)** Number of circulating T cells in recipient *Rag2*$^{-/-}$ mice injected with either Ctrl or *Ebi3*$^{-/-}$ CD3^{+} T cells **(C)** Percentage of CLL cells in the spleen of recipient *Rag2*$^{-/-}$ mice **(D)** Percentage of CD8^{+}, Tconv, and regulatory T cells among the injected Ctrl and *Ebi3*$^{-/-}$ CD3^{+} T cells. **(E-F)** HSNE clustering analysis of Ctrl and *Ebi3*$^{-/-}$ CD8^{+} T cells based on PD1, CD25, LAG3, CD127, TIGIT and CD44 expression measured by FC. **(E)** Heatmap comprising the clusters generated by HSNE analysis (top) and HSNE plots depicting the expression of each individual marker (bottom). **(F)** Percentages of cluster distribution on WT and *Ebi3*$^{-/-}$ CD4^{+} T cells. Unpaired t test, * P< .05, **** *P*< .0001.

Figure 4: CD8^{+} T cells from *Ebi3*$^{-/-}$ mice have altered expression of genes involved in activation and functionality.

(A) *Foxp3*$^{YFP/Cre}$ and *Foxp3*$^{YFP/Cre}$ *Ebi3*$^{-/-}$ mice (n=3 per group) were euthanized at 8 weeks of age and CD3^{+} T cells were isolated from the splenocytes. T cells were activated for 72 hours, sorted into CD8^{+} T cells, CD4^{+} Tconv, and Tregs (YFP^{+}) by FC, and subjected to RNA sequencing. **(B)** Volcano plot depicting differentially expressed genes (DEG) between Ctrl and *Ebi3*$^{-/-}$ CD8^{+} T cells. **(C)** Heatmap comparing the transcriptome of Ctrl and *Ebi3*$^{-/-}$ CD8^{+} T cells. **(D)** Heatmap and score of transmembrane transporters in Ctrl and *Ebi3*$^{-/-}$ CD8^{+} T cells. **(E)** Heatmap depicting the similarity of *Ebi3*$^{-/-}$ CD8^{+} T cells with the subset of proliferating progenitor exhausted T cells described in (Beltra *et al.*, 2020b). **(F)** Expression profiles of single genes in CD8^{+} T cells from Ctrl and *Ebi3*$^{-/-}$ mice. Unpaired t test, * *P*< .05, ** *P*< .01.

Figure 5: *Ebi3*$^{-/-}$ CD8^{+} T cells present impacted cytotoxic activity while IL-27 enhances their potential both in murine and human.

(A) Ctrl and *Ebi3*$^{-/-}$ mice (n=3 per group) were euthanized at 8 weeks and CD3^{+} T cells were isolated from splenocytes. T cells were activated *in vitro* for 6 days and analyzed after 3 days by FC and after 6 days by FC and confocal microscopy. **(B)** MFI of TOX in Ctrl vs *Ebi3*$^{-/-}$ CD8^{+} T cells after 3 days of activation. **(C)** Frequency of cells expressing the selected markers in Ctrl vs *Ebi3*$^{-/-}$ CD8^{+} T cells after

6 days of activation. **(D-E)** HSNE clustering analysis of Ctrl and *Ebi3*$^{-/-}$ CD8^{+} T cells based on IL-2, Ki-67, IFN-γ, CD44, CD39 and Granzyme B expression measured by FC. **(D)** Heatmap comprising the clusters generated by HSNE and HSNE plots depicting the expression of each individual marker. **(E)** Percentages of CD8^{+} T-cell cluster distribution on WT vs *Ebi3*$^{-/-}$ CD8^{+} T cells. **(F)** Detection and quantification of Profilin1 (red) between Ctrl vs *Ebi3*$^{-/-}$ activated CD8^{+} T cells (green) after 6 days of activation (scale bar, 5µm). **(G)** *In vitro* cytotoxic assay. CD3^{+} T cells were isolated from Ctrl mice (n=6) and incubated with or without IL-27 for 48h (left). TCL1-derived CLL cells loaded with the sAg were co-cultured with T cells for 4h and stained to investigate cytotoxicity efficiency by FC (right). **(H)** Experimental design of the 3D killing assay. Human PBMCs were isolated from four healthy donors and activated *in vitro* for 6 days in presence or absence of rhIL-27. At day 6, pulsed NALM6 cells transfected with the viability pCasper vector were added to the culture for 30h and live cell imaging was recorded. (scale bar, 50µm) **(I)** Percentage of living target cells was calculated in the 3 conditions (activated PBMCs only, and in presence or absence of IL-27). Representative plot of one donor. **(J)** Bar chart showing the percentage of living target cells 10 hours after the start of the killing activity of CD8^{+} T cells. Unpaired t test, * P< .05, ** P< .01, *** P< .001, **** *P*< .0001.

Figure 6: IL-27 level is reduced in the blood of leukemic mice and CLL patients and IL-27 neutralization enhanced CLL development as observed in *Ebi3*$^{-/-}$ mice. (A) (Left) Serum levels of IL-27 in mice before and after CLL development. (Right) Correlation between IL-27 serum levels and CLL development in mice measured by ELISA. **(B)** Serum levels of IL-27 in CLL patients (n=53) and healthy controls (n=16) measured by ELISA. **(C-G)** A cohort of recipient Ctrl mice was i.p. injected with α-IL-27 or isotype control antibodies and subsequently adoptively transferred with splenocytes from leukemic *Eμ-TCL1* mice. Mice were bled weekly to evaluate peripheral disease development. The injection of antibodies was maintained once per week until euthanasia. Percentages of circulating leukemic CD5^{+} CD19^{+} cells in the two groups (n=7 for isotype group and n=8 for α-IL-27 group, two-way ANOVA test. **(D-G)** Mice were euthanized and their splenocytes were analyzed by FC. **(D)** Number of CLL cells in the spleen of both experimental conditions. **(E)** Percentage of CD8^{+} T among total T cells. **(F-G)** HSNE clustering analysis of CD8^{+} T cells from isotype- and α-IL-27-treated mice based on CD44, Ki-67, PD1, KLRG1, TIGIT and CD62L expression measured by FC. **(F)** Heatmap comprising the clusters generated by HSNE and HSNE plots depicting the expression of each individual marker. **(G)** Distribution of cluster C1 among CD8^{+} T cells from isotype- and α-IL-27- treated mice. Unpaired t test, * P< .05, ** P< .01, **** P< .0001.

Discussion

Given the pleiotropic function of IL-27 in the tumorigenesis of multiple solid and hematologic malignancies, we investigated the role of this cytokine in the development and progression of CLL. Using a wide range of mouse models and patient samples, we demonstrated that IL-27 has a striking anti-tumoral role in CLL pathobiology. Moreover, we explored the microenvironment, cellular, and transcriptional mediators responsible for this observation.

A number of studies have previously assessed the role of IL-27 in chronic lymphocytic leukemia using a variety of cell lines and clinical samples (Hemati *et al.*, 2020; Jia *et al.*, 2016; Manouchehri-Doulabi *et al.*, 2020). Nevertheless, the existing research remains contradictory and inconclusive. Here, using adoptive transfer of TCL1 leukemia cells in C57BL/6 as well as transgenic mouse models, we demonstrate for the first time that the lack of IL-27 results in a much faster CLL development and earlier death. Additionally, extensive phenotypic characterization of the splenic immune subsets revealed an increasingly immunosuppressive TME in the absence of IL-27, suggesting that this cytokine has a role in modulating the anti-tumor response in CLL.

In line with the varying effects of IL-27 reported in the literature, the serum levels of this cytokine have been found to be either significantly elevated or decreased in a wide range of malignancies (Diakowska *et al.*, 2013; Duan *et al.*, 2015; Lu *et al.*, 2014), contributing to disease progression or control respectively. In consonance with our previous findings, our data revealed a significant and consistent decrease of IL-27 serum levels as CLL progresses in both murine and patient samples. This observation highlights both the involvement of this cytokine in CLL development as well as further supports its anti-tumor role in this malignancy.

Even though the EBI3 subunit is shared by IL-35, EBI3-deficient C57BL/6 mice are often used to investigate the role of IL-27 as they reportedly result in a dominant IL-27-deficient phenotype due to the higher expression of IL-27 and the wider range of cells producing the cytokine. This is evidenced by the presence of functional Tregs expressing high levels of IL-10 (Fabbi *et al.*, 2017). Nevertheless, the interpretation of data obtained from KO mouse models of cytokine subunits or their receptors is often complicated due to the promiscuous usage of chains among the different members of each family. In order to overcome this source of variability, we further validated the role of IL-27 by neutralizing this cytokine in an *in vivo* leukemia model.

Previous studies reported a direct anti-tumor role of IL-27 in several tumors, including hematological malignancies such as pediatric AML and CLL (Manouchehri-Doulabi *et al.*, 2020; Zorzoli *et al.*, 2012). Nonetheless, our data indicated that there are no significant changes in the viability or phenotype of murine and patient CLL cells, both *in vivo* and following *in vitro* treatment with IL-27. Alternatively, we provided evidence that T cells are the main mediators in the observed

enhanced CLL development in the absence of IL-27, as $CD3^+$ T cells controlled CLL development more efficiently in the presence of this cytokine.

The T-cell compartment has a critical function in anti-tumor immunity, and has been widely reported to show a significant functional impairment in CLL (Roessner and Seiffert, 2020). Using gene expression analysis, we identified transcriptional changes in $CD8^+$ T cells in presence or absence of IL-27. Interestingly, we detected a decreased expression of crucial transporters key in T-cell activation, proliferation, and cytotoxicity, most notably SLC7a5, which could potentially contribute to the altered T-cell activity described in the IL-27 depleted environment. Moreover, the expression of profilin-1, a known inhibitor of T-cell synapse formation (Schoppmeyer *et al.*, 2017), was dramatically increased in this setting. Altogether, these results suggest that the progressively decreasing levels of IL-27 in CLL patients leads to dysfunctional T-cell dynamics through different mechanisms, including the downregulation of crucial metabolic pathways and the inability to mount an appropriate immune response due to the lack of a functional lytic immune synapse.

A number of studies suggest that the immune enhancing properties of IL-27 lead to a potent anti-tumor response through the upregulation of Th1 and CTL responses (Salcedo *et al.*, 2009; Takeda *et al.*, 2003). Here, we show that IL-27 enhances the cytotoxicity of $CD8^+$ T cells in mice and in humans. These observations are consistent with previous reports in the literature suggesting that IL-27 acts on $CD8^+$ T cells through the activation of STAT1 and induces the T-bet and EOMES transcription factors, which are in turn critical for induction of effector molecules, and hence, the anti-tumor immune response (Mayer *et al.*, 2008; Morishima *et al.*, 2005b; Schneider *et al.*, 2011). Here we identified IL-27 as a major mediator in CLL pathogenesis, highlighting its correlation with disease progression and suggesting a potential role as disease biomarker. Collectively, our data unveiled a novel mechanism by which IL-27 promotes anti-tumor immunity in CLL by enhancing $CD8^+$ T-cell cytotoxicity, and established this cytokine as a promising immunotherapeutic agent in CLL. Further research should assess its efficacy in a pre-clinical setting in combination with other existing treatments, such as chemotherapy and immunotherapy agents, paving the path towards an affordable and effective personalized medicine regimen for the treatment of CLL.

Data Availability Statement: The data set presented in this study is openly available in the Gene Expression Omnibus with the accession number GSE216131 (reviewer token: mrepawauzlwdzeb).

Funding: This work was supported by grants from FNRS-Télévie to GP (7.4501.18, 7.6518.20), IFB (7.4529.19, 7.6603.21), MW (7.4508.16, 7.6504.18), SG (7.4502.19, 7.6604.21), and AL (7.4502.17, 7.4503.19), and from the Luxembourg National Research Fund (FNR) and Fondation Cancer to EG, EM and JP (PRIDE15/10675146/CANBIO, C20/BM/14582635, and C20/BM/14592342).

Figure S1

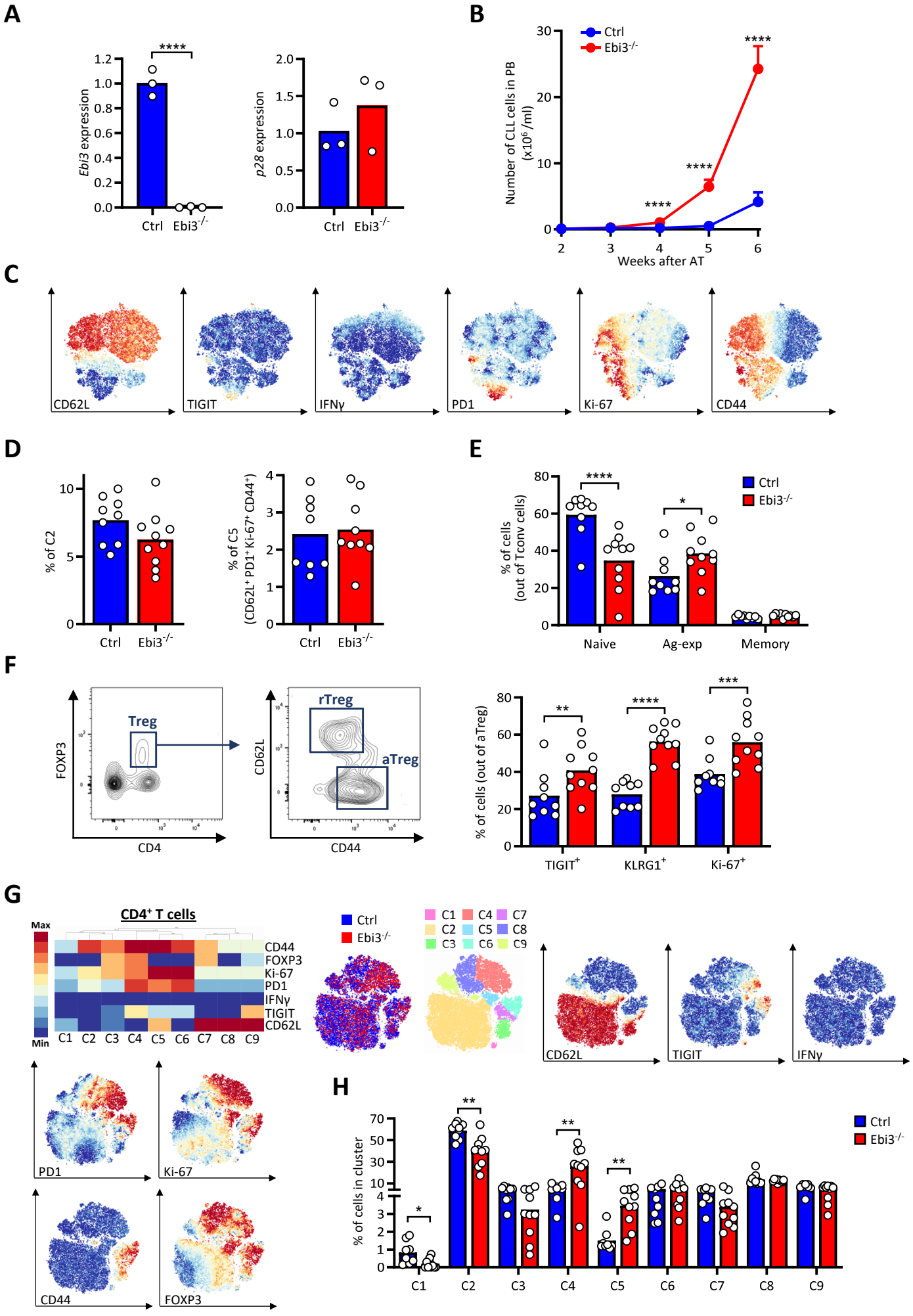
A
Ebi3 expression
p28 expression
Ctrl
Ebi3-/-
****
B
Ctrl
Ebi3-/-
Number of CLL cells in PB (x10⁶ /ml)
Weeks after AT
****
C
CD62L
TIGIT
IFNγ
PD1
Ki-67
CD44
D
% of C2
% of C5 (CD62L+ PD1+ Ki-67+ CD44+)
E
% of cells (out of Tconv cells)
Naive
Ag-exp
Memory
F
Treg
rTreg
aTreg
FOXP3
CD4
CD62L
CD44
% of cells (out of aTreg)
TIGIT+
KLRG1+
Ki-67+
G
CD4+ T cells
Max
Min
CD44
FOXP3
Ki-67
PD1
IFNγ
TIGIT
CD62L
C1 C2 C3 C4 C5 C6 C7 C8 C9
H
% of cells in cluster

Figure S2

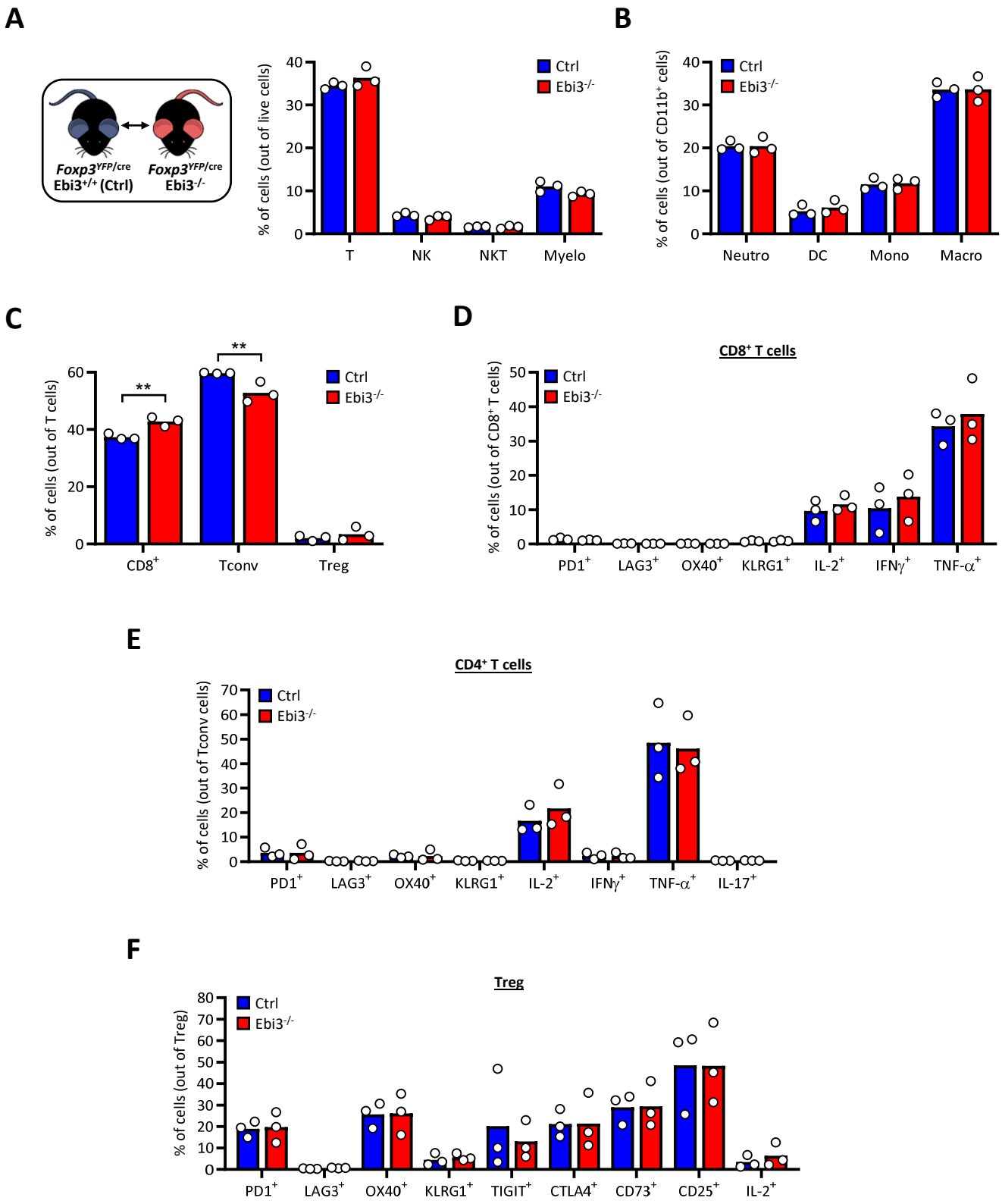
A
Foxp3YFP/cre Ebi3+/+ (Ctrl)
Foxp3YFP/cre Ebi3-/-
% of cells (out of live cells)
Ctrl
Ebi3-/-
T
NK
NKT
Myelo
B
% of cells (out of CD11b+ cells)
Neutro
DC
Mono
Macro
C
% of cells (out of T cells)
**
**
CD8+
Tconv
Treg
D
CD8+ T cells
% of cells (out of CD8+ T cells)
PD1+
LAG3+
OX40+
KLRG1+
IL-2+
IFNγ+
TNF-α+
E
CD4+ T cells
% of cells (out of Tconv cells)
PD1+
LAG3+
OX40+
KLRG1+
IL-2+
IFNγ+
TNF-α+
IL-17+
F
Treg
% of cells (out of Treg)
PD1+
LAG3+
OX40+
KLRG1+
TIGIT+
CTLA4+
CD73+
CD25+
IL-2+

Figure S3

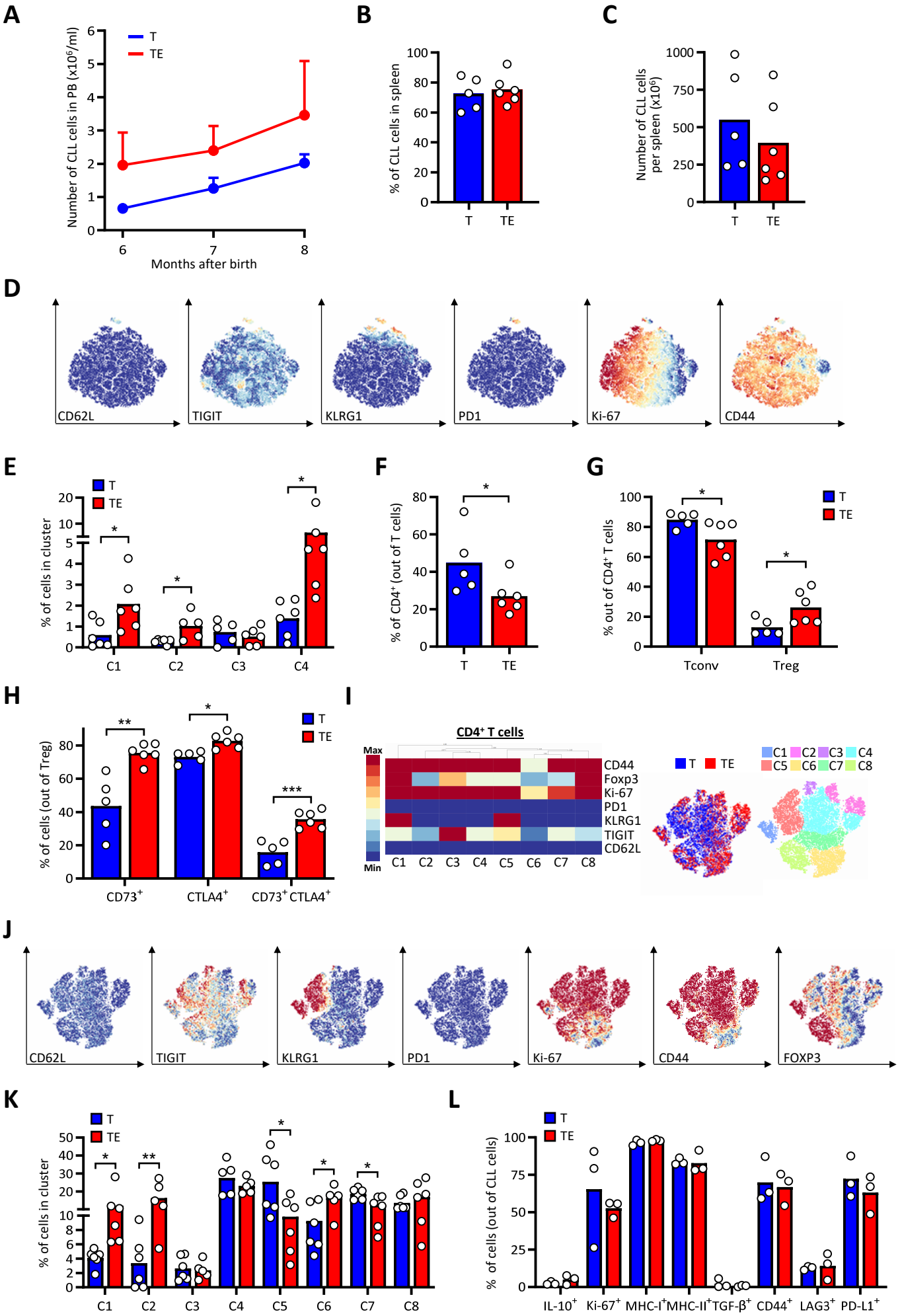
A
Number of CLL cells in PB (x10⁶/ml)
T
TE
Months after birth
B
% of CLL cells in spleen
C
Number of CLL cells per spleen (x10⁶)
D
CD62L
TIGIT
KLRG1
PD1
Ki-67
CD44
E
% of cells in cluster
C1
C2
C3
C4
F
% of CD4⁺ (out of T cells)
G
% out of CD4⁺ T cells
Tconv
Treg
H
% of cells (out of Treg)
CD73⁺
CTLA4⁺
CD73⁺ CTLA4⁺
I
CD4⁺ T cells
Max
Min
CD44
Foxp3
Ki-67
PD1
KLRG1
TIGIT
CD62L
C1 C2 C3 C4 C5 C6 C7 C8
J
CD62L
TIGIT
KLRG1
PD1
Ki-67
CD44
FOXP3
K
% of cells in cluster
L
% of cells (out of CLL cells)
IL-10⁺
Ki-67⁺
MHC-I⁺
MHC-II⁺
TGF-β⁺
CD44⁺
LAG3⁺
PD-L1⁺

Figure S4

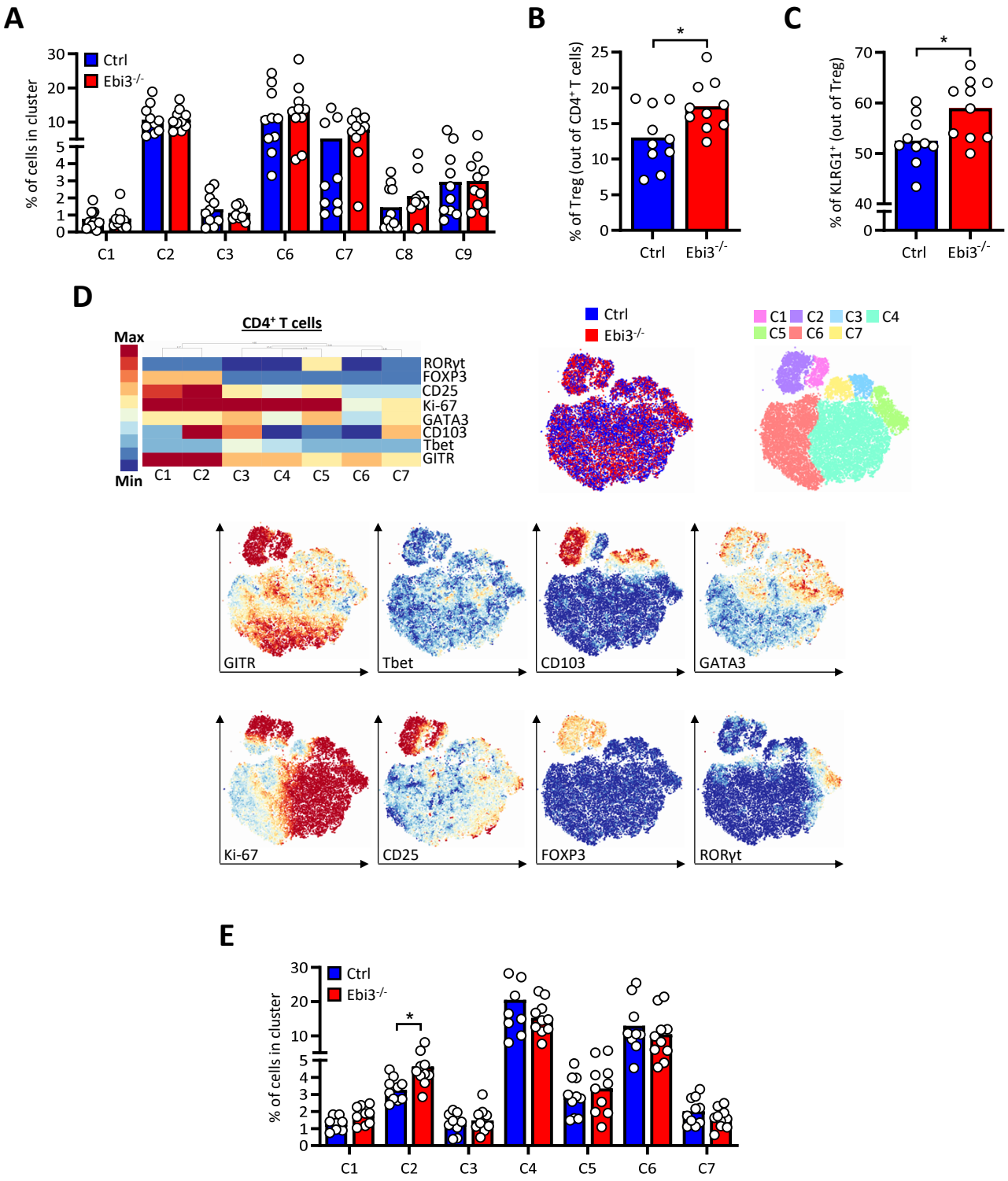
A
Ctrl
Ebi3-/-
% of cells in cluster
C1
C2
C3
C6
C7
C8
C9
B
% of Treg (out of CD4+ T cells)
Ctrl
Ebi3-/-
C
% of KLRG1+ (out of Treg)
Ctrl
Ebi3-/-
D
CD4+ T cells
Max
Min
RORγt
FOXP3
CD25
Ki-67
GATA3
CD103
Tbet
GITR
C1 C2 C3 C4 C5 C6 C7
Ctrl
Ebi3-/-
C1 C2 C3 C4
C5 C6 C7
GITR
Tbet
CD103
GATA3
Ki-67
CD25
FOXP3
RORγt
E
Ctrl
Ebi3-/-
% of cells in cluster
C1
C2
C3
C4
C5
C6
C7

Figure S5

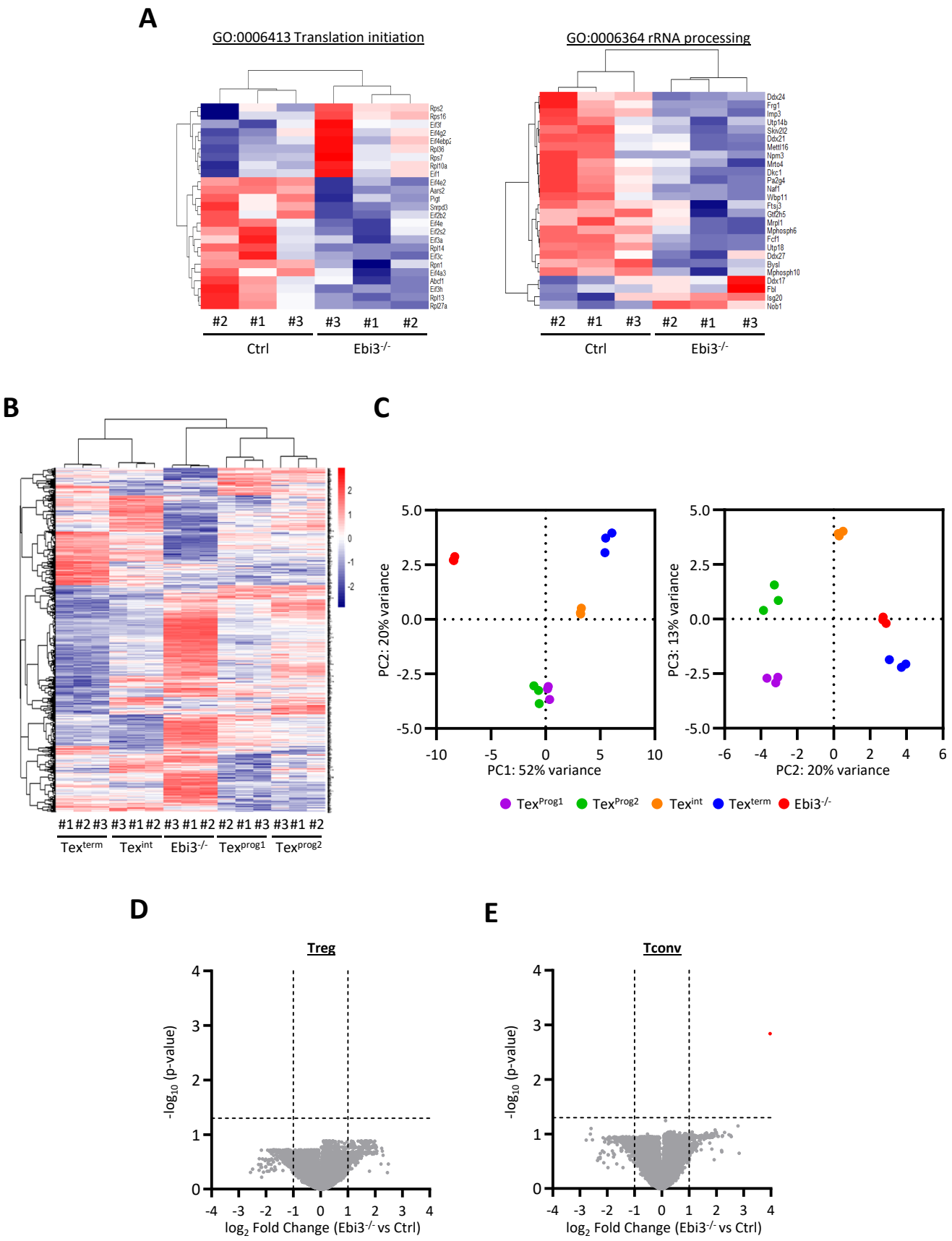
A
GO:0006413 Translation initiation
GO:0006364 rRNA processing
#2 #1 #3 #3 #1 #2
Ctrl
Ebi3-/-
B
#1 #2 #3 #3 #1 #2 #3 #1 #2 #2 #1 #3 #3 #1 #2
Texterm
Texint
Ebi3-/-
Texprog1
Texprog2
C
PC2: 20% variance
PC1: 52% variance
PC3: 13% variance
PC2: 20% variance
Texprog1
Texprog2
Texint
Texterm
Ebi3-/-
D
Treg
-log10 (p-value)
log2 Fold Change (Ebi3-/- vs Ctrl)
E
Tconv
-log10 (p-value)
log2 Fold Change (Ebi3-/- vs Ctrl)

Figure S6

A

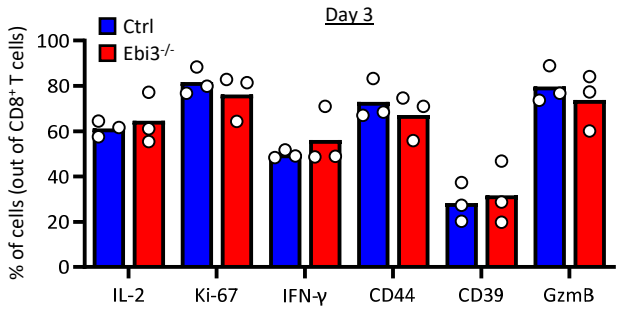

B

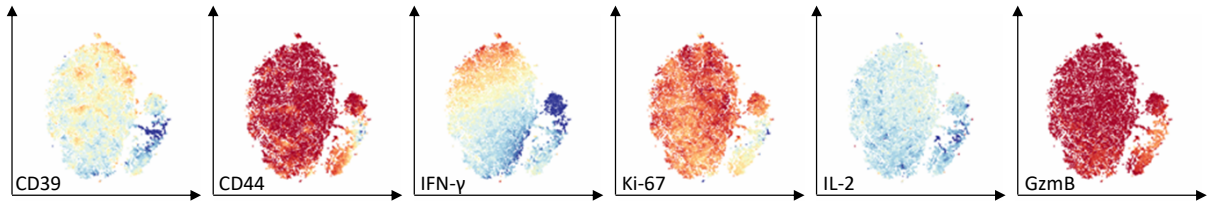

C

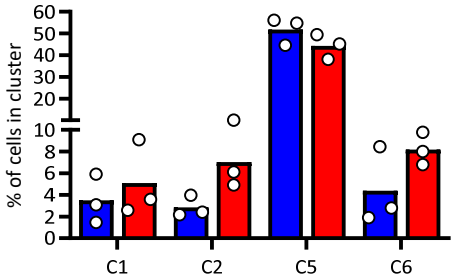

D

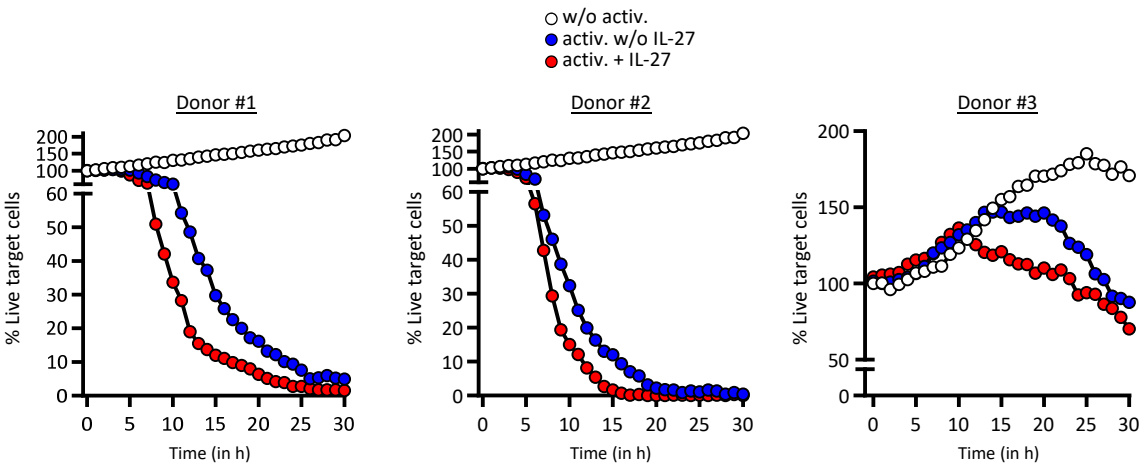

Figure S7

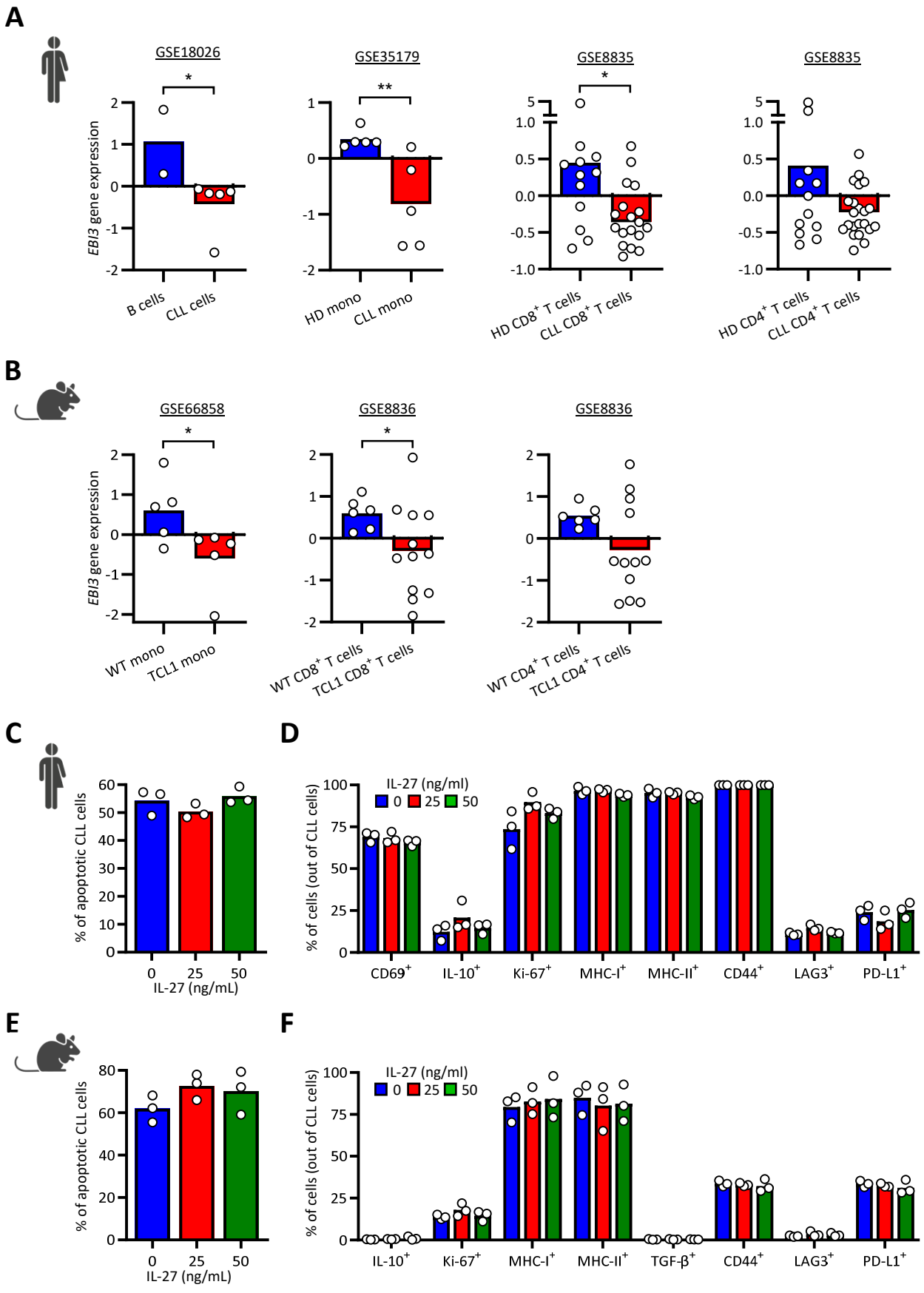
A
GSE18026
GSE35179
GSE8835
GSE8835
EBI3 gene expression
B cells
CLL cells
HD mono
CLL mono
HD CD8+ T cells
CLL CD8+ T cells
HD CD4+ T cells
CLL CD4+ T cells
B
GSE66858
GSE8836
GSE8836
WT mono
TCL1 mono
WT CD8+ T cells
TCL1 CD8+ T cells
WT CD4+ T cells
TCL1 CD4+ T cells
C
% of apoptotic CLL cells
IL-27 (ng/mL)
D
IL-27 (ng/ml)
0 25 50
% of cells (out of CLL cells)
CD69+
IL-10+
Ki-67+
MHC-I+
MHC-II+
CD44+
LAG3+
PD-L1+
E
% of apoptotic CLL cells
IL-27 (ng/mL)
F
IL-27 (ng/ml)
0 25 50
% of cells (out of CLL cells)
IL-10+
Ki-67+
MHC-I+
MHC-II+
TGF-β+
CD44+
LAG3+
PD-L1+

Figure S8

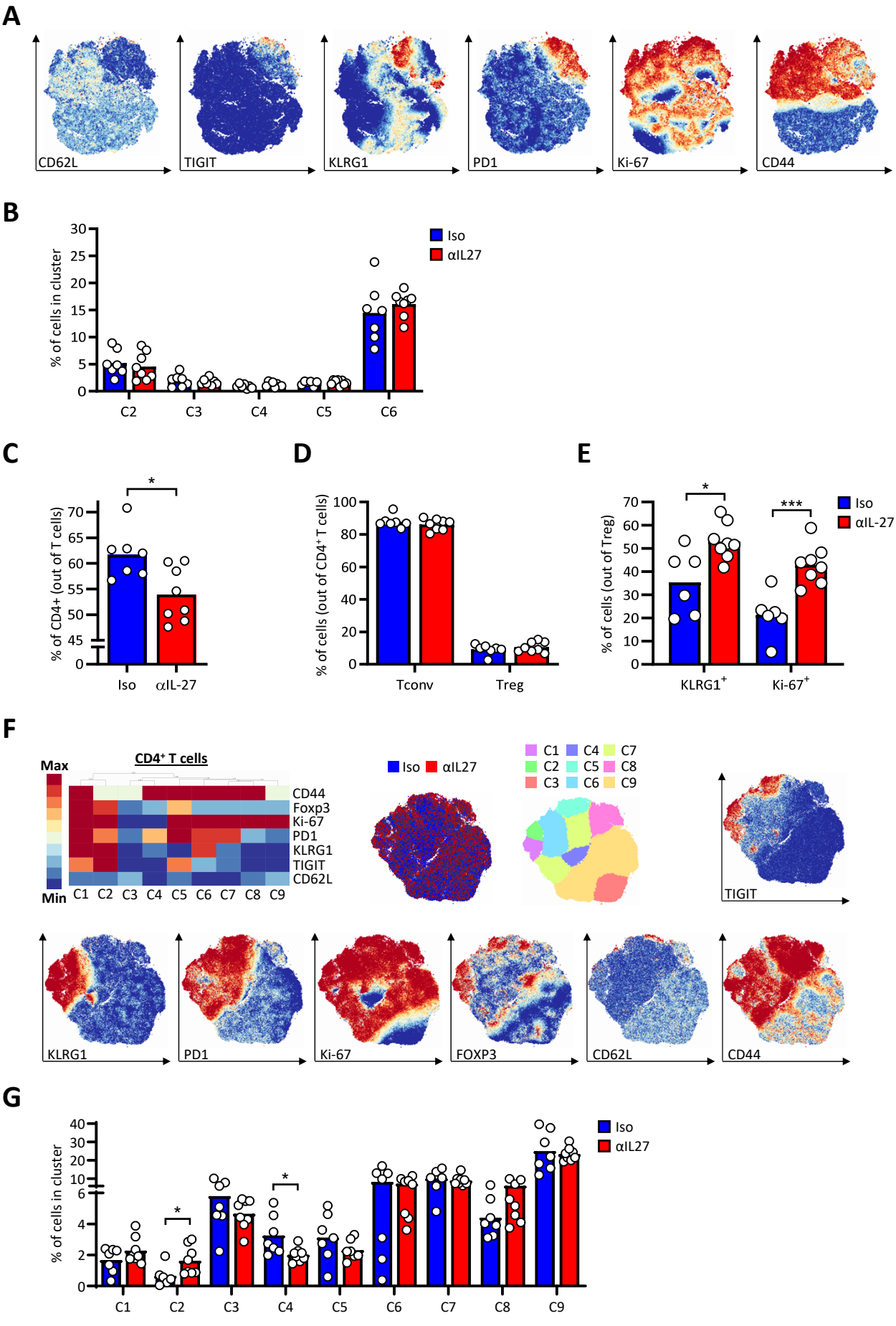
A
CD62L
TIGIT
KLRG1
PD1
Ki-67
CD44
B
% of cells in cluster
Iso
αIL27
C2
C3
C4
C5
C6
C
% of CD4+ (out of T cells)
Iso
αIL-27
D
% of cells (out of CD4+ T cells)
Tconv
Treg
E
% of cells (out of Treg)
KLRG1+
Ki-67+
F
CD4+ T cells
Max
Min
CD44
Foxp3
Ki-67
PD1
KLRG1
TIGIT
CD62L
C1 C2 C3 C4 C5 C6 C7 C8 C9
FOXP3
G
% of cells in cluster
C1
C2
C3
C4
C5
C6
C7
C8
C9

Figure legends

Figure S1: *Ebi3*$^{-/-}$ transgenic mice do not produce IL-27 and display a TME with immunosuppressive features.

(A) Relative mRNA levels of the IL-27 subunits, p28 and Ebi3, in WT and *Ebi3* $^{-/-}$ mice. **(B)** Number of circulating neoplastic CD5^{+} CD19^{+} cells (n=18 for Ctrl and n=19 for *Ebi3*$^{-/-}$, two-way ANOVA), same mice as Fig 1A. **(C-H)** The data shown corresponds to one experimental cohort (n=9 for Ctrl and n=10 for *Ebi3*$^{-/-}$). **(C)** HSNE plots (Cytosplore) depicting the expression of CD44, Ki-67, PD1, IFN-γ, TIGIT and CD62L on CD8^{+} T cells. **(D)** Percentages of CD8^{+} T-cell cluster distribution on Ctrl and *Ebi3*$^{-/-}$ CD8^{+} T cells**. (E)** Frequency of CD4^{+} Tconv with a naive (CD62L^{+} CD44^{-}), effector (CD62L^{-} CD44^{+}) or memory (CD62L^{+} CD44^{+}) phenotype among Ctrl and *Ebi3*$^{-/-}$ mice. **(F)** (Left) Representative flow cytometry plot depicting the gating strategy used to analyze activated Tregs (aTreg, CD62L^{hi} CD44^{lo}). Resting Tregs (rTregs, CD62L^{lo} CD44^{hi}) are also shown. (Right) Frequency of the indicated populations in Ctrl and *Ebi3*$^{-/-}$ Tregs. **(G-H)** HSNE clustering analysis of WT and *Ebi3*$^{-/-}$ CD4^{+} T cells based on CD44, Foxp3, Ki-67, PD-1, IFN-γ, TIGIT and CD62L expression measured by FC. **(G)** Heatmap comprising the clusters generated by HSNE and HSNE plots depicting the expression of each individual marker. **(H)** Percentages of cluster distribution on Ctrl and *Ebi3*$^{-/-}$ CD4^{+} T cells. Unpaired t test, * *P*< .05, ** *P*< .01, *** *P*< .001, **** *P*< .0001.

Figure S2: EBI3 depletion does not affect myeloid cell compartment and mildly affects T-cell distribution in a non-tumoral context.

(A-F) Healthy *Foxp3*$^{YFP/Cre}$ and *Foxp3*$^{YFP/Cre}$ *Ebi3*$^{-/-}$ mice (n=3 per group) were euthanized at 8 weeks of age and their splenocytes analyzed using FC. **(A)** Frequency of indicated cell populations among total live cells. T= T cells; NK= Natural killer cells; NKT= natural killer T cells; Myelo= myeloid cells. **(B)** Frequency of indicated cell populations out of CD11b^{+} cells. Neutro=neutrophils; DCs=dendritic cells; Mono=monocytes; Macro=macrophages. **(C)** Frequency of T-cell subpopulations among total T cells. **(D-F)** CD8^{+} and CD4^{+} T cells were isolated from *Foxp3*$^{YFP/Cre}$ and *Foxp3*$^{YFP/Cre}$ *Ebi3*$^{-/-}$ splenocytes, stimulated *ex vivo* with PMA, ionomycin and brefeldin A and analyzed by FC. Frequency of indicated immune checkpoints and cytokines in **(D)** CD8^{+} effector T cells, **(E)** CD4^{+} Tconv cells and **(F)** Tregs after *ex vivo* stimulation. Unpaired t test, ** P< .01.

Figure S3: EBI3 depletion in transgenic Eμ-TCL1 mice promotes an immunosuppressive TME.

(A-L) Leukemic T and TE mice were euthanized and their splenocytes were processed and analyzed by FC. **(A)** Number of circulating leukemic cells in T and TE mice. **(B)** Percentage of CLL cells among splenocytes of T and TE mice. **(C)** Number of CLL cells in the spleen of T and TE mice. **(D)** HSNE plots depicting the expression of each individual marker included in the clustering analysis of CD8^{+} T cells

derived from T and TE transgenic mice based on the expression of CD44, Ki-67, PD1, KLRG1 and CD62L measured by FC. (**E)** Percentages of $CD8^+$ T-cell clusters distribution on T and TE. **(F)** Percentage of $CD4^+$ T cells in the spleen of T and TE transgenic mice. **(G)** Percentage of Tconv and Treg populations among $CD4^+$ T cells. **(H)** Frequency of indicated cell populations among Tregs **(I-K)** HSNE clustering analysis of T and TE $CD4^+$ T cells based on the expression of CD44, FOXP3, Ki-67, PD1, KLRG1 and CD62L measured by FC. **(I)** Heatmap comprising the clusters generated by HSNE. **(J)** HSNE plots depicting the expression of each individual marker. (**K)** Percentages of cluster distribution in T and TE $CD4^+$ T cells. **(L)** CLL cells were isolated from T and TE mice (n=3 mice per group) and activated for 48h *in vitro*. CLL cells were stained and analyzed by FC. Unpaired t test, * *P*< .05, ** *P*< .01.

Figure S4: Specific T-cell-EBI3 depletion leads to a more immunosuppressive TME.

(A) Percentages of $CD8^+$ T-cell clusters distribution on Ctrl and *Ebi3*$^{-/-}$ isolated from the spleen of recipient *Rag2*$^{-/-}$ mice. **(B)** Percentage of Tregs among $CD4^+$ T cells in the spleen of recipient *Rag2*$^{-/-}$ mice. **(C)** Frequency of $KLRG1^+$ Tregs in the spleen of recipient *Rag2*$^{-/-}$ mice. **(D-E)** HSNE clustering analysis of Ctrl and *Ebi3*$^{-/-}$ $CD4^+$ T cells based on ROR-γt, FOXP3, CD25, Ki-67, GATA3, CD103, T-bet, and GITR expression measured by FC. **(D)** Heatmap comprising the clusters generated by HSNE (top) and HSNE plots depicting the expression of each individual marker (bottom). **(E)** Percentages of cluster distribution on WT and *Ebi3*$^{-/-}$ $CD4^+$ T cells. Unpaired t test, * P< .05.

Figure S5: $CD8^+$ T cells, but not Tconv or Tregs, show major transcriptional changes in the absence of EBI3.

(A) Heatmaps depicting the transcriptional changes associated with translation initiation (left) and rRNA processing (right) between Ctrl and *Ebi3*$^{-/-}$ $CD8^+$ T cells. **(B)** Heatmap depicting the similarity of *Ebi3*$^{-/-}$ $CD8^+$ T cells with subsets of exhausted T cells described in (Beltra *et al.*, 2020b). **(C)** Principal component analysis (PCA) of *Ebi3*$^{-/-}$ $CD8^+$ T cells with the aforementioned subsets. **(D-E)** Volcano plot showing differentially expressed genes (DEG) in Ctrl and *Ebi3*$^{-/-}$ Tregs **(D)** and Tconv **(E)**.

Figure S6: *Ebi3* depletion in $CD8^+$ T cells does not affect cytokine production after 3 days of activation.

(A) Frequency of cells expressing the selected markers in Ctrl vs *Ebi3*$^{-/-}$ $CD8^+$ T cells after 3 days of activation. **(B)** HSNE clustering analysis of Ctrl and *Ebi3*$^{-/-}$ $CD8^+$ T cells based on IL-2, Ki-i67, IFN-γ, CD44, CD39 and Granzyme B expression measured by FC at day 3 post activation. **(C)** Percentages of cluster distribution of Ctrl vs *Ebi3*$^{-/-}$ $CD8^+$ T cells. **(D)** Individual plots representing the viability of target cells over time for the 3D killing assay for each donor.

Figure S7: IL-27 does not affect human and murine CLL cells

(A) Relative gene expression of *Ebi3* in different cell subsets in CLL patients and healthy controls. **(B)** Relative gene expression of *Ebi3* in different cell subsets in Ctrl and *Eμ-TCL1* mice. **(C-D)** Viability **(C)** and phenotype **(D)** of patient-derived CLL cells after 48h of treatment with increasing levels of IL-27. **(E-F)** Viability **(E)** and phenotype **(F)** of *Eμ-TCL1*-derived splenocytes after 48h of treatment with increasing levels of IL-27. Unpaired T test, * P< .05, ** P< .01.

Figure S8: IL-27 neutralization partially recapitulates the less immunosuppressive microenvironment observed in the transgenic mouse model.

(A) HSNE clustering analysis of splenic $CD8^+$ T cells from isotype- and α-IL-27-treated mice based on CD62L, TIGIT, KRLG1, PD1, Ki-67, and CD44 expression measured by FC. **(B)** Percentages of cluster distribution between $CD8^+$ T cells derived from the spleen of isotype- or α-IL-27-treated mice. **(C)** Percentage of $CD4^+$ T cells out of total T cells. **(D)** Percentage of Tconv and Tregs out of $CD4^+$ T cells. **(E)** Frequency of the indicated Treg populations. **(F)** HSNE clustering analysis of splenic $CD4^+$ T cells from isotype- and α-IL-27-treated mice based on CD62L, TIGIT, KRLG1, PD1, Ki-67, and CD44 expression measured by FC. **(G)** Percentages of cluster distribution between splenic $CD4^+$ T cells from isotype- or α-IL-27-treated mice.

Supplementary Information – Pagano, Fernandez-Botana, *et al*.

Materials and Methods

Animal experiments

Leukemic cells derived from *Eμ-TCL1* mice were adoptively transferred (AT) by i.p. or i.v. transplantation (1-2x10^7/100µl DMEM) into C57BL/6 wild type (WT), *Ebi3*$^{-/-}$ and *Rag2*$^{-/-}$ mice. In specific experiments, CLL cells were injected after isolation from the spleen using the MojoSort™ Mouse Pan B Cell Isolation Kit (Biolegend) according to the manufacturer's instructions. Unless stated otherwise, all AT experiments were performed on sex and age-matched mice ranging from six to ten weeks of age. When applicable, CD3$^+$ T cells were isolated from WT and *Ebi3*$^{-/-}$ splenocytes using the MojoSort™ Mouse CD3 T-cell Isolation Kit (Biolegend) according to the manufacturer's instructions, and co-injected with the *Eμ-TCL1* splenocytes. CLL progression in leukemic mice was monitored weekly by assessment of the percentage of CD5$^+$ CD19$^+$ cells in the PB. The blood cell count was determined using the MS4e Vet haematology analyser (Melet-Schloesing, France).
Mice were euthanized by cervical dislocation before reaching the established humane end-point, and the leukemic spleens were dissected and processed as previously described.
In vivo treatment with IL-27 neutralising antibody or isotype IgG control (BioXcell, NH) was performed *i.p.* in *Eμ-TCL1*-AT mice. Antibody administration started two days prior to CLL AT and was repeated twice a week throughout the course of the experiment. For the first two injections, 500µg of anti-IL-27 neutralizing antibody were administered per mouse in 200µl of buffer (Day -2 and day 0). The following injections comprised 250µg of anti-IL-27 antibody in 100µl buffer. Blood serum was obtained weekly during routine blood checks by centrifuging the coagulated PB (2000g, 4°C, 20').

Flow cytometry

Cell sorting

CD3$^+$ T cells were isolated from *FoxP3*$^{YFP/Cre}$ and *FoxP3*$^{YFP/Cre}$ *Ebi3*$^{-/-}$ mice using MojoSort™ Mouse CD3 T-cell Isolation Kit (Biolegend), and activated with plate-bound anti-CD3 (2µg/ml), anti-CD28 (2µg/ml) and IL-2 (10 ng/mL) for 72 hours. Cells were harvested after three days, stained for surface markers and FACS-sorted using a FACSAria sorter III (BD Biosciences) in three fractions: CD8$^+$ T cells, CD4$^+$ conventional T cells and FOXP3$^+$ regulatory T cells (Treg, YFP$^+$). The samples were immediately spun down (500g, 10') and frozen at -80°C.

Cell clustering

Clustering analysis of live lymphocytes was performed with Cytosplore software. Briefly, samples were randomly down-sampled and subjected to Hierarchical Stochastic Neighbor Embedding

(HSNE) to generate clusters based on phenotypic similarities. Clusters were generated using the Gaussian mean shift algorithm using the density estimate as input.

T-cell-mediated cytotoxicity assay on murine CLL

Assessment of the cytotoxicity of IL-27-treated T cells on murine CLL cells was performed as previously described (Ioannou *et al.*, 2021). Briefly, $CD3^+$ T cells were isolated from C57BL/6 mice, cultured in RPMI1640 medium supplemented with 10% FBS, 1% P/S, and stimulated with coated anti-CD3 (1µg/ml) and soluble anti-CD28 (1µg/ml) for 48h at 37°C. Treatment with IL-27 was performed daily (25ng/ml). CLL cells ($CD5^+CD19^+$) isolated from *Eμ-TCL1* mice were stained with CellTrace CFSE (200nM, Thermo Fisher) and pulsed with 2µg/ml of super antigen (sAg; SEA and SEB; Sigma-Aldrich) for 30' at 37°C. The generated target CLL cells ($2.5x10^4$) were then loaded with sAg were added to the pre-treated $CD3^+$ T cells at a 1:20 (target: effector). Cell mixtures were centrifuged, and incubated for 4h at 37°C. Cells were stained with TO-PRO-3 viability dye (Thermo Fisher) according to the manufacturer's instructions and T-cell-mediated cytotoxicity against CLL target cells was determined by flow cytometry. Cytotoxicity was calculated as: % target cell death = (% CFSE+ TO-PRO-3+ target cells incubated with effector T cells - % of $CFSE^+$ TO-PRO-3^+ target cells incubated alone) × 100/(100 - % of $CFSE^+$ TO-PRO-3^+ target cells incubated alone).

Three-dimensional killing assay on human samples

The real-time killing assay was performed as previously described (Zhao *et al.*, 2021). In summary, Human CD3/CD28 activator beads (ThermoFisher Scientific) were used to stimulate PBMCs (0.7:1 ratio Beads/PBMCs) with or without IL-27 (100 ng/ml) for 6 days at 37 °C with 5% CO2. On day 4, half of the media was replaced by fresh media. For the 3D killing assay, NALM6-pCasper cells (Knorck *et al.*, 2022) were pulsed with SEA and SEB (1µg/ml) at 37 °C with 5% CO2 for 30 min. The pulsed NALM6-pCapser cells were then embedded into 2 mg/mL Type I bovine collagen (Advanced Biomatrix) and centrifuged down to the bottom as described before (Zhao *et al.*, 2021). After gel solidification, PBMCs were placed on top of the collagen matrix at a 20:1 effector: target ratio. Live cell imaging was carried out using a high-content imaging system (ImageXpress, Molecular Devices) at 37 °C with 5% CO2 for 30 hours. Images were analyzed with ImageJ.

Bulk-RNA sequencing

Previously sorted cells were thawed and RNA was isolated using the Nucleosol RNA isolation kit (Macherey-Nagel) prior to bulk-RNAseq. Librairies were prepared with the QuantSeq 3' mRNA-Seq Library Prep Kit FWD for Illumina (Lexogen), according to manufacturer's instructions, with the

addition of UMI. Barcoded samples were pooled, diluted, loaded onto a NextSeq 500/500 Mid Output flowcell (130M reads, Illumina) and single-end sequencing was performed on a NextSeq 550 (Illumina).

RNA sequencing analysis

After initial QCs using FastQC and FastQ Screen tools made available by the Babraham Bioinformatics group (https://www.bioinformatics.babraham.ac.uk/projects), fastq files were processed using a local Snakemake workflow including the following main steps. First, raw reads were trimmed from their UMI index, poly A and adapter sequences using a combination of dedicated scripts and cutadapt (v2.10). Next, filtered reads were submitted for mapping (STAR v2.5.3a) on the Mouse Reference genome (GRCm38). Collapsing of reads originating from the same fragment was achieved with umi_tools (v 1.0.0) and counting was performed with featureCounts (subread v2.0.0).

Counts were filtered and transformed with EdgeR for clustering and principal component analysis (PCA). Differential expression of genes (DEG) across $CD8^+$ T cells, Tconv and Treg cell samples was assessed using the NOISeq R/Bioconductor packages, and a FDR of 0.05 and a log2 fold change cut-off of 1 were imposed.

Cytokine measurements

The levels of IL-27 in patient blood serum, as well as in murine blood serum and spleen plasma were quantified by ELISA using the LEGEND MAX™ Human IL-27 ELISA Kit (Biolegend) and LEGEND MAX™ Mouse IL-27 Heterodimer ELISA Kit (Biolegend), respectively, according to the manufacturer's instructions. Equal volumes of serum or spleen plasma were loaded across conditions.

Analysis of publicly available data sets

For the analysis of Ebi3 gene expression, we collected raw or processed data from the GSE18026, GSE35179, GSE66858, GSE8835, and GSE8836 datasets (GEO database, NCBI). We obtained Ebi3 gene expression data from healthy Human B cells and CLL cells from Ferreira *et al.,* supplemental File 2 (Ferreira *et al.*, 2014). We used gene expression data from several $CD8^+$ T-cell populations for comparison (Beltra *et al.*, 2020b). Expression of differentially expressed genes from clusters 1-10 was gathered for PCA and clustering analysis.

Supplemental Table 1: List of antibodies used in flow cytometry

Antigen	Fluorochrome	Clone	Specificity	Manufacturer	Product #	Other name	RRIDs
CD103	APC	2E7	Mouse	Biolegend	121414		AB_1227502
CD11b	PE-Cy7	M1/70	Mouse/Human	Biolegend	101215		AB_312798
CD11c	APC-V770	1B29	Mouse	Miltenyi	130-107-461		AB_2783921
CD134	APC	REA625	Mouse	Miltenyi	130-109-742	OX40	AB_2654942
CD152	PE	UC10-4B9	Mouse	Biolegend	106305	CTLA4	AB_313255
CD19	FITC	eBio1D3	Mouse	ThermoFisher	11-0193-86		AB_657665
CD19	PE-Cy7	eBio1D3	Mouse	ThermoFisher	25-0193-82		AB_657663
CD19	APC	6D5	Mouse	Biolegend	115512		AB_313647
CD19	Biotin	6D5	Mouse	Miltenyi	130-101-951		AB_2801732
CD25	BV421	PC61	Mouse	Biolegend	102043	IL-2Rα	AB_11203373
CD25	FITC	REA568	Mouse	Miltenyi	130-108-999		AB_2656653
CD25	BV421	PC61	Mouse	Biolegend	102043		AB_2562611
CD279	BV510	29F.1A12	Mouse	Biolegend	135241	PD-1	AB_2715761
CD3	PerCP	1B8	Mouse	Biolegend	100326		AB_893317
CD3	Biotin	1B3	Mouse	Miltenyi	130-109-835		AB_2751822
CD357	PerCP/Cy5.5	DTA-1	Mouse	Biolegend	126316	GITR	AB_2563384
CD39	PE-Cy7	Duha59	Mouse	Biolegend	143805		AB_2563393
CD4	APC-Fire 750	1B13	Mouse	Biolegend	100568		AB_2629699
CD4	APC-Cy7	RM4-5	Mouse	Biolegend	100526		AB_312727
CD44	FITC	IM7	Mouse	Biolegend	103022		AB_312957
CD44	AF700	IM7	Mouse	Biolegend	103026		AB_493713
CD44	PE	IM7	Mouse	Biolegend	103008		AB_312959
CD44	APC	IM7	Mouse/Human	Biolegend	103012		AB_312963
CD5	PE	53-7.3	Mouse	Biolegend	100608		AB_312737
CD5	APC	53-7.3	Mouse	Biolegend	100626		AB_2563929
CD62L	PE-Cy7	MEL-14	Mouse	Biolegend	104418		AB_313103
CD69	AF700	FN50	Human	Biolegend	310922		AB_493775
CD73	APC	TY/11.8	Mouse	Biolegend	127209		AB_11218786
CD8	BV650	1B21	Mouse	Biolegend	100742		AB_2563056
F4/80	BV421	BM8	Mouse	Biolegend	123137		AB_11203717
Foxp3	APC	REA788	Mouse	Miltenyi	130-111-601		AB_2651766
Foxp3	BV488	MF-14	Mouse	Biolegend	126406		AB_1089113
GATA3	BV421	16E10A23	Mouse/Human	Biolegend	653814		AB_2563221
Granzyme B	PE	QA16A02	Mouse/Human	Biolegend	372208		AB_2687032
HLA-A,B,C	PE-Cy7	W6/32	Human	Biolegend	311430		AB_2561617
IFNy	BV711	XMG1.2	Mouse	Biolegend	505836		AB_2650928
IL-10	BV421	JES3-9D7	Human	Biolegend	501421		AB_10896947

IL17A	PE	TC11-18H10	Mouse	Miltenyi	130-102-344		AB_2660786
IL2	PE-Cy7	JES6-5H4	Mouse	Biolegend	503832		AB_2561750
Ki-67	BV421	16A8	Mouse	Biolegend	652411		AB_2562663
Ki-67	APC	16A8	Mouse	Biolegend	652406		AB_2561930
Ki-67	BV421	16A8	Mouse	Biolegend	652411		AB_2562663
KLRG1	BV711	2F1/KLRG1	Mouse	Biolegend	138427	MAFA	AB_2629721
LAG-3	BV421	C9B7W	Mouse	Biolegend	125221	CD223	AB_2572080
LAG-3	APC	7H2C65	Human	Biolegend	369211	CD223	AB_2728372
Ly6c	PE	1G7.G10	Mouse	Miltenyi	130-102-391		AB_2857638
Ly6G	Biotin	REA526	Mouse	Miltenyi	130-107-911	Gr-1	AB_2727584
MHC-DR	APC	L243	Human	Biolegend	980406		AB_2650655
MHC-I	PE	28-8-6	Mouse	Biolegend	114607		AB_313598
MHC-II	BV650	M5/114.15.2	Mouse	Biolegend	107641	I-A/I-E	AB_2565975
NK1.1	Biotin	PK136	Mouse	Miltenyi	130-101-888	CD161	AB_2727573
PD-L1	APC	29E2A3	Human	Biolegend	329707	CD274	AB_940358
PD-L1	APC	29E2A3	Human	Biolegend	329707	CD274	AB_940358
RORg (t)	PE	B2D	Mouse	eBioscience	2054914		AB_10805392
Tbet	PE-Cy7	4B10	Mouse/Human	Biolegend	644823		AB_2561760
TGF-β	PerCP/Cy5.5	TW7-16B4	Mouse	Biolegend	141409		AB_2561591
TIGIT	PE	GIGD7	Mouse	eBiosciences	12-950182		AB_11042152
TNFa	APC	MP6-XT22	Mouse	Biolegend	506308		AB_315429
TOX	PE	TXRX10	Mouse	eBioscience	12-6502-82		AB_10855034

eBioscience™ Fixable Viability Dye eFluor® 506	ThermoFisher	65-0866-18	
Zombie Green™ Fixable Viability Kit	Biolegend	423111	
Zombie RED™ Fixable Viability Kit	Biolegend	423109	
Zombie UV™ Fixable Viability Kit	Biolegend	423108	
Zombie NIR™ Fixable Viability Kit	Biolegend	423106	

Conclusions

By injecting CLL cells in *Ebi3*$^{-/-}$ and control mice we demonstrated a strong anti-tumor activity of IL-27 in CLL, as its absence led to an enhanced CLL progression and impacted anti-tumor immune response. In addition, via RNA sequencing, we could identify CD8^{+} T cells as the T-cell subtype mainly affected by IL-27 depletion, characterized by major transcriptional changes associated with impacted T-cell activation, proliferation, and synapse formation. In line with these findings, we observed increased cytotoxic activity of *ex vivo*-cultured CD8^{+} T cells in presence of IL-27 both in murine and human primary cells. The anti-tumor activity of IL-27 in CLL development was confirmed by neutralizing *in vivo* this cytokine during CLL development, where we could partially recapitulate the enhanced leukemia progression observed in *Ebi3*$^{-/-}$ mice. In addition, the concentration of this cytokine was decreased during CLL development in both pre-clinical murine and patient samples. Altogether, these data demonstrate the anti-tumoral role of IL-27 during CLL development *via* enhanced CD8^{+} T-cell-mediated cytotoxic activity during the anti-tumor immune response.

Discussion and perspectives

It is widely established that the interactions between cancer cells and TME to sustain tumor progression is even more emphasized in CLL. Indeed, within the proliferation centers of the lymph nodes, bone marrow and other lymphoid organs, CLL cells receive a chronic stimulation from stromal cells and immune cells that sustain their survival and promote their proliferation by stimulating the BCRs (Svanberg et al., 2021). In line with this, the introduction of drugs that inhibit BCR signaling in CLL cells (e.g. BTK and PI3K inhibitors) represents a turning point in the treatment of CLL patients, as their main activity is to block the interaction between CLL cells and the TME-mediated stimuli. The central objective of this PhD project was to unravel the mechanisms and dynamics that allow the interaction between CLL cells and immune cells and ultimately lead to leukemia progression. In the first part, we focused on regulatory T cells, asking whether depleting specific transcription factors in this T-cell subpopulation could affect their suppressive feature and lead to an impacted leukemia progression. In the second part we studied a specific cytokine, IL-27, trying to understand its role in CLL development and to characterize the effects that this cytokine produce on T-cell mediated anti-tumor immune response.

Part I - Microenvironment-Regulated Transcriptions Factors AHR and HIF-1α Expression in Regulatory T cells promotes Chronic Lymphocytic Leukemia Progression by impairing $CD8^+$ T-cell-mediated Anti-Tumor Immunity

1. ROLE OF REGULATORY T CELLS IN CLL AND THE IMPORTANCE OF AHR AND HIF-1α IN CANCER

Among the different immune cells of the TME, T cells play a complex role within CLL development, as they can have both pro-tumor and anti-tumor activities (Vlachonikola et al., 2020). As such, both $CD4^+$ and $CD8^+$ T cells appear dysfunctional in CLL patients, with $CD4^+$ T cells involved in CLL cell stimulation and $CD8^+$ T cells being functionally exhausted and with impaired anti-tumor cytotoxic activity (Roessner and Seiffert, 2020). In this scenario, treated CLL patients also present a higher number of Tregs compared to untreated patients and to healthy individuals (Maharaj et al., 2022; Palma et al., 2017), and this T cell subtype contributes to inhibit the anti-tumor immune response while promoting an immunosuppressive environment. In addition, Tregs of CLL patients display increased expression of immunosuppressive markers, e.g. IL-10 and CTLA4 (Beyer et al., 2005; Biancotto et al., 2012). We could confirm these findings in the adoptive transfer (AT) model of CLL (AT-TCL1 mice), where we observed an increased expression of immunosuppressive markers, such as LAG-3, CTLA-4 and KLRG1 in CLL-Tregs compared to HC-Tregs (Wierz et al., 2018). Very recently, we have also demonstrated in vivo the pro-tumoral role of Tregs in CLL, as we observed a decreased

CLL development in absence of Tregs in DEREG leukemic mice (Goral et al., 2022). However, the systemic depletion of Tregs in patients is not a perusable therapeutic strategy, as Tregs are fundamental for maintaining homeostasis and avoid autoimmunity (Bayati et al., 2020). For these reasons, there is the urgent need in studying specific molecules that mediate tumor-infiltrated Treg immunosuppressive functions, in order to selectively target them and help restoring a functional anti-tumor immunity. It is also important to underline that Tregs represent a heterogeneous population, with specific subsets able to inhibit different immune cell types. For example, we demonstrated that during CLL progression, a specific $CD44^{lo}$ $CD25^{lo}$ $LAG3^{hi}$ Treg subpopulation, which has a more immunosuppressive transcriptional program compared to normal Tregs, can be observed. Another Treg subpopulation with enhanced inhibitory activities was characterized by Joller and colleagues, who described a Treg subset expressing the immune checkpoint (IC) TIGIT and showing enhanced immunosuppressive abilities towards $CD4^+$ T cells, both in mice and humans (Joller et al., 2014). Among the different genes overexpressed by murine TIGIT+ Tregs, the transcription factors (TF) Ahr and Hif1a were the most upregulated ones after Ikzf2 (encoding for Helios). Due to their microenvironment-dependent activation, we wanted to investigate in the first part of the present project whether AHR and HIF-1α were involved in maintaining the suppressive phenotype and functions of Tregs during CLL development. Since there has been a conspicuous number of preclinical studies published over the last decade, AHR and HIF-1α are gaining increasing importance in the field of oncoimmunology and have an active role in cancer progression (Balamurugan, 2016; Wang *et al.*, 2020b). Indeed, both transcription factors are overexpressed and/or chronically active in many tumors, including DLBCL, T-cell leukemias and some solid tumors, and after promising in vivo results, some clinical trials are evaluating the therapeutic efficacy of their inhibition during cancer development (NCT04999202, NCT04069026, NCT04200963, (Fallah and Rini, 2019).

2. IMMUNOPHENOTYPING OF SPLEEN IN AHR/HIF-1α CKO AND CONTROL MICE

After having generated conditional knock-out (cKO) mice lacking the two TFs only in FOXP3+ Tregs, we characterized the newly generated colonies. When Tregs are depleted in vivo, as well as when FOXP3 or other fundamental factors are knocked out in Tregs, mice develop severe autoimmunity and decreased survival rate (Di Pilato et al., 2019; Kim et al., 2009; Zhang et al., 2009). Our AHR and HIF-1α cKO mice had no differences in survival (Fig.8F) and did not show any phenotype related to immune dysregulation and autoimmunity, demonstrating that the depletion of these two TFs does not impair Treg physiological development and function, most likely because AHR and HIF-1α are not or mildly transcriptionally active in physiological conditions. In line with this, no differences were observed in the thymic Treg frequency (Fig.10C) and thymocytes number (Fig.10B) between

the different models, demonstrating that the two TFs have marginal role in Treg survival and homeostasis. Nonetheless, when analyzing the spleen, we observed that the T-cell compartment was affected by AHR and HIF-1α depletion in Tregs in physiological conditions, and KO-Tregs already appeared less suppressive compared to WT ones. Indeed, increase in $CD4^+$ Tconv and $CD8^+$ T cells was observed in cKO mice (Fig.9D), together with a decrease in FOXP3 expression (Fig.9E) and in the frequency of Tregs expressing the immunosuprressive molecules CD25 and CD73 in Ahr-cKO mice (Fig.9F). It is important to underline that, in general, Ahr-depleted Tregs have bigger differences with control-Tregs compared to Hif-1α-KO Tregs, and this might be due to the presence of Hif-2α that might compensate the loss of Hif-1α. Indeed, Hsu and colleagues demonstrated that Hif-2α KO-Tregs have increased levels of Hif1a (Hsu *et al*., 2020).

Very interestingly, AHR and HIF-1α depletion in Tregs did not alter the myeloid cell compartment of the spleen (Fig.10), except for the number of inflammatory monocytes, which increased in absence of the two TFs. Even though there are no studies describing a direct relationship between Tregs and myeloid cells, this result could reflect the indirect effect that Tregs have on myeloid cells through other T-cell subpopulations (Bieber et al., 2017).

3. ROLE OF AHR AND HIF-1α IN TREGS DURING CLL DEVELOPMENT

The AT of CLL cells into the three models in two different cohorts injected with different primary CLL clones revealed a striking difference in tumor development among the cKO mice and the controls, demonstrating the impacted immunosuppressive ability of KO-Tregs in the tumoral contexts, where a strong activation of AHR and HIF-1α is most likely to happen. It has been demonstrated that AHR is overexpressed in the serum of CLL patients (Sanna et al., 2017), and HIF-1α is constitutively expressed in CLL patients (Ghosh et al., 2009). In addition, several works indirectly demonstrated the strong activation of these two TFs in CLL. First of all, IDO1, the key enzyme involved in the conversion of Trp into Kyn (endogenous AHR ligand) is upregulated in CLL patients (Lindström et al., 2012) and leukemic Eμ-TCL1 mice (Öztürk et al., 2021), similarly to IL4l1, another enzyme recently discovered to convert Trp into kynurenic acid and activate AHR (Sadik et al., 2020). Regarding HIF-1α, a clinical study demonstrated the correlation between HIF1A mRNA overexpression and poor overall survival of CLL patients (Kontos et al., 2017). However, an important question to address is whether the two TFs are upregulated in Tregs of CLL patients and animals compared to healthy counterparts, especially to try to predict the efficacy of a targeted therapy against these molecules in CLL.

In our cKO mice, the decreased tumor load correlated with increased frequency of $CD8^+$ T cells and increased expression of pro-inflammatory cytokines in Tconv, pointing towards an impacted immunosuppressive ability and consequent increased anti-tumor immune response in absence of

AHR and HIF-1α in Tregs. Surprisingly, no differences were detected in $CD8^+$ T cell cytokine production in leukemic mice; this result could be due to other cytotoxic molecules involved in mediating the anti-tumor immune response (e.g. Perforin or Granzymes). In line with a reduced immunosuppression, AHR-cKO mice injected with CLL displayed an accumulation of resting Tregs (rTregs) over activated Tregs (aTregs) together with a decreased frequency in TIGIT+ and CTLA-4+ Tregs (Fig.11J). With the analysis of the myeloid compartment we could recapitulate what we already observed at steady state: a skewing from patrolling to inflammatory monocytes in absence of AHR and HIF-1α in Tregs together with an increased DCs frequency, in line with an enhanced anti-tumor immune response in cKO mice.

It is important to highlight that among myeloid cells, Tregs have an important crosstalk with myeloid-derived suppressor cells (MDSCs). This cell type represent another immunosuppressive population and is fundamental in promoting tumor development by suppressing anti-tumor immune response. Tregs and MDSCs activate in a mutual way, and they cross-activate through the PD-1/PD-L1 axis. Very interestingly, both AHR and HIF-1α are involved in PD-L1 upregulation in different cell types (Noman *et al.*, 2014; Wang *et al.*, 2019a). For these reasons, analysis of MDSCs in the CLL-TME would be useful to reveal whether changes occur in this cell population upon AHR and HIF-1α depletion in Tregs. If changes are observable, it would be worthy to investigate PD-1 expression in MDSCs and PD-L1 expression in Tregs to understand whether KO-Tregs activate less MDSCs and contribute to a less immunosuppressive TME.

We also demonstrated the direct effect of Tregs on $CD8^+$ T cells in CLL in vivo, as we could diminish the differences observed in tumor load between cKO and control mice by depleting $CD8^+$ T cells (fig. 12C). Nonetheless, we could not completely abrogate the differences in the tumor load by depleting $CD8^+$ T cells, meaning that beside this T-cell subtype, Tregs affect CLL development by modulating the activity of other cells. Good candidates could be DCs, as cKO leukemic mice had an increased frequency of DCs (Fig.11R). As Tregs can indirectly affect effector T-cell function by regulating DC activation and maturation (Schildknecht et al., 2010), the difference in DC frequency may be linked to the enhanced T-cell mediated anti-tumor response observed in cKO mice. To address whether KO-Tregs have a different impact on DCs maturation compared to the WT ones, it is necessary to further characterize intra-tumor DCs in the AT model of CLL of cKO and control mice, analyzing not only DCs frequency and number, but also their APC abilities and maturation status (e.g. by measuring the expression of CD80, CD86, IL-10, CD40, MHC molecules). Moreover, it would be interesting to co-culture Tregs isolated from the three models and DCs in vitro. In this way, it would be possible to understand whether the lack of the two TFs in Tregs affects Treg function towards DCs.

As in other tumors, the mechanisms of Treg accumulation in the CLL TME remain unknown, especially whether Tregs in CLL-TME are attracted from the periphery to the tumor site (nTregs) or are polarized from $CD4^+$ Tconv (iTregs). CLL cells are known to release IL-10, which promotes FOXP3 upregulation and subsequent iTreg differentiation (DiLillo et al., 2013). In addition, PD-L1 expression by cancer cells induces the generation of iTregs from Tconv (Francisco et al., 2009), so PD-L1-expressing CLL cells might contribute to the induction of Tregs within the CLL TME, as it was demonstrated in non-Hodgkin's lymphoma (nHL) (Han et al., 2011). However, nTregs from the periphery can also be recruited to the CLL TME. In order to understand the origin of intra-tumor Tregs in CLL TME, it would be useful to analyze the expression of discriminative markers of nTregs and iTregs (e.g. Nrp1 and Helios). In addition, Tregs express several chemokine receptors that allow them homing to the tumor site, mainly attracted by chemokines released by tumor cells, thus analyzing the expression of these receptors might be an effective way to explore Treg origin.

It is also fundamental to underline that inhibiting AHR and HIF-1α with two antagonists reduced CLL development in vivo (Fig.14), confirming the importance of AHR and HIF-1α in CLL pathogenesis. In addition, we demonstrated that depletion of AHR and HIF-1α in CLL cells using $CD19^{Cre}$ $Ahr^{fx/fx}$/ $Hif1a^{fx/fx}$ mice does not affect leukemogenesis (Gonder et al., 2021), suggesting that AHR and HIF-1α expression by cells composing the TME promotes tumor development and is mainly affected by the inhibition of the two TFs in vivo. Regarding AHR, it is widely established that the IDO1-Kyn-Trp-AHR axis is upregulated in different tumors and its blockade reduces tumor load in melanoma, colon cancer and breast cancer (Campesato *et al.*, 2020a; Zhang *et al.*, 2021). For HIF-1α, its inhibition improves the efficacy of ICB in melanoma and non-small cell lung cancer by enhancing NK-cell and T-cell-mediated cytotoxicity (Lequeux et al., 2021; Luo et al., 2022). With our data, we confirmed the relevance of AHR and HIF-1α in CLL, and demonstrated that their pharmacological inhibition controls tumor development and their depletion in Tregs, but not in CLL cells, is able to control disease progression. An interesting aspect to consider is that inhibitors do not target any specific cell type, so it would be highly relevant to investigate how to specifically target AHR and HIF-1α only in Tregs, for example by combining these inhibitors with targeted drug delivery strategies.

4. ROLE OF AHR AND HIF-1α IN TREGS DURING MELANOMA DEVELOPMENT

We wanted to investigate whether the impacted immunosuppressive ability of Tregs in absence of AHR and HIF-1α was maintained in another tumor model, or whether it was specific for CLL development. It is known that Tregs play a crucial role in melanoma and accumulate in melanoma patients (Huang et al., 2021). Indeed, the ratio of $CD8^+$ T cells/Tregs in the TME is used to predict

melanoma patient OS (Jacobs et al., 2012). In addition, one clinical trial is evaluating the efficacy of Treg depletion in melanoma patients (NCT02823405), in particular by reducing Treg recruitment with X4P-001 (CXCR4 antagonist), hence blocking chemokines receptors. Moreover, anti-CCR4 antibody KM2160 effectively depletes effector Tregs and promotes the immune response of $CD8^+$ T cells in melanoma and T-cell leukemia patients (Sugiyama *et al.*, 2013b).

For preclinical studies, s.c. injection of B16F10 melanoma cells into syngenic mice is often used as melanoma model for studying immune cell infiltration and novel therapies, and FOXP3+ Treg depletion enhances immune cell infiltration in this model. For these reasons, we decided to investigate the impact of AHR and HIF-1α in Treg immunosuppression in melanoma by injecting B16F10 melanoma cells into cKO and control mice. Here, we could confirm that also in melanoma AHR- and HIF-1α depletion in Tregs decreases tumor load. A second cohort of AHR-KO and control mice confirmed these results and revealed a decrease expression of immunosuppressive IC in KO Tregs. $CD8^+$ T-cell depletion confirmed that the differences in tumor growth between cKO and control mice are mediated by $CD8^+$ T cells. To have a better idea of the molecular dynamics in melanoma, it would be useful to inspect the T cells in the TME and understand which particular mechanisms are affected by AHR and HIF-1α depletion in Tregs (e.g. DC activation, cytokine production of $CD8^+$ or $CD4^+$ T cells, NK cell infiltration).

It is important to underline that several studies highlighted the crucial role of NK cells in the anti-tumor immune response in this model, and NK cell depletion in melanoma-bearing mice resulted in higher tumor load compared to non-NK cell depleted mice (Kurosawa et al., 1995). NK cells and $CD8^+$ T cells have being described as the main mediators of the anti-tumor immune response in melanoma model (Xu et al., 2004), and Tregs are able to suppress NK activity both in vitro and in vivo. It would be then useful to inspect whether the depletion of NK cells in cKO and control mice eliminates differences in tumor growth as observed in absence of $CD8^+$ T cells. In case NK cells appear involved in mediating this effect, it would also be useful to compare the single depletion of either NK or $CD8^+$ T cells with the double depletion, to inspect whether the two cell types synergically mediate the anti-tumor immune response and are both affected by Treg immunosuppression, also because NK cells are important for attracting $CD8^+$ T cells in the TME through IFN-γ release. In this setting Tregs might also indirectly affect $CD8^+$ T cells by modulating NK cell functions.

Even if we showed that AHR and HIF-1α depletion in Tregs affect tumor development in both CLL and melanoma, it is important to highlight that the dynamics within the two tumors are very different. In accordance with this, Lequeux et al. recently demonstrated that HIF-1α depletion in B16F10 melanoma cells prior to in vivo injection led to decreased tumor load in mice with consequent infiltration of NK and $CD8^+$ T cells, suggesting that hypoxia and HIF-1α upregulation

have a direct impact on melanoma cells and on their ability to attract immune cells at the tumor site (Lequeux et al., 2021). Instead, we saw that HIF-1α depletion in CLL cells did not affect leukemogenesis, probably because of the increased hypoxia levels in solid tumors (and in particular in melanoma) and the different cellular and molecular composition of the TME, such as the involvement of NK cells in CLL and melanoma anti-tumor immune response.

5. MOUSE MODELS MIMICKING AHR AND HIF-1α DEPLETION OR UPREGULATION

Due to the relevance of AHR and HIF-1α in cancer development and in immune cell metabolic control, different models have been used to study these TFs.

Regarding hypoxia, it is known that it can promote inflammation during infections, while during cancer development low oxygen levels cause unresponsiveness of immune effectors, thus favoring tumor growth. Also, HIF activation displays often opposite effects on the activity of immune cells, and the complexity is expanded if we consider the different models and the technical approached used to address specific questions. Indeed, due to all these reasons, very often the results of different works seem contradictive and lead to opposite conclusions. For example, in order to mimic HIF-1α overexpression in Tregs, Lee et al. developed *Foxp3*^{Cre} *Vhl*$^{fx/fx}$ mice, and observed that HIF-1α stabilization through VHL depletion in Tregs leads to Th-1 like Treg conversion and impacted immunosuppression in a colitis model (Lee *et al.*, 2015b). These results are opposite to our findings, suggesting that VHL depletion in Tregs not only leads to HIF-1α stabilization, but it also regulates HIF-1α-independent mechanisms, such as HIF-2α stabilization (Hoefflin et al., 2020). In another work performed by Clever and colleagues, HIF-1α upregulation was achieved by depleting the three PHD hydroxylases in CD4$^+$ T cells (*CD4*^{Cre} *Egln1*$^{fl/fl}$ *Egln2*$^{fl/fl}$ *Egln3*$^{fl/fl}$) (Clever et al., 2016). In this way, HIF-1α depletion happened in the whole CD4$^+$ T cell compartment and not only in Tregs. In vitro polarization of PHD-KO-CD4$^+$ T cells into iTregs led to a decreased FOXP3 expression and increase in T-bet and IFN-γ expression in polarized Tregs, suggesting an impacted Treg immunosuppressive ability when PHDs are depleted and HIF-1α is stabilized. Also in this case, the results obtained in this work point towards opposite conclusion compared to our analysis (Fig.16E-K). It is then important to analyze the differences in the models used, which could explain the divergent results. First, PHDs depletion not only leads to HIF-1α stabilization, but it also affects HIF-2α and might have other functions not related to the HIF proteins. Another fundamental aspect to underline is that the depletion/upregulation of HIF-1α in Tregs (using Foxp3Cre mice) is not comparable with depletion of the same TF in CD4$^+$ T cells (achieved with CD4^{Cre} mice). This difference becomes crucial in experiments where the development or the differentiation process of Tregs is evaluated, such as during in vitro iTreg polarization. Indeed, in Foxp3Cre mice, the gene of interest is inactivated only upon FOXP3 expression, thus once Tregs are already differentiated. Instead, in CD4^{Cre} mice, PHDs

are depleted in $CD4^+$ T cells, hence are already absent during iTreg polarization. Knowing that both AHR and HIF-1α are fundamental for iTreg development (Dang et al., 2011; Quintana et al., 2008) and play different roles in specific phases of Tr1 generation (Mascanfroni et al., 2015), it is not surprising that the development stage chosen to deplete the same genes can have a huge impact on the results outcome.

Similar findings can be observed when studying the role of AHR in Tregs, as some works describe this TF as activator of FOXP3 (de Araújo et al., 2021; Gandhi et al., 2010), while other publications highlight how AHR inhibits Treg development (Dant et al., 2017; Kimura et al., 2008). Another aspect to consider is the presence of different tissue-specific Treg subsets, where AHR plays different roles according to the ligand that activates it.

6. METABOLIC CHANGES IN AHR AND HIF-1α-KO iTREGS

Through our in vitro experiments, we demonstrated that KO-iTregs have decreased expression of immunosuppressive markers (Fig.16) which correlate with a decreased immunosuppressive ability towards $CD8^+$ T cells (Fig.17), adding more evidence to the positive role of AHR and HIF-1α in regulating the immunosuppressive functions of Tregs.

It is known that AHR and HIF-1α control the transcription of different genes involved in metabolic changes and adaptation to the microenvironment. For this reason, to better understand the mechanisms by which AHR and HIF-1α regulate the immunosuppressive ability of Tregs, we inspected the metabolic behavior of polarized Tregs in vitro. Seahorse analysis revealed an enhanced oxygen consumption rate (OCR) of KO-iTregs compared to WT ones (Fig.18), although more replicates are needed to confirm these findings. Since OCR is used to measure mitochondrial oxidative phosphorylation (OXPHOS), our results demonstrate that KO-iTregs have increased OXPHOS but decreased immunosuppressive abilities, which seems to contradict the notion that enhanced OXPHOS correlates with increased immunosuppressive function of Tregs. Indeed, Tregs mainly rely on fatty acid oxidation (FAO) and OXPHOS (Angelin et al., 2017), and this metabolic advantage is mainly regulated by the expression of FOXP3, which is responsible of inhibiting the transcription of glycolytic enzymes-related genes and MYC (involved in glycolysis), thus promoting OXPHOS and enhancing Treg suppressive ability. Nonetheless, our data could reflect another scenario: regarding AHR, it is known that the activation of this TF decreased OCR in mouse hepatoma cells lines (Hwang et al., 2016), so it is possible that the depletion of AHR leads to a decreased FOXP3 expression but increased OXPHOS. HIF-1α, instead, is one of the main responsible of the metabolic switch to glycolysis, as it induces the expression of glycolytic genes and increases LDH enzyme activity, thus enhancing the conversion of pyruvate to lactate and leading to a glycolytic shift (Kempkes et al., 2019). It is also known that upon TCR and CD28 engagement, HIF-1α

is activated in normoxic conditions through mTORC1 engagement (Kurniawan et al., 2020). In our conditions, it is possible that HIF-1α gets activated in WT-iTregs, leading to low OCR rate. Instead, in HIF-1α KO-iTregs, switch to glycolysis is prevented with a consequent increase in OCR, as iTregs can only rely on this pathway for their metabolic activity.

As Tregs mainly rely on glutaminolysis to fuel the TCA cycle (Kurniawan et al., 2020), we analyzed the incorporation of labelled glutamine into TCA cycle metabolites and observed an increased relative flux of glutamine-derived carbon into citrate and α-ketoglutarate (α-KG) in KO-iTregs (Fig.18). Very interestingly, a recent study showed that increased α-KG in iTregs leads to a decrease in FOXP3 expression and consequent shift of Treg phenotype into Th1-like T cells (Matias et al., 2021). Indeed, glutamine enters in the T-cell mitochondria, and is converted into glutamate and α-ketoglutarate (α-KG). α-KG enters the TCA cycle to drive OXPHOS and leads to enhanced inflammatory phenotype of Tregs. Similar mechanisms could happen in our KO-iTregs, where AHR and HIF-1α depletion leads to α-KG accumulation and enhanced OXPHOS. It would be interesting to investigate whether KO-iTregs have enhanced expression of pro-inflammatory molecules (e.g. IFN-γ and T-bet) and whether it is possible to rescue their phenotype and function by inhibiting the enzymes that catalyze the reaction of glutamine into α-KG, such as glutamate dehydrogenase (GDH).

7. MOLECULAR MECHANISMS UNDERLYING BIOLOGICAL DIFFERENCES OBSERVED IN KO TREGS

With this project we provided evidence of the role of AHR and HIF-1α in contributing to the immunosuppressive function of Tregs. Nonetheless, the mechanisms used by these two TFs to mediate Treg-immunosuppression remain unknown. For this reason, we are currently performing bulk RNA sequencing of iTregs to explore the differentially expressed pathways in WT and KO-iTregs, aiming to define specific genes that we could target and better characterize to unravel the molecular mechanisms of Treg immunosuppression on presence and absence of AHR and HIF-1α. Another valid possibility would be to perform single-cell RNAseq of tumor-infiltrated Tregs in the spleen of leukemic control and cKO mice. In this way, not only differentially expressed genes in tumor-specific Tregs could be identified, but also Treg subpopulations characterized by the expression of specific genes that could be specifically enriched or depleted in KO Tregs compared to control ones. It is also important to underline that AHR and HIF-1α have different transcriptional activity (which may partially overlap since they share the same dimerization partner ARNT), but their depletion leads to similar biological effects in Tregs. These transcriptional differences might

explain the differences observed between AHR and HIF-1α KO iTregs in vitro and between the two cKO mice in vivo.

Another very important matter to address is to validate the activation of AHR and HIF-1α in our in vitro experiment settings. As we observe differences in the different conditions, we hypothesized that the two TFs are transcriptionally active in control iTregs, but qPCR of target genes of the two transcription factors in control and KO-iTregs or immunofluorescence of AHR and HIF-1α to detect their nuclear localization and consequent transcriptional activation are valid options to verify their transcriptional status. In addition, performing iTreg polarization in presence or absence of AHR- and HIF-1α- stabilizing molecules (Kyn/TCDD/FICZ for AHR and hypoxia/CoCl2 for HIF-1α) would allow us to understand whether the presence of the activators leads to different outcomes in the in vitro results.

Part II - Ebi3/IL-27 depleted microenvironment favors leukemia progression in CLL by impairing $CD8^+$ T-cell-mediated anti-tumor immunity

The involvement of the TME in promoting tumor progression is mainly due to a dysfunctional anti-tumor immunity, characterized by $CD8^+$ T-cell exhaustion, infiltration of immunosuppressive cells and secretion of soluble factors, such as metabolites and cytokines. Nonetheless, some cytokines present pleiotropic functions in different tumors, meaning that they are described with both pro-tumor and anti-tumor effects, making the characterization of a specific cytokine in different tumors of great importance. This substantial complexity becomes even wider when considering that some discrepancies in the literature are due to the distinct technical and experimental settings and to the different preclinical models used to address similar questions.

One of the cytokines characterized by all these features is IL-27, a pleiotropic cytokine belonging to the IL-12 family composed by two subunits: EBI3 and p28 (Carl and Bai, 2008). The receptor of this cytokine is also heterodimeric, formed by IL-27Rα and gp130. IL-27 has been described with both pro- and anti-tumor roles (Fabbi et al., 2017), and able to affect both cancer cells (ovarian cancer, AML and MM cells) and immune cells (mainly affecting T-cell function and differentiation processes). As a consequence of the complexity and peculiarity of each tumor, IL-27 might have opposite roles according to the tumor type and composition of the TME. For all these reasons, we wanted to investigate the role of IL-27 during CLL development, using different in vivo and in vitro approaches.

1. ROLE OF EBI3/IL-27 DURING MURINE CLL DEVELOPMENT

To address our question, we used C57BL/6 (WT) and *Ebi3*$^{-/-}$ mice (which lack the EBI3 subunit of IL-27). First of all, we injected CLL cells in both WT and *Ebi3*$^{-/-}$ mice and observed an enhanced tumor development in absence of EBI3 (Fig.1-S2). This difference was accompanied with increased CD8^{+} T cell exhaustion and Treg-mediated immunosuppression in *Ebi3*$^{-/-}$ mice, strongly suggesting an anti-tumor role of IL-27 in this context. Moreover, in line with an increased tumor load in KO mice, a major switch from naïve to antigen-experienced CD8^{+} and CD4^{+} T cells was observed in KO animals. Similar results were found when analyzing the survival and the splenic TME of leukemic Eμ-TCL1 and Eμ-TCL1 *Ebi3*$^{-/-}$ mice, where decreased survival, enhanced CD8^{+} T-cell exhaustion and increased immunosuppressive Tregs were found in leukemic mice lacking EBI3 (Fig.2-S3), confirming the anti-tumor role of IL-27 in CLL. In agreement with these findings, we also demonstrated that IL-27 is reduced in the blood of leukemic mice and CLL patients (Fig.6A-B), and that CLL progression correlates with decreased IL-27 concentration in the PB of AT-TCL1 mice.

We then wanted to understand which cell type was the main mediator of the enhanced CLL development in EBI3-KO mice. Since previous studies reported a direct anti-tumor role of IL-27 in several tumors, including hematological malignancies such as pediatric AML and CLL (Manouchehri-Doulabi et al., 2020; Zorzoli et al., 2012), EBI3 was initially depleted only in CLL cells (Fig.2G) and no differences were observed in CLL progression. These data suggested that IL-27 depletion does not directly affect CLL cells in vivo, and we confirmed these findings in vitro by treating mouse and human primary CLL cells with different concentrations of IL-27, which showed no differences in survival nor in the expression of CLL functional markers (Fig.S7C-F). The differences between our results and the data present in the literature might be explained by the different tumor cells, the concentrations and the time points chosen. Indeed, the physiological concentration of IL-27 in human PB is around 500 pg/ml, while the concentration used to treat CLL cells in vitro is between 25 and 50 ng/ml. For this reason, even though an effect is observed upon IL-27 treatment on cancer cells, it is probably due to the concentration used, which is far from the physiological settings.

As it is known that IL-27 has a fundamental role in T-cell differentiation and activation (Wehrens et al., 2018), and T cells expresses high levels of IL-27R, we evaluated the effect of EBI3 depletion in T cells during CLL development. For this purpose, *Ebi3*$^{-/-}$ T cells injected in Rag2-/- mice together with CLL could recapitulate the increased CLL development observed in *Ebi3*$^{-/-}$ mice (Fig.3-S4), with features of enhanced CD8^{+} T-cell exhaustion and Treg-mediated immunosuppression, thus demonstrating that IL-27 depletion in T cells is responsible of mediating the enhanced CLL development observed in *Ebi3*$^{-/-}$ mice. These findings are in accordance with several studies

published in the literature, where IL-27 is shown to regulate anti-tumor immune response by enhancing T-cell mediated functions, in particular Th1 cell development and CTL responses (Hisada et al., 2004; Schneider et al., 2011). Nonetheless, some studies came to opposite conclusions, showing that IL-27 enhances T-cell exhaustion by promoting T-cell expression of multiple inhibitory receptors (LAG-3, TIGIT; TIM-3, CTLA-4) in mouse $CD4^+$ and $CD8^+$ T cells during toxoplasmosis (DeLong et al., 2019). In line with this, by injecting melanoma cells in IL-27Rα-/- and WT mice, Chihara and colleagues also demonstrated with scRNAseq of $CD8^+$ TILs that the expression of TIM-3, LAG-3, and TIGIT was reduced in IL-27R-deficient mice (Chihara et al., 2018). These results clearly demonstrate the complex role of this cytokine during cancer development, which largely depends on the tumor type and on the TME-mediated stimuli, as it is plausible to hypothesise that the presence of other cytokines, metabolites and specific immune cells influence the final outcome of IL-27 in exerting its pro- or anti-tumor role. As the TME changes throughout tumor development, it is also possible that IL-27 has different functions depending on the tumor stage.

2. EBI3-DEPLETION MAINLY AFFECTS $CD8^+$ T-CELL CYTOTOXICITY

To better understand the role of EBI3 depletion on T cells, we analyzed the transcriptome of activated $CD8^+$ T cells, $CD4^+$ Tconv and Tregs through RNAseq. The majority of the transcriptional changes among WT and *Ebi3*$^{-/-}$ T cells concerned $CD8^+$ T cells (Fig4B) rather than $CD4^+$ Tconv and Tregs (Fig.S5D-E). Indeed, EBI3-depleted $CD8^+$ T cells displayed a decreased expression of crucial transporters involved in T-cell activation, proliferation, and cytotoxicity. In particular, SLC7a5, an amino-acid transporter involved in T-cell differentiation which could potentially contribute to the altered T-cell activity (Ren *et al.*, 2017a), was downregulated in EBI3-depleted $CD8^+$ T cells. Moreover, Profilin-1, a known inhibitor of T-cell synapse formation (Schoppmeyer et al., 2017), was overexpressed in this T-cell population in absence of EBI3. Another overexpressed gene was Wnt10a, involved in T-cell proliferation through the Wnt-β-catenin pathway. Collectively, the transcriptional analysis of $CD8^+$ T cells revealed that EBI3 depletion alters the transcriptional program of $CD8^+$ T cells with an increased expression of immune synapse inhibitor, increased proliferation and decreased expression of crucial transporters, suggesting an impacted function of this T-cell subtype in absence of EBI3. For this reason, we decided to investigate the functional activity of $CD8^+$ T cells, and observed that the treatment of murine and human $CD8^+$ T cells with IL-27 led to enhanced cytotoxic activity. Altogether, these results suggest that the progressively decreasing levels of IL-27 in CLL patients and leukemic mice lead to dysfunctional T-cell dynamics through different mechanisms, including the downregulation of crucial metabolic pathways and the inability to mount an appropriate immune response due to the lack of a functional lytic immune synapse.

As IL-27 acts on $CD8^+$ T cells through the activation of STAT1 and induces IFN-γ and EOMES, which are critical for induction of effector molecules during the anti-tumor immune response (Mayer *et al.*, 2008; Morishima *et al.*, 2005b; Schneider *et al.*, 2011), it would be interesting to evaluate whether in EBI3-KO T cells have decreased STAT1 phosphorylation that leads to an impacted cytotoxic activity.

3. *Ebi3*$^{-/-}$ MICE AS A MODEL TO RECAPITULATE IL-27 DEFICIENCY

Among the different members of IL-12 heterodimeric family, some cytokines share the same subunits. To this regard, IL-35 belongs to the same family, and is composed by EBI3 and p35 subunits, but has been described as a pro-tumoral cytokine (Niedbala et al., 2007). Indeed, IL-35 is secreted by activated and highly immunosuppressive Tregs in the TME and acts on different immune cells to impair their proliferation and activation status (Olson et al., 2013; Shao et al., 2021). For this reason, the usage of *Ebi3*$^{-/-}$ mice results in the depletion of both IL-27 and IL-35, which have opposite roles in many tumors.

When we observed an enhanced CLL development in absence of EBI3, we excluded a putative role of IL-35 because this cytokine has a pro-tumor role, but to confirm that the effect observed in *Ebi3*$^{-/-}$ mice was dependent on IL-27, we performed IL-27 neutralization during CLL development in WT mice. In this settings, we could recapitulate the enhanced CLL growth observed in *Ebi3*$^{-/-}$ mice. Nonetheless, there were minor differences between controls and IL-27-neutralized mice (Fig.6C) compared to WT vs *Ebi3*$^{-/-}$ mice in terms of tumor development and $CD8^+$ T cell exhaustion. This effect could be explained by the fact that antibody neutralization is not as efficient as genetic depletion, and that each injection of a primary CLL clone isolated from a diseased Eμ-TCL1 mouse has unique dynamics and specific features of the TME-immune landscape.

Since EBI3 subunit is shared between the two cytokines, EBI3-deficient mice are often used to investigate the role of IL-27 and IL-35 in different contexts, in particular to understand which group of forces is dominant during anti-tumor immune response (the IL-35-mediated pro-tumoral role or the IL-27-mediated anti-tumor effect). In line with our findings, Liu and colleagues demonstrated that *Ebi3*$^{-/-}$ mice present enhanced melanoma growth compared to control animals. In addition, our characterization of WT and *Ebi3*$^{-/-}$ mice at steady state revealed no differences in the Treg frequency (in line with a functional Treg compartment in absence of IL-35). On the contrary, even though in a minimal extent, frequencies of $CD8^+$ T cells and $CD4^+$ Tconv were altered in EBI3-deficient mice, and IL-27 (but not IL-35) is known to affect both T cell subpopulations. (Hibbert et al., 2003; Schneider et al., 2011).

In order to overcome the impairment of several cytokines in *Ebi3*$^{-/-}$ mice, some researchers study the effects of IL-27 by using *Il27ra*$^{-/-}$ mice, which lack one subunit of IL-27 receptor, impeding IL-27-

mediated signaling. Since we demonstrated that the lack of IL-27 affects $CD8^+$ T cell cytotoxic activity, we could further explore the role of IL-27 specifically on $CD8^+$ T cells by using *CD8^{Cre} Il27ra$^{fx/fx}$* mice, in which only $CD8^+$ T cells would be unresponsive to IL-27 binding. Moreover, with this approach, it would be possible to evaluate whether IL-27 acts on $CD8^+$ T cells in an autocrine or paracrine way (hence whether the effects observed in EBI3-KO mice are due to the lack of EBI3 in T cells, or to the lack of IL-27 in the splenic microenvironment). Nonetheless, a paracrine signaling remains the preferred hypothesis, as IL-27 is mainly produced by antigen presenting cells (APCs), which do not include T cells, and since we observed differences in cytotoxic activity of $CD8^+$ T cells upon IL-27 treatment.

Another important question to address is whether leukemic cells produce the same amount of IL-27 than normal B cells. In this way, a decreased IL-27 concentration in the leukemic TME could be explained by the impacted ability of CLL cells in producing this cytokine. In addition, in order to further inspect the anti-tumor activity of IL-27, it would be interesting to overexpress IL-27 during CLL development and verify whether this condition leads to a decrease in CLL development in recipient WT mice. To this purpose, a CLL mouse cell line, called TCL1-355, could be engineered to secrete IL-27 and injected in vivo to recapitulate a constant IL-27 production throughout CLL development. Our efforts to generate this IL-27 overexpressing cell line remain unsuccessful until today.

4. COMBINE IL-27 THERAPY WITH AHR AND HIF-1α INHIBITORS IN CLL

In the first part of the present PhD project we identified AHR and HIF-1α as fundamental players of Treg-mediated immunosuppression, thus highlighting the pro-tumor role of these two TFs in Tregs during CLL development. In the second part of the project, instead, we characterized IL-27 as an anti-tumoral cytokine in CLL that promotes $CD8^+$ T cell cytotoxic activity. To this regard, a combined therapy with AHR and/or HIF-1α inhibitors together with IL-27 could be a therapeutic strategy to initially test on leukemic animals. Particular attention should be given to the crosstalk between IL-27 and AHR: indeed, in Tr1 development, IL-27 is able to activate AHR via STAT3 engagement, leading to IL-10+ immunosuppressive FOXP3+ Tr1 T-cell development (Apetoh et al., 2010). For this reason, IL-27 treatment could be particularly effective in combination with AHR inhibitors, as the anti-tumor effect of IL-27 could be reached without the activation of Tr1 cells via AHR. Moreover, IL-27 is able to block HIF-1α-mediated VEGF activation in macrophages (Zhang et al., 2019). Also in this case, co-administration of IL-27 and HIF-1α inhibitors could be beneficial against leukemia, as HIF-1α inhibition and IL-27 administration could synergistically block VEGF expression in tumors, which contributes to tumor progression and recruitment of Tregs at the tumor site.

Final remarks

Since AHR and HIF-1α impact different mechanisms of Treg biology, we are now adopting a multi-omics approach to understand how these two TFs mediate Treg-immunosuppression: by metabolomic analysis, we are currently trying to assess the metabolic changes in KO-Tregs that could explain their impacted immunosuppressive abilities. At the same time, the transcriptomic differences are being analyzed through RNAseq to detect the changes in gene expression between the control and KO-Tregs. In addition, proteomic analysis would be very useful to understand whether post-transcriptional mechanisms mediate the function of AHR and HIF-1α in promoting the suppressive ability of Tregs. By adopting this multi-omics approach, our goal is to define the mechanisms used by these two TFs in controlling Treg function and perform further experiments to test the involvement of specific molecules.

With different in vivo and in vitro approaches, we also demonstrated the anti-tumoral role of IL-27 in CLL, as its depletion promotes CLL development by hampering $CD8^+$ T-cell mediated anti-tumor immune response. In addition, this cytokine promotes $CD8^+$ T-cell cytotoxic activity both in murine and human primary cells, and the same findings were observed in different tumors (Hisada et al., 2004; Hu et al., 2009). For this reason, IL-27 can be used in combination with immunotherapy to restore a functional anti-tumor immune response. To this regard, Hu and colleagues demonstrated that intra-tumor delivery of IL-27 through Adeno-Associated Virus in vivo is able to stimulate anti-tumor immunity and enhances the efficacy of anti-PD1 therapy in melanoma and myeloma (Hu et al., 2020). In order to test the therapeutic employability of IL-27 in CLL, we want to combine it with immune checkpoint blockade, in particular with anti-PD1, as it is known that single anti-PD1 blockade is not sufficient to control leukemia growth in preclinical mouse models and CLL patients.

Conclusions

The main goal of this PhD project was to unravel the mechanisms and dynamics that allow the interaction between CLL cells and the surrounding cells of the TME, in particular immune cells, which have an active contribution to CLL progression.

In the first part, we focused on regulatory T cells (Tregs), asking whether depleting specific transcription factors in this T-cell subpopulation could affect their suppressive feature and lead to an impacted leukemia progression. In particular, we depleted AHR and HIF-1α in vivo, generating conditional knock out (cKO) mice that lack either TF only in Tregs. These new mouse models allowed us to inspect the role of AHR and HIF-1α in the suppressive ability of Tregs. After validating the suitability of these models for further analysis, we performed adoptive transfer of CLL cells into cKO and control mice, obtaining a drastic delay in CLL growth upon depletion of AHR and HIF-1α, and a decrease in immune checkpoints expression in Tregs compared to controls. In vivo injection of AHR and HIF-1α antagonists recapitulated the decreased CLL development when the two TFs are functionally inactive. These findings already strongly suggested an important role of AHR and HIF-1α in contributing to the immunosuppressive activity of Tregs during CLL development. Similar results were obtained when injecting B16F10 melanoma cells in the cKO and control mice, with intra-tumoral AHR-KO Tregs expressing less TIGIT and PD-1 compared to WT Tregs. In both cases, the decrease in CLL and melanoma development were mitigated when $CD8^+$ T cells were depleted, demonstrating the importance of $CD8^+$ T cells in mediating the differences in the tumor load observed in cKO mice. We then evaluated the suppressive ability of ex vivo induced Tregs (iTregs) using suppression assay, observing an enhanced proliferation of $CD8^+$ T cells in presence KO-iTregs. Finally, we observed an altered oxygen consumption rate and glutamine uptake in KO-iTregs, pointing towards an altered metabolic behavior of Tregs in absence of the two TFs. Altogether, these results indicate that AHR and HIF-1α have a key role in the suppressive ability of Tregs, and are of particular importance for sustaining the immunosuppressive ability of intra-tumor Tregs during CLL development.

In the second part of the present project, we characterized the role of IL-27 in CLL development and identified the mechanisms used by this cytokine to promote T-cell-mediated anti-tumor immune response. For this purpose, we used the Eμ-TCL1 and *Ebi3*$^{-/-}$ transgenic mouse models as well as clinical samples from CLL patients. By injecting CLL cells in *Ebi3*$^{-/-}$ and control mice we demonstrated a strong anti-tumor activity of IL-27 in CLL, as its absence led to an enhanced CLL progression and impacted anti-tumor immune response. In addition, using RNA sequencing, we could identify $CD8^+$ T cells as the T-cell subtype mainly affected by IL-27 depletion, characterized by major transcriptional changes associated with impacted T-cell activation, proliferation, and synapse formation. In line with these findings, we observed increased cytotoxic activity of ex vivo-cultured

$CD8^+$ T cells in presence of IL-27 both in murine and human primary cells. The anti-tumor activity of IL-27 in CLL development was confirmed by neutralizing in vivo this cytokine during CLL development, where we could partially recapitulate the enhanced leukemia progression observed in *Ebi3*$^{-/-}$ mice. In addition, the concentration of this cytokine was decreased during CLL development in both pre-clinical murine and patient samples. Altogether, these data demonstrate the anti-tumoral role of IL-27 during CLL development via enhanced $CD8^+$ T-cell-mediated cytotoxic activity during the anti-tumor immune response.

Annexes

Preface

In addition to the work described in the "Experimental data" section, during my PhD I contributed to different publications in the field of tumor immunology and Chronic Lymphocitic Leukemia development. In particular, I participated in one project led by Susanne Gonder (PhD student of the TSI group at LIH), reported in Annex I. The main biological question underlying this project was to understand the role of *Ahr* and *Hif1a* in CLL pathophysiology. For this reason, she obtained conditional knock-out mice lacking these two transcription factos in CLL cells (Eμ-TCL1-CD19^{Cre}Ahr$^{fx/fx}$ or Hif1a$^{fx/fx}$ mice). By analysing the RNA-sequencing data and the CLL development of the cKO mice compared to the controls, we could demonstrate that the depletion of *Ahr* and *Hif1a* does not impact CLL development. The second work I was involved in (reported in Annex II) unravels the role of Tregs in CLL development. In this work, we took advantage of the DEREG mice to deplete Tregs during CLL development, demonstrating that Treg depletion leads to a controlled disease progression compared to control mice. Lastly, I participated in writing a review about the role of healthy B cells in tumor development (reported in Annex III), observing that little is known about this cell type in the field of tumor immunology. In particular, we describe how B cells can have both pro-tumoral and anti-tumoral roles during tumor development, underlying the necessity of identifying different B cell subpopulations that could have opposite roles in cancer progression (e.g. plasmacells and Bregs).

Annex I - The Tumor Microenvironment-Dependent Transcription Factors AHR and HIF-1α Are Dispensable for Leukemogenesis in the Eμ-TCL1 Mouse Model of Chronic Lymphocytic Leukemia.

Susanne Gonder[1,2], Anne Largeot[1], Ernesto Gargiulo[1], Sandrine Pierson[1], Iria Fernandez Botana[1,2], **Giulia Pagano[1,2]**, Jerome Paggetti[1,*] and Etienne Moussay [1,*]

[1] Tumor Stroma Interactions, Department of Oncology, Luxembourg Institute of Health; 84, val fleuri, L-1526 Luxembourg

[2] Faculty of Science, Technology and Medicine, University of Luxembourg, Esch-sur-Alzette, Luxembourg

* These authors share senior authorship.

Correspondence: etienne.moussay@lih.lu; jerome.paggetti@lih.lu;

Author Contributions

S.G. designed and performed experiments, analyzed the results, and wrote the manuscript. E.G., A.L., S.P., I.F.B. and **G.P.** helped in performing experiments and writing the manuscript. E.M. and J.P. designed and supervised the study and wrote the final version of the manuscript. All authors have read and agreed to the published version of the manuscript.

I contributed to the experiments shown in figure 2 (panels D-G), and figure 3 (panels D-G).

cancers

MDPI

Article

The Tumor Microenvironment-Dependent Transcription Factors AHR and HIF-1α Are Dispensable for Leukemogenesis in the Eμ-TCL1 Mouse Model of Chronic Lymphocytic Leukemia

Susanne Gonder [1,2], Anne Largeot [1], Ernesto Gargiulo [1], Sandrine Pierson [1], Iria Fernandez Botana [1,2], Giulia Pagano [1,2], Jerome Paggetti [1,*,†] and Etienne Moussay [1,*,†]

[1] Tumor Stroma Interactions, Department of Oncology, Luxembourg Institute of Health, L-1526 Luxembourg, Luxembourg; susanne.gonder@lih.lu (S.G.); anne.largeot@lih.lu (A.L.); ernesto.gargiulo@lih.lu (E.G.); sandrine.pierson@lih.lu (S.P.); iria.fernandezbotana@lih.lu (I.F.B.); giulia.pagano@lih.lu (G.P.)
[2] Faculty of Science, Technology and Medicine, University of Luxembourg, L-4365 Esch-sur-Alzette, Luxembourg
* Correspondence: jerome.paggetti@lih.lu (J.P.); etienne.moussay@lih.lu (E.M.)
† These authors contributed equally to this paper as senior authors.

Simple Summary: Chronic lymphocytic leukemia (CLL) is the most common leukemia in Western countries, mostly affecting the elderly. The survival of leukemic cells depends on multiple soluble factors and on the stimulation of the BCR signaling pathway. Microenvironment-dependent transcription factors also contribute to CLL biology. Here, we generated new transgenic murine conditional knock-out models of CLL to study the role of the two transcription factors HIF-1α and AHR. Unexpectedly, we observed that both factors are dispensable for leukemia development in these models.

Abstract: Chronic lymphocytic leukemia (CLL) is the most frequent leukemia in the elderly and is characterized by the accumulation of mature B lymphocytes in peripheral blood and primary lymphoid organs. In order to proliferate, leukemic cells are highly dependent on complex interactions with their microenvironment in proliferative niches. Not only soluble factors and BCR stimulation are important for their survival and proliferation, but also the activation of transcription factors through different signaling pathways. The aryl hydrocarbon receptor (AHR) and hypoxia-inducible factor (HIF)-1α are two transcription factors crucial for cancer development, whose activities are dependent on tumor microenvironment conditions, such as the presence of metabolites from the tryptophan pathway and hypoxia, respectively. In this study, we addressed the potential role of AHR and HIF-1α in chronic lymphocytic leukemia (CLL) development in vivo. To this end, we crossed the CLL mouse model Eμ-TCL1 with the corresponding transcription factor-conditional knock-out mice to delete one or both transcription factors in CD19+ B cells only. Despite AHR and HIF-1α being activated in CLL cells, deletion of either or both of them had no impact on CLL progression or survival in vivo, suggesting that these transcription factors are not crucial for leukemogenesis in CLL.

Keywords: chronic lymphocytic leukemia; tumor microenvironment; AHR; HIF1α

Citation: Gonder, S.; Largeot, A.; Gargiulo, E.; Pierson, S.; Fernandez Botana, I.; Pagano, G.; Paggetti, J.; Moussay, E. The Tumor Microenvironment-Dependent Transcription Factors AHR and HIF-1α Are Dispensable for Leukemogenesis in the Eμ-TCL1 Mouse Model of Chronic Lymphocytic Leukemia. *Cancers* **2021**, *13*, 4518. https://doi.org/10.3390/cancers13184518

Academic Editor: Fabrice Gouilleux

Received: 20 August 2021
Accepted: 3 September 2021
Published: 8 September 2021

1. Introduction

In western countries, chronic lymphocytic leukemia (CLL) is the most common B cell malignancy in adults [1]. The disease occurs mostly in elderly patients and is characterized by the accumulation of mature monoclonal CD5+ B cells in peripheral blood, bone marrow, and lymphoid organs [2].

Genome instability is a well-known hallmark of cancer [3]. Indeed, alterations in the DNA and, by consequence, transcriptional programs increase the probability of neoplastic

transformation and potentially enhance tumor immune evasion [4]. Also in CLL, gene mutations and dysfunction affecting transcriptional programs are essential prognostic factors for the disease outcome. In particular, given multiple its molecular abnormalities, CLL is considered a highly heterogeneous disease, including patients not requiring any therapy and patients having an aggressive course with poor response to therapy [5]. Major mutations in CLL affect many cellular components including inflammatory receptors (e.g., MYD88), kinases such as MAPK (e.g., BRAF), NF-kB-related molecules (e.g., BIRC3), transcription (e.g., EGR2 and NOTCH1) and splicing factors (e.g., SF3B1), DNA damage and cell cycle control factors (e.g., ATM and TP53) [6]. These genetic abnormalities have supported the generation of novel agents against CLL which have been translated into the clinical practice towards a more targeted treatment strategy for patients [7]. Treatments for CLL patients include chemotherapy, chemoimmunotherapy, and small molecules mostly targeting important signaling pathways in CLL cells (e.g., BCR and BCL2) [8]. Even after a long remission phase, patients can relapse and develop resistance to treatments. For this reason, investigating new strategies for the development of treatments against CLL is key for the improvement of patients' health.

In the past decades, the transcription factors (TFs) aryl hydrocarbon receptor (AHR) and hypoxia inducible factor-1α (HIF-1α) have been recognized to strongly impact cancer progression and escape mechanisms [9–12]. AHR is a ligand-activated TF involved in many biological processes, such as cell division, quiescence, and inflammation [13]. The most known agonist of AHR is 2,3,7,8 tetrachlorodibenzo-*p*-dioxin (TCDD); however, more importantly for the field of tumor immunology, is the endogenous agonist kynurenine, which originates from tryptophan, in a reaction catalyzed by indoleamine 2,3-dioxygenase 1 (IDO1) and tryptophan 2,3-dioxygenase 2 (TDO2) [14]. Importantly, AHR activation by this pathway has been shown to contribute to immune escape mechanisms leading to an immunosuppressive tumor microenvironment (TME) [15,16].

On the other hand, HIF-1α is an oxygen-sensitive TF, stabilized in a hypoxic environment and by certain non-canonical mechanisms, called pseudohypoxia [17]. Here, for example, metabolites of the Krebs cycle can block prolyl hydroxylases (PHDs), which under normoxic conditions, hydoxylate HIF-1α in order to trigger ubiquitination by the von Hippel–Lindau protein (pVHL) and to start proteasomal degradation [18]. HIF-1α is known to be involved in tumor progression and is mostly associated with poor patient's outcome [19]. Interestingly, AHR and HIF-1α share the dimerization partner ARNT/HIF1β, showing linked processes of tumor progression, metabolic pathways, and vascular development [20]. Moreover, these TFs have an impact on proliferation and functions of B lymphocytes and CLL cells [21,22]. Villa et al. showed that AHR is necessary for B cell proliferation and that cyclin O is directly impacted by AHR deficiency [23]. Furthermore, AHR seems to contribute to the transcriptional program of IL-10-producing regulatory B cells [24], which is a B cell subset sharing regulatory functions with CLL cells [25]. On the other hand, HIF-1α has been already described as highly involved in CLL pathogenesis and in the interaction with the TME. In 2016, Valsecchi and colleagues showed that this interaction is regulated by HIF-1α and promotes tumor survival and tumor propagation [26]. Indeed, HIF-1α is overexpressed in leukemic cells from TP53-disrupted patients and, thus, would be an interesting target for new therapies for CLL [27].

Currently, the impact of AHR and HIF1α in CLL development in vivo has not been fully evaluated. In this article, we generated conditional knock-out mice for Ahr, Hif1a, or both genes restricted to B cells of the Eμ-TCL1 transgenic mouse model, the most extensively used and studied animal model for CLL [28].

2. Materials and Methods

2.1. Mice

Animals were kept in a specific pathogen-free facility, and animal experiments were approved by the internal Animal Welfare Structure and the Luxembourg Ministry for Agriculture. Mice were treated in accordance with the European Union guidelines.

C57BL/6 mice were purchased from Janvier Labs (France). To generate B cell-specific *Ahr*-, *Hif1a*-, and *Ahr-Hif1a*-deficient mice, $Ahr^{fl/fl}$(#006203), $Hif1a^{fl/fl}$ (#007561), and $Ahr^{fl/fl}$ $Hif1a^{fl/fl}$ were crossed with $CD19^{WT/Cre}$ (#006785) mice. These mice were bred with Eμ-TCL1 mice to introduce the TCL1 oncogene under the IgVH promoter. These mice were described previously [28]. The mice were bred and maintained on a C57BL/6 background, and Eμ-TCL1 $CD19^{Cre/WT}Hif1a^{WT/WT}Ahr^{WT/WT}$ mice were used as WT controls. CLL progression in the transgenic mouse models was monitored over several months by determining the percentage of CD5+CD19+ CLL cells in peripheral blood mononuclear cells (PBMC) by flow cytometry analysis on a Cytoflex (Beckman Coulter, Brea, CA, USA) using CD19-APC and CD5-PE (Biolegend, San Diego, CA, USA). Mice reaching the humane endpoint were euthanized by cervical dislocation. All deaths unrelated to leukemia were excluded from this study. To perform adoptive transfer in healthy conditional knock-out mice, CLL cells were isolated from the spleen of diseased Eμ-TCL1 mice. Then, 10×10^6 CLL cells were injected intravenously in 100 μL of DMEM, and CLL progression was followed by weekly bleeding, as described previously.

2.2. B Cell Isolation

B cells were purified from the spleen by negative selection using the MojoSort™ Mouse Pan B Cell Isolation Kit II (Biolegend, San Diego, CA, USA) following the manufacturer's instructions. The isolated B cell population contained at least 90% of CD19+CD5+-double positive cells. B cells were cultured in RPMI supplemented with 10% FBS, 50 μM 2-β-mercaptoethanol, 100 U/mL penicillin, and 100 μg/mL streptomycin. To mimic hypoxia, 150 μM cobalt chloride (Sigma-Aldrich, Burlington, MA, USA) was added, and the cells were cultured overnight at 37 °C and 5% CO_2. In order to activate AHR, the cells were incubated with 250 nM FICZ (Sigma-Aldrich, Burlington, MA, USA) for 2 hours at 37 °C and 5% CO_2.

2.3. Validation of the Models at the gDNA, RNA, and Protein Levels

Genomic DNA was extracted using NucleoSpin Tissue Mini kit for DNA from cells and tissue (Macherey-Nagel, Düren, Germany) following the manufacturer's instructions. To perform the PCR on gDNA for *Ahr*, the PCR mix 2x M-PCR OPTI™ Mix (Bimake, Houston, TX, USA) was used as described in the instructions, and the specific primer sequences were: 5′-GTCACTCAGCATTACACTTTCTA-3′, 5′-CAGTGGGAATAAGGCAAGAGTGA-3′, and 5′-GGTACAAGTGCACATGCCTGC-3′. The use of these three primers enables the detection of wild-type (106 bp), floxed (140 bp), and excised (180 bp) alleles. The amplification of *Ahr* was performed with the following program: 94 °C for 5 min, 30 cycles of 94 °C for 15 s, 56 °C for 15 s, and 72 °C for 30 s. After amplification, the product was run on a 3% agarose gel with SYBR™ Safe DNA Gel Stain (ThermoFisher, Waltham, MA, USA) and visualized by Image Quant Las 4000 (GE Healthcare, Chicago, IL, USA). For *Hif1a*, we used the HIF1a TaqMan copy number assay Mm00375032_cn with the TaqMan™ Copy Number Reference Assay, mouse, Tfrc (Thermo Scientific, Waltham, MA, USA). Quantitative PCRs were performed using Takyon Low Rox Probe 2X mastermix (Eurogentec, Seraing, Belgium) according to manufacturer's instructions. The qPCRs were run on the QuantStudio™ 3 or 5 (Applied Biosystems, Waltham, MA, USA) with the following program for the Taqman assay: 50 °C 2 min, 95 °C for 10 min, 40 cycles of 95 °C for 15 s, and 60 °C for 1 min.

RNA from B cells was extracted using Nucleozol reagent and the NucleoSpin® RNA Set for NucleoZOL (Macherey-Nagel, Düren, Germany) and quantified using the Nanophotometer N60 (Implen, München, Germany). The complementary DNA was synthesized from 500 ng of RNA by using FastGene Scriptase II cDNA 5x ReadyMix (Nippon Genetics, Düren, Germany) according to the manufacturer's instructions. Quantitative PCRs were performed using Takyon for SYBR Assay Low Rox or Takyon Low Rox Probe 2X mastermix (Eurogentec, Seraing, Belgium). The specific primer sequences were: *Ahr*: 5′-AGCCGGTGCAGAAAACAGTAA-3′ and 5′-AGGCGGTCTAACTCTGTGTTC-3′; *Hprt*:

5′-TGGATACAGGCCAGACTTTGTTF-3′ and 5′-CAGATTCAACTTGCGCTCATC-3′; *Tbp*: 5′-GTCATTTTCTCCGCAGTGCC-3′ and 5′-GCTGTTGTTCTGGTCCATGAT-3′. For *Hif1a*, we used the HIF1a TaqMan assay Mm00375032_cn (Thermo Scientific, Waltham, MA, USA). The qPCR was performed similarly as described above.

The comparative Ct method was used to calculate gene expression relative to housekeeping gene *Hprt* and *Tpb*.

For protein isolation, cultured B cells were washed twice with ice-cold PBS, and proteins were extracted using RIPA buffer including the cOmplete™ Protease Inhibitor Cocktail (Roche, Basel, Switzerland) and the Phosphatase Inhibitor Cocktail 2 and 3 (Sigma-Aldrich, Burlington, MA, USA). Then, 10 µg of cell lysates were resolved on 10% SDS-PAGE and transferred to a nitrocellulose membrane. To confirm equivalent loading between lanes, a Ponceau red staining was performed. Membranes were incubated in 1x PBS-T (0.1%) and fat-free dry milk (5%, Roth) blocking buffer during one hour at room temperature. Membranes were then incubated with primary antibodies against HIF-1α (#36169, Cell Signaling), AHR (#694502, Biolegend, San Diego, CA, USA), and beta-actin-HRP (#A3854, Sigma-Aldrich, Burlington, MA, USA) in blocking buffer at 4 °C overnight. Membranes were washed three times in 1xPBS-T (0.1%) for 10 min each time. Secondary antibodies coupled to HRP were from Jackson ImmunoResearch. For detection, the ECL western blot detection kit was purchased from Amersham, and the radiographic films from Santa Cruz Biotechnology.

2.4. Sample Preparation for RNA Sequencing

Control C57BL/6 and diseased Eμ-TCL1, or Eμ-TCL1 *CD19* $^{Cre/WT}$ *Hif1α*$^{fl/fl}$, Eμ-TCL1 *CD19*$^{Cre/WT}$ *Ahr*$^{fl/fl}$, Eμ-TCL1 *CD19*$^{Cre/WT}$ *Hif1α*$^{fl/fl}$ *Ahr*$^{fl/fl}$, and the corresponding control mice Eμ-TCL1 *CD19*$^{Cre/WT}$ *Hif1α*$^{WT/WT}$ *Ahr*$^{WT/WT}$ were euthanized at humane endpoint by CO_2 inhalation or cervical dislocation. Spleens were collected, and single cell suspensions were prepared as previously described [29,30]. CD19+ B cells or CD5+CD19+ CLL cells were sorted with a BD FACSAria III at 4 °C. Then, 1–5 × 10^6 sorted cells were centrifuged and resuspended in 500 µL of Nucleozol reagent. Total cellular RNA was extracted using the NucleoSpin RNA Set for NucleoZOL and eluted in 30 µL of RNAse-free water. Libraries were prepared with the QuantSeq 3′ mRNA-Seq Library Prep Kit FWD for Illumina (Lexogen, Vienna, Austria) with dual indexing, according to the manufacturer's instructions, with the addition of UMI. Barcoded samples were diluted, pooled, loaded onto a NextSeq 500/500 Mid Output flowcell or a NovaSeq SP flowcell (Illumina, San Diego, CA, USA), and single-end sequencing was performed using a NextSeq 550 or a NovaSeq 6000 system (Illumina, San Diego, CA, USA).

2.5. RNA Sequencing Analysis

After initial QCs using FastQC (www.bioinformatics.babraham.ac.uk/projects/fastqc/, accessed on 19 March 2021) and FastQ Screen (www.bioinformatics.babraham.ac.uk/projects/fastq_screen/, accessed on 19 March 2021), fastq files were processed using a local Snakemake workflow including the following main steps. First, raw reads were trimmed from their UMI index, poly A, and adapter sequences using a combination of dedicated scripts and cutadapt (v2.10). Next, the filtered reads were submitted for mapping (STAR v2.5.3a) on the Mouse Reference genome (GRCm38). Collapsing of reads originating from the same fragment was achieved with umi_tools (v 1.0.0), and counting was performed with featureCounts (subread v2.0.0).

Counts were filtered and transformed with EdgeR for clustering and principal component analysis (PCA). For k-means clustering, the 2500 most variable genes were included, and 6 clusters were defined according to the elbow method (online tool iDEP.93). Top genes were mapped with the dimension reduction algorithm t-SNE. Differential expression of genes across C57BL/6 and Eμ-TCL1 samples (DEG) was assessed using the DESeq2 package, and FDR < 0.05 and log2 fold change cut-off of 1 were imposed. Raw and processed data were deposited in the NCBI GEO database (GSE175564).

Differential expression of genes across Eμ-TCL1 *CD19*$^{Cre/WT}$ *Hif1a*$^{WT/WT}$*Ahr*$^{WT/WT}$, Eμ-TCL1 *CD19*$^{Cre/WT}$*Hif1α*$^{fl/fl}$, Eμ-TCL1 *CD19*$^{Cre/WT}$*Ahr*$^{fl/fl}$, Eμ-TCL1 *CD19*$^{Cre/WT}$ *Hif1a*$^{fl/fl}$ *Ahr*$^{fl/fl}$ samples (DEG) was assessed using the EdgeR package, and FDR < 0.05 and log2 fold change cut-off of 1 were imposed. Pheatmap and EnhancedVolcano packages were used for data visualization. Raw and processed data were deposited in the NCBI GEO database (GSE179196).

2.6. Murine B Cell-Specific Ahr-Induced Gene Signature

The murine B cell-specific *Ahr*-induced gene signature (mouse_B_Ahr) was defined based on the gene expression data from Kovalova et al. (2017, GSE80953). Briefly, CEL files corresponding to murine B cells treated with vehicle (VH) or TCDD (2,3,7,8-tetrachlorodibenzo-p-dioxin) for 4 h, 8 h, or 24 h were loaded into the Transcriptome Analysis Console (TAC 4.0, Applied Biosystems), and the 153 genes induced by TCDD (fold change >1.5 and FDR < 0.05) at any time points (TCDD vs. VH) were included in the signature.

2.7. Gene Set Enrichment Analysis

We performed GSEA using the GSEA Broad Institute stand-alone software (http://www.gsea-msigdb.org/gsea/index.jsp, accessed on 20 April 2021). Gene counts from both groups (C57BL/6 and Eμ-TCL1) were loaded into GSEA according to recommendations. Data were tested against the above-described mouse_B_Ahr signature and the GSEA Hallmarks signatures. Normalized enrichment scores (NES) and FDR < 0.1 were taken into consideration.

2.8. Transcription Factor Enrichment Analysis

DEGs significantly upregulated in leukemic B cells from Eμ-TCL1 were subjected to transcription factor enrichment analysis with the online tool ChEA3 (Ma'ayan Laboratory, Icahn School of Medicine at Mount Sinai) predicting transcription factors associated with user-input sets of genes. DEGs were also submitted for Integrated System for Motif Activity Response Analysis performed with the free online ISMARA tool that recognizes the most important transcription factors impacting on the transcription profiles of a set of samples. The network of protein–protein interactions for transcription factors was constructed with string-db (v11.0, STRING Database).

2.9. Statistical Analysis

Statistical analysis was performed using GraphPad Prism software (version 9.1.2). The unpaired t test was used for Z-values analyses and qPCRs (Figures 1H, 2B, 2C, 3C and 4B,D,E). The log-rank test was used for the survival curves (Figures 2E, 3E and 4G). For the percentage of CLL cells in the transgenic mouse models overtime (Figure 2F, Figure 3F, and Figure 4H), we used mixed-effects analysis followed by Bonferroni's multiple comparison test. The percentage of CLL in the blood at one time point (Figures 2G, 3G and 4I) was tested with the unpaired t test. To test significance in the adoptive transfer models (Figures 2J, 3J and 4L), we performed two-way ANOVA followed by Bonferroni's multiple comparison test. A *p*-value lower than 0.05 was considered statistically significant.

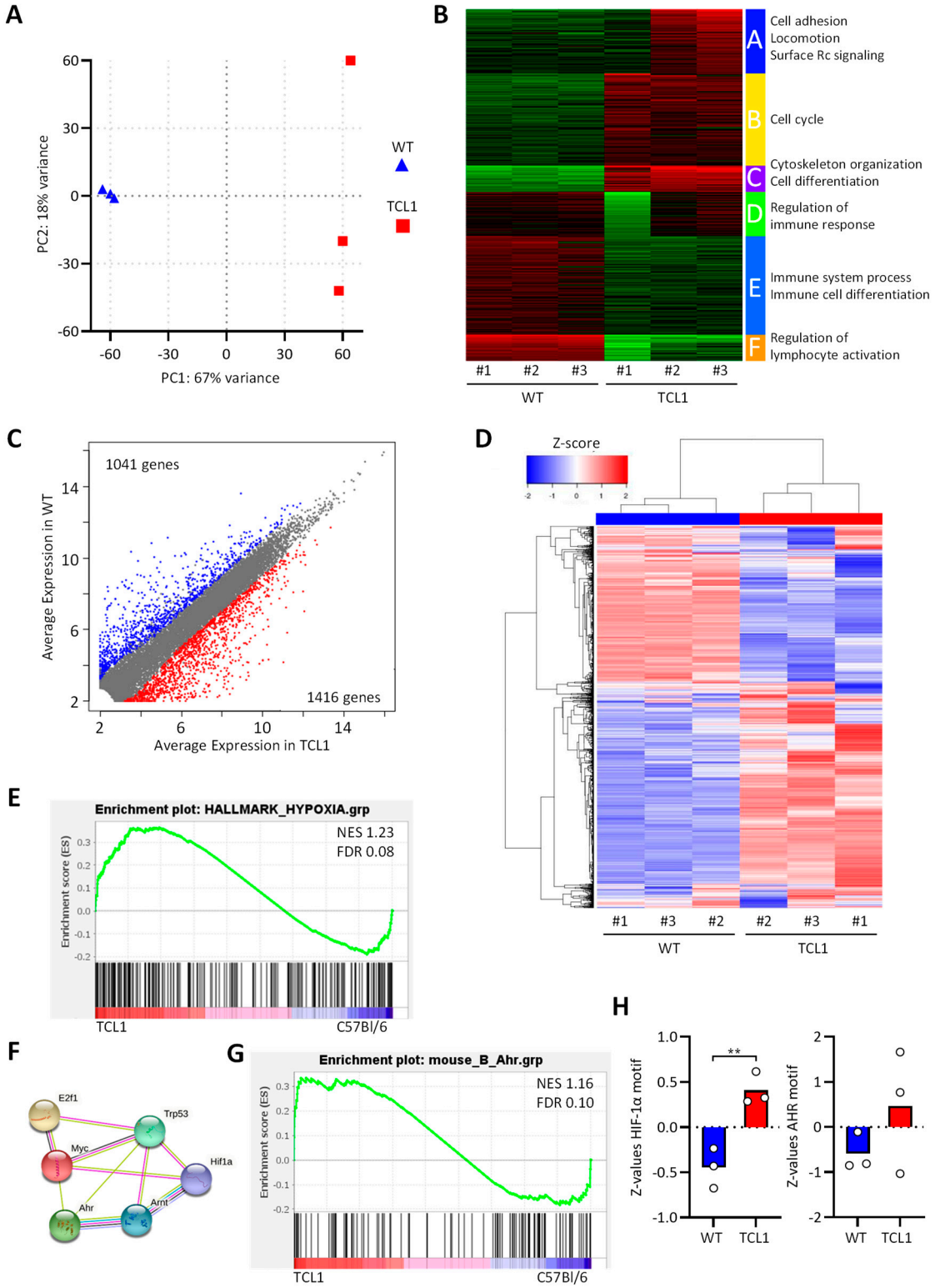

Figure 1. RNA sequencing of B cells from C57BL/6 and Eμ-TCL1 mice. Splenic B cells were FACS-sorted from three mice of each genotype, and mRNA was sequenced. (**A**) Principal component analysis of individual animals. (**B**) K-means clustering and Gene Ontology enrichment analysis. (**C**) Scatterplot depicting the expression of genes in the groups. (**D**) Unsupervised hierarchical clustering showing 1416 genes upregulated and 1041 genes downregulated in TCL1. (**E**,**G**) Gene Set Enrichment Analysis showing the enrichment of hypoxia (**E**) and AHR (**G**) signatures in Eμ-TCL1 versus C57BL/6 mice. (**F**) Protein–protein interactions network (STRING) for transcription factors involved in enriched hallmark pathways (GSEA). (**H**) Transcription factor activity (Z-values, ISMARA) for HIF-1α and AHR motifs in WT and TCL1 B cells.

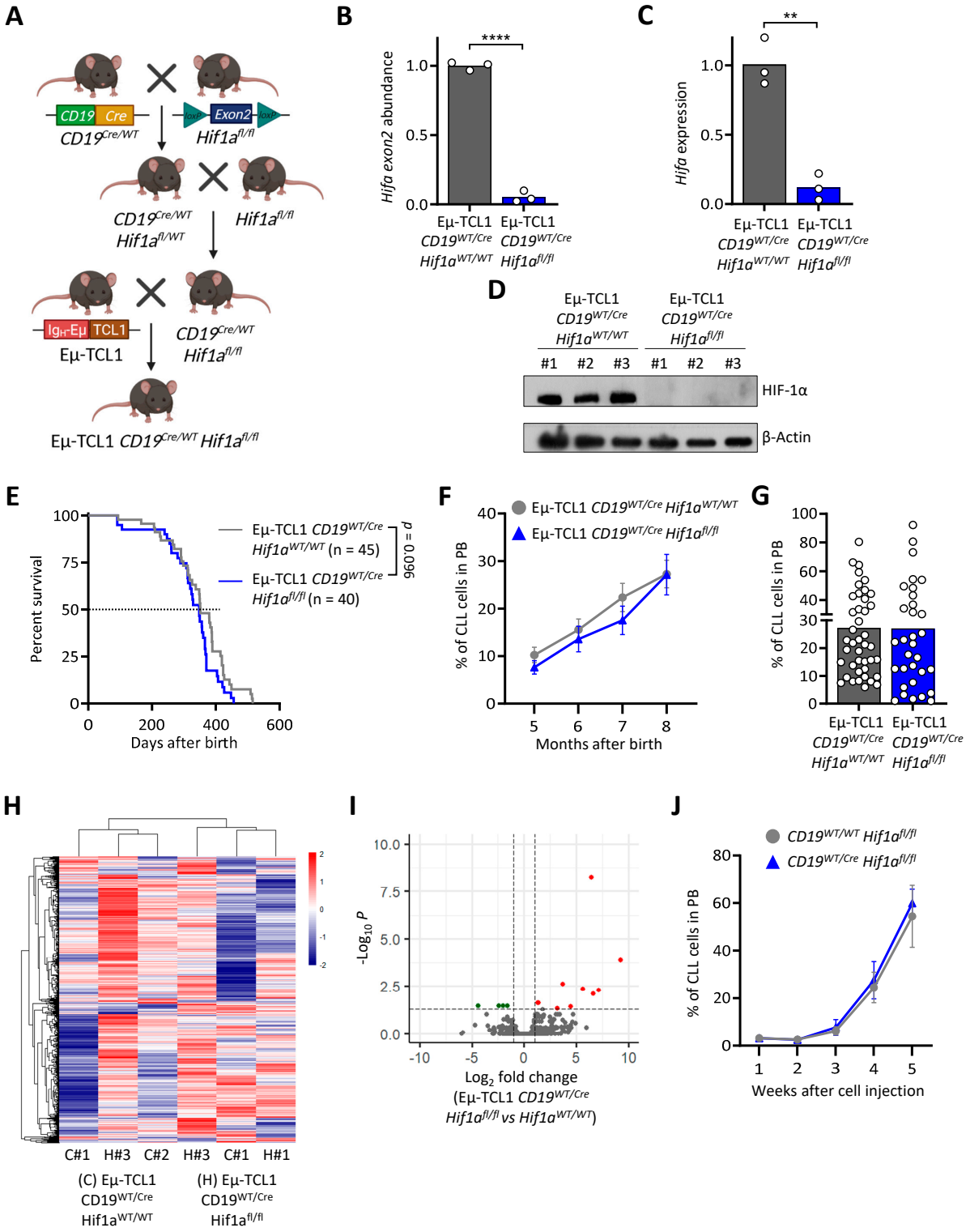

Figure 2. Knocking out HIF-1α does not show an effect on the leukemogenesis of CLL cells in the murine Eμ-TCL1 model. (**A**) Scheme of the breeding strategy to generate Eμ-TCL1 *CD19*$^{Cre/WT}$ *Hif1a*$^{fl/fl}$ (cKO). (**B**–**D**) Validation of the knock-out of exon 2 of *Hif1a* in isolated B cells from cKO mice incubated with $CoCl_2$ at the DNA (**B**), RNA (**C**), and protein (**D**) levels compared to control mice (n = 3). ** $p < 0.01$, **** $p < 0.0001$. (**E**) Survival curve of cKO compared to control mice shows no significant difference. (**F**–**G**) Flow cytometry analysis of CLL cells (CD19+ CD5+) in the peripheral blood (PB) of cKO and control mice over time (Ctrl: n = 45, cKO: n = 39) (**F**) and at month 8 (Ctrl: n = 42, cKO: n = 35) (**G**). (**H**–**I**) CLL cells from cKO and control mice (n = 3) were subjected to RNA sequencing. (**H**) Unsupervised hierarchical clustering showing the top 10,000 most expressed genes. (**I**) Volcano plot showing DEG between cKO and control mice. (**J**) CLL development of the adoptive transfer of Eμ-TCL1 CLL cells in CD19$^{Cre/WT}$ *Hif1a*$^{fl/fl}$ mice (Ctrl: n = 5, cKO: n = 6).

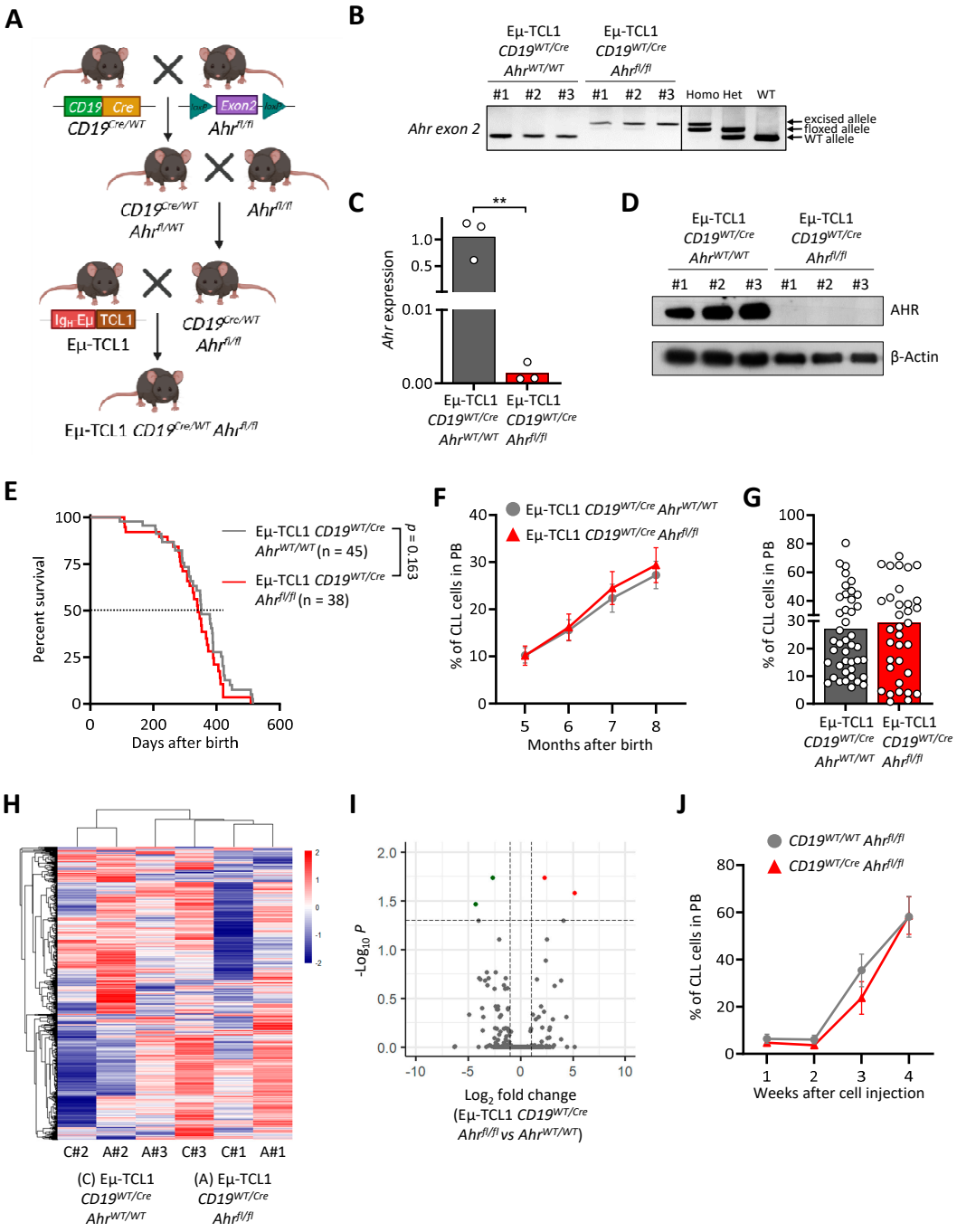

Figure 3. AHR knock-out does not influence CLL development in the murine Eμ-TCL1 model. (**A**) Scheme of the breeding strategy to generate Eμ-TCL1 CD19$^{Cre/WT}$ *Ahr*$^{fl/fl}$ (cKO) mice. (**B**–**D**) Validation of the knock-out of exon 2 of *Ahr* in isolated B cells from cKO mice incubated with FICZ at the DNA (**B**), RNA (**C**), and protein (**D**) levels compared to control mice (n = 3). ** $p < 0.01$. (**E**) Survival curve of cKO compared to control mice shows no significant difference. (Ctrl: n = 45, cKO: n = 38). (**F**,**G**) Flow cytometry analysis of CLL cells (CD19+ CD5+) in the peripheral blood (PB) of cKO and control mice over time (Ctrl: n = 45, cKO: n = 38) (**F**) and at month 8 (Ctrl: n = 42, cKO: n = 34) (**G**). (**H**,**I**) CLL cells from cKO and control mice (n = 3) were subjected to RNA sequencing. (**H**) Unsupervised hierarchical clustering showing the top 10,000 most expressed genes. (**I**) Volcano plot showing DEG between cKO and control mice. (**J**) CLL development of the adoptive transfer of Eμ-TCL1 CLL cells in *CD19*$^{Cre/WT}$ *Ahr*$^{fl/fl}$ mice (Ctrl: n = 5, cKO: n = 5).

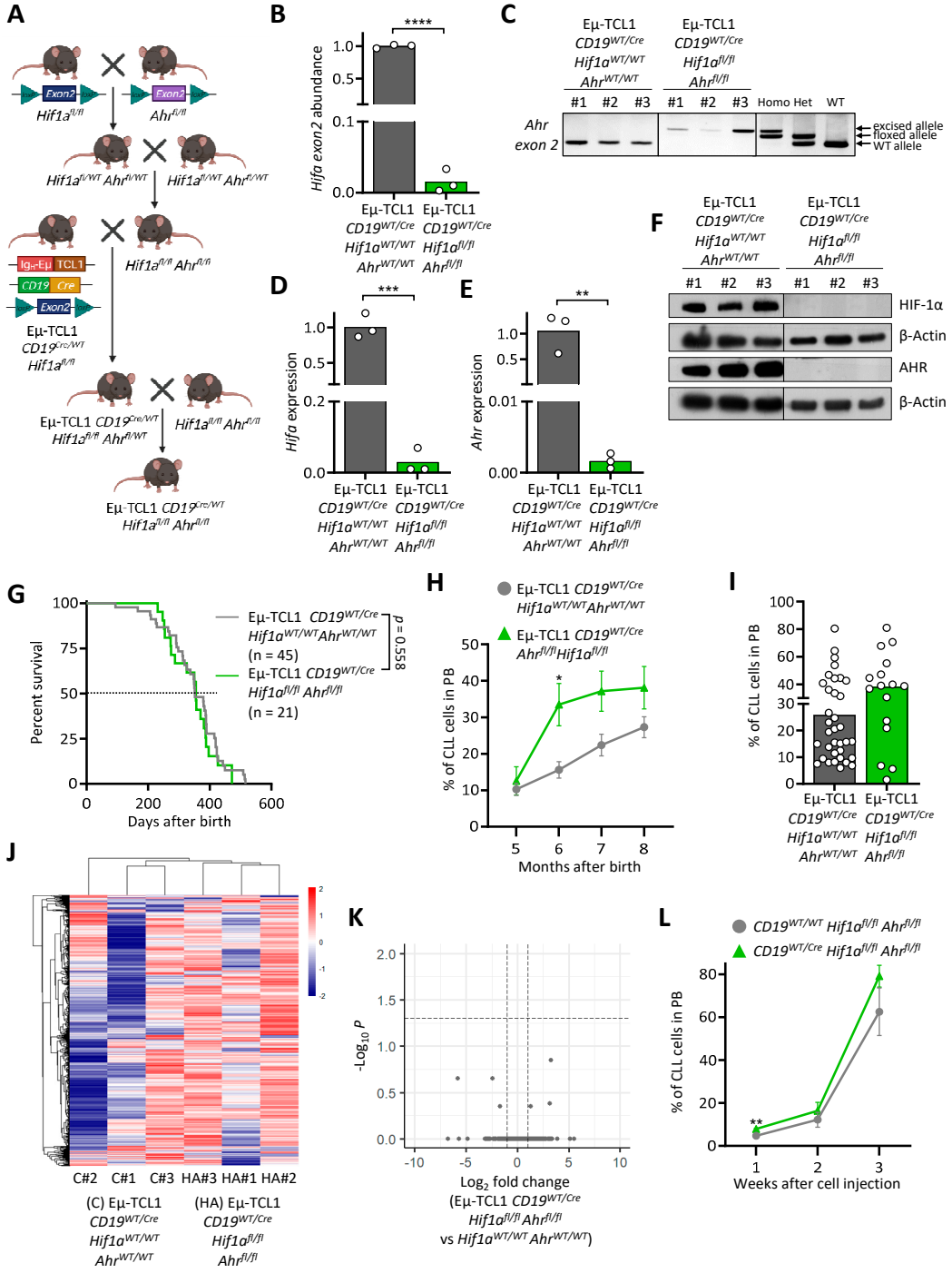

Figure 4. Double knock-out of AHR and HIF-1α does not appear to have an impact on the development of neoplastic B cells. (**A**) Scheme of the breeding strategy to generate Eμ-TCL1 *CD19*$^{Cre/WT}$ *Hif1a*$^{fl/fl}$ *Ahr*$^{fl/fl}$ (cDKO) mice. (**B**–**F**) Validation of the knock-out of exon 2 of *Hif1a* and *Ahr*, respectively, in isolated B cells from cDKO mice incubated with $CoCl_2$ and FICZ at the DNA (**B**,**C**), RNA (**D**,**E**), and protein (**F**) levels compared to control mice (n = 3). ** $p < 0.01$, *** $p < 0.001$, **** $p < 0.0001$. (**G**) Survival curve of cDKO compared to control mice shows no significant difference. (Ctrl: n = 45, cDKO: n = 21). (**H**,**I**) Flow cytometry analysis of CLL cells (CD19+ CD5+) in the peripheral blood (PB) of cDKO and control mice over time (Ctrl: n = 45, cDKO: n = 21) (**H**) and at month 8 (Ctrl: n = 35, cDKO: n = 16) (**I**). (**J**,**K**) CLL cells from cDKO and control mice (n = 3) were subjected to RNA sequencing. (**L**) Unsupervised hierarchical clustering showing the top 10,000 most expressed genes. (**I**) Volcano plot showing DEG between cDKO and control mice. (**J**) CLL development of the adoptive transfer of Eμ-TCL1 CLL cells in CD19$^{Cre/WT}$ *Hif1a*$^{fl/fl}$ *Ahr*$^{fl/fl}$ mice (Ctrl: n = 4, cDKO: n = 4).

3. Results

3.1. RNA Sequencing of CD5+CD19+ Leukemic B Cells from Eμ-TCL1 Mice

The development of leukemia involves the regulation of complex transcriptional programs allowing the cancer cells to proliferate, benefit from the support of the microenvironment, and escape the anti-tumor immune response [31,32]. In order to understand the biology of the leukemic cells in vivo, we performed RNA sequencing analysis of B cells sorted from control C57BL/6 (WT) and leukemic Eμ-TCL1 (TCL1) mice. Principal component analysis and correlation analysis showed a distinct transcriptional profile in leukemic B cells when compared with WT B cells, the gene expression profiles of leukemic B cells being more variable (Figure 1A and Supplementary Materials Figure S1A). Cluster analysis identified six clusters of deregulated genes in TCL1 B cells (K-means clustering, Figure 1B and Supplementary Materials Figure S1B–C). In particular, a decreased expression of genes involved in immune functions and lymphocyte activation was noticed, while genes involved in cell cycle, cell adhesion, locomotion, and cytoskeleton were upregulated. About 2457 genes were found statistically differentially expressed between WT and TCL1, with 1416 genes being more expressed in leukemic B cells, and 1041 genes being more expressed in WT B cells (Figure 1C,D).

Next, we performed a Gene Set Enrichment Analysis (GSEA) to identify hallmark pathways regulated in TCL1 and WT B cells. Among the 33 gene sets upregulated in TCL1 B cells and presenting a nominal enrichment score (NES > 1), we selected 22 gene sets as relevant for immune cells (Table 1). The most regulated gene sets were related to the TFs MYC, E2F, and TP53 and to several metabolic pathways linked to energy production, cholesterol/lipids, and glucose metabolism, indicating highly activated and proliferating cells. In addition, many signaling pathways involved in immune functions and cytokine secretion were enriched (IL-2/STAT5, mTORC1, IL-6/JAK/STAT3, and β-catenin). Finally, we observed the regulation of the two microenvironment-modulated pathways (hypoxia and xenobiotic stress) regulated by the TFs HIF family members and AHR, respectively (Figure 1E and Table 1). These two pathways are often regulated in cancer by a reduced oxygen concentration (hypoxia) and by tryptophan derivatives such as kynurenine [20]. Protein–protein interaction analysis (STRING) confirmed the tight connection between the transcription factors regulating these pathways (Figure 1F).

While the response to hypoxia and glycolysis are both mediated by HIF-1α [33], the response to xenobiotic stress is complex and more diverse, in terms of transcriptional regulation. To confirm the potential role of AHR in TCL1 leukemic cells, we established a murine B cell-specific AHR gene signature from the publicly available gene expression dataset GSE80953 [34]. A list of 153 genes was identified as induced by the AHR agonist TCDD in murine B cells and used as a gene set database to run a GSEA. The analysis confirmed the enrichment of the AHR gene signature in TCL1 leukemic cells compared to normal B cells (NES = 1.16, FDR = 0.1, Figure 1G).

Then, we performed a transcription factor enrichment analysis (TFEA) with the online tool ChEA3 to better understand the regulation of transcriptional programs in leukemic cells. Again, both AHR and HIF-1α were listed among the top 50 TFs contributing to the regulation of DEGs in leukemic B cells (ranked 37 and 43 over 1632 TFs, respectively, Table 2). A second analysis with the ISMARA tool detected the use of specific and different TFs in WT and TCL1 B cells. For example, TAF1 was specifically used in WT cells, while Fos was more used by leukemic TCL1 cells (Supplementary Materials Figure S1D). Concerning HIF-1α and AHR, an enrichment of binding motifs was detected in DEGs from TCL1 leukemic cells compared to WT cells (Figure 1H).

Given the enrichment of HIF-1α and AHR gene signatures in Eμ-TCL1 mice compared to WT mice, their important role in cancer, and their ability to heterodimerize with the same binding partner called HIF-1β/Arnt [35,36], we decided to study the role of both AHR and HIF-1α in leukemogenesis in the Eμ-TCL1 murine model of CLL.

Table 1. Relevant Gene Sets enriched in leukemic B cells compared to normal B cells as revealed by RNA sequencing analysis and GSEA. NES, normalized enrichment score. NOM *p*-val, nominal *p*-value.

Rank	GeneSets	SIZE	NES	NOM *p*-Val
1	HALLMARK_MYC_TARGETS_V1	200	1.46	0.000
2	HALLMARK_CHOLESTEROL_HOMEOSTASIS	73	1.45	0.000
3	HALLMARK_GLYCOLYSIS	200	1.4	0.000
4	HALLMARK_E2F_TARGETS	200	1.4	0.185
6	HALLMARK_MYC_TARGETS_V2	57	1.38	0.000
7	HALLMARK_OXIDATIVE_PHOSPHORYLATION	197	1.35	0.000
8	HALLMARK_REACTIVE_OXYGEN_SPECIES_PATHWAY	49	1.34	0.000
9	HALLMARK_FATTY_ACID_METABOLISM	157	1.34	0.000
10	HALLMARK_G2M_CHECKPOINT	196	1.29	0.185
11	HALLMARK_UV_RESPONSE_UP	156	1.28	0.000
15	**HALLMARK_HYPOXIA**	198	1.22	0.000
16	HALLMARK_P53_PATHWAY	200	1.22	0.084
18	HALLMARK_IL2_STAT5_SIGNALING	199	1.2	0.094
20	HALLMARK_MTORC1_SIGNALING	199	1.18	0.287
21	HALLMARK_UNFOLDED_PROTEIN_RESPONSE	112	1.15	0.185
24	HALLMARK_MITOTIC_SPINDLE	199	1.13	0.269
25	HALLMARK_DNA_REPAIR	148	1.13	0.084
28	**HALLMARK_XENOBIOTIC_METABOLISM**	196	1.09	0.299
30	HALLMARK_APOPTOSIS	161	1.01	0.376
31	HALLMARK_IL6_JAK_STAT3_SIGNALING	87	1.01	0.381
32	HALLMARK_PROTEIN_SECRETION	96	1.01	0.472
33	HALLMARK_WNT_BETA_CATENIN_SIGNALING	41	1	0.362

3.2. HIF-1α Knock-Out in Murine CLL Cells Does Not Impact Leukemogenesis

HIF-1α is important in many cancers, also in CLL. However, the impact of HIF-1α on CLL leukemogenesis in vivo has not been fully investigated yet. For this purpose, we generated conditional transgenic knock-out mice using the Cre-*loxP* system (Figure 2A). First, by crossing *CD19*$^{Cre/WT}$ mice with *Hif1a*$^{fl/fl}$ mice, we ensured the gene knock-out specifically in B cells, then we crossed the newly generated strain (*CD19*$^{Cre/WT}$ *Hif1a*$^{fl/fl}$) with Eμ-TCL1, creating the Eμ-TCL1 *CD19*$^{Cre/WT}$ *Hif1a*$^{fl/fl}$ transgenic model. In order to validate if HIF1α knock-out in Eμ-TCL1 *CD19*$^{Cre/WT}$ *Hif1a*$^{fl/fl}$ was efficient compared to the control mice (Eμ-TCL1 *CD19*$^{Cre/WT}$ *Hif1a*$^{WT/WT}$), we isolated DNA, RNA, and proteins from CD19+ cells. As shown in Figure 2B–D and Supplementary Materials Figure S2, the knock-out of HIF-1α in the mice was validated on all levels. To further investigate the impact of HIF-1α knock-out in leukemic cells, we monitored CLL development in the transgenic mice over several months. In the Eμ-TCL1 *CD19*$^{Cre/WT}$*Hif1a*$^{fl/fl}$ mouse model, we could not observe any difference in the survival compared to the control mice (Figure 2E). This finding was in accordance with the percentage of the circulating neoplastic cells in the peripheral blood, progressively accumulating over time (Figure 2F,G). Additionally, we performed RNA sequencing of leukemic B cells, comparing Eμ-TCL1 *CD19*$^{Cre/WT}$ *Hif1a*$^{fl/fl}$ mice with the control mice. Here, we could not observe any major differences in the gene expression profiles (Figure 2H,I and Supplementary Materials Table S1).

Table 2. Top50 ranking of transcription factors whose putative transcriptional targets are most closely similar to those in the query set. CHEA3 results for transcription factors enrichment analysis (TFEA). Lower scores indicate more relevancy to the related transcription factor. Full query = 1632 TFs.

Rank	TF	Score	Rank	TF	Score
1	FOXM1	4.333	26	CEBPB	88.83
2	CENPA	5.0	27	NFE2L2	89.4
3	ZNF367	8.333	28	ARNTL2	94.67
4	PA2G4	15.5	29	JDP2	95.67
5	HMGA2	24.67	30	ZNF888	97.0
6	AHRR	26.5	31	BHLHE40	97.75
7	ZNF695	29.0	32	ZNF670	98.5
8	E2F7	29.2	33	OSR1	99.5
9	E2F1	33.83	34	GLMP	101.5
10	FOSL1	35.4	35	HMGN3	105.0
11	ELK3	49.0	36	ZNF93	106.7
12	FOXD1	51.5	37	**AHR**	107.4
13	MYBL2	55.17	38	PPARG	108.0
14	TFDP1	56.0	39	TAL1	109.0
15	E2F2	65.33	40	ATF3	110.3
16	RFX8	68.0	41	TEAD4	119.8
17	CENPX	68.0	42	NR1H3	120.0
18	KLF6	72.0	43	**HIF1A**	120.2
19	CREB3L2	75.33	44	VDR	120.8
20	ETV4	76.5	45	KLF9	123.8
21	ZNF878	78.0	46	GLIS2	126.3
22	E2F8	80.0	47	RELB	128.3
23	DNMT1	81.0	48	PLSCR1	131.0
24	NR2F6	85.5	49	TEAD3	132.7
25	KLF4	87.0	50	HLX	136.3

To investigate the importance of HIF-1α in healthy B cells in the CLL tumor microenvironment, we adoptively transferred Eμ-TCL1 CLL cells into mice lacking HIF-1α in healthy B cells, $CD19^{Cre/WT}$ $Hif1a^{fl/fl}$. Here, we could not observe any difference in the development of CLL in knock-out compared to control mice (Figure 2J).

These results led us to conclude that in this model of CLL, HIF-1α seems not to be an important transcription factor in healthy and leukemic B cells for proliferation in WT mice and leukemogenesis in the transgenic murine model.

3.3. AHR Knock-Out in Murine CLL Cells Does Not Impact Leukemogenesis

The transcription factor AHR plays a role in B cell proliferation and development [23,37]. Here, we investigated the importance of AHR in the development of leukemic B cells. To do so, we used the same strategy as described above for the HIF-1α knock-out model (Figure 3A). In accordance with this, DNA, RNA, and proteins from CD19+ cells of the Eμ-TCL1 $CD19^{Cre/WT}Ahr^{fl/fl}$ mice were isolated for the validation of the knock-out. Compared to the control mice Eμ-TCL1 $CD19^{Cre/WT}Ahr^{WT/WT}$, the knock-out mice showed the excised allele of exon 2 of Ahr at the DNA level in B cells, no expression of exon 2 at the RNA level, and absence of the corresponding protein (Figure 3B–D and Supplementary Materials Figure S2), confirming that the knock-out was efficient.

Next, in order to analyze the impact of AHR knock-out in leukemic B cells, CLL development in the new transgenic model (Eμ-TCL1 $CD19^{Cre/WT}$ $Ahr^{fl/fl}$) and corresponding control (Eμ-TCL1 $CD19^{Cre/WT}$ $Ahr^{WT/WT}$) was monitored over several months. Eμ-TCL1 $CD19^{Cre/WT}$ $Ahr^{fl/fl}$ mice compared to the control mice did not show any difference in survival (Figure 3E). In addition, the percentage of the AHR knock-out CLL cells in the blood did not differ compared to the control at different time points (Figure 3F,G). RNA sequencing performed on CLL cells did not reveal any relevant changes in the RNA profile

of the knock-out mice compared to the control (Figure 3H, I and Supplementary Materials Table S2).

Furthermore, in order to investigate whether AHR knock-out in normal B cells could impact CLL development, we injected Eμ-TCL1 CLL cells into mice lacking AHR in normal B cells ($CD19^{Cre/WT}$ $Ahr^{fl/fl}$). As observed for the transgenic model, we could not detect any difference in CLL development for the adoptive transfer in either $CD19^{Cre/WT}$ $Ahr^{fl/fl}$ or $CD19^{WT/WT}$ $Ahr^{fl/fl}$ recipient mice (Figure 3J).

Based on the results of our AHR knock-out experiments in leukemic and in healthy B cells, AHR does not appear to be an essential factor in CLL development.

3.4. AHR and HIF-1α Double Knock-Out Does Not Interfere with Murine CLL Development

The dimerization partner ARNT/HIF1β connects the pathways of HIF-1α and AHR, as both TFs share it in order to bind to DNA. As we could not observe a difference by removing these two TFs separately, we decided to investigate the potential synergistic role of HIF-1α and AHR in leukemogenesis by knocking them out together in our CLL murine model.

To achieve this, we crossed the $Ahr^{fl/fl}$ and $Hif1\alpha^{fl/fl}$ mice, and the resulting strain was further crossed with the Eμ-TCL1 $CD19^{Cre/WT}$ $Hif1\alpha^{fl/fl}$ model (Figure 4A). This strain was further bred with $Hif1\alpha^{fl/fl}$ $Ahr^{fl/fl}$ mice. After obtaining the double knock-out mice (Eμ-TCL1 $CD19^{Cre/WT}$ $Hif1a^{fl/fl}$ $Ahr^{fl/fl}$), we validated the conditional knock-out at DNA (Figure 4B,C), RNA (Figure 4D,E), and protein (Figure 4F and Supplementary Materials Figure S2) levels in CD19+ B cells. Similar to the previous results in single conditional knock-out mice, we could not observe any difference between Eμ-TCL1 $CD19^{Cre/WT}$ $Hif1a^{fl/fl}$ $Ahr^{fl/fl}$ and the control mice (Figure 4G). Although a slight increase in CLL cells in the blood of Eμ-TCL1 $CD19^{Cre/WT}$ $Hif1\alpha^{fl/fl}$ $Ahr^{fl/fl}$ mice was visible at month 6, this difference evened out in the following months (Figure 4H,I). RNA sequencing of CLL cells did not reveal differences in gene expression between Eμ-TCL1 $CD19^{Cre/WT}Hif1\alpha^{fl/fl}$ $Ahr^{fl/fl}$ and the control mice (Figure 4J,K and Supplementary Materials Table S3). Finally, adoptive transfer of Eμ-TCL1 CLL cells into mice carrying the double knock-out in normal B cells showed no differences in disease development (Figure 4L).

Taken together, the deletion of the transcription factors HIF1α and AHR does not appear to be crucial in our murine CLL models. It is possible that the two TFs are not involved in CLL development and are not crucial for the function of healthy B cells in the clearance of CLL.

4. Discussion

In recent years, targeted therapy has shown to be highly efficient against CLL, improving patients living conditions and overall survival. Most of the current treatments are focusing on anti-apoptotic molecules (Bcl-2) and BCR-signaling kinases (BTK, PI3K), due to the highly stimulated state of CLL cells in the microenvironment. Innovative molecular therapy also aims to target leukemic cells' vulnerabilities more precisely. The use of conventional DNA-damage-based chemotherapy drugs in the past decades and the understanding of molecular mechanisms led to the discovery of potential new targets (e.g., WEE1 kinase) [38].

As heavily mutated and regulated in cancers, transcription factors naturally attracted attention for the development of new therapeutics. Around 300 TFs were described as oncogenes and could therefore become druggable candidates (e.g., TP53, MYC, and Stat family members) [39]. AHR and HIF-1α are not oncogenes but are crucial regulators of transcription programs in the microenvironment as sensors/responders to microenvironment conditions in both cancer and immune cells [40].

Previous research has shown that AHR and HIF-1α are important in hematological malignancies [13,41]. The impairment of HIF-1α and AHR provided promising results against leukemia and myeloma. Indeed, HIF-1α silencing by shRNA impaired the homing of CLL cells to the bone marrow and spleen, and the chemical inhibition of HIF-1α with

EZN-2208 prolonged the survival of mice challenged with MEC-1 cells [26]. In addition, the FDA-approved AHR antagonist clofazimine showed high efficacy in a transgenic model of multiple myeloma [42]. However, these observations are not sufficient to understand the exact mechanism of action and the cells targeted by the therapy. Whether the molecule directly kills cancer cells or impacts the immune microenvironment should be understood to refine treatments and propose new combinatory therapeutics for improved patient outcome. Therefore, we made use of transgenic murine models to specifically study the importance of both TFs in in leukemic cells in the context of CLL. We used the well-established Eμ-TCL1 murine model, where we showed that both AHR and HIF-1α transcriptional programs are enriched. We crossed this model with *Hif1a* or *Ahr* conditional knock-out mice to delete these genes only in $CD19^+$ B cells and investigated their role in the leukemogenesis of CLL. The unexpected results in this article show that knocking-out these two transcription factors does not affect the development of CLL in vivo. The gene expression profile of leukemic cells compared to that of cells from the control group was also unaffected by both knock-outs. Although we cannot rule out that there might be a different expression profile at early stages of the disease, this does not affect the final outcome of CLL progression. In addition, using our adoptive transfer model of TCL1 CLL cells into *Hif1a* or *Ahr* conditional knock-out, we could infer their role in normal B cells in the leukemic microenvironment. Indeed, the role of B cells in the context of cancer is still poorly defined and needs more investigations to better elucidate B cells pro-tumoral or anti-tumoral impact in different types of cancer [43]. Here, we could show that knocking out AHR and HIF-1α in healthy B cells did not impact the progression of CLL, which led to the conclusion that AHR and HIF-1α do not play a crucial role either in the development of CLL B cells or in the function of B cells in the TME.

From the literature, HIF-1α seems to be an interesting new target for CLL therapy, as it regulates the interaction of CLL cells with the TME and is upregulated in unmutated immunoglobulin heavy-chain variable region genes (IGHV) and TP53-disrupted CLL patients [26,27]. Interestingly, Meng et al. showed that the HIF-1α pathway directly affects IL-10 production in B cells [33], a feature also used by CLL B cells to favor an immunosuppressive tumor microenvironment and increase their survival [44]. Despite this, deletion of HIF-1α in leukemic cells of the Eμ-TCL1 mouse model had no impact on disease development, leading to the hypotheses that the importance of HIF-1α could depend on the oncogenic drivers and/or on compensatory mechanism (e.g., HIF-2α and/or on other cells of the TME). Griggio et al. nicely showed that the combination of an HIF-1α inhibitor with ibrutinib, a BTK inhibitor, showed a synergistic cytotoxic effect in TP53-disrupted CLL cells [27]. Considering this, it would be interesting to further investigate the effect of TP53 mutation in the TCL1 mouse model including the HIF-1α knock-out. Further, the use of a HIF-1α inhibitor in a co-culture of CLL cells and stromal cells in vitro showed that the inhibition also affected the stromal cells, resulting in decreased transcriptional regulation of target genes in the stromal compartment [45]. Considering the intricate regulation of the immune response by HIF-1α/A2A adenosine receptor signaling pathways [46], it would be worth investigating HIF-1α and its inhibition in the tumor microenvironment, including T cells, regulatory T cells, and nurse-like cells.

Regarding AHR, it also plays an important role in carcinogenesis and other diseases, especially the IDO–Kyn–AHR axis [47]. IDO activity is increased in CLL patients [48]. Furthermore, AHR is important in B cell development by controlling cell proliferation and apoptosis [21,23] and is involved in regulatory B cell (Bregs) differentiation and in the regulation of IL-10 production [24]. As CLL cells and Bregs share similar functions [25], AHR appears as an interesting therapeutic target in CLL. Nevertheless, and similarly to HIF-1α, its deletion did not influence disease outcome in the Eμ-TCL1 mouse model. According to previous studies, AHR is an important player in the establishment of an immunosuppressive TME. Jitschin et al. showed that untreated CLL patients have increased $IDO^{hi}CD62L^{hi}PD\text{-}L1^{hi}HLA\text{-}G^{hi}$ $CD11b^+CD33^+CD14^+HLA\text{-}DR^{lo}$ monocytic cells, supporting an immune suppression [49]. In addition, Sadik et al. recently demonstrated

that IL4I1, which catalyzes the formation of the AHR-activating ligand kynurenine, enhances CLL development due to a highly immunosuppressive TME [50]. Thus, increased AHR activation could influence disease outcome by an enhanced suppressive environment, by regulating the function of regulatory T cells (Tregs), and by turning the phenotype of effector $CD8^+$ T cells into an exhausted one [10,50]. Hence, targeting AHR in the TME of the proliferative CLL niche might still represent an interesting therapeutic option.

As HIF-1α and AHR share the dimerization partner ARNT/HIF1β, we could speculate on a reciprocal compensation, as for instance, both were shown to regulate IL-10 expression in B cells [24,33]. Therefore, we asked whether knocking out both factors would then be effective in decreasing CLL progression. However, as for single knock-outs, the survival of the mice did not differ compared to the control group. The percentage of CLL cells in the blood showed a slight increase in the double knock-out mice. However, this difference evened out when the disease was progressing. A possible explanation for CLL growth in the double knock-out might be the presence of an immunosuppressive tumor microenvironment. Indeed, CLL cells may overcompensate the loss of both HIF-1α and AHR, by another TF. For instance, Sp1 can regulate IL-10 production in CLL following BCR activation and signaling. It could supply CLL cells with enough survival signals and provide an IL-10-mediated suppression of the host immune system [44].

5. Conclusions

In conclusion, our results demonstrate that targeting HIF-1α or AHR by deleting them in CLL cells does not influence disease development in the Eμ-TCL1 mouse model. However, our results are not contradictory to previous results, as targeting the surrounding cells by specific inhibitors of these TFs could decrease the pro-survival signals for CLL cells and restore a more active anti-tumor immunity leading to reduced tumor burden. In vivo studies in relevant mouse models are therefore crucial to determine the importance of specific targets and also to investigate the effect of targeted inhibitors on tumor cells as well as on surrounding TME cells. This is crucial to validate interesting new targets and determine the mode of action of targeted treatments.

Supplementary Materials: The following are available online at https://www.mdpi.com/article/10.3390/cancers13184518/s1, Figure S1: RNA sequencing data of B cells from C57BL/6 and Eμ-TCL1 mice. Figure S2: Full gel pictures corresponding to Figures 2D, 3D and 4F, Table S1: Differentially expressed genes in leukemic cells from TCL1 $CD19^{Cre/WT}Hif1a^{fl/fl}$ versus Eμ-TCL1 $CD19^{Cre/WT}Hif1a^{WT/WT}$, Table S2: Differentially expressed genes in leukemic cells from TCL1 $CD19^{Cre/WT}Ahr^{fl/fl}$ versus Eμ-TCL1 $CD19^{Cre/WT}Ahr^{WT/WT}$, Table S3: Differentially expressed genes in leukemic cells from TCL1 $CD19^{Cre/WT}Ahr^{fl/fl}Hif1a^{fl/fl}$ versus Eμ-TCL1 $CD19^{Cre/WT}Ahr^{WT/WT}Hif1a^{WT/WT}$.

Author Contributions: S.G. designed and performed experiments, analyzed the results, and wrote the manuscript. E.G., A.L., S.P., I.F.B. and G.P. helped in performing experiments and writing the manuscript. E.M. and J.P. designed and supervised the study and wrote the final version of the manuscript. All authors have read and agreed to the published version of the manuscript.

Funding: This work was supported by grants from FNRS "Télévie" to S.G., A.L., I.F.B. and G.P. (7.4502.19, 7.4503.19, 7.4529.19, 7.6518.20), from Fonds National de la Recherche Luxembourg to E.G., S.P., J.P, and E.M. (PRIDE15/10675146/CANBIO, C20/BM/14592342, and C20/BM/14582635).

Institutional Review Board Statement: Animal experimentation protocols were approved by the by the local ethics committee (Animal Welfare Structure) and by the Luxembourg Ministry for Agriculture (protocols LUPA 2019/57 and LUPA 2019/71).

Informed Consent Statement: Not applicable.

Data Availability Statement: The data presented in this study are openly available in the public functional genomics data repository GEO under the references GSE175564 and GSE179196.

Acknowledgments: We thank Carlo Croce and John Byrd (OSU, OH) for the kind gift of Eμ-TCL1 mouse.

Conflicts of Interest: The authors declare no conflict of interest. The funders had no role in the design of the study; in the collection, analyses, or interpretation of data; in the writing of the manuscript, or in the decision to publish the results.

References

1. Chiorazzi, N.; Chen, S.S.; Rai, K.R. Chronic Lymphocytic Leukemia. *Cold Spring Harb. Perspect. Med.* **2021**, *11*, a035220. [CrossRef] [PubMed]
2. Herishanu, Y.; Katz, B.Z.; Lipsky, A.; Wiestner, A. Biology of chronic lymphocytic leukemia in different microenvironments: Clinical and therapeutic implications. *Hematol. Oncol. Clin.* **2013**, *27*, 173–206. [CrossRef]
3. Hanahan, D.; Weinberg, R.A. Hallmarks of Cancer: The Next Generation. *Cell* **2011**, *144*, 646–674. [CrossRef]
4. Belluti, S.; Rigillo, G.; Imbriano, C. Transcription Factors in Cancer: When Alternative Splicing Determines Opposite Cell Fates. *Cells* **2020**, *9*, 760. [CrossRef]
5. Kandoth, C.; McLellan, M.D.; Vandin, F.; Ye, K.; Niu, B.; Lu, C.; Xie, M.; Zhang, Q.; McMichael, J.F.; Wyczalkowski, M.; et al. Mutational landscape and significance across 12 major cancer types. *Nat. Cell Biol.* **2013**, *502*, 333–339. [CrossRef]
6. Venkatraman, S.; Meller, J.; Hongeng, S.; Tohtong, R.; Chutipongtanate, S. Transcriptional Regulation of Cancer Immune Checkpoints: Emerging Strategies for Immunotherapy. *Vaccines* **2020**, *8*, 735. [CrossRef] [PubMed]
7. Moia, R.; Patriarca, A.; Deambrogi, C.; Rasi, S.; Favini, C.; Kodipad, A.A.; Schipani, M.; Gaidano, G. An update on: Molecular genetics of high-risk chronic lymphocytic leukemia. *Expert Rev. Hematol.* **2019**, *13*, 109–116. [CrossRef]
8. Hallek, M. Chronic lymphocytic leukemia: 2020 update on diagnosis, risk stratification and treatment. *Am. J. Hematol.* **2019**, *94*, 1266–1287. [CrossRef]
9. Vito, A.; El-Sayes, N.; Mossman, K. Hypoxia-Driven Immune Escape in the Tumor Microenvironment. *Cells* **2020**, *9*, 992. [CrossRef] [PubMed]
10. Campesato, L.F.; Budhu, S.; Tchaicha, J.; Weng, C.-H.; Gigoux, M.; Cohen, I.J.; Redmond, D.; Mangarin, L.; Pourpe, S.; Liu, C.; et al. Blockade of the AHR restricts a Treg-macrophage suppressive axis induced by L-Kynurenine. *Nat. Commun.* **2020**, *11*, 4011. [CrossRef] [PubMed]
11. Irigoyen, M.; Garcia-Ruiz, J.C.; Berra, E. The hypoxia signalling pathway in haematological malignancies. *Oncotarget* **2017**, *8*, 36832–36844. [CrossRef]
12. Paris, A.; Tardif, N.; Galibert, M.-D.; Corre, S. AhR and Cancer: From Gene Profiling to Targeted Therapy. *Int. J. Mol. Sci.* **2021**, *22*, 752. [CrossRef]
13. Gentil, M.; Hugues, P.; Desterke, C.; Telliam, G.; Sloma, I.; Souza, L.E.B.; Baykal, S.; Artus, J.; Griscelli, F.; Guerci, A.; et al. Aryl hydrocarbon receptor (AHR) is a novel druggable pathway controlling malignant progenitor proliferation in chronic myeloid leukemia (CML). *PLoS ONE* **2018**, *13*, e0200923. [CrossRef]
14. Cheong, J.E.; Sun, L. Targeting the IDO1/TDO2-KYN-AhR Pathway for Cancer Immunotherapy—Challenges and Opportunities. *Trends Pharmacol. Sci.* **2018**, *39*, 307–325. [CrossRef]
15. Liu, Y.; Liang, X.; Dong, W.; Fang, Y.; Lv, J.; Zhang, T.; Fiskesund, R.; Xie, J.; Liu, J.; Yin, X.; et al. Tumor-Repopulating Cells Induce PD-1 Expression in CD8+ T Cells by Transferring Kynurenine and AhR Activation. *Cancer Cell* **2018**, *33*, 480–494. [CrossRef]
16. Xue, P.; Fu, J.; Zhou, Y. The Aryl Hydrocarbon Receptor and Tumor Immunity. *Front. Immunol.* **2018**, *9*, 286. [CrossRef]
17. Iommarini, L.; Porcelli, A.M.; Gasparre, G.; Kurelac, I. Non-Canonical Mechanisms Regulating Hypoxia-Inducible Factor 1 Alpha in Cancer. *Front. Oncol.* **2017**, *7*, 286. [CrossRef]
18. Selak, M.A.; Armour, S.M.; MacKenzie, E.D.; Boulahbel, H.; Watson, D.G.; Mansfield, K.D.; Pan, Y.; Simon, M.C.; Thompson, C.B.; Gottlieb, E. Succinate links TCA cycle dysfunction to oncogenesis by inhibiting HIF-α prolyl hydroxylase. *Cancer Cell* **2005**, *7*, 77–85. [CrossRef] [PubMed]
19. Kontos, C.; Papageorgiou, S.G.; Diamantopoulos, M.A.; Scorilas, A.; Bazani, E.; Vasilatou, D.; Gkontopoulos, K.; Glezou, E.; Stavroulaki, G.; Dimitriadis, G.; et al. mRNA overexpression of the hypoxia inducible factor 1 alpha subunit gene (HIF1A): An independent predictor of poor overall survival in chronic lymphocytic leukemia. *Leuk. Res.* **2016**, *53*, 65–73. [CrossRef] [PubMed]
20. Wagage, S.; Hunter, C.A. Interrelated Roles for the Aryl Hydrocarbon Receptor and Hypoxia Inducible Factor-1α in the Immune Response to Infection. *Curr. Med. Chem.* **2015**, *11*, 43–54. [CrossRef]
21. Sherr, D.H.; Monti, S. The role of the aryl hydrocarbon receptor in normal and malignant B cell development. *Semin. Immunopathol.* **2013**, *35*, 705–716. [CrossRef] [PubMed]
22. Burrows, N.; Maxwell, P.H. Hypoxia and B cells. *Exp. Cell Res.* **2017**, *356*, 197–203. [CrossRef] [PubMed]
23. Villa, M.; Gialitakis, M.; Tolaini, M.; Ahlfors, H.; Henderson, C.J.; Wolf, C.R.; Brink, R.; Stockinger, B. Aryl hydrocarbon receptor is required for optimal B-cell proliferation. *EMBO J.* **2017**, *36*, 116–128. [CrossRef] [PubMed]
24. Piper, C.J.; Rosser, E.C.; Oleinika, K.; Nistala, K.; Krausgruber, T.; Rendeiro, A.; Banos, A.; Drozdov, I.; Villa, M.; Thomson, S.; et al. Aryl Hydrocarbon Receptor Contributes to the Transcriptional Program of IL-10-Producing Regulatory B Cells. *Cell Rep.* **2019**, *29*, 1878–1892. [CrossRef]
25. DiLillo, D.J.; Weinberg, J.B.; Yoshizaki, A.; Horikawa, M.; Bryant, J.M.; Iwata, Y.; Matsushita, T.; Matta, K.M.; Chen, Y.; Venturi, G.M.; et al. Chronic lymphocytic leukemia and regulatory B cells share IL-10 competence and immunosuppressive function. *Leukemia* **2013**, *27*, 170–182. [CrossRef]

26. Valsecchi, R.; Coltella, N.; Belloni, D.; Ponente, M.; Hacken, E.T.; Scielzo, C.; Scarfo', L.; Bertilaccio, M.T.S.; Brambilla, P.; Lenti, E.; et al. HIF-1α regulates the interaction of chronic lymphocytic leukemia cells with the tumor microenvironment. *Blood* **2016**, *127*, 1987–1997. [CrossRef]
27. Griggio, V.; Vitale, C.; Todaro, M.; Riganti, C.; Kopecka, J.; Salvetti, C.; Bomben, R.; Bo, M.D.; Magliulo, D.; Rossi, D.; et al. HIF-1α is over-expressed in leukemic cells from TP53-disrupted patients and is a promising therapeutic target in chronic lymphocytic leukemia. *Haematologica* **2019**, *105*, 1042–1054. [CrossRef] [PubMed]
28. Bichi, R.; Shinton, S.A.; Martin, E.S.; Koval, A.; Calin, G.; Cesari, R.; Russo, G.; Hardy, R.R.; Croce, C.M. Human chronic lymphocytic leukemia modeled in mouse by targeted TCL1 expression. *Proc. Natl. Acad. Sci. USA* **2002**, *99*, 6955–6960. [CrossRef]
29. Gonder, S.; Botana, I.F.; Wierz, M.; Pagano, G.; Gargiulo, E.; Cosma, A.; Moussay, E.; Paggetti, J.; Largeot, A. Method for the Analysis of the Tumor Microenvironment by Mass Cytometry: Application to Chronic Lymphocytic Leukemia. *Front. Immunol.* **2020**, *11*, 578176. [CrossRef]
30. Wierz, M.; Pierson, S.; Chouha, N.; Désaubry, L.; François, J.-H.; Berchem, G.; Paggetti, J.; Moussay, E. The prohibitin-binding compound fluorizoline induces apoptosis in chronic lymphocytic leukemia cells ex vivo but fails to prevent leukemia development in a murine model. *Haematologica* **2018**, *103*, e154–e157. [CrossRef]
31. Wierz, M.; Janji, B.; Berchem, G.; Moussay, E.; Paggetti, J. High-dimensional mass cytometry analysis revealed microenvironment complexity in chronic lymphocytic leukemia. *OncoImmunology* **2018**, *7*, e1465167. [CrossRef]
32. Wierz, M.; Pierson, S.; Guyonnet, L.; Viry, E.; Lequeux, A.; Oudin, A.; Niclou, S.P.; Ollert, M.; Berchem, G.; Janji, B.; et al. Dual PD1/LAG3 immune checkpoint blockade limits tumor development in a murine model of chronic lymphocytic leukemia. *Blood* **2018**, *131*, 1617–1621. [CrossRef]
33. Meng, X.; Grötsch, B.; Luo, Y.; Knaup, K.X.; Wiesener, M.S.; Chen, X.-X.; Jantsch, J.; Fillatreau, S.; Schett, G.; Bozec, A. Hypoxia-inducible factor-1α is a critical transcription factor for IL-10-producing B cells in autoimmune disease. *Nat. Commun.* **2018**, *9*, 251. [CrossRef]
34. Kovalova, N.; Nault, R.; Crawford, R.; Zacharewski, T.R.; Kaminski, N.E. Comparative analysis of TCDD-induced AhR-mediated gene expression in human, mouse and rat primary B cells. *Toxicol. Appl. Pharmacol.* **2017**, *316*, 95–106. [CrossRef]
35. Wang, G.L.; Jiang, B.-H.; Rue, E.A.; Semenza, G.L. Hypoxia-inducible factor 1 is a basic-helix-loop-helix-PAS heterodimer regulated by cellular O2 tension. *Proc. Natl. Acad. Sci. USA* **1995**, *92*, 5510–5514. [CrossRef] [PubMed]
36. Bacsi, S.G.; Reisz-Porszasz, S.; Hankinson, O. Orientation of the heterodimeric aryl hydrocarbon (dioxin) receptor complex on its asymmetric DNA recognition sequence. *Mol. Pharmacol.* **1995**, *47*, 432–438. [PubMed]
37. Vaidyanathan, B.; Chaudhry, A.; Yewdell, W.T.; Angeletti, D.; Yen, W.-F.; Wheatley, A.; Bradfield, C.A.; McDermott, A.B.; Yewdell, J.W.; Rudensky, A.Y.; et al. The aryl hydrocarbon receptor controls cell-fate decisions in B cells. *J. Exp. Med.* **2017**, *214*, 197–208. [CrossRef] [PubMed]
38. Vakili-Samiani, S.; Jalil, A.T.; Abdelbasset, W.K.; Yumashev, A.V.; Karpisheh, V.; Jalali, P.; Adibfar, S.; Ahmadi, M.; Feizi, A.A.H.; Jadidi-Niaragh, F. Targeting Wee1 kinase as a therapeutic approach in Hematological Malignancies. *DNA Repair* **2021**, *107*, 103203. [CrossRef]
39. Lambert, M.; Jambon, S.; Depauw, S.; David-Cordonnier, M.-H. Targeting Transcription Factors for Cancer Treatment. *Molecules* **2018**, *23*, 1479. [CrossRef] [PubMed]
40. Ramsay, G.; Cantrell, D. Environmental and metabolic sensors that control T cell biology. *Front. Immunol.* **2015**, *6*, 99. [CrossRef] [PubMed]
41. Magliulo, D.; Bernardi, R. HIF-α factors as potential therapeutic targets in leukemia. *Expert Opin. Ther. Targets* **2018**, *22*, 917–928. [CrossRef]
42. Bianchi-Smiraglia, A.; Bagati, A.; Fink, E.E.; Affronti, H.C.; Lipchick, B.C.; Moparthy, S.; Long, M.D.; Rosario, S.R.; Lightman, S.M.; Moparthy, K.; et al. Inhibition of the aryl hydrocarbon receptor/polyamine biosynthesis axis suppresses multiple myeloma. *J. Clin. Investig.* **2018**, *128*, 4682–4696. [CrossRef]
43. Largeot, A.; Pagano, G.; Gonder, S.; Moussay, E.; Paggetti, J. The B-side of Cancer Immunity: The Underrated Tune. *Cells* **2019**, *8*, 449. [CrossRef] [PubMed]
44. Alhakeem, S.; McKenna, M.K.; Oben, K.Z.; Noothi, S.K.; Rivas, J.R.; Hildebrandt, G.C.; Fleischman, R.A.; Rangnekar, V.M.; Muthusamy, N.; Bondada, S. Chronic Lymphocytic Leukemia–Derived IL-10 Suppresses Antitumor Immunity. *J. Immunol.* **2018**, *200*, 4180–4189. [CrossRef] [PubMed]
45. Vitale, C.; Griggio, V.; Riganti, C.; Todaro, M.; Kopecka, J.; Jones, R.; Salvetti, C.; Boccellato, E.; Perutelli, F.; Voena, C.; et al. Targeting HIF-1α Regulatory Pathways as a Strategy to Hamper Tumor-Microenvironment Interactions in CLL. *Cancers* **2021**, *13*, 2883. [CrossRef]
46. Serra, S.; Vaisitti, T.; Audrito, V.; Bologna, C.; Buonincontri, R.; Chen, S.-S.; Arruga, F.; Brusa, D.; Coscia, M.; Jaksic, O.; et al. Adenosine signaling mediates hypoxic responses in the chronic lymphocytic leukemia microenvironment. *Blood Adv.* **2016**, *1*, 47–61. [CrossRef] [PubMed]
47. Ye, Z.; Yue, L.; Shi, J.; Shao, M.; Wu, T. Role of IDO and TDO in Cancers and Related Diseases and the Therapeutic Implications. *J. Cancer* **2019**, *10*, 2771–2782. [CrossRef]
48. Lindström, V.; Aittoniemi, J.; Jylhävä, J.; Eklund, C.; Hurme, M.; Paavonen, T.; Oja, S.S.; Itälä-Remes, M.; Sinisalo, M. Indoleamine 2,3-Dioxygenase Activity and Expression in Patients with Chronic Lymphocytic Leukemia. *Clin. Lymphoma Myeloma Leuk.* **2012**, *12*, 363–365. [CrossRef] [PubMed]

49. Jitschin, R.; Braun, M.; Büttner, M.; Dettmer-Wilde, K.; Bricks, J.; Berger, J.; Eckart, M.J.; Krause, S.; Oefner, P.J.; Le Blanc, K.; et al. CLL-cells induce IDOhi CD14+HLA-DRlo myeloid-derived suppressor cells that inhibit T-cell responses and promote TRegs. *Blood* **2014**, *124*, 750–760. [CrossRef]
50. Sadik, A.; Patterson, L.F.S.; Öztürk, S.; Mohapatra, S.R.; Panitz, V.; Secker, P.F.; Pfänder, P.; Loth, S.; Salem, H.; Prentzell, M.T.; et al. IL4I1 Is a Metabolic Immune Checkpoint that Activates the AHR and Promotes Tumor Progression. *Cell* **2020**, *182*, 1252–1270. [CrossRef]

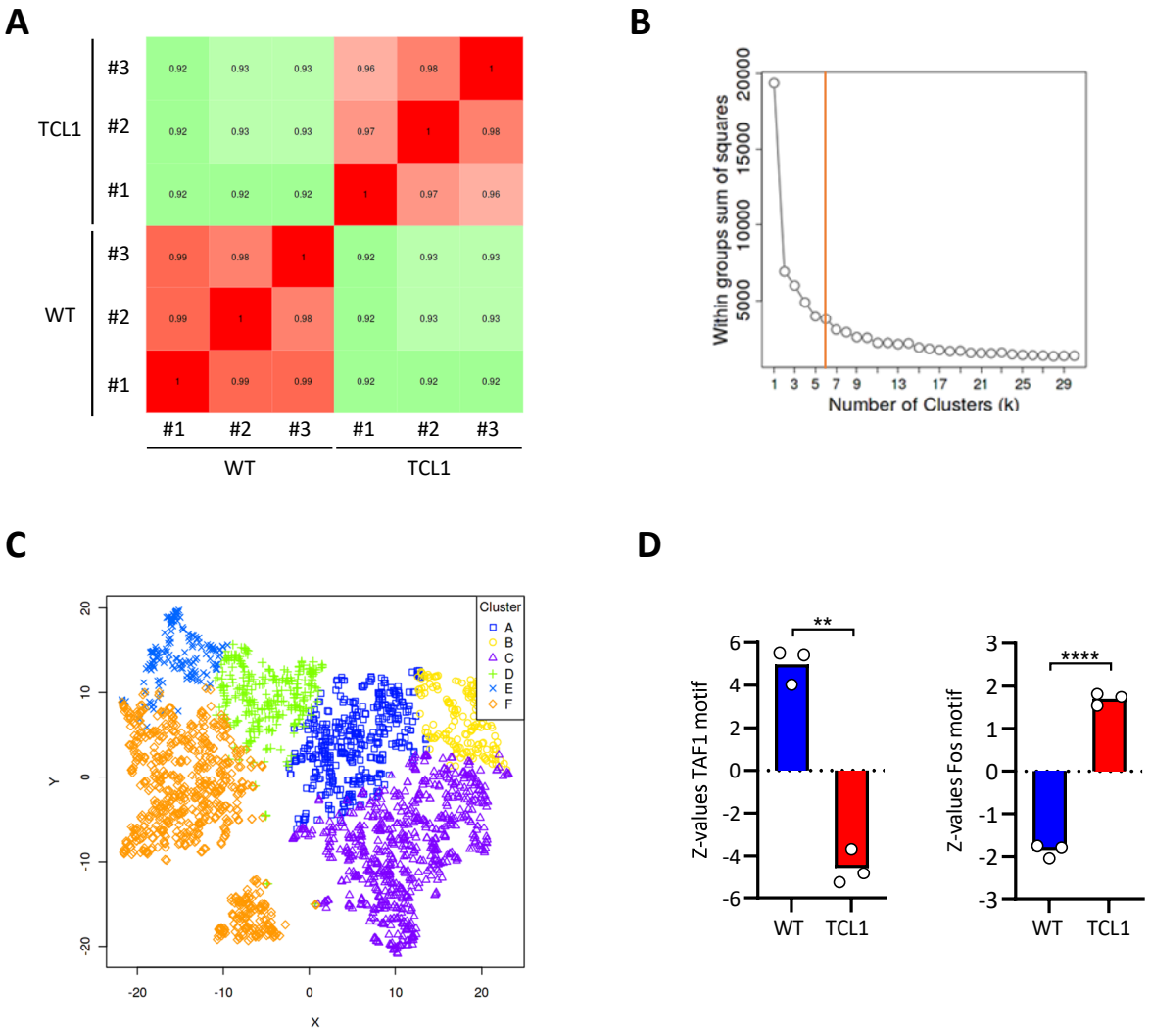

Supplemental Figure 1: RNA sequencing data of B cells from C57BL/6 and Eμ-TCL1 mice. **(A)** Correlation matrix for all biological replicates. **(B)** Estimate of the number of clusters (K value) using the elbow method. **(C)** Mapping of the top genes to k-means clusters with the dimension reduction algorithm t-SNE. **(D)** Transcription factor activity (Z-values, ISMARA) for TAF1 and Fos motifs among WT and TCL1 B cells.

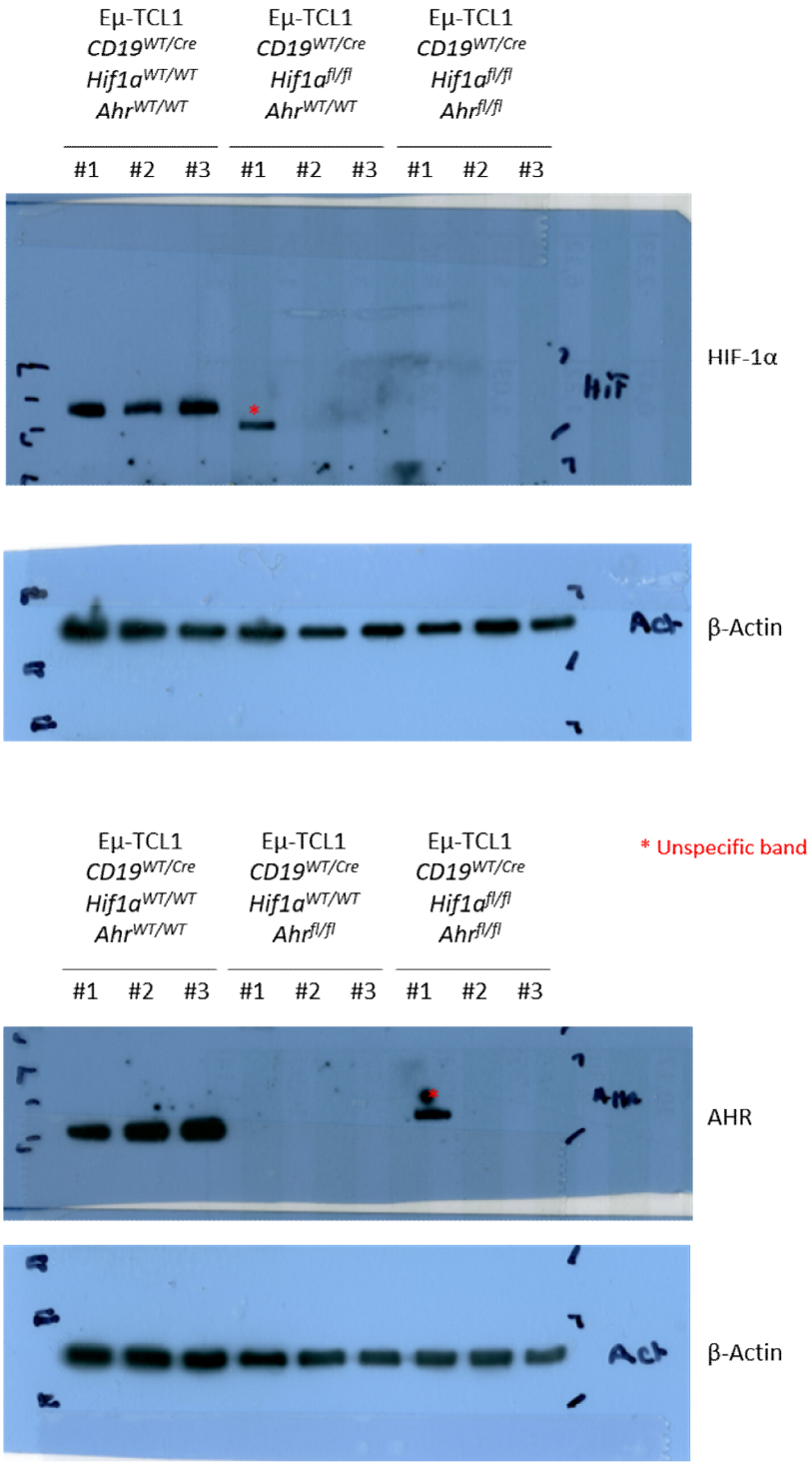

* Unspecific band

Supplemental Figure 2: Full gel pictures corresponding to Figure 2D, 3D, and 4F

Gene	logFC	FDR
Gstt1	6.47	5.487e-09
Prdm16	9.27	0.0001
Mcts2	3.69	0.0025
Igkv12-89	5.61	0.0043
Ighv1-55	7.14	0.0052
Cntln	6.60	0.0081
Scfd1	1.33	0.0248
Mnat1	1.35	0.0248
Peak1os	-4.38	0.0350
Gm20767	-1.57	0.0350
St6gal1	-1.97	0.0350
Cd36	-2.40	0.0350
Calcrl	4.45	0.0387
Ctnna1	3.21	0.0471

Supplemental Table 1. Differentially expressed genes in leukemic cells from TCL1 *CD19*$^{Cre/WT}$*Hif1a*$^{fl/fl}$ versus Eμ-TCL1 *CD19*$^{Cre/WT}$*Hif1a*$^{WT/WT}$.

Gene	logFC	FDR
Leprotl1	2.33	0.0185
Alox5ap	-2.65	0.0185
Prdm16	5.22	0.0265
Icos	-4.30	0.0342

Supplemental Table 2. Differentially expressed genes in leukemic cells from TCL1 *CD19*$^{Cre/WT}$*Ahr*$^{fl/fl}$ versus Eμ-TCL1 *CD19*$^{Cre/WT}$*Ahr*$^{WT/WT}$.

Gene	logFC	FDR
none		

Supplemental Table 3. Differentially expressed genes in leukemic cells from TCL1 *CD19*$^{Cre/WT}$*Ahr*$^{fl/fl}$*Hif1a*$^{fl/fl}$ versus Eμ-TCL1 *CD19*$^{Cre/WT}$*Ahr*$^{WT/WT}$*Hif1a*$^{WT/WT}$.

In this paper, we demonstrated that *Ahr* and *Hif1a* depletion in CLL cells does not impact CLL development in the TCL1 mouse model (which spontaneusly develops a CLL-like disease within 6 months. This finding is fundamental as a proof of concept of the importance of the TME in CLL pathogenesis. In fact, the same transcription factors depleted in Tregs caused a drastic delay in CLL development (as shown in the results section). It is important to underline that the models used in the two experiments are different: the Eμ-TCL1 mouse model was used when depleting the two TFs in CLL cells, while the Adoptive Transfer (AT) CLL model was used in depleting the same factors in Tregs. Nonetheless, it would be interesting to verify whether the data obtained in the AT model can be recapitulated in the *TCL1-Foxp3*^{Cre}*-Ahr*^{fx}*/Hif1α*^{fx} mice (until now this has not been done because of the large number of mice to use for this purpose).

In addition, the experiment in which we used inhibitors against AHR and HIF-1α partilly reproduced the delay in CLL development observed in the mice with KO-Tregs. It would be particularly interesting to inspect the TME of the mice injected with the inhibitors to observe whether major differences can be found in the CLL compartment, which are not expected.

Annex II - A Specific CD44^{lo} CD25^{lo} Subpopulation of Regulatory T cells Inhibits Anti-Leukemic Immune Response and Promotes the Progression in a Mouse Model of Chronic Lymphocytic Leukemia.

Agnieszka Goral1, Malgorzata Firczuk1, Klaudyna Fidyt 1, Marta Sledz1, Francesca Simoncello2, Karolina Siudakowska1, **Giulia Pagano3**, Etienne Moussay3, Jerome Paggetti3, Patrycja Nowakowska1, Stefania Gobessi4, Joanna Barankiewicz5, Aleksander Salomon-Perzynski5, Federica Benvenuti2, Dimitar G. Efremov4, Przemyslaw Juszczynski5, Ewa Lech-Maranda5 and Angelika Muchowicz1*

1 Department of Immunology, Medical University of Warsaw, Warsaw, Poland,
2 Cellular Immunology, International Centre for Genetic Engineering and Biotechnology, Trieste, Italy,
3 Tumor-Stroma Interactions, Department of Cancer Research, Luxembourg Institute of Health, Luxembourg, Luxembourg,
4 Molecular Hematology, International Centre for Genetic Engineering and Biotechnology, Trieste, Italy,
5 Department of Experimental Hematology, Institute of Hematology and Transfusion Medicine, Warsaw, Poland

Author Contributions

Conceptualization, AM, AG, and MF. Investigation, AG, KF, MS, KS, PN, FS, **GP**, JP, and EM. Resources, JB, AS-P, SG, EL-M, and DE. Writing and visualization AM, AG, KF, JP, and EM. Critical revision, SG, FB, DE, PJ, MF, JP, and EM. Supervision, project administration AM. All authors contributed to the article and approved the submitted version.

I contributed to the experiments shown in figure 3, panels D-E (library preparation for the RNA-seq experiment and help in data analysis).

frontiers in Immunology

ORIGINAL RESEARCH
published: 28 February 2022
doi: 10.3389/fimmu.2022.781364

A Specific CD44lo CD25lo Subpopulation of Regulatory T Cells Inhibits Anti-Leukemic Immune Response and Promotes the Progression in a Mouse Model of Chronic Lymphocytic Leukemia

*Agnieszka Goral[1], Malgorzata Firczuk[1], Klaudyna Fidyt[1], Marta Sledz[1], Francesca Simoncello[2], Karolina Siudakowska[1], Giulia Pagano[3], Etienne Moussay[3], Jérôme Paggetti[3], Patrycja Nowakowska[1], Stefania Gobessi[4], Joanna Barankiewicz[5], Aleksander Salomon-Perzynski[5], Federica Benvenuti[2], Dimitar G. Efremov[4], Przemyslaw Juszczynski[5], Ewa Lech-Maranda[5] and Angelika Muchowicz[1]**

[1] Department of Immunology, Medical University of Warsaw, Warsaw, Poland, [2] Cellular Immunology, International Centre for Genetic Engineering and Biotechnology, Trieste, Italy, [3] Tumor-Stroma Interactions, Department of Cancer Research, Luxembourg Institute of Health, Luxembourg, Luxembourg, [4] Molecular Hematology, International Centre for Genetic Engineering and Biotechnology, Trieste, Italy, [5] Department of Experimental Hematology, Institute of Hematology and Transfusion Medicine, Warsaw, Poland

OPEN ACCESS

Edited by:
Eyad Elkord,
University of Salford, United Kingdom

Reviewed by:
Daniel Gray,
Walter and Eliza Hall Institute of Medical Research, Australia
Mingfeng Zhao,
Tianjin First Central Hospital, China

***Correspondence:**
Angelika Muchowicz
angelika.muchowicz@wum.edu.pl

Specialty section:
This article was submitted to Cancer Immunity and Immunotherapy, a section of the journal Frontiers in Immunology

Received: *22 September 2021*
Accepted: *07 February 2022*
Published: *28 February 2022*

Citation:
Goral A, Firczuk M, Fidyt K, Sledz M, Simoncello F, Siudakowska K, Pagano G, Moussay E, Paggetti J, Nowakowska P, Gobessi S, Barankiewicz J, Salomon-Perzynski A, Benvenuti F, Efremov DG, Juszczynski P, Lech-Maranda E and Muchowicz A (2022) A Specific CD44lo CD25lo Subpopulation of Regulatory T Cells Inhibits Anti-Leukemic Immune Response and Promotes the Progression in a Mouse Model of Chronic Lymphocytic Leukemia. Front. Immunol. 13:781364. doi: 10.3389/fimmu.2022.781364

Regulatory T cells (Tregs) are capable of inhibiting the proliferation, activation and function of T cells and play an important role in impeding the immune response to cancer. In chronic lymphocytic leukemia (CLL) a dysfunctional immune response and elevated percentage of effector-like phenotype Tregs have been described. In this study, using the Eμ-TCL1 mouse model of CLL, we evaluated the changes in the Tregs phenotype and their expansion at different stages of leukemia progression. Importantly, we show that Tregs depletion in DEREG mice triggered the expansion of new anti-leukemic cytotoxic T cell clones leading to leukemia eradication. In TCL1 leukemia-bearing mice we identified and characterized a specific Tregs subpopulation, the phenotype of which suggests its role in the formation of an immunosuppressive microenvironment, supportive for leukemia survival and proliferation. This observation was also confirmed by the gene expression profile analysis of these TCL1-specific Tregs. The obtained data on Tregs are consistent with those described so far, however, above all show that the changes in the Tregs phenotype described in CLL result from the formation of a specific, described in this study Tregs subpopulation. In addition, functional tests revealed the ability of Tregs to inhibit T cells that recognize model antigens expressed by leukemic cells. Moreover, inhibition of Tregs with a MALT1 inhibitor provided a therapeutic benefit, both as monotherapy and also when combined with an immune checkpoint inhibitor. Altogether, activation of Tregs appears to be crucial for CLL progression.

Keywords: Tregs, CLL, Eμ-TCL1, MALT1, TCR repertoire, anti-leukemic immune response

INTRODUCTION

Despite the extensive research and the development of new treatment modalities, the number of chronic lymphocytic leukemia (CLL) cases with clinical resistance to therapy is constantly rising (1). The newest achievement in immunotherapy – chimeric antigen receptor T cells (CAR-T cells) – are less effective in CLL as compared to other B cell malignancies, including B cell acute lymphoblastic leukemia or diffuse large B cell lymphoma (2–4). Similarly, immune checkpoint inhibitors have a limited efficacy in relapsed/refractory CLL (3). In preclinical studies, antibodies against lymphocyte activation gene 3 (LAG-3), programmed cell death protein 1 (PD-1) or programmed death-ligand 1 (PD-L1) are only effective when administrated in the initial stage of leukemia development (5–7). Importantly, the immune system dysfunctions observed in CLL patients, suggest that CLL cells modulate the microenvironment to their own benefit (8–10). The exhausted phenotype of T cells that display high expression of PD-1, LAG-3, or T cell immunoglobulin domain and mucin domain (TIM-3) is a hallmark of CLL (11, 12). In order to improve the therapeutic strategies for CLL, it is crucial to understand the mechanisms that shape the leukemia microenvironment.

Naturally occurring, thymic, Forkhead box protein P3 $(FoxP3)^+$, $CD4^+$ regulatory T cells (Tregs), are sensitive to activation by self-antigens and tumor neoantigens, and are main players of the neoplastic microenvironment (13). Tregs can affect T cells in all stages of immune response development: priming, proliferation, and T cell effector functions (14). Increased frequency of Tregs correlates with poor prognosis of CLL patients (15). The expression patterns of Tregs-associated markers (CD25, LAG-3, killer cell lectin like receptor G1, CD69, Eomesodermin - EOMES) that determines their suppressive functions was recently presented in both CLL patients and leukemia-bearing mice (5, 16, 17). Nevertheless, the function of Tregs in CLL has not been elucidated and the approaches for Tregs elimination have shown to be insufficient. For instance, the administration of anti-CD25 antibodies or phosphoinositide 3-kinase δ (PI3Kδ) inhibitors affected not only Tregs but also abrogated the activation and function of $CD8^+$ lymphocytes (18).

In order to evaluate the role of Tregs in the development and shaping of immunosuppressive microenvironment of CLL, in this work we used Eμ-TCL1 transgenic mice model (19, 20). We characterized a novel, TCL1-derived Tregs subpopulation and assessed Tregs suppressive activity in functional tests. Furthermore, TCR sequencing allowed us to better understand the influence of leukemia on Tregs and $CD8^+$ T lymphocytes activation and clonality. Finally, we used the inhibitor of mucosa-associated lymphoid tissue lymphoma translocation protein 1 (MALT1) to block the activation of Tregs. MALT1 protease is a component of CARMA1-BCL10-MALT1 (CBM) complex which was shown to be crucial for Tregs activity (21). The results obtained in this study provide the evidence that Tregs are essential for leukemia progression in immunocompetent mice and can be efficiently targeted to block CLL progression.

MATERIALS AND METHODS

Reagents

MI-2 (Malt1 inhibitor, Selleckchem.com) was dissolved in DMSO (Sigma-Aldrich, St Louis, MA, USA), aliquoted and stored at -20°C. Albumin from chicken egg white (OVA, Sigma-Aldrich, St Louis, MA, USA) and Poly (I:C) (HMW) (*In vivo*Gen, San Diego, CA, USA) were aliquoted and stored at -20°C. Diphtheria Toxin (DT) from *Corynebacterium diphtheriae* (Sigma-Aldrich, St Louis, MA, USA) was aliquoted and stored at -80°C. Anti-mouse PD-L1 antibody InVivoPlus (B7-H1) (BioXcell, Lebanon, NH, USA) and InVivoPlus rat IgG2b isotype control, (BioXcell, Lebanon, NH, USA) were stored at 4°C.

Animals Studies

All *in vivo* studies were performed in accordance with the EU Directive 2010/63/EU and the Polish legislation for animal experiments of the Polish Ministry of Science and Higher Education (February 26, 2015) and approved by the Local Ethics Committee for the Animal Experimentation in Warsaw. The *in vivo* experiments were carried out in Animal Facility of the Medical University of Warsaw.

For the study, 6-12 weeks old female or male (never mixed in one experiment) mice were used. Mouse strains include: C57BL6/J (wild-type, immunocompetent mice) (Medical University of Bialystok or Mossakowski Medical Research Centre), B6.Cg-Foxp3tm2(EGFP)Tch/J (B6 $Foxp3^{EGFP}$, Tregs express GFP) (University of Warsaw), C57BL/6-Tg(Foxp3-DTR/EGFP)23.2Spar/Mmjax (DEREG, Tregs express GFP and receptor for diphtheria toxin) (The International Centre for Genetic Engineering and Biotechnology, Trieste, Italy) B6(Cg)-Rag2tm1.1Cgn/J (RAG2-KO, immunodeficient mice) and C57BL/6-Tg(TcraTcrb)1100Mjb/J (OT-1) (Medical University of Warsaw). Splenocytes or leukemic $CD5^+CD19^+$ TCL1 cells (5×10^6 – 1×10^7) isolated from spleens of female Eμ-TCL1 transgenic mice (The International Centre for Genetic Engineering and Biotechnology, Trieste, Italy) were adoptively transferred *via* tail vein injection. In described experiments we used cells isolated from two different Eμ-TCL1 transgenic mice, either TCL1-1159 or TCL1-1013. These cells were propagated in mice maximally twice, with the exception of genetically modified TCL1 cells expressing OVA (due to the procedure of generating modified cells, they required additional propagation in RAG2-KO mice).

In Vivo Treatments

Eμ-TCL1 mice model of CLL was used in this study. To monitor leukemia development and progression, the percentage of leukemic TCL1 cells ($CD5^+CD19^+$) among white blood cells (WBC) in the peripheral blood (PB) collected from cheek vein was assessed by flow cytometry. The consistency in the assessment of leukemia was ensured and blinding practice was not applicable. Mice with detected leukemia were randomly selected and further used in the experiments. The sample size was calculated with power analysis test (22).

DEREG mice were treated with DT (50 μg/kg) administered intraperitoneally (i.p.) every four days. MI-2 was administered

i.p. daily, at dose 20 mg/kg and the control mice were injected with the DMSO as a solvent. Anti-PD-L1 antibody or the appropriate isotype control were administered i.p. every second day at a dose 200 μg/mouse. The schemes of the treatments are presented in details in the appropriate figures.

Cell Isolation

In order to prepare a single cell suspension, spleens (SPL) or lymph nodes (LNs) were cut in small pieces and passed through a 150 μm cell strainer. To remove red blood cells the isolated splenocytes were lysed with ACK Lysing Buffer (Thermofisher Scientific, Waltham, MA, USA) according to the manufacturer's instructions. $CD19^+$, $CD4^+$ and $CD8^+$ cell subpopulations were isolated by immunomagnetic negative selection using EasySep™ Mouse B Cell Isolation Kit, EasySep™ Mouse $CD4^+$ T cell Isolation Kit and EasySep™ Mouse $CD8^+$ Cell Isolation Kit (STEMCELL Technologies, Vancouver, Canada), respectively, according to the manufacturer's protocols. The efficacy of the isolation was over 90%.

$CD8^+$ Cells Proliferation Assay

$CD8^+$ cells isolated from spleens were incubated with CellTrace™ Violet Cell Proliferation kit (CT) (Invitrogen/Thermo Fisher Scientific, Waltham, MA, USA) for 20 min at 37°C, washed with cell culture medium and seeded onto 96-well U-bottom plates coated with anti-CD3 antibody (eBioscience, San Diego, CA, USA) together with sorted Tregs-GFP (either all GFP^+ or GFP^+ $CD69^{high}$ $CD44^{-/low}$) in various ratios (1:0.125, 1:0.25, 1:0.5, 1:1 and 1:2). For stimulation, anti-CD28 (eBioscience, San Diego, CA, USA) antibody was added to the culture medium. The proliferation of $CD8^+$ cells was evaluated upon 72h using BD FACSCanto™ II Flow Cytometer and BD FACSDiva Software (v8.0.1) (BD Biosciences, La Jolla, CA, USA).

TCL1 OVA-Expressing Cells

The sequence encoding ovalbumin (Addgene, cat. number 25097) was inserted into mammalian expression vector pCDH-EF1-MCS-T2A-copGFP (System Biosciences). The pCDH-EF1-OVA-GFP and a packaging (psPAX2) and an envelope (pMD2.G) plasmids (gifts from prof. Didier Trono, École Polytechnique Fédérale de Lausanne, Switzerland) were introduced into HEK-293T cells using Polyethylenimine (Polysciences). Then freshly isolated TCL1 cells ($CD5^+CD19^+$) from mouse spleens were seeded into 24-well plates with M2-10B4 murine stroma cells. Next, medium containing lentiviral particles was added into TCL1 and M2-10B4 cells co-culture. Then TCL1 cells were washed and inoculated into RAG2-KO mice for leukemic cells propagation. Finally, OVA^+ GFP^+ cells were sorted and used for further experiments. In all performed experiments at least 60% of injected leukemic cells exerted OVA^+ GFP^+ phenotype as evaluated by flow cytometry.

In Vivo Functional Assays

Two weeks following TCL1 cells adoptive transfer, leukemia-bearing DEREG transgenic mice were treated with DT and on the following day, injected with CT-positive $CD8^+$ T cells isolated from spleens and lymph nodes of OT-1 mice. 4-5 hours later, the mice were i.v. inoculated with OVA protein (50 μg). The proliferation of $CD8^+$ OT-1 cells isolated from spleens was assessed upon 3 days using flow cytometry. In the second approach, DEREG mice were injected with genetically modified TCL1 leukemic cells expressing OVA-GFP (TCL1-OVA). Three days later, the mice were treated with DT and on the following day, injected with CT-positive $CD8^+$ OT-1 T cells. The proliferation of $CD8^+$ OT-1 cells was evaluated following 3 or 4 days using flow cytometry. The schemes of described experiments are presented in detail on appropriate figures.

Flow Cytometry

The isolated cells were stained with Zombie NIR™ Fixable Viability kit or Zombie Violet™ Fixable Viability Kit (BioLegend, San Diego, CA, USA) for 20 min at room temperature (RT) and washed with PBS. Next, the cells were incubated with Purified Rat Anti-Mouse CD16/CD32 (Mouse BD Fc Block™; clone 2.4G2, BD Biosciences, La Jolla, CA, USA) for 15 min at RT and stained for surface markers with proper fluorochrome-conjugated antibodies (all antibodies used in this study are listed in **Supplementary Table 1**) for 20-30 min at RT. After final washing with PBS, the cells were analysed using BD FACS Canto™ II Flow Cytometer and BD FACS Diva Software (v8.0.1)(BD Biosciences, La Jolla, CA, USA). For further analyses, including t-SNE (with markers: CD44, CD25, LAG-3, CD69), FlowJo Software (v. 10.6.1) (FlowJo LLC, Ashland, OR, USA) was used.

Cell Sorting

In order to sort Tregs ($CD4^+$, GFP^+) from spleens of B6 $Foxp3^{EGFP}$ or DEREG mice, $CD4^+$ cell subpopulation was enriched prior to sorting. To this end, isolated splenocytes were subjected to immunomagnetic positive selection for $CD19^+$ using EasySep™ Mouse CD19 Positive Selection Kit II (STEMCELL Technologies) and then the negative fraction was subsequently subjected to negative selection using EasySep™ Mouse $CD4^+$ T cell Isolation Kit (STEMCELL Technologies). When needed, $CD4^+$ cells were additionally stained with anti-CD69-PE and anti-CD44-PE-Cy7 monoclonal antibodies as described above. To sort $CD8^+$ cells, the fraction of splenocytes devoid of $CD19^+$ cells was stained with anti-CD8a-PerCP-Cy5.5 monoclonal antibody. Then the cells were sorted using BD FACS Aria™ III Cell Sorter (BD Biosciences).

DNA Isolation and Analysis of TCRβ Repertoire

Tregs A (GFP^+, $CD69^{high}$, $CD44^{-/low}$, gated as presented in **Figure 5** CD69/CD44 right panel) and $CD8^+$ cells were sorted as described above. Then the genomic DNA was isolated from the sorted cells using DNA Micro Kit (QIAGEN, Hilden, Germany) according to the manufacturer's instructions. The concentration and purity of extracted DNA was assessed using NanoDrop 2000 Spectrophotometer (Thermo Fisher Scientific). Immunosequencing of the CDR3 regions of TCRβ chains was performed with immunoSEQ® Assay and analysed by immunoSEQ® Analyzer (Adaptive Biotechnologies, Seatlle, WA, USA).

RNA Sequencing

When percentage of leukemic cells in mouse blood reached at least 20% of all PBMC, the GFP$^+$ Tregs: A (GFP$^+$, CD69^{high}, CD44$^{-/low}$) and B (GFP$^+$ excluding fraction A) were sorted from TCL1 leukemia-injected DEREG mice. Additionally, GFP$^+$ Tregs were also sorted from control DEREG mice. The mRNA was isolated from 4.5×10^5 cells with the RNeasy Micro Kit (Qiagen, Hilden, Germany). Libraries were prepared with the QuantSeq 3' mRNA-Seq Library Prep Kit FWD for Illumina (Lexogen), according to manufacturer's instructions, with the addition of UMI. Barcoded samples were pooled, diluted, loaded onto a NextSeq 500/550 Mid Output flowcell (130M reads, Illumina) and single-end 150bp sequencing was performed on a NextSeq 550 (Illumina).

After initial QCs using FastQC (https://www.bioinformatics.babraham.ac.uk/projects/fastqc/) and FastQ Screen (https://www.bioinformatics.babraham.ac.uk/projects/fastq_screen/), fastq files were processed using a local Snakemake workflow including the following main steps. First, raw reads were trimmed from their UMI index, poly A and adapter sequences using a combination of dedicated scripts and cutadapt (v2.10). Next, filtered reads were submitted for mapping (STAR v2.5.3a) on the Mouse Reference genome (GRCm38). Collapsing of reads originating from the same fragment was achieved with umi_tools (v 1.0.0) and counting was performed with featureCounts (subread v2.0.0).

Counts were filtered and transformed with edgeR (cpm > 5 and presence in at least 3 samples). For data visualization, heatmaps, sample distance matrix, and volcano plots were drawn with EdgeR, heatmap, and EnhancedVolcano R packages. For differential expression of genes across samples (DEGs), FDR < 0.05 and log2 fold change cut-off of 1 were imposed. For clustering, DEGs were selected as important for immune functions in Tregs. Gene expression values were z-scored and subjected to correlation-based clustering with complete linkage. Raw and processed data were deposited at the NCBI GEO database (GSE179121). The following secure token has been created to allow review of record GSE179121 while it remains in private status: qlchuysazpinjed. To better understand the nature of Tregs A and Tregs B, we re-analyzed the public dataset GSE72494 describing the transcriptome of naive, activated, and effector Treg (23) and performed a Gene Set Enrichment Analysis (GSEA, Hallmark and curated gene sets) with the stand-alone software (GSEA v4.2.1, Broad Institute, Boston, MA). Normalized enrichment scores (NES) and p-values < 0.05 were taken into consideration.

Statistical Analysis

GraphPad Prism 6 Software (GraphPad Software Inc., San Diego, CA, USA) was used for data analysis. The statistical significance was calculated by Mann-Whitney U test. The mice survival rate was analyzed by log-rank survival test. For gene expression data (RNA sequencing), one-way ANOVA with multiple comparisons was calculated for single genes and histograms were drawn with GraphPad Prism 9 Software.

Additional experimental procedures are described in details in the **Supplementary Material**.

RESULTS

Depletion of Tregs in Mice With Adoptively Transferred TCL1 Leukemia Results in the Expansion of Functional CD8$^+$ Cells and Leukemia Clearance

To evaluate the significance of Tregs for CLL progression we used DEREG transgenic mice with depletion of FoxP3$^+$ CD4$^+$ Tregs by treatment with diphtheria toxin (DT) (**Figure 1** and **Supplementary Figure 1A, B**). DEREG mice were treated with DT one day prior to adoptive transfer of malignant (CD5$^+$CD19$^+$) B cells, isolated from an Eμ-TCL1 transgenic mouse. Effective depletion of Tregs was observed in spleens and peripheral blood of DEREG mice and was maintained by additional DT injections every four days (**Figure 1A** and **Supplementary Figure 1A**). As monitored in peripheral blood twice a week, injection of DT did not affect the progression of leukemia during the first fifteen days of experiments. However, starting from day 18th after TCL1 leukemia inoculation, we detected a significant decrease in the percentage of leukemic cells (CD5$^+$CD19$^+$), in the peripheral blood, of DT-treated mice as compared to untreated TCL1 leukemia-bearing animals (**Figure 1B**, left panel). In line with these results, we observed a significant reduction of previously established leukemia in the spleens of Tregs-depleted mice (**Figure 1B**, right panel). The same observations were made when DEREG mice were injected with TCL1 leukemia isolated from another transgenic mouse (**Supplementary Figure 1B**). The decrease in the percentage of leukemic cells in spleens of DT-treated mice was accompanied by the extensive increase of the percentage in both CD4$^+$ and CD8$^+$ T lymphocytes (**Figure 1C**). These observations prompted us to investigate the putative changes in the phenotype of splenic CD4$^+$ and CD8$^+$ T cells mediated by Tregs-depletion. We observed the enrichment of effector (EFF; CD44$^+$CD62L$^-$) and central memory (CM; CD44$^+$CD62L$^+$) cells in both CD4$^+$ and CD8$^+$ T cell subpopulations in mice deprived of Tregs (**Figures 1D, E**). A significant increase in the percentage of effector (CD4$^+$ and CD8$^+$) and central memory (CD8$^+$) T cells was also observed in lymph nodes (axillary, brachial, inguinal) of DT-treated mice (**Figure 1F**). Depletion of Tregs resulted in the elevation of CD69 on both, CD4$^+$ and CD8$^+$ T cells in the lymph nodes, and reduced the percentage of naïve cells, suggesting the activation of a systemic immune response. Nevertheless, the depletion of Tregs, performed at an advanced stage of the disease (first dose of DT was administered when 30% of malignant B cells were detected among all white blood cells in peripheral blood) did not affect the progression of leukemia (**Supplementary Figure 1C**). Tregs depletion at an advanced stage of leukemia progression increased the percentage of effector and IFN-γ-positive CD4$^+$ and CD8$^+$ T lymphocytes, significantly elevated IFN-γ concentration and reduced the concentration of IL-10 in the sera (**Supplementary Figure 1D, E**). Importantly, three weeks of DT injections of control (without leukemia) DEREG mice lead to a minor activation of T cells, mostly CD4$^+$ T cell subpopulation (**Supplementary Figure 1F**, upper panel). However, no changes were observed in the level of CD69 in lymphatic T cells upon

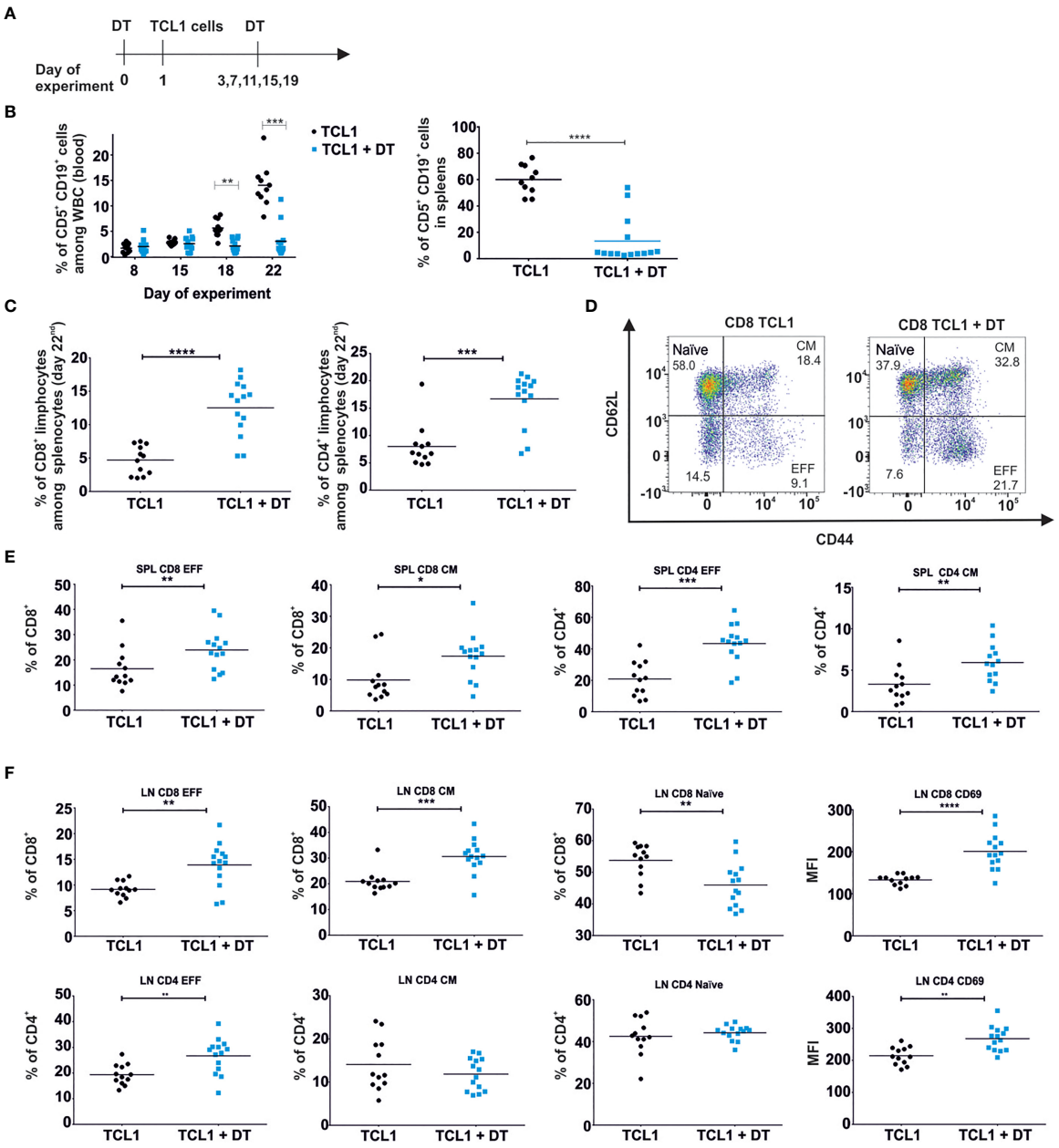

FIGURE 1 | Depletion of Tregs diminishes the progression of leukemia in DEREG mice and affects the relative frequency of conventional T cell subpopulations. **(A)** The graph presenting a scheme of the experiment. Tregs were depleted with DT and on the next day mice were injected with TCL1 CD19$^+$ leukemic cells. The depletion of Tregs (DT administration) was repeated every 4 days. **(B)** The percentage of leukemic cells (CD5$^+$CD19$^+$) among all white blood cells (WBC) assessed by flow cytometry in blood (at indicated time points of the experiment, left) and spleens (day 22nd of experiment, right) of untreated (TCL1) and DT-treated (TCL1+DT) TCL1 leukemia-bearing mice. The graphs represent mean results from two independent experiments. Each dot represents an individual sample (mouse), n = 10-12, Mann-Whitney U test *p ≤ 0.05. **(C)** The Percentage of CD8$^+$ (left) and CD4$^+$ (right) T cells in spleens of untreated and DT-treated TCL1 leukemia-bearing mice. The graphs present mean results from two independent experiments. Each dot represents an individual sample (mouse), n = 12-14, Mann-Whitney U test ***p ≤ 0.001, ****p < 0.0001. **(D–F)** The percentage of CD4$^+$ and CD8$^+$ T cells with phenotype of naïve, effector (EFF) and central memory (CM) subpopulations according to the expression of CD44 and CD62L surface markers. Representative dot plots with a gating strategy **(D)** and the graphs present the results from spleens (SPL) **(E)** and lymph nodes (LN) **(F)** of untreated and DT-treated TCL1 leukemia-bearing mice. In **(F)** the graphs presenting the expression of CD69 surface marker on CD4$^+$ and CD8$^+$ T cells in LN are also shown. The data from two independent experiments are showing mean values. Each dot represents an individual sample (mouse), n = 12-14, Mann-Whitney U test *p ≤ 0.05, **p ≤ 0.01, ***p ≤ 0.001, ****p < 0.0001.

DT-treatment (**Supplementary Figure 1F**, lower panel). The activation of $CD4^+$ T cells may be the result of anti-DT immune response as it was described before (24).

To understand more deeply the anti-leukemia immune response induced by Tregs depletion, we investigated the impact of $CD8^+$ T lymphocytes derived from the mice after DT injections on leukemia progression. We limited these experiments to the subset of $CD8^+$ T cells as it was shown that these cells play a superior role in anti-leukemia immune response over $CD4^+$ T lymphocytes (25). Importantly, an effective Tregs depletion in DEREG mice is transient. At day 22 after TCL1 injection we observed that the Tregs population was restored in murine blood despite continuous injections of DT (**Supplementary Figure 1A**, right panel), as was also reported by others (26). Thus, to examine the impact of the $CD8^+$ lymphocytes on leukemia progression and mice survival, the cells were isolated from spleens of untreated or DT-treated TCL1 leukemia-bearing mice (the same scheme of experiment as shown in **Figure 1A**), and adoptively transferred into TCL1-injected RAG2-KO mice (**Figure 2A**). Next, the expansion of TCL1 leukemic cells was monitored in murine blood twice a week. Interestingly, $CD8^+$ T lymphocytes, isolated from Tregs-depleted mice effectively prevented leukemia progression, and in some mice even lead to complete elimination of TCL1 cells (**Figures 2B, C**). In contrast, the $CD8^+$ T lymphocytes adoptively transferred from mice with intact Tregs population did not significantly affect the progression of the disease in RAG2-KO mice. Consequently, in TCL1-injected RAG2-KO mice, the adoptive transfer of $CD8^+$ T cells isolated from DEREG mice after Tregs depletion, translated into prolonged survival and complete leukemia eradication in three out of nine mice. (**Figure 2D**).

The results obtained from the experiments described above revealed that the lack of Tregs in the leukemia microenvironment triggers the expansion of anti-leukemic $CD8^+$ T cells. To address the differences in the investigated T cells, the $CD8^+$ T cells from spleens of TCL1-injected DEREG mice treated with DT or untreated were sorted for DNA isolation and the T cell receptor beta chain (TCRβ) third complementarity-determining regions (CDR3) sequences analysis. An increase of $CD8^+$ T cell clonality was observed in three out of five TCL1 leukemia-bearing mice with Tregs depletion, but overall, the observed differences were not statistically significant between the two examined groups (**Figure 2E**). Strikingly though, we observed distinct amino acid sequences of TCRβ CDR3 regions in the tested $CD8^+$ T cells, suggesting different specificity of the T cells among untreated and DT-treated mice (**Figure 2F**). Indeed, only one sequence is shared in the top fifteen rearrangements between both analyzed $CD8^+$ T cell populations (**Figure 2F**). Altogether, these data indicate that the elimination of Tregs from the TCL1 leukemia microenvironment resulted in the expansion of a distinct set of cytotoxic $CD8^+$ T effector cells, capable of clearing leukemia in DEREG and RAG2-KO mice.

CLL Leads to the Formation of a Specific Population of Tregs

We analyzed the phenotype and function of Tregs in TCL1-injected B6 $FoxP3^{EGFP}$ transgenic mice that express *EGFP* and *FOXP3* under the control of endogenous promoter. Based on the results of phenotyping with a set of markers (FoxP3, LAG-3, CD69, CD44, CD25), we performed t-distributed stochastic neighbor embedding (tSNE) analysis, which allowed us to distinguish a specific Tregs subpopulation that exerts the phenotype characteristic only for Tregs isolated from TCL1 leukemia-bearing mice (Tregs A) (**Figure 3A**). This particular Tregs A subpopulation can be defined by high level of CD69, LAG-3 and low of CD44 and CD25 on their surface.

In order to investigate whether the observed changes in Tregs phenotype are mediated by the interactions with malignant B cells, we co-cultured the control Tregs-GFP^+ (sorted from spleens of control B6 $Foxp3^{EGFP}$ mice) with leukemic (TCL1) or normal (CD19) B cells. After three days, significantly higher level of LAG-3 was observed on Tregs-GFP^+ co-cultured with TCL1 cells, but not with the control $CD19^+$ cells (**Supplementary Figure 2A**). The elevated expression of LAG-3 was achieved only when Tregs-GFP+ and TCL1 leukemia cells were cultured in direct contact. On contrary, the level of CD44 in Tregs-GFP^+ co-cultured with TCL1 leukemia cells (but not normal $CD19^+$ cells) was reduced regardless the separation of the cells by transwells (**Supplementary Figure 2B**).

Next, the clonality of Tregs A subpopulation was examined, based on the TCRβ CDR3 region sequences. Importantly, the TCL1-associated Tregs A subpopulation sorted from spleens of TCL1-leukemia bearing DEREG mice exhibits increased clonality and elevated frequency of particular clones, compared to whole Treg-GFP^+ subpopulation sorted from the control animals (CTR Tregs) (**Figures 3B, C**).

Finally, in order to characterize the TCL1-associated Tregs at the transcriptomic level, we performed RNA sequencing on two subpopulations of Tregs sorted from the spleens of TCL1-injected DEREG mice: Tregs A (specific to Eμ-TCL1 model, sorted as GFP^+ $CD44^{-/lo}$ and $CD69^{hi}$) and Tregs B (the remaining GFP^+ Tregs, which did not meet the criteria of subpopulation A). The transcriptome of both TCL1-associated subpopulations was compared with Tregs-GFP^+ population sorted from spleens of control mice. Interestingly, the analysis of differentially expressed genes (DEGs), showed that Tregs A subpopulation was markedly different from both Tregs B as well as control Tregs populations (**Supplementary Figure 3, 4**). This data suggests that the specific Tregs A cells signature might be selectively induced within the conditions of leukemia progression. In Tregs A, we observed increased expression of genes responsible for immunosuppressive activity (*Gzmb, Prf1, Gzmk, Il10*), checkpoints (*Havcr 2, Lag-3, Tigit*), chemokines that may support leukemia progression and its microenvironment (*Ccl3, Csf1, Ccl5*), as well as genes that have been recently reported as unique for CLL-Tregs (*EOMES*) (**Figure 3D**). Importantly, the gene expression profile was in line with the phenotype observed in flow cytometry, apart from CD69, which seemed to be regulated post-transcriptionally (**Figure 3E**). Additionally, the elevated level of *Ikzf2* encoding Helios transcription factor suggests enhanced suppressive capacity of Tregs A subpopulation (27).

Next, we compared the gene expression profiles of Tregs A and B with a public dataset [GSE72494 (23)] describing the transcription profiles of naive, activated, and effector Tregs. We used a gene signature reported in that study (23), and built heat maps to

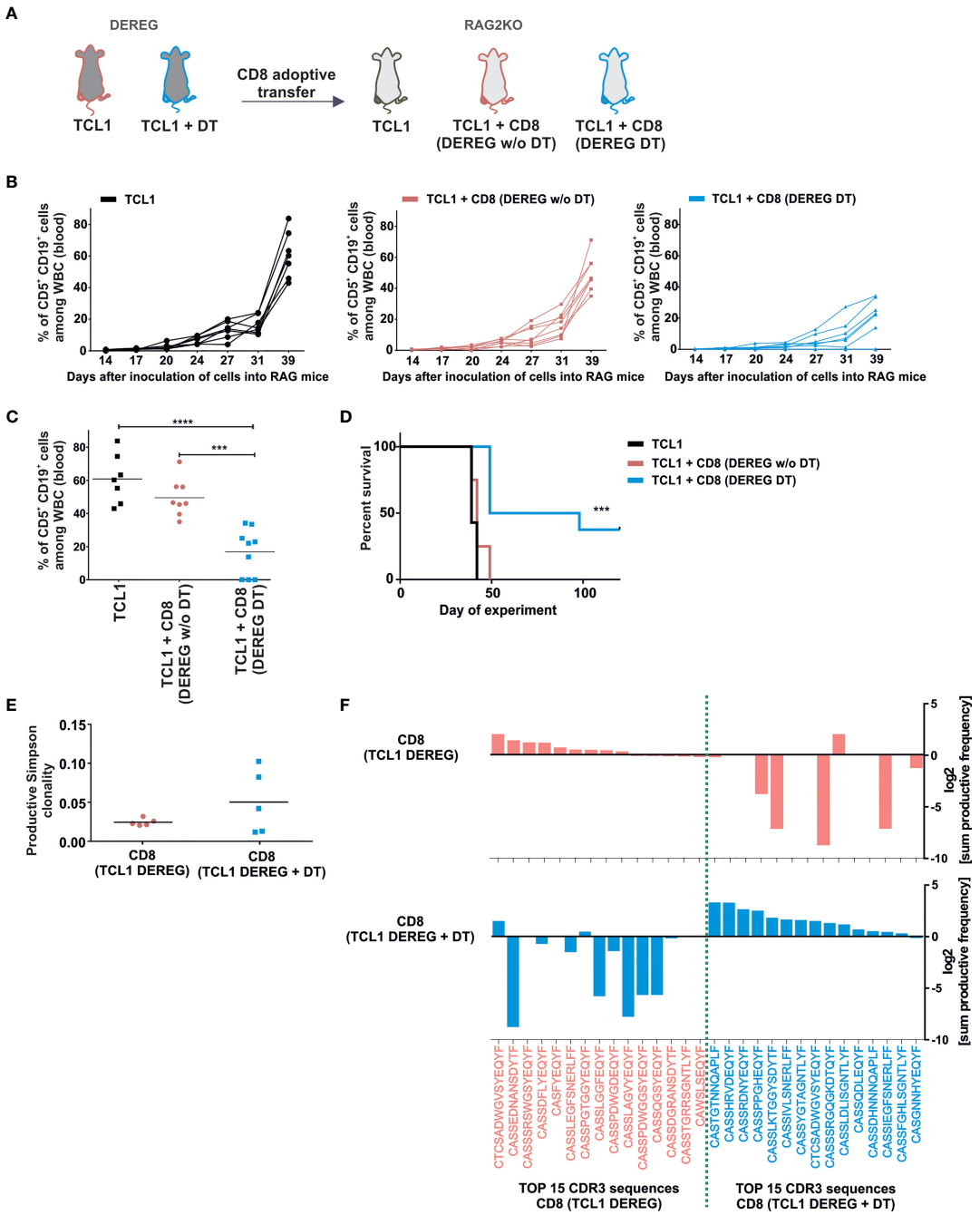

FIGURE 2 | Depletion of Tregs in TCL1 leukemia-bearing DEREG mice results in the expansion of CD8+ lymphocytes capable of eradicating leukemic cells. **(A)** The graph presenting a scheme of the experiment. DEREG mice were treated according to scheme from Fig1A. Then 5 x 10^6 of splenic $CD8^+$ T cells isolated with magnetic beads from untreated (DEREG w/o DT) or DT-treated (DEREG DT) leukemic DEREG mice were injected to RAG2-KO mice following the injection of TCL1 ($CD5^+CD19^+$) cells. **(B, C)** The percentage of leukemic cells ($CD5^+CD19^+$) assessed at indicated time points in the peripheral blood of RAG2-KO mice: TCL1 leukemia-injected mice (black lines), TCL1- and $CD8^+$-injected mice ($CD8^+$ isolated from TCL1 leukemia bearing-DEREG w/o DT, pink lines), and TCL1- and $CD8^+$-injected mice ($CD8^+$ isolated from leukemia-bearing DEREG treated with DT, blue lines). Each line represents an individual sample (mouse), **(B)** and on day 39^{th} **(C)**, each dot represents an individual sample (mouse). The graphs represent mean results from two independent experiments, n = 7-9, Mann-Whitney U test ***$p \leq 0.001$, ****$p < 0.0001$. **(D)** The survival plot summarizing the results from two independent experiments, n = 7-9, log-rank survival test ***$p \leq 0.001$. **(E)** The productive Simpson clonality of $CD8^+$ lymphocytes sorted from untreated or DT-treated mice analyzed in immunoSEQ Analyzer (from Adaptive Biotechnologies), n = 5. **(F)** The top 15 amino acid sequences of CDR3 TCRβ with the highest sum frequency (total amount of clones with a given sequence in all tested mice), of $CD8^+$ lymphocytes sorted from untreated (pink) or DT-treated TCL1 leukemia-bearing DEREG mice (blue). The Graphs present log2 transformation of % sum frequency of a given sequence in untreated (pink, upper graph) and DT- treated TCL1- injected DEREG mice (blue, lower graph), n = 5.

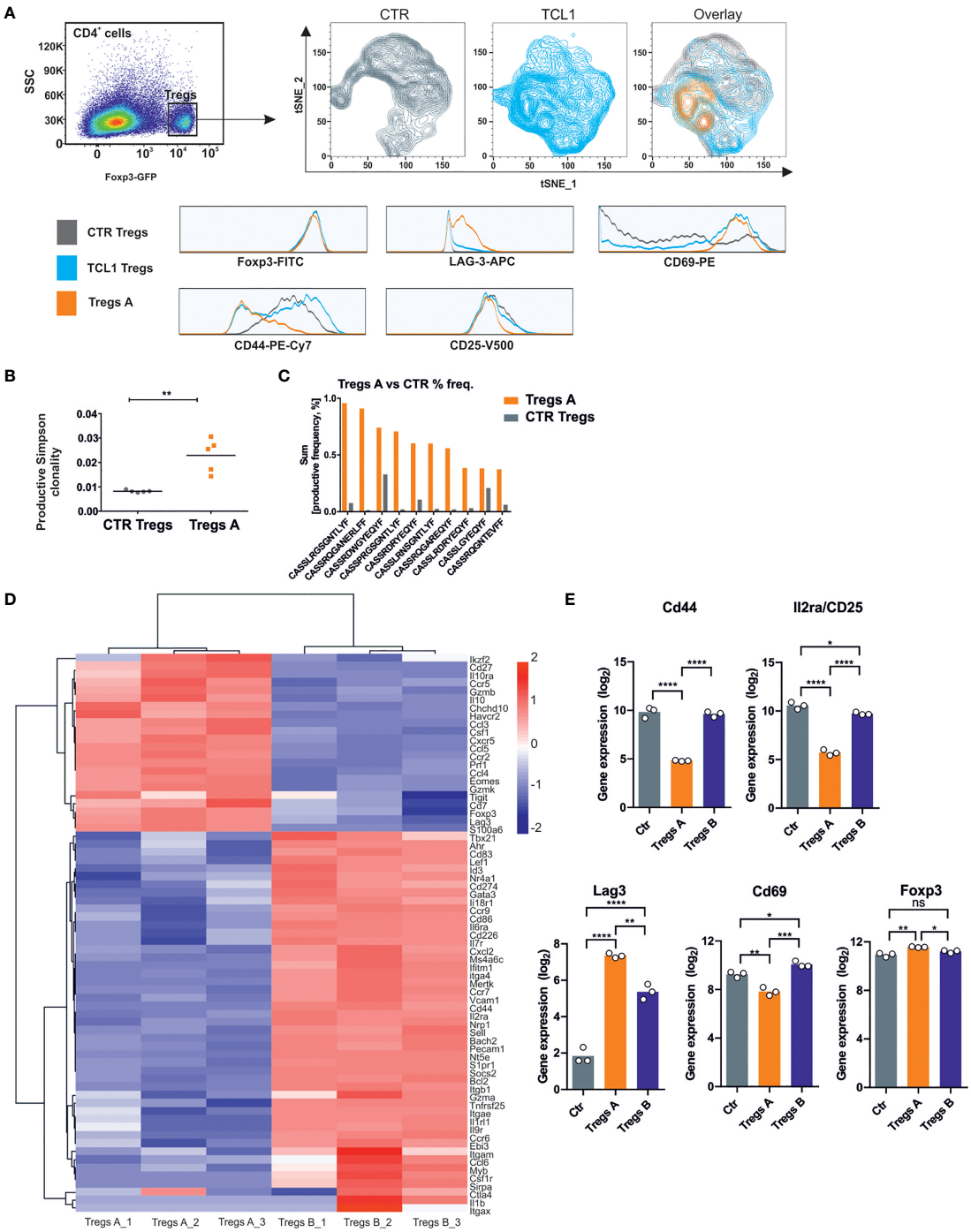

FIGURE 3 | A specific Tregs population is formed during the progression of TCL1 leukemia. **(A)** tSNE analysis of Tregs phenotype isolated from control (grey) and TCL1 leukemia-bearing (blue) B6 Foxp3^{EGFP} mice 14 days after injections with leukemic cells. The overlay of counterplots presents the Tregs subpopulation, specific for TCL1 leukemia-bearing mice (Tregs A, orange). The Tregs GFP^{+}-were plot on the graphs according to the expression of CD44, CD69, CD25, and LAG-3 that are presented on the histograms. The counter plots show representative analysis of Tregs from 2 control and 4 TCL1 leukemia-injected mice. **(B)** The productive Simpson clonality of Tregs sorted from control (all Tregs, CTR Tregs) and TCL1 leukemia-bearing (the specific TCL1-associated Tregs subpopulation, Tregs A) DEREG mice, n = 5. **(C)** The productive sum frequency of top 10 amino acid sequences of CDR3 TCRβ of Tregs A which were present in all of tested TCL1 leukemia-bearing DEREG mice, n = 5. **(D)** Clustering of selected DEGs between Tregs A and Tregs B (RNA sequencing with FDR < 0.05 and $\log_2$FC > 1) by correlation with complete linkage, n = 3. **(E)** Gene expression (log2, RNA sequencing) of genes from panel A in Tregs from CTR and TCL1 leukemia-bearing mice, n = 3. One-way ANOVA * p≤ 0.05, ** p< 0.01, *** p< 0.001.

compare Tregs subsets. The gene expression profiles indicated that our Ctrl Tregs population resembles naive Tregs and that Treg A and Tregs B exert similar expression patterns to effector Tregs and activated Tregs, respectively (**Supplementary Figure 4C**). Similar gene sets were identified as enriched in Tregs A (vs Treg B) and Effector Tregs (vs Activated Treg) (**Supplementary Tables 2** and **3**). Although Tregs A exhibited comparable transcription changes as compared to Effector Tregs (up-regulation of *Il10* and *Havcr2/Tim3* and down-regulation of *Sell* and *Ccr7*), we identified important differences suggesting a particular gene modulation in this specific Tregs population found in CLL (e.g. *Eomes, Prf1, Itgae, Cxcl10*) (**Supplementary Figure 4D**).

The TCL1-Induced Tregs Are Functionally Active

Next, we determined the ability of splenic Tregs population, sorted from control and TCL1 leukemia-bearing B6 FoxP3^{EGFP} mice to inhibit CD8$^+$ T cell proliferation in an antigen unspecific test, where T cells were activated *via* anti-CD3 and anti-CD28 antibodies. The obtained results indicated that whole Tregs population isolated from spleens of TCL1 leukemia-bearing mice is prone to inhibit CD8$^+$ T cells proliferation similarly to control Tregs (**Figure 4A**). Similarly, in a test with OVA peptide presented by the bone marrow-derived dendritic cells, Tregs isolated from leukemic mice inhibited CD8$^+$ OT1 cells proliferation as effectively as Tregs from control mice (**Supplementary Figure 5**). This data suggest that the effectiveness of antigen-independent suppression of Tregs from TCL leukemia-baring mice is similar to control Tregs.

In order to explore whether TCL1-associated Tregs suppress CD8$^+$ T cells in an antigen specific manner, we generated OVA-expressing TCL1 by means of lentiviral transduction. DEREG mice were inoculated with TCL1-OVA cells, and 3 days later, Tregs were depleted with DT in one group. On the following day, mice were injected with Cell Trace (CT)-positive OT1 CD8$^+$ T cells and the proliferation of these cells in the spleen was subsequently analyzed (**Figures 4B–D**). Interestingly, although the T cells were effectively activated in all tested TCL1 leukemia-bearing mice, in the group treated with DT, the proliferation was more efficient, suggesting that the Tregs population impeded OT1 CD8$^+$ T cells proliferation to some extent. Moreover, a significant drop in the percentage of leukemic cells in blood and spleens of DT-treated mice was observed after injection of OT1 CD8$^+$ T lymphocytes (**Figure 4B**). Conversely, when mice were inoculated with TCL1 cells (without OVA expression) and subsequently injected with OVA protein, no impact of Tregs depletion was observed on OT1 CD8$^+$ T cells proliferation (**Figure 4C**). Altogether, these results suggest that Tregs inhibit proliferation of leukemia-specific CD8$^+$ T cells in an antigen-dependent manner.

Treatment With MALT1 Inhibitor Disturbs the Formation of Tregs A Subpopulation in TCL1 Leukemia-Bearing Mice and Enhances the Effect of Immunotherapy

The analysis of Tregs phenotype at the various stages of leukemia revealed significant changes in the expression levels of Tregs surface proteins. The shift of Tregs into Tregs A phenotype escalated during leukemia progression and was accompanied by an increase in the percentage of splenic Tregs in leukemic mice (**Figure 5A**). Importantly, the Tregs A subpopulation was clearly formed at an advanced stage of the disease (when more than 40% of leukemic cells among all white blood cells were present in the spleens).

MI-2 has been described as a para-caspase MALT1 inhibitor that can selectively prevent the conversion of naïve Tregs into effector cells by decreasing the NFκB activity (21). MI-2 revealed its cytotoxic effect on primary CLL cells *in vitro* (28). Moreover, RNA sequencing analysis indicated elevated expression of NFκB-related genes in Tregs of TCL1-injected mice (**Supplementary Figure 4B**). In order to verify the influence of MI-2 on development of Tregs subpopulations, the inhibitor was administered intraperitoneally to the control and TCL1 leukemia-bearing B6 FoxP3^{EGFP} mice for two weeks starting from day 5 following TCL1 leukemic cells inoculation (**Figure 5B**). Administration of MI-2 impeded the change of Tregs into Tregs A phenotype and elevated the percentage of naïve Tregs (CD62L$^+$ CD44$^-$) (**Figure 5C**). MI-2 inhibited the progression of leukemia and increased significantly the percentage of central memory and effector CD4$^+$ and CD8$^+$ T lymphocytes (**Figures 5C–E**). Importantly, the effectiveness of MI-2 treatment was impaired in TCL1 leukemia-bearing RAG2-KO mice as compared to immunocompetent, wild type mice, suggesting a key role of T cells in the mechanism of action of this drug (**Supplementary Figures 6A, B**).

Since the PD1/PD-L1 axis was already shown to contribute to T cells dysregulations in both human and mouse models of CLL, we used MI-2 therapy as a pretreatment for checkpoint blockade with anti-PD-L1 antibody in immunocompetent TCL1-leukemia bearing mice (6, 29). Considering that long-term inhibition of Tregs functions can lead to autoimmune pathology (30), MI-2 inhibitor was used only before anti-PD-L1 therapy (**Figure 6A**). The anti-PD-L1 therapy did not affect the percentage of T cells already elevated by MI-2 (**Figure 6B**). However, the combined treatment decreased the percentage of naive cells and increased the percentage of effector cells of both CD4$^+$ and CD8$^+$ T lymphocytes (**Figure 6B**) Anti-PD-L1 antibodies administered 16 days post TCL1 inoculation decreased the percentage of leukemic cells in blood and spleen when applied after treatment with MI-2 (**Figure 6C**). These results indicate that the combination of Tregs inhibition with anti-PD-L1 antibody can bring beneficial treatment outcome in leukemia.

DISCUSSION

The anti-tumor strategy reducing the number of Tregs has been reported since 1999 (31). Nevertheless, targeting Tregs can yield differential responses in cancer models (32). In this study, we revealed that in the CLL mouse model, the depletion of Tregs population can lead to the expansion of CD8$^+$ T cells with the ability to completely eradicate leukemia.

Published studies have consistently demonstrated elevated levels of Tregs in the peripheral blood collected from CLL

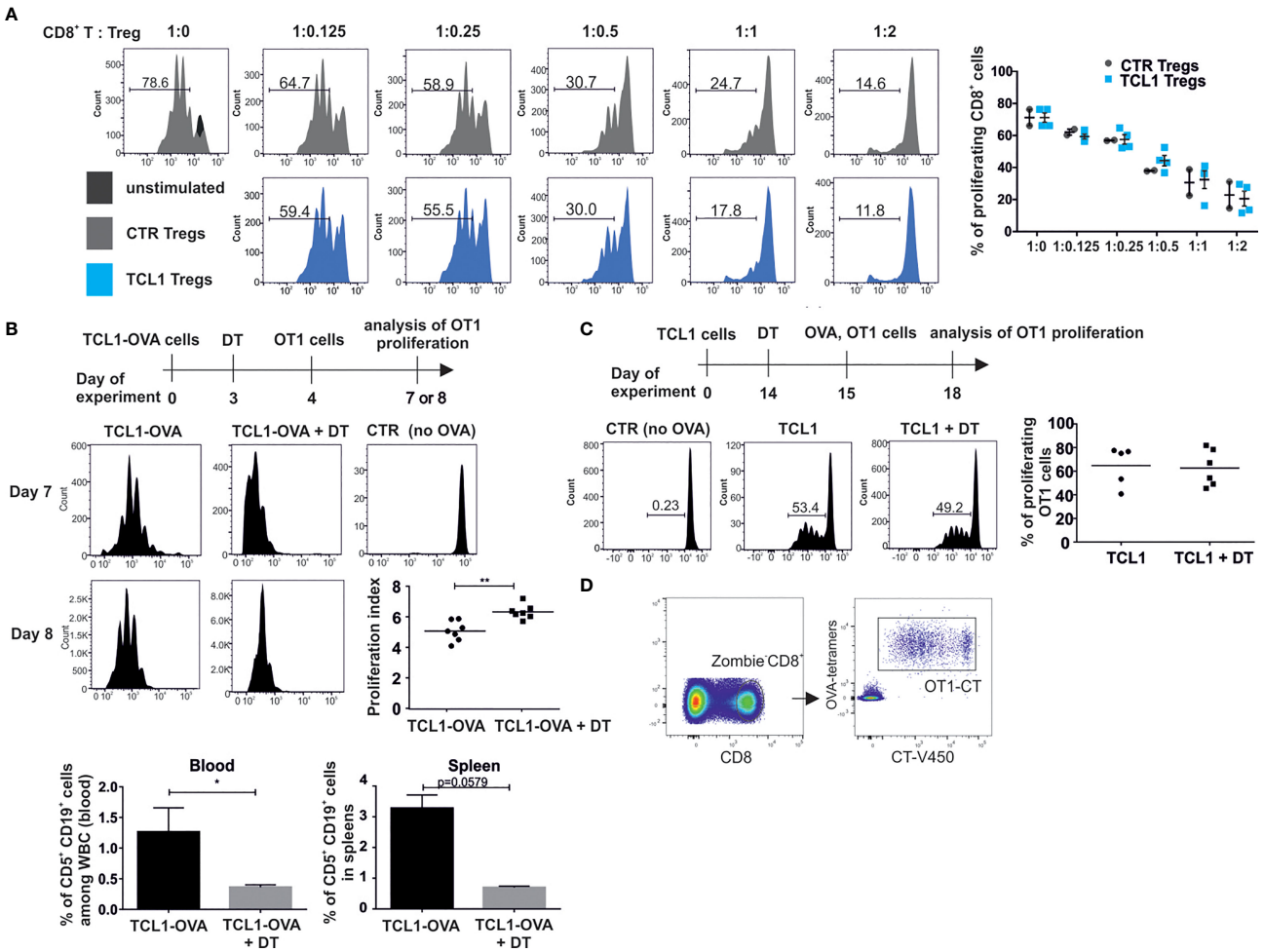

FIGURE 4 | Tregs from TCL1 leukemia-bearing mice are capable of inhibiting T cells proliferation. **(A)** All Tregs-GFP$^+$ sorted from spleens of control (CTR Tregs) and TCL1-injected (TCL1 Tregs) B6-Foxp3^{EGFP} mice, were added to the Cell Trace Violet (CT) stained CD8$^+$ lymphocytes isolated from control mice and activated with αCD3 and αCD28 antibodies. The proliferation of – CT-stained CD8$^+$ T cells was assessed by flow cytometry. Graphs show the results from two independent experiments, mean ± SD, n = 2-4 **(B)** OT1 CD8$^+$ cell proliferation in mice injected with TCL1-OVA cells. After TCL1-OVA cells inoculation the mice were treated with DT and injected with CT-positive OT1 CD8$^+$ lymphocytes (scheme of the experiment, upper panel). The proliferation of OT1 CD8$^+$ cells from untreated or DT-treated mice was evaluated on the same day (7th or 8th). The representative histograms of proliferation measured on days 7th and 8th are shown (left panel) and the proliferation index, from two independent experiments, is shown on the graph (middle right panel), n = 7 **p ≤ 0.01. Proliferation index was calculated by FlowJo software as the total number of divisions divided by the number of cells that went into division. The percentage of leukemic cells was assessed in blood and spleens of DEREG mice on day 8th of the experiment (lower panel), data is presented as mean ± SD, n = 3-4, Mann-Whitney U test * p ≤ 0.05. **(C)** OT1 CD8$^+$ cell proliferation in mice injected with TCL1 cells and vaccinated with OVA protein. The representative histograms (left panel) and graph summarizing the results from two independent experiments (right panel), n = 5-6. **(D)** Gating strategy incorporated for analysis of CT-positive OT1 CD8$^+$ T cells proliferation in functional *in vivo* tests.

patients compared to healthy subjects (33). The phenotype of analyzed Tregs was described as effector-like in both CLL patients and the Eμ-TCL1 mouse model of CLL (5, 16, 18). Our results indicate that the phenotype of Tregs changes during the course of leukemia to establish a subpopulation of CD4$^+$, FoxP3$^+$, LAG-3$^+$, CD69^{hi}, and surprisingly, CD44^{lo} and CD25^{lo} cells. A low expression of CD25 in Tregs has been already reported by another group (34), yet the CD44^{lo} phenotype is rather a characteristic feature of naïve lymphocytes. Our *ex vivo* experiments revealed that the level of cell-surface glycoprotein CD44 decreased in Tregs as a result of leukemia progression. At the transcriptomic level, however, the reduced amount of mRNA for CD44 was seen only in Tregs A, a specific TCL1-associated Tregs subpopulation distinguished for the first time in this study. Interestingly, the Tregs A subpopulation is positive for already reported markers of CLL-related Tregs, including IL-10, LAG-3, granzyme B, EOMES, as well as share a unique gene expression signature of chemokines that may support leukemia progression and formation of leukemic microenvironment (35, 36). Moreover, the overexpression of mRNA encoding HELIOS, TIGIT, TIM-3 and CD27 suggests that TCL1-related Tregs may possess immunosuppressive activity (27, 37–39).

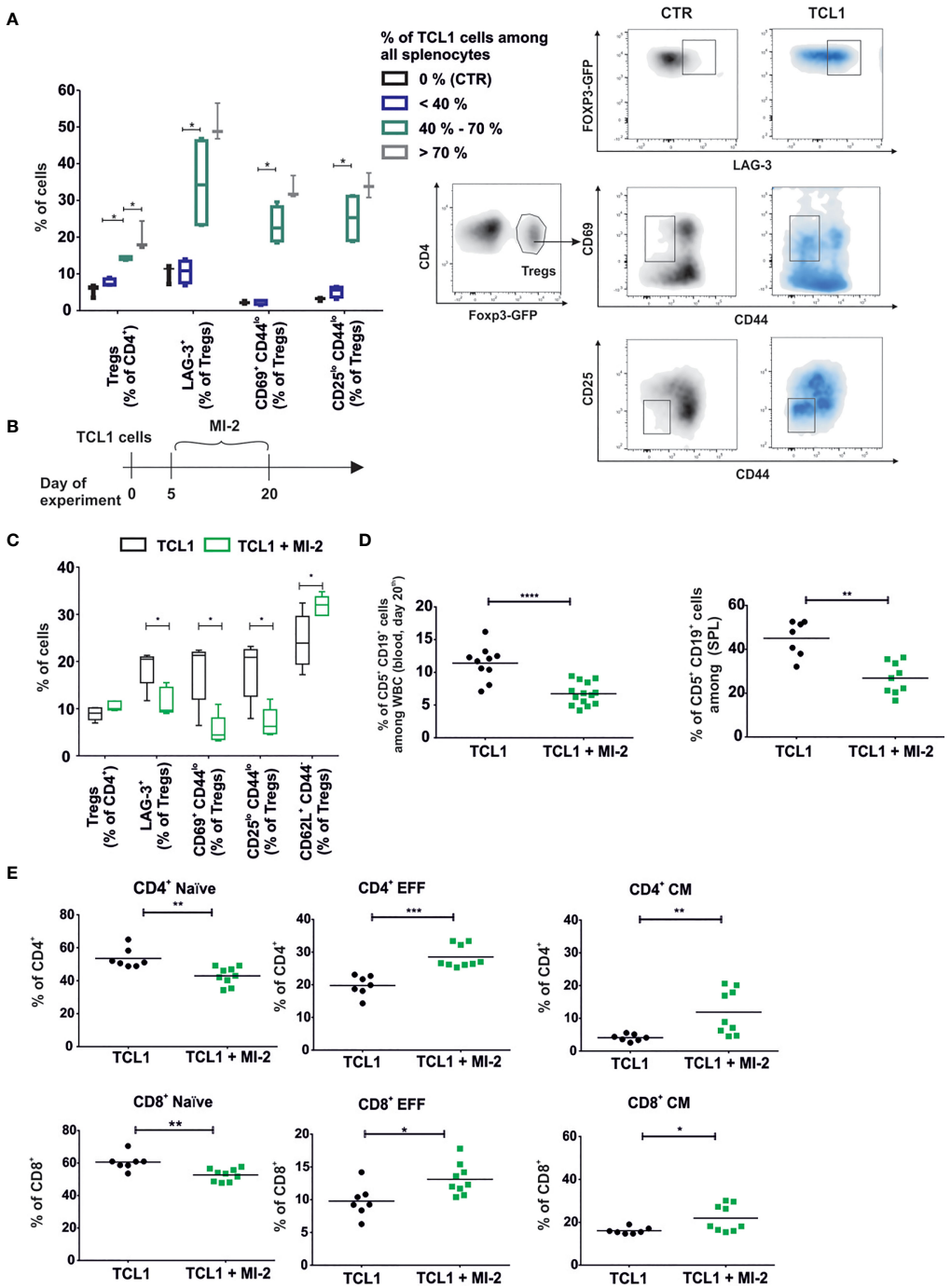

FIGURE 5 | Development of a specific TCL1-related Tregs (Tregs A) population is correlated with the stage of the disease and can be blocked by MALT-1 inhibitor. **(A)** The box plot min-max graph (left panel) and density plots with gating strategy (right panel) present phenotype of Tregs in relation to the percentage of leukemic cells ($CD5^+CD19^+$) in the spleens. Mean ± SD, n=11, Mann-Whitney U test *$p \leq 0.05$. **(B)** The graph presenting a scheme of the experiment. MI-2 was administered daily at dose 20 mg/kg *via* intraperitoneal injections for two weeks. **(C)** The phenotype of Tregs collected from spleens of TCL1 leukemia-bearing B6 $Foxp3^{EGFP}$ mice, untreated (TCL1) or treated with MI-2(TCL1 + MI-2). Mean ± SD, Mann-Whitney U test n = 5, *$p \leq 0.05$. **(D)** Percentage of leukemic cells ($CD5^+CD19^+$) assessed by flow cytometry in blood (left graph) and spleens (right graph) on day 21^{st} of the experiment. The graph presents data from three (blood, n = 10-14) or two (spleens, n = 7-8) independent experiments. Each dot represents an individual sample (mouse), means, Mann-Whitney U test **$p \leq 0.01$, ***$p \leq 0.001$, **** $p < 0.0001$. **(E)** The percent of naïve, effector (EFF), central memory (CM), subpopulations of $CD4^+$ and $CD8^+$ T cells. Cells were collected from spleens of untreated and MI-2-treated TCL1 leukemia-bearing B6 $Foxp3^{EGFP}$ mice in two independent experiments, n = 7-12. Each dot represents an individual sample (mouse), means, Mann-Whitney U test *$p \leq 0.05$, **$p \leq 0.01$, ***$p \leq 0.001$.

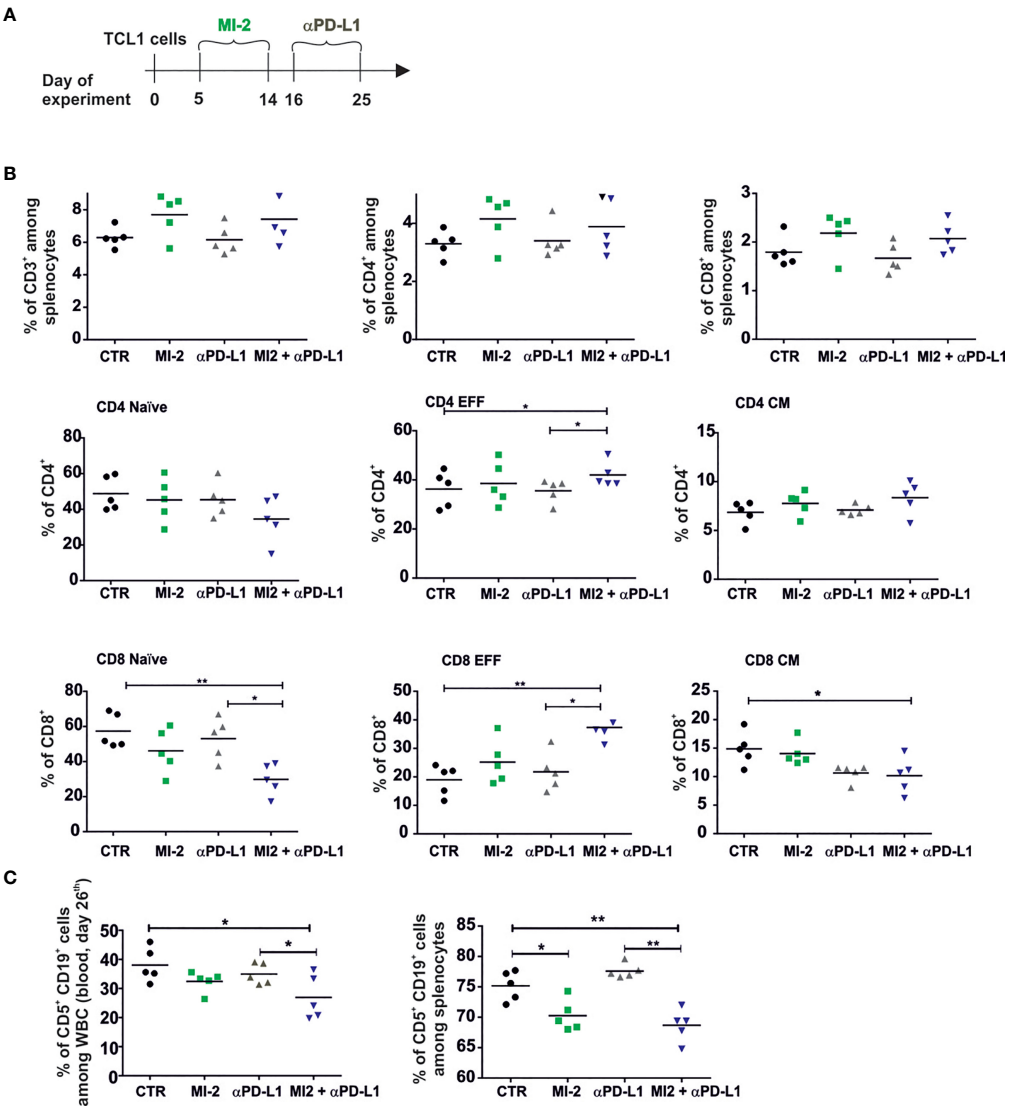

FIGURE 6 | The pretreatment with MALT-1 inhibitor sensitizes leukemia to the therapy with anti-PD-L1 at the advanced stage of the disease. **(A)** The graphs presenting a scheme of the experiment. **(B)** The percentage of $CD3^+$, $CD4^+$, $CD8^+$ and naïve, effector (EFF), and central memory (CM) subpopulations of $CD4^+$ and $CD8^+$. Cells were collected from spleens of untreated (CTR), MI-2 and/or aPD-L1-treated TCL1 leukemia-bearing mice, n = 4-5, each dot represents an individual sample (mouse), means, Mann-Whitney U test *p ≤ 0.05, **p ≤ 0.01. **(C)** The Percentage of leukemic cells ($CD5^+CD19^+$) assessed by flow cytometry in blood (left panel) and spleens (right panel) at day 26th of the experiment, n = 5, each dot represents an individual sample (mouse), means, Mann-Whitney U test *p ≤ 0.05, **p ≤ 0.01.

Importantly, our results prove that the observed change in the Tregs phenotype occurring during the progression of CLL results from the formation of a specific Tregs subpopulation (Tregs A).

Mpakou and colleagues show that Tregs isolated from CLL patients have an ability to inhibit $CD8^+$ T cell proliferation (34). Likewise, according to our results, TCL1-derived Tregs are able to inhibit proliferation of T cells *ex vivo*. In *ex vivo* assays, T cells were activated in unspecific and specific manner, accordingly with the cognate antigen or by OVA peptide presented by dendritic cells thus the observed effect was not related to leukemia-specific antigens. The CLL-related Tregs functionality was finally confirmed in the *in vivo* experiment with TCL1-OVA cells, indicating that Tregs inhibit the proliferation of $CD8^+$ cells upon recognition of tumor-expressed antigen.

The variable CDR3 regions of TCR interact with the peptide presented by MHC. The analysis of CDR3 sequence provides information about the diversity and clonality of investigated T cell populations and has become a valuable research tool in immunology (40). Thus, the higher oligoclonal composition of TCL1-derived Tregs compared to Tregs sorted from control mice, suggests that only selected clones of Tregs have undergone the expansion in TCL1 leukemia-bearing mice.

The expansion of exhausted T cells is a hallmark of human CLL and is also recapitulated in the Eμ-TCL1 mouse model (11).

The $CD8^+$ lymphocytes, which are present in spleens of TCL1 leukemia-bearing mice, have been described as antigen-experienced, oligoclonal cells that expand during the progression of the disease (12). In our experiments, upon depletion of Tregs, the $CD8^+$ T cells became more oligoclonal and were effective in the elimination of leukemic cells. Surprisingly, anti-leukemic $CD8^+$ T cells expressed different CDR3 sequences compared to the CDR3 sequences of lymphocytes from non-DT-treated, leukemia-bearing mice. It has been reported that in some tumors, based on the TCR sequences functional T cells formed a distinct group from dysfunctional, transitional tumor - infiltrating lymphocytes (41). Our results suggest that the depletion of Tregs in leukemia-bearing mice triggers the expansion of functional $CD8^+$ T cell clones through the presentation of different epitopes than those used for splenic, exhausted $CD8^+$ T cells. Elimination of Tregs primed the activation of T cells not only in spleens but also in the lymph nodes. The expansion of $CD8^+$ T lymphocytes capable of killing leukemic cells occurred due to Tregs depletion, thus revealing their role in the maintenance of tumor antigen tolerance in CLL. The limitation of these studies is the fact that the antigens that led to the activation of anti-leukemic T lymphocytes were not identified yet. However, we suspect that these antigens could be associated with mutations typical for CLL. Importantly, we cannot rule out the possibility that these antigens are of other origins, for example derived due to genetic differences between mouse strains. Nevertheless, the depletion of Tregs seems to be a trigger for the expansion of effector T lymphocytes.

As it was also shown for other malignances, the inhibition of Tregs activation must occur early in the course of the disease to bring the beneficial outcome (42, 43). It has also been shown that the efficacy of adoptive T cell therapy is dependent on the tumor burden and is high in the early stages of tumor development or after chemotherapy (44, 45). To address this observation we conducted treatment with the MALT1 inhibitor, MI-2, when the leukemic cells were already detectable in blood but at a low level. MI-2 disrupted Tregs activation, prevented the formation of the specific TCL1-derived Tregs A subpopulation and inhibited the progression of leukemia in immunocompetent mice. Since the MI-2 was shown to exert a cytotoxic effect on leukemic cells (28), it is difficult to conclude from our experiments, whether it affects Tregs directly or only delays their activation due to the inhibition of leukemia progression. Though, the relatively small anti-leukemia efficacy of MI-2 obtained in RAG2-KO mice model may bring to the conclusion that T cells are important component in anti-leukemic MI-2 mechanism of action. Moreover, the decrease in the frequency of activated Tregs provided the therapeutic window to reduce the percentage of leukemic cells in mouse blood even two weeks after inoculation of leukemic cells.

Our results underline the role of Tregs in the progression of CLL and more importantly suggest that reactivation of the existing, exhausted T cell populations with anti-PD-L1 therapy, might be insufficient to block the disease progression. Notably, the presented results indicate that one approach to obtain an effective anti-leukemia immune response is to reorganize the CLL microenvironment, in order to create an opportunity for the expansion of a population of cytotoxic $CD8^+$ T cells.

DATA AVAILABILITY STATEMENT

The datasets presented in this study can be found in online repositories. The names of the repository/repositories and accession number(s) can be found below: https://www.ncbi.nlm.nih.gov/, GSE179121.

ETHICS STATEMENT

The animal study was reviewed and approved by The Local Ethics Committee for the Animal Experimentation in Warsaw, Warsaw University of Life Sciences, Warsaw, Poland.

AUTHOR CONTRIBUTIONS

Conceptualization, AM, AG, and MF. Investigation, AG, KF, MS, KS, PN, FS, GP, JP, and EM. Resources, JB, AS-P, SG, EL-M, and DE. Writing and visualization AM, AG, KF, JP, and EM. Critical revision, SG, FB, DE, PJ, MF, JP, and EM. Supervision, project administration AM. All authors contributed to the article and approved the submitted version.

FUNDING

This work was supported by: the Polish National Science Centre grants 2018/29/B/NZ6/01962 (AM) and 2016/21/B/NZ7/02041 (MF) and the Ministry of Science and Higher Education within "Regional Initiative of Excellence" program in the years 2019-2022 - 013/RID/2018/19, the FNRS "Télévie" 7.6518.20 (GP), and the Fonds National de la Recherche Luxembourg TIME-CLL: C20/BM/14582635 (EM).

ACKNOWLEDGMENTS

We wish to thank Ewa Kozlowska from University of Warsaw for providing Treg-Foxp3EGFP mice, Serena Zacchigna and Simone Vodret from ICGEB, Trieste for their support with DEREG mice experiments and sharing the DEREG colony, and Nathalie Nicot, Elise Mommaerts, Arnaud Muller (LUXGEN Platform, LIH) for RNA sequencing.

SUPPLEMENTARY MATERIAL

The Supplementary Material for this article can be found online at: https://www.frontiersin.org/articles/10.3389/fimmu.2022.781364/full#supplementary-material

REFERENCES

1. Sedlarikova L, Petrackova A, Papajik T, Turcsanyi P, Kriegova E. Resistance-Associated Mutations in Chronic Lymphocytic Leukemia Patients Treated With Novel Agents. *Front Oncol* (2020) 10:894. doi: 10.3389/fonc.2020.00894
2. Lemal R, Tournilhac O. State-Of-the-Art for CAR T-Cell Therapy for Chronic Lymphocytic Leukemia in 2019. *J Immunother Cancer* (2019) 7 (1):202. doi: 10.1186/s40425-019-0686-x
3. Cox MJ, Lucien F, Sakemura R, Boysen JC, Kim Y, Horvei P, et al. Leukemic Extracellular Vesicles Induce Chimeric Antigen Receptor T Cell Dysfunction in Chronic Lymphocytic Leukemia. *Mol Ther J Am Soc Gene Ther* (2020) 29 (4):1529–40. doi: 10.1016/j.bbmt.2019.12.137
4. June CH, Sadelain M. Chimeric Antigen Receptor Therapy. *N Engl J Med* (2018) 379(1):64–73. doi: 10.1056/NEJMra1706169
5. Wierz M, Pierson S, Guyonnet L, Viry E, Lequeux A, Oudin A, et al. Dual PD1/LAG3 Immune Checkpoint Blockade Limits Tumor Development in a Murine Model of Chronic Lymphocytic Leukemia. *Blood* (2018) 131 (14):1617–21. doi: 10.1182/blood-2017-06-792267
6. McClanahan F, Hanna B, Miller S, Clear AJ, Lichter P, Gribben JG, et al. PD-L1 Checkpoint Blockade Prevents Immune Dysfunction and Leukemia Development in a Mouse Model of Chronic Lymphocytic Leukemia. *Blood* (2015) 126(2):203–11. doi: 10.1182/blood-2015-01-622936
7. Wierz M, Janji B, Berchem G, Moussay E, Paggetti J. High-Dimensional Mass Cytometry Analysis Revealed Microenvironment Complexity in Chronic Lymphocytic Leukemia. *Oncoimmunology* (2018) 7(8):e1465167. doi: 10.1080/2162402X.2018.1465167
8. Archibald WJ, Meacham PJ, Williams AM, Baran AM, Victor AI, Barr PM, et al. Management of Melanoma in Patients With Chronic Lymphocytic Leukemia. *Leukemia Res* (2018) 71:43–6. doi: 10.1016/j.leukres.2018.07.003
9. Falchi L, Vitale C, Keating MJ, Lerner S, Wang X, Elhor Gbito KY, et al. Incidence and Prognostic Impact of Other Cancers in a Population of Long-Term Survivors of Chronic Lymphocytic Leukemia. *Ann Oncol* (2016) 27 (6):1100–6. doi: 10.1093/annonc/mdw072
10. Teh BW, Tam CS, Handunnetti S, Worth LJ, Slavin MA. Infections in Patients With Chronic Lymphocytic Leukaemia: Mitigating Risk in the Era of Targeted Therapies. *Blood Rev* (2018) 32(6):499–507. doi: 10.1016/j.blre.2018.04.007
11. Palma M, Gentilcore G, Heimersson K, Mozaffari F, Nasman-Glaser B, Young E, et al. T Cells in Chronic Lymphocytic Leukemia Display Dysregulated Expression of Immune Checkpoints and Activation Markers. *Haematologica* (2017) 102(3):562–72. doi: 10.3324/haematol.2016.151100
12. Llao Cid L, Hanna BS, Iskar M, Roessner PM, Ozturk S, Lichter P, et al. CD8 (+) T-Cells of CLL-Bearing Mice Acquire a Transcriptional Program of T-Cell Activation and Exhaustion. *Leuk Lymphoma* (2020) 61(2):351–6. doi: 10.1080/10428194.2019.1660972
13. Han S, Toker A, Liu ZQ, Ohashi PS. Turning the Tide Against Regulatory T Cells. *Front Oncol* (2019) 9:279. doi: 10.3389/fonc.2019.00279
14. Gajewski TF, Meng Y, Blank C, Brown I, Kacha A, Kline J, et al. Immune Resistance Orchestrated by the Tumor Microenvironment. *Immunol Rev* (2006) 213:131–45. doi: 10.1111/j.1600-065X.2006.00442.x
15. D'Arena G, Vitale C, Coscia M, Festa A, Di Minno NMD, De Feo V, et al. Regulatory T Cells and Their Prognostic Relevance in Hematologic Malignancies. *J Immunol Res* (2017) 2017:1832968. doi: 10.1155/2017/1832968
16. De Matteis S, Molinari C, Abbati G, Rossi T, Napolitano R, Ghetti M, et al. Immunosuppressive Treg Cells Acquire the Phenotype of Effector-T Cells in Chronic Lymphocytic Leukemia Patients. *J Transl Med* (2018) 16(1):172. doi: 10.1186/s12967-018-1545-0
17. Roessner PM, Llao Cid L, Lupar E, Roider T, Bordas M, Schifflers C, et al. EOMES and IL-10 Regulate Antitumor Activity of T Regulatory Type 1 CD4 (+) T Cells in Chronic Lymphocytic Leukemia. *Leukemia* (2021) 35:2311–24. doi: 10.1101/2020.03.09.983098
18. Hanna BS, Roessner PM, Scheffold A, Jebaraj BMC, Demerdash Y, Ozturk S, et al. PI3Kdelta Inhibition Modulates Regulatory and Effector T-Cell Differentiation and Function in Chronic Lymphocytic Leukemia. *Leukemia* (2019) 33(6):1427–38. doi: 10.1038/s41375-018-0318-3
19. Bichi R, Shinton SA, Martin ES, Koval A, Calin GA, Cesari R, et al. Human Chronic Lymphocytic Leukemia Modeled in Mouse by Targeted TCL1 Expression. *Proc Natl Acad Sci USA* (2002) 99(10):6955–60. doi: 10.1073/pnas.102181599
20. Johnson AJ, Lucas DM, Muthusamy N, Smith LL, Edwards RB, De Lay MD, et al. Characterization of the TCL-1 Transgenic Mouse as a Preclinical Drug Development Tool for Human Chronic Lymphocytic Leukemia. *Blood* (2006) 108(4):1334–8. doi: 10.1182/blood-2005-12-011213
21. Rosenbaum M, Gewies A, Pechloff K, Heuser C, Engleitner T, Gehring T, et al. Bcl10-Controlled Malt1 Paracaspase Activity Is Key for the Immune Suppressive Function of Regulatory T Cells. *Nat Commun* (2019) 10 (1):2352. doi: 10.1038/s41467-019-10203-2
22. Charan J, Kantharia ND. How to Calculate Sample Size in Animal Studies? *J Pharmacol Pharmacother* (2013) 4(4):303–6. doi: 10.4103/0976-500X.119726
23. Dias S, D'Amico A, Cretney E, Liao Y, Tellier J, Bruggeman C, et al. Effector Regulatory T Cell Differentiation and Immune Homeostasis Depend on the Transcription Factor Myb. *Immunity* (2017) 46(1):78–91. doi: 10.1016/j.immuni.2016.12.017
24. Wang J, Siffert M, Spiliotis M, Gottstein B. Repeated Long-Term DT Application in the DEREG Mouse Induces a Neutralizing Anti-DT Antibody Response. *J Immunol Res* (2016) 2016:1450398. doi: 10.1155/2016/1450398
25. Hanna BS, Roessner PM, Yazdanparast H, Colomer D, Campo E, Kugler S, et al. Control of Chronic Lymphocytic Leukemia Development by Clonally-Expanded CD8(+) T-Cells That Undergo Functional Exhaustion in Secondary Lymphoid Tissues. *Leukemia* (2019) 33(3):625–37. doi: 10.1038/s41375-018-0250-6
26. Lahl K, Sparwasser T. *In Vivo* Depletion of FoxP3+ Tregs Using the DEREG Mouse Model. *Methods Mol Biol* (2011) 707:157–72. doi: 10.1007/978-1-61737-979-6_10
27. Thornton AM, Lu J, Korty PE, Kim YC, Martens C, Sun PD, et al. Helios(+) and Helios(-) Treg Subpopulations Are Phenotypically and Functionally Distinct and Express Dissimilar TCR Repertoires. *Eur J Immunol* (2019) 49 (3):398–412. doi: 10.1002/eji.201847935
28. Saba NS, Wong DH, Tanios G, Iyer JR, Lobelle-Rich P, Dadashian EL, et al. MALT1 Inhibition Is Efficacious in Both Naive and Ibrutinib-Resistant Chronic Lymphocytic Leukemia. *Cancer Res* (2017) 77(24):7038–48. doi: 10.1158/0008-5472.CAN-17-2485
29. Brusa D, Serra S, Coscia M, Rossi D, D'Arena G, Laurenti L, et al. The PD-1/PD-L1 Axis Contributes to T-Cell Dysfunction in Chronic Lymphocytic Leukemia. *Haematologica* (2013) 98(6):953–63. doi: 10.3324/haematol.2012.077537
30. Martin K, Junker U, Tritto E, Sutter E, Rubic-Schneider T, Morgan H, et al. Pharmacological Inhibition of MALT1 Protease Leads to a Progressive IPEX-Like Pathology. *Front Immunol* (2020) 11:745. doi: 10.3389/fimmu.2020.00745
31. Onizuka S, Tawara I, Shimizu J, Sakaguchi S, Fujita T, Nakayama E. Tumor Rejection by *In Vivo* Administration of Anti-CD25 (Interleukin-2 Receptor Alpha) Monoclonal Antibody. *Cancer Res* (1999) 59(13):3128–33.
32. Hu G, Li Z, Wang S. Tumor-Infiltrating FoxP3(+) Tregs Predict Favorable Outcome in Colorectal Cancer Patients: A Meta-Analysis. *Oncotarget* (2017) 8 (43):75361–71. doi: 10.18632/oncotarget.17722
33. D'Arena G, Simeon V, D'Auria F, Statuto T, Sanzo PD, Martino LD, et al. Regulatory T-Cells in Chronic Lymphocytic Leukemia: Actor or Innocent Bystander? *Am J Blood Res* (2013) 3(1):52–7.
34. Mpakou VE, Ioannidou HD, Konsta E, Vikentiou M, Spathis A, Kontsioti F, et al. Quantitative and Qualitative Analysis of Regulatory T Cells in B Cell Chronic Lymphocytic Leukemia. *Leukemia Res* (2017) 60:74–81. doi: 10.1016/j.leukres.2017.07.004
35. Sivina M, Hartmann E, Kipps TJ, Rassenti L, Krupnik D, Lerner S, et al. CCL3 (MIP-1alpha) Plasma Levels and the Risk for Disease Progression in Chronic Lymphocytic Leukemia. *Blood* (2011) 117(5):1662–9. doi: 10.1182/blood-2010-09-307249
36. Patterson SJ, Pesenacker AM, Wang AY, Gillies J, Mojibian M, Morishita K, et al. T Regulatory Cell Chemokine Production Mediates Pathogenic T Cell Attraction and Suppression. *J Clin Invest* (2016) 126(3):1039–51. doi: 10.1172/JCI83987
37. Arroyo Hornero R, Georgiadis C, Hua P, Trzupek D, He LZ, Qasim W, et al. CD70 Expression Determines the Therapeutic Efficacy of Expanded Human Regulatory T Cells. *Commun Biol* (2020) 3(1):375. doi: 10.1038/s42003-020-1097-8
38. Gautron AS, Dominguez-Villar M, de Marcken M, Hafler DA. Enhanced Suppressor Function of TIM-3+ FoxP3+ Regulatory T Cells. *Eur J Immunol* (2014) 44(9):2703–11. doi: 10.1002/eji.201344392

39. Joller N, Lozano E, Burkett PR, Patel B, Xiao S, Zhu C, et al. Treg Cells Expressing the Coinhibitory Molecule TIGIT Selectively Inhibit Proinflammatory Th1 and Th17 Cell Responses. *Immunity* (2014) 40 (4):569–81. doi: 10.1016/j.immuni.2014.02.012
40. De Simone M, Rossetti G, Pagani M. Single Cell T Cell Receptor Sequencing: Techniques and Future Challenges. *Front Immunol* (2018) 9:1638. doi: 10.3389/fimmu.2018.01638
41. Li H, van der Leun AM, Yofe I, Lubling Y, Gelbard-Solodkin D, van Akkooi ACJ, et al. Dysfunctional CD8 T Cells Form a Proliferative, Dynamically Regulated Compartment Within Human Melanoma. *Cell* (2019) 176(4):775–89.e18. doi: 10.1016/j.cell.2018.11.043
42. Teng MW, Ngiow SF, von Scheidt B, McLaughlin N, Sparwasser T, Smyth MJ. Conditional Regulatory T-Cell Depletion Releases Adaptive Immunity Preventing Carcinogenesis and Suppressing Established Tumor Growth. *Cancer Res* (2010) 70(20):7800–9. doi: 10.1158/0008-5472.CAN-10-1681
43. Fisher SA, Aston WJ, Chee J, Khong A, Cleaver AL, Solin JN, et al. Transient Treg Depletion Enhances Therapeutic Anti-Cancer Vaccination. *Immun Inflammation Dis* (2017) 5(1):16–28. doi: 10.1002/iid3.136
44. Prato S, Zhan Y, Mintern JD, Villadangos JA. Rapid Deletion and Inactivation of CTLs Upon Recognition of a Number of Target Cells Over a Critical Threshold. *J Immunol* (2013) 191(7):3534–44. doi: 10.4049/jimmunol.1300803
45. Segal G, Prato S, Zehn D, Mintern JD, Villadangos JA. Target Density, Not Affinity or Avidity of Antigen Recognition, Determines Adoptive T Cell Therapy Outcomes in a Mouse Lymphoma Model. *J Immunol* (2016) 196 (9):3935–42. doi: 10.4049/jimmunol.1502187

Conflict of Interest: The authors declare that the research was conducted in the absence of any commercial or financial relationships that could be construed as a potential conflict of interest.

Publisher's Note: All claims expressed in this article are solely those of the authors and do not necessarily represent those of their affiliated organizations, or those of the publisher, the editors and the reviewers. Any product that may be evaluated in this article, or claim that may be made by its manufacturer, is not guaranteed or endorsed by the publisher.

Supplementary Material

1 Supplementary Figures and Tables

1.1 Supplementary Figures

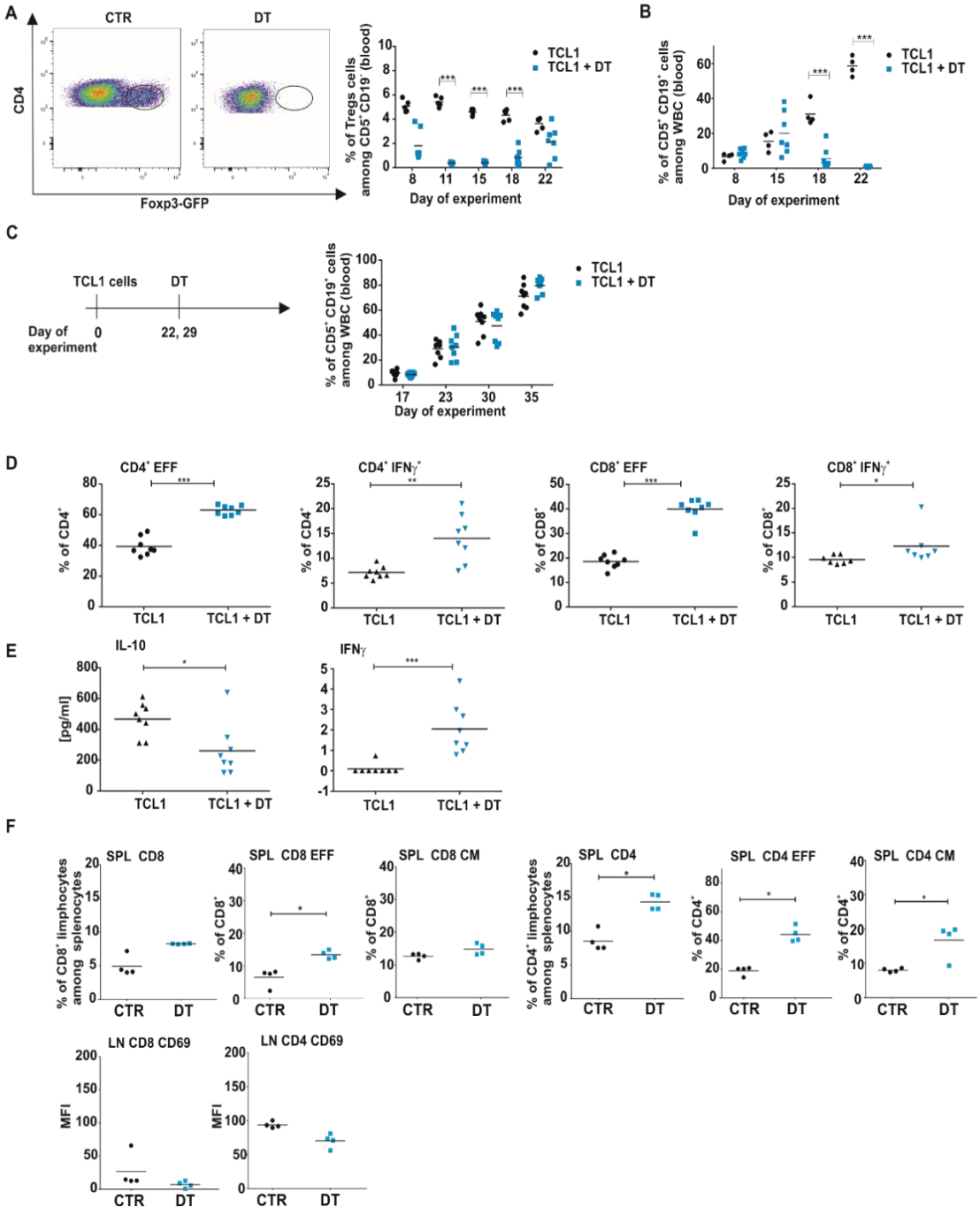

Supplementary Figure 1. (**A**) The representative dot plots showing the efficacy of Tregs depletion in DEREG mice spleens 24 hours upon DT injection (left) and graph presenting the percentage of Tregs (among CD5+ cells) assessed by flow cytometry at indicated time points in peripheral blood collected from untreated and DT-treated TCL1 leukemia-bearing DEREG mice (right panel). Each dot represents an individual sample (mouse), n=4-7, mean *p≤0.05, ***p≤ 0.001.

(**B**) Percentage of leukemic cells ($CD5^+CD19^+$) assessed with flow cytometry in blood collected from untreated and DT-treated TCL1 leukemia-bearing DEREG mice a different batch of TCL1 leukemic

cells were used (isolated from Eμ-TCL1-1013 transgenic mouse) than those presented on Figure 1, Each dot represents an individual sample (mouse) n=4-7, ***p≤ 0.001.

(**C**) Scheme of the experiment showing different time points for Tregs depletion as compared to data presented on Figure 1 (left panel) and graph presenting the percentage of leukemic cells ($CD5^+CD19^+$) assessed by flow cytometry at indicated time points in blood collected from untreated and DT-treated TCL1 leukemia-bearing DEREG mice, each dot represents an individual sample (mouse), n=8.

(**D**) The percentage of effector (EFF) and IFN-γ^+ subpopulations of $CD4^+$ and $CD8^+$ T cells. Cells were collected from spleens of untreated and DT-treated TCL1 leukemia-bearing DEREG mice and stained for CD44 and CD62L, each dot represents an individual sample (mouse), n=8, *p≤0.05, ** p≤ 0.01, ***p≤ 0.001.

(**E**) The analysis of IL-10 and IFN- γ concentrations in mouse serum, collected from untreated and DT-treated TCL1-injected DEREG mice, each dot represents an individual sample (mouse), n=8, *p≤0.05, ***p≤ 0.001.

(**F**) The percentage of $CD8^+$ and $CD4^+$, effector (EFF) and central memory (CM) subpopulations in spleens (upper panel) and CD69 level in $CD8^+$ and $CD4^+$ of lymph nodes (lower panel) of DEREG control and DT-treated mice (both without leukemia), each dot represents an individual sample (mouse) n=4, *p≤0.05.

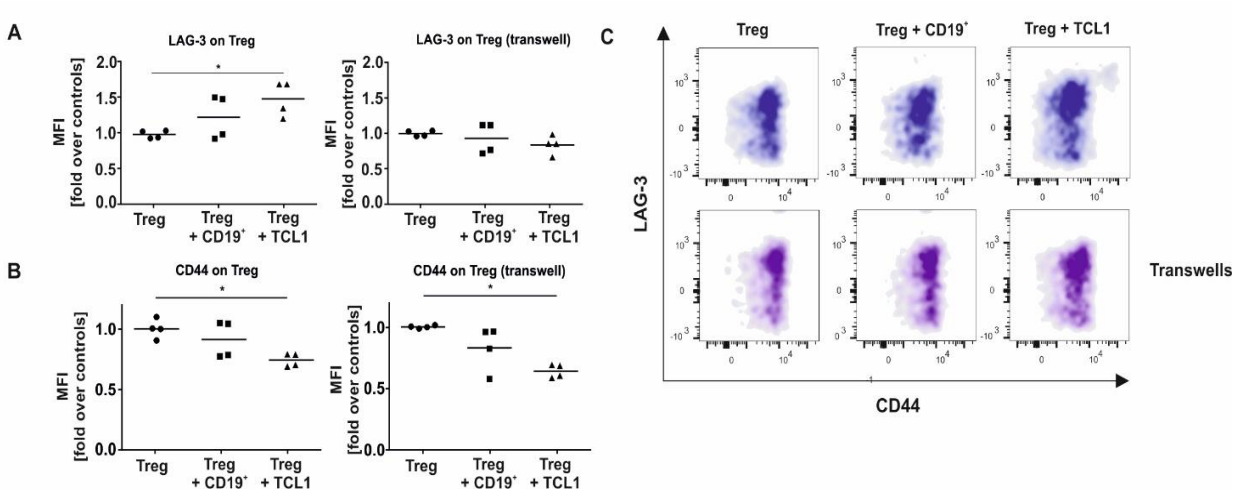

Supplementary Figure 2. The expression of LAG-3 (**A**) or CD44 (**B**) and representative density plots (**C**) of Tregs sorted and co-cultured *ex vivo* with $CD19^+$ isolated from control ($CD19^+$) and TCL1 leukemia-bearing (TCL1) mice. Cells were mixed (left graphs) or separated by transwells (right graphs) and cultured for 72 hours. The graphs show results from two independent experiments, mean ±SD, $p \leq 0.05$.

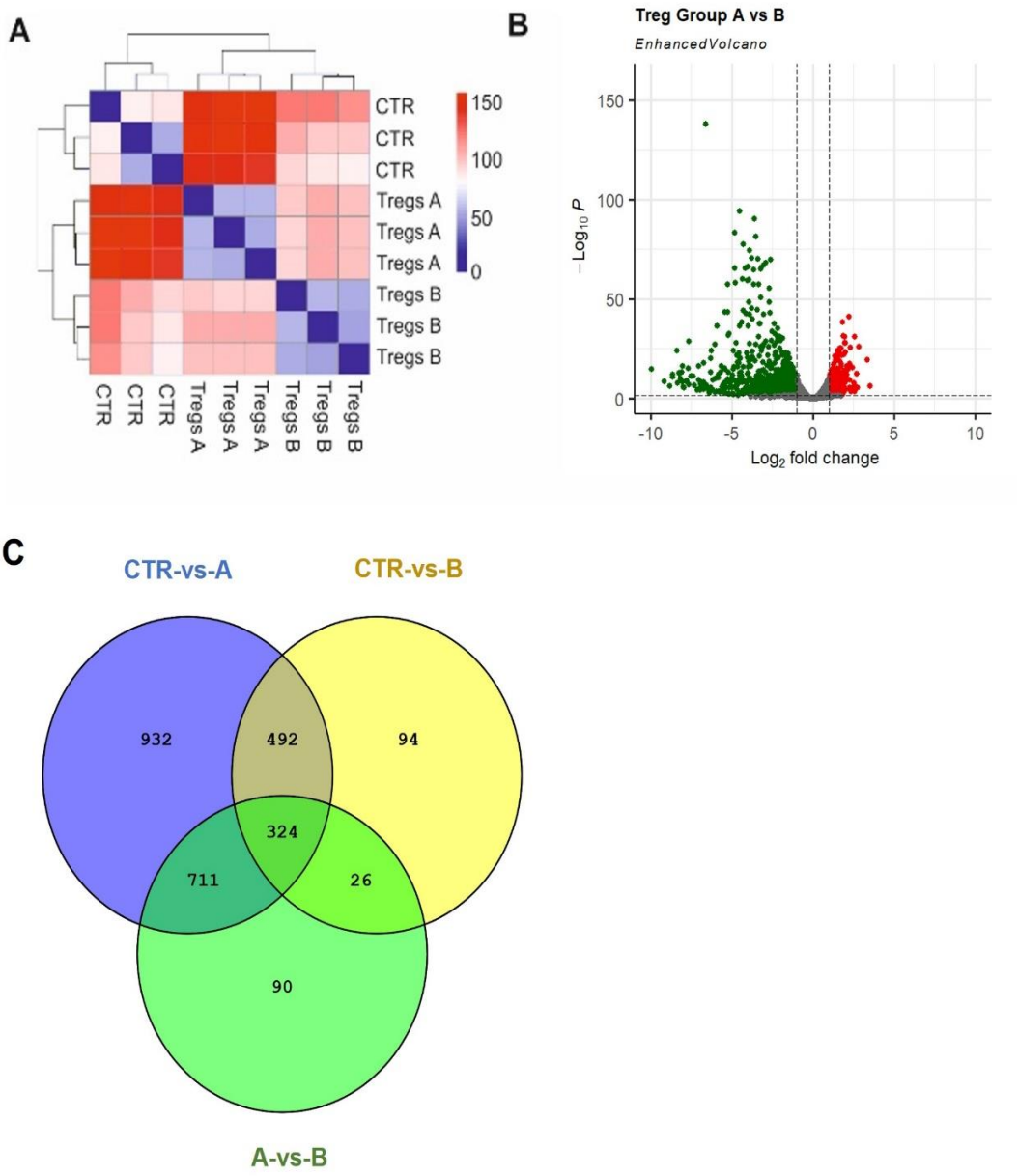

Supplementary Figure 3. (**A**) The Euclidean distance was used to assess the overall similarity between samples. Log2-transformed gene expressions were used to compute distances in a matrix that were visualized in a heatmap. CTR and Tregs A appear as the most different conditions.
(**B**) Volcano plot showing gene expression comparison between Tregs A and Tregs B. Most of DEGs are down-regulated in Tregs A vs Tregs B from TCL1-bearing mice.
(**C**) Venn diagram indicating the number of DEGs common between the comparisons. Most DEGs belonged to the CTR-Tregs A comparison, confirming these conditions as the most different.

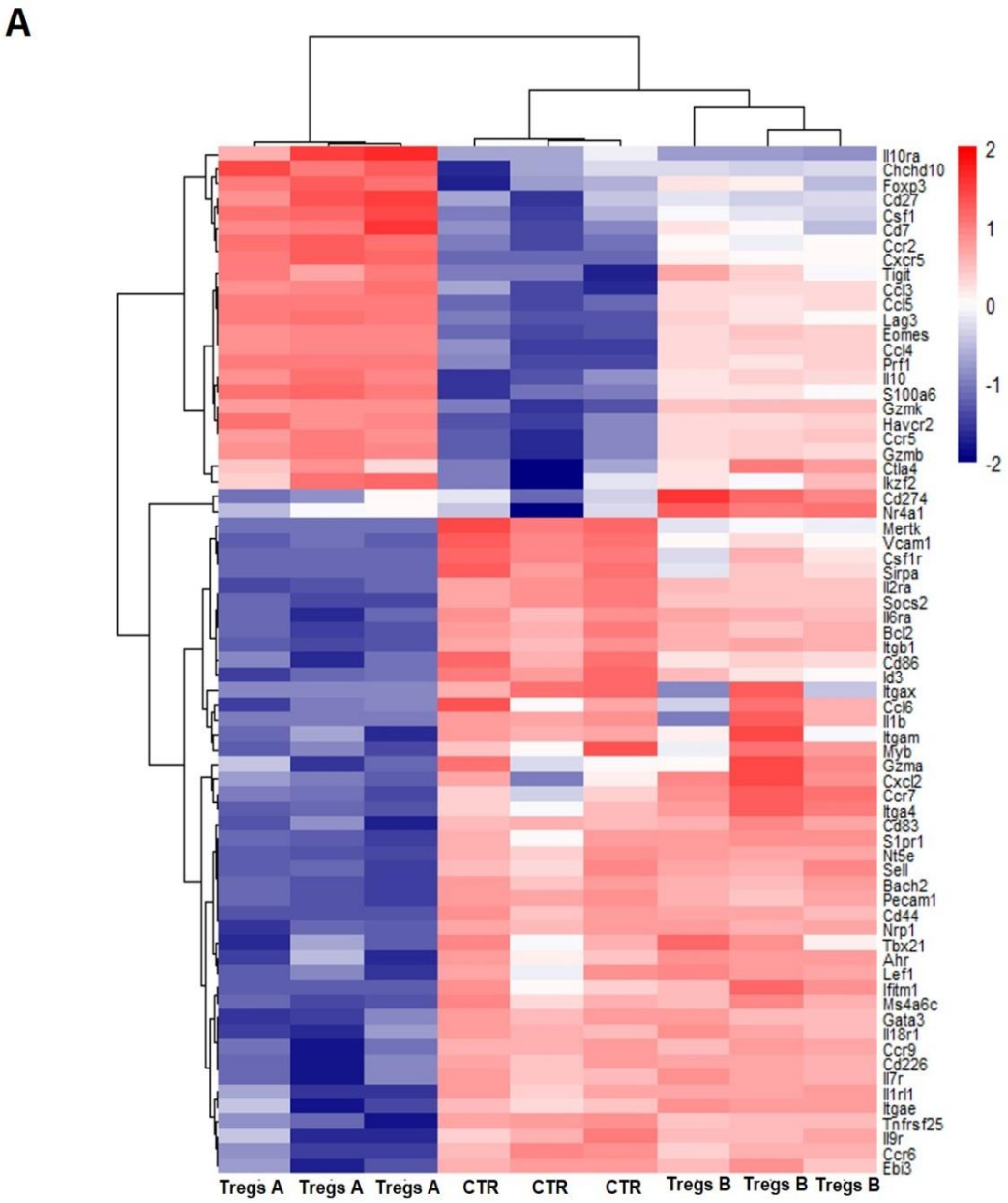
A
Il10ra
Chchd10
Foxp3
Cd27
Csf1
Cd7
Ccr2
Cxcr5
Tigit
Ccl3
Ccl5
Lag3
Eomes
Ccl4
Prf1
Il10
S100a6
Gzmk
Havcr2
Ccr5
Gzmb
Ctla4
Ikzf2
Cd274
Nr4a1
Mertk
Vcam1
Csf1r
Sirpa
Il2ra
Socs2
Il6ra
Bcl2
Itgb1
Cd86
Id3
Itgax
Ccl6
Il1b
Itgam
Myb
Gzma
Cxcl2
Ccr7
Itga4
Cd83
S1pr1
Nt5e
Sell
Bach2
Pecam1
Cd44
Nrp1
Tbx21
Ahr
Lef1
Ifitm1
Ms4a6c
Gata3
Il18r1
Ccr9
Cd226
Il7r
Il1rl1
Itgae
Tnfrsf25
Il9r
Ccr6
Ebi3
2
1
0
-1
-2
Tregs A
Tregs A
Tregs A
CTR
CTR
CTR
Tregs B
Tregs B
Tregs B
B
Malt1
RelA
RelB
NFKB1
Gene expression (log2)
Gene expression (log2)
Gene expression (log2)
Gene expression (log2)
Ctr
Tregs A
Tregs B

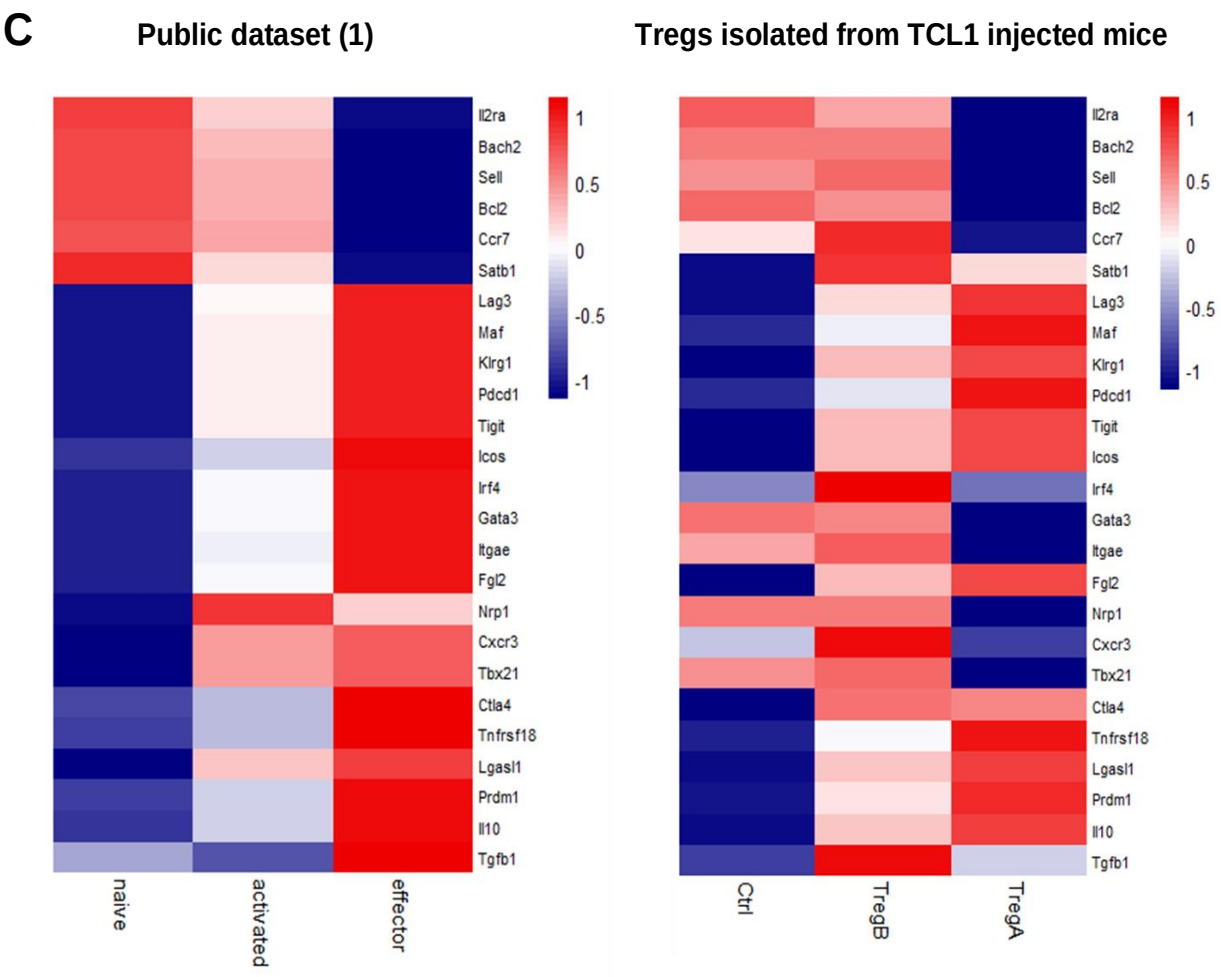

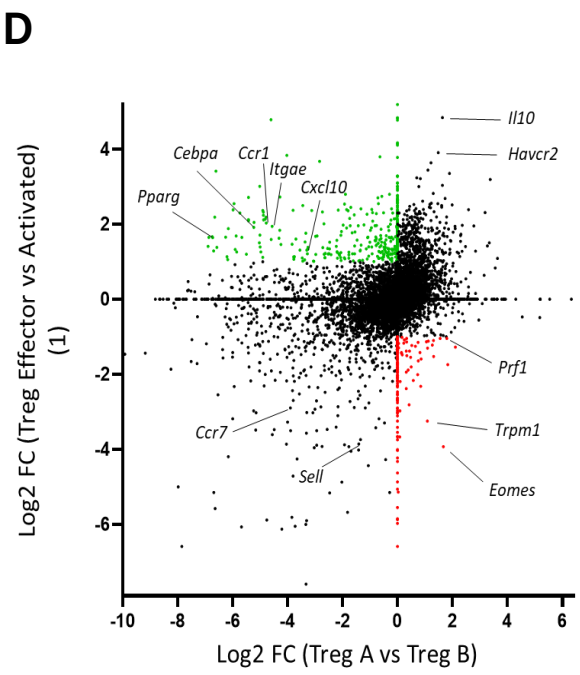

Supplementary Figure 4. (**A**) Clustering of selected DEGs in Tregs from control and TCL1-bearing mice (RNA sequencing with FDR < 0.05 and log2FC > 1) by correlation with complete linkage, n=3 for each Tregs subpopulation.
(**B**) The expression (log2, RNA sequencing) of genes regulating the NF-κB pathway in Tregs from control and TCL1-bearing mice, n=3. One-way ANOVA * $p \leq 0.05$, ** $p < 0.01$, *** $p < 0.001$.

(**C**) Heatmaps showing the expression of genes selected from a publicly available dataset ((1), GSE72494) in naïve, activated and effector Tregs (left panel) and from our RNA-seq data among control, Tregs A, and Tregs B subpopulations isolated from TCL1 injected DEREG mice (described in details in Figure 3).
(**D**) Plot showing gene expression comparison between effector vs activated Tregs (GSE72494), and Tregs A vs Tregs B. Green dots represent genes upregulated in effector vs activated Tregs (log FC>1) and downregulated (or not different) in Tregs A vs Tregs B (total of 442 genes). Red dots represent genes downregulated in effector vs activated Tregs (logFC<-1) and downregulated (or not different) in Tregs A vs Tregs B (total of 172 genes). Black dots represent genes that moves similarly between the 2 comparisons..

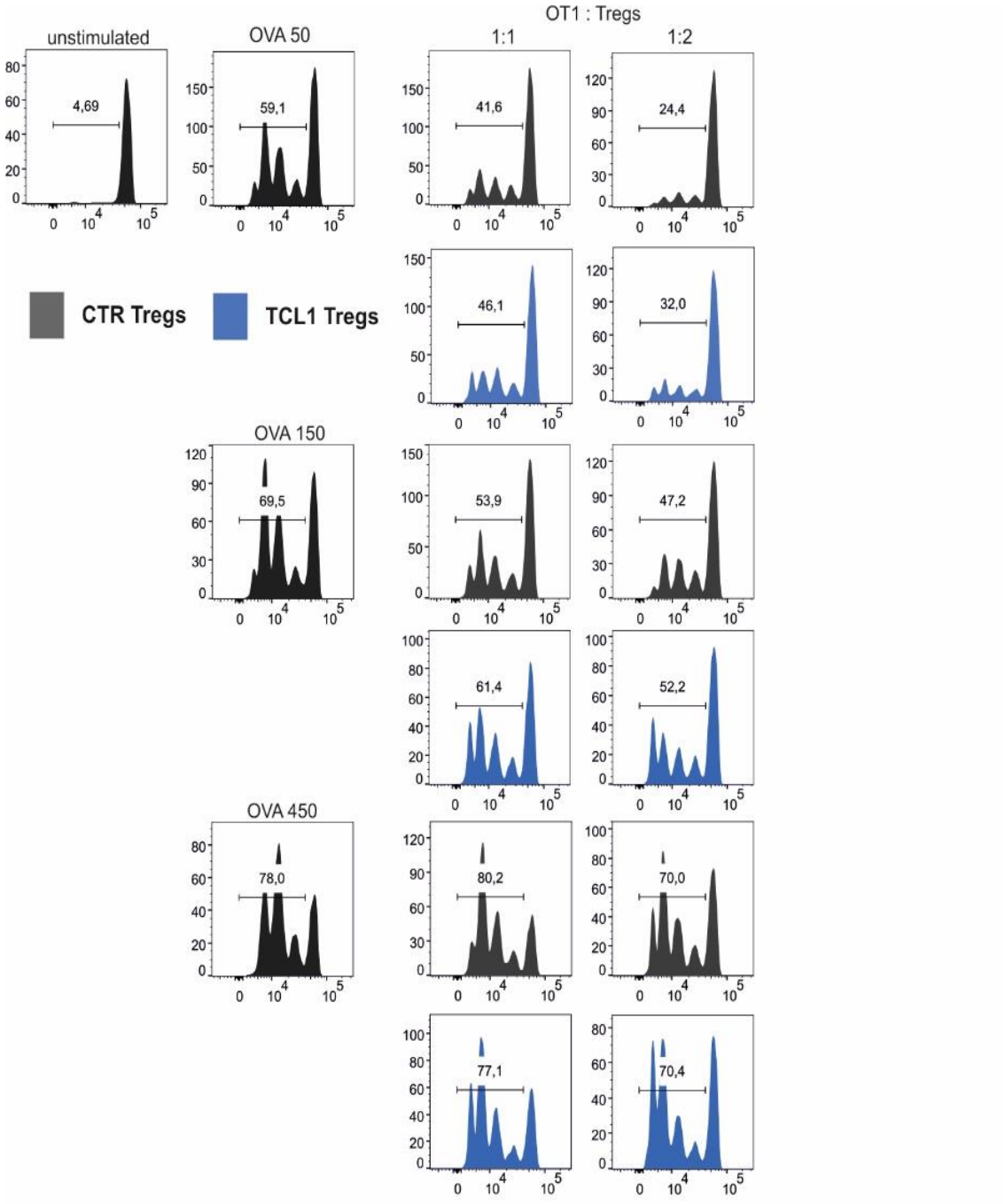

Supplementary Figure 5. OT1 T cell proliferation primed by bone marrow derived-dendritic cells after incubation with OVA peptide (50, 150, 450 μM). Dendritic cells were co-cultured with Tregs, sorted from control and TCL1-injected B6 Foxp^{EGFP} mice. Subsequently, the OT1 CD8^{+} cells stained with Cell Trace Violet were added and their proliferation was assessed with flow cytometry after 72 hours.

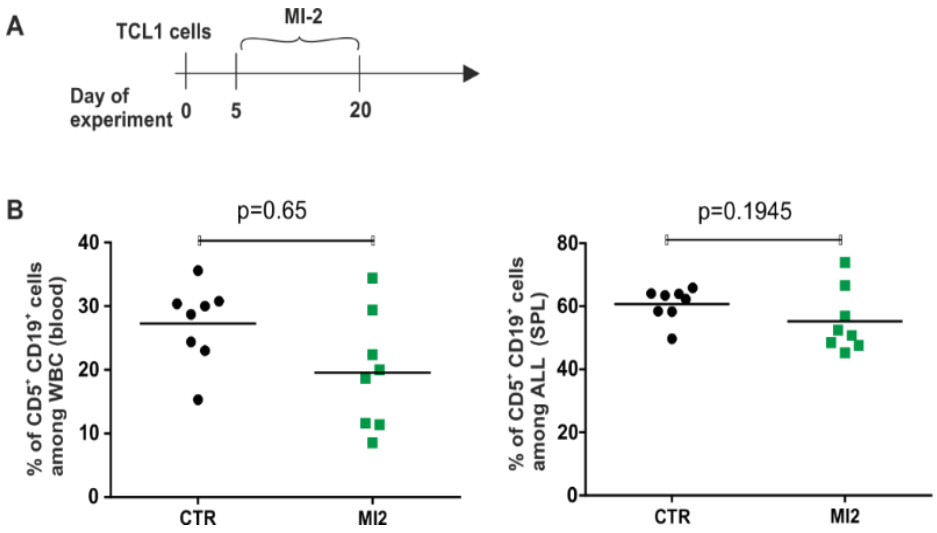

Supplementary Figure 6. (**A**) Scheme of experiment. RAG2-KO were injected with TCL1 cells and treated with MI-2 for two weeks at dose 20 mg/kg.
(**B**) Percentage of leukemic cells ($CD5^+CD19^+$) assessed with flow cytometry in blood collected from untreated and MI-2-treated TCL1 leukemia-bearing RAG2-KO mice. The experiment was repeated twice, each dot represents an individual sample (mouse) n=7-8.

1.2 Supplementary Tables

Supplementary Table 1. Antibodies used in this study

ANTIBODY	SOURCE	IDENTIFIER
BD Pharmingen™ PE Rat Anti-Mouse CD5, clone: 53-7.3	BD Biosciences	Cat# 553023; RRID:AB_394561
BD Pharmingen™ APC Rat Anti-Mouse CD19; clone: 1D3	BD Biosciences	Cat# 550992; RRID:AB_398483
CD3 Monoclonal Antibody (17A2), eFluor 450	eBioscience/Thermo Fisher Scientific	Cat# 48-0032-82; RRID:AB_1272193
BD Pharmingen™ APC-Cy™7 Rat Anti-Mouse CD4, clone: GK1.5	BD Biosciences	Cat#: 552051; RRID:AB_394331
BD Pharmingen™ PE-Cy™7 Rat Anti-Mouse CD4, clone: GK1.5	BD Biosciences	Cat#: 563933; RRID:AB_2738492
CD8a Monoclonal Antibody (53-6.7), PerCP-Cyanine5.5	eBioscience/Thermo Fisher Scientific	Cat#: 45-0081-82
BD Horizon™ BV510 Rat Anti-Mouse CD25, clone: C61	BD Biosciences	Cat#: 563037; RRID:AB_2737969
CD44 Monoclonal Antibody (IM7), PE-Cyanine7	eBioscience/Thermo Fisher Scientific	Cat#: 25-0441-81; RRID:AB_469622
CD62L (L-Selectin) Monoclonal Antibody (MEL-14), APC	eBioscience/Thermo Fisher Scientific	Cat#: 17-0621-81; RRID:AB_469409
CD69 Monoclonal Antibody (H1.2F3), PE	eBioscience/Thermo Fisher Scientific	Cat#: 12-0691-81; RRID:AB_465731
PerCP-Cy™5.5 Rat Anti-Mouse Ly-6C, clone: AL-21	BD Biosciences	Cat#: 560525; RRID:AB_1727558
BD Horizon™ V450 Rat Anti-Mouse Ly-6C, clone: AL-21	BD Biosciences	Cat#: 560594; RRID:AB_1727559
BD Pharmingen™ PE Rat Anti-Mouse IFN-γ, clone: XMG1.2	BD Biosciences	Cat#: 554412; RRID:AB_395376
BD Pharmingen™ APC Rat Anti-Mouse CD223, clone: C9B7W	BD Biosciences	Cat#: 562346
BD Pharmingen™ PerCP-Cy™5.5 Rat Anti-Mouse CD223, clone: C9B7W	BD Biosciences	Cat#: 564673, RRID:AB_2734764
Brilliant Violet 421™ anti-mouse CD274 (B7-H1, PD-L1) Antibody, clone: 10F.9G2	BioLegend	Cat#: 124315; RRID:AB_10897097
BD Pharmingen™ APC Rat Anti-Mouse IL-10, clone: JES5-16E3	BD Biosciences	Cat#: 554468; RRID:AB_398558
CD3e Monoclonal Antibody (145-2C11), Functional Grade	eBioscience/Thermo Fisher Scientific	Cat#: 16-0031-85; RRID:AB_468848
CD28 Monoclonal Antibody (37.51), Functional Grade	eBioscience/Thermo Fisher Scientific	Cat#: 16-0281-85; RRID:AB_468922
InVivoPlus anti-mouse PD-L1 (B7-H1), clone: 10F.9G2	BioXcell	Cat#: BP0101; RRID:AB_10949073
InVivoPlus rat IgG2b isotype control, anti-keyhole limpet hemocyanin, clone: LTF-2	BioXcell	Cat#: BP0090; RRID:AB_1107780

Supplementary Table 2. Gene Set Enrichment Analysis (GSEA) of Tregs A and Tregs B gene expression.

Tregs A	GeneSet	NES	NOM p-val
	GAVIN_FOXP3_TARGETS_CLUSTER_P6	1,91	0,000
	MARSON_FOXP3_CORE_DIRECT_TARGETS	1,8	0,007
	HALLMARK_E2F_TARGETS	1,73	0,000
	HALLMARK_G2M_CHECKPOINT	1,58	0,000
	WP_OXIDATIVE_PHOSPHORYLATION	1,39	0,028
	HALLMARK_MTORC1_SIGNALING	1,36	0,000
	MARSON_FOXP3_TARGETS_UP	1,35	0,031
	KEGG_OXIDATIVE_PHOSPHORYLATION	1,32	0,000
	HALLMARK_CHOLESTEROL_HOMEOSTASIS	1,29	0,049

Tregs B	GeneSet	NES	NOM p-val
	GAVIN_FOXP3_TARGETS_CLUSTER_P7	-1,8	0,000
	ZHENG_FOXP3_TARGETS_IN_T_LYMPHOCYTE_DN	-1,76	0,000
	GAVIN_FOXP3_TARGETS_CLUSTER_T4	-1,68	0,000
	ZHENG_BOUND_BY_FOXP3	-1,67	0,000
	ZHENG_FOXP3_TARGETS_IN_THYMUS_UP	-1,66	0,000
	HALLMARK_TNFA_SIGNALING_VIA_NFKB	-1,65	0,000
	HALLMARK_IL6_JAK_STAT3_SIGNALING	-1,63	0,000
	HALLMARK_TGF_BETA_SIGNALING	-1,61	0,003
	HALLMARK_INFLAMMATORY_RESPONSE	-1,58	0,000
	HALLMARK_IL2_STAT5_SIGNALING	-1,56	0,000
	HALLMARK_INTERFERON_GAMMA_RESPONSE	-1,38	0,002
	HALLMARK_HYPOXIA	-1,33	0,011

Supplementary Table 3. Gene Set Enrichment Analysis (GSEA) of Effector Tregs and Activated Tregs gene expression (1).

Effector	GeneSet	NES	NOM p-val
	FISCHER_G2_M_CELL_CYCLE	2,43	0
	KONG_E2F3_TARGETS	2,43	0
	GAVIN_FOXP3_TARGETS_CLUSTER_P6	2,36	0
	HALLMARK_G2M_CHECKPOINT	2,25	0
	HALLMARK_E2F_TARGETS	2,24	0
	HALLMARK_MITOTIC_SPINDLE	1,73	0
	GAVIN_FOXP3_TARGETS_CLUSTER_P3	1,54	0,003
	HALLMARK_MTORC1_SIGNALING	1,47	0,003
	HALLMARK_GLYCOLYSIS	1,36	0,019
	HALLMARK_P53_PATHWAY	1,34	0,025

	HALLMARK_TNFA_SIGNALING_VIA_NFKB	1,33	0,025
	HALLMARK_IL2_STAT5_SIGNALING	1,27	0,048

Active	GeneSet	NES	NOM p-val
	ZHENG_FOXP3_TARGETS_IN_T_LYMPHOCYTE_DN	-2,13	0
	GAVIN_FOXP3_TARGETS_CLUSTER_P7	-1,93	0
	ZHENG_BOUND_BY_FOXP3	-1,48	0
	GAVIN_FOXP3_TARGETS_CLUSTER_P2	-1,47	0,007
	GAVIN_FOXP3_TARGETS_CLUSTER_P4	-1,42	0,011
	GAVIN_FOXP3_TARGETS_CLUSTER_T7	-1,39	0,028

2 Supplementary Methods

2.1 Cell culture

Murine bone marrow stromal M2-10B4 and human embryonic kidney (HEK 293T) cell lines were purchased from American Type Culture Collection (ATCC) (Manassas, VA, USA) The genetic characteristics of HEK293T cells was determined by PCR-single-locus-technology in 2020. The cells were cultured in Roswell Park Memorial Institute (RPMI-1640) medium (Gibco/Thermo Fisher Scientific, Waltham, MA, USA) or Dulbecco's Minimal Eagle's Medium (DMEM) (Sigma Aldrich, St Louis, MA, USA), respectively. Mouse hybridoma cell line Sp2.0 transfected with gene for soluble Fms Related Receptor Tyrosine Kinase 3 Ligand (FLT3L secreting cells) (2), were cultured in Iscove's Modified Dulbecco's Medium (IMDM) (Gibco/Thermo Fisher Scientific, Waltham, MA, USA). All media were supplemented with 10% (v/v) heat-inactivated fetal bovine serum (FBS) (HyClone Laboratories, Logan, Utah, USA) gentamycin (50 μg/ml) (Sigma-Aldrich, St Louis, MA, USA) and cells were cultured at 37°C, 5% CO_2, in a humidified atmosphere. For *ex vivo* experiments, the medium was supplemented with 2 mM L-glutamine (Sigma-Aldrich, St Louis, MA, USA) and 50 μM B-mercaptoethanol (Gibco/Thermo Fisher Scientific, Waltham, MA, USA). The cell lines were tested for Mycoplasma spp. contamination once a week.

2.2. Co-cultures of Tregs and CD19/TCL1 cells

M2-10B4 murine stroma cells were seeded onto 24-well plates at the density 5.0×10^3 cell per well. Next day, B cells isolated from spleens of control ($CD19^+$) and leukemia bearing mice (TCL1) were seeded into wells (1.0×10^6 cells per well). Then Tregs sorted from spleens of control FoxP3-GFP mice were added to the wells (1.5×10^4 cells /well) directly or seeded on cell culture inserts (FALCON/Corning, Corning, NY, USA). For phenotyping of Tregs, upon three days of co-culture the cells were stained with proper antibodies and analysed by flow cytometry.

2.3. Mouse serum preparation and assessment of cytokine concentration in mouse serum

Blood samples were collected from cheek vein into anticoagulant-free tubes and left for 1h at RT to form a cloth. Then the tubes were centrifuged at 1000 x g for 10 min. Collected serum was aliquoted and stored at -80°C. BD Cytometric Bead Array (CBA) Mouse Th1/Th2/Th17 CBA Kit (BD Biosciences) was applied according to the manufacturer's protocol and analysed by flow cytometry .

2.4. Dendritic cells differentiation

Bone marrow immune cells were isolated from femurs and tibia of 5-6 weeks old, wild type C57BL6/J mice and dendritic cells (DCs) were differentiated as described before (3). Briefly, the isolated bone marrow cells were seeded onto non-tissue culture treated 6-well plates at the density 1.0×10^6/ml and cultured in IMDM medium (Gibco/Thermo Fisher Scientific, Waltham, MA, USA) supplemented with 10% (v/v) heat-inactivated FBS (HyClone Laboratories,) gentamycin (50 μg/ml) (Sigma-Aldrich,), 50 μM β-mercaptoethanol (Gibco/Thermo Fisher Scientific,) and 15% of FLT3L-containing supernatant (complete IMDM medium) at 37°C, 5% CO_2, in a humidified atmosphere for 7 days. At day 3^{rd} and 6^{th} the half volume of the medium was removed and replaced by the complete fresh medium. DCs were used for priming experiments between 7^{th} and 9^{th} day.

2.5. Priming assay

Bone marrow-derived DCs were seeded onto tissue treated 96-well plates (2.0×10^4 cells/well) in complete IMDM medium supplemented with Poly(I:C)(HMW) (1 μg/ml) (InvivoGen, San Diego, CA, USA), pulsed with OVA protein (Albumin from chicken egg white, Sigma-Aldrich) (50, 150 or 450 μg) for 3 hours and washed twice with RPMI medium supplemented with 10% (v/v) heat-inactivated FBS (HyClone Laboratories,), gentamycin (50 μg/ml) (Sigma-Aldrich), 50 μM B-mercaptoethanol (Gibco/Thermo Fisher Scientific) and 2 mM L-glutamine (Sigma-Aldrich). Next, Tregs sorted as described in main text, from spleens of control or TCL1 leukemia-bearing B6 $Foxp3^{EGFP}$ mice were added to the proper wells together with 4×10^4 cells/well) $CD8^+$ T cells isolated by magnetic separation (EasySep™ Mouse $CD8^+$ Cell Isolation Kit; STEMCELL Technologies) from spleens of OT1 mice and stained with CT as described above. The $CD8^+$: Tregs-GFP ratio was 1:1 or 1:2. The proliferation of $CD8^+$ cells was evaluated upon 72 hours using flow cytometry.

Supplementary References

1. Dias S, D'Amico A, Cretney E, Liao Y, Tellier J, Bruggeman C, et al. Effector Regulatory T Cell Differentiation and Immune Homeostasis Depend on the Transcription Factor Myb. Immunity. 2017;46(1):78-91.

2. Dehlin M, Bokarewa M, Rottapel R, Foster SJ, Magnusson M, Dahlberg LE, et al. Intra-articular fms-like tyrosine kinase 3 ligand expression is a driving force in induction and progression of arthritis. PLoS One. 2008;3(11):e3633.

3. Caronni N, Simoncello F, Stafetta F, Guarnaccia C, Ruiz-Moreno JS, Opitz B, et al. Downregulation of Membrane Trafficking Proteins and Lactate Conditioning Determine Loss of Dendritic Cell Function in Lung Cancer. Cancer Res. 2018;78(7):1685-99.

This publication represents a fundamental contribution in the study of regulatory T cells during CLL development because it demonstrates for the first time the importance that Tregs have in favouring CLL development. Indeed, in absence of this T cell subtype, CLL development decreases in the adoptive transfer (AT)- CLL model. In addition, it is also demonstrated that Tregs isolated from CLL mice have an enhanced suppression in an antigen-specific manner. These discoveries fully support the data I produced during my PhD, as we observed that Ahr and Hif1a regulate the suppressive function of Tregs. As a result, depleting these two transcription factors in Tregs drastically impacts CLL development in the AT model. It would be very interesting to further characterize regulatory T cells in CLL, analysing the RNA seq results performed in this publication and verifying whether Ahr and Hif1a are overexpressed in Tregs of leukemic mice compared to Tregs of healty mice. Very interestingly, in this publication it is reportated that a specific subpopulation of Tregs (defined as $CD44^{low}$ $CD25^{low}$) are enriched in CLL. These two proteins are consifered an activation and suppression marker, respectively, and we would expect Tregs to express high levels of these proteins during CLL development, due to their enhanced activation and suppressive activity. In order to understand more about this finding, it would be useful to perform a single-cell RNA sequencing of Tregs, as different Treg supopulations are important in the CLL context, and these populations might change during the different stages of CLL development.

Annex III - The B-side of Cancer Immunity: The Underrated Tune.

Anne Largeot #, **Giulia Pagano #**, Susanne Gonder, Etienne Moussay z,* and Jerome Paggetti z,*

Tumor Stroma Interactions, Department of Oncology, Luxembourg Institute of Health, L-1526 Luxenbourg, Luxembourg;

anne.largeot@lih.lu (A.L.); giulia.pagano@lih.lu (G.P.); susanne.gonder@lih.lu (S.G.)

***** Correspondence: etienne.moussay@lih.lu (E.M); jerome.paggetti@lih.lu (J.P.);

Tel.: +35226970-232 (E.M.); +35226970-344 (J.P.)

# These authors contributed equally.

z These authors share senior authorship.

Author Contributions

A.L., **G.P.**, S.G., E.M. and J.P. contributed to the writing of the manuscript and the conception of the figures.

I revised the literature and gave a major contribution in writing and correcting the manuscript. I entirely wrote the chapter 3 “Tumor Microenvironment Factors Influencing B Cells Functions”.

cells

MDPI

Review

The B-Side of Cancer Immunity: The Underrated Tune

Anne Largeot [†], Giulia Pagano [†], Susanne Gonder, Etienne Moussay [‡,*] and Jerome Paggetti [‡,*]

Tumor Stroma Interactions, Department of Oncology, Luxembourg Institute of Health, L-1526 Luxenbourg, Luxembourg; anne.largeot@lih.lu (A.L.); giulia.pagano@lih.lu (G.P.); susanne.gonder@lih.lu (S.G.)

* Correspondence: etienne.moussay@lih.lu (E.M); jerome.paggetti@lih.lu (J.P.); Tel.: +35226970-232 (E.M.); +35226970-344 (J.P.)

† These authors contributed equally.

‡ These authors share senior authorship.

Received: 1 April 2019; Accepted: 10 May 2019; Published: 13 May 2019

Abstract: Tumor-infiltrating lymphocytes are known to be critical in controlling tumor progression. While the role of T lymphocytes has been extensively studied, the function of B cells in this context is still ill-defined. In this review, we propose to explore the role of B cells in tumor immunity. First of all we define their dual role in promoting and inhibiting cancer progression depending on their phenotype. To continue, we describe the influence of different tumor microenvironment factors such as hypoxia on B cells functions and differentiation. Finally, the role of B cells in response to therapy and as potential target is examined. In accordance with the importance of B cells in immuno-oncology, we conclude that more studies are required to throw light on the precise role of B cells in the tumor microenvironment in order to have a better understanding of their functions, and to design new strategies that efficiently target these cells by immunotherapy.

Keywords: B lymphocytes; tumor microenvironment; immunotherapy; tumor immunity; Breg

1. Introduction

Immunity is a complex and finely regulated process which involves the coordinated action of different cell types. B cells (Bursal–derived lymphocytes) are the central players of the humoral immunity through their capacity of immunoglobulins (antibodies) production. In first instance, antigens are recognized by the B cell receptor (BCR) composed of membrane anchored-immunoglobulin and co-receptor molecules. Upon first antigen encounter, naïve mature B cells are turned into activated B cells, capable of proliferation and differentiation into plasma cells (PCs), which produce and release antibodies [1]. Mature B cells are divided into three main subsets: B1 B cells, mainly found in peritoneal and pleural cavities; B2 or follicular (FO) B cells, which are the most abundant and are located in the B cell areas of lymph nodes, Peyer's patches and spleen; and marginal zone (MZ) B cells, sitting in the marginal sinus of the spleen [2]. B cells of different subsets vary in terms of their location and in the way they are activated in a T-dependent or a T-independent way. Polysaccharides or lipidic antigens mostly cause a T-independent response, which leads to the production of short-lived plasma cells. This is the case of B1 and MZ B cells that mostly bind non-proteic antigens. On the other side, the T-dependent response executed by FO B cells (and in some cases by MZ B cells), provides for the presentation of the antigen to follicular T helper cells (Tfh) through MHC class II molecules, which in turn through CD40, IL-21 and IL-4 production, stimulate B cell activation and maturation into short-lived plasma cells [3]. FO B cells can also undergo further maturation in the germinal centers (GCs) where they become either long-lived plasma cells or memory B cells. Contrary to MZ and B-1 B cells, FO B cells produce high affinity antibodies which are very specific to one antigen [4]. Interestingly, B cells play an important role in immunity independently of their antibody production function, particularly through

secretion of cytokines which can affect T cells, dendritic cells (DC), lymphoid tissue reorganization and neogenesis.

A poorly characterized but important B cell subset is represented by regulatory B cells (Bregs), functionally defined by their capacity to inhibit T cell mediated immunity. However, different types of Bregs have been depicted, arising from different B cell subpopulations, making their studies difficult. One of the major hallmark of this population is the production of inhibitory cytokines such as interleukin-10 (IL-10), IL-35 or transforming growth factor beta (TGF-β) [5–7]. For this review, we will consider Bregs as cells which can suppress immunity independently of their phenotype.

In the context of tumor immunity, T cells are widely studied and characterized. Indeed, they attracted the main attention for several reasons: infiltration of cytolytic T cells is associated with good prognosis [8] while regulatory T lymphocytes (Tregs) suppress anti-tumor response [9]. Moreover, the different T cell subpopulations have been well characterized during the last decades both functionally and phenotypically. Notably, current immunotherapies based on the immune checkpoint blockade are designed to target these cells and reactivate the anti-tumor immunity [10]. Despite the great advance that these new therapies represent, a certain number of patients do not benefit from them, and efforts should be made to better understand other immune players in this tumor battlefield in order to develop better alternatives. In some cancer types, B cells represent an important proportion of infiltrating cells, as shown in breast cancer [11–13], epithelial ovarian cancer [14], melanoma [15], non-small-cell lung carcinoma [16,17], renal cell carcinoma [18]. B cells can associate with T cells and organize in tertiary lymphoid structures (TLS) within the tumor, where it is believed that naïve T cells can be activated [19], which highlights the potential role of B cells in modulating anti-tumor immunity. In the majority of cancer types, the infiltration of B cells is associated with a good prognosis [20], as for T cells however, B cells are associated with different activities depending on their phenotype, which does not facilitate their study.

In this review we explore the dual role of B cells in tumor immunity, then depict the tumor microenvironment factors that influence their functions and finally examine the role of B cells in therapy.

2. Role of B Cells in Pro- and Anti-Tumor Immunity

Recently, the importance of B cells in the tumor microenvironment (TME) has been more and more investigated and discussed, which has led to controversial evidences in the field of tumor immunology. The role of B cells in the TME is diverse and besides the secretion of antibodies and cytokines, B cells are able to modulate T cell and innate immune responses and also, recognize antigens, regulate antigen processing and presentation [21]. The balance between B cell subtypes (which are characterized by the expression of specific markers) and their activities affects pro– or anti–tumorigenic function. In light of these contradictory activities, it is thus not surprising that discrepancies are observed when the prognostic value of B cells is studied. Indeed, B cells have been described as being markers of both good and bad prognosis [20]. Here, we will summarize the dual role of the heterogeneous B cell populations in pro- and anti-tumor immunity (Figure 1, Table 1).

Table 1. Overview of the molecules produced by B cells in the context of cancer and their effect on tumor immunity.

Effector Molecules/Mechanism	Function		Reference
	Pro-Tumorigenic	Anti-Tumorigenic	
Antibodies	Circulating immune complexes activate Fcγ receptors on immunosupressive myeloid cells, facilitate angiogenesis	Antibodies against tumor antigens, mediate complement -dependent lysis, ADCC, FcR-mediated phagocytosis, antigen presentation by DCs	[22–25]
Fas/FasL	Bregs inducing apoptosis in $CD4^+$ T cells	Killing of tumor cells	[6]
TRAIL/Apo2L		Killing of tumor cells	[26]

Table 1. *Cont.*

Effector Molecules/Mechanism	Function		Reference
	Pro-Tumorigenic	Anti-Tumorigenic	
IL-10	Produced by Bregs, exacerbate inflammation and support cancer growth, inhibit $CD4^+$ T cells		[5–7,22,23,27]
TGF-β	Convert naïve $CD4^+$ T cells into $Foxp3^+$ Tregs, upregulate reactive oxygen species (ROS) and nitric oxide (NO) in MDSCs		[28]
Granzyme B	Transfer to T cells, degrading the T cell receptor ξ chain without inducing T cell apoptosis	Induce apoptosis in B-chronic lymphocytic leukemia cells	[29,30]
Lymphotoxin	Activates non-canonical and canonical NF-κB signaling and STAT3, inhibitory effect of B cells, survival signals to tumor cells		[27]
IL-35	Stimulates tumor growth		[31]
IFN-y		Facilitate the killing of tumor cells by NK cells, polarize T cells towards Th1 or Th2 response	[5–7]

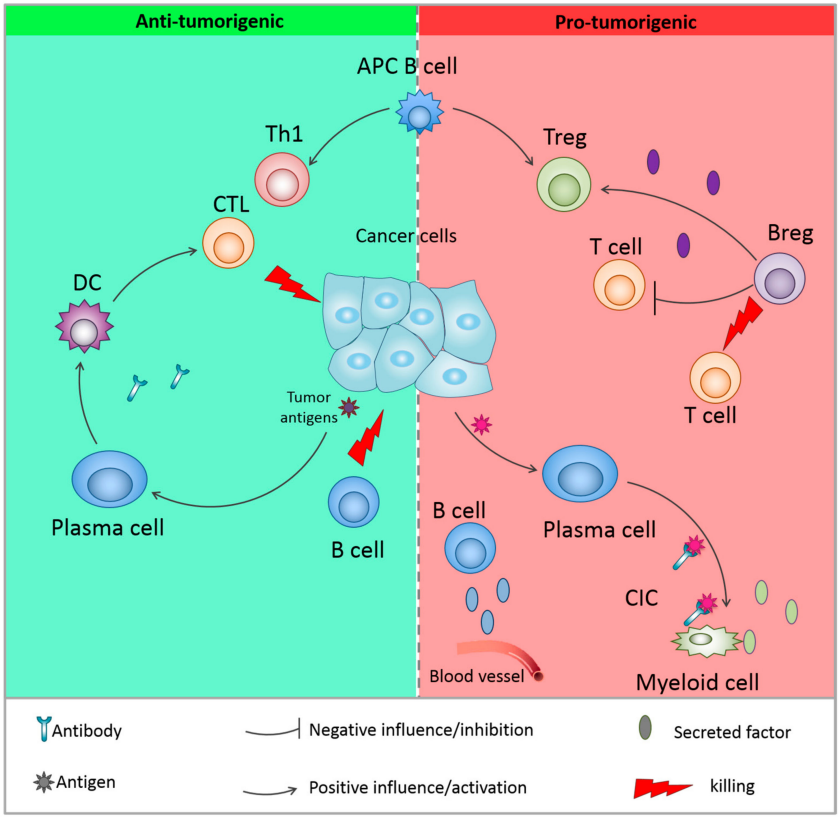

Figure 1. Dual role of B cells in the tumor microenvironment. B cells can have anti-tumor activities through the recognition of tumor-specific antigens and antibody production, antigen presenting cell (APC) function or direct killing of cancer cells. They can also be associated to pro-tumorigenic activities, through activation of myeloid-derived suppression cells (MDSC), production of pro-tumorigenic cytokines and activation of immunosuppressive regulatory T cells. The pro-tumoral activity is mainly mediated by regulatory B cells. DC = dendritic cells; CTL = cytotoxic T cells; Th1 = type 1 T helper cell; APC = antigen presenting cell; CIC: circulating immune complex.

2.1. Anti-Tumor Activity of B Cells

2.1.1. Antibody Production

Tumor cells can trigger a humoral response due to the expression of specific antigens, which can be a consequence of mutations (neoantigens), the overexpression of genes, aberrant post-translational modification, the expression of a specific differentiation marker (for example CD20 in B related lymphoma/leukemia) or the expression of marker normally found in a restricted tissue, such as the Cancer–testis antigens, normally restricted to testis, which are found in melanoma and other tumors [32]. B cell-mediated antibodies production can lead to killing of tumor cells through the complement cascade activation, phagocytosis by macrophages and activation of tumor killing activity of NK [24]. In 2009, Reuschenbach and collaborators exploited published data from 145 articles in order to better describe the humoral response developed against tumor antigens. A majority of the antigens that have been studied were derived from overexpressed or mutated antigens. Nevertheless, as mentioned in this study, it is not clear if antibody production reflects a proper B cell response against the tumor, or is just an irrelevant consequence of exposure to the antigens [33]. However, several lines of experimental evidence tend to support the idea that antibody production could efficiently target and control tumor growth. In vitro–activated B cells obtained from tumor draining lymph nodes produce high quantity of antibodies when co-cultured with tumor cells, which can mediate complement–dependent specific killing of the tumor. When injected in tumor-bearing mice, these cells lead to a regression of the tumor [25]. The injection of tumor specific antibodies induces complement–dependent tumor regression in a model of large cell lung carcinoma [34]. More recently, Carmi et al., using an allogenic tumor rejection model (B16F10 melanoma cells, originated from C57BL/6 mice, injected in 129S1 mice), elegantly demonstrated that B cells-produced antibodies at the very early stage of tumor development activate dendritic cells (DC) which in turn trigger a cytotoxic T cell response to control tumor growth [35].

2.1.2. Other Functions of B Cells

B cells have the capacity to directly kill tumor cells. Indeed, Tao and colleagues showed that $CD19^+$ $IL10^-$ B cells derived from tumor-draining lymph nodes (and in vitro activated) express FASL which triggers the apoptotic signal in 4T1 murine breast cancer cells expressing FAS [6]. This direct killing activity of $CD19^+$ B cells is exacerbated by the production of IL-17A in the TME [36]. Another example of direct cytotoxicity is represented by CpG–activated B cells, which are able of killing cancer cells through TRAIL/Apo-2L–related pathway [26]. Moreover, upon IL-21 stimulation, B cells are capable of producing granzyme B. In chronic lymphocytic leukemia (CLL), IL-21–stimulated leukemic B cells can kill non stimulated ones [30].

In addition, specific B cell subtype expressing B220, CD19 and CD11c can act as antigen presenting cells (APCs) [37,38]. $CD20^+$ B cells can be found in close proximity of T cells in several types of cancer, including when dendritic cells are not present, such as ovarian cancer, which suggest that they can play the role of APC in this case [14]. In non–small–cell lung cancer, infiltrating B cells can act as APC to $CD4^+$ T cells. Interestingly, 2 classes of APCs were identified in this setting: activated ($CD69^+$ $HLA\text{-}DR^+$ $CD27^+$ $CD21^+$) or exhausted ($CD69^+$ $HLA\text{-}DR^+$ $CD27^-$ $CD21^-$), both displaying opposite functions. Whereas the activated B cell APCs were able to induce Th1 differentiation, exhausted ones led to the generation of Tregs [39]. Other B cell functions have been described such as secretion of cytokines, which can trigger an active T cell response. However, there is no evidence that they are associated with anti-tumor activity.

2.2. Pro-Tumor Activity of B Cells

2.2.1. Conventional B Cells

Whereas B cells display anti-tumor activity, mainly sustained by their antibody production function, B cells can also be a crucial mediator of tumor growth. Indeed, circulating immune complexes (CICs) are composed of antibodies bound to a soluble antigen, and these complexes are known to induce inflammation through their recognition by the receptor of the fragment crystallizable region (FcR) [22]. Lisa Coussens' lab demonstrated in a model of epithelium carcinogenesis (K14-HPV16 mice) that CICs produced by B cells, induced chronic inflammation by the activation of myeloid cells *via* engagement of the FcR [22,23]. Furthermore, B cell antibody production in the tumor-draining lymph nodes of melanoma (B16F10) bearing mice promotes tumor growth, which can be dampened by macrophages [40]. In addition to antibody production, Ammirante et al. demonstrated that tumor-infiltrating mature B2 cells ($CD19^+$ $B220^+$ $CD5^-$ $CD11b^-$) produce lymphotoxin (LT) which is crucial for castration-resistant prostate cancer tumor development. Tumor implantation in a mice specifically deficient for LT in B cells is associated with a significant growth delay [27]. Moreover, tumor-associated $CD19^+$ B cells expressing the activated signal transducer and activator of transcription 3 (STAT3) can produce vascular endothelial growth factor (VEGF) at the tumor site, which leads to an increased angiogenesis and supports tumor progression [41].

2.2.2. Regulatory B Cells

Besides the above-mentioned pro-tumorigenic activities, the tumor-promoting ability of B cells is mainly mediated by diverse populations of B cells known as regulatory B cells or Bregs. These cells are functionally defined by their capacity to mediate and maintain immune tolerance. Conventionally, Bregs were defined as $CD5^+$ $CD24^{hi}$ $CD27^+$ $CD38^{hi}$ B cells [42], but in the last few years different types of Bregs have been depicted, arising from different B cell subpopulations. It is also suspected that virtually all B cell subtypes could acquire a regulatory activity upon appropriate stimulation. Furthermore, some of Bregs subpopulations differ between mice and humans, making their characterization even harder. Nevertheless, one of the main feature of Bregs is the production of suppressive cytokines such as IL-10, IL-35 and TGF-β [5–7]. Lindner and colleagues showed that a Breg subset ($CD19^+$ $CD38^+$ $CD1d^+$ IgM^+ $CD147^+$ granzyme B-expressing B cells) suppresses $CD4^+$ T cell proliferation and causes Foxp3 expression in Tregs through secretion of IL-10 and TGF-β. This phenomenon is happening in several types of tumors, in particular in breast, ovarian, colorectal, cervical and prostate carcinomas [29]. In a very recent study performed on acute myeloid leukemia (AML) patients, Bregs are defined as $CD19^+$ $CD24^+$ $CD38^+$. In this work, the authors show that AML patients display a higher frequency of Bregs and the presence of these cells predicts a short survival and poor prognosis [43]. Importantly, among the different phenotypic markers associated with mouse Bregs, immune checkpoints such as PD-1 and PD-L1 were recently pointed out. Xiao et al., described a Breg subset expressing high levels of PD-1 ($PD\text{-}1^{hi}$ Bregs) in human hepatocellular carcinoma (HCC) samples. They showed how this Breg subset is able to suppress T-cell specific antitumor response and to promote tumor development through IL-10 signals [44]. Studying a mouse model of HCC, Shalapour et al. showed that class-switched IL-10-producing B cells are able to inhibit the anti-tumor response mediated by cytotoxic T cells through the interaction between PD-L1 expressed by Bregs and PD-1 expressed by T cells [45]. Olkhanud et al. define a previously undescribed subpopulation of "tumor-evoked" $CD19^+$ $B220^+$ $CD25^+$ B cells (named tBregs) that promotes the development of tumor metastasis in the lungs of a breast cancer mouse model (4T1) [28]. A subpopulation of IL-10-producing $CD19^+$ $CD21^+$ Bregs able to suppress $CD8^+$ IFN-γ^+ T cells was also described in a murine model of skin carcinoma, and the differentiation of these cells is TNF-α–dependent [46]. A recent work by Das and Bar-Sagi demonstrated that Bruton's tyrosine kinase (BTK) is able to promote Bregs differentiation, hence driving pancreatic carcinogenesis [47].

As already mentioned, one of the main feature of Bregs is the production of suppressive cytokines such as IL-10, IL-35 and TGF-β, and/or high level of expression of negative immune checkpoint

molecules such as PD-L1. There are also several mechanisms used by Bregs to inhibit other immune cells, however their functional characterization is limited in the context of cancer. Shao et al. published an interesting work about the role of Bregs in directly promoting HCC development. Through in vivo and in vitro experiments, they observed that Bregs induce HCC cells proliferation, protect them from apoptosis and increase their migration capacities via the CD40/CD154 pathway [48]. Signals leading to differentiation of Bregs are multiple and not fully understood; however, examples of those signals can be find in the next sections.

3. Tumor Microenvironment Factors Influencing B Cells Functions

As discussed in the previous section, different B cell subpopulations can behave differently and have opposing functions. This can explain the dual role of B cells in both promoting cancer progression and anti-tumor immunity. In this section we will discuss the different factors of the TME that can influence these functions (Figure 2). The TME is highly immunosuppressive and a multitude of factors contribute to this status that can be sustained by cell-cell contacts, cytokine production or metabolic factors.

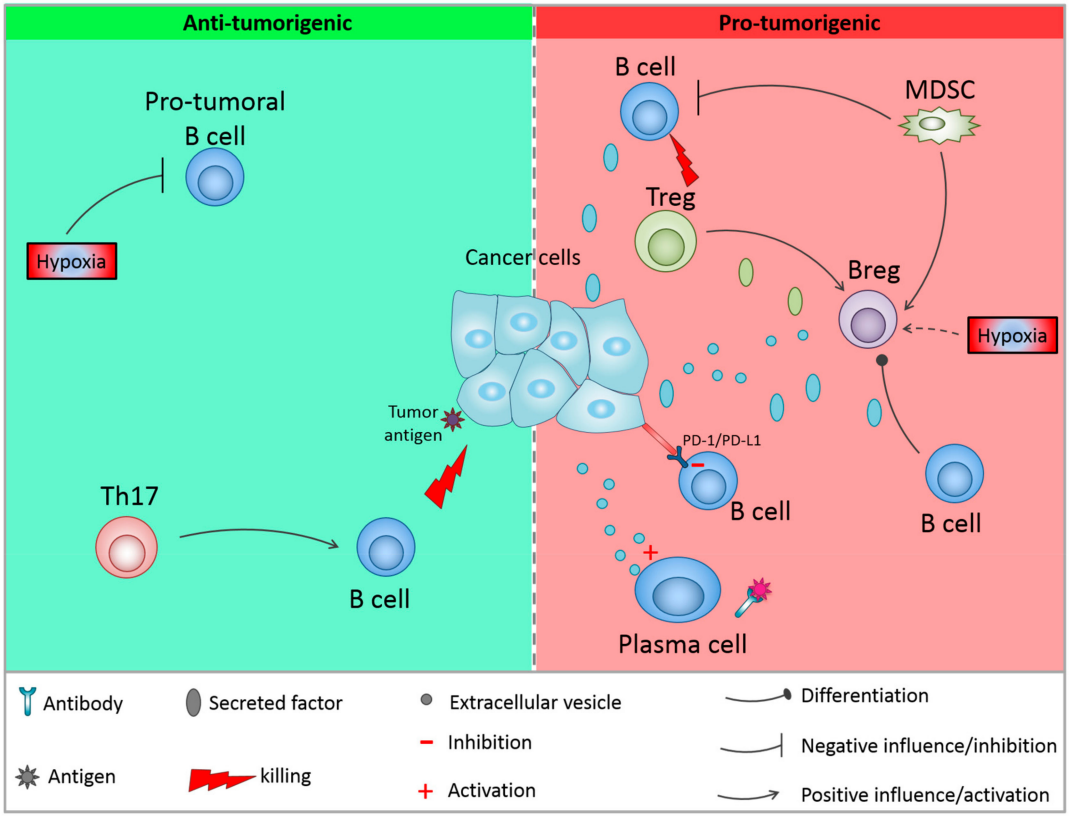

Figure 2. Influence of the microenvironment on B cells functions. Anti-tumor activities can be reinforced by different factors such as hypoxia or IL-17 production by T cells. On the other hand, other immune cells from the microenvironment can activate Bregs and kill anti-tumor B cells. In addition, the tumor cells themselves can influence B cells activity. CTL = cytotoxic T cells; Th17 = IL-17 producing T helper cell; MDSC = myeloid derived suppressive cell.

3.1. Influence of Different TME Cells on B Cell Functions

3.1.1. Immune Cells Component Influencing B Cells

Tregs, which represent major players in tumor evasion, can directly influence B cells. A study performed by Lindner et al. showed that IL-21-producing Tregs found in human breast, ovarian, cervical,

colorectal, and prostate carcinomas, induce $CD19^+$ B cells differentiation into Bregs ($CD19^+$ $CD38^+$ $CD1d^+$ IgM^+ $CD147^+$) expressing IL-10, indoleamine 2,3-dioxygenase 1 (IDO1), and granzyme B (GrB). The transfer of active GrB to T cells promotes the degradation of the T-cell receptor (TCR), which blocks T cell proliferation [29]. In addition, the in vitro study performed by Zhao et al. described how $CD4^+$ $CD25^+$ Tregs, once activated, are able to suppress B cells proliferation by inducing granzyme-dependent cell death, affecting preferentially antigen–pulsed B cells (with APC capacities) [49]. These studies highlight the different behavior of Tregs in promoting B cells pro-tumoral activities by different means. Besides Tregs, other cell types support immune evasion such as myeloid-derived suppressor cells (MDSCs). In a model of breast cancer (4T1–bearing mice), it has been shown that these cells can induce the emergence of a Breg subset expressing PD-L1 but not PD-1 [50]. In addition, MDSCs cells can also impair B cells function through IL-7 secretion which is associated with a decreased antibody production [51]. Notably, different cell types of the TME (T cells, DC, stromal cells, myeloid cells, NK cells) are able to secrete specific cytokines that can target B cells and potentially modulate their activity [52]. On the other hand, the cells found in the TME can also promote the anti-tumor functions of B cells. Interestingly, it has been described that tumor-infiltrating T cells expressing IL-17 can induce B cells migration and increase FAS/FASL–dependent direct tumor cell killing by B cells [36].

3.1.2. Direct Action of Tumor Cells on B Cells

Tumor cells themselves can produce factors, cytokines or metabolites which directly influence B cells. Wejksza and colleagues, demonstrated that metabolites of the arachidonate 5-lipoxygenase (ALOX5) enzyme such as leukotriene B4 (LTB4) can activate the peroxisome proliferator–activated receptor α (PPARα) in B cells, inducing their differentiation in Bregs [53]. Furthermore, human breast cancer cells MDA-MB-231 express high level of chemokine (C-X-C motif) ligand 13 (CXCL13) which enable the migration of C-X-C chemokine receptor type 5 (CXCR5)–expressing B cells to the tumor [54]. Ricciardi et al. showed that co-culture of B cells with the cancer cells MCF7 induces apoptosis of B cells and appearance of a Breg population ($CD56^+$ $CD24^{hi}$ $CD34^{hi}$) only when MCF7 underwent epithelial-to-mesenchymal transition (EMT), a process involved in cancer progression and metastasis and involving broad transcriptional and secretome changes [55]. Regarding melanoma cells, it has been demonstrated that they produce basic fibroblast growth factor (FGF2) which triggers the production of the tumor-supportive insulin-like growth factor 1 (IGF-1) by B cells present in the tumor niche [56]. Besides cytokines or soluble factor secretion, tumor cells communicate with their microenvironment through the secretion of extracellular vesicles (EVs), small structures which allow the trafficking of mRNAs or proteins. EVs derived from several tumor cell lines promote the expansion of a population of regulatory B cells expressing T-cell immunoglobulin and mucin-domain containing-1 (TIM-1) through a Toll-like receptor (TLR) dependent mechanism [57]. In addition, glioblastoma cells produce EVs carrying placenta growth factor (PIGF), which can convert naïve $CD19^+$ B cells into regulatory B cells expressing TGFβ. This effect is antigen dependent as it is restricted to B cells infiltrating the tumor and not to peripheral B cells [58]. In vivo, tumor derived-EVs can induce increased antibody production by $CD19^-$ $CD138^+$ plasma cells in the tumor draining lymph node, which promote tumor growth [40].

3.2. Immune Checkpoint Stimulation on B Cells

One mechanism for tumor-induced immunosuppression is based on the expression of immune checkpoint molecules acting as receptor/ligand, including PD-L1/PD-1, galectin-9/TIM-3, IDO1, lymphocyte-activation gene 3 (LAG-3), and cytotoxic T-lymphocyte-associated protein 4 (CTLA4), which can inhibit the activation of effector lymphocytes. It is well described that PD-L1 is abnormally highly expressed on tumor cells [59]. On the other hand, PD-1 is expressed on a wide range of immune cells, including B cells [60]. When binding to its ligand, PD-1 can activate intracellular signaling pathways and inhibit the activation of B cells [61]. Okazaki et al. proposed a model explaining the PD-1-mediated B cell inhibition. They used a chimeric molecule composed of the extracellular region of the IgG Fc IIB receptor and the intracellular region of PD-1. They found that PD-1 prevented B cell

receptor (BCR) signaling transduction through the recruitment and phosphorylation of tyrosine-protein phosphatase non-receptor type 11 (PTPN11). Once activated, PTPN11 dephosphorylates BCR-signaling molecules such as spleen tyrosine kinase (SYK), and impairs the downstream cascade, causing decrease in activation of phosphoinositide 3-kinase (PI3K), phosphoinositide-specific phospholipase C γ2 (PLCγ2), and extracellular signal–regulated kinases (ERK). This process impacts on calcium release and signaling [62]. In accordance with this work, Haas and colleagues showed that PD-1 interaction with PD-L1 suppresses antigen-specific proliferation of B1-b cells ($B220^{lo}$ $CD19^{hi}$ $CD1d^{int}$ $CD21/35^{lo}$ $CD11b^{+}$ $CD5^{neg\text{-}lo}$) and their secretion of antibodies during T cell independent activation [63]. Moreover, PD-1 prevents the production of antibodies by B cells in a model of immunization against the Thomsen-nouvelle (Tn) antigen in tumor-bearing mice [64].

3.3. Effect of Hypoxia on B Cells

One hallmark of cancer is hypoxia, which is a major difference between tumor and normal tissues [65]. At the tumor site, the cell number increases, immune cells infiltrate the tumor and a general vascular disorganization occurs. All these mechanisms cause an increased oxygen consumption and decreased oxygen supply, leading to a hypoxic condition which affects both the tumor cells and the tumor-infiltrating immune cells. Hypoxia-inducible factors (HIFs) regulate a transcriptional network crucial for the adaptation of cells to this environment, involving metabolism adaptation from oxidative phosphorylation to glycolysis. In tumor cells, HIF induces the secretion of factors that can regulate immune cell recruitment to support tumor growth [66]. In addition, hypoxia and the HIF signaling pathway can modulate metabolism and impact on a wide variety of cellular processes in immune cells [67,68]. The influence of these mechanisms on B cells is poorly elucidated in the context of cancer, however several lines of evidence suggest that hypoxia influences B cells functions. B cell-specific deletion of glucose transporter 1 (Glut1), a HIF-1α target gene, leads to a decrease in B cells proliferation and antibody production capacities [69]. TWIK–related acid–sensitive K^{+} channel 2 (TASK-2) is a potassium channel, the expression of which is controlled by HIF-1α in B cells under hypoxic conditions. TASK-2 hypoxia-dependent expression is correlated with elevated calcium flux, suggesting that this protein could be crucial for B cells functions [70]. An interesting study performed by Meng and colleagues demonstrated that HIF-1α contributes to IL-10 production by $CD1d^{hi}$ $CD5^{+}$ B cells, as it directly regulates IL-10 expression during autoimmune disease [71]. As described previously, IL-10 is one of the key immunosuppressive cytokines released by Bregs within the TME. Hence, the same mechanism may occur in the tumor context, where sustained hypoxia may support the immunosuppressive functions of regulatory B and T lymphocytes. In the context of cancer, it has been reported that HIF-1α stabilization under hypoxic conditions prevents $CD19^{+}$ B cells from colonizing the tumor site and is associated with a slower development of the tumor in the early stage of pancreatic cancer development [72].

4. Role of B Cells in Cancer Therapy

Considering the role of B cells in tumor development, it is not surprising that B cells could also have an impact on cancer therapy. It has been described that B cells could help to predict response to some therapies, or immune-related adverse effect (irAE). In addition, B cells can directly impact the efficiency of some cancer treatments (Figure 3, Table 2). Efforts have been made in order to target these cells, either through their activation or, on the contrary, through their depletion/inhibition (Figure 3, Table 3).

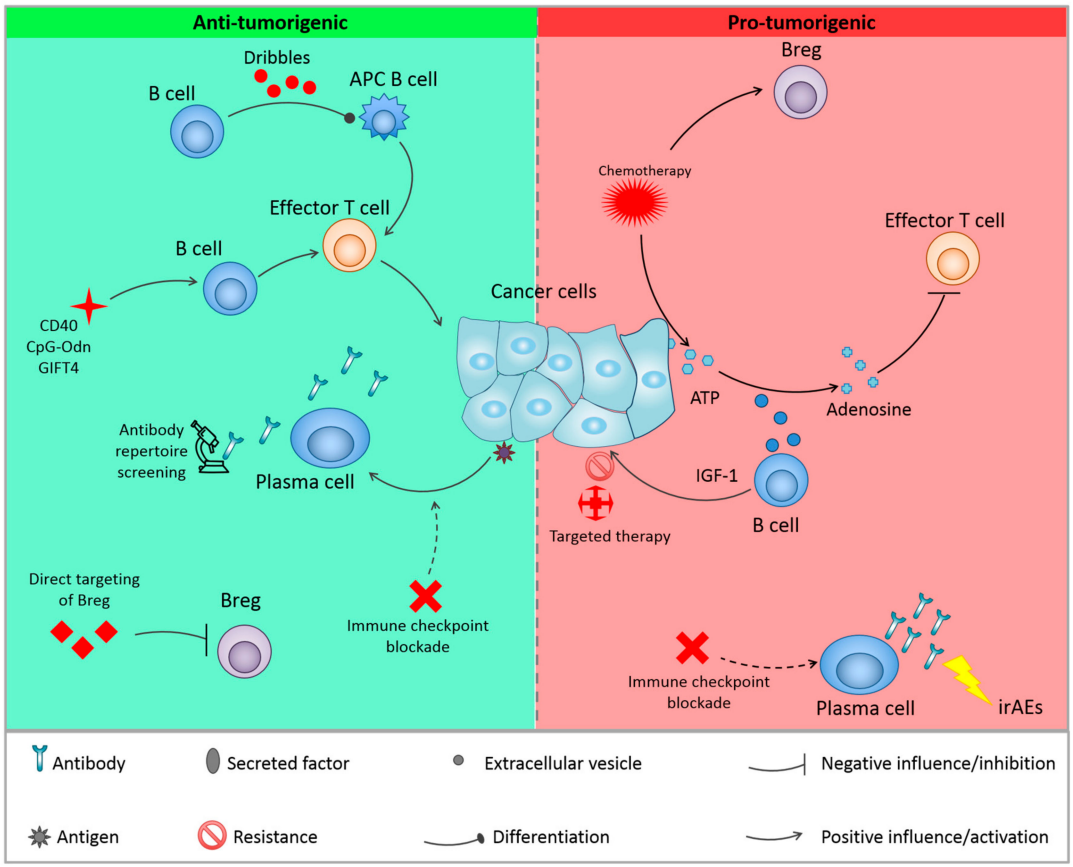

Figure 3. Cancer therapies and B cells. Current therapies can influence B cells functions, leading to resistance to therapy by the activation of Breg, or release of ATP which is converted into adenosine by B cells Extracellular vesicles, leading to the inhibition of T cells. Activation of antibody production is associated with adverse side effects in immunotherapy. On the other hand, other therapies activate anti-tumoral activities of B cells either by activating B cells with anti-tumorigenic functions or by inhibitions of Bregs. APC = antigen presenting cell; irAEs: immune-related adverse effects; IGF-1: insulin-like growth factor 1.

4.1. B Cells in Therapy: Implication in Resistance and Correlation with Response

In addition to their direct effect on tumor cells, chemotherapies induce an immune response, which is triggered by the induction of immunogenic cell death [73]. The tumor immuno-suppressive microenvironment can then impede the efficiency of these therapies. Oxaliplatin treatment was reported to be associated with an increased infiltration of immunosuppressive B cells expressing IgA, IL-10 and PD-L1 in the transgenic adenocarcinoma of the mouse prostate (TRAMP) model of metastatic prostate cancer (PC). In Human, these cells are also found enriched in therapy resistant patients [74]. Squamous cell carcinomas (SCC) are also highly enriched in $CD20^+$ B cells, which are at least in part responsible for the resistance to platinum- (cisplatin and carboplatin) and taxol-based (paclitaxel) chemotherapy as their removal using an anti-CD20 antibody prevents this resistance [75]. Very recently, Zhang et al. elegantly demonstrated that chemotherapy-induced ATP released from damaged tumor cells is hydrolysed into adenosine by B cells-derived EVs in the TME. This elevated rate of adenosine inhibits the activation of effector T cells, preventing efficient response to chemotherapy in mice model of melanoma (B16F10) and colon adenocarcinoma (MC38). In a cohort of colon cancer patients, the authors observed that these CD19+ EVs are associated with bad prognosis and suggested that they could be used as a biomarker for chemotherapy resistance [76]. As opposed to chemotherapy, targeted therapy involves the modulation of specific pathways involved in oncogenic processes, such as signaling kinases. In melanoma, v-Raf murine sarcoma viral oncogene homolog B (BRAF) and

MAPK (mitogen-activated protein kinase)/ERK kinase (MEK) inhibitors are widely used. However, despite high level of initial response rate, a high percentage of patients will develop resistance [77]. Somasundaram and colleagues demonstrated that tumor-associated B cells induce resistance to these inhibitors in vitro through the secretion of IGF-1 and confirmed an increase of CD20 and IGF-1 gene expression in tumor of resistant patients [56].

Immunotherapy constitutes the reactivation of the immune system which is mainly immunosuppressive in the TME [78]. Despite the fact that immunotherapy has revolutionized the field of oncology in the last few years, a high proportion of patients still don't benefit from this advance. Majority of these therapies are designed to target effector T cells. However, it is increasingly clear that B cells can also be affected by these treatments, and that these cells play a role in the response to these therapies. Indeed, pre-existing antibodies against the tumor antigen NY-ESO-1 in the serum of patients with melanoma correlate with an improved clinical benefit following anti-CTLA4 immunotherapy [79]. In the blood of non-progressing patients with different forms of metastatic cancers (melanoma, lung adenocarcinoma, non-small cell lung carcinoma and renal cell carcinoma) treated with immune checkpoint blockade immunotherapy (anti-CTLA4, anti-PD-1) or by chemotherapy, an active humoral immune response could be detected, characterized by somatic hypermutation, IgG class switch and clonal expansion of plasmablast ($CD20^-$ $CD19^+$ $CD38^{hi}$ $CD27^+$ $CD3^-$ $CD14^-$ IgA^- IgM^-). Interestingly, the antibodies produced in these patients recognized antigens found in several types of cancer and across patients [80]. In 2018, Sade-Feldman et al. analyzed at single-cell level the immune microenvironment of melanoma patients responding, or not responding, to immunotherapy by the use of cutting-edge technologies (mass cytometry and single-cell RNA sequencing). They observed an enrichment of B cells in responder patients [81]. These reports suggest a beneficial role of B cell activation for immunotherapy efficiency. However, expression of immune checkpoints is not restricted to T cells, and these molecules are also found at the surface of B cells, like PD-1 [82], CTLA4 [83], or LAG-3 [84,85], implying that the immune checkpoint blockade could directly affect B lymphocytes activity.

The interruption of treatment due to side effect is a major pitfall of immunotherapy. These side effects are known as immune-related adverse effects (irAEs) and they are due to the overactivation of the immune system which can then attack different organs [86]. The prediction of patients who will develop irAEs, and the understanding of the mechanisms involved are viewed as main challenges to bring forward this new class of treatment. Das et al. observed a decrease in the total number of B cells in the blood of melanoma patients treated with combination checkpoint blockade (CCB) therapy (anti-CTLA4 and anti-PD-1 antibodies). However, $CD21^{lo}$ B cells expressing a high level of PD-1 were, in contrast, enriched and activated, and patients with this specific B-cell response have a higher risk to develop irAEs [87]. In melanoma patients treated with bacillus Calmette-Guerin (BCG) followed by CTLA4 blockade, increase in tumor autoantibody repertoire precedes high grade irAEs [88,89]. These results highlight the potential roles played by B cells in immunotherapy side effects, and their potential role as biomarkers.

Table 2. The roles of B cells in response to current therapies are summarized accordingly to the type of therapy and B cell subsets.

Effect	Type of Therapy	B Cell Subtype/Function	Cancer Type/Mouse Model/Cell Line	References
Resistance	Oxaliplatin	IgA^+ $IL10^+$ $PD\text{-}L1^+$	Prostate	[74]
	Platinum/Taxol-based chemotherapy	$CD20^+$	Carcinoma	[75]
	Chemotherapy (oxaliplatin, doxorubicin, phosphoramide mustard, cyclophosphamide	$CD20^+$ EVs	B16F10, MC38	[76]
	BRAF/MEK inhibitor	IGF-1 producing $CD20^+$	B16F10	[56]
Positive impact on response	Anti-CTLA4	Presence of tumor specific antibodies	Melanoma	[79]
	Anti-CTLA4, anti-PD-1, chemotherapy	Somatic hypermutation, IgG class switch, clonal expansion of B cells	Melanoma, lung and renal cell carcinomas	[80]
	immunotherapy	$CD20^+$ enrichment	Melanoma	[81]
Prediction of irAEs	Anti-CTLA4 and anti-PD-1	$CD21^{lo}$ $PD\text{-}1^{hi}$ enrichment	Melanoma	[87]
	BCG + anti-CTLA4	Increase in anti–tumor antibodies repertoire	Melanoma	[88,89]

4.2. Therapies Activating B Cells

The activation of B cells appears to be a promising approach in the fight against cancer, and several strategies have been developed in order to fully unleash the anti-tumor potential of B cells. B cell–based cancer vaccines consist in the stimulation of B cells in order to activate cytotoxic T cells against tumors. In this context, the use of CD40 stimulation has been widely studied. Indeed, the ligation of CD40 with its ligand CD40L induces the expression of co-stimulatory molecules and cytokines, and CD40-activated B cells gain the potential to promote the activation of naïve and memory T cells [90,91]. In addition, it has been shown that these CD40-activated B cells are not sensitive to the immunosuppressive microenvironment [92], and that they can efficiently reach secondary lymphoid organs when injected in vivo, where they can efficiently activate T cells [93]. The potential of these CD40-activated B cells have been tested and validated in vivo in models of Human papillomavirus 16 (HPV16) E6 and E7 expressing TC-1 tumor [94], B16-F10 melanoma, E.G7 lymphoma [95], 4T1 breast tumor metastasis [96], sarcoma [25] and in spontaneous non-Hodgkin's lymphoma in dogs [97]. In conclusion, CD40-activated B cells represent an interesting tool in cancer immunotherapy, and further studies, including clinical trials, should be performed to confirm this potential. Cytosine guanine dinucleotide-oligodeoxynucleotides (CpG-ODN), is a Toll-like receptor 9 (TLR9) ligand that can also be used to activate B cells. In a model of B16-F10 derived lung metastases, injection of CpG-activated B cells induces a regression of metastases and a less immunosuppressive microenvironment [98]. The "fusiokine" GIFT4, is a fusion between GM-CSF and IL-4 cytokines which unexpectedly cluster the respective receptors on B cells and leads to the activation of Janus kinase (JAK)/STAT pathway in these cells. This clustering triggers the proliferation of B cells and their differentiation from naïve B cells to activated helper B cells up-regulating CD19, CD25, CD27, CD40, CD69, MHC class I and II, CD80, CD83 and CD86 expression. These activated B cells act as APCs, secrete cytokines and express co-stimulatory markers, leading to the activation of T cells into cytotoxic T cells. Treatment of mice bearing melanoma with GIFT4 leads to an efficient control of tumor growth. This effect is B cell-dependent as tumors are resistant to GIFT4 in B cell-deficient mice [99]. Otherwise, tumor-derived autophagosomes enriched in defective ribosomal products (DRibbles) can be captured and internalized by B cells. These DRibbles contain tumor specific antigens, and lead to the activation of B cells associated with increased expression of MHC class I and II molecules, CD86 and CD40. These cells can then

present DRibbles-derived antigens to stimulate tumor specific T cell response. The combined injection of DRibbles and DRibble-loaded B cells in mice bearing lymphoma and hepatocellular carcinoma induce the control of tumor growth [100,101].

Antibodies produced by B cells are associated with therapeutic efficiency. Several examples of antibody-based therapies can be cited, with various clinical outcome, some of them targeting directly tumor antigens (anti-CD20 in B-cell related lymphoma/leukemia, anti-HER2 in breast cancer), others having immunomodulatory effects such as the one used for immune checkpoint blockade (anti-CTLA4, anti-PD-1/PDL-1, anti-LAG) (reviews on the subject can be found in [102–104]). Indeed, antibodies have the capacity to activate antibody-dependent cellular cytotoxicity, phagocytosis, and complement-dependent cytotoxicity and can modulate signaling in target cells by activation or inhibition of cell surface receptors [102]. The antibodies produced by B cells found in the tumor and in tumor-draining lymph nodes have in theory the capacity to induce these effects but are certainly produced at too low a concentration to be effective. One strategy under investigation to increase the antibody repertoire available in the clinic aims at identifying tumor–reactive antibodies by the characterization of antibody repertoire of these tumor–infiltrating B cells by screening a phage–display library [105,106] or by next–generation sequencing (NGS) [107–109].

4.3. Therapies Depleting/Inhibiting B Cells

As some B cell populations are associated with pro-tumoral activities, the idea of depleting or inhibiting B cells has also been explored by the scientific community. Anti-CD20 antibodies were initially design for the treatment of autoimmune diseases and B cell lymphomas. However, it became clear that these antibodies could be used to deplete B cells in solid tumors. Depletion of B cells using an anti-CD20 antibody in small cohorts of patients with advanced colon cancer [110], melanoma [111,112], cutaneous T cell lymphoma [113] was associated with health benefit. However, it can also be deleterious in another context. For example, it leads to an increased tumor growth in B16-F10 melanoma bearing mice [114] and in the lung of mice intravenously injected with melanoma B16-F10 cells [98]. In addition, a study reported no clinical benefit in patients with renal cell carcinoma and melanoma treated with anti-CD20 antibody [115]. These contradictory results could be explained by the cell populations targeted by the anti-CD20 antibody. Indeed, it has been reported that these antibodies could efficiently cleared B cells expressing high level of CD20, without affecting cells with a low level of expression, which leads to an enrichment in regulatory B cells and to an even more immunosuppressive environment [116].

It is worth noting that Bruton's tyrosine kinase (BTK) inhibitor ibrutinib used for the treatment of some B cell-associated lymphomas/leukemias has been tested in solid tumors [117]. Indeed, BTK activity is not restricted to B cells, but is also involved in oncogenic pathways in solid tumors, and is activated in myeloid cells, including MDSCs [118]. However, it is clear that BTK activity in these solid tumors could also be at least partially explained by its direct activity on B cells. In that respect, in a mouse model of pancreatic ductal adenocarcinoma, treatment with BTK inhibitor induces a reduction in tumor growth which was associated with a depletion or decreased presence of $IgM^{lo}CD23^{+}CD5^{-}$ follicular and IgM^{lo} $CD23^{-}$ memory B cells [119].

Table 3. The different anti-cancer therapies targeting B cells, either through their activation or on the contrary through their depletion/inhibition are summarized.

Type of Therapy	Target Cells/Effect on B Cells	Consequence	Cancer Type/Animal Model/Cell Line	References
Activation of B cells				
B cell–based vaccine–CD40 dependent activation	$CD19^+$	Activation of T cells, migration to secondary lymphoid organs	HPV16, B16-F10, E.G7, 4T1 metastasis, sarcoma, spontaneous NHL.	[25,92,94–97]
CpG-ODN	$CD19^+$	Metastasis regression, decrease immunosuppressive TME	B16-F10	[98]
GIFT4	Up-regulation of CD25, CD27, CD40, CD69, MHC class I/II, CD80, CD83 and CD86 expression	Activation of CTL	B16-F10	[99]
DRibbles	MHC class I and II molecules, CD86 and CD40	Activation of tumor specific T cells	Lymphoma, HCC	[100,101]
Inhibition/Depletion of B cells				
Anti-CD20 antibody	Depletion of $CD20^+$ cells	Health benefit	colon cancer, melanoma, cutaneous T cell lymphoma	[110–113]
		No effect or deleterious effect	B16-F10 Renal cell carcinoma, melanoma	[98,114–116]
BTK inhibitor	Depletion of IgM^{lo} $CD23^+$ $CD5^-$ and IgM^{lo} $CD23^-$ B cells	Reduction in tumor growth	Pancreatic ductal adenocarcinoma	[117]
CXCL13-CpG-ODN	Depletion of CXCR5+ Bregs	Activation of CTL	4T1	[116]
Anti-IL10 antibody	Inhibition of Bregs	Increase efficiency of CD40-activated B cells	4T1	[6]
Resveratrol	Decrease in Breg number	Block metastasis formation	4T1	[120]
Total glucosides of paeony (TGP)	Decrease in Breg number	Improved survival	HCC	[121]
Lipoxin A4	Inhibition of Breg conversion from naïve B cells	Decrease tumor growth	B16-F10, H22	[122]
MK886	Inhibition of Breg conversion from naïve B cells	Decrease tumor growth	B16-F10	[53]

Specific inhibition of Bregs is perceived as a sensitive way to divert the immunosuppressive TME, without affecting the B cells populations that could be, on the contrary, beneficial for anti-tumor immunity. The Biragyn's lab managed to efficiently deplete CXCR5+ Bregs in vivo by coupling CXCL13 (CXCR5 ligand) to CpG-ODN. After injection in tumor-bearing mice, the number of Bregs was reduced, and in contrast, remaining B cells had the capacity to induce activation of cytotoxic T cells [116]. Another strategy described is the specific inhibition of Bregs with a blocking antibody against IL-10 which leads to an increase efficiency of CD40–activated B cells transfer [6]. Some molecules have also been associated with inhibition of Bregs cells. The phytoalexin resveratrol, which is known to inhibit STAT3 phosphorylation, induces a decreased proportion of Bregs in breast tumor (4T1)–bearing mice and blocks lung metastases formation [120]. It is known that the components of the total glucosides of paeony (TGP), extracted from plant, are important for their anti-inflammatory and immunomodulatory activities. In a model of diethylnitrosamine (DEN)-induced hepatocellular carcinoma in rats, TGP treatment leads to a reduction of nodules and improvement of survival through a reduction of Breg

numbers [121]. Lipoxin A4 (LXA4), a metabolite of the arachidonic acid pathway, inhibits B16F10 melanoma and H22 hepatocarcinoma tumor growth which could be at least partially explained by a decrease in Bregs. In vitro, LXA4 prevents differentiation in Bregs but also Breg-induced Tregs differentiation [122]. Interestingly, another metabolite from this pathway has the opposite effect: the LTB4 is able to induce conversion of naïve B cells into Bregs. MK886, an inhibitor of ALOX5 enzyme, required for LTB4 production, leads to reduced differentiation capacities of B cells into Bregs and control the growth of B16F10 tumors. Transfer of Bregs restores the tumor growth, whereas MK886-treated ones fail to do so [53]. All these molecules represent interesting potential therapeutic approaches in cancer, however their efficiency and mechanism of action need to be attested into more details and in a higher variety of models.

5. Conclusions and Perspectives

B cells tend to be overlooked for their role in the anti–tumor immunity. Nevertheless, they represent fundamental players in the TME, where they can either enhance an efficient immune response by activating cytotoxic T cell response, producing anti-tumor antibodies and cytokines, or inhibit immunity and participating in cancer immune evasion. These contradictory activities are achieved by different B cell populations, which can be induced or on the contrary inhibit in the TME. Interestingly, they are also involved in the response to therapy. In this context, efforts should be done in order to either activate B cells with anti-tumor activities or inhibit the regulatory B cells. In fact, a better understanding of the B cell sub-populations appears to be essential in order to be able to develop new strategies to target them specifically. The identification of specific signaling pathways, expression of cell surface markers and immune checkpoint molecules, or dependency to cytokines could serve as targets for the development of these therapies. In addition, limiting identification of B cell to a single marker (generally CD20 or CD19) when studying prognosis/predictive value of B cells appears to restrict the comprehensive utility of such studies. In this context it is clear that more markers should be included in order to distinguish different B cells populations. In the last few years, with the development of cutting-edge technologies such as mass cytometry or single-cell RNA-sequencing, the fine analysis of immune sub-populations has become possible. In the context of TME, dozens of publications analyzed immune infiltration using these technologies. Unfortunately, the majority of the analyses investigated T or myeloid cells, with very little focus on the B cell populations, even in the case where they represented an important fractions of the immune cells [12–18,81]. The use of these powerful tools should be applied to B lymphocytes, as they remain mysteries that need to be solved in order to fully develop their potential in the fight against cancer.

Author Contributions: A.L., G.P., S.G., E.M. and J.P. contributed to the writing of the manuscript and the conception of the figures.

Funding: This work was supported by grants from FNRS "Télévie" (7.4502.17 and 7.4501.18) and FNR Luxembourg (INTER/DFG/16/11509946).

Conflicts of Interest: The authors declare no conflict of interest.

References

1. Packard, T.A.; Cambier, J.C. B lymphocyte antigen receptor signaling: Initiation, amplification, and regulation. *F1000Prime Rep.* **2013**, *5*, 40. [CrossRef] [PubMed]
2. Allman, D.; Pillai, S. Peripheral B cell subsets. *Curr. Opin. Immunol.* **2008**, *20*, 149–157. [CrossRef] [PubMed]
3. Zubler, R.H. Naive and memory B cells in T-cell-dependent and T-independent responses. *Springer Semin. Immun.* **2001**, *23*, 405–419. [CrossRef]
4. Mesin, L.; Ersching, J.; Victora, G.D. Germinal Center B Cell Dynamics. *Immunity* **2016**, *45*, 471–482. [CrossRef] [PubMed]
5. Sarvaria, A.; Madrigal, J.A.; Saudemont, A. B cell regulation in cancer and anti-tumor immunity. *Cell Mol. Immunol.* **2017**, *14*, 662–674. [CrossRef] [PubMed]

6. Tao, H.; Lu, L.; Xia, Y.; Dai, F.; Wang, Y.; Bao, Y.; Lundy, S.K.; Ito, F.; Pan, Q.; Zhang, X.; et al. Antitumor effector B cells directly kill tumor cells via the Fas/FasL pathway and are regulated by IL-10. *Eur. J. Immunol.* **2015**, *45*, 999–1009. [CrossRef] [PubMed]
7. Schwartz, M.; Zhang, Y.; Rosenblatt, J.D. B cell regulation of the anti-tumor response and role in carcinogenesis. *J. Immunother. Cancer* **2016**, *4*, 40. [CrossRef] [PubMed]
8. Pages, F.; Kirilovsky, A.; Mlecnik, B.; Asslaber, M.; Tosolini, M.; Bindea, G.; Lagorce, C.; Wind, P.; Marliot, F.; Bruneval, P.; et al. In situ cytotoxic and memory T cells predict outcome in patients with early-stage colorectal cancer. *J. Clin. Oncol.* **2009**, *27*, 5944–5951. [CrossRef]
9. Zou, W. Regulatory T cells, tumour immunity and immunotherapy. *Nat. Rev. Immunol.* **2006**, *6*, 295–307. [CrossRef]
10. O'Donnell, J.S.; Teng, M.W.L.; Smyth, M.J. Cancer immunoediting and resistance to T cell-based immunotherapy. *Nat. Rev. Clin. Oncol.* **2019**, *16*, 151–167. [CrossRef]
11. Coronella-Wood, J.A.; Hersh, E.M. Naturally occurring B-cell responses to breast cancer. *Cancer Immunol. Immunother.* **2003**, *52*, 715–738. [CrossRef] [PubMed]
12. Azizi, E.; Carr, A.J.; Plitas, G.; Cornish, A.E.; Konopacki, C.; Prabhakaran, S.; Nainys, J.; Wu, K.; Kiseliovas, V.; Setty, M.; et al. Single-Cell Map of Diverse Immune Phenotypes in the Breast Tumor Microenvironment. *Cell* **2018**, *174*, 1293–1308. [CrossRef] [PubMed]
13. Chung, W.; Eum, H.H.; Lee, H.O.; Lee, K.M.; Lee, H.B.; Kim, K.T.; Ryu, H.S.; Kim, S.; Lee, J.E.; Park, Y.H.; et al. Single-cell RNA-seq enables comprehensive tumour and immune cell profiling in primary breast cancer. *Nat. Commun.* **2017**, *8*, 15081. [CrossRef]
14. Milne, K.; Kobel, M.; Kalloger, S.E.; Barnes, R.O.; Gao, D.; Gilks, C.B.; Watson, P.H.; Nelson, B.H. Systematic analysis of immune infiltrates in high-grade serous ovarian cancer reveals CD20, FoxP3 and TIA-1 as positive prognostic factors. *PLoS ONE* **2009**, *4*, e6412. [CrossRef] [PubMed]
15. Tirosh, I.; Izar, B.; Prakadan, S.M.; Wadsworth, M.H., 2nd; Treacy, D.; Trombetta, J.J.; Rotem, A.; Rodman, C.; Lian, C.; Murphy, G.; et al. Dissecting the multicellular ecosystem of metastatic melanoma by single-cell RNA-seq. *Science* **2016**, *352*, 189–196. [CrossRef]
16. Lambrechts, D.; Wauters, E.; Boeckx, B.; Aibar, S.; Nittner, D.; Burton, O.; Bassez, A.; Decaluwe, H.; Pircher, A.; Van den Eynde, K.; et al. Phenotype molding of stromal cells in the lung tumor microenvironment. *Nat. Med.* **2018**, *24*, 1277–1289. [CrossRef]
17. Lavin, Y.; Kobayashi, S.; Leader, A.; Amir, E.D.; Elefant, N.; Bigenwald, C.; Remark, R.; Sweeney, R.; Becker, C.D.; Levine, J.H.; et al. Innate Immune Landscape in Early Lung Adenocarcinoma by Paired Single-Cell Analyses. *Cell* **2017**, *169*, 750–765. [CrossRef] [PubMed]
18. Chevrier, S.; Levine, J.H.; Zanotelli, V.R.T.; Silina, K.; Schulz, D.; Bacac, M.; Ries, C.H.; Ailles, L.; Jewett, M.A.S.; Moch, H.; et al. An Immune Atlas of Clear Cell Renal Cell Carcinoma. *Cell* **2017**, *169*, 736–749. [CrossRef]
19. Dieu-Nosjean, M.C.; Goc, J.; Giraldo, N.A.; Sautes-Fridman, C.; Fridman, W.H. Tertiary lymphoid structures in cancer and beyond. *Trends Immunol.* **2014**, *35*, 571–580. [CrossRef]
20. Wouters, M.C.A.; Nelson, B.H. Prognostic Significance of Tumor-Infiltrating B Cells and Plasma Cells in Human Cancer. *Clin. Cancer Res.* **2018**, *24*, 6125–6135. [CrossRef] [PubMed]
21. Tsou, P.; Katayama, H.; Ostrin, E.J.; Hanash, S.M. The Emerging Role of B Cells in Tumor Immunity. *Cancer Res.* **2016**, *76*, 5597–5601. [CrossRef]
22. Andreu, P.; Johansson, M.; Affara, N.I.; Pucci, F.; Tan, T.; Junankar, S.; Korets, L.; Lam, J.; Tawfik, D.; DeNardo, D.G.; et al. FcRgamma activation regulates inflammation-associated squamous carcinogenesis. *Cancer Cell* **2010**, *17*, 121–134. [CrossRef] [PubMed]
23. De Visser, K.E.; Korets, L.V.; Coussens, L.M. De novo carcinogenesis promoted by chronic inflammation is B lymphocyte dependent. *Cancer Cell* **2005**, *7*, 411–423. [CrossRef]
24. Yuen, G.J.; Demissie, E.; Pillai, S. B lymphocytes and cancer: A love-hate relationship. *Trends Cancer* **2016**, *2*, 747–757. [CrossRef]
25. Li, Q.; Teitz-Tennenbaum, S.; Donald, E.J.; Li, M.; Chang, A.E. In vivo sensitized and in vitro activated B cells mediate tumor regression in cancer adoptive immunotherapy. *J. Immunol.* **2009**, *183*, 3195–3203. [CrossRef]
26. Kemp, T.J.; Moore, J.M.; Griffith, T.S. Human B cells express functional TRAIL/Apo-2 ligand after CpG-containing oligodeoxynucleotide stimulation. *J. Immunol.* **2004**, *173*, 892–899. [CrossRef] [PubMed]
27. Ammirante, M.; Luo, J.L.; Grivennikov, S.; Nedospasov, S.; Karin, M. B-cell-derived lymphotoxin promotes castration-resistant prostate cancer. *Nature* **2010**, *464*, 302–305. [CrossRef] [PubMed]

28. Olkhanud, P.B.; Damdinsuren, B.; Bodogai, M.; Gress, R.E.; Sen, R.; Wejksza, K.; Malchinkhuu, E.; Wersto, R.P.; Biragyn, A. Tumor-evoked regulatory B cells promote breast cancer metastasis by converting resting CD4(+) T cells to T-regulatory cells. *Cancer Res.* **2011**, *71*, 3505–3515. [CrossRef]
29. Lindner, S.; Dahlke, K.; Sontheimer, K.; Hagn, M.; Kaltenmeier, C.; Barth, T.F.; Beyer, T.; Reister, F.; Fabricius, D.; Lotfi, R.; et al. Interleukin 21-induced granzyme B-expressing B cells infiltrate tumors and regulate T cells. *Cancer Res.* **2013**, *73*, 2468–2479. [CrossRef]
30. Jahrsdorfer, B.; Blackwell, S.E.; Wooldridge, J.E.; Huang, J.; Andreski, M.W.; Jacobus, L.S.; Taylor, C.M.; Weiner, G.J. B-chronic lymphocytic leukemia cells and other B cells can produce granzyme B and gain cytotoxic potential after interleukin-21-based activation. *Blood* **2006**, *108*, 2712–2719. [CrossRef] [PubMed]
31. Pylayeva-Gupta, Y.; Das, S.; Handler, J.S.; Hajdu, C.H.; Coffre, M.; Koralov, S.B.; Bar-Sagi, D. IL35-Producing B Cells Promote the Development of Pancreatic Neoplasia. *Cancer Dis.* **2016**, *6*, 247–255. [CrossRef]
32. Da Gama Duarte, J.; Peyper, J.M.; Blackburn, J.M. B cells and antibody production in melanoma. *Mamm. Genome.* **2018**, *29*, 790–805. [CrossRef]
33. Reuschenbach, M.; von Knebel Doeberitz, M.; Wentzensen, N. A systematic review of humoral immune responses against tumor antigens. *Cancer Immunol. Immunother.* **2009**, *58*, 1535–1544. [CrossRef] [PubMed]
34. Mizukami, M.; Hanagiri, T.; Yasuda, M.; Kuroda, K.; Shigematsu, Y.; Baba, T.; Fukuyama, T.; Nagata, Y.; So, T.; Ichiki, Y.; et al. Antitumor effect of antibody against a SEREX-defined antigen (UOEH-LC-1) on lung cancer xenotransplanted into severe combined immunodeficiency mice. *Cancer Res.* **2007**, *67*, 8351–8357. [CrossRef] [PubMed]
35. Carmi, Y.; Spitzer, M.H.; Linde, I.L.; Burt, B.M.; Prestwood, T.R.; Perlman, N.; Davidson, M.G.; Kenkel, J.A.; Segal, E.; Pusapati, G.V.; et al. Allogeneic IgG combined with dendritic cell stimuli induce antitumour T-cell immunity. *Nature* **2015**, *521*, 99–104. [CrossRef]
36. Lu, L.; Weng, C.; Mao, H.; Fang, X.; Liu, X.; Wu, Y.; Cao, X.; Li, B.; Chen, X.; Gan, Q.; et al. IL-17A promotes migration and tumor killing capability of B cells in esophageal squamous cell carcinoma. *Oncotarget* **2016**, *7*, 21853–21864. [CrossRef]
37. Rubtsov, A.V.; Rubtsova, K.; Kappler, J.W.; Jacobelli, J.; Friedman, R.S.; Marrack, P. CD11c-Expressing B Cells Are Located at the T Cell/B Cell Border in Spleen and Are Potent APCs. *J. Immunol.* **2015**, *195*, 71–79. [CrossRef] [PubMed]
38. Rodriguez-Pinto, D. B cells as antigen presenting cells. *Cell Immunol.* **2005**, *238*, 67–75. [CrossRef] [PubMed]
39. Bruno, T.C.; Ebner, P.J.; Moore, B.L.; Squalls, O.G.; Waugh, K.A.; Eruslanov, E.B.; Singhal, S.; Mitchell, J.D.; Franklin, W.A.; Merrick, D.T.; et al. Antigen-Presenting Intratumoral B Cells Affect CD4(+) TIL Phenotypes in Non-Small Cell Lung Cancer Patients. *Cancer Immunol. Res.* **2017**, *5*, 898–907. [CrossRef]
40. Pucci, F.; Garris, C.; Lai, C.P.; Newton, A.; Pfirschke, C.; Engblom, C.; Alvarez, D.; Sprachman, M.; Evavold, C.; Magnuson, A.; et al. SCS macrophages suppress melanoma by restricting tumor-derived vesicle-B cell interactions. *Science* **2016**, *352*, 242–246. [CrossRef]
41. Yang, C.; Lee, H.; Pal, S.; Jove, V.; Deng, J.; Zhang, W.; Hoon, D.S.; Wakabayashi, M.; Forman, S.; Yu, H. B cells promote tumor progression via STAT3 regulated-angiogenesis. *PLoS ONE* **2013**, *8*, e64159. [CrossRef]
42. Iwata, Y.; Matsushita, T.; Horikawa, M.; Dilillo, D.J.; Yanaba, K.; Venturi, G.M.; Szabolcs, P.M.; Bernstein, S.H.; Magro, C.M.; Williams, A.D.; et al. Characterization of a rare IL-10-competent B-cell subset in humans that parallels mouse regulatory B10 cells. *Blood* **2011**, *117*, 530–541. [CrossRef]
43. Lv, Y.; Wang, H.; Liu, Z. The Role of Regulatory B Cells in Patients with Acute Myeloid Leukemia. *Med. Sci. Monit.* **2019**, *25*, 3026–3031. [CrossRef] [PubMed]
44. Xiao, X.; Lao, X.M.; Chen, M.M.; Liu, R.X.; Wei, Y.; Ouyang, F.Z.; Chen, D.P.; Zhao, X.Y.; Zhao, Q.; Li, X.F.; et al. PD-1hi Identifies a Novel Regulatory B-cell Population in Human Hepatoma That Promotes Disease Progression. *Cancer Dis.* **2016**, *6*, 546–559. [CrossRef]
45. Shalapour, S.; Lin, X.J.; Bastian, I.N.; Brain, J.; Burt, A.D.; Aksenov, A.A.; Vrbanac, A.F.; Li, W.; Perkins, A.; Matsutani, T.; et al. Inflammation-induced IgA+ cells dismantle anti-liver cancer immunity. *Nature* **2017**, *551*, 340–345. [CrossRef] [PubMed]
46. Schioppa, T.; Moore, R.; Thompson, R.G.; Rosser, E.C.; Kulbe, H.; Nedospasov, S.; Mauri, C.; Coussens, L.M.; Balkwill, F.R. B regulatory cells and the tumor-promoting actions of TNF-alpha during squamous carcinogenesis. *Proc. Natl. Acad. Sci. USA* **2011**, *108*, 10662–10667. [CrossRef] [PubMed]
47. Das, S.; Bar-Sagi, D. BTK signaling drives CD1d(hi)CD5(+) regulatory B-cell differentiation to promote pancreatic carcinogenesis. *Oncogene* **2019**. [CrossRef]

48. Shao, Y.; Lo, C.M.; Ling, C.C.; Liu, X.B.; Ng, K.T.; Chu, A.C.; Ma, Y.Y.; Li, C.X.; Fan, S.T.; Man, K. Regulatory B cells accelerate hepatocellular carcinoma progression via CD40/CD154 signaling pathway. *Cancer Lett.* **2014**, *355*, 264–272. [CrossRef]
49. Zhao, D.M.; Thornton, A.M.; DiPaolo, R.J.; Shevach, E.M. Activated CD4+CD25+ T cells selectively kill B lymphocytes. *Blood* **2006**, *107*, 3925–3932. [CrossRef]
50. Shen, M.; Wang, J.; Yu, W.; Zhang, C.; Liu, M.; Wang, K.; Yang, L.; Wei, F.; Wang, S.E.; Sun, Q.; et al. A novel MDSC-induced PD-1(-)PD-L1(+) B-cell subset in breast tumor microenvironment possesses immuno-suppressive properties. *Oncoimmunology* **2018**, *7*, e1413520. [CrossRef]
51. Wang, Y.; Schafer, C.C.; Hough, K.P.; Tousif, S.; Duncan, S.R.; Kearney, J.F.; Ponnazhagan, S.; Hsu, H.C.; Deshane, J.S. Myeloid-Derived Suppressor Cells Impair B Cell Responses in Lung Cancer through IL-7 and STAT5. *J. Immunol.* **2018**, *201*, 278–295. [CrossRef]
52. Lee, S.; Margolin, K. Cytokines in cancer immunotherapy. *Cancers* **2011**, *3*, 3856–3893. [CrossRef] [PubMed]
53. Wejksza, K.; Lee-Chang, C.; Bodogai, M.; Bonzo, J.; Gonzalez, F.J.; Lehrmann, E.; Becker, K.; Biragyn, A. Cancer-produced metabolites of 5-lipoxygenase induce tumor-evoked regulatory B cells via peroxisome proliferator-activated receptor alpha. *J. Immunol.* **2013**, *190*, 2575–2584. [CrossRef]
54. Pimenta, E.M.; De, S.; Weiss, R.; Feng, D.; Hall, K.; Kilic, S.; Bhanot, G.; Ganesan, S.; Ran, S.; Barnes, B.J. IRF5 is a novel regulator of CXCL13 expression in breast cancer that regulates CXCR5(+) B- and T-cell trafficking to tumor-conditioned media. *Immunol. Cell Biol.* **2015**, *93*, 486–499. [CrossRef]
55. Ricciardi, M.; Zanotto, M.; Malpeli, G.; Bassi, G.; Perbellini, O.; Chilosi, M.; Bifari, F.; Krampera, M. Epithelial-to-mesenchymal transition (EMT) induced by inflammatory priming elicits mesenchymal stromal cell-like immune-modulatory properties in cancer cells. *Br. J. Cancer* **2015**, *112*, 1067–1075. [CrossRef]
56. Somasundaram, R.; Zhang, G.; Fukunaga-Kalabis, M.; Perego, M.; Krepler, C.; Xu, X.; Wagner, C.; Hristova, D.; Zhang, J.; Tian, T.; et al. Tumor-associated B-cells induce tumor heterogeneity and therapy resistance. *Nat. Commun.* **2017**, *8*, 607. [CrossRef] [PubMed]
57. Ye, L.; Zhang, Q.; Cheng, Y.; Chen, X.; Wang, G.; Shi, M.; Zhang, T.; Cao, Y.; Pan, H.; Zhang, L.; et al. Tumor-derived exosomal HMGB1 fosters hepatocellular carcinoma immune evasion by promoting TIM-1(+) regulatory B cell expansion. *J. Immunother. Cancer* **2018**, *6*, 145. [CrossRef]
58. Han, S.; Feng, S.; Ren, M.; Ma, E.; Wang, X.; Xu, L.; Xu, M. Glioma cell-derived placental growth factor induces regulatory B cells. *Int. J. Biochem. Cell Biol.* **2014**, *57*, 63–68. [CrossRef]
59. Escors, D.; Gato-Canas, M.; Zuazo, M.; Arasanz, H.; Garcia-Granda, M.J.; Vera, R.; Kochan, G. The intracellular signalosome of PD-L1 in cancer cells. *Signal. Transduct. Target Ther.* **2018**, *3*, 26. [CrossRef]
60. Keir, M.E.; Butte, M.J.; Freeman, G.J.; Sharpe, A.H. PD-1 and its ligands in tolerance and immunity. *Annu. Rev. Immunol.* **2008**, *26*, 677–704. [CrossRef] [PubMed]
61. Nishimura, H.; Minato, N.; Nakano, T.; Honjo, T. Immunological studies on PD-1 deficient mice: Implication of PD-1 as a negative regulator for B cell responses. *Int. Immunol.* **1998**, *10*, 1563–1572. [CrossRef]
62. Okazaki, T.; Maeda, A.; Nishimura, H.; Kurosaki, T.; Honjo, T. PD-1 immunoreceptor inhibits B cell receptor-mediated signaling by recruiting src homology 2-domain-containing tyrosine phosphatase 2 to phosphotyrosine. *Proc. Natl. Acad. Sci. USA* **2001**, *98*, 13866–13871. [CrossRef]
63. Haas, K.M. Programmed cell death 1 suppresses B-1b cell expansion and long-lived IgG production in response to T cell-independent type 2 antigens. *J. Immunol.* **2011**, *187*, 5183–5195. [CrossRef]
64. Haro, M.A.; Littrell, C.A.; Yin, Z.; Huang, X.; Haas, K.M. PD-1 Suppresses Development of Humoral Responses That Protect against Tn-Bearing Tumors. *Cancer Immunol. Res.* **2016**, *4*, 1027–1037. [CrossRef] [PubMed]
65. Balkwill, F.; Mantovani, A. Inflammation and cancer: Back to Virchow? *Lancet* **2001**, *357*, 539–545. [CrossRef]
66. Triner, D.; Shah, Y.M. Hypoxia-inducible factors: A central link between inflammation and cancer. *J. Clin. Investig.* **2016**, *126*, 3689–3698. [CrossRef]
67. Gnanaprakasam, J.N.R.; Sherman, J.W.; Wang, R. MYC and HIF in shaping immune response and immune metabolism. *Cytokine Growth Factor Rev.* **2017**, *35*, 63–70. [CrossRef] [PubMed]
68. Corcoran, S.E.; O'Neill, L.A. HIF1alpha and metabolic reprogramming in inflammation. *J. Clin. Investig.* **2016**, *126*, 3699–3707. [CrossRef] [PubMed]
69. Caro-Maldonado, A.; Wang, R.; Nichols, A.G.; Kuraoka, M.; Milasta, S.; Sun, L.D.; Gavin, A.L.; Abel, E.D.; Kelsoe, G.; Green, D.R.; et al. Metabolic reprogramming is required for antibody production that is suppressed in anergic but exaggerated in chronically BAFF-exposed B cells. *J. Immunol.* **2014**, *192*, 3626–3636. [CrossRef]

70. Shin, D.H.; Lin, H.; Zheng, H.; Kim, K.S.; Kim, J.Y.; Chun, Y.S.; Park, J.W.; Nam, J.H.; Kim, W.K.; Zhang, Y.H.; et al. HIF-1alpha-mediated upregulation of TASK-2 K(+) channels augments Ca(2)(+) signaling in mouse B cells under hypoxia. *J. Immunol.* **2014**, *193*, 4924–4933. [CrossRef] [PubMed]
71. Meng, X.; Grotsch, B.; Luo, Y.; Knaup, K.X.; Wiesener, M.S.; Chen, X.X.; Jantsch, J.; Fillatreau, S.; Schett, G.; Bozec, A. Hypoxia-inducible factor-1alpha is a critical transcription factor for IL-10-producing B cells in autoimmune disease. *Nat. Commun.* **2018**, *9*, 251. [CrossRef] [PubMed]
72. Lee, K.E.; Spata, M.; Bayne, L.J.; Buza, E.L.; Durham, A.C.; Allman, D.; Vonderheide, R.H.; Simon, M.C. Hif1a Deletion Reveals Pro-Neoplastic Function of B Cells in Pancreatic Neoplasia. *Cancer Dis.* **2016**, *6*, 256–269. [CrossRef]
73. Kroemer, G.; Galluzzi, L.; Kepp, O.; Zitvogel, L. Immunogenic cell death in cancer therapy. *Annu. Rev. Immunol.* **2013**, *31*, 51–72. [CrossRef] [PubMed]
74. Shalapour, S.; Font-Burgada, J.; Di Caro, G.; Zhong, Z.; Sanchez-Lopez, E.; Dhar, D.; Willimsky, G.; Ammirante, M.; Strasner, A.; Hansel, D.E.; et al. Immunosuppressive plasma cells impede T-cell-dependent immunogenic chemotherapy. *Nature* **2015**, *521*, 94–98. [CrossRef]
75. Affara, N.I.; Ruffell, B.; Medler, T.R.; Gunderson, A.J.; Johansson, M.; Bornstein, S.; Bergsland, E.; Steinhoff, M.; Li, Y.; Gong, Q.; et al. B cells regulate macrophage phenotype and response to chemotherapy in squamous carcinomas. *Cancer Cell* **2014**, *25*, 809–821. [CrossRef] [PubMed]
76. Zhang, F.; Li, R.; Yang, Y.; Shi, C.; Shen, Y.; Lu, C.; Chen, Y.; Zhou, W.; Lin, A.; Yu, L.; et al. Specific Decrease in B-Cell-Derived Extracellular Vesicles Enhances Post-Chemotherapeutic CD8(+) T Cell Responses. *Immunity* **2019**. [CrossRef]
77. Griffin, M.; Scotto, D.; Josephs, D.H.; Mele, S.; Crescioli, S.; Bax, H.J.; Pellizzari, G.; Wynne, M.D.; Nakamura, M.; Hoffmann, R.M.; et al. BRAF inhibitors: Resistance and the promise of combination treatments for melanoma. *Oncotarget* **2017**, *8*, 78174–78192. [CrossRef] [PubMed]
78. Wierz, M.; Pierson, S.; Guyonnet, L.; Viry, E.; Lequeux, A.; Oudin, A.; Niclou, S.P.; Ollert, M.; Berchem, G.; Janji, B.; et al. Dual PD1/LAG3 immune checkpoint blockade limits tumor development in a murine model of chronic lymphocytic leukemia. *Blood* **2018**, *131*, 1617–1621. [CrossRef]
79. Yuan, J.; Gnjatic, S.; Li, H.; Powel, S.; Gallardo, H.F.; Ritter, E.; Ku, G.Y.; Jungbluth, A.A.; Segal, N.H.; Rasalan, T.S.; et al. CTLA-4 blockade enhances polyfunctional NY-ESO-1 specific T cell responses in metastatic melanoma patients with clinical benefit. *Proc. Natl. Acad. Sci. USA* **2008**, *105*, 20410–20415. [CrossRef]
80. DeFalco, J.; Harbell, M.; Manning-Bog, A.; Baia, G.; Scholz, A.; Millare, B.; Sumi, M.; Zhang, D.; Chu, F.; Dowd, C.; et al. Non-progressing cancer patients have persistent B cell responses expressing shared antibody paratopes that target public tumor antigens. *Clin. Immunol.* **2018**, *187*, 37–45. [CrossRef]
81. Sade-Feldman, M.; Yizhak, K.; Bjorgaard, S.L.; Ray, J.P.; de Boer, C.G.; Jenkins, R.W.; Lieb, D.J.; Chen, J.H.; Frederick, D.T.; Barzily-Rokni, M.; et al. Defining T Cell States Associated with Response to Checkpoint Immunotherapy in Melanoma. *Cell* **2018**, *175*, 998.e1020–1013.e1020. [CrossRef] [PubMed]
82. Thibult, M.L.; Mamessier, E.; Gertner-Dardenne, J.; Pastor, S.; Just-Landi, S.; Xerri, L.; Chetaille, B.; Olive, D. PD-1 is a novel regulator of human B-cell activation. *Int. Immunol.* **2013**, *25*, 129–137. [CrossRef] [PubMed]
83. Kuiper, H.M.; Brouwer, M.; Linsley, P.S.; van Lier, R.A. Activated T cells can induce high levels of CTLA-4 expression on B cells. *J. Immunol.* **1995**, *155*, 1776–1783.
84. Kisielow, M.; Kisielow, J.; Capoferri-Sollami, G.; Karjalainen, K. Expression of lymphocyte activation gene 3 (LAG-3) on B cells is induced by T cells. *Eur. J. Immunol.* **2005**, *35*, 2081–2088. [CrossRef] [PubMed]
85. Lino, A.C.; Dang, V.D.; Lampropoulou, V.; Welle, A.; Joedicke, J.; Pohar, J.; Simon, Q.; Thalmensi, J.; Baures, A.; Fluhler, V.; et al. LAG-3 Inhibitory Receptor Expression Identifies Immunosuppressive Natural Regulatory Plasma Cells. *Immunity* **2018**, *49*, 120–133. [CrossRef] [PubMed]
86. Winer, A.; Bodor, J.N.; Borghaei, H. Identifying and managing the adverse effects of immune checkpoint blockade. *J. Thorac. Dis.* **2018**, *10*, S480–S489. [CrossRef]
87. Das, R.; Bar, N.; Ferreira, M.; Newman, A.M.; Zhang, L.; Bailur, J.K.; Bacchiocchi, A.; Kluger, H.; Wei, W.; Halaban, R.; et al. Early B cell changes predict autoimmunity following combination immune checkpoint blockade. *J. Clin. Investig.* **2018**, *128*, 715–720. [CrossRef] [PubMed]

88. Da Gama Duarte, J.; Parakh, S.; Andrews, M.C.; Woods, K.; Pasam, A.; Tutuka, C.; Ostrouska, S.; Blackburn, J.M.; Behren, A.; Cebon, J. Autoantibodies May Predict Immune-Related Toxicity: Results from a Phase I Study of Intralesional Bacillus Calmette-Guerin followed by Ipilimumab in Patients with Advanced Metastatic Melanoma. *Front. Immunol.* **2018**, *9*, 411. [CrossRef]
89. Gowen, M.F.; Giles, K.M.; Simpson, D.; Tchack, J.; Zhou, H.; Moran, U.; Dawood, Z.; Pavlick, A.C.; Hu, S.; Wilson, M.A.; et al. Baseline antibody profiles predict toxicity in melanoma patients treated with immune checkpoint inhibitors. *J. Trans. Med.* **2018**, *16*, 82. [CrossRef]
90. Ahmadi, T.; Flies, A.; Efebera, Y.; Sherr, D.H. CD40 Ligand-activated, antigen-specific B cells are comparable to mature dendritic cells in presenting protein antigens and major histocompatibility complex class I- and class II-binding peptides. *Immunology* **2008**, *124*, 129–140. [CrossRef]
91. Carpenter, E.L.; Mick, R.; Ruter, J.; Vonderheide, R.H. Activation of human B cells by the agonist CD40 antibody CP-870,893 and augmentation with simultaneous toll-like receptor 9 stimulation. *J. Trans. Med.* **2009**, *7*, 93. [CrossRef]
92. Shimabukuro-Vornhagen, A.; Draube, A.; Liebig, T.M.; Rothe, A.; Kochanek, M.; von Bergwelt-Baildon, M.S. The immunosuppressive factors IL-10, TGF-beta, and VEGF do not affect the antigen-presenting function of CD40-activated B cells. *J. Exp. Clin. Cancer Res.* **2012**, *31*, 47. [CrossRef]
93. Gonzalez, N.K.; Wennhold, K.; Balkow, S.; Kondo, E.; Bolck, B.; Weber, T.; Garcia-Marquez, M.; Grabbe, S.; Bloch, W.; von Bergwelt-Baildon, M.; et al. In vitro and in vivo imaging of initial B-T-cell interactions in the setting of B-cell based cancer immunotherapy. *Oncoimmunology* **2015**, *4*, e1038684. [CrossRef]
94. Rossetti, R.A.M.; Lorenzi, N.P.C.; Yokochi, K.; Rosa, M.; Benevides, L.; Margarido, P.F.R.; Baracat, E.C.; Carvalho, J.P.; Villa, L.L.; Lepique, A.P. B lymphocytes can be activated to act as antigen presenting cells to promote anti-tumor responses. *PLoS ONE* **2018**, *13*, e0199034. [CrossRef]
95. Wennhold, K.; Weber, T.M.; Klein-Gonzalez, N.; Thelen, M.; Garcia-Marquez, M.; Chakupurakal, G.; Fiedler, A.; Schlosser, H.A.; Fischer, R.; Theurich, S.; et al. CD40-activated B cells induce anti-tumor immunity in vivo. *Oncotarget* **2017**, *8*, 27740–27753. [CrossRef] [PubMed]
96. Li, Q.; Lao, X.; Pan, Q.; Ning, N.; Yet, J.; Xu, Y.; Li, S.; Chang, A.E. Adoptive transfer of tumor reactive B cells confers host T-cell immunity and tumor regression. *Clin. Cancer Res.* **2011**, *17*, 4987–4995. [CrossRef]
97. Sorenmo, K.U.; Krick, E.; Coughlin, C.M.; Overley, B.; Gregor, T.P.; Vonderheide, R.H.; Mason, N.J. CD40-activated B cell cancer vaccine improves second clinical remission and survival in privately owned dogs with non-Hodgkin's lymphoma. *PLoS ONE* **2011**, *6*, e24167. [CrossRef] [PubMed]
98. Sorrentino, R.; Morello, S.; Forte, G.; Montinaro, A.; De Vita, G.; Luciano, A.; Palma, G.; Arra, C.; Maiolino, P.; Adcock, I.M.; et al. B cells contribute to the antitumor activity of CpG-oligodeoxynucleotide in a mouse model of metastatic lung carcinoma. *Am. J. Respir. Crit. Care Med.* **2011**, *183*, 1369–1379. [CrossRef] [PubMed]
99. Deng, J.; Yuan, S.; Pennati, A.; Murphy, J.; Wu, J.H.; Lawson, D.; Galipeau, J. Engineered fusokine GIFT4 licenses the ability of B cells to trigger a tumoricidal T-cell response. *Cancer Res.* **2014**, *74*, 4133–4144. [CrossRef] [PubMed]
100. Li, W.; Zhou, M.; Ren, H.; Hu, H.M.; Lu, L.; Cao, M.; Wang, L.X. Tumor-derived autophagosomes (DRibbles) induce B cell activation in a TLR2-MyD88 dependent manner. *PLoS ONE* **2013**, *8*, e53564. [CrossRef]
101. Ren, H.; Zhao, S.; Li, W.; Dong, H.; Zhou, M.; Cao, M.; Hu, H.M.; Wang, L.X. Therapeutic antitumor efficacy of B cells loaded with tumor-derived autophagasomes vaccine (DRibbles). *J. Immunother.* **2014**, *37*, 383–393. [CrossRef] [PubMed]
102. Hendriks, D.; Choi, G.; de Bruyn, M.; Wiersma, V.R.; Bremer, E. Antibody-Based Cancer Therapy: Successful Agents and Novel Approaches. *Int. Rev. Cell Mol. Biol.* **2017**, *331*, 289–383. [CrossRef]
103. Scott, A.M.; Allison, J.P.; Wolchok, J.D. Monoclonal antibodies in cancer therapy. *Cancer Immun.* **2012**, *12*, 14.
104. Scott, A.M.; Wolchok, J.D.; Old, L.J. Antibody therapy of cancer. *Nat. Rev. Cancer* **2012**, *12*, 278–287. [CrossRef]
105. Pavoni, E.; Monteriu, G.; Santapaola, D.; Petronzelli, F.; Anastasi, A.M.; Pelliccia, A.; D'Alessio, V.; De Santis, R.; Minenkova, O. Tumor-infiltrating B lymphocytes as an efficient source of highly specific immunoglobulins recognizing tumor cells. *BMC Biotechnol.* **2007**, *7*, 70. [CrossRef]
106. Kotlan, B.; Simsa, P.; Teillaud, J.L.; Fridman, W.H.; Toth, J.; McKnight, M.; Glassy, M.C. Novel ganglioside antigen identified by B cells in human medullary breast carcinomas: The proof of principle concerning the tumor-infiltrating B lymphocytes. *J. Immunol.* **2005**, *175*, 2278–2285. [CrossRef] [PubMed]

107. Katoh, H.; Komura, D.; Konishi, H.; Suzuki, R.; Yamamoto, A.; Kakiuchi, M.; Sato, R.; Ushiku, T.; Yamamoto, S.; Tatsuno, K.; et al. Immunogenetic Profiling for Gastric Cancers Identifies Sulfated Glycosaminoglycans as Major and Functional B Cell Antigens in Human Malignancies. *Cell Rep.* **2017**, *20*, 1073–1087. [CrossRef] [PubMed]
108. Zhang, W.; Feng, Q.; Wang, C.; Zeng, X.; Du, Y.; Lin, L.; Wu, J.; Fu, L.; Yang, K.; Xu, X.; et al. Characterization of the B Cell Receptor Repertoire in the Intestinal Mucosa and of Tumor-Infiltrating Lymphocytes in Colorectal Adenoma and Carcinoma. *J. Immunol.* **2017**, *198*, 3719–3728. [CrossRef] [PubMed]
109. Robinson, W.H. Sequencing the functional antibody repertoire—Diagnostic and therapeutic discovery. *Nat. Rev. Rheumatol.* **2015**, *11*, 171–182. [CrossRef]
110. Barbera-Guillem, E.; Nelson, M.B.; Barr, B.; Nyhus, J.K.; May, K.F., Jr.; Feng, L.; Sampsel, J.W. B lymphocyte pathology in human colorectal cancer. Experimental and clinical therapeutic effects of partial B cell depletion. *Cancer Immunol. Immunother.* **2000**, *48*, 541–549. [CrossRef]
111. Winkler, J.K.; Schiller, M.; Bender, C.; Enk, A.H.; Hassel, J.C. Rituximab as a therapeutic option for patients with advanced melanoma. *Cancer Immunol. Immunother.* **2018**, *67*, 917–924. [CrossRef]
112. Pinc, A.; Somasundaram, R.; Wagner, C.; Hormann, M.; Karanikas, G.; Jalili, A.; Bauer, W.; Brunner, P.; Grabmeier-Pfistershammer, K.; Gschaider, M.; et al. Targeting CD20 in melanoma patients at high risk of disease recurrence. *Mol. Ther.* **2012**, *20*, 1056–1062. [CrossRef]
113. Theurich, S.; Schlaak, M.; Steguweit, H.; Heukamp, L.C.; Wennhold, K.; Kurschat, P.; Rabenhorst, A.; Hartmann, K.; Schlosser, H.; Shimabukuro-Vornhagen, A.; et al. Targeting Tumor-Infiltrating B Cells in Cutaneous T-Cell Lymphoma. *J. Clin. Oncol.* **2016**, *34*, e110–e116. [CrossRef] [PubMed]
114. DiLillo, D.J.; Yanaba, K.; Tedder, T.F. B cells are required for optimal CD4+ and CD8+ T cell tumor immunity: Therapeutic B cell depletion enhances B16 melanoma growth in mice. *J. Immunol.* **2010**, *184*, 4006–4016. [CrossRef] [PubMed]
115. Aklilu, M.; Stadler, W.M.; Markiewicz, M.; Vogelzang, N.J.; Mahowald, M.; Johnson, M.; Gajewski, T.F. Depletion of normal B cells with rituximab as an adjunct to IL-2 therapy for renal cell carcinoma and melanoma. *Ann. Oncol.* **2004**, *15*, 1109–1114. [CrossRef] [PubMed]
116. Bodogai, M.; Lee Chang, C.; Wejksza, K.; Lai, J.; Merino, M.; Wersto, R.P.; Gress, R.E.; Chan, A.C.; Hesdorffer, C.; Biragyn, A. Anti-CD20 antibody promotes cancer escape via enrichment of tumor-evoked regulatory B cells expressing low levels of CD20 and CD137L. *Cancer Res.* **2013**, *73*, 2127–2138. [CrossRef]
117. Pal Singh, S.; Dammeijer, F.; Hendriks, R.W. Role of Bruton's tyrosine kinase in B cells and malignancies. *Mol. Cancer* **2018**, *17*, 57. [CrossRef] [PubMed]
118. Molina-Cerrillo, J.; Alonso-Gordoa, T.; Gajate, P.; Grande, E. Bruton's tyrosine kinase (BTK) as a promising target in solid tumors. *Cancer Treat Rev.* **2017**, *58*, 41–50. [CrossRef]
119. Gunderson, A.J.; Kaneda, M.M.; Tsujikawa, T.; Nguyen, A.V.; Affara, N.I.; Ruffell, B.; Gorjestani, S.; Liudahl, S.M.; Truitt, M.; Olson, P.; et al. Bruton Tyrosine Kinase-Dependent Immune Cell Cross-talk Drives Pancreas Cancer. *Cancer Dis.* **2016**, *6*, 270–285. [CrossRef]
120. Lee-Chang, C.; Bodogai, M.; Martin-Montalvo, A.; Wejksza, K.; Sanghvi, M.; Moaddel, R.; de Cabo, R.; Biragyn, A. Inhibition of breast cancer metastasis by resveratrol-mediated inactivation of tumor-evoked regulatory B cells. *J. Immunol.* **2013**, *191*, 4141–4151. [CrossRef]
121. Song, S.S.; Yuan, P.F.; Li, P.P.; Wu, H.X.; Ni, W.J.; Lu, J.T.; Wei, W. Protective Effects of Total Glucosides of Paeony on N-nitrosodiethylamine-induced Hepatocellular Carcinoma in Rats via Down-regulation of Regulatory B Cells. *Immunol. Investig.* **2015**, *44*, 521–535. [CrossRef] [PubMed]
122. Wang, Z.; Cheng, Q.; Tang, K.; Sun, Y.; Zhang, K.; Zhang, Y.; Luo, S.; Zhang, H.; Ye, D.; Huang, B. Lipid mediator lipoxin A4 inhibits tumor growth by targeting IL-10-producing regulatory B (Breg) cells. *Cancer Lett.* **2015**, *364*, 118–124. [CrossRef] [PubMed]

In this publication, we described the dual role of B cells in the context of tumor development (as they can have either pro- or anti-tumoral role), while highlighting the need of more studies to throw light on this complex cell type. Interestingly, while for T cells it is very clear the separation between the pro-inflammatory and anti-inflammatory subtypes, for B cells this distinction is not yet clear. Indeed, the same subtypes have been described as protoming and inhibiting tumor development. Moreover, it is important to highlight that regulatory B cells (Bregs), a subtype of B cells with immunoregulatory functions, have a pro-tumoral role and are known to inhibit T cell activity. It would hence be very interesting to further study the crosstalk between Tregs and Bregs in suppressing the anti-tumor immune response. In addition, different studies suggest that CLL cells have a Breg-like phenotype (they share phenotypical and functional characteristics) and negatively control the T-cell activation and immune responses (Mohr *et al*., 2019). By characterizing Bregs and their crosstalk with Tregs, it would be then possible to compare their features and cross-talks with CLL cells and Tregs.

References

1. Abou Khouzam, R., Goutham, H.V., Zaarour, R.F., Chamseddine, A.N., Francis, A., Buart, S., Terry, S., and Chouaib, S. (2020). Integrating tumor hypoxic stress in novel and more adaptable strategies for cancer immunotherapy. Semin Cancer Biol *65*, 140-154.
2. Ahmed, H.A., Maklad, A.M., Khaled, S.A., and Elyamany, A. (2019). Interleukin-27 and interleukin-35 in de novo acute myeloid leukemia: expression and significance as biological markers. J Blood Med *10*, 341-349.
3. Ahn, E., Araki, K., Hashimoto, M., Li, W., Riley, J.L., Cheung, J., Sharpe, A.H., Freeman, G.J., Irving, B.A., and Ahmed, R. (2018). Role of PD-1 during effector CD8 T cell differentiation. Proc Natl Acad Sci U S A *115*, 4749-4754.
4. Ahrends, T., Spanjaard, A., Pilzecker, B., Babala, N., Bovens, A., Xiao, Y., Jacobs, H., and Borst, J. (2017). CD4(+) T Cell Help Confers a Cytotoxic T Cell Effector Program Including Coinhibitory Receptor Downregulation and Increased Tissue Invasiveness. Immunity *47*, 848-861 e845.
5. Al-Ghezi, Z.Z., Singh, N., Mehrpouya-Bahrami, P., Busbee, P.B., Nagarkatti, M., and Nagarkatti, P.S. (2019). AhR Activation by TCDD (2,3,7,8-Tetrachlorodibenzo-p-dioxin) Attenuates Pertussis Toxin-Induced Inflammatory Responses by Differential Regulation of Tregs and Th17 Cells Through Specific Targeting by microRNA. Front Microbiol *10*, 2349.
6. Al-Sawaf, O., Zhang, C., Tandon, M., Sinha, A., Fink, A.M., Robrecht, S., Samoylova, O., Liberati, A.M., Pinilla-Ibarz, J., Opat, S.*, et al.* (2020). Venetoclax plus obinutuzumab versus chlorambucil plus obinutuzumab for previously untreated chronic lymphocytic leukaemia (CLL14): follow-up results from a multicentre, open-label, randomised, phase 3 trial. Lancet Oncol *21*, 1188-1200.
7. Alarcon, B., Mestre, D., and Martinez-Martin, N. (2011). The immunological synapse: a cause or consequence of T-cell receptor triggering? Immunology *133*, 420-425.
8. Allard, B., Longhi, M.S., Robson, S.C., and Stagg, J. (2017). The ectonucleotidases CD39 and CD73: Novel checkpoint inhibitor targets. Immunol Rev *276*, 121-144.
9. Amoah, S., Holbrook, B.C., Yammani, R.D., and Alexander-Miller, M.A. (2013). High viral burden restricts short-lived effector cell number at late times postinfection through increased natural regulatory T cell expansion. J Immunol *190*, 5020-5029.
10. Andersen, M.A., Vojdeman, F.J., Andersen, M.K., Brown Pde, N., Geisler, C.H., Weis Bjerrum, O., and Niemann, C.U. (2016). Hypogammaglobulinemia in newly diagnosed chronic lymphocytic leukemia is a predictor of early death. Leuk Lymphoma *57*, 1592-1599.
11. Anderson, G. (2020). Tumour Microenvironment: Roles of the Aryl Hydrocarbon Receptor, O-GlcNAcylation, Acetyl-CoA and Melatonergic Pathway in Regulating Dynamic Metabolic Interactions across Cell Types-Tumour Microenvironment and Metabolism. Int J Mol Sci *22*.
12. Andritsos, L.A., Byrd, J.C., B., H., Kipps, T.J., D., J., and Burger, J.A. (2010). Preliminary results from a phase I/II dose escalation study to determine the maximum tolerated dose of plerixafor in combination with rituximab in patients with relapsd chronic lymphocytic leukemia. ASH, Abstract 772.
13. Angelin, A., Gil-de-Gómez, L., Dahiya, S., Jiao, J., Guo, L., Levine, M.H., Wang, Z., Quinn, W.J., 3rd, Kopinski, P.K., Wang, L.*, et al.* (2017). Foxp3 Reprograms T Cell Metabolism to Function in Low-Glucose, High-Lactate Environments. Cell Metab *25*, 1282-1293.e1287.
14. Annunziato, F., Cosmi, L., Santarlasci, V., Maggi, L., Liotta, F., Mazzinghi, B., Parente, E., Fili, L., Ferri, S., Frosali, F.*, et al.* (2007). Phenotypic and functional features of human Th17 cells. J Exp Med *204*, 1849-1861.
15. Apert, C., Romagnoli, P., and van Meerwijk, J.P.M. (2018). IL-2 and IL-15 dependent thymic development of Foxp3-expressing regulatory T lymphocytes. Protein Cell *9*, 322-332.
16. Apetoh, L., Quintana, F.J., Pot, C., Joller, N., Xiao, S., Kumar, D., Burns, E.J., Sherr, D.H., Weiner, H.L., and Kuchroo, V.K. (2010). The aryl hydrocarbon receptor interacts with c-Maf to promote the differentiation of type 1 regulatory T cells induced by IL-27. Nat Immunol *11*, 854-861.

17. Arandi, N., Ramzi, M., Safaei, F., and Monabati, A. (2018). Overexpression of indoleamine 2,3-dioxygenase correlates with regulatory T cell phenotype in acute myeloid leukemia patients with normal karyotype. Blood Res *53*, 294-298.
18. Arneth, B. (2019). Tumor Microenvironment. Medicina (Kaunas) *56*.
19. Ashkar, S., Weber, G.F., Panoutsakopoulou, V., Sanchirico, M.E., Jansson, M., Zawaideh, S., Rittling, S.R., Denhardt, D.T., Glimcher, M.J., and Cantor, H. (2000). Eta-1 (osteopontin): an early component of type-1 (cell-mediated) immunity. Science *287*, 860-864.
20. Asslaber, D., Grössinger, E.M., Girbl, T., Hofbauer, S.W., Egle, A., Weiss, L., Greil, R., and Hartmann, T.N. (2013). Mimicking the microenvironment in chronic lymphocytic leukaemia - where does the journey go? Br J Haematol *160*, 711-714.
21. Asslaber, D., Qi, Y., Maeding, N., Steiner, M., Denk, U., Hopner, J.P., Hartmann, T.N., Zaborsky, N., Greil, R., and Egle, A. (2019). B-cell-specific IRF4 deletion accelerates chronic lymphocytic leukemia development by enhanced tumor immune evasion. Blood *134*, 1717-1729.
22. Attaf, M., Legut, M., Cole, D.K., and Sewell, A.K. (2015). The T cell antigen receptor: the Swiss army knife of the immune system. Clin Exp Immunol *181*, 1-18.
23. Bacsi, S.G., and Hankinson, O. (1996). Functional characterization of DNA-binding domains of the subunits of the heterodimeric aryl hydrocarbon receptor complex imputing novel and canonical basic helix-loop-helix protein-DNA interactions. J Biol Chem *271*, 8843-8850.
24. Badoux, X.C., Keating, M.J., Wen, S., Wierda, W.G., O'Brien, S.M., Faderl, S., Sargent, R., Burger, J.A., and Ferrajoli, A. (2013). Phase II study of lenalidomide and rituximab as salvage therapy for patients with relapsed or refractory chronic lymphocytic leukemia. J Clin Oncol *31*, 584-591.
25. Baghban, R., Roshangar, L., Jahanban-Esfahlan, R., Seidi, K., Ebrahimi-Kalan, A., Jaymand, M., Kolahian, S., Javaheri, T., and Zare, P. (2020). Tumor microenvironment complexity and therapeutic implications at a glance. Cell Commun Signal *18*, 59.
26. Bagnara, D., Kaufman, M.S., Calissano, C., Marsilio, S., Patten, P.E., Simone, R., Chum, P., Yan, X.J., Allen, S.L., Kolitz, J.E*., et al.* (2011). A novel adoptive transfer model of chronic lymphocytic leukemia suggests a key role for T lymphocytes in the disease. Blood *117*, 5463-5472.
27. Bailey, S.R., Nelson, M.H., Himes, R.A., Li, Z., Mehrotra, S., and Paulos, C.M. (2014). Th17 cells in cancer: the ultimate identity crisis. Front Immunol *5*, 276.
28. Balachandran, V.P., Cavnar, M.J., Zeng, S., Bamboat, Z.M., Ocuin, L.M., Obaid, H., Sorenson, E.C., Popow, R., Ariyan, C., Rossi, F*., et al.* (2011). Imatinib potentiates antitumor T cell responses in gastrointestinal stromal tumor through the inhibition of Ido. Nat Med *17*, 1094-1100.
29. Balamurugan, K. (2016). HIF-1 at the crossroads of hypoxia, inflammation, and cancer. Int J Cancer *138*, 1058-1066.
30. Baliakas, P., Hadzidimitriou, A., Agathangelidis, A., Rossi, D., Sutton, L.A., Kminkova, J., Scarfo, L., Pospisilova, S., Gaidano, G., Stamatopoulos, K*., et al.* (2015). Prognostic relevance of MYD88 mutations in CLL: the jury is still out. Blood *126*, 1043-1044.
31. Balkhi, M.Y. (2020). Receptor signaling, transcriptional, and metabolic regulation of T cell exhaustion. Oncoimmunology *9*, 1747349.
32. Banerjee, H., Nieves-Rosado, H., Kulkarni, A., Murter, B., McGrath, K.V., Chandran, U.R., Chang, A., Szymczak-Workman, A.L., Vujanovic, L., Delgoffe, G.M*., et al.* (2021). Expression of Tim-3 drives phenotypic and functional changes in Treg cells in secondary lymphoid organs and the tumor microenvironment. Cell Rep *36*, 109699.
33. Barak, A.F., Lewinsky, H., Perpinial, M., Huber, V., Radomir, L., Kramer, M.P., Sever, L., Wolf, Y., Shapiro, M., Herishanu, Y*., et al.* (2020). Bone marrow dendritic cells support the survival of chronic lymphocytic leukemia cells in a CD84 dependent manner. Oncogene *39*, 1997-2008.
34. Barrueto, L., Caminero, F., Cash, L., Makris, C., Lamichhane, P., and Deshmukh, R.R. (2020). Resistance to Checkpoint Inhibition in Cancer Immunotherapy. Transl Oncol *13*, 100738.
35. Bauer, V., Ahmetlic, F., Homberg, N., Geishauser, A., Rocken, M., and Mocikat, R. (2021). Immune checkpoint blockade impairs immunosuppressive mechanisms of regulatory T cells in B-cell lymphoma. Transl Oncol *14*, 101170.

36. Bayati, F., Mohammadi, M., Valadi, M., Jamshidi, S., Foma, A.M., and Sharif-Paghaleh, E. (2020). The Therapeutic Potential of Regulatory T Cells: Challenges and Opportunities. Front Immunol *11*, 585819.
37. Beizavi, Z., Zohouri, M., Asadipour, M., and Ghaderi, A. (2021). IL-27, a pleiotropic cytokine for fine-tuning the immune response in cancer. Int Rev Immunol *40*, 319-329.
38. Beltra, J.C., Manne, S., Abdel-Hakeem, M.S., Kurachi, M., Giles, J.R., Chen, Z., Casella, V., Ngiow, S.F., Khan, O., Huang, Y.J*., et al.* (2020a). Developmental Relationships of Four Exhausted CD8(+) T Cell Subsets Reveals Underlying Transcriptional and Epigenetic Landscape Control Mechanisms. Immunity *52*, 825-841.e828.
39. Beltra, J.C., Manne, S., Abdel-Hakeem, M.S., Kurachi, M., Giles, J.R., Chen, Z., Casella, V., Ngiow, S.F., Khan, O., Huang, Y.J*., et al.* (2020b). Developmental Relationships of Four Exhausted CD8(+) T Cell Subsets Reveals Underlying Transcriptional and Epigenetic Landscape Control Mechanisms. Immunity *52*, 825-841 e828.
40. Ben-Shoshan, J., Maysel-Auslender, S., Mor, A., Keren, G., and George, J. (2008). Hypoxia controls CD4+CD25+ regulatory T-cell homeostasis via hypoxia-inducible factor-1alpha. Eur J Immunol *38*, 2412-2418.
41. Bengsch, B., Johnson, A.L., Kurachi, M., Odorizzi, P.M., Pauken, K.E., Attanasio, J., Stelekati, E., McLane, L.M., Paley, M.A., Delgoffe, G.M*., et al.* (2016). Bioenergetic Insufficiencies Due to Metabolic Alterations Regulated by the Inhibitory Receptor PD-1 Are an Early Driver of CD8(+) T Cell Exhaustion. Immunity *45*, 358-373.
42. Bennett, S.R., Carbone, F.R., Karamalis, F., Flavell, R.A., Miller, J.F., and Heath, W.R. (1998). Help for cytotoxic-T-cell responses is mediated by CD40 signalling. Nature *393*, 478-480.
43. Beyer, M., Kochanek, M., Darabi, K., Popov, A., Jensen, M., Endl, E., Knolle, P.A., Thomas, R.K., von Bergwelt-Baildon, M., Debey, S*., et al.* (2005). Reduced frequencies and suppressive function of CD4+CD25hi regulatory T cells in patients with chronic lymphocytic leukemia after therapy with fludarabine. Blood *106*, 2018-2025.
44. Bianchi-Smiraglia, A., Bagati, A., Fink, E.E., Affronti, H.C., Lipchick, B.C., Moparthy, S., Long, M.D., Rosario, S.R., Lightman, S.M., Moparthy, K*., et al.* (2018). Inhibition of the aryl hydrocarbon receptor/polyamine biosynthesis axis suppresses multiple myeloma. J Clin Invest *128*, 4682-4696.
45. Biancotto, A., Dagur, P.K., Fuchs, J.C., Wiestner, A., Bagwell, C.B., and McCoy, J.P., Jr. (2012). Phenotypic complexity of T regulatory subsets in patients with B-chronic lymphocytic leukemia. Mod Pathol *25*, 246-259.
46. Bichi, R., Shinton, S.A., Martin, E.S., Koval, A., Calin, G.A., Cesari, R., Russo, G., Hardy, R.R., and Croce, C.M. (2002). Human chronic lymphocytic leukemia modeled in mouse by targeted TCL1 expression. Proc Natl Acad Sci U S A *99*, 6955-6960.
47. Bieber, K., Sun, S., Witte, M., Kasprick, A., Beltsiou, F., Behnen, M., Laskay, T., Schulze, F.S., Pipi, E., Reichhelm, N*., et al.* (2017). Regulatory T Cells Suppress Inflammation and Blistering in Pemphigoid Diseases. Front Immunol *8*, 1628.
48. Blackburn, S.D., Shin, H., Haining, W.N., Zou, T., Workman, C.J., Polley, A., Betts, M.R., Freeman, G.J., Vignali, D.A., and Wherry, E.J. (2009). Coregulation of CD8+ T cell exhaustion by multiple inhibitory receptors during chronic viral infection. Nat Immunol *10*, 29-37.
49. Blanco, G., Vardi, A., Puiggros, A., Gomez-Llonin, A., Muro, M., Rodriguez-Rivera, M., Stalika, E., Abella, E., Gimeno, E., Lopez-Sanchez, M*., et al.* (2018). Restricted T cell receptor repertoire in CLL-like monoclonal B cell lymphocytosis and early stage CLL. Oncoimmunology *7*, e1432328.
50. Blumberg, R.S., Alarcon, B., Sancho, J., McDermott, F.V., Lopez, P., Breitmeyer, J., and Terhorst, C. (1990). Assembly and function of the T cell antigen receptor. Requirement of either the lysine or arginine residues in the transmembrane region of the alpha chain. J Biol Chem *265*, 14036-14043.
51. Bock, K.W. (2019). Aryl hydrocarbon receptor (AHR): From selected human target genes and crosstalk with transcription factors to multiple AHR functions. Biochem Pharmacol *168*, 65-70.
52. Boise, L.H., Minn, A.J., Noel, P.J., June, C.H., Accavitti, M.A., Lindsten, T., and Thompson, C.B. (1995). CD28 costimulation can promote T cell survival by enhancing the expression of Bcl-XL. Immunity *3*, 87-98.

53. Borad, M.J., Reddy, S.G., Bahary, N., Uronis, H.E., Sigal, D., Cohn, A.L., Schelman, W.R., Stephenson, J., Jr., Chiorean, E.G., Rosen, P.J.*, et al.* (2015). Randomized Phase II Trial of Gemcitabine Plus TH-302 Versus Gemcitabine in Patients With Advanced Pancreatic Cancer. J Clin Oncol *33*, 1475-1481.
54. Bosch, F., and Dalla-Favera, R. (2019). Chronic lymphocytic leukaemia: from genetics to treatment. Nat Rev Clin Oncol *16*, 684-701.
55. Bosco, M.C., D'Orazi, G., and Del Bufalo, D. (2020). Targeting hypoxia in tumor: a new promising therapeutic strategy. J Exp Clin Cancer Res *39*, 8.
56. Bottcher, M., Bottcher-Loschinski, R., Kahlfuss, S., Aigner, M., Giessl, A., Mackensen, A., Schlotzer-Schrehardt, U., Tuting, T., Bruns, H., and Mougiakakos, D. (2022). CLL-Derived Extracellular Vesicles Impair T-Cell Activation and Foster T-Cell Exhaustion via Multiple Immunological Checkpoints. Cells *11*.
57. Breed, E.R., Lee, S.T., and Hogquist, K.A. (2018). Directing T cell fate: How thymic antigen presenting cells coordinate thymocyte selection. Semin Cell Dev Biol *84*, 2-10.
58. Bresin, A., D'Abundo, L., Narducci, M.G., Fiorenza, M.T., Croce, C.M., Negrini, M., and Russo, G. (2016). TCL1 transgenic mouse model as a tool for the study of therapeutic targets and microenvironment in human B-cell chronic lymphocytic leukemia. Cell Death Dis *7*, e2071.
59. Bromley, S.K., and Dustin, M.L. (2002). Stimulation of naive T-cell adhesion and immunological synapse formation by chemokine-dependent and -independent mechanisms. Immunology *106*, 289-298.
60. Brunkow, M.E., Jeffery, E.W., Hjerrild, K.A., Paeper, B., Clark, L.B., Yasayko, S.A., Wilkinson, J.E., Galas, D., Ziegler, S.F., and Ramsdell, F. (2001). Disruption of a new forkhead/winged-helix protein, scurfin, results in the fatal lymphoproliferative disorder of the scurfy mouse. Nat Genet *27*, 68-73.
61. Budhu, S., Schaer, D.A., Li, Y., Toledo-Crow, R., Panageas, K., Yang, X., Zhong, H., Houghton, A.N., Silverstein, S.C., Merghoub, T.*, et al.* (2017). Blockade of surface-bound TGF-beta on regulatory T cells abrogates suppression of effector T cell function in the tumor microenvironment. Sci Signal *10*.
62. Buggert, M., Tauriainen, J., Yamamoto, T., Frederiksen, J., Ivarsson, M.A., Michaelsson, J., Lund, O., Hejdeman, B., Jansson, M., Sonnerborg, A.*, et al.* (2014). T-bet and Eomes are differentially linked to the exhausted phenotype of CD8+ T cells in HIV infection. PLoS Pathog *10*, e1004251.
63. Burchill, M.A., Yang, J., Vogtenhuber, C., Blazar, B.R., and Farrar, M.A. (2007). IL-2 receptor beta-dependent STAT5 activation is required for the development of Foxp3+ regulatory T cells. J Immunol *178*, 280-290.
64. Burger, J.A. (2011). Nurture versus nature: the microenvironment in chronic lymphocytic leukemia. Hematology Am Soc Hematol Educ Program *2011*, 96-103.
65. Burger, J.A. (2020). Treatment of Chronic Lymphocytic Leukemia. N Engl J Med *383*, 460-473.
66. Burger, J.A., and Chiorazzi, N. (2013). B cell receptor signaling in chronic lymphocytic leukemia. Trends Immunol *34*, 592-601.
67. Burger, J.A., and Gribben, J.G. (2014). The microenvironment in chronic lymphocytic leukemia (CLL) and other B cell malignancies: insight into disease biology and new targeted therapies. Semin Cancer Biol *24*, 71-81.
68. Burger, J.A., Li, K.W., Keating, M.J., Sivina, M., Amer, A.M., Garg, N., Ferrajoli, A., Huang, X., Kantarjian, H., Wierda, W.G.*, et al.* (2017). Leukemia cell proliferation and death in chronic lymphocytic leukemia patients on therapy with the BTK inhibitor ibrutinib. JCI Insight *2*, e89904.
69. Burger, J.A., Tsukada, N., Burger, M., Zvaifler, N.J., Dell'Aquila, M., and Kipps, T.J. (2000). Blood-derived nurse-like cells protect chronic lymphocytic leukemia B cells from spontaneous apoptosis through stromal cell-derived factor-1. Blood *96*, 2655-2663.
70. Burke, K.P., Grebinoski, S., Sharpe, A.H., and Vignali, D.A.A. (2021). Understanding adverse events of immunotherapy: A mechanistic perspective. J Exp Med *218*.
71. Burns, M.C., O'Donnell, A., and Puzanov, I. (2016). Pembrolizumab for the treatment of advanced melanoma. Expert Opin Orphan Drugs *4*, 867-873.

72. Byrd, J.C., Harrington, B., O'Brien, S., Jones, J.A., Schuh, A., Devereux, S., Chaves, J., Wierda, W.G., Awan, F.T., Brown, J.R*., et al.* (2016). Acalabrutinib (ACP-196) in Relapsed Chronic Lymphocytic Leukemia. N Engl J Med *374*, 323-332.
73. Byrne, K.T., and Vonderheide, R.H. (2016). CD40 Stimulation Obviates Innate Sensors and Drives T Cell Immunity in Cancer. Cell Rep *15*, 2719-2732.
74. Cachot, A., Bilous, M., Liu, Y.C., Li, X., Saillard, M., Cenerenti, M., Rockinger, G.A., Wyss, T., Guillaume, P., Schmidt, J*., et al.* (2021). Tumor-specific cytolytic CD4 T cells mediate immunity against human cancer. Sci Adv *7*.
75. Cai, J., Wang, D., Zhang, G., and Guo, X. (2019). The Role Of PD-1/PD-L1 Axis In Treg Development And Function: Implications For Cancer Immunotherapy. Onco Targets Ther *12*, 8437-8445.
76. Calmon-Hamaty, F., Combe, B., Hahne, M., and Morel, J. (2011). Lymphotoxin alpha revisited: general features and implications in rheumatoid arthritis. Arthritis Res Ther *13*, 232.
77. Campesato, L.F., Budhu, S., Tchaicha, J., Weng, C.-H., Gigoux, M., Cohen, I.J., Redmond, D., Mangarin, L., Pourpe, S., Liu, C*., et al.* (2020a). Blockade of the AHR restricts a Treg-macrophage suppressive axis induced by L-Kynurenine. Nature Communications *11*, 4011.
78. Campesato, L.F., Budhu, S., Tchaicha, J., Weng, C.H., Gigoux, M., Cohen, I.J., Redmond, D., Mangarin, L., Pourpe, S., Liu, C*., et al.* (2020b). Blockade of the AHR restricts a Treg-macrophage suppressive axis induced by L-Kynurenine. Nat Commun *11*, 4011.
79. Cao, X., Cai, S.F., Fehniger, T.A., Song, J., Collins, L.I., Piwnica-Worms, D.R., and Ley, T.J. (2007). Granzyme B and perforin are important for regulatory T cell-mediated suppression of tumor clearance. Immunity *27*, 635-646.
80. Carbotti, G., Barisione, G., Airoldi, I., Mezzanzanica, D., Bagnoli, M., Ferrero, S., Petretto, A., Fabbi, M., and Ferrini, S. (2015). IL-27 induces the expression of IDO and PD-L1 in human cancer cells. Oncotarget *6*, 43267-43280.
81. Carenza, C., Calcaterra, F., Oriolo, F., Di Vito, C., Ubezio, M., Della Porta, M.G., Mavilio, D., and Della Bella, S. (2019). Costimulatory Molecules and Immune Checkpoints Are Differentially Expressed on Different Subsets of Dendritic Cells. Front Immunol *10*, 1325.
82. Carl, J.W., and Bai, X.F. (2008). IL27: its roles in the induction and inhibition of inflammation. Int J Clin Exp Pathol *1*, 117-123.
83. Cassioli, C., and Baldari, C.T. (2022). The Expanding Arsenal of Cytotoxic T Cells. Front Immunol *13*, 883010.
84. Castellano, F., Prevost-Blondel, A., Cohen, J.L., and Molinier-Frenkel, V. (2021). What role for AHR activation in IL4I1-mediated immunosuppression ? Oncoimmunology *10*, 1924500.
85. Castellino, F., Huang, A.Y., Altan-Bonnet, G., Stoll, S., Scheinecker, C., and Germain, R.N. (2006). Chemokines enhance immunity by guiding naive CD8+ T cells to sites of CD4+ T cell-dendritic cell interaction. Nature *440*, 890-895.
86. Catakovic, K., Gassner, F.J., Ratswohl, C., Zaborsky, N., Rebhandl, S., Schubert, M., Steiner, M., Gutjahr, J.C., Pleyer, L., Egle, A*., et al.* (2017). TIGIT expressing CD4+T cells represent a tumor-supportive T cell subset in chronic lymphocytic leukemia. Oncoimmunology *7*, e1371399.
87. Catovsky, D., Miliani, E., Okos, A., and Galton, D.A. (1974). Clinical significance of T-cells in chronic lymphocytic leukaemia. Lancet *2*, 751-752.
88. Caudy, A.A., Reddy, S.T., Chatila, T., Atkinson, J.P., and Verbsky, J.W. (2007). CD25 deficiency causes an immune dysregulation, polyendocrinopathy, enteropathy, X-linked-like syndrome, and defective IL-10 expression from CD4 lymphocytes. J Allergy Clin Immunol *119*, 482-487.
89. Chan, W.K., Chu, R., Jain, S., Reddy, J.K., and Bradfield, C.A. (1994). Baculovirus expression of the Ah receptor and Ah receptor nuclear translocater. Evidence for additional dioxin responsive element-binding species and factors required for signaling. J Biol Chem *269*, 26464-26471.
90. Chang, H., Shyu, K.G., Lee, C.C., Tsai, S.C., Wang, B.W., Hsien Lee, Y., and Lin, S. (2003). GL331 inhibits HIF-1alpha expression in a lung cancer model. Biochem Biophys Res Commun *302*, 95-100.
91. Chapoval, S., Dasgupta, P., Dorsey, N.J., and Keegan, A.D. (2010). Regulation of the T helper cell type 2 (Th2)/T regulatory cell (Treg) balance by IL-4 and STAT6. J Leukoc Biol *87*, 1011-1018.

92. Chawla, S.P., Cranmer, L.D., Van Tine, B.A., Reed, D.R., Okuno, S.H., Butrynski, J.E., Adkins, D.R., Hendifar, A.E., Kroll, S., and Ganjoo, K.N. (2014). Phase II study of the safety and antitumor activity of the hypoxia-activated prodrug TH-302 in combination with doxorubicin in patients with advanced soft tissue sarcoma. J Clin Oncol *32*, 3299-3306.
93. Chen, D.S., and Mellman, I. (2013). Oncology meets immunology: the cancer-immunity cycle. Immunity *39*, 1-10.
94. Chen, E.L.Y., Brauer, P.M., Martinez, E.C., Huang, X., Yu, N., Anderson, M.K., Li, Y., and Zuniga-Pflucker, J.C. (2021). Cutting Edge: TCR-beta Selection Is Required at the CD4(+)CD8(+) Stage of Human T Cell Development. J Immunol *206*, 2271-2276.
95. Chen, L., and Flies, D.B. (2013). Molecular mechanisms of T cell co-stimulation and co-inhibition. Nat Rev Immunol *13*, 227-242.
96. Chen, M.L., Pittet, M.J., Gorelik, L., Flavell, R.A., Weissleder, R., von Boehmer, H., and Khazaie, K. (2005). Regulatory T cells suppress tumor-specific CD8 T cell cytotoxicity through TGF-beta signals in vivo. Proc Natl Acad Sci U S A *102*, 419-424.
97. Chen, W., Jin, W., Hardegen, N., Lei, K.J., Li, L., Marinos, N., McGrady, G., and Wahl, S.M. (2003). Conversion of peripheral CD4+CD25- naive T cells to CD4+CD25+ regulatory T cells by TGF-beta induction of transcription factor Foxp3. J Exp Med *198*, 1875-1886.
98. Cheng, G., Yu, A., Dee, M.J., and Malek, T.R. (2013). IL-2R signaling is essential for functional maturation of regulatory T cells during thymic development. J Immunol *190*, 1567-1575.
99. Chigrinova, E., Rinaldi, A., Kwee, I., Rossi, D., Rancoita, P.M., Strefford, J.C., Oscier, D., Stamatopoulos, K., Papadaki, T., Berger, F.*, et al.* (2013). Two main genetic pathways lead to the transformation of chronic lymphocytic leukemia to Richter syndrome. Blood *122*, 2673-2682.
100. Chihara, N., Madi, A., Karwacz, K., Awasthi, A., and Kuchroo, V.K. (2016). Differentiation and Characterization of Tr1 Cells. Curr Protoc Immunol *113*, 3.27.21-23.27.10.
101. Chihara, N., Madi, A., Kondo, T., Zhang, H., Acharya, N., Singer, M., Nyman, J., Marjanovic, N.D., Kowalczyk, M.S., Wang, C.*, et al.* (2018). Induction and transcriptional regulation of the co-inhibitory gene module in T cells. Nature *558*, 454-459.
102. Chilosi, M., Pizzolo, G., Caligaris-Cappio, F., Ambrosetti, A., Vinante, F., Morittu, L., Bonetti, F., Fiore-Donati, L., and Janossy, G. (1985). Immunohistochemical demonstration of follicular dendritic cells in bone marrow involvement of B-cell chronic lymphocytic leukemia. Cancer *56*, 328-332.
103. Chiorazzi, N., and Ferrarini, M. (2011). Cellular origin(s) of chronic lymphocytic leukemia: cautionary notes and additional considerations and possibilities. Blood *117*, 1781-1791.
104. Choudhary, M., and Malek, G. (2020). The Aryl Hydrocarbon Receptor: A Mediator and Potential Therapeutic Target for Ocular and Non-Ocular Neurodegenerative Diseases. Int J Mol Sci *21*.
105. Clambey, E.T., McNamee, E.N., Westrich, J.A., Glover, L.E., Campbell, E.L., Jedlicka, P., de Zoeten, E.F., Cambier, J.C., Stenmark, K.R., Colgan, S.P.*, et al.* (2012). Hypoxia-inducible factor-1 alpha-dependent induction of FoxP3 drives regulatory T-cell abundance and function during inflammatory hypoxia of the mucosa. Proc Natl Acad Sci U S A *109*, E2784-2793.
106. Clever, D., Roychoudhuri, R., Constantinides, M.G., Askenase, M.H., Sukumar, M., Klebanoff, C.A., Eil, R.L., Hickman, H.D., Yu, Z., Pan, J.H.*, et al.* (2016). Oxygen Sensing by T Cells Establishes an Immunologically Tolerant Metastatic Niche. Cell *166*, 1117-1131 e1114.
107. Cocco, C., Giuliani, N., Di Carlo, E., Ognio, E., Storti, P., Abeltino, M., Sorrentino, C., Ponzoni, M., Ribatti, D., and Airoldi, I. (2010). Interleukin-27 acts as multifunctional antitumor agent in multiple myeloma. Clin Cancer Res *16*, 4188-4197.
108. Cocco, C., Pistoia, V., and Airoldi, I. (2012). Anti-leukemic properties of IL-12, IL-23 and IL-27: differences and similarities in the control of pediatric B acute lymphoblastic leukemia. Crit Rev Oncol Hematol *83*, 310-318.
109. Cohan, S.L., Lucassen, E.B., Romba, M.C., and Linch, S.N. (2019). Daclizumab: Mechanisms of Action, Therapeutic Efficacy, Adverse Events and Its Uncovering the Potential Role of Innate Immune System Recruitment as a Treatment Strategy for Relapsing Multiple Sclerosis. Biomedicines *7*.

110. Colamatteo, A., Carbone, F., Bruzzaniti, S., Galgani, M., Fusco, C., Maniscalco, G.T., Di Rella, F., de Candia, P., and De Rosa, V. (2019). Molecular Mechanisms Controlling Foxp3 Expression in Health and Autoimmunity: From Epigenetic to Post-translational Regulation. Front Immunol *10*, 3136.
111. Collins, R.J., Verschuer, L.A., Harmon, B.V., Prentice, R.L., Pope, J.H., and Kerr, J.F. (1989). Spontaneous programmed death (apoptosis) of B-chronic lymphocytic leukaemia cells following their culture in vitro. Br J Haematol *71*, 343-350.
112. Collison, L.W., Workman, C.J., Kuo, T.T., Boyd, K., Wang, Y., Vignali, K.M., Cross, R., Sehy, D., Blumberg, R.S., and Vignali, D.A. (2007). The inhibitory cytokine IL-35 contributes to regulatory T-cell function. Nature *450*, 566-569.
113. Corthay, A., Skovseth, D.K., Lundin, K.U., Rosjo, E., Omholt, H., Hofgaard, P.O., Haraldsen, G., and Bogen, B. (2005). Primary antitumor immune response mediated by CD4+ T cells. Immunity *22*, 371-383.
114. Cox, M.A., Harrington, L.E., and Zajac, A.J. (2011). Cytokines and the inception of CD8 T cell responses. Trends Immunol *32*, 180-186.
115. Cree, I.A. (2022). The WHO Classification of Haematolymphoid Tumours. Leukemia *36*, 1701-1702.
116. Croft, M. (2003). Costimulation of T cells by OX40, 4-1BB, and CD27. Cytokine Growth Factor Rev *14*, 265-273.
117. Crompot, E., Van Damme, M., Pieters, K., Vermeersch, M., Perez-Morga, D., Mineur, P., Maerevoet, M., Meuleman, N., Bron, D., Lagneaux, L.*, et al.* (2017). Extracellular vesicles of bone marrow stromal cells rescue chronic lymphocytic leukemia B cells from apoptosis, enhance their migration and induce gene expression modifications. Haematologica *102*, 1594-1604.
118. Cui, X., Ye, Z., Wang, D., Yang, Y., Jiao, C., Ma, J., Tang, N., and Zhang, H. (2022). Aryl hydrocarbon receptor activation ameliorates experimental colitis by modulating the tolerogenic dendritic and regulatory T cell formation. Cell & Bioscience *12*, 46.
119. Cullen, S.P., and Martin, S.J. (2008). Mechanisms of granule-dependent killing. Cell Death Differ *15*, 251-262.
120. D'Arena, G., Tarnani, M., Rumi, C., Vaisitti, T., Aydin, S., De Filippi, R., Perrone, F., Pinto, A., Chiusolo, P., Deaglio, S.*, et al.* (2007). Prognostic significance of combined analysis of ZAP-70 and CD38 in chronic lymphocytic leukemia. Am J Hematol *82*, 787-791.
121. Damle, R.N., Calissano, C., and Chiorazzi, N. (2010). Chronic lymphocytic leukaemia: a disease of activated monoclonal B cells. Best Pract Res Clin Haematol *23*, 33-45.
122. Dang, E.V., Barbi, J., Yang, H.Y., Jinasena, D., Yu, H., Zheng, Y., Bordman, Z., Fu, J., Kim, Y., Yen, H.R.*, et al.* (2011). Control of T(H)17/T(reg) balance by hypoxia-inducible factor 1. Cell *146*, 772-784.
123. Dant, T.A., Lin, K.L., Bruce, D.W., Montgomery, S.A., Kolupaev, O.V., Bommiasamy, H., Bixby, L.M., Woosley, J.T., McKinnon, K.P., Gonzalez, F.J.*, et al.* (2017). T-cell expression of AhR inhibits the maintenance of pTreg cells in the gastrointestinal tract in acute GVHD. Blood *130*, 348-359.
124. Das, M., Zhu, C., and Kuchroo, V.K. (2017). Tim-3 and its role in regulating anti-tumor immunity. Immunol Rev *276*, 97-111.
125. Davarinos, N.A., and Pollenz, R.S. (1999). Aryl hydrocarbon receptor imported into the nucleus following ligand binding is rapidly degraded via the cytosplasmic proteasome following nuclear export. J Biol Chem *274*, 28708-28715.
126. Dave, V.P. (2011). Role of CD3epsilon-mediated signaling in T-cell development and function. Crit Rev Immunol *31*, 73-84.
127. de Araújo, E.F., Loures, F.V., Preite, N.W., Feriotti, C., Galdino, N.A., Costa, T.A., and Calich, V.L.G. (2021). AhR Ligands Modulate the Differentiation of Innate Lymphoid Cells and T Helper Cell Subsets That Control the Severity of a Pulmonary Fungal Infection. Front Immunol *12*, 630938.
128. De Matteis, S., Molinari, C., Abbati, G., Rossi, T., Napolitano, R., Ghetti, M., Di Rora, A.G.L., Musuraca, G., Lucchesi, A., Rigolin, G.M.*, et al.* (2018). Immunosuppressive Treg cells acquire the phenotype of effector-T cells in chronic lymphocytic leukemia patients. J Transl Med *16*, 172.
129. de Weerdt, I., Hofland, T., de Boer, R., Dobber, J.A., Dubois, J., van Nieuwenhuize, D., Mobasher, M., de Boer, F., Hoogendoorn, M., Velders, G.A.*, et al.* (2019). Distinct immune

composition in lymph node and peripheral blood of CLL patients is reshaped during venetoclax treatment. Blood Adv *3*, 2642-2652.
130. DeLong, J.H., O'Hara Hall, A., Rausch, M., Moodley, D., Perry, J., Park, J., Phan, A.T., Beiting, D.P., Kedl, R.M., Hill, J.A*., et al.* (2019). IL-27 and TCR Stimulation Promote T Cell Expression of Multiple Inhibitory Receptors. Immunohorizons *3*, 13-25.
131. Dengler, V.L., Galbraith, M., and Espinosa, J.M. (2014). Transcriptional regulation by hypoxia inducible factors. Crit Rev Biochem Mol Biol *49*, 1-15.
132. Denison, M.S., and Heath-Pagliuso, S. (1998). The Ah receptor: a regulator of the biochemical and toxicological actions of structurally diverse chemicals. Bull Environ Contam Toxicol *61*, 557-568.
133. Denison, M.S., Pandini, A., Nagy, S.R., Baldwin, E.P., and Bonati, L. (2002). Ligand binding and activation of the Ah receptor. Chem Biol Interact *141*, 3-24.
134. Di Carlo, E., Sorrentino, C., Zorzoli, A., Di Meo, S., Tupone, M.G., Ognio, E., Mincione, G., and Airoldi, I. (2014). The antitumor potential of Interleukin-27 in prostate cancer. Oncotarget *5*, 10332-10341.
135. Di Pilato, M., Kim, E.Y., Cadilha, B.L., Prüßmann, J.N., Nasrallah, M.N., Seruggia, D., Usmani, S.M., Misale, S., Zappulli, V., Carrizosa, E*., et al.* (2019). Targeting the CBM complex causes Treg cells to prime tumours for immune checkpoint therapy. Nature *570*, 112-116.
136. Diakowska, D., Lewandowski, A., Markocka-Mączka, K., and Grabowski, K. (2013). Concentration of serum interleukin-27 increase in patients with lymph node metastatic gastroesophageal cancer. Adv Clin Exp Med *22*, 683-691.
137. DiLillo, D.J., Weinberg, J.B., Yoshizaki, A., Horikawa, M., Bryant, J.M., Iwata, Y., Matsushita, T., Matta, K.M., Chen, Y., Venturi, G.M*., et al.* (2013). Chronic lymphocytic leukemia and regulatory B cells share IL-10 competence and immunosuppressive function. Leukemia *27*, 170-182.
138. Ding, W., LaPlant, B.R., Call, T.G., Parikh, S.A., Leis, J.F., He, R., Shanafelt, T.D., Sinha, S., Le-Rademacher, J., Feldman, A.L*., et al.* (2017). Pembrolizumab in patients with CLL and Richter transformation or with relapsed CLL. Blood *129*, 3419-3427.
139. Diop, F., Moia, R., Favini, C., Spaccarotella, E., De Paoli, L., Bruscaggin, A., Spina, V., Terzi-di-Bergamo, L., Arruga, F., Tarantelli, C*., et al.* (2020). Biological and clinical implications of BIRC3 mutations in chronic lymphocytic leukemia. Haematologica *105*, 448-456.
140. Dobrzanski, M.J. (2013). Expanding roles for CD4 T cells and their subpopulations in tumor immunity and therapy. Front Oncol *3*, 63.
141. Duan, M., Ning, Z., Fu, Z., Zhang, J., Liu, G., Wei, Q., and Zheng, X. (2015). Decreased IL-27 Negatively Correlated with Th17 Cells in Non-Small-Cell Lung Cancer Patients. Mediators Inflamm *2015*, 802939.
142. Duan, Q., Zhang, H., Zheng, J., and Zhang, L. (2020). Turning Cold into Hot: Firing up the Tumor Microenvironment. Trends Cancer *6*, 605-618.
143. Dubois, N., Crompot, E., Meuleman, N., Bron, D., Lagneaux, L., and Stamatopoulos, B. (2020). Importance of Crosstalk Between Chronic Lymphocytic Leukemia Cells and the Stromal Microenvironment: Direct Contact, Soluble Factors, and Extracellular Vesicles. Front Oncol *10*, 1422.
144. Dunn, G.P., Bruce, A.T., Ikeda, H., Old, L.J., and Schreiber, R.D. (2002). Cancer immunoediting: from immunosurveillance to tumor escape. Nat Immunol *3*, 991-998.
145. Eichhorst, B., Fink, A.M., Bahlo, J., Busch, R., Kovacs, G., Maurer, C., Lange, E., Koppler, H., Kiehl, M., Sokler, M*., et al.* (2016). First-line chemoimmunotherapy with bendamustine and rituximab versus fludarabine, cyclophosphamide, and rituximab in patients with advanced chronic lymphocytic leukaemia (CLL10): an international, open-label, randomised, phase 3, non-inferiority trial. Lancet Oncol *17*, 928-942.
146. Ellmeier, W., Sawada, S., and Littman, D.R. (1999). The regulation of CD4 and CD8 coreceptor gene expression during T cell development. Annu Rev Immunol *17*, 523-554.
147. Elston, L., Fegan, C., Hills, R., Hashimdeen, S.S., Walsby, E., Henley, P., Pepper, C., and Man, S. (2020). Increased frequency of CD4+ PD-1+ HLA-DR+ T cells is associated with disease progression in CLL. British Journal of Haematology *188*, 872-880.

148. Esensten, J.H., Helou, Y.A., Chopra, G., Weiss, A., and Bluestone, J.A. (2016). CD28 Costimulation: From Mechanism to Therapy. Immunity *44*, 973-988.
149. Fabbi, M., Carbotti, G., and Ferrini, S. (2017). Dual Roles of IL-27 in Cancer Biology and Immunotherapy. Mediators Inflamm *2017*, 3958069.
150. Facciabene, A., Peng, X., Hagemann, I.S., Balint, K., Barchetti, A., Wang, L.P., Gimotty, P.A., Gilks, C.B., Lal, P., Zhang, L.*, et al.* (2011). Tumour hypoxia promotes tolerance and angiogenesis via CCL28 and T(reg) cells. Nature *475*, 226-230.
151. Faget, J., Biota, C., Bachelot, T., Gobert, M., Treilleux, I., Goutagny, N., Durand, I., Léon-Goddard, S., Blay, J.Y., Caux, C.*, et al.* (2011). Early detection of tumor cells by innate immune cells leads to T(reg) recruitment through CCL22 production by tumor cells. Cancer Res *71*, 6143-6152.
152. Fallah, J., and Rini, B.I. (2019). HIF Inhibitors: Status of Current Clinical Development. Curr Oncol Rep *21*, 6.
153. Famili, F., Wiekmeijer, A.S., and Staal, F.J. (2017). The development of T cells from stem cells in mice and humans. Future Sci OA *3*, FSO186.
154. Fantini, M.C., Becker, C., Monteleone, G., Pallone, F., Galle, P.R., and Neurath, M.F. (2004). Cutting edge: TGF-beta induces a regulatory phenotype in CD4+CD25- T cells through Foxp3 induction and down-regulation of Smad7. J Immunol *172*, 5149-5153.
155. Farinello, D., Wozinska, M., Lenti, E., Genovese, L., Bianchessi, S., Migliori, E., Sacchetti, N., di Lillo, A., Bertilaccio, M.T.S., de Lalla, C.*, et al.* (2018). A retinoic acid-dependent stroma-leukemia crosstalk promotes chronic lymphocytic leukemia progression. Nat Commun *9*, 1787.
156. Ferreira, P.G., Jares, P., Rico, D., Gomez-Lopez, G., Martinez-Trillos, A., Villamor, N., Ecker, S., Gonzalez-Perez, A., Knowles, D.G., Monlong, J.*, et al.* (2014). Transcriptome characterization by RNA sequencing identifies a major molecular and clinical subdivision in chronic lymphocytic leukemia. Genome Res *24*, 212-226.
157. Fischer, K., Al-Sawaf, O., Bahlo, J., Fink, A.M., Tandon, M., Dixon, M., Robrecht, S., Warburton, S., Humphrey, K., Samoylova, O.*, et al.* (2019). Venetoclax and Obinutuzumab in Patients with CLL and Coexisting Conditions. N Engl J Med *380*, 2225-2236.
158. Fischer, K., Bahlo, J., Fink, A.M., Goede, V., Herling, C.D., Cramer, P., Langerbeins, P., von Tresckow, J., Engelke, A., Maurer, C.*, et al.* (2016). Long-term remissions after FCR chemoimmunotherapy in previously untreated patients with CLL: updated results of the CLL8 trial. Blood *127*, 208-215.
159. Fischer, K., Cramer, P., Busch, R., Stilgenbauer, S., Bahlo, J., Schweighofer, C.D., Bottcher, S., Staib, P., Kiehl, M., Eckart, M.J.*, et al.* (2011). Bendamustine combined with rituximab in patients with relapsed and/or refractory chronic lymphocytic leukemia: a multicenter phase II trial of the German Chronic Lymphocytic Leukemia Study Group. J Clin Oncol *29*, 3559-3566.
160. Flinn, I.W., Hillmen, P., Montillo, M., Nagy, Z., Illes, A., Etienne, G., Delgado, J., Kuss, B.J., Tam, C.S., Gasztonyi, Z.*, et al.* (2018). The phase 3 DUO trial: duvelisib vs ofatumumab in relapsed and refractory CLL/SLL. Blood *132*, 2446-2455.
161. Fontenot, J.D., Gavin, M.A., and Rudensky, A.Y. (2003). Foxp3 programs the development and function of CD4+CD25+ regulatory T cells. Nat Immunol *4*, 330-336.
162. Forsythe, J.A., Jiang, B.H., Iyer, N.V., Agani, F., Leung, S.W., Koos, R.D., and Semenza, G.L. (1996). Activation of vascular endothelial growth factor gene transcription by hypoxia-inducible factor 1. Mol Cell Biol *16*, 4604-4613.
163. Francisco, L.M., Salinas, V.H., Brown, K.E., Vanguri, V.K., Freeman, G.J., Kuchroo, V.K., and Sharpe, A.H. (2009). PD-L1 regulates the development, maintenance, and function of induced regulatory T cells. J Exp Med *206*, 3015-3029.
164. Franzin, R., Netti, G.S., Spadaccino, F., Porta, C., Gesualdo, L., Stallone, G., Castellano, G., and Ranieri, E. (2020). The Use of Immune Checkpoint Inhibitors in Oncology and the Occurrence of AKI: Where Do We Stand? Front Immunol *11*, 574271.
165. Freedman, S.J., Sun, Z.Y., Poy, F., Kung, A.L., Livingston, D.M., Wagner, G., and Eck, M.J. (2002). Structural basis for recruitment of CBP/p300 by hypoxia-inducible factor-1 alpha. Proc Natl Acad Sci U S A *99*, 5367-5372.

166. Freudenberg, K., Lindner, N., Dohnke, S., Garbe, A.I., Schallenberg, S., and Kretschmer, K. (2018). Critical Role of TGF-beta and IL-2 Receptor Signaling in Foxp3 Induction by an Inhibitor of DNA Methylation. Front Immunol *9*, 125.
167. Funatake, C.J., Marshall, N.B., Steppan, L.B., Mourich, D.V., and Kerkvliet, N.I. (2005). Cutting edge: activation of the aryl hydrocarbon receptor by 2,3,7,8-tetrachlorodibenzo-p-dioxin generates a population of CD4+ CD25+ cells with characteristics of regulatory T cells. J Immunol *175*, 4184-4188.
168. Furman, R.R., Sharman, J.P., Coutre, S.E., Cheson, B.D., Pagel, J.M., Hillmen, P., Barrientos, J.C., Zelenetz, A.D., Kipps, T.J., Flinn, I.*, et al.* (2014). Idelalisib and rituximab in relapsed chronic lymphocytic leukemia. N Engl J Med *370*, 997-1007.
169. Gabriely, G., Wheeler, M.A., Takenaka, M.C., and Quintana, F.J. (2017). Role of AHR and HIF-1α in Glioblastoma Metabolism. Trends Endocrinol Metab *28*, 428-436.
170. Gagliani, N., Vesely, M.C.A., Iseppon, A., Brockmann, L., Xu, H., Palm, N.W., de Zoete, M.R., Licona-Limón, P., Paiva, R.S., Ching, T.*, et al.* (2015). Th17 cells transdifferentiate into regulatory T cells during resolution of inflammation. Nature *523*, 221-225.
171. Gaidano, G., and Rossi, D. (2017). The mutational landscape of chronic lymphocytic leukemia and its impact on prognosis and treatment. Hematology Am Soc Hematol Educ Program *2017*, 329-337.
172. Galletti, G., Scielzo, C., Barbaglio, F., Rodriguez, T.V., Riba, M., Lazarevic, D., Cittaro, D., Simonetti, G., Ranghetti, P., Scarfo, L.*, et al.* (2016). Targeting Macrophages Sensitizes Chronic Lymphocytic Leukemia to Apoptosis and Inhibits Disease Progression. Cell Rep *14*, 1748-1760.
173. Gambineri, E., Torgerson, T.R., and Ochs, H.D. (2003). Immune dysregulation, polyendocrinopathy, enteropathy, and X-linked inheritance (IPEX), a syndrome of systemic autoimmunity caused by mutations of FOXP3, a critical regulator of T-cell homeostasis. Curr Opin Rheumatol *15*, 430-435.
174. Gandhi, R., Kumar, D., Burns, E.J., Nadeau, M., Dake, B., Laroni, A., Kozoriz, D., Weiner, H.L., and Quintana, F.J. (2010). Activation of the aryl hydrocarbon receptor induces human type 1 regulatory T cell-like and Foxp3(+) regulatory T cells. Nat Immunol *11*, 846-853.
175. Gao, P., Zhang, H., Dinavahi, R., Li, F., Xiang, Y., Raman, V., Bhujwalla, Z.M., Felsher, D.W., Cheng, L., Pevsner, J.*, et al.* (2007). HIF-dependent antitumorigenic effect of antioxidants in vivo. Cancer Cell *12*, 230-238.
176. Garcia-Munoz, R., Roldan Galiacho, V., and Llorente, L. (2012). Immunological aspects in chronic lymphocytic leukemia (CLL) development. Ann Hematol *91*, 981-996.
177. Gargiulo, E., Viry, E., Morande, P.E., Largeot, A., Gonder, S., Xian, F., Ioannou, N., Benzarti, M., Kleine Borgmann, F., Mittelbronn, M.*, et al.* (2022a). S137: SMALL EXTRACELLULAR VESICLES IN THE LEUKEMIA MICROENVIRONMENT SUSTAIN CLL PROGRESSION BY HAMPERING T CELL-MEDIATED ANTI-TUMOR IMMUNITY. HemaSphere *6*, 38-39.
178. Gargiulo, E., Viry, E., Morande, P.E., Largeot, A., Gonder, S., Xian, F., Ioannou, N., Benzarti, M., Kleine Borgmann, F.B., Mittelbronn, M.*, et al.* (2022b). Extracellular vesicle secretion by leukemia cells in vivo promotes CLL progression by hampering antitumor T-cell responses. Blood Cancer Discov.
179. Gascoigne, N.R. (2008). Do T cells need endogenous peptides for activation? Nat Rev Immunol *8*, 895-900.
180. Gasiewicz, T.A., Singh, K.P., and Bennett, J.A. (2014). The Ah receptor in stem cell cycling, regulation, and quiescence. Ann N Y Acad Sci *1310*, 44-50.
181. Gaudino, S.J., and Kumar, P. (2019). Cross-Talk Between Antigen Presenting Cells and T Cells Impacts Intestinal Homeostasis, Bacterial Infections, and Tumorigenesis. Front Immunol *10*, 360.
182. Georgiev, P., Charbonnier, L.M., and Chatila, T.A. (2019). Regulatory T Cells: the Many Faces of Foxp3. J Clin Immunol *39*, 623-640.
183. Germain, R.N. (2002). T-cell development and the CD4-CD8 lineage decision. Nat Rev Immunol *2*, 309-322.

184. Gerriets, V.A., Kishton, R.J., Johnson, M.O., Cohen, S., Siska, P.J., Nichols, A.G., Warmoes, M.O., de Cubas, A.A., MacIver, N.J., Locasale, J.W.*, et al.* (2016). Foxp3 and Toll-like receptor signaling balance Treg cell anabolic metabolism for suppression. Nat Immunol *17*, 1459-1466.
185. Ghia, P., Pluta, A., Wach, M., Lysak, D., Kozak, T., Simkovic, M., Kaplan, P., Kraychok, I., Illes, A., de la Serna, J.*, et al.* (2020). ASCEND: Phase III, Randomized Trial of Acalabrutinib Versus Idelalisib Plus Rituximab or Bendamustine Plus Rituximab in Relapsed or Refractory Chronic Lymphocytic Leukemia. J Clin Oncol *38*, 2849-2861.
186. Ghosh, A.K., Shanafelt, T.D., Cimmino, A., Taccioli, C., Volinia, S., Liu, C.G., Calin, G.A., Croce, C.M., Chan, D.A., Giaccia, A.J.*, et al.* (2009). Aberrant regulation of pVHL levels by microRNA promotes the HIF/VEGF axis in CLL B cells. Blood *113*, 5568-5574.
187. Giannopoulos, K., Schmitt, M., Wlasiuk, P., Chen, J., Bojarska-Junak, A., Kowal, M., Rolinski, J., and Dmoszynska, A. (2008). The high frequency of T regulatory cells in patients with B-cell chronic lymphocytic leukemia is diminished through treatment with thalidomide. Leukemia *22*, 222-224.
188. Gladstone, D.E., and Fuchs, E. (2012). Hematopoietic stem cell transplantation for chronic lymphocytic leukemia. Curr Opin Oncol *24*, 176-181.
189. Goettel, J.A., Gandhi, R., Kenison, J.E., Yeste, A., Murugaiyan, G., Sambanthamoorthy, S., Griffith, A.E., Patel, B., Shouval, D.S., Weiner, H.L.*, et al.* (2016). AHR Activation Is Protective against Colitis Driven by T Cells in Humanized Mice. Cell Rep *17*, 1318-1329.
190. Gonder, S., Largeot, A., Gargiulo, E., Pierson, S., Fernandez Botana, I., Pagano, G., Paggetti, J., and Moussay, E. (2021). The Tumor Microenvironment-Dependent Transcription Factors AHR and HIF-1alpha Are Dispensable for Leukemogenesis in the Emicro-TCL1 Mouse Model of Chronic Lymphocytic Leukemia. Cancers (Basel) *13*.
191. Gonin, J., Carlotti, A., Dietrich, C., Audebourg, A., Radenen-Bussière, B., Caignard, A., Avril, M.F., Vacher-Lavenu, M.C., Larousserie, F., and Devergne, O. (2013). Expression of IL-27 by tumor cells in invasive cutaneous and metastatic melanomas [corrected]. PLoS One *8*, e75694.
192. Goral, A., Firczuk, M., Fidyt, K., Sledz, M., Simoncello, F., Siudakowska, K., Pagano, G., Moussay, E., Paggetti, J., Nowakowska, P.*, et al.* (2022). A Specific CD44lo CD25lo Subpopulation of Regulatory T Cells Inhibits Anti-Leukemic Immune Response and Promotes the Progression in a Mouse Model of Chronic Lymphocytic Leukemia. Front Immunol *13*, 781364.
193. Gorelik, L., and Flavell, R.A. (2000). Abrogation of TGFbeta signaling in T cells leads to spontaneous T cell differentiation and autoimmune disease. Immunity *12*, 171-181.
194. Gorgun, G., Holderried, T.A., Zahrieh, D., Neuberg, D., and Gribben, J.G. (2005). Chronic lymphocytic leukemia cells induce changes in gene expression of CD4 and CD8 T cells. J Clin Invest *115*, 1797-1805.
195. Göthert, J.R., Eisele, L., Klein-Hitpass, L., Weber, S., Zesewitz, M.-L., Sellmann, L., Röth, A., Pircher, H., Dührsen, U., and Dürig, J. (2013). Expanded CD8+ T cells of murine and human CLL are driven into a senescent KLRG1+ effector memory phenotype. Cancer Immunology, Immunotherapy *62*, 1697-1709.
196. Gramatzki, D., Pantazis, G., Schittenhelm, J., Tabatabai, G., Kohle, C., Wick, W., Schwarz, M., Weller, M., and Tritschler, I. (2009). Aryl hydrocarbon receptor inhibition downregulates the TGF-beta/Smad pathway in human glioblastoma cells. Oncogene *28*, 2593-2605.
197. Greene, L.I., Bruno, T.C., Christenson, J.L., D'Alessandro, A., Culp-Hill, R., Torkko, K., Borges, V.F., Slansky, J.E., and Richer, J.K. (2019). A Role for Tryptophan-2,3-dioxygenase in CD8 T-cell Suppression and Evidence of Tryptophan Catabolism in Breast Cancer Patient Plasma. Mol Cancer Res *17*, 131-139.
198. Greten, F.R., and Grivennikov, S.I. (2019). Inflammation and Cancer: Triggers, Mechanisms, and Consequences. Immunity *51*, 27-41.
199. Griggio, V., Vitale, C., Todaro, M., Riganti, C., Kopecka, J., Salvetti, C., Bomben, R., Bo, M.D., Magliulo, D., Rossi, D.*, et al.* (2020). HIF-1α is over-expressed in leukemic cells from TP53-disrupted patients and is a promising therapeutic target in chronic lymphocytic leukemia. Haematologica *105*, 1042-1054.

200. Grioni, M., Brevi, A., Cattaneo, E., Rovida, A., Bordini, J., Bertilaccio, M.T.S., Ponzoni, M., Casorati, G., Dellabona, P., Ghia, P.*, et al.* (2021). CD4+ T cells sustain aggressive chronic lymphocytic leukemia in Eμ-TCL1 mice through a CD40L-independent mechanism. Blood Advances *5*, 2817-2828.
201. Grossman, W.J., Verbsky, J.W., Barchet, W., Colonna, M., Atkinson, J.P., and Ley, T.J. (2004). Human T regulatory cells can use the perforin pathway to cause autologous target cell death. Immunity *21*, 589-601.
202. Guieze, R., and Wu, C.J. (2015). Genomic and epigenomic heterogeneity in chronic lymphocytic leukemia. Blood *126*, 445-453.
203. Gupta, N., Mittal, A., Duggal, R., Dadu, T., Agarwal, A., and Handoo, A. (2021). Hodgkin Variant of Richter's Transformation in Chronic Lymphocytic Leukemia (CLL): An Illustrative Case Report and Literature Review. Int J Hematol Oncol Stem Cell Res *15*, 249-254.
204. Gupta, S.S., Wang, J., and Chen, M. (2020). Metabolic Reprogramming in CD8(+) T Cells During Acute Viral Infections. Front Immunol *11*, 1013.
205. Gustafson, M.P., Abraham, R.S., Lin, Y., Wu, W., Gastineau, D.A., Zent, C.S., and Dietz, A.B. (2012). Association of an increased frequency of CD14+ HLA-DR lo/neg monocytes with decreased time to progression in chronic lymphocytic leukaemia (CLL). Br J Haematol *156*, 674-676.
206. Guven, H., Gilljam, M., Chambers, B.J., Ljunggren, H.G., Christensson, B., Kimby, E., and Dilber, M.S. (2003). Expansion of natural killer (NK) and natural killer-like T (NKT)-cell populations derived from patients with B-chronic lymphocytic leukemia (B-CLL): a potential source for cellular immunotherapy. Leukemia *17*, 1973-1980.
207. Guzzo, C., Ayer, A., Basta, S., Banfield, B.W., and Gee, K. (2012). IL-27 enhances LPS-induced proinflammatory cytokine production via upregulation of TLR4 expression and signaling in human monocytes. J Immunol *188*, 864-873.
208. Hallek, M. (2019). Chronic lymphocytic leukemia: 2020 update on diagnosis, risk stratification and treatment. Am J Hematol *94*, 1266-1287.
209. Hallek, M., and Al-Sawaf, O. (2021). Chronic lymphocytic leukemia: 2022 update on diagnostic and therapeutic procedures. Am J Hematol *96*, 1679-1705.
210. Han, Y., Wu, J., Bi, L., Xiong, S., Gao, S., Yin, L., Jiang, L., Chen, C., Yu, K., and Zhang, S. (2011). Malignant B cells induce the conversion of CD4+CD25- T cells to regulatory T cells in B-cell non-Hodgkin lymphoma. PLoS One *6*, e28649.
211. Hanna, B.S., McClanahan, F., Yazdanparast, H., Zaborsky, N., Kalter, V., Rossner, P.M., Benner, A., Durr, C., Egle, A., Gribben, J.G.*, et al.* (2016). Depletion of CLL-associated patrolling monocytes and macrophages controls disease development and repairs immune dysfunction in vivo. Leukemia *30*, 570-579.
212. Hanna, B.S., Roessner, P.M., Scheffold, A., Jebaraj, B.M.C., Demerdash, Y., Ozturk, S., Lichter, P., Stilgenbauer, S., and Seiffert, M. (2019a). PI3Kdelta inhibition modulates regulatory and effector T-cell differentiation and function in chronic lymphocytic leukemia. Leukemia *33*, 1427-1438.
213. Hanna, B.S., Roessner, P.M., Yazdanparast, H., Colomer, D., Campo, E., Kugler, S., Yosifov, D., Stilgenbauer, S., Schmidt, M., Gabriel, R.*, et al.* (2019b). Control of chronic lymphocytic leukemia development by clonally-expanded CD8(+) T-cells that undergo functional exhaustion in secondary lymphoid tissues. Leukemia *33*, 625-637.
214. Hassin, D., Garber, O.G., Meiraz, A., Schiffenbauer, Y.S., and Berke, G. (2011). Cytotoxic T lymphocyte perforin and Fas ligand working in concert even when Fas ligand lytic action is still not detectable. Immunology *133*, 190-196.
215. Hemati, M., Rasouli Nejad, Z., Shokri, M.R., Ghahremanfard, F., Mir Mohammadkhani, M., and Kokhaei, P. (2020). IL-27 impact on NK cells activity: Implication for a robust anti-tumor response in chronic lymphocytic leukemia. Int Immunopharmacol *82*, 106350.
216. Hennecke, J., and Wiley, D.C. (2001). T cell receptor-MHC interactions up close. Cell *104*, 1-4.
217. Herishanu, Y., Katz, B.Z., Lipsky, A., and Wiestner, A. (2013). Biology of chronic lymphocytic leukemia in different microenvironments: clinical and therapeutic implications. Hematol Oncol Clin North Am *27*, 173-206.

218. Herishanu, Y., Perez-Galan, P., Liu, D., Biancotto, A., Pittaluga, S., Vire, B., Gibellini, F., Njuguna, N., Lee, E., Stennett, L.*, et al.* (2011). The lymph node microenvironment promotes B-cell receptor signaling, NF-kappaB activation, and tumor proliferation in chronic lymphocytic leukemia. Blood *117*, 563-574.
219. Herling, M., Patel, K.A., Khalili, J., Schlette, E., Kobayashi, R., Medeiros, L.J., and Jones, D. (2005). TCL1 shows a regulated expression pattern in chronic lymphocytic leukemia that correlates with molecular subtypes and proliferative state. Leukemia *(2006)*, 280–285.
220. Herndon, T.M., Chen, S.S., Saba, N.S., Valdez, J., Emson, C., Gatmaitan, M., Tian, X., Hughes, T.E., Sun, C., Arthur, D.C.*, et al.* (2017). Direct in vivo evidence for increased proliferation of CLL cells in lymph nodes compared to bone marrow and peripheral blood. Leukemia *31*, 1340-1347.
221. Herrmann, F., Lochner, A., Philippen, H., Jauer, B., and Ruhl, H. (1982). Imbalance of T cell subpopulations in patients with chronic lymphocytic leukaemia of the B cell type. Clin Exp Immunol *49*, 157-162.
222. Hibbert, L., Pflanz, S., De Waal Malefyt, R., and Kastelein, R.A. (2003). IL-27 and IFN-alpha signal via Stat1 and Stat3 and induce T-Bet and IL-12Rbeta2 in naive T cells. J Interferon Cytokine Res *23*, 513-522.
223. Higuchi, T., Matsuo, K., Hashida, Y., Kitahata, K., Ujihara, T., Taniguchi, A., Yoshie, O., Nakayama, T., and Daibata, M. (2019). Epstein-Barr virus-positive pyothorax-associated lymphoma expresses CCL17 and CCL22 chemokines that attract CCR4-expressing regulatory T cells. Cancer Lett *453*, 184-192.
224. Hillmen, P., Robak, T., Janssens, A., Babu, K.G., Kloczko, J., Grosicki, S., Doubek, M., Panagiotidis, P., Kimby, E., Schuh, A.*, et al.* (2015). Chlorambucil plus ofatumumab versus chlorambucil alone in previously untreated patients with chronic lymphocytic leukaemia (COMPLEMENT 1): a randomised, multicentre, open-label phase 3 trial. Lancet *385*, 1873-1883.
225. Hisada, M., Kamiya, S., Fujita, K., Belladonna, M.L., Aoki, T., Koyanagi, Y., Mizuguchi, J., and Yoshimoto, T. (2004). Potent antitumor activity of interleukin-27. Cancer Res *64*, 1152-1156.
226. Hodi, F.S., O'Day, S.J., McDermott, D.F., Weber, R.W., Sosman, J.A., Haanen, J.B., Gonzalez, R., Robert, C., Schadendorf, D., Hassel, J.C.*, et al.* (2010). Improved survival with ipilimumab in patients with metastatic melanoma. N Engl J Med *363*, 711-723.
227. Hoefflin, R., Harlander, S., Schäfer, S., Metzger, P., Kuo, F., Schönenberger, D., Adlesic, M., Peighambari, A., Seidel, P., Chen, C.-y.*, et al.* (2020). HIF-1α and HIF-2α differently regulate tumour development and inflammation of clear cell renal cell carcinoma in mice. Nature Communications *11*, 4111.
228. Hoellenriegel, J., Meadows, S.A., Sivina, M., Wierda, W.G., Kantarjian, H., Keating, M.J., Giese, N., O'Brien, S., Yu, A., Miller, L.L.*, et al.* (2011). The phosphoinositide 3'-kinase delta inhibitor, CAL-101, inhibits B-cell receptor signaling and chemokine networks in chronic lymphocytic leukemia. Blood *118*, 3603-3612.
229. Hofbauer, J.P., Heyder, C., Denk, U., Kocher, T., Holler, C., Trapin, D., Asslaber, D., Tinhofer, I., Greil, R., and Egle, A. (2011). Development of CLL in the TCL1 transgenic mouse model is associated with severe skewing of the T-cell compartment homologous to human CLL. Leukemia *25*, 1452-1458.
230. Honey, K. (2006). CCL3 and CCL4 actively recruit CD8+ T cells. Nature Reviews Immunology *6*, 427-427.
231. Hoogeboom, R., van Kessel, K.P., Hochstenbach, F., Wormhoudt, T.A., Reinten, R.J., Wagner, K., Kater, A.P., Guikema, J.E., Bende, R.J., and van Noesel, C.J. (2013). A mutated B cell chronic lymphocytic leukemia subset that recognizes and responds to fungi. J Exp Med *210*, 59-70.
232. Hornyak, L., Dobos, N., Koncz, G., Karanyi, Z., Pall, D., Szabo, Z., Halmos, G., and Szekvolgyi, L. (2018). The Role of Indoleamine-2,3-Dioxygenase in Cancer Development, Diagnostics, and Therapy. Front Immunol *9*, 151.
233. Hovelmeyer, N., Schmidt-Supprian, M., and Ohnmacht, C. (2022). NF-kappaB in control of regulatory T cell development, identity, and function. J Mol Med (Berl) *100*, 985-995.

234. Hsu, TS., Lin, YL., Wang, YA. et al. HIF-2α is indispensable for regulatory T cell function. Nat Commun 11, 5005 (2020). https://doi.org/10.1038/s41467-020-18731-y
235. https://seer.cancer.gov/statfacts/html/clyl.html.
236. https://www.lls.org/leukemia/chronic-lymphocytic-leukemia/treatment/clinical-trials.
237. Hu, A., Ding, M., Zhu, J., Liu, J.Q., Pan, X., Ghoshal, K., and Bai, X.F. (2020). Intra-Tumoral Delivery of IL-27 Using Adeno-Associated Virus Stimulates Anti-tumor Immunity and Enhances the Efficacy of Immunotherapy. Front Cell Dev Biol *8*, 210.
238. Hu, M., Li, Y., Lu, Y., Wang, M., Li, Y., Wang, C., Li, Q., and Zhao, H. (2021). The regulation of immune checkpoints by the hypoxic tumor microenvironment. PeerJ *9*, e11306.
239. Hu, P., Hu, H.D., Chen, M., Peng, M.L., Tang, L., Tang, K.F., Matsui, M., Belladonna, M.L., Yoshimoto, T., Zhang, D.Z*., et al.* (2009). Expression of interleukins-23 and 27 leads to successful gene therapy of hepatocellular carcinoma. Mol Immunol *46*, 1654-1662.
240. Huang, C.T., Workman, C.J., Flies, D., Pan, X., Marson, A.L., Zhou, G., Hipkiss, E.L., Ravi, S., Kowalski, J., Levitsky, H.I*., et al.* (2004). Role of LAG-3 in regulatory T cells. Immunity *21*, 503-513.
241. Huang, L., Guo, Y., Liu, S., Wang, H., Zhu, J., Ou, L., and Xu, X. (2021). Targeting regulatory T cells for immunotherapy in melanoma. Mol Biomed *2*, 11.
242. Huang, L.E., Gu, J., Schau, M., and Bunn, H.F. (1998). Regulation of hypoxia-inducible factor 1alpha is mediated by an O2-dependent degradation domain via the ubiquitin-proteasome pathway. Proc Natl Acad Sci U S A *95*, 7987-7992.
243. Huang, Y.C., Huang, F.I., Mehndiratta, S., Lai, S.C., Liou, J.P., and Yang, C.R. (2015). Anticancer activity of MPT0G157, a derivative of indolylbenzenesulfonamide, inhibits tumor growth and angiogenesis. Oncotarget *6*, 18590-18601.
244. Huber, M., Steinwald, V., Guralnik, A., Brüstle, A., Kleemann, P., Rosenplänter, C., Decker, T., and Lohoff, M. (2008). IL-27 inhibits the development of regulatory T cells via STAT3. Int Immunol *20*, 223-234.
245. Hwang, H.J., Dornbos, P., Steidemann, M., Dunivin, T.K., Rizzo, M., and LaPres, J.J. (2016). Mitochondrial-targeted aryl hydrocarbon receptor and the impact of 2,3,7,8-tetrachlorodibenzo-p-dioxin on cellular respiration and the mitochondrial proteome. Toxicol Appl Pharmacol *304*, 121-132.
246. Ichiyama, K., Yoshida, H., Wakabayashi, Y., Chinen, T., Saeki, K., Nakaya, M., Takaesu, G., Hori, S., Yoshimura, A., and Kobayashi, T. (2008). Foxp3 inhibits RORgammat-mediated IL-17A mRNA transcription through direct interaction with RORgammat. J Biol Chem *283*, 17003-17008.
247. Inman, B.A., Longo, T.A., Ramalingam, S., and Harrison, M.R. (2017). Atezolizumab: A PD-L1-Blocking Antibody for Bladder Cancer. Clin Cancer Res *23*, 1886-1890.
248. International-CLL-IPI-working-group (2016). An international prognostic index for patients with chronic lymphocytic leukaemia (CLL-IPI): a meta-analysis of individual patient data. Lancet Oncol *17*, 779-790.
249. Ioannou, N., Hagner, P.R., Stokes, M., Gandhi, A.K., Apollonio, B., Fanous, M., Papazoglou, D., Sutton, L.A., Rosenquist, R., Amini, R.M*., et al.* (2021). Triggering interferon signaling in T cells with avadomide sensitizes CLL to anti-PD-L1/PD-1 immunotherapy. Blood *137*, 216-231.
250. Jacobs, J.F., Nierkens, S., Figdor, C.G., de Vries, I.J., and Adema, G.J. (2012). Regulatory T cells in melanoma: the final hurdle towards effective immunotherapy? Lancet Oncol *13*, e32-42.
251. Jago, C.B., Yates, J., Camara, N.O., Lechler, R.I., and Lombardi, G. (2004). Differential expression of CTLA-4 among T cell subsets. Clin Exp Immunol *136*, 463-471.
251. Jahrsdörfer, B., Blackwell, S.E., Wooldridge, J.E., Huang, J., Andreski, M.W., Jacobus, L.S., Taylor, C.M., and Weiner, G.J. (2006). B-chronic lymphocytic leukemia cells and other B cells can produce granzyme B and gain cytotoxic potential after interleukin-21-based activation. Blood *108*, 2712-2719.
252. Jeong, J.W., Bae, M.K., Ahn, M.Y., Kim, S.H., Sohn, T.K., Bae, M.H., Yoo, M.A., Song, E.J., Lee, K.J., and Kim, K.W. (2002). Regulation and destabilization of HIF-1alpha by ARD1-mediated acetylation. Cell *111*, 709-720.

253. Jia, H., Dilger, P., Bird, C., and Wadhwa, M. (2016). IL-27 Promotes Proliferation of Human Leukemic Cell Lines Through the MAPK/ERK Signaling Pathway and Suppresses Sensitivity to Chemotherapeutic Drugs. J Interferon Cytokine Res *36*, 302-316.
254. Jing, X., Yang, F., Shao, C., Wei, K., Xie, M., Shen, H., and Shu, Y. (2019). Role of hypoxia in cancer therapy by regulating the tumor microenvironment. Mol Cancer *18*, 157.
255. Jitschin, R., Braun, M., Buttner, M., Dettmer-Wilde, K., Bricks, J., Berger, J., Eckart, M.J., Krause, S.W., Oefner, P.J., Le Blanc, K.*, et al.* (2014). CLL-cells induce IDOhi CD14+HLA-DRlo myeloid-derived suppressor cells that inhibit T-cell responses and promote TRegs. Blood *124*, 750-760.
256. Johnson, A.J., Lucas, D.M., Muthusamy, N., Smith, L.L., Edwards, R.B., De Lay, M.D., Croce, C.M., Grever, M.R., and Byrd, J.C. (2006). Characterization of the TCL-1 transgenic mouse as a preclinical drug development tool for human chronic lymphocytic leukemia. Blood *108*, 1334-1338.
257. Joller, N., Lozano, E., Burkett, P.R., Patel, B., Xiao, S., Zhu, C., Xia, J., Tan, T.G., Sefik, E., Yajnik, V.*, et al.* (2014). Treg cells expressing the coinhibitory molecule TIGIT selectively inhibit proinflammatory Th1 and Th17 cell responses. Immunity *40*, 569-581.
258. Jones, J.M., and Gellert, M. (2004). The taming of a transposon: V(D)J recombination and the immune system. Immunol Rev *200*, 233-248.
259. Joshi, N.S., Cui, W., Chandele, A., Lee, H.K., Urso, D.R., Hagman, J., Gapin, L., and Kaech, S.M. (2007). Inflammation directs memory precursor and short-lived effector CD8(+) T cell fates via the graded expression of T-bet transcription factor. Immunity *27*, 281-295.
260. Kachroo, P., Lee, M.H., Zhang, L., Baratelli, F., Lee, G., Srivastava, M.K., Wang, G., Walser, T.C., Krysan, K., Sharma, S.*, et al.* (2013). IL-27 inhibits epithelial-mesenchymal transition and angiogenic factor production in a STAT1-dominant pathway in human non-small cell lung cancer. J Exp Clin Cancer Res *32*, 97.
261. Kamada, T., Togashi, Y., Tay, C., Ha, D., Sasaki, A., Nakamura, Y., Sato, E., Fukuoka, S., Tada, Y., Tanaka, A.*, et al.* (2019). PD-1(+) regulatory T cells amplified by PD-1 blockade promote hyperprogression of cancer. Proc Natl Acad Sci U S A *116*, 9999-10008.
262. Kandarakov, O., Belyavsky, A., and Semenova, E. (2022). Bone Marrow Niches of Hematopoietic Stem and Progenitor Cells. Int J Mol Sci *23*.
263. Karin, N. (2021). Chemokines in the Landscape of Cancer Immunotherapy: How They and Their Receptors Can Be Used to Turn Cold Tumors into Hot Ones? Cancers (Basel) *13*.
264. Kaser, T., Mair, K.H., Hammer, S.E., Gerner, W., and Saalmuller, A. (2015). Natural and inducible Tregs in swine: Helios expression and functional properties. Dev Comp Immunol *49*, 323-331.
265. Katrinakis, G., Kyriakou, D., Papadaki, H., Kalokyri, I., Markidou, F., and Eliopoulos, G.D. (1996). Defective natural killer cell activity in B-cell chronic lymphocytic leukaemia is associated with impaired release of natural killer cytotoxic factor(s) but not of tumour necrosis factor-alpha. Acta Haematol *96*, 16-23.
266. Kay, N.E., Hampel, P.J., Van Dyke, D.L., and Parikh, S.A. (2022). CLL update 2022: A continuing evolution in care. Blood Rev, 100930.
267. Keith, B., Johnson, R.S., and Simon, M.C. (2011). HIF1α and HIF2α: sibling rivalry in hypoxic tumour growth and progression. Nat Rev Cancer *12*, 9-22.
268. Kempkes, R.W.M., Joosten, I., Koenen, H., and He, X. (2019). Metabolic Pathways Involved in Regulatory T Cell Functionality. Front Immunol *10*, 2839.
269. Khalaf, K., Hana, D., Chou, J.T., Singh, C., Mackiewicz, A., and Kaczmarek, M. (2021). Aspects of the Tumor Microenvironment Involved in Immune Resistance and Drug Resistance. Front Immunol *12*, 656364.
270. Khalid, K., Padda, J., Syam, M., Moosa, A., Kakani, V., Sanka, S., Zubair, U., Padda, S., Cooper, A.C., and Jean-Charles, G. (2021). 13q14 Deletion and Its Effect on Prognosis of Chronic Lymphocytic Leukemia. Cureus *13*, e16839.
271. Kilgore, A.M., Pennock, N.D., and Kedl, R.M. (2020). cDC1 IL-27p28 Production Predicts Vaccine-Elicited CD8(+) T Cell Memory and Protective Immunity. J Immunol *204*, 510-517.
272. Kim, H.S., Zhang, X., and Choi, Y.S. (1994). Activation and proliferation of follicular dendritic cell-like cells by activated T lymphocytes. J Immunol *153*, 2951-2961.

273. Kim, J., Lahl, K., Hori, S., Loddenkemper, C., Chaudhry, A., deRoos, P., Rudensky, A., and Sparwasser, T. (2009). Cutting edge: depletion of Foxp3+ cells leads to induction of autoimmunity by specific ablation of regulatory T cells in genetically targeted mice. J Immunol *183*, 7631-7634.
274. Kim, J.H., Kim, B.S., and Lee, S.K. (2020). Regulatory T Cells in Tumor Microenvironment and Approach for Anticancer Immunotherapy. Immune Netw *20*, e4.
275. Kimura, A., Naka, T., Nohara, K., Fujii-Kuriyama, Y., and Kishimoto, T. (2008). Aryl hydrocarbon receptor regulates Stat1 activation and participates in the development of Th17 cells. Proc Natl Acad Sci U S A *105*, 9721-9726.
276. Kipps, T.J., Stevenson, F.K., Wu, C.J., Croce, C.M., Packham, G., Wierda, W.G., O'Brien, S., Gribben, J., and Rai, K. (2017). Chronic lymphocytic leukaemia. Nat Rev Dis Primers *3*, 17008.
277. Kiweler, N., Delbrouck, C., Pozdeev, V.I., Neises, L., Soriano-Baguet, L., Eiden, K., Xian, F., Benzarti, M., Haase, L., Koncina, E*., et al.* (2022). Mitochondria preserve an autarkic one-carbon cycle to confer growth-independent cancer cell migration and metastasis. Nature Communications *13*, 2699.
278. Klysz, D., Tai, X., Robert, P.A., Craveiro, M., Cretenet, G., Oburoglu, L., Mongellaz, C., Floess, S., Fritz, V., Matias, M.I*., et al.* (2015). Glutamine-dependent α-ketoglutarate production regulates the balance between T helper 1 cell and regulatory T cell generation. Sci Signal *8*, ra97.
279. Kneitz, B., Herrmann, T., Yonehara, S., and Schimpl, A. (1995). Normal clonal expansion but impaired Fas-mediated cell death and anergy induction in interleukin-2-deficient mice. Eur J Immunol *25*, 2572-2577.
280. Knorck, A., Schafer, G., Alansary, D., Richter, J., Thurner, L., Hoth, M., and Schwarz, E.C. (2022). Cytotoxic Efficiency of Human CD8(+) T Cell Memory Subtypes. Front Immunol *13*, 838484.
281. Kochetkova, I., Golden, S., Holderness, K., Callis, G., and Pascual, D.W. (2010). IL-35 stimulation of CD39+ regulatory T cells confers protection against collagen II-induced arthritis via the production of IL-10. J Immunol *184*, 7144-7153.
282. Kolijn, P.M., Hosnijeh, F.S., Spath, F., Hengeveld, P.J., Agathangelidis, A., Saleh, M., Casabonne, D., Benavente, Y., Jerkeman, M., Agudo, A*., et al.* (2022). High-risk subtypes of chronic lymphocytic leukemia are detectable as early as 16 years prior to diagnosis. Blood *139*, 1557-1563.
283. Kontos, C.K., Papageorgiou, S.G., Diamantopoulos, M.A., Scorilas, A., Bazani, E., Vasilatou, D., Gkontopoulos, K., Glezou, E., Stavroulaki, G., Dimitriadis, G*., et al.* (2017). mRNA overexpression of the hypoxia inducible factor 1 alpha subunit gene (HIF1A): An independent predictor of poor overall survival in chronic lymphocytic leukemia. Leuk Res *53*, 65-73.
284. Kourko, O., Seaver, K., Odoardi, N., Basta, S., and Gee, K. (2019). IL-27, IL-30, and IL-35: A Cytokine Triumvirate in Cancer. Front Oncol *9*, 969.
285. Kovacs, J.J., Murphy, P.J., Gaillard, S., Zhao, X., Wu, J.T., Nicchitta, C.V., Yoshida, M., Toft, D.O., Pratt, W.B., and Yao, T.P. (2005). HDAC6 regulates Hsp90 acetylation and chaperone-dependent activation of glucocorticoid receptor. Mol Cell *18*, 601-607.
286. Kranich, J., and Krautler, N.J. (2016). How Follicular Dendritic Cells Shape the B-Cell Antigenome. Front Immunol *7*, 225.
287. Krummel, M.F., and Allison, J.P. (1996). CTLA-4 engagement inhibits IL-2 accumulation and cell cycle progression upon activation of resting T cells. J Exp Med *183*, 2533-2540.
288. Kumar, P., Marinelarena, A., Raghunathan, D., Ragothaman, V.K., Saini, S., Bhattacharya, P., Fan, J., Epstein, A.L., Maker, A.V., and Prabhakar, B.S. (2019). Critical role of OX40 signaling in the TCR-independent phase of human and murine thymic Treg generation. Cell Mol Immunol *16*, 138-153.
289. Kung, J.T., Beller, D., and Ju, S.T. (1998). Lymphokine regulation of activation-induced apoptosis in T cells of IL-2 and IL-2R beta knockout mice. Cell Immunol *185*, 158-163.
290. Kurniawan, H., Soriano-Baguet, L., and Brenner, D. (2020). Regulatory T cell metabolism at the intersection between autoimmune diseases and cancer. Eur J Immunol *50*, 1626-1642.
291. Kurosawa, S., Harada, M., Matsuzaki, G., Shinomiya, Y., Terao, H., Kobayashi, N., and Nomoto, K. (1995). Early-appearing tumour-infiltrating natural killer cells play a crucial role in the generation of anti-tumour T lymphocytes. Immunology *85*, 338-346.

292. Lad, D., Hoeppli, R., Huang, Q., Garcia, R., Xu, L., Toze, C., Broady, R., and Levings, M. (2018). Regulatory T-cells drive immune dysfunction in CLL. Leuk Lymphoma *59*, 486-489.
293. Lakshmi Narendra, B., Eshvendar Reddy, K., Shantikumar, S., and Ramakrishna, S. (2013). Immune system: a double-edged sword in cancer. Inflamm Res *62*, 823-834.
294. Lando, D., Peet, D.J., Whelan, D.A., Gorman, J.J., and Whitelaw, M.L. (2002). Asparagine hydroxylation of the HIF transactivation domain a hypoxic switch. Science *295*, 858-861.
295. Largeot, A., Pagano, G., Gonder, S., Moussay, E., and Paggetti, J. (2019). The B-side of Cancer Immunity: The Underrated Tune. Cells *8*.
296. Larigot, L., Juricek, L., Dairou, J., and Coumoul, X. (2018). AhR signaling pathways and regulatory functions. Biochim Open *7*, 1-9.
297. Larousserie, F., Charlot, P., Bardel, E., Froger, J., Kastelein, R.A., and Devergne, O. (2006). Differential effects of IL-27 on human B cell subsets. J Immunol *176*, 5890-5897.
298. Larousserie, F., Pflanz, S., Coulomb-L'Herminé, A., Brousse, N., Kastelein, R., and Devergne, O. (2004). Expression of IL-27 in human Th1-associated granulomatous diseases. J Pathol *202*, 164-171.
299. Lee, H.M., Bautista, J.L., and Hsieh, C.S. (2011). Thymic and peripheral differentiation of regulatory T cells. Adv Immunol *112*, 25-71.
300. Lee, J.H., Elly, C., Park, Y., and Liu, Y.C. (2015a). E3 Ubiquitin Ligase VHL Regulates Hypoxia-Inducible Factor-1alpha to Maintain Regulatory T Cell Stability and Suppressive Capacity. Immunity *42*, 1062-1074.
301. Lee, J.H., Elly, C., Park, Y., and Liu, Y.C. (2015b). E3 Ubiquitin Ligase VHL Regulates Hypoxia-Inducible Factor-1α to Maintain Regulatory T Cell Stability and Suppressive Capacity. Immunity *42*, 1062-1074.
302. Lee, P., Chandel, N.S., and Simon, M.C. (2020). Cellular adaptation to hypoxia through hypoxia inducible factors and beyond. Nature Reviews Molecular Cell Biology *21*, 268-283.
303. Lequeux, A., Noman, M.Z., Xiao, M., Van Moer, K., Hasmim, M., Benoit, A., Bosseler, M., Viry, E., Arakelian, T., Berchem, G.*, et al.* (2021). Targeting HIF-1 alpha transcriptional activity drives cytotoxic immune effector cells into melanoma and improves combination immunotherapy. Oncogene *40*, 4725-4735.
304. Li, B., Samanta, A., Song, X., Iacono, K.T., Bembas, K., Tao, R., Basu, S., Riley, J.L., Hancock, W.W., Shen, Y.*, et al.* (2007). FOXP3 interactions with histone acetyltransferase and class II histone deacetylases are required for repression. Proc Natl Acad Sci U S A *104*, 4571-4576.
305. Li, C., Jiang, P., Wei, S., Xu, X., and Wang, J. (2020). Regulatory T cells in tumor microenvironment: new mechanisms, potential therapeutic strategies and future prospects. Mol Cancer *19*, 116.
306. Li, F., Li, C., Cai, X., Xie, Z., Zhou, L., Cheng, B., Zhong, R., Xiong, S., Li, J., Chen, Z.*, et al.* (2021a). The association between CD8+ tumor-infiltrating lymphocytes and the clinical outcome of cancer immunotherapy: A systematic review and meta-analysis. EClinicalMedicine *41*, 101134.
307. Li, K., Yuan, Z., Lyu, J., Ahn, E., Davis, S.J., Ahmed, R., and Zhu, C. (2021b). PD-1 suppresses TCR-CD8 cooperativity during T-cell antigen recognition. Nat Commun *12*, 2746.
308. Li, M.O., and Rudensky, A.Y. (2016). T cell receptor signalling in the control of regulatory T cell differentiation and function. Nat Rev Immunol *16*, 220-233.
309. Li, Z.D., Wang, K., Yang, X.W., Zhuang, Z.G., Wang, J.J., and Tong, X.W. (2014). Expression of aryl hydrocarbon receptor in relation to p53 status and clinicopathological parameters in breast cancer. Int J Clin Exp Pathol *7*, 7931-7937.
310. Liang, B., Workman, C., Lee, J., Chew, C., Dale, B.M., Colonna, L., Flores, M., Li, N., Schweighoffer, E., Greenberg, S.*, et al.* (2008). Regulatory T cells inhibit dendritic cells by lymphocyte activation gene-3 engagement of MHC class II. J Immunol *180*, 5916-5926.
311. Lim, H.W., Lee, J., Hillsamer, P., and Kim, C.H. (2008). Human Th17 cells share major trafficking receptors with both polarized effector T cells and FOXP3+ regulatory T cells. J Immunol *180*, 122-129.

312. Lim, T.S., Goh, J.K., Mortellaro, A., Lim, C.T., Hammerling, G.J., and Ricciardi-Castagnoli, P. (2012). CD80 and CD86 differentially regulate mechanical interactions of T-cells with antigen-presenting dendritic cells and B-cells. PLoS One *7*, e45185.
313. Lim, T.X., Ahamed, M., and Reutens, D.C. (2022). The aryl hydrocarbon receptor: A diagnostic and therapeutic target in glioma. Drug Discov Today *27*, 422-435.
314. Lindau, D., Gielen, P., Kroesen, M., Wesseling, P., and Adema, G.J. (2013). The immunosuppressive tumour network: myeloid-derived suppressor cells, regulatory T cells and natural killer T cells. Immunology *138*, 105-115.
315. Lindström, V., Aittoniemi, J., Jylhävä, J., Eklund, C., Hurme, M., Paavonen, T., Oja, S.S., Itälä-Remes, M., and Sinisalo, M. (2012). Indoleamine 2,3-dioxygenase activity and expression in patients with chronic lymphocytic leukemia. Clin Lymphoma Myeloma Leuk *12*, 363-365.
316. Lio, C.W., and Hsieh, C.S. (2008). A two-step process for thymic regulatory T cell development. Immunity *28*, 100-111.
317. Lipsky, A., and Lamanna, N. (2020). Managing toxicities of Bruton tyrosine kinase inhibitors. Hematology Am Soc Hematol Educ Program *2020*, 336-345.
318. Litzenburger, U.M., Opitz, C.A., Sahm, F., Rauschenbach, K.J., Trump, S., Winter, M., Ott, M., Ochs, K., Lutz, C., Liu, X*., et al.* (2014). Constitutive IDO expression in human cancer is sustained by an autocrine signaling loop involving IL-6, STAT3 and the AHR. Oncotarget *5*, 1038-1051.
319. Liu, E., Marin, D., Banerjee, P., Macapinlac, H.A., Thompson, P., Basar, R., Nassif Kerbauy, L., Overman, B., Thall, P., Kaplan, M*., et al.* (2020). Use of CAR-Transduced Natural Killer Cells in CD19-Positive Lymphoid Tumors. N Engl J Med *382*, 545-553.
320. Liu, H., and Rohowsky-Kochan, C. (2011). Interleukin-27-mediated suppression of human Th17 cells is associated with activation of STAT1 and suppressor of cytokine signaling protein 1. J Interferon Cytokine Res *31*, 459-469.
321. Liu, H.T., Jiang, M.J., Deng, Z.J., Li, L., Huang, J.L., Liu, Z.X., Li, L.Q., and Zhong, J.H. (2021). Immune Checkpoint Inhibitors in Hepatocellular Carcinoma: Current Progresses and Challenges. Front Oncol *11*, 737497.
322. Liu, J., Zhou, Y., Huang, Q., and Qiu, L. (2015a). CD14(+)HLA-DR(low/-) expression: A novel prognostic factor in chronic lymphocytic leukemia. Oncol Lett *9*, 1167-1172.
323. Liu, L., Cheng, X., Yang, H., Lian, S., Jiang, Y., Liang, J., Chen, X., Mo, S., Shi, Y., Zhao, S*., et al.* (2022). BCL-2 expression promotes immunosuppression in chronic lymphocytic leukemia by enhancing regulatory T cell differentiation and cytotoxic T cell exhaustion. Mol Cancer *21*, 59.
324. Liu, Y., Liang, X., Dong, W., Fang, Y., Lv, J., Zhang, T., Fiskesund, R., Xie, J., Liu, J., Yin, X*., et al.* (2018). Tumor-Repopulating Cells Induce PD-1 Expression in CD8(+) T Cells by Transferring Kynurenine and AhR Activation. Cancer Cell *33*, 480-494 e487.
325. Liu, Z., Liu, J.Q., Shi, Y., Zhu, X., Liu, Z., Li, M.S., Yu, J., Wu, L.C., He, Y., Zhang, G*., et al.* (2015b). Epstein-Barr virus-induced gene 3-deficiency leads to impaired antitumor T-cell responses and accelerated tumor growth. Oncoimmunology *4*, e989137.
326. Liu, Z., Liu, J.Q., Talebian, F., Wu, L.C., Li, S., and Bai, X.F. (2013a). IL-27 enhances the survival of tumor antigen-specific CD8+ T cells and programs them into IL-10-producing, memory precursor-like effector cells. Eur J Immunol *43*, 468-479.
327. Liu, Z., Wu, L., Zhu, J., Zhu, X., Zhu, J., Liu, J.Q., Zhang, J., Davis, J.P., Varikuti, S., Satoskar, A.R*., et al.* (2017). Interleukin-27 signalling induces stem cell antigen-1 expression in T lymphocytes in vivo. Immunology *152*, 638-647.
328. Liu, Z., Yu, J., Carson, W.E., 3rd, and Bai, X.F. (2013b). The role of IL-27 in the induction of anti-tumor cytotoxic T lymphocyte response. Am J Transl Res *5*, 470-480.
329. Liu, Z.M., Wang, K.P., Ma, J., and Guo Zheng, S. (2015c). The role of all-trans retinoic acid in the biology of Foxp3+ regulatory T cells. Cell Mol Immunol *12*, 553-557.
330. Livak, F., and Schatz, D.G. (1996). T-cell receptor alpha locus V(D)J recombination by-products are abundant in thymocytes and mature T cells. Mol Cell Biol *16*, 609-618.
331. Lu, D., Zhou, X., Yao, L., Liu, C., Jin, F., and Wu, Y. (2014). Clinical Implications of the Interleukin 27 Serum Level in Breast Cancer. Journal of Investigative Medicine *62*, 627-631.

332. Lucas, S., Ghilardi, N., Li, J., and de Sauvage, F.J. (2003). IL-27 regulates IL-12 responsiveness of naive CD4+ T cells through Stat1-dependent and -independent mechanisms. Proc Natl Acad Sci U S A *100*, 15047-15052.
333. Luo, F., Lu, F.T., Cao, J.X., Ma, W.J., Xia, Z.F., Zhan, J.H., Zeng, K.M., Huang, Y., Zhao, H.Y., and Zhang, L. (2022). HIF-1α inhibition promotes the efficacy of immune checkpoint blockade in the treatment of non-small cell lung cancer. Cancer Lett *531*, 39-56.
334. Lutzny, G., Kocher, T., Schmidt-Supprian, M., Rudelius, M., Klein-Hitpass, L., Finch, A.J., Durig, J., Wagner, M., Haferlach, C., Kohlmann, A.*, et al.* (2013). Protein kinase c-beta-dependent activation of NF-kappaB in stromal cells is indispensable for the survival of chronic lymphocytic leukemia B cells in vivo. Cancer Cell *23*, 77-92.
335. Ma, D.Y., and Clark, E.A. (2009). The role of CD40 and CD154/CD40L in dendritic cells. Semin Immunol *21*, 265-272.
336. Maharaj, K., Uriepero, A., Sahakian, E., and Pinilla-Ibarz, J. (2022). Regulatory T cells (Tregs) in lymphoid malignancies and the impact of novel therapies. Front Immunol *13*, 943354.
337. Mahmud, S.A., Manlove, L.S., and Farrar, M.A. (2013). Interleukin-2 and STAT5 in regulatory T cell development and function. JAKSTAT *2*, e23154.
338. Makino, Y., Cao, R., Svensson, K., Bertilsson, G., Asman, M., Tanaka, H., Cao, Y., Berkenstam, A., and Poellinger, L. (2001). Inhibitory PAS domain protein is a negative regulator of hypoxia-inducible gene expression. Nature *414*, 550-554.
339. Malek, T.R., Yu, A., Vincek, V., Scibelli, P., and Kong, L. (2002). CD4 regulatory T cells prevent lethal autoimmunity in IL-2Rbeta-deficient mice. Implications for the nonredundant function of IL-2. Immunity *17*, 167-178.
340. Manouchehri-Doulabi, E., Abbaspour, S., Rostami, S., Faranoush, M., Ghahramanfard, F., Pak, F., Barati, M., Kokhaei, P., and Momtazi-Borojeni, A.A. (2020). Evaluating the mechanism underlying antitumor effect of interleukin 27 on B cells of chronic lymphocytic leukemia patients. J Cell Physiol *235*, 9424-9431.
341. Mansouri, L., Papakonstantinou, N., Ntoufa, S., Stamatopoulos, K., and Rosenquist, R. (2016). NF-kappaB activation in chronic lymphocytic leukemia: A point of convergence of external triggers and intrinsic lesions. Semin Cancer Biol *39*, 40-48.
342. Mantel, P.Y., Ouaked, N., Ruckert, B., Karagiannidis, C., Welz, R., Blaser, K., and Schmidt-Weber, C.B. (2006). Molecular mechanisms underlying FOXP3 induction in human T cells. J Immunol *176*, 3593-3602.
343. Mariuzza, R.A., Agnihotri, P., and Orban, J. (2020). The structural basis of T-cell receptor (TCR) activation: An enduring enigma. J Biol Chem *295*, 914-925.
344. Marquez, M.E., Hernandez-Uzcategui, O., Cornejo, A., Vargas, P., and Da Costa, O. (2015). Bone marrow stromal mesenchymal cells induce down regulation of CD20 expression on B-CLL: implications for rituximab resistance in CLL. Br J Haematol *169*, 211-218.
345. Marti, G.E., Faguet, G., Bertin, P., Agee, J., Washington, G., Ruiz, S., Carter, P., Zenger, V., Vogt, R., and Noguchi, P. (1992). CD20 and CD5 expression in B-chronic lymphocytic leukemia. Ann N Y Acad Sci *651*, 480-483.
346. Maruhashi, T., Okazaki, I.M., Sugiura, D., Takahashi, S., Maeda, T.K., Shimizu, K., and Okazaki, T. (2018). LAG-3 inhibits the activation of CD4(+) T cells that recognize stable pMHCII through its conformation-dependent recognition of pMHCII. Nat Immunol *19*, 1415-1426.
347. Mascanfroni, I.D., Takenaka, M.C., Yeste, A., Patel, B., Wu, Y., Kenison, J.E., Siddiqui, S., Basso, A.S., Otterbein, L.E., Pardoll, D.M.*, et al.* (2015). Metabolic control of type 1 regulatory T cell differentiation by AHR and HIF1-α. Nat Med *21*, 638-646.
348. Matias, M.I., Yong, C.S., Foroushani, A., Goldsmith, C., Mongellaz, C., Sezgin, E., Levental, K.R., Talebi, A., Perrault, J., Rivière, A.*, et al.* (2021). Regulatory T cell differentiation is controlled by αKG-induced alterations in mitochondrial metabolism and lipid homeostasis. Cell Rep *37*, 109911.
349. Mato, A.R., Shah, N.N., Jurczak, W., Cheah, C.Y., Pagel, J.M., Woyach, J.A., Fakhri, B., Eyre, T.A., Lamanna, N., Patel, M.R.*, et al.* (2021). Pirtobrutinib in relapsed or refractory B-cell malignancies (BRUIN): a phase 1/2 study. Lancet *397*, 892-901.

350. Matsui, M., Kishida, T., Nakano, H., Yoshimoto, K., Shin-Ya, M., Shimada, T., Nakai, S., Imanishi, J., Yoshimoto, T., Hisa, Y.*, et al.* (2009). Interleukin-27 activates natural killer cells and suppresses NK-resistant head and neck squamous cell carcinoma through inducing antibody-dependent cellular cytotoxicity. Cancer Res *69*, 2523-2530.
351. Maxwell, P.H., Wiesener, M.S., Chang, G.W., Clifford, S.C., Vaux, E.C., Cockman, M.E., Wykoff, C.C., Pugh, C.W., Maher, E.R., and Ratcliffe, P.J. (1999). The tumour suppressor protein VHL targets hypoxia-inducible factors for oxygen-dependent proteolysis. Nature *399*, 271-275.
352. Mayer, K.D., Mohrs, K., Reiley, W., Wittmer, S., Kohlmeier, J.E., Pearl, J.E., Cooper, A.M., Johnson, L.L., Woodland, D.L., and Mohrs, M. (2008). Cutting Edge: T-bet and IL-27R Are Critical for In Vivo IFN-γ Production by CD8 T Cells during Infection. The Journal of Immunology *180*, 693-697.
353. McClanahan, F., Riches, J.C., Miller, S., Day, W.P., Kotsiou, E., Neuberg, D., Croce, C.M., Capasso, M., and Gribben, J.G. (2015). Mechanisms of PD-L1/PD-1-mediated CD8 T-cell dysfunction in the context of aging-related immune defects in the Emicro-TCL1 CLL mouse model. Blood *126*, 212-221.
354. Meiser, J., Schuster, A., Pietzke, M., Vande Voorde, J., Athineos, D., Oizel, K., Burgos-Barragan, G., Wit, N., Dhayade, S., Morton, J.P.*, et al.* (2018). Increased formate overflow is a hallmark of oxidative cancer. Nat Commun *9*, 1368.
355. Melenhorst, J.J., Chen, G.M., Wang, M., Porter, D.L., Chen, C., Collins, M.A., Gao, P., Bandyopadhyay, S., Sun, H., Zhao, Z.*, et al.* (2022). Decade-long leukaemia remissions with persistence of CD4+ CAR T cells. Nature *602*, 503-509.
356. Merkenschlager, M., Graf, D., Lovatt, M., Bommhardt, U., Zamoyska, R., and Fisher, A.G. (1997). How many thymocytes audition for selection? J Exp Med *186*, 1149-1158.
357. Mescher, M.F., Curtsinger, J.M., Agarwal, P., Casey, K.A., Gerner, M., Hammerbeck, C.D., Popescu, F., and Xiao, Z. (2006). Signals required for programming effector and memory development by CD8+ T cells. Immunol Rev *211*, 81-92.
358. Mesturini, R., Nicola, S., Chiocchetti, A., Bernardone, I.S., Castelli, L., Bensi, T., Ferretti, M., Comi, C., Dong, C., Rojo, J.M.*, et al.* (2006). ICOS cooperates with CD28, IL-2, and IFN-gamma and modulates activation of human naive CD4+ T cells. Eur J Immunol *36*, 2601-2612.
359. Mezrich, J.D., Fechner, J.H., Zhang, X., Johnson, B.P., Burlingham, W.J., and Bradfield, C.A. (2010). An interaction between kynurenine and the aryl hydrocarbon receptor can generate regulatory T cells. J Immunol *185*, 3190-3198.
360. Mi, J.L., Xu, M., Liu, C., and Wang, R.S. (2020). Interactions between tumor mutation burden and immune infiltration in ovarian cancer. Int J Clin Exp Pathol *13*, 2513-2523.
361. Michalek, R.D., Gerriets, V.A., Jacobs, S.R., Macintyre, A.N., MacIver, N.J., Mason, E.F., Sullivan, S.A., Nichols, A.G., and Rathmell, J.C. (2011). Cutting edge: distinct glycolytic and lipid oxidative metabolic programs are essential for effector and regulatory CD4+ T cell subsets. J Immunol *186*, 3299-3303.
362. Michalek, R.D., and Rathmell, J.C. (2010). The metabolic life and times of a T-cell. Immunol Rev *236*, 190-202.
363. Mimura, J., Ema, M., Sogawa, K., and Fujii-Kuriyama, Y. (1999). Identification of a novel mechanism of regulation of Ah (dioxin) receptor function. Genes Dev *13*, 20-25.
364. Miska, J., Lee-Chang, C., Rashidi, A., Muroski, M.E., Chang, A.L., Lopez-Rosas, A., Zhang, P., Panek, W.K., Cordero, A., Han, Y.*, et al.* (2019). HIF-1α Is a Metabolic Switch between Glycolytic-Driven Migration and Oxidative Phosphorylation-Driven Immunosuppression of Tregs in Glioblastoma. Cell Rep *27*, 226-237.e224.
365. Mitchell, D.M., Ravkov, E.V., and Williams, M.A. (2010). Distinct roles for IL-2 and IL-15 in the differentiation and survival of CD8+ effector and memory T cells. J Immunol *184*, 6719-6730.
366. Molica, S. (2010). A systematic review on Richter syndrome: what is the published evidence? Leuk Lymphoma *51*, 415-421.
367. Mohr, A., Cumin, M., Bagacean, M.C., Pochard, P., Le Dantec, C., Hillion, S., Renaudineau, Y., Berthou C., Tempescul, A., Saad, H., Pers, J.C., Bordron, A., and Jamina, C., (2019). The regulatory capacity of B cells directs the aggressiveness of CLL. Oncoimmunology Dec 12;8(3):1554968.

368. Molle, C., Nguyen, M., Flamand, V., Renneson, J., Trottein, F., De Wit, D., Willems, F., Goldman, M., and Goriely, S. (2007a). IL-27 synthesis induced by TLR ligation critically depends on IFN regulatory factor 3. J Immunol *178*, 7607-7615.
369. Molle, C., Nguyen, M., Flamand, V., Renneson, J., Trottein, F., De Wit, D., Willems, F., Goldman, M., and Goriely, S. (2007b). IL-27 Synthesis Induced by TLR Ligation Critically Depends on IFN Regulatory Factor 3. The Journal of Immunology *178*, 7607-7615.
370. Montoya, M., Schiavoni, G., Mattei, F., Gresser, I., Belardelli, F., Borrow, P., and Tough, D.F. (2002). Type I interferons produced by dendritic cells promote their phenotypic and functional activation. Blood *99*, 3263-3271.
371. Morishima, N., Owaki, T., Asakawa, M., Kamiya, S., Mizuguchi, J., and Yoshimoto, T. (2005a). Augmentation of effector CD8+ T cell generation with enhanced granzyme B expression by IL-27. J Immunol *175*, 1686-1693.
372. Morishima, N., Owaki, T., Asakawa, M., Kamiya, S., Mizuguchi, J., and Yoshimoto, T. (2005b). Augmentation of Effector CD8⁺ T Cell Generation with Enhanced Granzyme B Expression by IL-27. The Journal of Immunology *175*, 1686-1693.
373. Morita, Y., Masters, E.A., Schwarz, E.M., and Muthukrishnan, G. (2021). Interleukin-27 and Its Diverse Effects on Bacterial Infections. Front Immunol *12*, 678515.
374. Motta, M., Rassenti, L., Shelvin, B.J., Lerner, S., Kipps, T.J., Keating, M.J., and Wierda, W.G. (2005). Increased expression of CD152 (CTLA-4) by normal T lymphocytes in untreated patients with B-cell chronic lymphocytic leukemia. Leukemia *19*, 1788-1793.
374. Murray, H.W., Rubin, B.Y., Carriero, S.M., Harris, A.M., and Jaffee, E.A. (1985). Human mononuclear phagocyte antiprotozoal mechanisms: oxygen-dependent vs oxygen-independent activity against intracellular Toxoplasma gondii. J Immunol *134*, 1982-1988.
375. Murray, I.A., Patterson, A.D., and Perdew, G.H. (2014). Aryl hydrocarbon receptor ligands in cancer: friend and foe. Nat Rev Cancer *14*, 801-814.
376. Nagarsheth, N., Wicha, M.S., and Zou, W. (2017). Chemokines in the cancer microenvironment and their relevance in cancer immunotherapy. Nat Rev Immunol *17*, 559-572.
377. Nakamura, H., Makino, Y., Okamoto, K., Poellinger, L., Ohnuma, K., Morimoto, C., and Tanaka, H. (2005). TCR engagement increases hypoxia-inducible factor-1 alpha protein synthesis via rapamycin-sensitive pathway under hypoxic conditions in human peripheral T cells. J Immunol *174*, 7592-7599.
378. Neophytou, C.M., Panagi, M., Stylianopoulos, T., and Papageorgis, P. (2021). The Role of Tumor Microenvironment in Cancer Metastasis: Molecular Mechanisms and Therapeutic Opportunities. Cancers (Basel) *13*.
379. Nguyen, N.T., Kimura, A., Nakahama, T., Chinen, I., Masuda, K., Nohara, K., Fujii-Kuriyama, Y., and Kishimoto, T. (2010). Aryl hydrocarbon receptor negatively regulates dendritic cell immunogenicity via a kynurenine-dependent mechanism. Proc Natl Acad Sci U S A *107*, 19961-19966.
380. Nicholson, S.E., Keating, N., and Belz, G.T. (2019). Natural killer cells and anti-tumor immunity. Mol Immunol *110*, 40-47.
381. Niedbala, W., Wei, X.Q., Cai, B., Hueber, A.J., Leung, B.P., McInnes, I.B., and Liew, F.Y. (2007). IL-35 is a novel cytokine with therapeutic effects against collagen-induced arthritis through the expansion of regulatory T cells and suppression of Th17 cells. Eur J Immunol *37*, 3021-3029.
382. Noman, M.Z., Desantis, G., Janji, B., Hasmim, M., Karray, S., Dessen, P., Bronte, V., and Chouaib, S. (2014). PD-L1 is a novel direct target of HIF-1α, and its blockade under hypoxia enhanced MDSC-mediated T cell activation. J Exp Med *211*, 781-790.
383. Noyes, D., Bag, A., Oseni, S., Semidey-Hurtado, J., Cen, L., Sarnaik, A.A., Sondak, V.K., and Adeegbe, D. (2022). Tumor-associated Tregs obstruct antitumor immunity by promoting T cell dysfunction and restricting clonal diversity in tumor-infiltrating CD8+ T cells. Journal for ImmunoTherapy of Cancer *10*, e004605.

384. Nunes, C., Wong, R., Mason, M., Fegan, C., Man, S., and Pepper, C. (2012). Expansion of a CD8(+)PD-1(+) replicative senescence phenotype in early stage CLL patients is associated with inverted CD4:CD8 ratios and disease progression. Clin Cancer Res *18*, 678-687.
385. Ohkura, N., and Sakaguchi, S. (2010). Foxo1 and Foxo3 help Foxp3. Immunity *33*, 835-837.
386. Ohkura, N., and Sakaguchi, S. (2020). Transcriptional and epigenetic basis of Treg cell development and function: its genetic anomalies or variations in autoimmune diseases. Cell Research *30*, 465-474.
387. Okeke, E.B., and Uzonna, J.E. (2019). The Pivotal Role of Regulatory T Cells in the Regulation of Innate Immune Cells. Front Immunol *10*, 680.
388. Olson, B.M., Sullivan, J.A., and Burlingham, W.J. (2013). Interleukin 35: a key mediator of suppression and the propagation of infectious tolerance. Front Immunol *4*, 315.
389. Oniki, S., Nagai, H., Horikawa, T., Furukawa, J., Belladonna, M.L., Yoshimoto, T., Hara, I., and Nishigori, C. (2006). Interleukin-23 and interleukin-27 exert quite different antitumor and vaccine effects on poorly immunogenic melanoma. Cancer Res *66*, 6395-6404.
390. Opitz, C.A., Litzenburger, U.M., Sahm, F., Ott, M., Tritschler, I., Trump, S., Schumacher, T., Jestaedt, L., Schrenk, D., Weller, M.*, et al.* (2011). An endogenous tumour-promoting ligand of the human aryl hydrocarbon receptor. Nature *478*, 197-203.
391. Orsini, E., Guarini, A., Chiaretti, S., Mauro, F.R., and Foa, R. (2003). The circulating dendritic cell compartment in patients with chronic lymphocytic leukemia is severely defective and unable to stimulate an effective T-cell response. Cancer Res *63*, 4497-4506.
392. Owaki, T., Asakawa, M., Kamiya, S., Takeda, K., Fukai, F., Mizuguchi, J., and Yoshimoto, T. (2006). IL-27 suppresses CD28-mediated [correction of medicated] IL-2 production through suppressor of cytokine signaling 3. J Immunol *176*, 2773-2780.
393. Öztürk, S., Kalter, V., Roessner, P.M., Sunbul, M., and Seiffert, M. (2021). IDO1-Targeted Therapy Does Not Control Disease Development in the Eμ-TCL1 Mouse Model of Chronic Lymphocytic Leukemia. Cancers (Basel) *13*.
394. Paduano, F., Gaudio, E., Mensah, A.A., Pinton, S., Bertoni, F., and Trapasso, F. (2018). T-Cell Leukemia/Lymphoma 1 (TCL1): An Oncogene Regulating Multiple Signaling Pathways. Front Oncol *8*, 317.
395. Pagé, E.L., Robitaille, G.A., Pouysségur, J., and Richard, D.E. (2002). Induction of hypoxia-inducible factor-1alpha by transcriptional and translational mechanisms. J Biol Chem *277*, 48403-48409.
396. Paggetti, J., Haderk, F., Seiffert, M., Janji, B., Distler, U., Ammerlaan, W., Kim, Y.J., Adam, J., Lichter, P., Solary, E.*, et al.* (2015). Exosomes released by chronic lymphocytic leukemia cells induce the transition of stromal cells into cancer-associated fibroblasts. Blood *126*, 1106-1117.
397. Palazon, A., Goldrath, A.W., Nizet, V., and Johnson, R.S. (2014). HIF transcription factors, inflammation, and immunity. Immunity *41*, 518-528.
398. Palazon, A., Tyrakis, P.A., Macias, D., Veliça, P., Rundqvist, H., Fitzpatrick, S., Vojnovic, N., Phan, A.T., Loman, N., Hedenfalk, I.*, et al.* (2017). An HIF-1α/VEGF-A Axis in Cytotoxic T Cells Regulates Tumor Progression. Cancer Cell *32*, 669-683.e665.
399. Palma, M., Gentilcore, G., Heimersson, K., Mozaffari, F., Nasman-Glaser, B., Young, E., Rosenquist, R., Hansson, L., Osterborg, A., and Mellstedt, H. (2017). T cells in chronic lymphocytic leukemia display dysregulated expression of immune checkpoints and activation markers. Haematologica *102*, 562-572.
400. Pang, N., Alimu, X., Chen, R., Muhashi, M., Ma, J., Chen, G., Zhao, F., Wang, L., Qu, J., and Ding, J. (2021). Activated Galectin-9/Tim3 promotes Treg and suppresses Th1 effector function in chronic lymphocytic leukemia. FASEB J *35*, e21556.
401. Pang, N., Zhang, R., Li, J., Zhang, Z., Yuan, H., Chen, G., Zhao, F., Wang, L., Cao, H., Qu, J.*, et al.* (2016). Increased IL-10/IL-17 ratio is aggravated along with the prognosis of patients with chronic lymphocytic leukemia. Int Immunopharmacol *40*, 57-64.
402. Pang, Y., Yang, C., Schovanek, J., Wang, H., Bullova, P., Caisova, V., Gupta, G., Wolf, K.I., Semenza, G.L., Zhuang, Z.*, et al.* (2017). Anthracyclines suppress pheochromocytoma cell

characteristics, including metastasis, through inhibition of the hypoxia signaling pathway. Oncotarget *8*, 22313-22324.
403. Parikh, S.A., and Shanafelt, T.D. (2014). Risk factors for Richter syndrome in chronic lymphocytic leukemia. Curr Hematol Malig Rep *9*, 294-299.
404. Patel, K., and Pagel, J.M. (2021). Current and future treatment strategies in chronic lymphocytic leukemia. J Hematol Oncol *14*, 69.
405. Patrussi, L., Capitani, N., Ulivieri, C., Manganaro, N., Granai, M., Cattaneo, F., Kabanova, A., Mundo, L., Gobessi, S., Frezzato, F.*, et al.* (2019). p66Shc deficiency in the Emu-TCL1 mouse model of chronic lymphocytic leukemia enhances leukemogenesis by altering the chemokine receptor landscape. Haematologica *104*, 2040-2052.
406. Patsoukis, N., Bardhan, K., Weaver, J., Herbel, C., Seth, P., Li, L., and Boussiotis, V.A. (2016). The role of metabolic reprogramming in T cell fate and function. Curr Trends Immunol *17*, 1-12.
407. Pauken, K.E., and Wherry, E.J. (2015). Overcoming T cell exhaustion in infection and cancer. Trends Immunol *36*, 265-276.
408. Pekarsky, Y., Palamarchuk, A., Maximov, V., Efanov, A., Nazaryan, N., Santanam, U., Rassenti, L., Kipps, T., and Croce, C.M. (2008). Tcl1 functions as a transcriptional regulator and is directly involved in the pathogenesis of CLL. Proc Natl Acad Sci U S A *105*, 19643-19648.
409. Pellegrino, M., Crino, A., Rosado, M.M., and Fierabracci, A. (2019). Identification and functional characterization of CD8+ T regulatory cells in type 1 diabetes patients. PLoS One *14*, e0210839.
410. Perkins, D., Wang, Z., Donovan, C., He, H., Mark, D., Guan, G., Wang, Y., Walunas, T., Bluestone, J., Listman, J.*, et al.* (1996). Regulation of CTLA-4 expression during T cell activation. J Immunol *156*, 4154-4159.
411. Petitprez, F., Meylan, M., de Reynies, A., Sautes-Fridman, C., and Fridman, W.H. (2020). The Tumor Microenvironment in the Response to Immune Checkpoint Blockade Therapies. Front Immunol *11*, 784.
412. Pflanz, S., Hibbert, L., Mattson, J., Rosales, R., Vaisberg, E., Bazan, J.F., Phillips, J.H., McClanahan, T.K., de Waal Malefyt, R., and Kastelein, R.A. (2004). WSX-1 and glycoprotein 130 constitute a signal-transducing receptor for IL-27. J Immunol *172*, 2225-2231.
413. Pflanz, S., Timans, J.C., Cheung, J., Rosales, R., Kanzler, H., Gilbert, J., Hibbert, L., Churakova, T., Travis, M., Vaisberg, E.*, et al.* (2002). IL-27, a heterodimeric cytokine composed of EBI3 and p28 protein, induces proliferation of naive CD4+ T cells. Immunity *16*, 779-790.
414. Pilotte, L., Larrieu, P., Stroobant, V., Colau, D., Dolusic, E., Frédérick, R., De Plaen, E., Uyttenhove, C., Wouters, J., Masereel, B.*, et al.* (2012). Reversal of tumoral immune resistance by inhibition of tryptophan 2,3-dioxygenase. Proc Natl Acad Sci U S A *109*, 2497-2502.
415. Pinheiro, M.B., Antonelli, L.R., Sathler-Avelar, R., Vitelli-Avelar, D.M., Spindola-de-Miranda, S., Guimaraes, T.M., Teixeira-Carvalho, A., Martins-Filho, O.A., and Toledo, V.P. (2012). CD4-CD8-alphabeta and gammadelta T cells display inflammatory and regulatory potentials during human tuberculosis. PLoS One *7*, e50923.
416. Pohar, J., Simon, Q., and Fillatreau, S. (2018). Antigen-Specificity in the Thymic Development and Peripheral Activity of CD4(+)FOXP3(+) T Regulatory Cells. Front Immunol *9*, 1701.
417. Ponader, S., Chen, S.S., Buggy, J.J., Balakrishnan, K., Gandhi, V., Wierda, W.G., Keating, M.J., O'Brien, S., Chiorazzi, N., and Burger, J.A. (2012). The Bruton tyrosine kinase inhibitor PCI-32765 thwarts chronic lymphocytic leukemia cell survival and tissue homing in vitro and in vivo. Blood *119*, 1182-1189.
418. Popmihajlov, Z., and Smith, K.A. (2008). Negative feedback regulation of T cells via interleukin-2 and FOXP3 reciprocity. PLoS One *3*, e1581.
419. Postow, M.A., Chesney, J., Pavlick, A.C., Robert, C., Grossmann, K., McDermott, D., Linette, G.P., Meyer, N., Giguere, J.K., Agarwala, S.S.*, et al.* (2015). Nivolumab and ipilimumab versus ipilimumab in untreated melanoma. N Engl J Med *372*, 2006-2017.
420. Povroznik, J.M., and Robinson, C.M. (2020). IL-27 regulation of innate immunity and control of microbial growth. Future Sci OA *6*, Fso588.

421. Qin, S., Xu, L., Yi, M., Yu, S., Wu, K., and Luo, S. (2019). Novel immune checkpoint targets: moving beyond PD-1 and CTLA-4. Mol Cancer *18*, 155.
422. Qiu, G.Z., Jin, M.Z., Dai, J.X., Sun, W., Feng, J.H., and Jin, W.L. (2017). Reprogramming of the Tumor in the Hypoxic Niche: The Emerging Concept and Associated Therapeutic Strategies. Trends Pharmacol Sci *38*, 669-686.
423. Quintana, F.J., Basso, A.S., Iglesias, A.H., Korn, T., Farez, M.F., Bettelli, E., Caccamo, M., Oukka, M., and Weiner, H.L. (2008). Control of T(reg) and T(H)17 cell differentiation by the aryl hydrocarbon receptor. Nature *453*, 65-71.
424. Quintana, F.J., Murugaiyan, G., Farez, M.F., Mitsdoerffer, M., Tukpah, A.M., Burns, E.J., and Weiner, H.L. (2010). An endogenous aryl hydrocarbon receptor ligand acts on dendritic cells and T cells to suppress experimental autoimmune encephalomyelitis. Proc Natl Acad Sci U S A *107*, 20768-20773.
425. Ramsay, A.G., Johnson, A.J., Lee, A.M., Gorgün, G., Le Dieu, R., Blum, W., Byrd, J.C., and Gribben, J.G. (2008). Chronic lymphocytic leukemia T cells show impaired immunological synapse formation that can be reversed with an immunomodulating drug. J Clin Invest *118*, 2427-2437.
426. Rannug, A., and Rannug, U. (2018). The tryptophan derivative 6-formylindolo[3,2-b]carbazole, FICZ, a dynamic mediator of endogenous aryl hydrocarbon receptor signaling, balances cell growth and differentiation. Crit Rev Toxicol *48*, 555-574.
427. Rassenti, L.Z., Jain, S., Keating, M.J., Wierda, W.G., Grever, M.R., Byrd, J.C., Kay, N.E., Brown, J.R., Gribben, J.G., Neuberg, D.S*., et al.* (2008). Relative value of ZAP-70, CD38, and immunoglobulin mutation status in predicting aggressive disease in chronic lymphocytic leukemia. Blood *112*, 1923-1930.
428. Rech, A.J., and Vonderheide, R.H. (2009). Clinical use of anti-CD25 antibody daclizumab to enhance immune responses to tumor antigen vaccination by targeting regulatory T cells. Ann N Y Acad Sci *1174*, 99-106.
429. Ren, W., Liu, G., Yin, J., Tan, B., Wu, G., Bazer, F.W., Peng, Y., and Yin, Y. (2017a). Amino-acid transporters in T-cell activation and differentiation. Cell Death & Disease *8*, e2655-e2655.
430. Ren, W., Liu, G., Yin, J., Tan, B., Wu, G., Bazer, F.W., Peng, Y., and Yin, Y. (2017b). Amino-acid transporters in T-cell activation and differentiation. Cell Death Dis *8*, e2655.
431. Reyes, A., Corrales, N., Gálvez, N.M.S., Bueno, S.M., Kalergis, A.M., and González, P.A. (2020). Contribution of hypoxia inducible factor-1 during viral infections. Virulence *11*, 1482-1500.
432. Riches, J.C., Davies, J.K., McClanahan, F., Fatah, R., Iqbal, S., Agrawal, S., Ramsay, A.G., and Gribben, J.G. (2013). T cells from CLL patients exhibit features of T-cell exhaustion but retain capacity for cytokine production. Blood *121*, 1612-1621.
433. Riha, P., and Rudd, C.E. (2010). CD28 co-signaling in the adaptive immune response. Self Nonself *1*, 231-240.
434. Rius, J., Guma, M., Schachtrup, C., Akassoglou, K., Zinkernagel, A.S., Nizet, V., Johnson, R.S., Haddad, G.G., and Karin, M. (2008). NF-kappaB links innate immunity to the hypoxic response through transcriptional regulation of HIF-1alpha. Nature *453*, 807-811.
435. Robak, T., and Robak, P. (2013). BCR signaling in chronic lymphocytic leukemia and related inhibitors currently in clinical studies. Int Rev Immunol *32*, 358-376.
436. Rocamora-Reverte, L., Melzer, F.L., Wurzner, R., and Weinberger, B. (2020). The Complex Role of Regulatory T Cells in Immunity and Aging. Front Immunol *11*, 616949.
437. Roessner, P.M., Hanna, B.S., Öztürk, S., Schulz, R., Llaó Cid, L., Yazdanparast, H., Scheffold, A., Colomer, D., Stilgenbauer, S., Lichter, P*., et al.* (2020). TBET-expressing Th1 CD4+ T cells accumulate in chronic lymphocytic leukaemia without affecting disease progression in Eμ-TCL1 mice. British Journal of Haematology *189*, 133-145.
438. Roessner, P.M., and Seiffert, M. (2020). T-cells in chronic lymphocytic leukemia: Guardians or drivers of disease? Leukemia *34*, 2012-2024.
439. Rosati, E., Baldoni, S., De Falco, F., Del Papa, B., Dorillo, E., Rompietti, C., Albi, E., Falzetti, F., Di Ianni, M., and Sportoletti, P. (2018). NOTCH1 Aberrations in Chronic Lymphocytic Leukemia. Front Oncol *8*, 229.

440. Rossi, D., Rasi, S., Fabbri, G., Spina, V., Fangazio, M., Forconi, F., Marasca, R., Laurenti, L., Bruscaggin, A., Cerri, M*., et al.* (2012a). Mutations of NOTCH1 are an independent predictor of survival in chronic lymphocytic leukemia. Blood *119*, 521-529.
441. Rossi, D., Rasi, S., Spina, V., Fangazio, M., Monti, S., Greco, M., Ciardullo, C., Fama, R., Cresta, S., Bruscaggin, A*., et al.* (2012b). Different impact of NOTCH1 and SF3B1 mutations on the risk of chronic lymphocytic leukemia transformation to Richter syndrome. Br J Haematol *158*, 426-429.
442. Rossi, D., Spina, V., Cerri, M., Rasi, S., Deambrogi, C., De Paoli, L., Laurenti, L., Maffei, R., Forconi, F., Bertoni, F*., et al.* (2009). Stereotyped B-cell receptor is an independent risk factor of chronic lymphocytic leukemia transformation to Richter syndrome. Clin Cancer Res *15*, 4415-4422.
443. Rotbain, E.C., Frederiksen, H., Hjalgrim, H., Rostgaard, K., Egholm, G.J., Zahedi, B., Poulsen, C.B., Enggard, L., da Cunha-Bang, C., and Niemann, C.U. (2020). IGHV mutational status and outcome for patients with chronic lymphocytic leukemia upon treatment: a Danish nationwide population-based study. Haematologica *105*, 1621-1629.
444. Roy, S., Kumaravel, S., Sharma, A., Duran, C.L., Bayless, K.J., and Chakraborty, S. (2020). Hypoxic tumor microenvironment: Implications for cancer therapy. Exp Biol Med (Maywood) *245*, 1073-1086.
445. Rozman, C., Hernandez-Nieto, L., Montserrat, E., and Brugues, R. (1981). Prognostic significance of bone-marrow patterns in chronic lymphocytic leukaemia. Br J Haematol *47*, 529-537.
446. RV, L., R, Z., AV, V., and B, X. (2012). $CD4^+$T cells: differentiation and functions. Clin Dev Immunol *2012:925135*.
447. Sadik, A., Somarribas Patterson, L.F., Öztürk, S., Mohapatra, S.R., Panitz, V., Secker, P.F., Pfänder, P., Loth, S., Salem, H., Prentzell, M.T*., et al.* (2020). IL4I1 Is a Metabolic Immune Checkpoint that Activates the AHR and Promotes Tumor Progression. Cell *182*, 1252-1270.e1234.
448. Saito, S., Lin, Y.C., Tsai, M.H., Lin, C.S., Murayama, Y., Sato, R., and Yokoyama, K.K. (2015). Emerging roles of hypoxia-inducible factors and reactive oxygen species in cancer and pluripotent stem cells. Kaohsiung J Med Sci *31*, 279-286.
449. Saito, T., Kurose, K., Kojima, T., Funakoshi, T., Sato, E., Nishikawa, H., Nakajima, J., Seto, Y., Kakimi, K., Iida, S*., et al.* (2021). Phase Ib study on the humanized anti-CCR4 antibody, KW-0761, in advanced solid tumors. Nagoya J Med Sci *83*, 827-840.
450. Sakaguchi, S., Sakaguchi, N., Asano, M., Itoh, M., and Toda, M. (1995). Immunologic self-tolerance maintained by activated T cells expressing IL-2 receptor alpha-chains (CD25). Breakdown of a single mechanism of self-tolerance causes various autoimmune diseases. J Immunol *155*, 1151-1164.
451. Salcedo, R., Hixon, J.A., Stauffer, J.K., Jalah, R., Brooks, A.D., Khan, T., Dai, R.M., Scheetz, L., Lincoln, E., Back, T.C*., et al.* (2009). Immunologic and therapeutic synergy of IL-27 and IL-2: enhancement of T cell sensitization, tumor-specific CTL reactivity and complete regression of disseminated neuroblastoma metastases in the liver and bone marrow. J Immunol *182*, 4328-4338.
452. Salcedo, R., Stauffer, J.K., Lincoln, E., Back, T.C., Hixon, J.A., Hahn, C., Shafer-Weaver, K., Malyguine, A., Kastelein, R., and Wigginton, J.M. (2004). IL-27 mediates complete regression of orthotopic primary and metastatic murine neuroblastoma tumors: role for CD8+ T cells. J Immunol *173*, 7170-7182.
453. Samelson, L.E. (2002). Signal transduction mediated by the T cell antigen receptor: the role of adapter proteins. Annu Rev Immunol *20*, 371-394.
454. Sanchez-Correa, B., Valhondo, I., Hassouneh, F., Lopez-Sejas, N., Pera, A., Bergua, J.M., Arcos, M.J., Banas, H., Casas-Aviles, I., Duran, E*., et al.* (2019). DNAM-1 and the TIGIT/PVRIG/TACTILE Axis: Novel Immune Checkpoints for Natural Killer Cell-Based Cancer Immunotherapy. Cancers (Basel) *11*.
455. Sanna, S., Satta, G., Padoan, M., Piro, S., Gambelunghe, A., Miligi, L., Ferri, G.M., Magnani, C., Muzi, G., Rigacci, L*., et al.* (2017). Activation of the aryl hydrocarbon receptor and risk of lymphoma subtypes. Int J Mol Epidemiol Genet *8*, 40-44.
456. Sansom, D.M. (2000). CD28, CTLA-4 and their ligands: who does what and to whom? Immunology *101*, 169-177.

457. Santamaria, J.C., Borelli, A., and Irla, M. (2021). Regulatory T Cell Heterogeneity in the Thymus: Impact on Their Functional Activities. Front Immunol *12*, 643153.
458. Savoia, P., Astrua, C., and Fava, P. (2016). Ipilimumab (Anti-Ctla-4 Mab) in the treatment of metastatic melanoma: Effectiveness and toxicity management. Hum Vaccin Immunother *12*, 1092-1101.
459. Sawant, D.V., Yano, H., Chikina, M., Zhang, Q., Liao, M., Liu, C., Callahan, D.J., Sun, Z., Sun, T., Tabib, T.*, et al.* (2019). Adaptive plasticity of IL-10(+) and IL-35(+) Treg cells cooperatively promotes tumor T cell exhaustion. Nat Immunol *20*, 724-735.
460. Schiavinato, J.L.d.S., Haddad, R., Saldanha-Araujo, F., Baiochi, J., Araujo, A.G., Santos Scheucher, P., Covas, D.T., Zago, M.A., and Panepucci, R.A. (2017). TGF-beta/atRA-induced Tregs express a selected set of microRNAs involved in the repression of transcripts related to Th17 differentiation. Scientific Reports *7*, 3627.
461. Schietinger, A., and Greenberg, P.D. (2014). Tolerance and exhaustion: defining mechanisms of T cell dysfunction. Trends Immunol *35*, 51-60.
462. Schildknecht, A., Brauer, S., Brenner, C., Lahl, K., Schild, H., Sparwasser, T., Probst, H.C., and van den Broek, M. (2010). FoxP3⁺ regulatory T cells essentially contribute to peripheral CD8⁺ T-cell tolerance induced by steady-state dendritic cells. Proceedings of the National Academy of Sciences *107*, 199-203.
463. Schlenner, S.M., Weigmann, B., Ruan, Q., Chen, Y., and von Boehmer, H. (2012). Smad3 binding to the foxp3 enhancer is dispensable for the development of regulatory T cells with the exception of the gut. J Exp Med *209*, 1529-1535.
464. Schmidt, A., Oberle, N., and Krammer, P.H. (2012). Molecular mechanisms of treg-mediated T cell suppression. Front Immunol *3*, 51.
465. Schmidt, J.V., and Bradfield, C.A. (1996). Ah receptor signaling pathways. Annu Rev Cell Dev Biol *12*, 55-89.
466. Schneider, R., Yaneva, T., Beauseigle, D., El-Khoury, L., and Arbour, N. (2011). IL-27 increases the proliferation and effector functions of human naïve CD8+ T lymphocytes and promotes their development into Tc1 cells. Eur J Immunol *41*, 47-59.
467. Schofield, C.J., and Ratcliffe, P.J. (2005). Signalling hypoxia by HIF hydroxylases. Biochem Biophys Res Commun *338*, 617-626.
468. Schoppmeyer, R., Zhao, R., Cheng, H., Hamed, M., Liu, C., Zhou, X., Schwarz, E.C., Zhou, Y., Knörck, A., Schwär, G.*, et al.* (2017). Human profilin 1 is a negative regulator of CTL mediated cell-killing and migration. Eur J Immunol *47*, 1562-1572.
469. Schulz, A., Durr, C., Zenz, T., Dohner, H., Stilgenbauer, S., Lichter, P., and Seiffert, M. (2013). Lenalidomide reduces survival of chronic lymphocytic leukemia cells in primary cocultures by altering the myeloid microenvironment. Blood *121*, 2503-2511.
470. Schuster, M., Plaza-Sirvent, C., Visekruna, A., Huehn, J., and Schmitz, I. (2019). Generation of Foxp3(+)CD25(-) Regulatory T-Cell Precursors Requires c-Rel and IkappaBNS. Front Immunol *10*, 1583.
471. Sckisel, G.D., Mirsoian, A., Minnar, C.M., Crittenden, M., Curti, B., Chen, J.Q., Blazar, B.R., Borowsky, A.D., Monjazeb, A.M., and Murphy, W.J. (2017). Differential phenotypes of memory CD4 and CD8 T cells in the spleen and peripheral tissues following immunostimulatory therapy. J Immunother Cancer *5*, 33.
472. Scott, A.C., Dündar, F., Zumbo, P., Chandran, S.S., Klebanoff, C.A., Shakiba, M., Trivedi, P., Menocal, L., Appleby, H., Camara, S.*, et al.* (2019). TOX is a critical regulator of tumour-specific T cell differentiation. Nature *571*, 270-274.
473. Scurr, M., Pembroke, T., Bloom, A., Roberts, D., Thomson, A., Smart, K., Bridgeman, H., Adams, R., Brewster, A., Jones, R.*, et al.* (2017). Low-Dose Cyclophosphamide Induces Antitumor T-Cell Responses, which Associate with Survival in Metastatic Colorectal Cancer. Clin Cancer Res *23*, 6771-6780.

474. Sedlarikova, L., Petrackova, A., Papajik, T., Turcsanyi, P., and Kriegova, E. (2020). Resistance-Associated Mutations in Chronic Lymphocytic Leukemia Patients Treated With Novel Agents. Front Oncol *10*, 894.
475. Seiffert, M. (2020). HIF-1α: a potential treatment target in chronic lymphocytic leukemia. Haematologica *105*, 856-858.
476. Sekiya, T., Nakatsukasa, H., Lu, Q., and Yoshimura, A. (2016). Roles of transcription factors and epigenetic modifications in differentiation and maintenance of regulatory T cells. Microbes Infect *18*, 378-386.
477. Semenza, G.L., Agani, F., Booth, G., Forsythe, J., Iyer, N., Jiang, B.H., Leung, S., Roe, R., Wiener, C., and Yu, A. (1997). Structural and functional analysis of hypoxia-inducible factor 1. Kidney Int *51*, 553-555.
478. Sen, D.R., Kaminski, J., Barnitz, R.A., Kurachi, M., Gerdemann, U., Yates, K.B., Tsao, H.W., Godec, J., LaFleur, M.W., Brown, F.D.*, et al.* (2016). The epigenetic landscape of T cell exhaustion. Science *354*, 1165-1169.
479. Seok, S.H., Lee, W., Jiang, L., Molugu, K., Zheng, A., Li, Y., Park, S., Bradfield, C.A., and Xing, Y. (2017). Structural hierarchy controlling dimerization and target DNA recognition in the AHR transcriptional complex. Proc Natl Acad Sci U S A *114*, 5431-5436.
480. Seymour, J.F., Kipps, T.J., Eichhorst, B., Hillmen, P., D'Rozario, J., Assouline, S., Owen, C., Gerecitano, J., Robak, T., De la Serna, J.*, et al.* (2018). Venetoclax-Rituximab in Relapsed or Refractory Chronic Lymphocytic Leukemia. N Engl J Med *378*, 1107-1120.
481. Shah, D.K., and Zuniga-Pflucker, J.C. (2014). An overview of the intrathymic intricacies of T cell development. J Immunol *192*, 4017-4023.
482. Shao, Y., Yang, W.Y., Saaoud, F., Drummer, C.t., Sun, Y., Xu, K., Lu, Y., Shan, H., Shevach, E.M., Jiang, X.*, et al.* (2021). IL-35 promotes CD4+Foxp3+ Tregs and inhibits atherosclerosis via maintaining CCR5-amplified Treg-suppressive mechanisms. JCI Insight *6*.
483. Sharma, S., and Rai, K.R. (2019). Chronic lymphocytic leukemia (CLL) treatment: So many choices, such great options. Cancer *125*, 1432-1440.
484. Shehade, H., Acolty, V., Moser, M., and Oldenhove, G. (2015). Cutting Edge: Hypoxia-Inducible Factor 1 Negatively Regulates Th1 Function. The Journal of Immunology *195*, 1372-1376.
485. Shi, L.Z., Wang, R., Huang, G., Vogel, P., Neale, G., Green, D.R., and Chi, H. (2011). HIF1alpha-dependent glycolytic pathway orchestrates a metabolic checkpoint for the differentiation of TH17 and Treg cells. J Exp Med *208*, 1367-1376.
486. Shibru, B., Fey, K., Fricke, S., Blaudszun, A.R., Furst, F., Weise, M., Seiffert, S., Weyh, M.K., Kohl, U., Sack, U.*, et al.* (2021). Detection of Immune Checkpoint Receptors - A Current Challenge in Clinical Flow Cytometry. Front Immunol *12*, 694055.
487. Shimizu, J., Yamazaki, S., and Sakaguchi, S. (1999). Induction of tumor immunity by removing CD25+CD4+ T cells: a common basis between tumor immunity and autoimmunity. J Immunol *163*, 5211-5218.
488. Simon-Gabriel, C.P., Foerster, K., Saleem, S., Bleckmann, D., Benkisser-Petersen, M., Thornton, N., Umezawa, K., Decker, S., Burger, M., Veelken, H.*, et al.* (2018). Microenvironmental stromal cells abrogate NF-kappaB inhibitor-induced apoptosis in chronic lymphocytic leukemia. Haematologica *103*, 136-147.
489. Simonetta, F., and Bourgeois, C. (2013). CD4+FOXP3+ Regulatory T-Cell Subsets in Human Immunodeficiency Virus Infection. Front Immunol *4*, 215.
490. Simonetti, G., Bertilaccio, M.T., Ghia, P., and Klein, U. (2014). Mouse models in the study of chronic lymphocytic leukemia pathogenesis and therapy. Blood *124*, 1010-1019.
491. Simpson, T.R., Li, F., Montalvo-Ortiz, W., Sepulveda, M.A., Bergerhoff, K., Arce, F., Roddie, C., Henry, J.Y., Yagita, H., Wolchok, J.D.*, et al.* (2013). Fc-dependent depletion of tumor-infiltrating regulatory T cells co-defines the efficacy of anti-CTLA-4 therapy against melanoma. J Exp Med *210*, 1695-1710.
492. Slaney, C.Y., Kershaw, M.H., and Darcy, P.K. (2014). Trafficking of T cells into tumors. Cancer Res *74*, 7168-7174.

493. Smith, E.N., Ghia, E.M., DeBoever, C.M., Rassenti, L.Z., Jepsen, K., Yoon, K.A., Matsui, H., Rozenzhak, S., Alakus, H., Shepard, P.J.*, et al.* (2015). Genetic and epigenetic profiling of CLL disease progression reveals limited somatic evolution and suggests a relationship to memory-cell development. Blood Cancer J *5*, e303.
494. Sojka, D.K., Huang, Y.H., and Fowell, D.J. (2008). Mechanisms of regulatory T-cell suppression - a diverse arsenal for a moving target. Immunology *124*, 13-22.
495. Sokol, C.L., Chu, N.Q., Yu, S., Nish, S.A., Laufer, T.M., and Medzhitov, R. (2009). Basophils function as antigen-presenting cells for an allergen-induced T helper type 2 response. Nat Immunol *10*, 713-720.
496. Solomon, I., Amann, M., Goubier, A., Arce Vargas, F., Zervas, D., Qing, C., Henry, J.Y., Ghorani, E., Akarca, A.U., Marafioti, T.*, et al.* (2020). CD25-T(reg)-depleting antibodies preserving IL-2 signaling on effector T cells enhance effector activation and antitumor immunity. Nat Cancer *1*, 1153-1166.
497. Soma, L.A., Craig, F.E., and Swerdlow, S.H. (2006). The proliferation center microenvironment and prognostic markers in chronic lymphocytic leukemia/small lymphocytic lymphoma. Hum Pathol *37*, 152-159.
498. Song, Y., Wang, N., Chen, L., and Fang, L. (2021). Tr1 Cells as a Key Regulator for Maintaining Immune Homeostasis in Transplantation. Front Immunol *12*, 671579.
499. Spits, H. (2002). Development of alphabeta T cells in the human thymus. Nat Rev Immunol *2*, 760-772.
500. Srinivasan, V.K., Naseem, S., Varma, N., Lad, D.P., and Malhotra, P. (2020). Genomic alterations in chronic lymphocytic leukemia and their correlation with clinico-hematological parameters and disease progression. Blood Res *55*, 131-138.
501. Stanford, E.A., Ramirez-Cardenas, A., Wang, Z., Novikov, O., Alamoud, K., Koutrakis, P., Mizgerd, J.P., Genco, C.A., Kukuruzinska, M., Monti, S.*, et al.* (2016). Role for the Aryl Hydrocarbon Receptor and Diverse Ligands in Oral Squamous Cell Carcinoma Migration and Tumorigenesis. Mol Cancer Res *14*, 696-706.
502. Stankovic, T., and Skowronska, A. (2014). The role of ATM mutations and 11q deletions in disease progression in chronic lymphocytic leukemia. Leuk Lymphoma *55*, 1227-1239.
503. Staron, M.M., Gray, S.M., Marshall, H.D., Parish, I.A., Chen, J.H., Perry, C.J., Cui, G., Li, M.O., and Kaech, S.M. (2014). The transcription factor FoxO1 sustains expression of the inhibitory receptor PD-1 and survival of antiviral CD8(+) T cells during chronic infection. Immunity *41*, 802-814.
504. Stevenson, F.K., Krysov, S., Davies, A.J., Steele, A.J., and Packham, G. (2011). B-cell receptor signaling in chronic lymphocytic leukemia. Blood *118*, 4313-4320.
505. Stockinger, B., Di Meglio, P., Gialitakis, M., and Duarte, J.H. (2014). The aryl hydrocarbon receptor: multitasking in the immune system. Annu Rev Immunol *32*, 403-432.
506. Stockinger, B., Veldhoen, M., and Hirota, K. (2009). Modulation of Th17 development and function by activation of the aryl hydrocarbon receptor--the role of endogenous ligands. Eur J Immunol *39*, 652-654.
507. Strati, P., Abruzzo, L.V., Wierda, W.G., O'Brien, S., Ferrajoli, A., and Keating, M.J. (2015). Second cancers and Richter transformation are the leading causes of death in patients with trisomy 12 chronic lymphocytic leukemia. Clin Lymphoma Myeloma Leuk *15*, 420-427.
508. Strati, P., and Shanafelt, T.D. (2015). Monoclonal B-cell lymphocytosis and early-stage chronic lymphocytic leukemia: diagnosis, natural history, and risk stratification. Blood *126*, 454-462.
509. Strowitzki, M.J., Ritter, A.S., Kimmer, G., and Schneider, M. (2019). Hypoxia-adaptive pathways: A pharmacological target in fibrotic disease? Pharmacol Res *147*, 104364.
510. Su, J.M., Lin, P., and Chang, H. (2013). Prognostic value of nuclear translocation of aryl hydrocarbon receptor for non-small cell lung cancer. Anticancer Res *33*, 3953-3961.
511. Sugiyama, D., Nishikawa, H., Maeda, Y., Nishioka, M., Tanemura, A., Katayama, I., Ezoe, S., Kanakura, Y., Sato, E., Fukumori, Y.*, et al.* (2013a). Anti-CCR4 mAb selectively depletes effector-type

FoxP3+CD4+ regulatory T cells, evoking antitumor immune responses in humans. Proc Natl Acad Sci U S A *110*, 17945-17950.
512. Sugiyama, D., Nishikawa, H., Maeda, Y., Nishioka, M., Tanemura, A., Katayama, I., Ezoe, S., Kanakura, Y., Sato, E., Fukumori, Y.*, et al.* (2013b). Anti-CCR4 mAb selectively depletes effector-type FoxP3+CD4+ regulatory T cells, evoking antitumor immune responses in humans. Proc Natl Acad Sci U S A *110*, 17945-17950.
513. Svanberg, R., Janum, S., Patten, P.E.M., Ramsay, A.G., and Niemann, C.U. (2021). Targeting the tumor microenvironment in chronic lymphocytic leukemia. Haematologica *106*, 2312-2324.
514. Swerdlow, S.H., Campo, E., Pileri, S.A., Harris, N.L., Stein, H., Siebert, R., Advani, R., Ghielmini, M., Salles, G.A., Zelenetz, A.D.*, et al.* (2016). The 2016 revision of the World Health Organization classification of lymphoid neoplasms. Blood *127*, 2375-2390.
515. Tadmor, T., and Levy, I. (2021). Richter Transformation in Chronic Lymphocytic Leukemia: Update in the Era of Novel Agents. Cancers (Basel) *13*.
516. Taghiloo, S., Allahmoradi, E., Tehrani, M., Hossein-Nataj, H., Shekarriz, R., Janbabaei, G., Abediankenari, S., and Asgarian-Omran, H. (2017). Frequency and functional characterization of exhausted CD8(+) T cells in chronic lymphocytic leukemia. Eur J Haematol *98*, 622-631.
517. Tai, X., Erman, B., Alag, A., Mu, J., Kimura, M., Katz, G., Guinter, T., McCaughtry, T., Etzensperger, R., Feigenbaum, L.*, et al.* (2013). Foxp3 transcription factor is proapoptotic and lethal to developing regulatory T cells unless counterbalanced by cytokine survival signals. Immunity *38*, 1116-1128.
518. Takahama, Y. (2006). Journey through the thymus: stromal guides for T-cell development and selection. Nat Rev Immunol *6*, 127-135.
519. Takeda, A., Hamano, S., Yamanaka, A., Hanada, T., Ishibashi, T., Mak, T.W., Yoshimura, A., and Yoshida, H. (2003). Cutting edge: role of IL-27/WSX-1 signaling for induction of T-bet through activation of STAT1 during initial Th1 commitment. J Immunol *170*, 4886-4890.
520. Takenaka, M.C., Gabriely, G., Rothhammer, V., Mascanfroni, I.D., Wheeler, M.A., Chao, C.C., Gutiérrez-Vázquez, C., Kenison, J., Tjon, E.C., Barroso, A.*, et al.* (2019). Control of tumor-associated macrophages and T cells in glioblastoma via AHR and CD39. Nat Neurosci *22*, 729-740.
521. Takeuchi, A., and Saito, T. (2017). CD4 CTL, a Cytotoxic Subset of CD4(+) T Cells, Their Differentiation and Function. Front Immunol *8*, 194.
522. Tam, C.S., Trotman, J., Opat, S., Burger, J.A., Cull, G., Gottlieb, D., Harrup, R., Johnston, P.B., Marlton, P., Munoz, J.*, et al.* (2019). Phase 1 study of the selective BTK inhibitor zanubrutinib in B-cell malignancies and safety and efficacy evaluation in CLL. Blood *134*, 851-859.
523. Tang, K., Wu, Y.-H., Song, Y., and Yu, B. (2021). Indoleamine 2,3-dioxygenase 1 (IDO1) inhibitors in clinical trials for cancer immunotherapy. Journal of Hematology & Oncology *14*, 68.
524. Tangye, S.G., Liu, Y.J., Aversa, G., Phillips, J.H., and de Vries, J.E. (1998). Identification of functional human splenic memory B cells by expression of CD148 and CD27. J Exp Med *188*, 1691-1703.
525. Tao, X., Constant, S., Jorritsma, P., and Bottomly, K. (1997). Strength of TCR signal determines the costimulatory requirements for Th1 and Th2 CD4+ T cell differentiation. J Immunol *159*, 5956-5963.
526. Tappenden, D.M., Hwang, H.J., Yang, L., Thomas, R.S., and Lapres, J.J. (2013). The Aryl-Hydrocarbon Receptor Protein Interaction Network (AHR-PIN) as Identified by Tandem Affinity Purification (TAP) and Mass Spectrometry. J Toxicol *2013*, 279829.
527. Tekguc, M., Wing, J.B., Osaki, M., Long, J., and Sakaguchi, S. (2021). Treg-expressed CTLA-4 depletes CD80/CD86 by trogocytosis, releasing free PD-L1 on antigen-presenting cells. Proc Natl Acad Sci U S A *118*.
528. Ten Hacken, E., Gounari, M., Ghia, P., and Burger, J.A. (2019). The importance of B cell receptor isotypes and stereotypes in chronic lymphocytic leukemia. Leukemia *33*, 287-298.
529. Thompson, P.A., Tam, C.S., O'Brien, S.M., Wierda, W.G., Stingo, F., Plunkett, W., Smith, S.C., Kantarjian, H.M., Freireich, E.J., and Keating, M.J. (2016). Fludarabine, cyclophosphamide, and

rituximab treatment achieves long-term disease-free survival in IGHV-mutated chronic lymphocytic leukemia. Blood *127*, 303-309.
530. Thornton, A.M., and Shevach, E.M. (1998). CD4+CD25+ immunoregulatory T cells suppress polyclonal T cell activation in vitro by inhibiting interleukin 2 production. J Exp Med *188*, 287-296.
531. Thorsby, E. (1984). The role of HLA in T cell activation. Hum Immunol *9*, 1-7.
532. Timar, B., Fulop, Z., Csernus, B., Angster, C., Bognar, A., Szepesi, A., Kopper, L., and Matolcsy, A. (2004). Relationship between the mutational status of VH genes and pathogenesis of diffuse large B-cell lymphoma in Richter's syndrome. Leukemia *18*, 326-330.
533. Timofeeva, N., and Gandhi, V. (2021). Ibrutinib combinations in CLL therapy: scientific rationale and clinical results. Blood Cancer J *11*, 79.
534. Togashi, Y., Shitara, K., and Nishikawa, H. (2019). Regulatory T cells in cancer immunosuppression - implications for anticancer therapy. Nat Rev Clin Oncol *16*, 356-371.
535. Trimarco, V., Ave, E., Facco, M., Chiodin, G., Frezzato, F., Martini, V., Gattazzo, C., Lessi, F., Giorgi, C.A., Visentin, A.*, et al.* (2015). Cross-talk between chronic lymphocytic leukemia (CLL) tumor B cells and mesenchymal stromal cells (MSCs): implications for neoplastic cell survival. Oncotarget *6*, 42130-42149.
536. Trinchieri, G., Pflanz, S., and Kastelein, R.A. (2003). The IL-12 family of heterodimeric cytokines: new players in the regulation of T cell responses. Immunity *19*, 641-644.
537. Tsuji, N., Fukuda, K., Nagata, Y., Okada, H., Haga, A., Hatakeyama, S., Yoshida, S., Okamoto, T., Hosaka, M., Sekine, K.*, et al.* (2014). The activation mechanism of the aryl hydrocarbon receptor (AhR) by molecular chaperone HSP90. FEBS Open Bio *4*, 796-803.
538. Tsukada, N., Burger, J.A., Zvaifler, N.J., and Kipps, T.J. (2002). Distinctive features of "nurselike" cells that differentiate in the context of chronic lymphocytic leukemia. Blood *99*, 1030-1037.
539. Valsecchi, R., Coltella, N., Belloni, D., Ponente, M., Ten Hacken, E., Scielzo, C., Scarfò, L., Bertilaccio, M.T., Brambilla, P., Lenti, E.*, et al.* (2016). HIF-1α regulates the interaction of chronic lymphocytic leukemia cells with the tumor microenvironment. Blood *127*, 1987-1997.
540. van der Veeken, J., Gonzalez, A.J., Cho, H., Arvey, A., Hemmers, S., Leslie, C.S., and Rudensky, A.Y. (2016). Memory of Inflammation in Regulatory T Cells. Cell *166*, 977-990.
541. van der Windt, G.J., and Pearce, E.L. (2012). Metabolic switching and fuel choice during T-cell differentiation and memory development. Immunol Rev *249*, 27-42.
542. Vardi, A., Stamatopoulos, K., and Hadzidimitriou, A. (2017a). T cells in chronic lymphocytic leukemia: can they fight? Oncotarget *8*, 99209-99210.
543. Vardi, A., Vlachonikola, E., Karypidou, M., Stalika, E., Bikos, V., Gemenetzi, K., Maramis, C., Siorenta, A., Anagnostopoulos, A., Pospisilova, S.*, et al.* (2017b). Restrictions in the T-cell repertoire of chronic lymphocytic leukemia: high-throughput immunoprofiling supports selection by shared antigenic elements. Leukemia *31*, 1555-1561.
544. Veldhoen, M., Hirota, K., Westendorf, A.M., Buer, J., Dumoutier, L., Renauld, J.C., and Stockinger, B. (2008a). The aryl hydrocarbon receptor links TH17-cell-mediated autoimmunity to environmental toxins. Nature *453*, 106-109.
545. Veldhoen, M., Uyttenhove, C., van Snick, J., Helmby, H., Westendorf, A., Buer, J., Martin, B., Wilhelm, C., and Stockinger, B. (2008b). Transforming growth factor-β 'reprograms' the differentiation of T helper 2 cells and promotes an interleukin 9–producing subset. Nature Immunology *9*, 1341-1346.
546. Venturi, V., and Thomas, P.G. (2018). The expanding role of systems immunology in decoding the T cell receptor repertoire. Curr Opin Syst Biol *12*, 37-45.
547. Veuillen, C., Aurran-Schleinitz, T., Castellano, R., Rey, J., Mallet, F., Orlanducci, F., Pouyet, L., Just-Landi, S., Coso, D., Ivanov, V.*, et al.* (2012). Primary B-CLL resistance to NK cell cytotoxicity can be overcome in vitro and in vivo by priming NK cells and monoclonal antibody therapy. J Clin Immunol *32*, 632-646.
548. Vignali, D.A., Collison, L.W., and Workman, C.J. (2008). How regulatory T cells work. Nat Rev Immunol *8*, 523-532.

549. Villarino, A.V., Larkin, J., 3rd, Saris, C.J., Caton, A.J., Lucas, S., Wong, T., de Sauvage, F.J., and Hunter, C.A. (2005). Positive and negative regulation of the IL-27 receptor during lymphoid cell activation. J Immunol *174*, 7684-7691.
550. Visentin, A., Bonaldi, L., Rigolin, G.M., Mauro, F.R., Martines, A., Frezzato, F., Pravato, S., Gargarella, L.R., Bardi, M.A., Cavallari, M.*, et al.* (2022). The complex karyotype landscape in chronic lymphocytic leukemia allows the refinement of the risk of Richter syndrome transformation. Haematologica *107*, 868-876.
551. Vlachonikola, E., Stamatopoulos, K., and Chatzidimitriou, A. (2020). T Cells in Chronic Lymphocytic Leukemia: A Two-Edged Sword. Front Immunol *11*, 612244.
552. Vogel, C.F., Goth, S.R., Dong, B., Pessah, I.N., and Matsumura, F. (2008). Aryl hydrocarbon receptor signaling mediates expression of indoleamine 2,3-dioxygenase. Biochem Biophys Res Commun *375*, 331-335.
553. Volpe, E., Servant, N., Zollinger, R., Bogiatzi, S.I., Hupe, P., Barillot, E., and Soumelis, V. (2008). A critical function for transforming growth factor-beta, interleukin 23 and proinflammatory cytokines in driving and modulating human T(H)-17 responses. Nat Immunol *9*, 650-657.
554. von Boehmer, H., Teh, H.S., and Kisielow, P. (1989). The thymus selects the useful, neglects the useless and destroys the harmful. Immunol Today *10*, 57-61.
555. Waldman, A.D., Fritz, J.M., and Lenardo, M.J. (2020). A guide to cancer immunotherapy: from T cell basic science to clinical practice. Nat Rev Immunol *20*, 651-668.
556. Wang, D., Quiros, J., Mahuron, K., Pai, C.C., Ranzani, V., Young, A., Silveria, S., Harwin, T., Abnousian, A., Pagani, M.*, et al.* (2018a). Targeting EZH2 Reprograms Intratumoral Regulatory T Cells to Enhance Cancer Immunity. Cell Rep *23*, 3262-3274.
557. Wang, G.L., Jiang, B.H., Rue, E.A., and Semenza, G.L. (1995). Hypoxia-inducible factor 1 is a basic-helix-loop-helix-PAS heterodimer regulated by cellular O2 tension. Proc Natl Acad Sci U S A *92*, 5510-5514.
558. Wang, G.Z., Zhang, L., Zhao, X.C., Gao, S.H., Qu, L.W., Yu, H., Fang, W.F., Zhou, Y.C., Liang, F., Zhang, C.*, et al.* (2019a). The Aryl hydrocarbon receptor mediates tobacco-induced PD-L1 expression and is associated with response to immunotherapy. Nat Commun *10*, 1125.
559. Wang, L., Lawrence, M.S., Wan, Y., Stojanov, P., Sougnez, C., Stevenson, K., Werner, L., Sivachenko, A., DeLuca, D.S., Zhang, L.*, et al.* (2011). SF3B1 and other novel cancer genes in chronic lymphocytic leukemia. N Engl J Med *365*, 2497-2506.
560. Wang, L., Simons, D.L., Lu, X., Tu, T.Y., Solomon, S., Wang, R., Rosario, A., Avalos, C., Schmolze, D., Yim, J.*, et al.* (2019b). Connecting blood and intratumoral Treg cell activity in predicting future relapse in breast cancer. Nat Immunol *20*, 1220-1230.
561. Wang, Q., Ning, H., Peng, H., Wei, L., Hou, R., Hoft, D.F., and Liu, J. (2017). Tristetraprolin inhibits macrophage IL-27-induced activation of antitumour cytotoxic T cell responses. Nature Communications *8*, 867.
562. Wang, W.T., Zhu, H.Y., Wu, Y.J., Xia, Y., Wu, J.Z., Wu, W., Liang, J.H., Wang, L., Fan, L., Li, J.Y.*, et al.* (2018b). Elevated absolute NK cell counts in peripheral blood predict good prognosis in chronic lymphocytic leukemia. J Cancer Res Clin Oncol *144*, 449-457.
563. Wang, Y., Tschautscher, M.A., Rabe, K.G., Call, T.G., Leis, J.F., Kenderian, S.S., Kay, N.E., Muchtar, E., Van Dyke, D.L., Koehler, A.B.*, et al.* (2020a). Clinical characteristics and outcomes of Richter transformation: experience of 204 patients from a single center. Haematologica *105*, 765-773.
564. Wang, Z., Snyder, M., Kenison, J.E., Yang, K., Lara, B., Lydell, E., Bennani, K., Novikov, O., Federico, A., Monti, S.*, et al.* (2020b). How the AHR Became Important in Cancer: The Role of Chronically Active AHR in Cancer Aggression. Int J Mol Sci *22*.
565. Ward-Kavanagh, L.K., Lin, W.W., Sedy, J.R., and Ware, C.F. (2016). The TNF Receptor Superfamily in Co-stimulating and Co-inhibitory Responses. Immunity *44*, 1005-1019.
566. Wehrens, E.J., Wong, K.A., Gupta, A., Khan, A., Benedict, C.A., and Zuniga, E.I. (2018). IL-27 regulates the number, function and cytotoxic program of antiviral CD4 T cells and promotes cytomegalovirus persistence. PLoS One *13*, e0201249.

567. Whiteside, T.L. (2013). Immune modulation of T-cell and NK (natural killer) cell activities by TEXs (tumour-derived exosomes). Biochem Soc Trans *41*, 245-251.
568. Wierz, M., Pierson, S., Guyonnet, L., Viry, E., Lequeux, A., Oudin, A., Niclou, S.P., Ollert, M., Berchem, G., Janji, B.*, et al.* (2018). Dual PD1/LAG3 immune checkpoint blockade limits tumor development in a murine model of chronic lymphocytic leukemia. Blood *131*, 1617-1621.
569. Wilson, A., Hodgson-Garms, M., Frith, J.E., and Genever, P. (2019). Multiplicity of Mesenchymal Stromal Cells: Finding the Right Route to Therapy. Front Immunol *10*, 1112.
570. Wilson, W.R., and Hay, M.P. (2011). Targeting hypoxia in cancer therapy. Nat Rev Cancer *11*, 393-410.
571. Wing, J.B., Tanaka, A., and Sakaguchi, S. (2019). Human FOXP3(+) Regulatory T Cell Heterogeneity and Function in Autoimmunity and Cancer. Immunity *50*, 302-316.
572. Wirtz, S., Becker, C., Fantini, M.C., Nieuwenhuis, E.E., Tubbe, I., Galle, P.R., Schild, H.J., Birkenbach, M., Blumberg, R.S., and Neurath, M.F. (2005). EBV-induced gene 3 transcription is induced by TLR signaling in primary dendritic cells via NF-kappa B activation. J Immunol *174*, 2814-2824.
573. Wolchok, J.D., Kluger, H., Callahan, M.K., Postow, M.A., Rizvi, N.A., Lesokhin, A.M., Segal, N.H., Ariyan, C.E., Gordon, R.A., Reed, K.*, et al.* (2013). Nivolumab plus ipilimumab in advanced melanoma. N Engl J Med *369*, 122-133.
574. Wolf, A.A., Yáñez, A., Barman, P.K., and Goodridge, H.S. (2019). The Ontogeny of Monocyte Subsets. Front Immunol *10*, 1642.
575. Wong, W.K., Leem, J., and Deane, C.M. (2019). Comparative Analysis of the CDR Loops of Antigen Receptors. Front Immunol *10*, 2454.
576. Workman, C.J., Szymczak-Workman, A.L., Collison, L.W., Pillai, M.R., and Vignali, D.A. (2009). The development and function of regulatory T cells. Cell Mol Life Sci *66*, 2603-2622.
577. Wucherpfennig, K.W., Gagnon, E., Call, M.J., Huseby, E.S., and Call, M.E. (2010). Structural biology of the T-cell receptor: insights into receptor assembly, ligand recognition, and initiation of signaling. Cold Spring Harb Perspect Biol *2*, a005140.
578. Wurzer, H., Filali, L., Hoffmann, C., Krecke, M., Biolato, A.M., Mastio, J., De Wilde, S., Francois, J.H., Largeot, A., Berchem, G.*, et al.* (2021). Intrinsic Resistance of Chronic Lymphocytic Leukemia Cells to NK Cell-Mediated Lysis Can Be Overcome In Vitro by Pharmacological Inhibition of Cdc42-Induced Actin Cytoskeleton Remodeling. Front Immunol *12*, 619069.
579. Wykes, R.C., and Lignani, G. (2018). Gene therapy and editing: Novel potential treatments for neuronal channelopathies. Neuropharmacology *132*, 108-117.
580. Xia, A., Zhang, Y., Xu, J., Yin, T., and Lu, X.J. (2019). T Cell Dysfunction in Cancer Immunity and Immunotherapy. Front Immunol *10*, 1719.
581. Xiao, S., Jin, H., Korn, T., Liu, S.M., Oukka, M., Lim, B., and Kuchroo, V.K. (2008). Retinoic acid increases Foxp3+ regulatory T cells and inhibits development of Th17 cells by enhancing TGF-beta-driven Smad3 signaling and inhibiting IL-6 and IL-23 receptor expression. J Immunol *181*, 2277-2284.
582. Xu, D., Gu, P., Pan, P.-Y., Li, Q., Sato, A.I., and Chen, S.-H. (2004). NK and CD8+ T cell-mediated eradication of poorly immunogenic B16-F10 melanoma by the combined action of IL-12 gene therapy and 4-1BB costimulation. International Journal of Cancer *109*, 499-506.
583. Xu, W., Yang, S., Zhou, K., Pan, L., Li, Z., Zhou, J., Gao, S., Zhou, D., Hu, J., Feng, R.*, et al.* (2020). Treatment of relapsed/refractory chronic lymphocytic leukemia/small lymphocytic lymphoma with the BTK inhibitor zanubrutinib: phase 2, single-arm, multicenter study. J Hematol Oncol *13*, 48.
584. Yan, Y., Huang, L., Liu, Y., Yi, M., Chu, Q., Jiao, D., and Wu, K. (2022). Metabolic profiles of regulatory T cells and their adaptations to the tumor microenvironment: implications for antitumor immunity. Journal of Hematology & Oncology *15*, 104.
585. Yang, R., Cai, Z., Zhang, Y., Yutzy, W.H.t., Roby, K.F., and Roden, R.B. (2006). CD80 in immune suppression by mouse ovarian carcinoma-associated Gr-1+CD11b+ myeloid cells. Cancer Res *66*, 6807-6815.

586. Yao, L., Wang, M., Niu, Z., Liu, Q., Gao, X., Zhou, L., Liao, Q., and Zhao, Y. (2017). Interleukin-27 inhibits malignant behaviors of pancreatic cancer cells by targeting M2 polarized tumor associated macrophages. Cytokine *89*, 194-200.
587. Ye, Z., Yue, L., Shi, J., Shao, M., and Wu, T. (2019). Role of IDO and TDO in Cancers and Related Diseases and the Therapeutic Implications. J Cancer *10*, 2771-2782.
588. Yeste, A., Mascanfroni, I.D., Nadeau, M., Burns, E.J., Tukpah, A.M., Santiago, A., Wu, C., Patel, B., Kumar, D., and Quintana, F.J. (2014). IL-21 induces IL-22 production in CD4+ T cells. Nat Commun *5*, 3753.
589. Yonekura, S. (2022). Epstein-Barr Virus-induced Gene 3 as a Novel Biomarker in Metastatic Melanoma With Infiltrating CD8(+) T Cells: A Study Based on The Cancer Genome Atlas (TCGA). Anticancer Res *42*, 511-517.
590. Yoshida, H., and Hunter, C.A. (2015). The immunobiology of interleukin-27. Annu Rev Immunol *33*, 417-443.
591. Yoshimoto, T., Morishima, N., Mizoguchi, I., Shimizu, M., Nagai, H., Oniki, S., Oka, M., Nishigori, C., and Mizuguchi, J. (2008). Antiproliferative activity of IL-27 on melanoma. J Immunol *180*, 6527-6535.
592. Yoshimoto, T., Okada, K., Morishima, N., Kamiya, S., Owaki, T., Asakawa, M., Iwakura, Y., Fukai, F., and Mizuguchi, J. (2004). Induction of IgG2a class switching in B cells by IL-27. J Immunol *173*, 2479-2485.
593. Zaborsky, N., Holler, C., Geisberger, R., Asslaber, D., Gassner, F.J., Egger, V., Piñón-Hofbauer, J., Kocher, T., Hartmann, T.N., Greil, R*., et al.* (2015). B-cell receptor usage correlates with the sensitivity to CD40 stimulation and the occurrence of CD4+ T-cell clonality in chronic lymphocytic leukemia. Haematologica *100*, e307-310.
594. Zelenetz, A.D., Gordon, L.I., Wierda, W.G., Abramson, J.S., Advani, R.H., Andreadis, C.B., Bartlett, N., Byrd, J.C., Czuczman, M.S., Fayad, L.E*., et al.* (2015). Chronic lymphocytic leukemia/small lymphocytic lymphoma, version 1.2015. J Natl Compr Canc Netw *13*, 326-362.
595. Zhang, C., Wang, Y., Xun, X., Wang, S., Xiang, X., Hu, S., Cheng, Q., Guo, J., Li, Z., and Zhu, J. (2020a). TIGIT Can Exert Immunosuppressive Effects on CD8+ T Cells by the CD155/TIGIT Signaling Pathway for Hepatocellular Carcinoma In Vitro. J Immunother *43*, 236-243.
596. Zhang, H., Madi, A., Yosef, N., Chihara, N., Awasthi, A., Pot, C., Lambden, C., Srivastava, A., Burkett, P.R., Nyman, J*., et al.* (2020b). An IL-27-Driven Transcriptional Network Identifies Regulators of IL-10 Expression across T Helper Cell Subsets. Cell Rep *33*, 108433.
597. Zhang, J., Qian, X., Ning, H., Yang, J., Xiong, H., and Liu, J. (2010). Activation of IL-27 p28 gene transcription by interferon regulatory factor 8 in cooperation with interferon regulatory factor 1. J Biol Chem *285*, 21269-21281.
598. Zhang, M., Hu, Y., Yang, F., Zhang, J., Zhang, J., Yu, W., Wang, M., Lv, X., Li, J., Bai, T*., et al.* (2022). Interaction between AhR and HIF-1 signaling pathways mediated by ARNT/HIF-1β. BMC Pharmacology and Toxicology *23*, 26.
599. Zhang, N., and Bevan, M.J. (2011). CD8(+) T cells: foot soldiers of the immune system. Immunity *35*, 161-168.
600. Zhang, Q., Cunha, A.P.D., Li, S., Hao, Q., Kainz, V., Huang, Q., and Wu, H.Y. (2019). IL-27 regulates HIF-1α-mediated VEGFA response in macrophages of diabetic retinopathy patients and healthy individuals. Cytokine *113*, 238-247.
601. Zhang, Q., Wang, L., Jiang, J., Lin, S., Luo, A., Zhao, P., Tan, W., and Zhang, M. (2020c). Critical Role of AdipoR1 in Regulating Th17 Cell Differentiation Through Modulation of HIF-1α-Dependent Glycolysis. Front Immunol *11*, 2040.
602. Zhang, W., Sharma, R., Ju, S.T., He, X.S., Tao, Y., Tsuneyama, K., Tian, Z., Lian, Z.X., Fu, S.M., and Gershwin, M.E. (2009). Deficiency in regulatory T cells results in development of antimitochondrial antibodies and autoimmune cholangitis. Hepatology *49*, 545-552.
603. Zhang, X., Liu, X., Zhou, W., Du, Q., Yang, M., Ding, Y., and Hu, R. (2021). Blockade of IDO-Kynurenine-AhR Axis Ameliorated Colitis-Associated Colon Cancer via Inhibiting Immune Tolerance. Cell Mol Gastroenterol Hepatol *12*, 1179-1199.

604. Zhao, R., Zhou, X., Khan, E.S., Alansary, D., Friedmann, K.S., Yang, W., Schwarz, E.C., Del Campo, A., Hoth, M., and Qu, B. (2021). Targeting the Microtubule-Network Rescues CTL Killing Efficiency in Dense 3D Matrices. Front Immunol *12*, 729820.
605. Zhou, L., Lopes, J.E., Chong, M.M., Ivanov, II, Min, R., Victora, G.D., Shen, Y., Du, J., Rubtsov, Y.P., Rudensky, A.Y.*, et al.* (2008). TGF-beta-induced Foxp3 inhibits T(H)17 cell differentiation by antagonizing RORgammat function. Nature *453*, 236-240.
606. Zhou, X., Kong, N., Wang, J., Fan, H., Zou, H., Horwitz, D., Brand, D., Liu, Z., and Zheng, S.G. (2010). Cutting edge: all-trans retinoic acid sustains the stability and function of natural regulatory T cells in an inflammatory milieu. J Immunol *185*, 2675-2679.
607. Zhu, J., Guo, L., Watson, C.J., Hu-Li, J., and Paul, W.E. (2001). Stat6 is necessary and sufficient for IL-4's role in Th2 differentiation and cell expansion. J Immunol *166*, 7276-7281.
608. Zhu, J., Liu, J.Q., Shi, M., Cheng, X., Ding, M., Zhang, J.C., Davis, J.P., Varikuti, S., Satoskar, A.R., Lu, L.*, et al.* (2018). IL-27 gene therapy induces depletion of Tregs and enhances the efficacy of cancer immunotherapy. JCI Insight *3*.
609. Ziello, J.E., Jovin, I.S., and Huang, Y. (2007). Hypoxia-Inducible Factor (HIF)-1 regulatory pathway and its potential for therapeutic intervention in malignancy and ischemia. Yale J Biol Med *80*, 51-60.
610. Zorzoli, A., Di Carlo, E., Cocco, C., Ognio, E., Ribatti, D., Ferretti, E., Dufour, C., Locatelli, F., Montagna, D., and Airoldi, I. (2012). Interleukin-27 inhibits the growth of pediatric acute myeloid leukemia in NOD/SCID/Il2rg-/- mice. Clin Cancer Res *18*, 1630-1640.